UNIVERSIDAD AUTÓNOMA DE MADRID

FACULTAD DE CIENCIAS

Departamento de Química-Física Aplicada

METABOLÓMICA DE COMPUESTOS BIOACTIVOS: NUEVOS DESARROLLOS METODOLÓGICOS Y APLICACIONES

TANIZE DOS SANTOS ACUNHA

Tesis Doctoral

Instituto de Investigación en Ciencias de la Alimentación

(CIAL, CSIC-UAM)

Madrid, 2017

UNIVERSIDAD AUTÓNOMA DE MADRID

FACULTAD DE CIENCIAS

Departamento de Química-Física Aplicada

METABOLÓMICA DE COMPUESTOS BIOACTIVOS: NUEVOS DESARROLLOS METODOLÓGICOS Y APLICACIONES

Memoria presentada por:

Tanize dos Santos Acunha

Para optar al grado de

Doctora en Biología y Ciencias de la Alimentación

Trabajo realizado bajo la dirección de:

Dr. Alejandro Cifuentes

Dra. Carolina Simó

Instituto de Investigación en Ciencias de la Alimentación (CIAL, CSIC)

Tutor Académico:

Dra.Tiziana Fornari Reale

Universidad Autónoma de Madrid (UAM)

D. Alejandro Cifuentes Gallego, Doctor en Ciencias Químicas, Profesor de Investigación en el Instituto de Investigación en Ciencias de la Alimentación (CIAL) del Consejo Superior de Investigaciones Científicas (CSIC)

y

Dª. Carolina Simó Ruiz, Doctora en Ciencias Químicas, Científico Titular en el Instituto de Investigación en Ciencias de la Alimentación (CIAL) del Consejo Superior de Investigaciones Científicas (CSIC).

CERTIFICAN:

Que la presente memoria: "**METABOLÓMICA DE COMPUESTOS BIOACTIVOS: NUEVOS DESARROLLOS METODOLÓGICOS Y APLICACIONES**", que presenta **Dña. Tanize dos Santos Acunha**, ha sido realizada bajo nuestra dirección en el Departamento de Bioactividad y Análisis de Alimentos del Instituto de Investigación en Ciencias de la Alimentación. Y para que así conste, firmamos el presente certificado en Madrid a 9 de junio de 2017.

Dr. Alejandro Cifuentes Gallego

Dra. Carolina Simó Ruiz

A mis padres...

Índice

Abreviaturas

^{13}C-NMR (*carbon-13 nuclear magnetic resonance*): resonancia magnética nuclear de carbono-13

^{1}H-NMR (*proton nuclear magnetic resonance*): resonancia magnética nuclear de protón

^{31}P-NMR (*phosphorus-31 nuclear magnetic resonance*): resonancia magnética nuclear de fósforo-31

ACC (*acetyl-CoA carboxylase*): acetil-CoA carboxilasa

AMPK (*adenosine monophosphate-activated protein kinase*): proteina quinasa activada por adenosín monofosfato

ANOVA (*analysis of variance*): análisis de la varianza

APCI (*atmospheric pressure chemical ionization*): ionización química a presión atmosférica

API (*atmospheric pressure ionization*): ionización a presión atmosférica

BGE (*background electrolyte*): electrolito de separación

BSTFA (*N,O-bis-trimethylsilyltrifluoroacetamide*): N,O-bis-trimetilsilil-trifluorocetamida

CCS (*collision cross section)*: sección transversal de colisión

CE (*capillary electrophoresis*): electroforesis capilar

CEC (*capillary electrochromatography*): electrocromatografía capilar

CGE (*capillary gel electrophoresis*): electroforesis capilar en gel

CI (*chemical ionization*): ionización química

CIEF (*capillary isoelectric focusing*): isoelectroenfoque capilar

CITP (*capillary isotachophoresis*): isotacoforesis capilar

CVA (*canonical variate analysis*): análisis canónico discriminante

CZE (*capillary zone electrophoresis*): electroforesis capilar zonal

DA (*discriminant analysis*): análisis discriminante

DART (*direct analysis in real time*): análisis directo en tiempo real

DESI (*desorption electrospray ionization*): ionización por desorción con electrospray

DI (*direct infusion*): infusión directa

DNA (*deoxyribonucleic acid*): ácido desoxirribonucleico

EI (*electron impact*): impacto electrónico

EOF (*electroosmotic flow*): flujo electroosmótico

ESI (*electrospray ionization*): ionización por electrospray

FI (*flow injection*): inyección de flujo

FT (*Fourier transform)*: transformada de Fourier

GC (*gas chromatography*): cromatografía de gases

GCxGC (*two dimensional gas chromatography*): cromatografía de gases bidimensional

GMD (*golm metabolome database*): base de datos metabolómico

GSH (*reduced glutathione*): glutatión reducido

GSSG (*oxidized glutathione*): glutatión oxidado

HILIC (*hydrophilic interaction chromatography*): cromatografía de interacción hidrófila

HMDB (*human metabolome database*): base de datos del metaboloma humano

HPLC (*high-performance liquid chromatography*): cromatografía de líquidos de alta resolucion

HPMA (*N-(2-hydroxypropyl) methacrylamide*): *N*-(2-hidroxipropil) metacrilamida

ICR (*ion cyclotron resonance*): resonancia de ion-ciclotrón

IMS (*ion mobility spectrometry*): espectrometría de movilidad iónica

IT (*ion trap*): trampa de iones

KEGG (*Kyoto encyclopedia of genes and genomes*): enciclopedia de genes y genomas de Kyoto

LC (*liquid chromatography*): cromatografía de líquidos

LDA (*linear discriminant analysis*): análisis lineal discriminante

LTQ (*linear trap quadrupole*): cuadrupolo de trampa lineal

m/z (*mass-to-charge ratio*): relación masa-carga

MALDI (*matrix-assisted laser desorption/ionization*): desorción/ionización por láser asistida por una matriz

MEKC (*micellar electrokinetic chromatography*): cromatografía electrocinética micelar

MPP: Mass Profiler Professional software

MS (*mass spectrometry*): espectrometría de masas

MS/MS (*tandem mass spectrometry*): espectrometría de masas en tándem

MSTFA (*N-methyl-trimethylsilyltrifluoroacetamide*): N-metil-trimetilsilil-trifluoroacetamida

NIST (*National Institute of Standards and Technology*): Instituto Nacional de Estándares y Tecnología

NMR (*nuclear magnetic resonance*): resonancia magnética nuclear

NRF2 (*nuclear factor (erythroid-derived 2)-like 2*): factor de transcripción nuclear eritroide-2

OPLS (*orthogonal partial least squares*): proyecciones ortogonales a estructuras latentes

OPLS-DA (*orthogonal partial least square discriminant analysis*): análisis discriminante por mínimos cuadrados parciales ortogonal

PCA (*principal component analysis*): análisis de componentes principales

PLS (*partial least squares*): mínimos cuadrados parciales

PLS-DA (*partial least square discriminant analysis*): análisis discriminante por mínimos cuadrados parciales

PREDIMED: Prevención con Dieta Mediterránea

PTR (*proton-transfer reaction*): reacción de transferencia de protones

Q (*quadrupole*): cuadrupolo

REACH (*European Regulation on Registration, Evaluation, Authorisation and Restriction of Chemicals*): registro, evaluación, autorización y restricción de las sustancias y preparados químicos

ROS (*reactive oxygen species*): especies reactivas del oxígeno

RP (*reversed-phase*): fase inversa

SFE (*supercritical fluid extraction*): extracción con fluidos supercríticos

SPE (*solid phase extraction*): extracción en fase sólida

TEDETAMA (*2-(3-(Bis(2(diethylamino)ethyl)amino) propanamido)ethyl methacrylate*): 2-(3-(bis(2-(dietilamino)etil)amino)propanamido)etil metacrilato

TMCS (*trimethylchlorosilane*): trimetilsililclorosilano

TOF (*time of flight*): tiempo de vuelo

UHPLC (*ultra high-performance liquid chromatography*): cromatografía de líquidos de ultra alta resolución

UV (*ultraviolet*): ultravioleta

VIP (*variable importance in the projection*): importancia de la variable en la proyección

VOCs (*volatile organic compounds*): compuestos orgánicos volátiles

Resumen

La secuenciación del genoma humano ha dado lugar a la llamada "era post-genómica" en la cual se plantea una visión integral de los procesos biológicos que se ha visto reflejada en el desarrollo de las denominadas "tecnologías ómicas". Las principales tecnologías ómicas desarrolladas durante los últimos años son la genómica, la transcriptómica, la proteómica y la metabolómica. Sin embargo, el sufijo "ómica" se está aplicando a numerosas ramificaciones y disciplinas que se están estableciendo a medida que se obtiene un mayor conocimiento de las múltiples posibilidades que dichas tecnologías ómicas presentan. En este sentido, la Alimentómica (también conocida como *Foodomics*) ha sido recientemente definida como una nueva disciplina, que haciendo uso de las técnicas ómicas (principalmente transcriptómica, proteómica y metabolómica), permite abordar de una forma global aspectos relacionados con la bioactividad, calidad, seguridad y trazabilidad de los alimentos e investigar la relación existente entre los alimentos y la salud. La Alimentómica ofrece un enfoque holístico de la investigación en alimentos y/o de los efectos a nivel molecular asociados a los mismos.

En esta Tesis Doctoral se presentan nuevas aproximaciones metodológicas para el desarrollo de herramientas metabolómicas utilizando diferentes técnicas analíticas, como la electroforesis capilar (CE), la cromatografía de líquidos (LC) y la cromatografía de gases (GC) acopladas a espectrometría de masas (MS), así como sus aplicaciones en aproximaciones relacionadas con la Alimentómica.

La memoria está dividida en seis capítulos, en el Capítulo 1 se presenta como Introducción una amplia visión de la temática objetivo de esta Tesis Doctoral, así como sus fundamentos teóricos más importantes, y en el Capítulo 2 se describen los principales objetivos del trabajo realizado.

El Capítulo 3 contiene cuatro Trabajos relacionados con el desarrollo de nuevas metodologías mediante CE y CE-MS y su aplicación en Alimentómica. En el primero (*Capillary Electrophoresis in Food and Foodomics*) y en el segundo (*CE-MS in Food Analysis y Foodomics*) de los trabajos contenidos en el Capítulo 3, se describe el potencial de las técnicas CE y CE-MS para el análisis de compuestos importantes en el área de la ciencia de los alimentos y se incluye una detallada descripción experimental y metodológica del uso de CE-MS para el análisis alimentómico. En el tercer trabajo del Capítulo 3 (*Potential of prodendronic polyamines with modulated segmental charge density as novel coating for fast and efficient analysis of peptides and basic proteins by CE and CE-MS*) se investiga el uso de una nueva familia de polímeros como recubrimientos adsorbidos físicamente a la pared del capilar para el análisis de péptidos y proteínas básicas por CE-UV y CE-MS. En concreto, se investigan diferentes recubrimientos poliméricos basados en un homopolímero de 2-(3 (bis(2(dietilamino)etil)amino)propanamido)etil metacrilato (TEDETAMA) y tres copolímeros de TEDETAMA, estos últimos sintetizados con unidades neutras de *N*-(2-hidroxipropil) metacrilamida (HPMA) en diferentes porcentajes molares. Además de prevenir las interacciones de proteínas y péptidos con la pared interna del capilar, los polímeros de

TEDETAMA también permiten invertir el flujo electroosmótico. Entre los polímeros investigados, el recubrimiento capilar con TEDETAMA-co-HPMA (50:50) presenta la capacidad de separar péptidos y proteínas en tiempos cortos de migración y con buena resolución. Además, el método desarrollado con este recubrimiento polimérico permite el análisis de proteínas básicas, tal como la lisozima, en muestras de alimentos como el queso.

El cuarto trabajo del Capítulo 3 (*Anionic metabolite profiling by capillary electrophoresis–mass spectrometry using a noncovalent polymeric coating. Orange juice and wine as case studies*) está dirigido al desarrollo de una nueva estrategia analítica para el análisis del perfil metabólico de aniones por CE-MS, empleando un recubrimiento capilar con el copolímero TEDETAMA-co-HPMA (50:50) con la finalidad de invertir y estabilizar el flujo electroosmótico. El empleo del mencionado copolímero como recubrimiento capilar catiónico permite la separación de metabolitos aniónicos en tiempos de análisis cortos y con alta reproducibilidad y eficacia.

En el Capítulo 4 se desarrolla una aproximación metabolómica para evaluar el efecto de los compuestos bioactivos de romero, ácido carnósico, carnosol y rosmanol, en un modelo *in vitro* de células de hígado humano (HepaRG). Con el fin de maximizar la cobertura del metaboloma analizado, se ha empleado una aproximación metabolómica multiplataforma basada en GC-MS y LC-MS. La combinación de los resultados de las diferentes plataformas analíticas permite aumentar el número de metabolitos identificados y evaluar su expresión significativamente diferente en células HepaRG tras el tratamiento con los mencionados diterpenos de romero.

En el Capítulo 5 se presenta una discusión general y en el Capítulo 6 se recogen las conclusiones finales de los principales trabajos realizados en esta Tesis Doctoral. Además, se incluyen como anexos a la memoria tres artículos de investigación que han sido realizados en colaboración con el Dr. Guillaume L. Erny, de la Universidade do Porto, durante el período de desarrollo de esta Tesis Doctoral.

Summary

The completion of the human genome sequence led to the "post-genomic era" that has made possible a better understanding of many biological processes through the development of the so-called "omics technologies". The main omics technologies developed so far have been genomics, transcriptomics, proteomics and metabolomics. However, the suffix "-omics" is being used more and more in other fields in parallel to our growing knowledge about the huge possibilities of these omics technologies. In this sense, Foodomics has recently been defined as a new discipline that studies the food and nutrition domains through the application of advanced omics technologies to improve consumer's well-being, health, and confidence. Foodomics offers a holistic approach to the study of food and/or their effects at molecular level.

This PhD Thesis presents new methodological developments for metabolomics based on different analytical techniques, such as capillary electrophoresis (CE), liquid chromatography (LC) and gas chromatography (GC) coupled to mass spectrometry (MS), as well as several applications in Foodomics.

The Thesis is divided into six chapters, Chapter 1 presents as Introduction a broad vision of the objective topic of this Doctoral Thesis, as well as its main theoretical fundamentals, and Chapter 2 describes the main objectives within the scope of this PhD work.

Chapter 3 contains four articles related to the development of new methodologies by means of CE and CE-MS and their application in Foodomics. The potential of CE and CE-MS for the analysis of important compounds in the area of food science is reviewed in the first (*Capillary Electrophoresis in Food and Foodomics*) and second (*CE-MS in Food Analysis y Foodomics*) article of this Chapter 3. In addition, it includes a detailed experimental and methodological description of the use of CE-MS in Foodomics. In the third article of Chapter 3 (*Potential of prodendronic polyamines with modulated segmental charge density as novel coating for fast and efficient analysis of peptides and basic proteins by CE and CE-MS*) the use of a new family of polymers has been investigated as capillary coatings for the analysis of peptides and basic proteins by CE-UV and CE-MS. Four different polymers have been evaluated, a homopolymer based on 2-(3-(bis(2(diethylamino)ethyl)amino) propanamido)ethyl methacrylate (TEDETAMA), and three copolymers that randomly incorporate TEDETAMA together with neutral units of N-(2-hydroxypropyl) methacrylamide (HPMA) at different molar percentages. The coatings based on TEDETAMA prevent protein and peptide interactions onto the capillary wall, and they have also demonstrated the ability to reverse the electroosmotic flow. Among the polymers studied, poly-(TEDETAMA-*co*-HPMA) 50:50 copolymer has the ability to separate peptides and proteins in short migration times and with good resolution. Moreover, the method developed with this capillary coating has also shown to be effective for the analysis of lysozyme in commercial cheese samples.

The fourth article of Chapter 3 (*Anionic metabolite profiling by capillary electrophoresis–mass spectrometry using a noncovalent polymeric coating. Orange juice and wine as case studies*) is focused on the development of an new analytical strategy for anionic metabolite profiling by CE-MS using the TEDETAMA-co-HPMA (50:50) copolymer as capillary coating to reverse and stabilize the electroosmotic flow. The use of this cationic capillary coating allows the analysis of anionic metabolites in a short migration time, with good reproducibility and high separation efficiency.

Chapter 4 addresses the development of a metabolomic approach to evaluate the toxicity of three bioactive compounds from rosemary (namely, the diterpenes carnosic acid, carnosol and rosmanol) on an *in vitro* model of human liver cells (HepaRG). In order to maximize the coverage of the analyzed metabolome, an analytical multiplatform based on GC-MS and LC-MS has been used. The combination of the results of the different analytical platforms enhances the number of identified metabolites that show a significant different expression in HepaRG cells after treatment with the aforementioned rosemary diterpenes.

In Chapter 5 a general discussion is presented and in Chapter 6 the main conclusions from this PhD work are summarized. Finally, the Appendix section presents three research articles that have been published in collaboration with Dr. Guillaume L. Erny, of the University of Porto, whilst developing this PhD Thesis.

CAPÍTULO 1

Introducción

1. INTRODUCCIÓN

1.1. COMPONENTES BIOACTIVOS DE LA DIETA

Se considera un componente bioactivo de la dieta aquel que influye en la actividad celular y en los mecanismos fisiológicos aportando un beneficio para la salud más allá de la nutrición básica. Un gran número de estudios de investigación indican la existencia de efectos positivos para la salud, por ejemplo mejora de ciertas funciones o reducción del riesgo de padecer enfermedades, originados por algunos componentes de los alimentos. Un ejemplo destacado es el de las propiedades saludables de la "Dieta Mediterránea" (Sofi y col., 2010; Gerber y Hoffman, 2015). La Dieta Mediterránea se caracteriza principalmente por un consumo elevado de compuestos fenólicos y ácidos grasos insaturados procedentes de fuentes vegetales (Gerber y Hoffman, 2015). Por ejemplo, los resultados preliminares del estudio PREDIMED (PREvención con DIeta MEDiterránea), en el que se evaluó la eficacia de la dieta mediterránea suplementada con aceite de oliva virgen extra o enriquecida con frutos secos (nueces, avellanas y almendras) en más de 7000 pacientes con riesgo cardiovascular, demostraron que los participantes presentaban menor frecuencia de infartos de miocardio, de accidentes vasculares cerebrales y de muerte por causa cardiovascular, que aquellos pacientes simplemente sometidos a una dieta baja en todo tipo de grasa (animal y vegetal) (Estruch y col., 2013).

La mayoría de los compuestos bioactivos de origen vegetal son compuestos derivados del metabolismo secundario de las plantas, los cuales se sintetizan como mecanismo de defensa o adaptación al medio (Azmir y col., 2013). También están relacionados con las características sensoriales, tales como amargor, astringencia, color, sabor y aroma, así como con la estabilidad oxidativa de los alimentos de origen vegetal (Naczk y col., 2006). Desde el punto de vista químico, los grupos más importantes de los fitoquímicos derivados del metabolismo secundario son los compuestos fenólicos, los terpenoides, las sustancias azufradas y los alcaloides. Entre ellos, los compuestos fenólicos son uno de los grupos de compuestos más estudiados por sus potenciales beneficios para la salud (Manach y col., 2004). De acuerdo con el número de anillos fenólicos que contienen y según los elementos estructurales que los une, los compuestos fenólicos pueden ser clasificados en cuatro grandes clases: ácidos fenólicos, estilbenos, flavonoides y lignanos (Spencer y col., 2008). Ya han sido descritos más de 8000 compuestos fenólicos diferentes (Pandey y Rizvi, 2009), los cuales presentan una gran diversidad de estructuras químicas y de funciones. Pueden encontrarse en su forma más sencilla como ácidos fenólicos simples o en forma conjugada con otras moléculas como azúcares, proteínas, lípidos, ácidos carboxílicos o incluso a otros compuestos fenólicos (Bravo y col., 1998). El contenido y sus formas estructurales pueden variar según la variedad cultivada, condiciones agronómicas, condiciones de almacenamiento, clima, entre otros (Klepacka y col., 2011). El gran interés por los compuestos fenólicos se debe fundamentalmente a las numerosas evidencias que indican que el consumo de alimentos ricos en compuestos fenólicos presentan protección contra el cáncer (Dai y Mumper, 2010; Galati y Brien, 2004; Fresco y col., 2006), enfermedades cardiovasculares (Morton y col., 2000; de Pascual-Teresa y col., 2010) y

neurodegenerativas (Ramassamy, 2006), entre otras. Muchos de los efectos beneficiosos de los compuestos fenólicos han sido atribuidos a su actividad antitumoral (Carocho y Ferreira, 2013), antiaterogénica (Visioli y Galli, 2001; Szmitko y Verma, 2005), antiinflamatoria (Ríos y col., 2009; Hernández-Aguilera y col., 2013), antimicrobiana (Alves y col., 2013), antioxidante (Kaur y Kapoor, 2001; Balasundram y col., 2006), etc. A pesar de este gran número de estudios, aún es necesario profundizar en el conocimiento de los mecanismos moleculares a través de los cuales los compuestos bioactivos de los alimentos ejercen su función; para ello, las técnicas masivas de análisis, como las técnicas ómicas, pueden proporcionar información de gran utilidad para profundizar en dicho conocimiento.

1.2. TECNOLOGÍAS ÓMICAS. METABOLÓMICA

Después de la secuenciación del genoma humano se inicia la llamada "era post-genómica" a partir de la cual se plantea una visión integral de los procesos biológicos, que se ha visto reflejada en el desarrollo de las denominadas "tecnologías ómicas". Las principales ómicas desarrolladas durante los últimos años son la genómica, la transcriptómica, la proteómica y la metabolómica. Sin embargo, el sufijo "ómica" se está aplicando a numerosas ramificaciones que se están estableciendo a medida que se obtiene un mayor número de datos, como por ejemplo, lipidómica, glicómica, peptidómica, farmacogenómica, epigenómica, nutrigenómica, interactómica, etc. Recientemente ha surgido el concepto de "*alimentómica*" (Cifuentes, 2009), definida como una nueva disciplina, que haciendo uso de las técnicas ómicas, permite abordar de una forma global aspectos relacionados con la calidad, seguridad y trazabilidad de los alimentos, y la relación existente entre los alimentos y la salud. Todas estas disciplinas están aportando avances sin precedentes en el conocimiento básico de los sistemas biológicos y su respuesta a factores ambientales como la dieta, la edad, la enfermedad, etc. Las diferentes tecnologías ómicas están permitiendo llevar a cabo nuevos enfoques en la investigación bioquímica y biomédica, ya que ya no es necesario partir de hipótesis de partida restringidas. De este modo, el uso de las técnicas ómicas permite iniciar nuevos estudios sin hipótesis previas y por lo tanto explorar de forma simultánea diversas vías y rutas metabólicas. A continuación se describe con más detalle la metabolómica al ser la técnica que se ha empleado en esta Tesis Doctoral.

La metabolómica es la más reciente de las tecnologías ómicas y tiene como objetivo el estudio sistemático del conjunto de metabolitos (metaboloma) de una determinada célula, tejido, fluido biológico u organismo (Fiehn, 2001). Los metabolitos son las moléculas de bajo peso molecular (normalmente < 1000-1500 Da), productos o intermedios de los procesos químicos o enzimáticos resultado del metabolismo celular. Se puede considerar que los metabolitos son los productos finales de la transcripción y la traducción. Sin embargo, los metabolitos también influyen sobre la transcripción genética a través de lo que se denomina circuito de retroalimentación, en el cual el flujo de información desde el genoma a través de transcriptoma y el proteoma hacia el metaboloma es bidireccional. El resultado de la compleja

interacción de los componentes de los diferentes niveles de expresión y los factores ambientales es lo que da lugar al fenotipo observado (**Figura 1.1**).

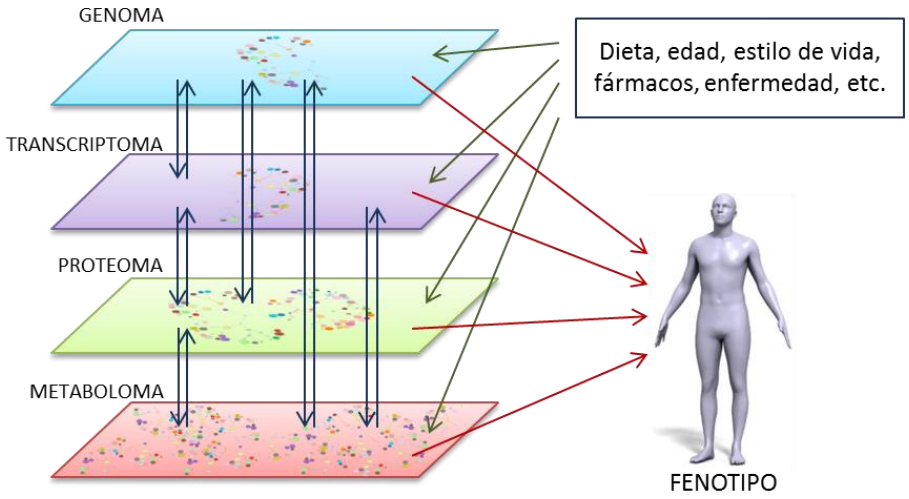

Figura 1.1. Niveles funcionales y sus interacciones en los sistemas biológicos.

A diferencia de los genes y las proteínas, los metabolitos no son específicos de una única ruta metabólica. En muchos casos, varias reacciones bioquímicas contribuyen a la producción de un determinado metabolito. Además, el metaboloma puede verse afectado por diferentes factores externos o internos, de modo que mediante la metabolómica podemos estudiar el efecto de un determinado estado del organismo debido a un estímulo exterior, a una enfermedad, etc. (**Figura 1.2**).

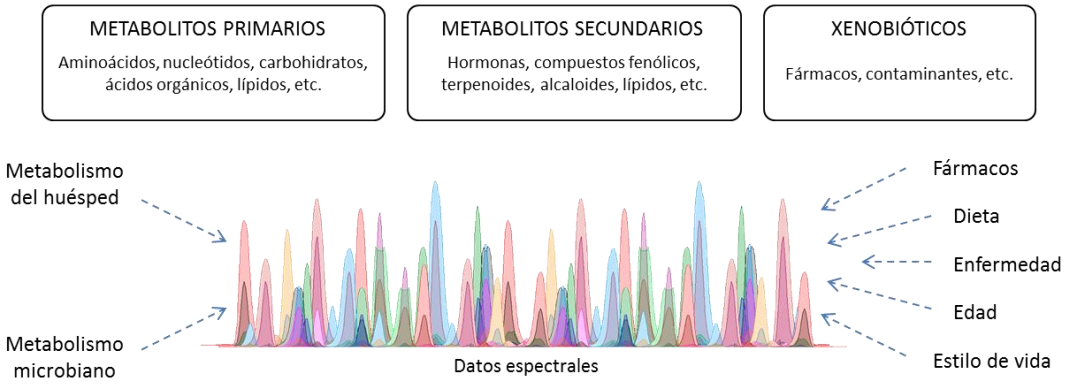

Figura 1.2. Perspectiva general de la complejidad de los estudios metabolómicos.

Las dos estrategias más ampliamente empleadas en metabolómica son el análisis del **perfil metabólico** y la determinación de la **huella metabólica**. En el perfil metabólico el análisis se dirige hacia un grupo de metabolitos con propiedades físico-químicas similares y/o que participan en una determinada ruta metabólica. En la huella metabólica el objetivo es la obtención del mayor número de señales analíticas de metabolitos de una determinada muestra. En este segundo caso no se conoce a priori qué metabolitos están presentes en la muestra, y típicamente, el objetivo del estudio es la clasificación de muestras y/o la búsqueda de biomarcadores.

Uno de los mayores desafíos de la metabolómica es afrontar la complejidad de cualquier metaboloma, normalmente compuesto por un gran número de moléculas con propiedades fisicoquímicas muy diversas. Otro factor importante es el amplio intervalo de concentración de los metabolitos, que se estima que puede ser de más de nueve órdenes de magnitud, desde pM a mM (Dunn y col., 2005). Toda esta diversidad hace que el análisis completo de los metabolitos que forman parte de un determinado sistema biológico sea un gran reto desde el punto de vista analítico.

Para abordar este reto analítico, las herramientas empleadas en metabolómica en la actualidad son la resonancia magnética nuclear (NMR) y la espectrometría de masas (MS). La NMR proporciona un método de análisis rápido, no destructivo, de alto rendimiento, y requiere una preparación mínima de la muestra (Lindon y col., 2003; Reo, 2002). En NMR la detección se basa en la frecuencia de resonancia de los núcleos de los átomos cuándo estos son expuestos a un campo magnético. Debido a la alta abundancia del núcleo de ^{1}H, la ^{1}H-NMR ha sido empleada considerablemente en metabolómica; de hecho, cualquier molécula que contenga hidrógenos en células, tejidos o fluidos biológicos es potencialmente detectable. En menor frecuencia, otros átomos como el carbono (^{13}C-NMR) y el fósforo (^{31}P-NMR) también son objeto de detección por NMR, proporcionando información adicional sobre grupos funcionales de metabolitos específicos (Reo, 2002). En NMR la identificación estructural de los metabolitos se puede llevar a cabo mediante la comparación de los espectros obtenidos con los espectros de librerías (Ellinger y col., 2013). Como se ha comentado anteriormente, en NMR el tratamiento de la muestra es mínimo comparado con el necesario para el análisis por MS (Brennan, 2014), lo que es de gran utilidad en aplicaciones metabolómicas, en las cuales el número de muestras a analizar puede ser muy elevado. No obstante, una de las principales limitaciones de la NMR es la baja sensibilidad (Lenz y col, 2004; Psychogios y col, 2011) lo que reduce su aplicabilidad al análisis de los metabolitos de mayor abundancia en los sistemas biológicos (Dettmer y col, 2007). Por otro lado, la mayor sensibilidad (niveles de detección en el orden de ng/mL-pg/mL o incluso menores) y la gran selectividad de la MS en la identificación y cuantificación de una amplia variedad de metabolitos, han convertido a esta técnica en una valiosa herramienta en metabolómica (Dettmer y col., 2007; Dunn y Ellis, 2005). En MS se lleva a cabo en primer lugar la vaporización e ionización de los metabolitos y a continuación la separación de los iones en función de su relación masa-carga (*m/z*). En metabolómica, el empleo de analizadores de masas de alta y ultra-alta resolución es imprescindible dada la gran complejidad del metaboloma de cualquier muestra biológica, para cuya elucidación se requiere una elevada exactitud en la determinación de los

valores de *m/z* de los iones y de su abundancia isotópica (Junot y col., 2014). El analizador de tiempo de vuelo (TOF), el de tipo Orbitrap® y el analizador de resonancia de ion-ciclotrón con transformada de Fourier (FT-ICR MS), son los espectrómetros de masas que en la actualidad proporcionan mayor resolución y por tanto son los más empleados en metabolómica a pesar de su elevado coste. Por otro lado, la espectrometría de masas en tándem (MS/MS) permite adquirir espectros de fragmentación proporcionando información estructural adicional para su aplicación posterior en el proceso de identificación de los metabolitos de interés. En la siguiente **Tabla 1.1** se muestra un resumen de los espectrómetros de masas de alta resolución más comúnmente utilizados en metabolómica.

Tabla 1.1. Resumen de los espectrómetros de masas de alta resolución más comúnmente utilizados en metabolómica. Fuente: Junot y col. 2014.

Tipo de analizador de masas		Poder de resolución (FWHM)[a]	Exactitud de la masa[b] (ppm)	Tasa de adquisición (Hz)	Intervalo de masas (m/z)	Intervalo dinámico
TOF						
	TOF	Hasta 20,000 (~ 1000 m/z)	< 1-2	Hasta 40	Hasta 20,000	10^4-10^5
	Q/TOF	Hasta 60,000 (~ 1222 m/z)	< 1-2	Hasta 100	Hasta 40,000	10^4-10^5
	IT/TOF	10,000 (~ 1000 m/z)	< 2	10	Hasta 5,000	10^3
Orbitrap						
	Orbitrap-Extractive	Hasta 140,000 (~ 200 m/z)	< 1-3	Hasta 12	Hasta 6,000	10^3-10^4
	LTQ-Orbitrap	Hasta 240,000 (~ 200 m/z)	< 1-3	Hasta 8	Hasta 4,000	10^3-10^4
	Q-Orbitrap	Hasta 140,000 (~ 200 m/z)	< 1-5	Hasta 12	Hasta 4,000	10^3-10^4
FT-ICR						
	LTQ-FT (7T)	> 750,000 (~ 400 m/z)	< 1-1.2	1	Hasta 4,000	10^3-10^4
	Q/FT (7T)	> 1,000,000 (~ 400 m/z)	< 1-1.5	1	Hasta 10,000	10^3-10^4

[a]Poder de resolución (FWHM): se define como la anchura a media altura que presenta un determinado pico/ion en un espectro de masas.

[b]Exactitud de la masa: mide la proximidad del valor registrado de m/z a su verdadero. Se calcula aplicando la siguiente fórmula ((m/z medido – m/z calculado) / m/z calculado) x 1,000,000.

A pesar de las ventajas e inconvenientes de cada una de estas técnicas, los resultados obtenidos mediante NMR y MS aportan generalmente información analítica complementaria, necesaria a la hora de llevar a cabo un análisis del metaboloma lo más completo posible (Dettmer y col., 2007; Lei y col., 2011; Barding y col., 2012; Smolinska y col., 2012). Dada la importancia de la MS en metabolómica y siendo además ésta la herramienta analítica que se ha utilizado en la presente Tesis Doctoral, a continuación se llevará a cabo una descripción de las estrategias analíticas más empleadas con MS.

1.2.1. Análisis directo mediante MS

El análisis directo mediante MS tiene cada vez más importancia en aplicaciones de "alto rendimiento" en metabolómica, en las cuales suele ser necesario el análisis rápido de un elevado número de muestras. Mediante el uso de una gran variedad de sistemas de introducción/ionización directa de la muestra en el

espectrómetro de masas se pueden obtener perfiles y huellas metabólicas en unos pocos segundos, al evitar cualquier etapa de separación previa a la detección por MS.

La **infusión directa** (DI) y la **inyección de flujo** (FI) son las principales técnicas empleadas para introducir muestras líquidas en el espectrómetro de masas. Mientras que la DI se refiere a la ionización continua de una muestra estática, la FI consiste en inyectar una muestra en un flujo continuo que fluye hacia la interfaz de ionización. Los sistemas de ionización a presión atmosférica (API) son los más empleados cuando la inyección de la muestra se lleva a cabo por DI y FI (Draper y col., 2013). Entre los sistemas API, las técnicas de ionización por electrospray (ESI) e ionización química a presión atmosférica (APCI), esta última en menor proporción, son las más utilizadas en el análisis directo por MS empleando DI y FI.

Para el análisis directo mediante MS de compuestos orgánicos en fase gaseosa, se utiliza principalmente la técnica de **reacción de transferencia de protones** (PTR) o la **APCI**. Ambos métodos se basan en la ionización por reacciones de las moléculas iónicas en fase gaseosa seguidas de su detección por MS. Los dos métodos difieren principalmente en la presión en el sistema; mientras que en APCI la ionización ocurre a presión atmosférica, en PTR la ionización se lleva a cabo a baja presión. Ambas técnicas se emplean para la obtención del perfil de compuestos orgánicos volátiles (VOCs) en una gran variedad de muestras biológicas (Biasioli y col, 2011; Dummer y col., 2011).

La técnica **MALDI** (desorción e ionización por láser asistida por una matriz) es una técnica de introducción directa bien establecida en MS. Además de su uso generalizado para el análisis de polímeros y biopolímeros, principalmente péptidos y proteínas, también está cobrando importancia para el análisis de compuestos de bajo peso molecular. Una de las ventajas de la técnica MALDI con respecto a otros sistemas de introducción de muestra es la mayor tolerancia a los contaminantes presentes en la matriz de la muestra. Por otro lado, una de las principales limitaciones de la aplicación de MALDI-MS para el análisis de moléculas de bajo peso molecular es la supresión de la señal debido a los numerosos iones que produce la matriz química añadida a la muestra para la realización del proceso de desorción/ionización por láser. Estrategias tales como la sustitución de las matrices normalmente empleadas en MALDI por matrices basadas en iones líquidos u otros compuestos tales como la 9-aminoacrimida que interfieren menos con la señal de los metabolitos, se han empleado con éxito en estudios con un enfoque metabolómico (Vaidyanathan y col., 2006; Edwards y Kennedy, 2005; Miura y col., 2010).

En los últimos años se han desarrollado numerosas **técnicas de ionización ambiental** con el objetivo de superar algunas de las limitaciones de los sistemas anteriormente mencionados, aumentando con ello el número de posibles aplicaciones metabolómicas mediante análisis directo por MS. La principal característica de las técnicas de ionización ambiental es la posibilidad de llevar a cabo el análisis directo de las muestras con poco o ningún pre-tratamiento de las mismas, y sin la necesidad del empleo de cámaras de nebulización cerradas sometidas a vacío como requiere por ejemplo la técnica MALDI. Diferentes tipos de técnicas basadas en distintos mecanismos de desorción/ionización, permiten llevar a

cabo el análisis directo de un gran número de compuestos con diferentes pesos moleculares y polaridades (Weston, 2010; Harris y col., 2011; Monge y col., 2013). Dos de los sistemas más prometedores en el campo de la metabolómica son **DESI** (desorción e ionización por electrospray) (Takats y col, 2004) y **DART** (análisis directo en tiempo real) (Gross, 2014). Mediante DESI un haz de microgotas cargadas eléctricamente es dirigido a una gran velocidad hacia la muestra de interés; al impactar sobre la superficie de la muestra, los analitos, que se disuelven en las microgotas cargadas eléctricamente, entran en el espectrómetro de masas donde son analizados (**Figura 1.3A**). Por otro lado, en la técnica DART se aplica un potencial eléctrico a una corriente de gas pre-calentado (normalmente helio o nitrógeno) para formar un plasma de iones y átomos excitados (**Figura 1.3B**). Este plasma, que se dirige a la superficie de la muestra, produce la desorción de las moléculas de bajo peso molecular (<1 kDa), que entran directamente al espectrómetro de masas para su análisis.

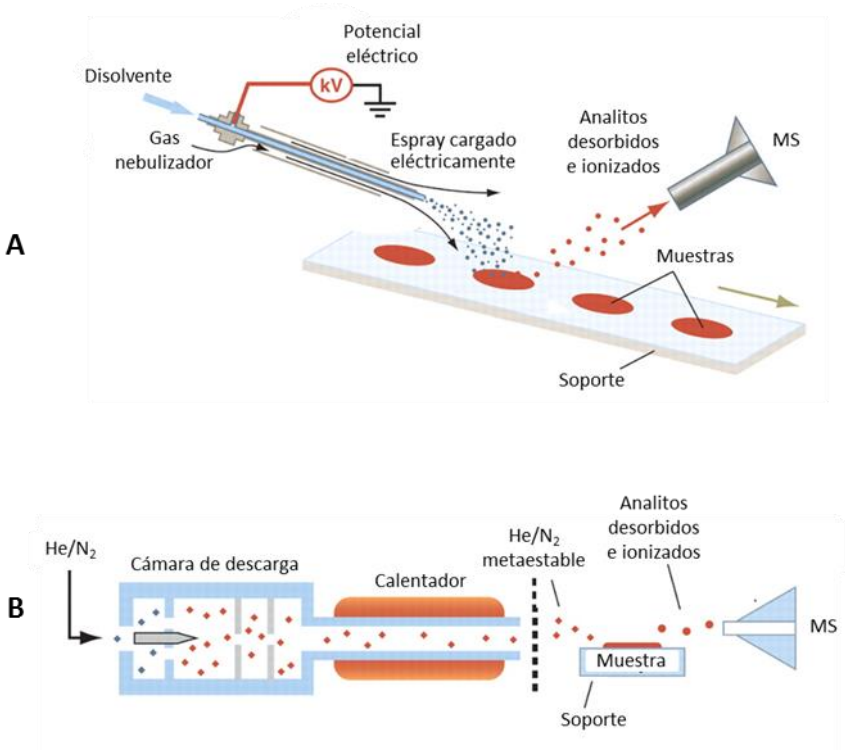

Figura 1.3. Representación esquemática del funcionamiento de las técnicas DESI (A) y DART (B). (extraída y adaptada de Cooks y col., 2006).

Las principales características de las técnicas de introducción directa de muestras en MS y sus principales aplicaciones en el análisis metabolómico, proteómico y peptidómico se describen en el **Trabajo 1.3.1** que lleva por título "*The role of direct high-resolution mass spectrometry in foodomics*" y que se anexa a este Capítulo. Además, en este trabajo se describen y se discuten las principales ventajas y limitaciones de cada técnica, así como los nuevos desarrollos en el área.

A pesar de las ventajas del análisis directo mediante MS, estas técnicas generalmente presentan limitaciones en su sensibilidad debido a los problemas de supresión iónica y baja eficiencia de ionización, así como a las interferencias que produce la matriz de las muestras biológicas normalmente analizadas en metabolómica. Además, no se van a poder diferenciar aquellos metabolitos que presenten el mismo valor m/z. La combinación de la MS con técnicas de separación de alta resolución reduce los efectos de la matriz, lo que lleva a una mejora en la sensibilidad, además de proporcionar información adicional sobre las propiedades fisicoquímicas de los compuestos, lo que ayuda a la identificación de los mismos (Dettmer y col., 2007). La cromatografía de líquidos (LC), la cromatografía de gases (GC) y la electroforesis capilar (CE) son las técnicas de separación más comúnmente empleadas en combinación con MS en metabolómica.

1.2.2. Cromatografía de gases-espectrometría de masas (GC-MS)

La técnica GC-MS ha tenido un papel fundamental en los inicios de la metabolómica, ya que este acoplamiento fue el primero en ser desarrollado debido a la compatibilidad entre la GC y la MS, ya que ambas operan en fase gaseosa. Todavía hoy la GC-MS se emplea ampliamente en metabolómica debido a su gran capacidad de separación, robustez instrumental y repetibilidad de los espectros de masas. En general la separación cromatográfica se lleva a cabo en columnas capilares de polaridad media-alta, a temperaturas de hasta 350 °C. La mayoría de los estudios metabolómicos basados en GC-MS emplean ionización por impacto electrónico (EI), y en menor medida ionización química (CI). En la ionización por EI el empleo de una alta energía de ionización (estandarizada a 70 eV) provoca que el proceso de ionización vaya acompañado por la fragmentación de los analitos. Una de las características más importantes del acoplamiento GC-MS es su capacidad para identificar picos desconocidos mediante el empleo de librerías de espectros, lo cual es posible gracias a la reproducibilidad de los procesos de fragmentación mediante el uso de condiciones estandarizadas en EI. En la actualidad hay diversas bases de datos espectrales, tales como NIST (Instituto Nacional de Estándares y Tecnología) (Babushok y col., 2007) y Wiley (Roessner y col., 2000), comercialmente disponibles, o bases de datos de acceso libre, como Golm Metabolome Database (GMD) (Kopka y col., 2005) o MassBank database (Horai y col., 2010), que permiten llevar a cabo la identificación de los metabolitos a través de la comparación del espectro de fragmentación experimental con los espectros de fragmentación contenidos en estas librerías. En algunos casos, estas bases de datos espectrales contienen también índices de retención altamente reproducibles, lo que aumenta la fiabilidad en la identificación de los metabolitos, dado que en este caso la identificación se lleva a cabo no solo por el patrón de fragmentación en MS, sino también por el índice de retención en GC (Kind y col., 2009). La CI es un método de ionización alternativo que puede ser utilizado para determinar el ion molecular, el cual en ocasiones no está presente en los espectros de EI-MS debido a la alta fragmentación que puede producir este modo de ionización. Sin embargo, la CI

presenta una menor reproducibilidad de la señal obtenida en MS por lo que es un modo de ionización aún poco utilizado en metabolómica.

Además de la reproducibilidad espectral anteriormente comentada, la GC es una técnica que proporciona alta resolución cromatográfica junto con una elevada reproducibilidad de los tiempos de retención. Sin embargo, es una técnica que solo permite el análisis de metabolitos que sean volátiles y térmicamente estables. Como la gran mayoría de los metabolitos primarios no son volátiles, para estos casos se requiere de una etapa de derivatización previa al análisis por GC. El objetivo principal de este proceso es la volatilización de compuestos polares, aunque también permite estabilizar metabolitos térmicamente lábiles y puede mejorar la eficiencia de la separación cromatográfica. El protocolo de derivatización más comúnmente empleado en metabolómica generalmente utiliza dos etapas (Koek y col., 2011). En una primera etapa se lleva a cabo la oximación de los grupos carbonilos, usando clorhidrato de metoxiamina, con el fin de inhibir la ciclación de los azúcares, proteger los compuestos α-cetoácidos frente a la descarboxilación y fijar los grupos carbonilos enolizables. A continuación le sigue un proceso de sililación de los grupos hidroxilo (-OH), carboxilo (-COOH), amino (-NH2), o tiol (-SH). En metabolómica los agentes derivatizantes más comunes son la N-metil-trimetilsilil-trifluoroacetamida (MSTFA) y la N,O-bis-trimetilsilil-trifluorocetamida (BSTFA). En algunas ocasiones, los agentes derivatizantes también pueden ir acompañados de un catalizador, como el trimetilsililclorosilano (TMCS), aunque algunos trabajos sugieren que su uso no produce mejoras significativas en el rendimiento de la derivatización (Koek y col., 2006). Otros procedimientos alternativos de derivatización como el uso de cloroformiato de etilo (Gao y col., 2009) son en general menos empleados en estudios metabolómicos. Una de las mayores limitaciones de esta estrategia analítica de sililación es que aumenta la complejidad de la etapa de preparación de la muestra e introduce mayor variabilidad en el análisis, además de producir en algunos casos más de un producto de derivatización lo que origina más de un pico cromatográfico para el mismo metabolito, dificultando el análisis posterior de los datos.

Los analizadores de masas tradicionalmente más empleados en los acoplamientos GC-MS son los analizadores cuadrupolo (Q) y trampa de iones (IT). Sin embargo la nueva generación de plataformas GC-TOF MS combina la reproducibilidad y el alto poder de resolución de la GC con la sensibilidad, alta resolución y velocidad de adquisición de datos de los analizadores TOF, y por lo tanto son los más comúnmente empleados en metabolómica (Theodoridis y col., 2011).

La configuración bidimensional completa GCxGC ofrece grandes oportunidades en metabolómica para mejorar la separación de los metabolitos que coeluyen en muestras muy complejas, aprovechando el poder de separación de dos modos de separación ortogonales. La configuración GCxGC más empleada en aplicaciones metabolómicas se basa en el empleo de una columna apolar seguida de una columna polar (Mondello y col., 2008). La tecnología bidimensional aporta grandes ventajas en cuanto a su poder de resolución, a expensas de tiempos de análisis más largos y la necesidad de instrumentación compleja y menos robusta (Jeong y col., 2013; Dettmer y col., 2013).

1.2.3. Cromatografía de líquidos-espectrometría de masas (LC-MS)

La cromatografía de líquidos acoplada a espectrometría de masas (LC-MS) es actualmente la técnica más utilizada en metabolómica, debido principalmente a su versatilidad, sensibilidad y su capacidad para analizar una gran variedad de metabolitos. La resolución cromatográfica de esta técnica es inferior a la que proporciona la cromatografía de gases, sin embargo, permite la separación de compuestos termolábiles, con un mayor peso molecular y mayor polaridad sin la necesidad de una etapa previa de derivatización. La ionización por electrospray (ESI) es el modo más ampliamente utilizado en el acoplamiento LC-MS en aplicaciones metabolómicas (Gika y col., 2014). Por otro lado, la APCI está más indicada para el análisis de metabolitos apolares y se suele emplear con menor frecuencia en metabolómica (Theodoridis y col., 2012). La separación por LC depende de las propiedades fisicoquímicas de los metabolitos, lo que determina el modo de separación (fase estacionaria) y la fase móvil que deben ser empleados. En los estudios de metabolómica por LC, la fase inversa (RP) y la cromatografía de interacción hidrófila (HILIC) son los modos de separación más empleados. Aunque las separaciones mediante RP permiten el análisis de una extensa gama de metabolitos, presenta limitaciones en el análisis de especies polares y/o iónicas como, por ejemplo, ácidos orgánicos, aminoácidos, aminas, etc., debido a la baja retención de estos compuestos en la fase estacionaria de naturaleza hidrofóbica. En estos casos, el modo de separación por HILIC proporciona una separación complementaria a la obtenida por RP, y con frecuencia en los estudios metabolómicos se emplea la combinación de ambas. Por otro lado, la introducción de la cromatografía de líquidos de ultra alta resolución (UHPLC) con columnas rellenas con partículas de diámetro <5µm ha provocado una mejora significativa en la resolución cromatográfica, ha aportado mayor sensibilidad y ha proporcionado una gran reducción de los tiempos de análisis en comparación con los análisis clásicos por cromatografía de líquidos de alta eficacia (HPLC) (Wilson y col., 2005; Guillarme y col., 2010). En metabolómica, estos parámetros desempeñan un papel importante dado que una resolución y/o sensibilidad superiores significan una mejor cobertura del metaboloma. Por otro lado, la reducción de los tiempos de análisis aumenta el rendimiento de la técnica. Cada vez son más los estudios metabolómicos que combinan UHPLC con espectrometría de masas de alta resolución (Rodriguez-Aller y col., 2012). En buena parte de los estudios metabolómicos con UHPLC (y HPLC), se emplean analizadores del tipo TOF MS, ya que de esta manera se combina la alta resolución y velocidad de análisis del sistema de UHPLC con la sensibilidad, la alta exactitud de las masas (y alta resolución) y la velocidad de adquisición de datos de los analizadores TOF (Gika y col., 2014). La última generación de analizadores Orbitrap® presentan gran resolución y exactitud en la medida de la masa, así como tiempos de adquisición compatibles con la técnica de UHPLC. Cada vez son más los estudios metabolómicos que emplean el acoplamiento UHPLC-Orbitrap MS (Ghaste y col., 2016), sin embargo, el número de aplicaciones es todavía inferior si se compara con UHPLC-TOF MS o UHPLC-Q/TOF MS. Por último, las desventajas de los equipos de FT-ICR MS son su menor velocidad de adquisición (~1Hz), lo que limita su aplicación en acoplamientos LC-MS y CE-MS, y su elevado coste (Ghaste y col., 2016; Junot y col., 2014).

Recientemente, la espectrometría de movilidad iónica (IMS), la cual proporciona una separación de los iones en fase gaseosa en función de su movilidad (que a su vez está relacionada con el tamaño del ion a través del parámetro denominado sección eficaz de colisión o "*collision cross section*, CCS"), se está empezando a utilizar en combinación con la espectrometría de masas (Shah y col., 2013; Paglia y Astarita, 2017) en aplicaciones metabolómicas.

En el **Trabajo 1.3.2** titulado "*Foodomics: LC and LC-MS-based omics strategies in food science and nutrition*", que se anexa al final de este primer Capítulo, se describe la importancia de la LC y del acoplamiento LC-MS en diferentes disciplinas ómicas como la proteómica, péptidomica, metabolómica, glicómica y lipidómica aplicadas en el área de la Ciencia y Tecnología de los Alimentos y la Nutrición.

1.2.4. Electroforesis capilar-espectrometría de masas (CE-MS)

La electroforesis capilar engloba a un conjunto de técnicas de separación basadas en la diferente movilidad electroforética de las especies a analizar en solución bajo la acción de un campo eléctrico, en el interior de un tubo capilar (Ewing y col., 1989). Ya se ha demostrado que el empleo de CE-MS en metabolómica es una potente herramienta analítica complementaria a LC-MS y GC-MS, ya que permite el análisis de los analitos iónicos y/o de mayor polaridad que son difíciles de analizar mediante las otras técnicas (Ibáñez y col., 2013). La interfase ESI es la más utilizada en la actualidad para el acoplamiento CE-MS, y a diferencia de la técnica LC-MS, la interfase ESI para CE-MS tiene como función, además de la vaporización e ionización de los analitos ya separados mediante CE, el cierre del circuito eléctrico a la salida del capilar.

Existen diversos modos de separación en CE: electroforesis capilar zonal (CZE), electrocromatografía (CEC), cromatografía electrocinética micelar (MEKC), electroforesis capilar en geles o redes poliméricas (CGE), isoelectroenfoque capilar (CIEF) e isotacoforesis capilar (CITP). Estas distintas modalidades se diferencian principalmente en la naturaleza del medio de separación que se encuentra dentro del capilar y en las características de los analitos que se pretenden separar. Los modos de CE más adecuados para su acoplamiento con MS son CZE y CEC ya que son los que emplean tampones de separación compatibles (electrolitos volátiles) con MS (Hirayama y col., 2014; García y col., 2017).

Al igual que ocurre con la técnica LC-MS, uno de los analizadores de masas más adecuados para el acoplamiento CE-MS es el analizador TOF MS, ya que proporciona, como se ha comentado anteriormente, una gran resolución y exactitud en la medida de las masas, junto con una alta velocidad de adquisición de los espectros de masas (Gika y col., 2014). De igual manera, los analizadores Orbitrap® y FT-ICR MS se emplean en menor medida en el acoplamiento CE-MS. En los últimos años se ha publicado un importante número de trabajos mostrando la capacidad de esta técnica para el análisis de perfiles y huellas metabólicas en una gran variedad de muestras (plantas, alimentos, fluidos biológicos, células, tejidos, organismos, etc.) (Ramautar y col., 2013; Ramautar y col., 2017).

En el Capítulo 3 de esta Tesis Doctoral se describe con mayor detalle el papel de la plataforma CE-MS en aplicaciones metabolómicas dentro del área de la alimentómica. Además, al final de este Capítulo 1 se incluye el **Trabajo 1.3.3** que presenta una revisión bibliográfica titulada "*Recent advances in the application of capillary electromigration methods for food analysis and Foodomics*" en la que se discuten las principales aplicaciones de la técnica de electroforesis capilar en el análisis de alimentos y en alimentómica, así como nuevos desarrollos y tendencias en esta área de investigación.

1.2.5. Estrategias metabolómicas multiplataforma

A pesar de los continuos avances y desarrollos en las diferentes técnicas analíticas anteriormente descritas, incluyendo sus múltiples acoplamientos, no existe una plataforma analítica universal que permita el estudio de todos los metabolitos presentes en el metaboloma de una determinada muestra biológica. A diferencia de otras tecnologías ómicas como la genómica, trascriptómica y la proteómica, en metabolómica es necesario emplear múltiples plataformas y configuraciones analíticas que maximicen la cobertura del metaboloma analizado. Por este motivo es cada vez más común en estudios metabolómicos la combinación de la información procedente de distintas plataformas analíticas (Ibáñez y col., 2012a, Ibáñez y col., 2012b). Esto se traduce en un aumento del conocimiento del metaboloma de los organismos o muestras en estudio y en el aumento de la probabilidad de éxito en el descubrimiento de potenciales biomarcadores. Por otro lado, la generación masiva de datos hace que el tratamiento de datos sea una etapa fundamental en cualquier estudio metabolómico. Cada vez más, las multiplataformas se están empleando en análisis metabolómicos en una gran variedad de campos de aplicación, como el clínico (Birungi y col., 2010; Suhre y col., 2010; Saric y col., 2012; Temmerman y col., 2012) y en investigación de los efectos de compuestos bioactivos de la dieta sobre la salud (Law y col., 2008; Martin y col., 2009; van Dorsten y col., 2010; Mellert y col., 2011; Jacobs y col., 2012). Este último aspecto se abordará con detalle en el Capítulo 4 de esta Tesis Doctoral.

1.3. PUBLICACIONES RELACIONADAS

1.3.1. The role of direct high-resolution mass spectrometry in foodomics

Ibáñez, C., Simó, C., García-Cañas, V., Acunha, T., Cifuentes, A.

Analytical and Bioanalytical Chemistry **407,** 6275–6287 (2015).
DOI: 10.1007/s00216-015-8812-1.

Anal Bioanal Chem (2015) 407:6275–6287
DOI 10.1007/s00216-015-8812-1

REVIEW

The role of direct high-resolution mass spectrometry in foodomics

Clara Ibáñez[1] · Carolina Simó[1] · Virginia García-Cañas[1] · Tanize Acunha[1,2] · Alejandro Cifuentes[1]

Received: 6 May 2015 / Accepted: 27 May 2015 / Published online: 5 July 2015

Abstract Foodomics has been defined as a global discipline in which advanced analytical techniques and bioinformatics are combined to address different questions in food science and nutrition. There is a growing number of works on the development and application of non-targeted omics methods in foodomics, which reflects that this emerging discipline is already considered by the scientific community to be a valuable approach to assess food safety, quality, and traceability as well as for the study of the links between food and health. As a result, there is a clear need for more rapid, high-throughput MS approaches for developing and applying non-targeted studies. Nowadays, direct MS analysis is one of the main choices to achieve high throughput, generating a set of information from the largest possible number of samples in a fast and straightforward way. The use of high- and ultrahigh-resolution MS greatly improves the analytical performance and offers a good combination of selectivity and sensitivity. By using a range of methods for direct sample introduction/desorption/ionization, high-throughput and non-target analysis of a variety of samples can be obtained in a few seconds by HRMS analysis. In this review, a general overview is presented of the main characteristics of direct HRMS-based approaches and their principal applications in foodomics.

Published in the topical collection *High-Resolution Mass Spectrometry in Food and Environmental Analysis* with guest editor Aldo Laganà.

✉ Carolina Simó
c.simo@csic.es

[1] Laboratory of Foodomics, CIAL, CSIC, Nicolas Cabrera 9, 28049 Madrid, Spain

[2] CAPES Foundation, Ministry of Education of Brazil, 70.040-020 Brasília, Distrito Federal do Brasil, Brazil

Keywords Foodomics · High-resolution mass spectrometry · Direct MS · Food analysis · Food bioactivity

Introduction

Food analysis is a field in continuous progress, which is particularly driven by consumers' rising demands for food safety and quality. Food safety assessment involves the examination of food for the presence of microbial hazards induced by bacteria, viruses, parasites, toxigenic molds, or microalgae, and also for the presence of chemical compounds such as agrochemicals, environmental contaminants, veterinary drugs, and allergens. Food quality focuses on the evaluation of those attributes and properties that make food acceptable to consumers. In an effort to improve food safety and quality, regulatory authorities have introduced the concept of traceability, which ensures control and management through all stages of food production, processing, and distribution [1]. Effective traceability systems help in the prevention of fraudulent practices which, in most cases, focus on illicit economic gain. Such practices may include adulteration, mislabeling, false use of geographical indications, and deliberate fraudulent practices (production, processing, and distribution), among others, that have direct implications for the quality and the safety of foods. Verification of compliance with food regulations in terms of food safety and quality has been traditionally approached using targeted analysis. This analytical strategy involves a combination of procedures for sample preparation and the subsequent analysis of one or a small number of compounds (pesticides, toxins, proteins, DNA, etc.) from a complex mixture. However, a major requirement to effectively apply the targeted approach is to know the identity of the compound before it can be detected, excluding its application to the analysis of unknown compounds. Considering that

limitation and the increasing requirements from administrative authorities for control of food safety and quality with scientifically based guarantees, the development of novel and complementary non-targeted analytical methodologies is highly advisable. Non-targeted methods combined with suitable chemometric tools have the potential to improve the breadth of traditional targeted analysis and open up new prospects for novel applications, providing the opportunity to explore formerly unanswered problems relevant to food science [2–4]. A good example of this revolutionary view of food analysis is the emerging discipline of foodomics. This discipline studies the food and nutrition domains through the application and integration of advanced omics technologies to improve consumers' well-being, health, and confidence [5]. Thus, foodomics can be conceptualized as a global discipline in which advanced analytical techniques and bioinformatics are combined to address different issues in food science and nutrition. Another area in which foodomics has found an important application is the investigation of the links between food and health [6–10]. In this regard, the growing number of published reports on the development and application of non-targeted methods in foodomics studies reflects that this emerging area is already considered by the scientific community to be a valuable approach to assess food safety, quality, and to study the links between food and health [11, 12].

Hyphenated mass spectrometry techniques such as gas chromatography–mass spectrometry (GC-MS), liquid chromatography–mass spectrometry (LC-MS), and, to a lesser extent, capillary electrophoresis-mass spectrometry (CE-MS) have achieved great success in non-targeted applications. Chromatographic or electrophoretic separation reduces ion suppression effects originating from the sample matrix. However, the major drawback of hyphenated MS-based techniques lies in their limitation to analyze large sets of samples to detect changes in composition in a fast and simple way. There is a clear need for more rapid, high-throughput MS approaches for non-targeted studies. Nowadays, direct MS analysis is the method of choice to achieve the maximum high-throughput production of information from the largest possible number of samples. In direct MS analysis, any separation step prior to MS detection is avoided and thus direct analysis of samples (previously processed or not) is carried out. Without a chromatographic or electrophoretic separation minimal data preprocessing is required, thereby simplifying the analysis and increasing the speed, which makes it particularly attractive when dealing with large sample sets.

The use of high-resolution mass spectrometry (HRMS) greatly improves the analytical performance and offers a good combination of selectivity and sensitivity. High mass resolution and mass accuracy together with measured relative isotopic abundance ratios are used to tentatively identify elemental formulae of thousands of different compounds. In practice, comparison against a database of accurate masses is also used to assign an identity. However, information other than just accurately measured mass is needed to support compound identification. Fragmentation of molecular ions produces a mass spectrum from which the fragments can be used to characterize the molecule of interest. However, MS/MS spectra might vary depending on the instrument used, the collision energy used, the collision gas used, etc. Moreover, fragmentation mass spectra are not always accurate in unequivocal identification of isomeric compounds. NMR, which would allow full structure elucidation, requires large amounts of material and thus low levels of unknown compounds are likely to remain difficult to identify. Matching against standards is also another strategy for identifying unknown compounds. However, in many cases, no authentic standards are available for comparison.

Several reports have recently reviewed the principles and techniques of high-resolution mass spectrometers [13–15]. Fourier transform ion cyclotron mass spectrometry (FTICR MS), especially at high fields, enables reliable assignment of molecular formula for completely unknown small molecules. The new generation of time-of-flight (TOF) instruments as well as the Orbitrap technology offers exceptional sensitivity at high resolution and sub-second scan speeds. By using a range of methods for direct sample introduction/desorption/ionization methods, high-throughput and non-target analysis of a variety of samples can be obtained in a few seconds by HRMS analysis. These direct methods provide innovative ways to utilize available ionization methods and are especially aided by high mass resolution and MS/MS capabilities. In this review, a general overview is presented of the main characteristics of direct HRMS-based approaches and their main applications in foodomics.

Direct injection

By using a variety of direct sample-introduction techniques, non-target analysis can be carried out in a short time by direct MS analysis. Direct infusion (DI) and flow injection (FI) are the main techniques used to introduce liquid samples into the mass spectrometer. While DI refers to the continuous ionization of a static sample, FI consists of injecting a sample into a continuous stream of organic phase flowing to the ionization interface. Among atmospheric pressure ionization (API) techniques, electrospray ionization (ESI) ion source and, to a lesser extent, atmospheric pressure chemical ionization (APCI) are the techniques typically employed in direct MS analysis using DI and FI [16]. When using both DI and FI sample typically needs to be treated to dissolve the compounds of interest in the appropriate solvent. On the other hand, for the direct analysis of organic compounds in gas-phase samples, proton-transfer reaction mass spectrometry (PTR-MS) is mainly used.

DI-HRMS and FI-HRMS

In the food quality and safety field, much research has been done on wine owing to its economic importance. Cooper and Marshall presented the first attempts to prove the capabilities of DI ESI-FTICR MS to fingerprint wine for classification purposes [17]. At that time, the authors suggested that negative ionization mode was preferable to positive ionization because of a dominant sucrose peak in the latter mode which led to limited mass spectral dynamic range. In a different work, a "metabologeographic signature" by DI ESI-FTICR MS of barrel-aged wines was suggested [18] following observation that the geographic origin and the species of oak wood influenced the quality of wines matured in oak barrels. On that occasion, the authors claimed that both positive- and negative-ion data showed the same discrimination capabilities. The same DI ESI-FTICR MS analytical platform was employed to study champagne [19], specifically the differences between the chemical fingerprints of the champagne bulk and the aerosol formed when a myriad of ascending bubbles collapse and radiate a multitude of tiny droplets. As expected, hundreds of chemical components with organoleptic properties or potential to be aroma precursors were observed to be preferentially partitioned in the champagne aerosols rather than in the champagne bulk. In a different report, DI ESI-FTICR MS was applied for wine classification samples obtained from different valleys, years of harvest, and processing techniques [20]. The obtained results reinforced the fact that the percentages of correct discrimination and classification of wines depend on the variability of the samples analyzed and the type of signals used for discrimination/classification. Moreover, the authors underlined the importance of the mathematical model (built with spectral information) to improve the percentages of classification. Fermentation process monitoring as well as the addition of sugar or unfermented must to wine has also been investigated with DI ESI-TOF MS [21]. Recently, FTICR MS spectra of grape extracts and wines were used to obtain complex chemical fingerprints of thousands of compounds [22]; as an example, Fig. 1 shows several of these complex chemical fingerprints. The importance of terroir and vintage effects on wine and grape chemodiversities was demonstrated by DI ESI-FTICR MS; however, the majority of the discriminant masses could not be annotated, exemplifying the yet unknown chemical complexity of grape and wine compositions [22]. Other beverages, such as coffee, have also attracted interest. As an example, DI ESI-FTICR MS was employed to analyze polar compounds from coffee aqueous extracts and to explore the capabilities of the technique as a fast method to predict the blend composition of the two most common varieties of the world's coffee production (robusta and arabica) [23].

Preliminary evidence of the utility of DI ESI-TOF MS for edible oil authentication purposes was shown in 2002 by Goodacre et al. [24]. Using minimal sample preparation, the authors clearly separated olive oil from oils commonly used as adulterants. Thereafter, characterization of edible oils by DI ESI-MS has continued to receive considerable interest because of the large increase in demand for high-quality edible oils. Compositional-based fingerprints of vegetable oils (canola, olive, and soybean) by DI ESI-FTICR MS were used to characterize them and to detect and identify adulterants [25]. While fatty acids were found to be the most abundant compounds in the negative-ion mass spectra, triacylglycerols and diacylglycerols dominated the positive-ion mass spectra. DI ESI-FTICR MS has also been applied to the study of rancidity in macadamia nut oil [26]. As expected, different methods of oil extraction and storage resulted in different levels of peroxides in the oil that are associated with rancidity. Moreover, non-target analysis of macadamia nut oil extracts indicated that, together with well-known free radical oxidation of fatty acids, enzymatic activity also played an important role in rancidity and, consequently, in oil quality. DI ESI-QqQ-TOF MS and FIA ESI-QqQ-TOF MS were also employed to analyze the lipid fraction and obtain a classification model to discriminate between different types of hams in relation to the feeding of the pigs [27].

DI ESI-FTICR MS also showed the potential to study genetically modified maize samples [28]. Based on the FTICR MS spectral data obtained in both positive and negative ESI modes, differences between the metabolic profiles of transgenic and wild maize could be highlighted and elementary compositions of specific GMO biomarkers were studied (Fig. 2). Electrophoretic mobilities and *m*/*z* values provided by the CE-TOF MS platform helped confirm the identity of various isomeric compounds that could not be unequivocally identified by FTICR MS, such as isomeric compounds.

Direct APCI-HRMS and PTR-HRMS

Dynamic measurements of the gas-phase volatile content are possible with direct APCI-MS and direct PTR-MS. Both methods are based on the ionization by gas-phase ion–molecule reactions followed by MS. The two methods mainly differ in the pressure in the system: atmospheric pressure for APCI-MS and low pressure for PTR-MS. APCI-MS has proved to be a valuable technique for direct monitoring of volatile organic compounds (VOCs). When using APCI for the direct analysis of complex food samples, one can sometimes differentiate overlapping ions by inducing limited fragmentation of the compound by increasing the voltage before the ions enter the mass filters, to obtain more spectral information.

In flavor release applications, traditional GC-MS is time consuming compared to direct APCI-MS. Ashraf et al. demonstrated good correlation between both techniques [29], and showed a rapid determination of key aroma compounds in

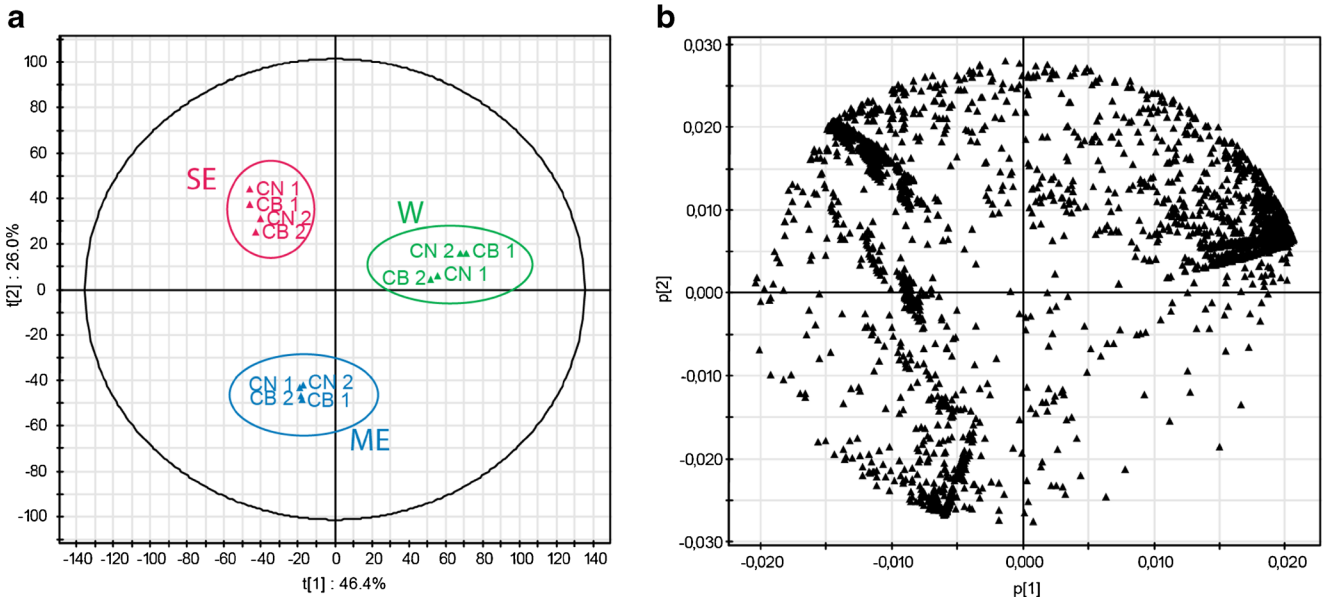

Fig. 1 (**a**) Scores plot and (**b**) loading plot of the PCA analysis of the FTICR-MS data for wines (*green*), skin (*pink*) and must (*blue*) extracts of the 2008 vintage from Côte de Nuits (*CN*) and Côte de Beaune (*CB*) locations. The first two components retained 72.4 % of the variation. Reprinted with permission from reference [22]

beer by APCI-MS. This method permitted the time course of flavor compound formation to be followed during fermentation and could also be used to differentiate beers [29]. Other interesting applications can be found in the literature, such as flavor release from French fries [30] and dried red bell peppers [31]. In the latter case, the accurate mass measurements by APCI-TOF MS allowed the differentiation between compounds with the same nominal mass, but with different elemental compositions.

PTR-MS, originally developed in the mid-1990s [32], is a very interesting technology for fast and sensitive direct measurement of volatile compounds in air, with no pretreatment of the sample. PTR is a form of chemical ionization based on the ionization by gas-phase ion–molecule reactions with the main

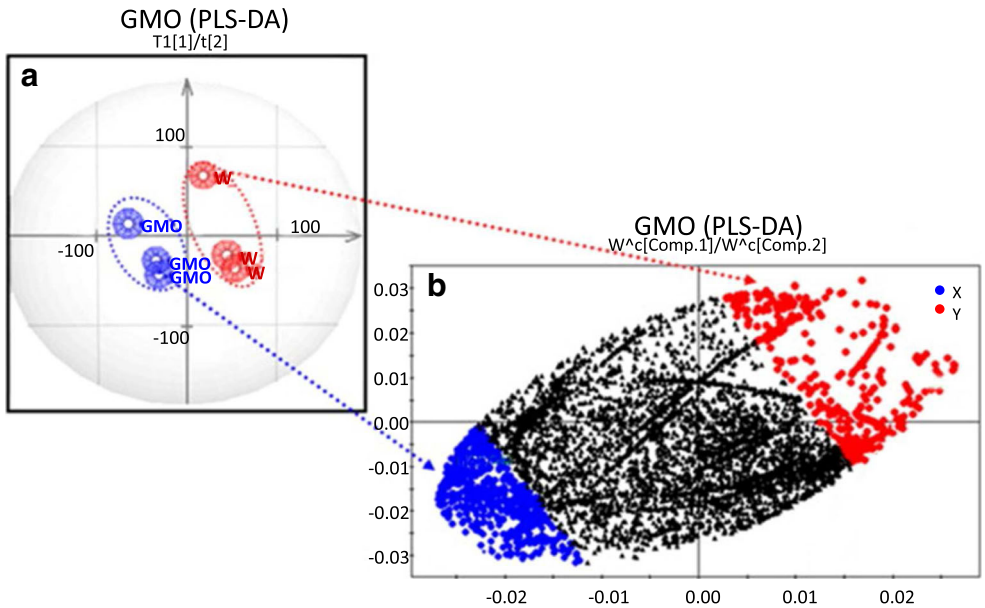

Fig. 2 2PLS-DA model (Q^2(cum) = 0.52 and R2(Y) = 0.99) with six different maize varieties analyzed by DI ESI-FTICR MS. Three *GMO* and three Wild type (*W*). The score scatter plot underlines a different pattern for the transgenic (they are represented in *blue* color) and isogenic lines (*red* color). The different properties of the discriminative masses (represented in *blue* and *red* in the loading plot) are investigated with MassTRIX (www.masstrix.org). Reprinted with permission from [28]

primary ions H_3O^+. The ionization principle is governed by the proton affinity (PA) of the sample molecule, which has to be higher than the PA of water, a criterion that is satisfied by most VOCs. This is a soft ionization method, which often does not lead to fragmentation of the product ions. It has been suggested that PTR-MS allows more accurate quantification owing to a controlled and efficient ionization, which also offers higher sensitivity. PTR-MS enables the continuous online detection of changes in the composition and quantity of volatiles in food [33], among other types of sample [34]. The application of this technique usually leads to a fingerprint of the emission of VOCs profile from food samples for the study of quality, fermentation, ripening, and processing. As an example, PTR-MS has been used to investigate volatile fingerprints of orange juices subjected to different thermal and pressure treatments [35], classification of milk fats of different qualities [36], prediction of freshness of bread [37], classification of infant formulas according to different brands and physical forms [38], and prediction of sensory profiles of coffee [39]. Special importance has been given to wine [40, 41] owing to the economic importance of this industry.

Quadrupole MS has been employed in most published PTR-MS works. The performance of the first PTR-TOF MS instrument was demonstrated by Blake et al. in 2004 [42]. Since then, improvements in mass resolution, mass range, and LOD have been achieved [43]. Since the pioneering works in 2010 involving the analysis of VOCs by PTR-TOF MS to study the effect of storage conditions of milk on the final quality of cheese [44] and for monitoring of lactic acid fermentation of milk [45, 46], a variety of applications have demonstrated the great potential of this approach in the field of food science and technology. Analysis of VOCs by PRT-TOF MS permitted the discrimination among different olive varieties and stage of ripeness [47], as well as the monitoring of VOC release during post-harvest ripening of different apple cultivars [48]. Classification of dry cured hams produced following the indications of different protected designations of origin (PDOs) [49] and different diet of the pigs [50] was also achieved with PTR-TOF MS. Profiling hundreds of peaks from volatile compounds to study the evolution of volatile compounds during storage of dried porcini was also possible by PTR-TOF MS [51]. Owing to the importance of coffee volatiles in flavor attributes of coffee the suitability of PTR-TOF MS has been demonstrated in several works. Thus, volatile profiles from ground coffees from different origins were obtained by PTR-TOF MS and used to classify samples according to geographic origin [52], to study the evolution of the roasting process [53], and to monitor changes in espresso coffee for investigating the impact of different parameters that affect extraction dynamics of flavor compounds (see Fig. 3) [54]. In another type of practical application, the effect of sugar concentration on the release of volatile compounds both from cereal bars and from mouth during consumption was investigated [55]. The influence of compositional and structural-mechanical properties of yogurt matrices on the release of flavor volatile compounds has also been studied by PTR-TOF MS [56].

PTR-TOF MS offers interesting advantages, which can be optimally used for online breath analysis [57]. Although there are some established and emerging clinical applications of breath analysis [58], the full potential of PTR-TOF MS to study complex effects of dietary factors on the generation of breath compounds has not yet been exploited. Some works have demonstrated the usefulness of PTR-TOF MS to investigate relationships between pathologies induced by dietary regime and breath composition [59]. Several marker compounds directly related to liver metabolism could be identified in the exhaled breath of rats. Recently, breath analysis in humans by PTR-TOF MS showed that coeliac disease patients on a gluten-free diet presented the same breath profile as healthy ones, demonstrating that at the time of breath analysis they did not show any symptom of the disease [60].

In a recent study, APCI-MS and PTR-MS provided equivalent results for the study of in vitro and in vivo flavor release [61]. Although a higher degree of fragmentation was observed with PTR-MS, similar response linearity and sensitivities were obtained. One of the drawbacks of PTR-MS is that only those compounds whose PA is larger than that of H_2O can be detected. Recently, with the introduction of the "switchable reagent ionization", it is possible to switch between H_3O^+ ions ionizing via proton-transfer reactions and NO^+ and O_2^+, or Kr^+ ions, thereby providing even greater analytical value and extending the range of measurable compounds [62, 63].

Matrix-assisted and matrix-free laser desorption/ionization

MALDI-MS is also a well-established tool and complementary to other soft ionization approaches, such as ESI. Unlike ESI, MALDI affords higher tolerance towards contaminants arising from the sample. Although the major research focus has been on the analysis of large molecules (proteins), MALDI-MS is also applicable to analytes with intermediate and smaller masses. The main limitation in the application of MALDI-MS to analyze small molecules is signal suppression due to matrix background ions. Strategies, such as use of ionic liquid-based matrices [64] or other matrix-assisted compounds, such as 9-aminoacridine [65, 66], have been presented for applications of high-throughput metabolomics. Other approaches involve the use of matrix-free strategies to counteract these interferences. The use of silicon surfaces has also been proved to be effective and simple for high-throughput analysis of small molecular weight compounds [67, 68].

MALDI-MS has been increasingly used in foodomics approaches because of its high sample throughput. Among other applications, it has been used to determine the origin of food

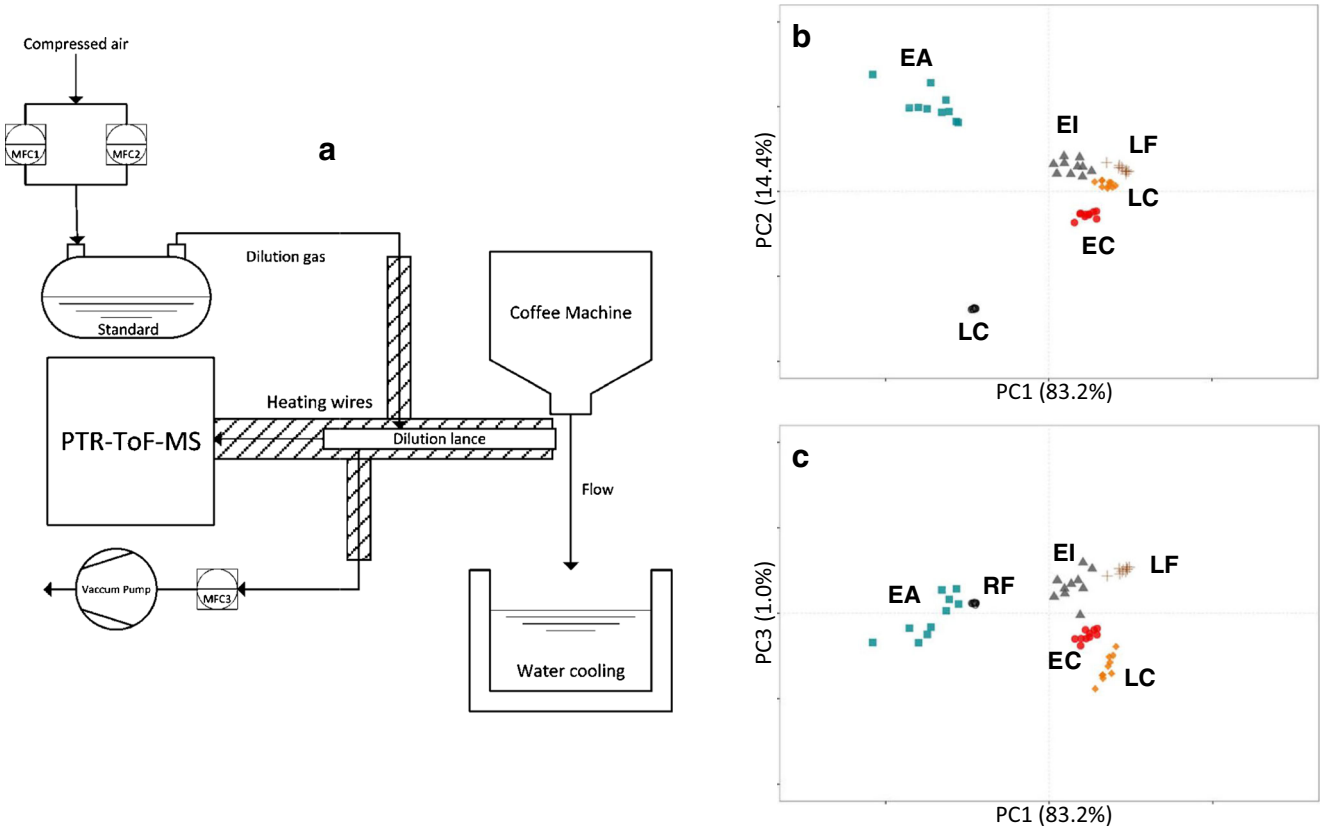

Fig. 3 (**a**) Set up for sampling VOCs from the coffee flow. Volatiles were introduced into the dilution lancet by a flow created with a vacuum pump and were then diluted 7.5 fold using dried compressed air containing a standard for mass calibration. (**b**, **c**) Score plots for the three first dimensions of PCA of the six capsule varieties: Ristretto Forte (*RF*), Espresso Intenso (*EI*), Espresso Alba (*EA*), Espresso Classico (*EC*), Lungo Fortissimo (*LF*), and Lungo Crema (*LC*)) using the full extraction time corrected by weight of extracted coffee (G, H, I). Reprinted with permission from [54]

[69–71] and food adulterations [72–77]. The discrimination of samples on the basis of their protein fingerprints using MALDI-MS is also an intense area of research [78–80]. For instance, protein and maltooligosaccharide fingerprints from 17 different brands of beer purchased at different time points were obtained with a rapid and simple MALDI-MS method [80]. Beers of the same brand but from different breweries were clearly discriminated and most beers could be assigned to their brands. Milk adulteration and contamination is also a topic of major interest and has been extensively evaluated using MALDI-MS. Thus, MALDI-TOF mass spectra were used to determine and quantify the protein components of various types of milks (from cow, sheep, and goat) with minimal sample pretreatment [73]. By using the whole spectrum of peaks obtained from the analysis, MALDI-TOF MS showed good potential for rapid detection of milk adulteration. Similarly the detection of fraudulent addition of cow milk to sheep and goat milks (of higher value) was investigated by MALDI-TOF MS [75]. Lipid profiles for the analyzed milks showed a different abundance ratio of the ions *m/z* 703 and 706 which was directly correlated with addition of cow milk into sheep or goat milks. Donkey milk was also analyzed by MALDI-TOF MS in order to detect contaminants and adulterations with bovine or goat milks [76]. Protein profiles were obtained for goat, cow, and donkey milks and their mixtures in the positive-ion mode without any pretreatment and thus the enhancing speed of the method; unintended contaminations up to a limit of 0.5–2 % were determined and fraudulent mixtures with goat or cow milks were detected using this method [76]. Similar limits of adulteration (ca. 0.5 %) were also obtained through MALDI-TOF MS making it possible to detect adulteration of both donkey and goat milks with other species' milks (cow, ewe, and buffalo) on the basis of their different proteomic profiles [77].

A MALDI-TOF MS method was also developed for the authentication and quality control of 29 hazelnut (*Corylus avellana* L.) cultivars based on the analysis of peptide and protein components [71]. Hazelnut kernel samples were analyzed in the positive-ion mode and acquired in the *m/z* 3500–15000 range. The unambiguous discrimination of the selected cultivars was achieved on the basis of specific biomarker patterns found in the kernels. Likewise, peptide profiles from the aqueous extract of peanut kernel were analyzed by MALDI-TOF MS [81]. The potential use of peanut extract as a food supplement was revealed owing to its rich peptide content and

low phytate levels [81]. More recently, the effect of encapsulation of fish oils on lipid oxidation was determined by MALDI-TOF MS [82]. Powders obtained from emulsions with different compositions were analyzed for water content, encapsulation efficiency, matrix crystallinity, and oxidation products. A trehalose/sodium caseinate matrix was shown to be the most efficient for microencapsulation of polyunsaturated oils providing a spectrum very similar to the original non-treated oil [82].

Ambient desorption/ionization

Recently, new ambient ionization techniques were introduced to overcome some of the intrinsic limitations of ESI and MALDI, thereby increasing the number of applications that can be addressed using direct MS. The main characteristic of ambient ionization techniques is that they allow direct sampling/ionization of samples in open air or ambient environment with little or no sample preparation. The sample is positioned at the entrance of a mass analyzer in the open environment and molecules released from the sample are ionized and transferred to the mass spectrometer. A variety of methods, based on different desorption/ionization mechanisms, allow the direct MS analysis of a gamut of compounds with a wide range of molecular weights and polarities [83–85]. Among them, direct and desorption electrospray ionization (DESI) and direct analysis in real time (DART) are still the two most prevalent techniques.

DESI-HRMS

In DESI, which is mechanistically related with ESI, electrosprayed aqueous droplets are directed to a surface of interest in air and act as projectiles desorbing ions from the surface as a result of electrostatic and pneumatic forces. Electrical charge applied to the solution produces charged droplets, which in aqueous solutions lead to an excess of hydronium ions (H_3O^+) or hydroxide ions (OH^-), and hence to protonated or deprotonated analytes, which are observable in the positive-ion and negative-ion modes, respectively [86]. This mechanism implies that the solubility of the analytes in the spray solvent is an important consideration in DESI analysis. DESI has shown better performance (i.e., higher tolerance to salts) than direct ESI [87]. It can be applied across an extensive mass range from small molecules to medium size proteins [88] and causes minimum fragmentation. DESI-HRMS has also been demonstrated to be a useful tool for multiresidue analysis of a wide range of agrochemical (insecticides, herbicides, and fungicides) in fruit surfaces [89].

Rapid DESI-TOF MS analysis (ca. 30 s) of sulfur volatiles in several onion varieties made it possible to distinguish phenotypes (tearless and normal) as demonstrated by Joyce et al. [90]. By using this approach, they confirmed decreased concentrations of the lachrymatory factor 3 and higher concentrations of sulfenic acid condensates in a tearless onion variety. Anthocyanin profile evaluation, used for detection of illicit wine coloring, was also carried out by DESI-TOF MS [91]. A variety of anthocyanins could be detected in red wine samples from different vintages and cultivars, as well as in berries. However, some isobaric compounds remained undistinguished, demonstrating the need for high mass accuracy measurements to improve the applicability of DESI in anthocyanin analysis [91]. Analysis of less polar compounds is also feasible by DESI-MS. Thus, Gerbig and Takáts [92] showed that it was possible to detect triglycerides as alkali metal or ammonium adducts by DESI-Orbitrap MS. Analysis of the triglyceride content in edible oils and fats was carried out by simply dispersing the oil on a glass slide which makes it an attractive approach in high-throughput quality control applications in the food industry [92]. Only a few studies have been undertaken to show the potential of DESI-MS for the investigation of proteins (both standards and biological samples) [93] and protein digests [94, 95]. Recently, Montowska et al. demonstrated the potential of surface desorption/ionization methods together with HRMS for meat protein/peptide analysis for authentication purposes [96]. After assessment of the methodology with standard proteins (myoglobin, troponin C, actin, bovine serum albumin, tropomyosin), ambient DESI and liquid extraction surface analysis (LESA) demonstrated the capability to discriminate subtle spectral differences between samples of meat from closely related species. The detection of unique peptides from the most abundant proteins specific to each species (bovine, horse, pig, chicken, and turkey) was achieved by both DESI- and LESA-Orbitrap. As can be seen in Fig. 4 unequivocal discrimination between species was achieved.

Paper spray [97], a technique with close connections to ESI and nanoelectrospray, is an alternative to DESI for the analysis of surfaces in foods [98]. The electrospray is induced from the sharp tip of a triangular shaped piece of paper containing a small amount of sample by applying a high voltage. Usually, sample is loaded by dropping or by wiping the surface of interest onto the triangular paper. It has also been modified to directly analyze leaves of plants. Following this approach, major sweet glycosides and their oxidation products were identified from a fresh triangular piece of stevia leaf by using an Orbitrap MS [99]. Among the stevia glycosides identified by MS and MS^n, rebaudioside D standard was used for semi-quantitative determinations.

DART-HRMS

In DART, an electrical potential is applied to a heated gas stream (typically helium or nitrogen) to form a plasma of excited-state atoms and ions that desorb low molecular weight

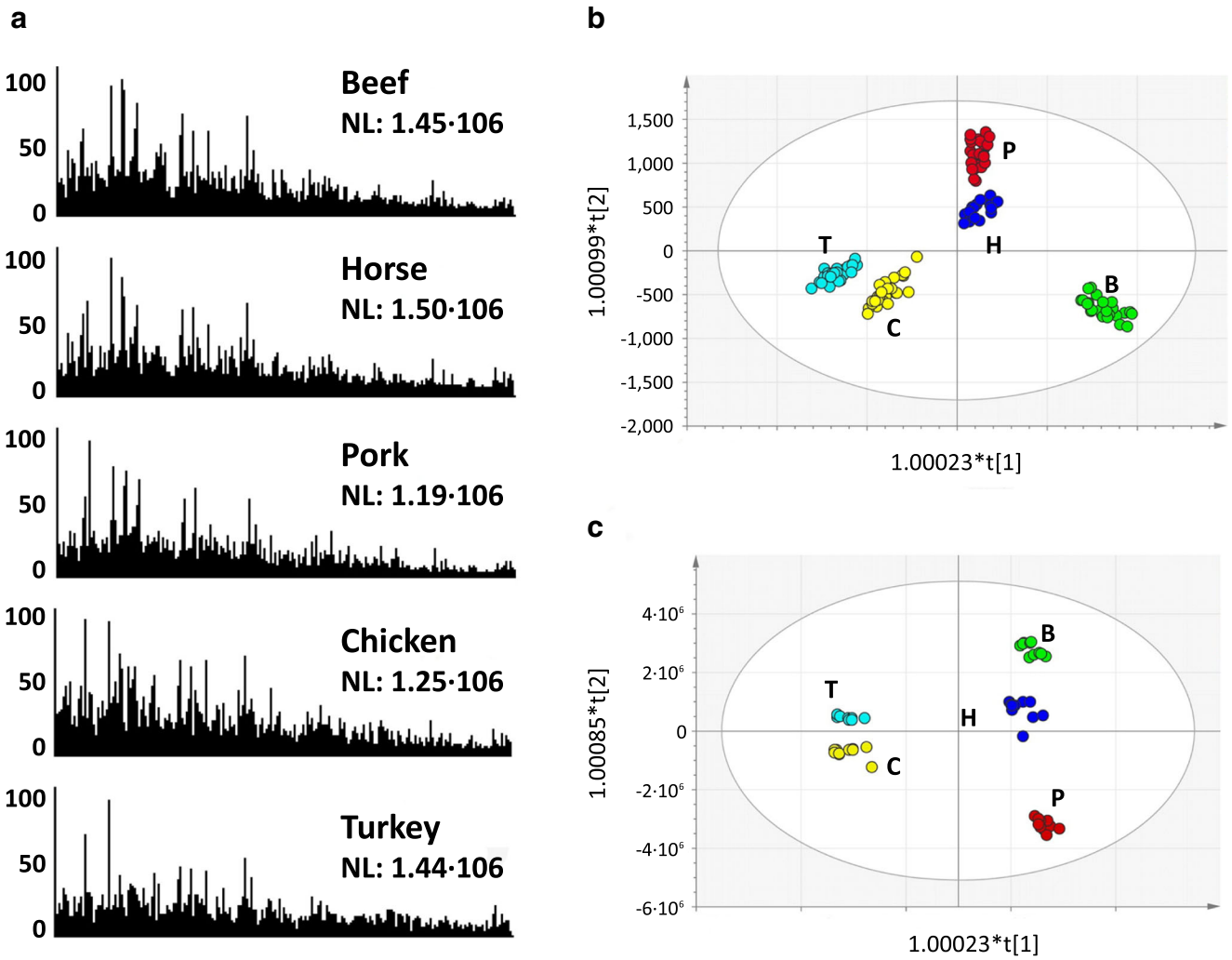

Fig. 4 Differentiation between beef, pork, horse, chicken, and turkey meat. **a** Average mass spectra of meat digest obtained using liquid extraction surface analysis mass spectrometry (LESA-MS); **b** OPLS-DA score plots of data sets collected using DESI-MS in the range of *m/z* 400−1600 (n=125); **c** OPLS-DA score plots of data sets collected using LESA-MS in the range of *m/z* 400−1000 (n=50). *B* beef, *H* horse meat, *P* pork, *C* chicken meat, *T* turkey meat. Reprinted with permission from [96]

molecules from the surface of a sample [100]. DART is capable of analyzing low to high polarity compounds (up to 1 kDa) in both negative- and positive-ion modes, either in solid or liquid samples. DART produces relatively simple mass spectra characterized in most cases by $[M+H]^+$ in positive-ion mode and $[M-H]^-$ in negative-ion mode. The majority of systems have interfaced the DART ionization source with TOF MS. DART-MS is gaining importance in foodomics, particularly within the areas of contamination, food packaging, authenticity, and adulteration [101, 102]. DART-HRMS has shown great potential for multiresidue screening. Study of contaminants present in fruits by exposing the peel (without any pretreatment) to DART-HRMS is particularly interesting owing to the high sample throughput and real-time identification of compounds [103]. A total of ten different xenobiotics could be tentatively identified in the different fruit samples. Among them, imazalil was selected to explore quantitative possibilities of the method and to carry out an unequivocal identification by matching the isotopic cluster with the analytical standard. If no specimen pretreatment is carried out to the surface, it might result in poor sensitivity. Thus, effective contaminant detection was possible by applying swabbing methods on the surfaces of fruits and vegetables [104, 105]. Thus, by spiking different pieces of fruits with a complex mixture of pesticides, it was demonstrated that swabs increased sample throughput by reducing sample preparation and analysis time [104]. A variety of contaminants, such as acrylamide, can also be produced during food processing. Mass spectral fingerprints obtained also by DART-Orbital ion trap MS enabled high-throughput fingerprinting of biscuit samples submitted to different heat-treatments applied during the baking process [106]. Models for prediction of acrylamide were obtained from chemical fingerprints by using partial least square regression (PLSR) analysis to accurately predict

the amounts of acrylamide formed during baking of biscuits under various conditions of time and temperature. DART-Orbitrap MS has also demonstrated potential in the study of other unintended processes, such as lipid oxidation, which may occur during processing/storage of vegetable oils and that can lead to deterioration of both their nutritional and sensory quality [107].

Mislabeling, adulteration, false use of geographical indications, deliberate fraudulent practices, among others, have important economic implications in the food industry; and in this field, DART-HRMS is undergoing rapid development. DART-TOF MS has demonstrated the capability to classify olive oils according to their quality grade, as well as adulteration of extra virgin olive oil with other cheaper oils [108]. In that work, triacylglycerols (TAGs) and TAGs together with polar compounds dominated the spectral profiles of whole oils and methanol-water extracts, respectively [108]. As expected, differentiation of positional isomers of TAGs with two or three different fatty acids was not possible by DART-TOF MS. Analysis of non-polar fractions obtained from cheese by DART-Orbitrap MS enabled fast recognition of cheese adulteration with poor quality vegetable oils. Discrimination was based on detection of compounds arising from oxidation of plant TAGs [109]. Authentication of animal fat through rapid profiling of TAGs was also feasible by DART-TOF MS and multivariate analysis [110]. Unequivocal identification of TAGs detected in the samples and/or the differentiation among their stereoisomers was not possible because of the simultaneous desorption/ionization of all compounds present; nevertheless, the resulting mass spectral fingerprints enabled the creation of predictive models for animal fat classification. Fraudulent practices of animal feeding [111], beer origin recognition [112], and identification of the origins of commercial cubeb fruits [113] were also feasible through chemical fingerprinting by DART-TOF MS and subsequent multivariate analysis. DART-HRMS is also gaining importance in food characterization of complex matrices, such as propolis [114] and mustard [115], as a fingerprint-based approach for fast qualitative evaluation of food products. In the latter work, major glucosinolates found in mustard were tentatively identified as sinigrin and sinalbin. Standards of sinalbin and sinigrin were then used for unambiguous identification and for semiquantitative determination purposes [115].

DAPPI-HRMS

Desorption atmospheric pressure photoionization (DAPPI) [116] is a different ambient ionization method that allows the surface analysis of neutral and non-polar compounds, opening up new possibilities for the analysis of compounds poorly ionized by DESI. DAPPI uses the reactive chemistry of APPI and the analytes from surfaces are desorbed by a heated jet of gas and vaporized spray solvent [117]. DAPPI was shown to have a better matrix tolerance and to cause less contamination of the ion source when compared with DESI [118]. DAPPI-MS has also been demonstrated to be a suitable technology in environmental and food analysis [119]. However, so far low resolution mass spectrometers have been used together with DAPPI and thus limited information could be obtained from the analysis of food products (fish oil and butter) [120].

Conclusions and final comments

Direct HRMS-based approaches combined with suitable chemometric tools are opening up new prospects in food science. Combination of HRMS with direct sample introduction/desorption/ionization methods is a promising approach in foodomics, especially in food safety, quality, and authenticity evaluation studies. Among direct MS-based approaches, ambient mass spectrometry is a very active area of research in which modifications to existing methodologies are continuously being introduced. Traditional barriers to MS analysis of samples in their native states are being overcome by these strategies, and analysis of surfaces in foods involving minimum sample preparation is now possible by these approaches. Non-destructive and real-time detection of volatile compound by PTR-HRMS for the measurement of flavor in complex food systems or in matrices undergoing time-dependent transformations, or of food mastication, is also a very interesting direct MS-based strategy. However, the inherent complexity of food samples presents significant analytical challenges. With the lack of chromatographic or electrophoretic separation prior to MS analysis, high-resolution mass spectrometers are compulsory for characterization of complex samples.

There are several critical points in direct HRMS-based approaches. Without a preceding separation step, the sample matrix can directly affect desorption and ionization processes. In addition, isobaric interferences in the mass spectrum adversely affect compound identification as well as other aspects of performance. On the other hand, the high throughput and the reduction of sample preparation time are the main advantages of direct HRMS-based approaches over conventional hyphenated techniques. These approaches are advancing the reliability and accuracy of high-throughput non-target direct MS analysis and are just the beginning of a new set of applications in foodomics. In this regard, we foresee the development and application of new direct HRMS methods that can help to improve our understanding of the links between food and health, a topic still to discover by direct HRMS practitioners.

Acknowledgments This work was supported by AGL2011-29857-C03-01 and AGL2014-53609-P projects (Ministerio de Economía y Competitividad, Spain). T. A. thanks the CAPES Foundation, Ministry of Education of Brazil for her predoctoral scholarship - Proc. N° 1532/13-8.

References

1. Parliament and Council Regulation No (EC) 178/2002
2. Valdés A, Ibáñez C, Simó C, García-Cañas V (2013) Recent transcriptomics advances and emerging applications in food science. Trac-Trend Anal Chem 52:142–154
3. Valdés A, Simó C, Ibáñez C, García-Cañas V (2013) Foodomics strategies for the analysis of transgenic foods. Trac-Trend Anal Chem 52:2–15
4. Ibáñez C, García-Cañas V, Valdés A, Simó C (2013) Novel MS-based approaches and applications in food metabolomics. Trac-Trend Anal Chem 52:100–111
5. Herrero M, Simó C, García-Cañas V, Ibáñez E, Cifuentes A (2012) Foodomics: MS-based strategies in modern food science and nutrition. Mass Spectrom Rev 31:49–69
6. Ibáñez C, Valdés A, García-Cañas V, Simó C, Celebier M, Rocamora-Reverte L, Gómez-Martínez A, Herrero M, Castro-Puyana M, Segura-Carretero A, Ibáñez E, Ferragut JA, Cifuentes A (2011) Global foodomics strategy to investigate the health benefits of dietary constituents. J Chromatogr A 1248:139–153
7. Valdés A, Simó C, Ibáñez C, Rocamora-Reverte L, Ferragut JA, García-Cañas V, Cifuentes A (2012) Effect of dietary polyphenols on K562 leukemia cells: a foodomics approach. Electrophoresis 33:2314–2327
8. Ibáñez C, Simó C, García-Cañas V, Gómez-Martínez A, Ferragut JA, Cifuentes A (2012) CE/LC-MS multiplatform for broad metabolomic analysis of dietary polyphenols effect on colon cancer cells proliferation. Electrophoresis 33:2328–2336
9. Valdés A, García-Cañas V, Rocamora-Reverte L, Gómez-Martínez A, Ferragut JA, Cifuentes A (2013) Effect of rosemary polyphenols on human colon cancer cells: transcriptomic profiling and functional enrichment analysis. Genes Nutr 8:43–60
10. Valdés A, García-Cañas V, Simó C, Ibáñez C, Micol V, Ferragut JA, Cifuentes A (2014) Comprehensive foodomics study on the mechanisms operating at various molecular levels in cancer cells in response to individual rosemary polyphenols. Anal Chem 86: 9807–9815
11. García-Cañas V, Simó C, Herrero M, Ibáñez E, Cifuentes A (2012) Present and future challenges in food analysis: foodomics. Anal Chem 84:10150–10159
12. García-Cañas V, Simó C, Castro-Puyana M, Cifuentes A (2014) Recent advances in the application of capillary electromigration methods for food analysis and foodomics. Electrophoresis 35: 147–169
13. Hu Q, Noll RJ, Li H, Makarov A, Hardman M, Cooks RG (2005) The Orbitrap: a new mass spectrometer. J Mass Spectrom 40:430–443
14. Marshall AG, Hendrickson CL (2008) High-resolution mass spectrometers. Annu Rev Anal Chem 1:579–599
15. Kaufmann A (2012) The current role of high-resolution mass spectrometry in food analysis. Anal Bioanal Chem 403:1233–1249
16. Draper J, Lloyd AJ, Goodacre R, Beckmann M (2013) Flow infusion electrospray ionisation mass spectrometry for high throughput, non-targeted metabolite fingerprinting: a review. Metabolomics 9:S4–S29
17. Cooper HJ, Marshall AG (2001) Electrospray ionization Fourier transform mass spectrometric analysis of wine. J Agric Food Chem 49:5710–5718
18. Gougeon RD, Lucio M, Frommberger M, Peyron D, Chassagne D, Alexandre H, Feuillat F, Voilley A, Cayot P, Gebefügi I, Hertkorn N, Schmitt-Kopplin P (2009) The chemodiversity of wines can reveal a metabologeography expression of cooperage oak wood. Proc Natl Acad Sci U S A 106:9174–9179
19. Liger-Belair G, Cilindre C, Gougeon RD, Lucio M, Gebefügi I, Jeandet P, Schmitt-Kopplin P (2009) Unraveling different chemical fingerprints between a champagne wine and its aerosols. Proc Natl Acad Sci U S A 106:16545–16549
20. Villagra E, Santos LS, Vaz BG, Eberlin MN, Laurie F (2012) Varietal discrimination of Chilean wines by direct injection mass spectrometry analysis combined with multivariate statistics. Food Chem 131:692–697
21. Catharino RR, Cunha IBS, Fogac AO, Facco EMP, Godoy HT, Daudt CE, Eberlin MN, Sawaya ACHF (2006) Characterization of must and wine of six varieties of grapes by direct infusion electrospray ionization mass spectrometry. J Mass Spectrom 41: 185–190
22. Roullier-Gall C, Boutegrabet L, Gougeon RD, Schmitt-Kopplin P (2014) A grape and wine chemodiversity comparison of different appellations in Burgundy: vintage vs terroir effects. Food Chem 152:100–107
23. Garrett R, Vaz BG, Hovell AMC, Eberlin MN, Rezende CM (2012) Arabica and robusta coffees: identification of major polar compounds and quantification of blends by direct-infusion electrospray ionization-mass spectrometry. J Agric Food Chem 60:4253–4258
24. Goodacre R, Vaidyanathan S, Bianchi G, Kell DB (2002) Metabolic profiling using direct infusion electrospray ionisation mass spectrometry for the characterisation of olive oils. Analyst 127:1457–1462
25. Wu Z, Rodgers RP, Marshall AG (2004) Characterization of vegetable oils: detailed compositional fingerprints derived from electrospray ionization Fourier transform ion cyclotron resonance mass spectrometry. J Agric Food Chem 52:5322–5328
26. Proschogo NW, Albertson PL, Bursle J, McConchie CA, Turner AG, Willett GD (2012) Aging effects on macadamia nut oil studied by electrospray ionization Fourier transform ion cyclotron resonance mass spectrometry. J Agric Food Chem 60:1973–1980
27. González-Dominguez R, García-Barrera T, Gómez-Ariza JL (2012) Iberian ham typification by direct infusion electrospray and photospray ionization mass spectrometry fingerprinting. Rapid Commun Mass Spectrom 26:835–844
28. León C, Rodríguez-Meizoso I, Lucio M, García-Cañas V, Ibáñez E, Schmitt-Kopplin P, Cifuentes A (2009) Metabolomics of transgenic maize combining Fourier transform-ion cyclotron resonance-mass spectrometry, capillary electrophoresis-mass spectrometry and pressurized liquid extraction. J Chromatogr A 1216:7314–7323
29. Ashraf N, Linforth RST, Bealin-Kelly F, Smart K, Taylor AJ (2010) Rapid analysis of selected beer volatiles by atmospheric pressure chemical ionisation-mass spectrometry. Int J Mass Spectrom 294:47–53
30. Van Loon WA, Linssen JP, Boelrijk AE, Burgering MJ, Voragen AG (2005) Real-time flavor release from French fries using atmospheric pressure chemical ionization-mass spectrometry. J Agric Food Chem 53:6438–6442
31. Van Ruth S, Boscaini E, Mayr D, Pugh J, Posthumus M (2003) Evaluation of three gas chromatography and two direct mass spectrometry techniques for aroma analysis of dried red bell peppers. Int J Mass Spectrom 223–224:55–65
32. Hansel A, Jordan A, Holzinger R, Prazeller P, Vogel W, Lindinger W (1995) Int J Mass Spectrom 149–150:609–619
33. Tsachaki M, Linforth RS, Taylor AJ (2009) Aroma release from wines under dynamic conditions. J Agric Food Chem 57:6976–6981
34. Blake RS, Monks PS, Ellis AM (2009) Proton-transfer reaction mass spectrometry. Chem Rev 109:861–896
35. Biasioli F, Gasperi F, Aprea E, Colato L, Boscaini E, Märk TD (2003) Fingerprinting mass spectrometry by PTR-MS: heat

treatment vs. pressure treatment of red orange juice-a case study. Int J Mass Spectrom 223–224:343–353
36. Van Ruth SM, Koot A, Akkermans W, Araghipour N, Rozijn M, Baltussen M, Wisthaler A, Märk TD, Frankhuizen R (2008) Butter and butter oil classification by PTR-MS. Eur Food Res Technol 227:307–317
37. Heenan SP, Dufour J-P, Hamid N, Harvey W, Delahunty CM (2009) Characterisation of fresh bread flavour: relationships between sensory characteristics and volatile composition. Food Chem 116:249–257
38. Van Ruth SM, Floris V, Fayoux S (2006) Characterisation of the volatile profiles of infant formulas by proton transfer reaction-mass spectrometry and gas chromatography-mass spectrometry. Food Chem 98:343–350
39. Lindinger C, Labbe D, Pollien P, Rytz A, Juillerat MA, Yeretzian C, Blank I (2008) When machine tastes coffee: instrumental approach to predict the sensory profile of espresso coffee. Anal Chem 80:1574–1581
40. Boscaini E, Mikoviny T, Wisthaler A, Von Hartungen E, Märk TD (2004) Characterization of wine with PTR-MS. Int J Mass Spectrom 239:215–219
41. Spitaler R, Araghipour N, Mikoviny T, Wisthaler A, Via DL, Märk TD (2007) PTR-MS in enology: advances in analytics and data analysis. Int J Mass Spectrom 266:1–7
42. Blake RS, Whyte C, Hughes CO, Ellis AM, Monks PS (2004) Demonstration of proton-transfer reaction time-of-flight mass spectrometry for real-time analysis of trace volatile organic compounds. Anal Chem 76:3841–3845
43. Tanimoto H, Aoki N, Inomata S, Hirokawa J, Sadanaga Y (2007) Development of a PTR-TOFMS instrument for real-time measurements of volatile organic compounds in air. Int J Mass Spectrom 26:1–11
44. Fabris A, Biasioli F, Granitto PM, Aprea E, Cappellin L, Schuhfried E, Soukoulis C, Märk TD, Gasperi F, Endrizzi I (2010) PTR-TOF-MS and data-mining methods for rapid characterisation of agro-industrial samples: influence of milk storage conditions on the volatile compounds profile of Trentingrana cheese. J Mass Spectrom 45:1065–1074
45. Soukoulis C, Aprea E, Biasioli F, Cappellin L, Schuhfried E, Märk TD, Gasperi F (2010) Proton transfer reaction time-of-flight mass spectrometry monitoring of the evolution of volatile compounds during lactic acid fermentation of milk. Rapid Commun Mass Spectrom 24:2127–3134
46. Tsevdou M, Soukoulis C, Cappellin L, Gasperi F, Taoukis PS, Biasioli F (2013) Monitoring the effect of high pressure and transglutaminase treatment of milk on the evolution of flavour compounds during lactic acid fermentation using PTR-ToF-MS. Food Chem 138:2159–2167
47. Masi E, Romani A, Pandolfi C, Heimler D, Mancuso S (2014) PTR-TOF-MS analysis of volatile compounds in olive fruits. J Sci Food Agric. doi:10.1002/jsfa.6837
48. Soukoulis C, Cappellin L, Aprea E, Costa F, Viola R, Märk TD, Gasperi F, Biasioli F (2013) PTR-ToF-MS, A novel, rapid, high sensitivity and non-invasive tool to monitor volatile compound release during fruit post-harvest storage: the case study of apple ripening. Food Bioprocess Technol 6:2831–2843
49. Sánchez del Pulgar J, Soukoulis C, Biasioli F, Cappellin L, García C, Gasperi F, Granitto P, Märk TD, Piasentier E, Schuhfried E (2011) Rapid characterization of dry cured ham produced following different PDOs by proton transfer reaction time of flight mass spectrometry (PTR-ToF-MS). Talanta 85:386–393
50. Sánchez del Pulgar J, Soukoulis C, Carrapiso AI, Cappellin L, Granitto P, Aprea E, Romano A, Gasperi F, Biasioli F (2013) Effect of the pig rearing system on the final volatile profile of Iberian dry-cured ham as detected by PTR-ToF-MS. Meat Sci 93:420–428
51. Aprea E, Romano A, Betta E, Biasioli F, Cappellin L, Fanti M, Gasperi F (2015) Volatile compound changes during shelf life of dried Boletus edulis: comparison between SPME-GC-MS and PTR-ToF-MS analysis. J Mass Spectrom 50:56–64
52. Yener S, Romano A, Cappellin L, Märk TD, Sánchez Del Pulgar J, Gasperi F, Navarini L, Biasioli F (2014) PTR-ToF-MS characterisation of roasted coffees (C. arabica) from different geographic origins. J Mass Spectrom 49:929–935
53. Wieland F, Gloess AN, Keller M, Wetzel A, Schenker S, Yeretzian C (2012) Online monitoring of coffee roasting by proton transfer reaction time-of-flight mass spectrometry (PTR-ToF-MS): towards a real-time process control for a consistent roast profile. Anal Bioanal Chem 402:2531–2543
54. Sánchez-López JA, Zimmermann R, Yeretzian C (2014) Insight into the time-resolved extraction of aroma compounds during espresso coffee preparation: online monitoring by PTR-ToF-MS. Anal Chem 86:11696–11704
55. Heenan S, Soukoulis C, Silcock P, Fabris A, Aprea E, Cappellin L, Märk TD, Gasperi F, Biasioli F (2012) PTR-TOF-MS monitoring of in vitro and in vivo flavour release in cereal bars with varying sugar composition. Food Chem 131:477–484
56. Soukoulis C, Biasioli F, Aprea E, Schuhfried E, Cappellin L, Märk TD, Gasperi F (2012) PTR-TOF-MS analysis for influence of milk base supplementation on texture and headspace concentration of endogenous volatile compounds in yogurt. Food Bioprocess Technol 5:2085–2097
57. Herbig J, Müller M, Schallhart S, Titzmann T, Graus M, Hansel A (2009) On-line breath analysis with PTR-TOF. J Breath Res 3: 027004
58. Ajibola OA, Smith D, Španěl P, Ferns GAA (2013) Effects of dietary nutrients on volatile breath metabolites. J Nutr Sci 2, e34. doi:10.1017/jns.2013.26
59. Aprea E, Morisco F, Biasioli F, Vitaglione P, Cappellin L, Soukoulis C, Lembo V, Gasperi F, D'Argenio G, Fogliano V, Caporaso N (2012) Analysis of breath by proton transfer reaction time of flight mass spectrometry in rats with steatohepatitis induced by high-fat diet. J Mass Spectrom 47:1098–1103
60. Aprea E, Cappellin L, Gasperi F, Morisco F, Lembo V, Rispo A, Tortora R, Vitaglione P, Caporaso N, Biasioli F (2014) Application of PTR-TOF-MS to investigate metabolites in exhaled breath of patients affected by coeliac disease under gluten free diet. J Chromatogr, B 966:208–213
61. Déléris I, Saint-Eve A, Sémon E, Guillemin H, Guichard E, Souchon I, Le Quéré JL (2013) Comparison of direct mass spectrometry methods for the on-line analysis of volatile compounds in foods. J Mass Spectrom 48:594–607
62. Biasioli F, Gasperi F (2011) PTR-MS monitoring of VOCs and BVOCs in food science and technology. Trac-Trend Anal Chem 7: 968–977
63. Sulzer P, Edtbauer A, Hartungen E, Jürschik S, Jordan A, Hanel G, Feil S, Jaksch S, Märk L, Märk TD (2012) From conventional proton-transfer-reaction mass spectrometry (PTR-MS) to universal trace gas analysis. Int J Mass Spectrom 321–322:66–70
64. Vaidyanathan S, Gaskell S, Goodacre R (2006) Matrix-suppressed laser desorption/ionisation mass spectrometry and its suitability for metabolome analyses. Rapid Commun Mass Spectrom 20: 1192–1198
65. Edwards JL, Kennedy RT (2005) Metabolomic analysis of eukaryotic tissue and prokaryotes using negative mode MALDI time-of-flight mass spectrometry. Anal Chem 77:2201–2209
66. Miura D, Fujimura Y, Tachibana H, Wariishi H (2010) Highly sensitive matrix-assisted laser desorption ionization-mass spectrometry for high-throughput metabolic profiling. Anal Chem 82:498–504
67. Vaidyanathan S, Jones D, Broadhurst DI, Ellis J, Jenkins T, Dunn WB, Hayes A, Burton N, Oliver SG, Kell DB (2005) A laser

desorption ionisation mass spectrometry approach for high throughput metabolomics. Metabolomics 1:243–250
68. Vaidyanathan S, Jones D, Ellis J, Jenkins T, Chong C, Anderson M, Goodacre R (2007) Laser desorption/ionization mass spectrometry on porous silicon for metabolome analyses: influence of surface oxidation. Rapid Commun Mass Spectrom 21:2157–2166
69. Careri M, Elviri L, Mangia A, Zagnoni I, Agrimonti C, Visioli G, Marmiroli N (2003) Analysis of protein profiles of genetically modified potato tubers by matrix-assisted laser desorption/ionization time-of-flight mass spectrometry. Rapid Commun Mass Spectrom 17:479–483
70. Cozzolino R, De Giulio B (2011) Application of ESI and MALDI-TOF MS for triacylglycerols analysis in edible oils. Eur J Lipid Sci Technol 113:160–167
71. Ciarmiello LF, Mazzeo MF, Minasi P, Peluso A, De Luca A, Piccirillo P, Siciliano RA, Carbone V (2014) Analysis of different European hazelnut (Corylus avellana L.) cultivars: authentication, phenotypic features, and phenolic profiles. J Agric Food Chem 62: 6236–6246
72. Cozzolino R, Passalacqua S, Salemi S, Malvagna P, Spina E, Garozzo D (2001) Identification of adulteration in milk by matrix-assisted laser desorption/ionization time-of-flight mass spectrometry. J Mass Spectrom 36:1031–1037
73. Nicolau N, Xu Y, Goodacre R (2011) MALDI-MS and multivariate analysis for the detection and quantification of different milk species. Anal Bioanal Chem 399:3491–3502
74. Garcia JS, Sanvido GB, Saraiva SA, Zacca JJ, Cosso RG, Eberlin MN (2012) Bovine milk powder adulteration with vegetable oils or fats revealed by MALDI-QTOF MS. Food Chem 131:722–726
75. Calvano CD, Monopoli A, Loizzo P, Faccia M, Zambonin C (2013) Proteomic approach based on MALDI-TOF MS to detect powdered milk in fresh cow's milk. J Agric Food Chem 61:1609–1617
76. Cunsolo V, Muccilli V, Saletti R, Foti S (2013) MALDI-TOF mass spectrometry for the monitoring of she-donkey's milk contamination or adulteration. J Mass Spectrom 48:148–153
77. Di Girolamo F, Masotti A, Salvatori G, Scapaticci M, Muraca M, Putignani L (2014) A sensitive and effective proteomic approach to identify she-donkey's and goat's milk adulterations by MALDI-TOF MS fingerprinting. Int J Mol Sci 15:13697–13719
78. Sabbadin S, Seraglia R, Allegri G, Bertazzo A, Traldi P (1999) Matrix-assisted laser desorption/ionization mass spectrometry in evaluation of protein profiles of infant formulae. Rapid Commun Mass Spectrom 13:1438–1443
79. Catinella S, Traldi P, Pinelli C, Dallaturca E (1996) Matrix-assisted laser desorption/ionization mass spectrometry: a valid analytical tool in the dairy industry. Rapid Commun Mass Spectrom 10:1123–1127
80. Sedo O, Márová I, Zdráhal Z (2012) Beer fingerprinting by matrix-assisted laser desorption-ionisation-time of flight mass spectrometry. Food Chem 135:473–478
81. Latif S, Pfannstiel J, Makkar HP, Becker K (2013) Amino acid composition, antinutrients and allergens in the peanut protein fraction obtained by an aqueous enzymatic process. Food Chem 136: 213–217
82. Cerimedo MSA, Candal RJ, Herrera ML (2014) Physical properties and oxidative status of concentrated-from-fish oils microencapsulated in trehalose/sodium caseinate matrix. Food Bioprocess Tech 7:3536–3547
83. Weston DJ (2010) Ambient ionization mass spectrometry: current understanding of mechanistic theory; analytical performance and application areas. Analyst 135:661–668
84. Harris GA, Galhena AS, Fernández FM (2011) Ambient sampling/ionization mass spectrometry: applications and current trends. Anal Chem 83:4508–4538
85. Monge ME, Harris GA, Dwivedi P, Fernández FM (2013) Mass spectrometry: recent advances in direct open air surface sampling/ionization. Chem Rev 113:2269–2308
86. Takats Z, Wiseman JM, Gologan B, Cooks RG (2004) Mass spectrometry sampling under ambient conditions with desorption electrospray ionization. Science 306:471–473
87. Jackson AU, Talaty N, Cooks RG, Van Berkel GJ (2007) Salt tolerance of desorption electrospray ionization (DESI). J Am Soc Mass Spectrom 18:2218–2225
88. Douglass KA, Venter AR (2013) Protein analysis by desorption electrospray ionization mass spectrometry and related methods. J Mass Spectrom 48:553–560
89. García-Reyes JF, Jackson AU, Molina-Díaz A, Cooks RG (2009) DESI-MS is demonstrating to be a promising tool in food safety control, for example, in multiresidue analysis of a wide range of agrochemical (insecticides, herbicides, and fungicides), even in fruit surface. Anal Chem 81:820–829
90. Joyce NI, Eady CC, Silcock P, Perry NB, van Klink JW (2013) Fast phenotyping of LFS-silenced (tearless) onions by desorption electrospray ionization mass spectrometry (DESI-MS). J Agric Food Chem 61:1449–1456
91. Hartmanova L, Ranc V, Papouskova B, Bednar P, Havlicek V, Lemr K (2010) Fast profiling of anthocyanins in wine by desorption nano-electrospray ionization mass spectrometry. J Chromatogr A 1217:4223–4228
92. Gerbig S, Takáts Z (2010) Analysis of triglycerides in food items by desorption electrospray ionization mass spectrometry. Rapid Commun Mass Spectrom 24:2186–2192
93. Shin YS, Drolet B, Mayer R, Dolence K, Basile F (2007) Desorption electrospray ionization-mass spectrometry of proteins. Anal Chem 79:3514–3518
94. Takats Z, Wiseman JM, Ifa DR, Cooks RG (2008) Desorption electrospray ionization (DESI) analysis of tryptic digests/peptides. CSH Protoc. doi:10.1101/pdb.prot4993
95. Takats Z, Wiseman JM, Ifa DR, Cooks RG (2008) Desorption electrospray ionization (DESI) analysis of intact proteins/oligopeptides. CSH Protoc. doi:10.1101/pdb.prot4992
96. Montowska M, Rao W, Alexander MR, Tucker GA, Barrett DA (2014) Tryptic digestion coupled with ambient desorption electrospray ionization and liquid extraction surface analysis mass spectrometry enabling identification of skeletal muscle proteins in mixtures and distinguishing between beef, pork, horse, chicken, and turkey meat. Anal Chem 86:4479–4487
97. Liu J, Wang H, Manicke NE, Lin J-M, Cooks RG, Ouyang Z (2010) Development, characterization, and application of paper spray ionization. Anal Chem 82:2463–2471
98. Zhang Z, Cooks RG, Ouyang Z (2012) Paper spray: a simple and efficient means of analysis of different contaminants in foodstuffs. Analyst 137:2556–2558
99. Zhang JI, Li X, Ouyang Z, Cooks RG (2012) Direct analysis of steviol glycosides from stevia leaves by ambient ionization mass spectrometry performed on whole leaves. Analyst 137:3091–3098
100. Cody RB, Laramée JA, Durst HD (2005) Versatile new ion source for the analysis of materials in open air under ambient conditions. Anal Chem 77:2297–2302
101. Hajslova J, Cajka T, Vaclavik L (2011) Challenging applications offered by direct analysis in real time (DART) in food-quality and safety analysis. Trac-Trend Anal Chem 30:204–218
102. Gross JH (2014) Direct analysis in real time - a critical review on DART-MS. Anal Bioanal Chem 406:63–80
103. Farré M, Picó Y, Barceló D (2013) Direct peel monitoring of xenobiotics in fruit by direct analysis in real time coupled to a linear quadrupole ion trap-orbitrap mass spectrometer. Anal Chem 85:638–644
104. Edison SE, Lin LA, Gamble BM, Wong J, Zhang K (2011) Surface swabbing technique for the rapid screening for pesticides

using ambient pressure desorption ionization with high-resolution mass spectrometry. Rapid Commun Mass Spectrom 25:127–139
105. Crawford E, Musselman B (2012) Evaluating a direct swabbing method for screening pesticides on fruit and vegetable surfaces using direct analysis in real time (DART) coupled to an exactive benchtop orbitrap mass spectrometer. Anal Bioanal Chem 403: 2807–2812
106. Vaclavik L, Capuano E, Gökmen V, Hajslova J (2015) Prediction of acrylamide formation in biscuits based on fingerprint data generated by ambient ionization mass spectrometry employing direct analysis in real time (DART) ion source. Food Chem 173:290–297
107. Vaclavik L, Belkova B, Reblova Z, Riddellova K, Hajslova J (2013) Rapid monitoring of heat-accelerated reactions in vegetable oils using direct analysis in real time ionization coupled with high resolution mass spectrometry. Food Chem 138:2312–2320
108. Vaclavik L, Cajka T, Hrbek V, Hajslova J (2009) Ambient mass spectrometry employing direct analysis in real time (DART) ion source for olive oil quality and authenticity assessment. Anal Chim Acta 645:56–63
109. Hrbek V, Vaclavik L, Elich O, Hajslova J (2014) Authentication of milk and milk-based foods by direct analysis in real time ionization-high resolution mass spectrometry (DART-HRMS) technique: a critical assessment. Food Control 36:138–145
110. Vaclavik L, Hrbek V, Cajka T, Rohlik BA, Pipek P, Hajslova J (2011) Authentication of animal fats using direct analysis in real time (DART) ionization-mass spectrometry and chemometric tools. J Agric Food Chem 59:5919–5926
111. Cajka T, Danhelova H, Zachariasova M, Riddellova K, Hajslova J (2013) Application of direct analysis in real time ionization-mass spectrometry (DART-MS) in chicken meat metabolomics aiming at the retrospective control of feed fraud. Metabolomics 9:545–557
112. Cajka T, Riddellova K, Tomaniova M, Hajslova J (2011) Ambient mass spectrometry employing a DART ion source for metabolomic fingerprinting/profiling: a powerful tool for beer origin recognition. Metabolomics 4:500–508
113. Kim HJ, Baek WS, Jang YP (2011) Identification of ambiguous cubeb fruit by DART-MS-based fingerprinting combined with principal component analysis. Food Chem 129:1305–1310
114. Chernetsova ES, Bromirski M, Scheibner O, Morlock GE (2012) DART-Orbitrap MS: a novel mass spectrometric approach for the identification of phenolic compounds in propolis. Anal Bioanal Chem 403:2859–2867
115. Prchalová J, Kovařík F, Ševčík R, Čížková H, Rajchl A (2014) Characterization of mustard seeds and paste by DART ionization with time-of-flight mass spectrometry. J Mass Spectrom 49:811–818
116. Haapala M, Pól J, Saarela V, Arvola V, Kotiaho T, Ketola RA, Franssila S, Kauppila TJ, Kostiainen R (2007) Desorption atmospheric pressure photoionization. Anal Chem 79:7867–7872
117. Luosujärvi L, Arvola V, Haapala M, Pól J, Saarela V, Franssila S, Kotiaho T, Kostiainen R, Kauppila TJ (2008) Desorption and ionization mechanisms in desorption atmospheric pressure photoionization. Anal Chem 80:7460–7466
118. Suni NM, Lindfors P, Laine O, Östman P, Ojanperä I, Kotiaho T, Kauppila TJ, Kostiainen R (2011) Matrix effect in the analysis of drugs of abuse from urine with desorption atmospheric pressure photoionization-mass spectrometry (DAPPI-MS) and desorption electrospray ionization-mass spectrometry (DESI-MS). Anal Chim Acta 699:73–80
119. Luosujärvi L, Kanerva S, Saarela V, Franssila S, Kostiainen R, Kotiaho T, Kauppila TJ (2010) Environmental and food analysis by desorption atmospheric pressure photoionization-mass spectrometry. Rapid Commun Mass Spectrom 24:1343–1350
120. Suni NM, Aalto H, Kauppila TJ, Kotiaho T, Kostiainen R (2012) Analysis of lipids with desorption atmospheric pressure photoionization-mass spectrometry (DAPPI-MS) and desorption electrospray ionization-mass spectrometry (DESI-MS). J Mass Spectrom 47:611–619

1.3.2. Foodomics: LC and LC-MS-based omics strategies in food science and nutrition

Gilbert-López, B., Valdés, A., Acunha, T., García-Cañas, V., Simó, C., Cifuentes, A.

In Liquid Chromatography. Volume Two: Applications, Second Edition, Edited by: Fanali, S., Poole, C., Haddad, P., and Riekkola, M-L. (2017) Elsevier Inc., Cambridge.
ISBN: 9780128053928.

Foodomics: LC and LC-MS-based omics strategies in food science and nutrition

Bienvenida Gilbert-López[1]*, Alberto Valdés[1], Tanize Acunha[1,2], Virginia García-Cañas[1], Carolina Simó[1], Alejandro Cifuentes[1]

[1] Foodomics Laboratory, CIAL, CSIC, Nicolas Cabrera 9, 28049 Madrid, Spain

[2] CAPES Foundation, Ministry of Education of Brazil, 70.040-020 Brasília, DF, Brazil

*corresponding author: b.gilbert.lopez@csic.es

Abstract

Foodomics is becoming a relevant approach to assess food quality, safety and traceability, in a robust, efficient, sensitive and cost-effective way. Omics technologies, as used in Foodomics, have the potential to improve the scope of traditional targeted analysis and open up new prospects for novel applications, providing the opportunity to explore formerly unanswered questions and problems relevant to food science. In this chapter, LC and LC-MS-based Foodomics techniques are described, and typical applications in food science are presented, including applications related to food composition, food safety, quality, nutrition and health.

Keywords

Foodomics, liquid chromatography, food safety, food quality, food traceability, food bioactivity

Introduction

Foodomics has been defined by our research group as a new discipline that studies the food and nutrition domains through the application and integration of advanced Omics technologies to

improve consumer's well-being, health, and confidence [1]. Omics technologies have the potential to improve the scope of traditional targeted analysis and open up new prospects for novel applications, providing the opportunity to explore formerly unanswered questions and problems relevant to food science. These technologies are becoming relevant procedures to assess food bioactivity, quality, safety and traceability. Another important issue of Foodomics is to improve our limited understanding of the roles of food compounds at molecular level and, therefore, their implications on human health and disease.

To carry out a Foodomics study, it is essential to make use of modern analytical approaches capable to provide molecular information on the different expression levels*, i.e.,* gene, transcript, protein or metabolite. In this situation, scientists involved in developing new analytical methods play a crucial role in order to give a correct answer to these new needs. Analytical separation techniques such as liquid chromatography (LC) play a key role in Foodomics [2]. In this regard, the latest developments on new columns enable the reduction of the analysis time without compromising resolution and separation efficiency [3, 4]. Separated compounds of complex samples, especially in short analysis runs, require the use of powerful detectors with low response time, which ensure the acquisition of a minimum number of points per chromatographic peak [5]. In this sense, the coupling of LC with mass spectrometry (MS) is nearly an obligation, and it is the key analytical methodology on which the established Omics technologies such as proteomics, peptidomics, and metabolomics are based.In this chapter, the capabilities of LC (HPLC, UHPLC, nanoLC) and LC-MS technologies in the field of Foodomics will be discussed including some key applications.

Fundamentals of Omics approaches based on LC

Proteomics

Proteomics involves the comprehensive study of the complete set of proteins expressed in a biological system at a particular time under defined conditions [6]. In Proteomics, the identification and the quantification of proteins, as well as the study of the primary structure, conformation, and the location of these proteins in a place, space or time, can be addressed. The structural diversity of proteins and the wide dynamic range of expression (up to 6 orders of magnitude), make the study of the proteome a complex task. In addition to these difficulties, Proteomics must deal with other problems such as the alternative splicing (the same RNA molecule may lead to different proteins), and the post-translational modifications (or chemical modifications affecting the functionality of proteins in terms of activity, location and interaction with other cellular components such as proteins, nucleic acids, lipids or cofactors), among others.

Sample preparation is the first critical step that affects the outcome of the entire proteomic analysis. Different extraction methods can be used depending on the matrix nature, protein target, and application. Tissue/cell disruption is the most common procedure when handling solid samples, followed by solubilization of proteins using different solvents. In addition, chaotropic agents, surfactants and reductants can also be employed to improve protein solubility. Because of the different nature of the proteins and the extreme complexity of biological/food samples, one or more fractionation, purification and/or separation steps are necessary prior to analysis by LC-MS. Moreover, sample clean-up is a critical step before protein analysis. Contaminants, such as salts, stabilizers, or detergents used in the extraction step can interfere with the results of LC-MS analysis, preventing the study of low-abundant proteins.

Depending on the analytical strategy selected for the protein analysis, the proteomics studies can be categorized in two different groups, “top-down” and “bottom-up” approaches. *Top-down* is used for the comprehensive and characterization of the post transcriptional modifications present in proteins. It is based on the study of intact proteins previously separated by two-dimensional

polyacrylamide gel electrophoresis (2-DE) or LC, and their subsequent detection by MS analysis. Ions derived from the intact protein are isolated after the analysis of their mass, and then fragmented in the collision cell and detected by MS/MS [7]. *Bottom-up* is characterized by the enzymatic digestion of the proteins in their respective peptides prior the analysis by MS-based analytical tools. Briefly, by using gel-based approaches, proteins are separated by 2-DE or sodium dodecyl sulfate polyacrylamide gel electrophoresis (SDS-PAGE), and once separated the proteins are submitted to an in-gel digestion before the analysis by MS-based approaches. Commonly, the spots of interest are excised from the gel and submitted to analysis by MALDI-TOF MS [8]. Alternatively, to achieve high-throughput analysis of proteomes, a "shotgun" proteomic approach can be used. By using this approach, digestion of proteins is carried out prior to separation process, and the resulting peptides are simultaneously analyzed by LC-MS [9].

In general, the separation of proteins by LC constitutes a slow process because of their high molecular weights and low diffusion coefficients, and as a consequence, long analysis times are usually required. Two different strategies have been developed in order to decrease analysis time by LC, and to enhance the resolution of proteins. The first one is to increase particle permeability by using wide pores, which enhance the mass transfer between the mobile and the stationary phases. The second option is to reduce the time required for molecules to diffuse in and out of the particle, which can be account by reducing the particle size. Other strategies developed to improve the protein analysis sensitivity are related to the dimension of separation columns. One approach is the use of longer columns and elution times [10], which has enabled the analysis of over 95 % of the yeast proteome in a single run. Another approach is to reduce the internal diameter from of 4.0-4.6 mm (conventional columns) to 1-2.1 mm (micro), 0.1-1 mm (capillary), and 25-100 µm (nano). By decreasing the internal diameter of the column, the dilution of the analyte is lowered resulting in an increased sensitivity. In addition, the reduction of the column's internal diameter

permits a decrease in flow-rate, with the consequent use of less mobile phase and the reduction of waste. Among the different chromatographic techniques used for protein/peptide separation, reverse phase (RP) chromatography is the most widely used, but other chromatographic modes such as strong cation exchange (SCX) [11], anion exchange (AEC) [12] or hydrophilic interaction liquid chromatography (HILIC) [13] have also been used.

Selection of the appropriate protein identification strategies depends on the type of proteomic approach. In *top-down*, identification uses the extremely accurate masses of intact proteins from high resolution MS as well as masses obtained from their subsequent collision-induced dissociation (CID) fragmentation. In the *bottom-up* approach, the identification of the original protein is determined by comparison of the experimental mass spectra of the peptides obtained in the digestion, with their corresponding theoretical masses stored in databases. Two strategies are mainly used here: the "peptide mass fingerprinting" and the "peptide sequencing". In *peptide mass fingerprinting*, the list of experimental peptide masses are compared to the list of theoretical peptide masses stored in databases. In *peptide sequencing*, the molecular mass and spectrum fragmentation of each peptide generated are compared with the molecular masses and theoretical fragmentation spectra contained in proteomic databases. A variety of peptide and protein databases have been created, where information such as the sequence, molecular weight or biological activity are stored: NCBI (http://www.ncbi.nlm.nih.gov), SwePep (http://www.swepep.org), Erop-Moscow (http://erop.inbi.ras.ru), PeptideDB (http://www.peptides.be), Peptidome (http://www.peptidome.jp), Pep-Bank (http://pepbank.mgh.harvard.edu), IPI human protein database (http://www.ebi.ac.uk/IPI), BioPep (http://www.uwm.edu.pl/biochemia/index_en.php) or BioPD (http://biopd.bjmu.edu.cn), among others. In addition, different search engines software have been developed to facilitate this task, such as MASCOT [14], SEQUEST [15], Andromeda [16] and X!Tandem [17]. Moreover,

advances in bioinformatics have enabled the development and the combination of computational tools for *in silico* prediction and discovery of functional peptides information from the genome sequence (known as “reverse-genome engineering” [18]).

Various approximations have been designed to quantify (absolute or relatively) the proteins [19]. These methods are generally divided into three main categories: “stable isotope labeling”, “label-free” methods, and “multiple reaction monitoring” (MRM). *Stable isotope labeling* is the most widely used approach and several labeling methods have been developed. The *isotope-labeling* can be used after protein extraction with chemical labeling (the most common methods are Isobaric tags for relative and absolute quantitation (iTRAQ) [20] and stable isotope dimethyl labeling (DML)[21]), or in cell culture with metabolic incorporation (Stable isotope labeling with amino acids in cell culture (SILAC)) [22]. This approach enables the quantitation of two or more sets of peptides simultaneously by LC-MS analysis. The quantification is performed determining the relative intensities of the different labels of the peptides. In the *label-free* approach, the quantification is carried out measuring the peak areas or using the spectral counts of the peptide in an MS/MS experiment. This approach has the advantages of simplicity, cost, and the reduction of steps and difficulty of multiplex experiments. However, the quality of the quantification is strongly dependent on the reproducibility of the LC-MS data and on the bioinformatics tools used for processing. The MRM method is applied for detection and quantification of predetermined specific peptides with known fragmentation properties in complex samples. It explores the *m/z* transitions of a precursor ion and their fragments, considering both the chromatographic retention time and the signal intensity in the mass spectrometer. The selective nature of this method increases sensitivity by one to two orders of magnitude and the dynamic range of detection in up to five orders as compared to conventional proteomics techniques.

Peptidomics

The term Peptidomics was introduced in 2001, and it is referred as the qualitative, quantitative and functional description of the whole biologically active peptides in a cell, tissue or organism [23]. The peptidome can be defined as the low-molecular weight subset of the proteome, including peptides and small proteins with molecular weights ranging from 0.5 to 15 kDa [24]. Many physiological functions in the organism are mediated by peptides, acting as neurotransmitters, hormones and antibiotics [25]. Peptides in the peptidome can be divided into two main categories: biomarker peptides cleaved by enzymes resulting from *in vivo* resident proteins, and bioactive peptides generated by all cell types in a specific microenvironment. On the one hand, biomarker peptides constitute a class of peptides which could reflect biological enzymatic states of individuals [26]. Their presence and concentration are used for diagnosis, prognosis and to monitor the treatment effectiveness of a disease. The primary resource for peptidome studies are body fluids because of their richness in disease-specific peptide and protein candidates. On the other hand, bioactive peptides are defined as specific protein fragments that have a positive impact on the functioning or conditions of living beings, thereby improving their health [27]. The bioactive peptides are encrypted as a part of a protein that remains inactive as long as it is confined within the protein, as it occurs in dietary proteins. Dietary proteins have gained an increased interest in the last years due to their possible health promoting effects [28]. These beneficial effects may occur because peptides from food sources can be structurally similar to the endogenous peptides and interact with the same receptors, acting as modifiers of food intake, growth factors, immune regulators, or antimicrobials in the host organism. Bioactive peptides can be released by *in vitro* or *in vivo* proteolysis or in a combination of both [29]. Traditionally, bioactive peptides in biological samples have been analyzed by immunoassay methods, which possess a high sensitivity. However, one of the mayor drawbacks of this method is

the requirement of previous isolation of the peptide to be analyzed to generate the antibody, which difficult the possibility of analyzing new peptides. Nevertheless, the development of different soft ionization methods such as ESI and MALDI enabled the ionization of peptides and their subsequent analysis through MS [30]. Among these two ionization methods, the ESI interface has become the method of choice in LC-MS coupling [31]. This hyphenation is a very selective and sensitive approach that enables the simultaneous analysis of a great number of peptides, as well as the identification of new ones. In addition, the ESI interface enables the use of small flow rates (below 200 nL/min) which improves the sensitivity (in the nanoliter/min range, electrospray can reach almost 100% ionization efficiency [32]).

One of the main problems when analyzing peptides is the high dynamic range and the physico-chemical diversity of peptides in biological or food samples, which make necessary the implementation of pretreatments to remove interfering components and a large reduction in sample complexity before the peptides enter the MS. The first step when analyzing peptides from a complex sample is their extraction. This extraction is usually carried out with acidic solutions of different organic solvents or water, followed by a deproteinization step through selective precipitation, filtration and/or centrifugation. Moreover, and because bioactive peptides are often present in biological samples at very low concentrations, enrichment procedures such as online solid-phase extraction (SPE) onto a pre-concentration column, can be used ([33]. After the extraction, purification and/or concentration of peptides, these are separated by LC before their analysis by MS. The most widely used material for this separation are columns with silica-based reversed-phase (RP) particles, among which, C18 phases are the most used when searching for bioactive peptides [34,35]. Ion-exchange chromatography (IEC) columns have also been extensively used [36-38]. The separation using these columns is based on the effective charge of the peptides. Among the different IEC columns available, the SCX columns are the most widely

used. In this case, all the peptides carry a net positive charge because of the use of acidic pH, and has been successfully applied in the analysis of endogenous bioactive peptides [36] or the isolation of bioactive peptides in food products [37,38]. Another chromatographic method that can be used to separate peptides is HILIC, in which a hydrophobic mobile phase and a polar column are used, and the retention increases with hydrophilicity of solutes. This method has been used for the analysis of Maillard reaction components in peptides [39], but it is not widely used because of the poor solubility of peptides in the high organic content solvents. LC methods can be used as stand-alone, but they can also be combined to increase the overall resolving power (multi-dimensional approaches). The most popular combination is SCX with RP [40-41], although RP-RP (under different pH conditions) and size exclusion chromatography (SEC) with RP [42] are also used (RP has a better resolution and is therefore used as the second dimension) [43]. Because RP is the most used separation mechanism, dozens of reversed-phase columns are commercially available designed to separate peptides, differing in length, particle diameter, internal diameter, pore size, hydrophobicity, pH stability, support material, etc. Acetonitrile is the most used mobile phase with trifluoroacetic acid (TFA) as an additive for separation of peptides. Nevertheless, TFA is usually replaced by other additives such as formic acid or acetic acid, because TFA can produce important losses of sensitivity in MS detection [44].

As it has been stated above, after the separation of the peptides using LC, the most common method to detect the peptides is MS. In Peptidomics, good sensitivity, mass accuracy, and the ability to fragment peptides through tandem MS are essential. Thus, the most common mass analyzers are quadrupole (Q), time-of-flight (TOF), ion trap (IT), Fourier transform ion cyclotron resonance (FT-ICR) and Orbitrap®. Quadrupole has a low resolving power but offers high reproducibility, and its combination with a TOF analyzer (with good sensitivity and resolving power) enables the MS/MS fragmentation. IT mass analyzer is characterized for the capability of

storing ions and the high detection speed, and its combination with a quadrupole offers the superior capability of specific modification detections [45]. FT-ICR MS has also been used to detect peptides biomarkers [46]. This analyzer has the highest mass accuracy and resolving power among all types of mass analyzers, and also provides MS/MS fragmentation function, although its high cost is an important limitation to consider. This fragmentation is imperative to determine the amino acid sequence of peptides, and can be achieved by various techniques such CID (collision-induced dissociation), HCD (Higher-energy collisional dissociation), ETD (Electron-transfer dissociation) or ECD (Electron-capture dissociation), being CID the most commonly used.

Quantification of small differences in peptide amounts between samples is also one of the most important and challenging tasks in Peptidomics. As already presented above, both labeled and label-free quantification strategies can be employed in Peptidomics [47,48].

Metabolomics

Metabolomics involves the comprehensive study of the complete set of metabolites (i.e., the metabolome) in a certain biological system at a particular time under defined conditions. The metabolome is the complete set of small compounds (< 1500 Da) found within a biological system. In metabolomics, two different approaches can be followed: “metabolic profiling” and “metabolic fingerprinting”. *Metabolic profiling* focuses on the study of a large group of metabolites that either is related to a class of compounds or a specific metabolic pathway. LC-MS-based metabolic profiling in metabolomics involves the use of wide polarity gradients to cover as many metabolites as possible combined with full scan MS [49]. *Metabolic fingerprinting* refers to obtain a rapid classification of samples. The aim is to compare patterns or metabolite *fingerprints* that might be changed in a given biological system in response to a certain condition [50].

The sample preparation is an important step in a metabolomics experiments. At the same time that fast and reproducible methods are required, these also should be able to cover a wide range of analytes with different polarities and/or select the aimed metabolite classes according to their chemical properties [51]. In order to prevent potential loss of metabolites in non-targeted metabolomics studies, biological samples should preferably be evaluated with minimal pretreatment. The sample pretreatment steps can be quite straightforward, separating low molecular weight compounds from proteins. The presence of proteins can influence the accuracy, precision, and instrument component lifetime (*e.g.* LC columns). In contrast, for targeted analysis some development and/or optimization procedures for sample pretreatment is generally necessary and the separation of metabolites from proteins often is followed by liquid extraction with organic solvents and/or solid-phase extraction for the selective isolation and enrichment of the target compounds, and removal of matrix interferences [52]. The final step during sample preparation generally involves evaporation in order to concentrate the analytes and reconstitution of the dry extracts using a smaller volume of analysis-compatible solvent [53].

Due to the complexity and dynamic nature of the metabolome, numerous analytical platforms have been used with the aim to cover the full spectrum of metabolites. Among them, nuclear magnetic resonances (NMR) and mass spectrometry (MS), the later often combined with a high-resolution separation technique (LC, GC or CE), are the most employed. The combination of MS with a separation technique reduces the matrix effects and delivers additional information on the physicochemical properties of the metabolites [54].

Liquid chromatography (LC) has become one of the most used chromatography-MS technique in metabolomics together with GC-MS and in a less extent CE−MS [55]. LC-MS allows for the collection of both quantitative and structural information, and can achieve ppt (part-per-trillion, 10^{-12}) sensitivities [49]. The resolution and sensitivity play an important role in metabolomics. The

use of UHPLC improves significantly peak resolution, together with an increase of speed and sensitivity compared to HPLC [56], and result in better MS data quality due to reduced background noise. In metabolomics experiments, RP and HILIC are the most frequent LC-based separation methods. RP separation covers a large range of metabolites and also provides the most robust and sophisticated LC stationary phases. However, RP-LC shows limitations in the analysis of polar and/or ionic species (e.g. amino acids, organic acids, amines, sugar, and carbohydrates) due to poor retention of these analytes. In this case, HILIC provides a complementary separation to that obtained by RP-LC [57], and frequently the combination of both is used in metabolomics experiments. The usual method in RP-LC-based metabolomics uses a gradient of methanol-water or acetonitrile-water, supplemented with 0.1% formic acid. Low proportions of organic modifiers are generally added to the mobile phase in order to improve the separation efficiency, meanwhile, the selection of the correctly organic modifier is not generally easy and the favored modifier condition varies for different metabolites and the detection ion mode used [58]. In this regard, the use of different mobile phase additives, as well as acetic acid, formic acid, ammonium fluoride, ammonium formate, ammonium acetate, ammonium hydroxide and ammonium carbonate, have been studied [58,59]. HILIC uses polar stationary phases (*e.g.*, bare or chemically modified silica, or polar polymers). In most cases, the mobile phase is polar organic solvent (most frequently acetonitrile and sometimes methanol) containing up to 30% water [60]. Generally, the applications use a gradient starting with a high percentage of acetonitrile (with at least 5% of water) followed by increasing the percentage of water. In this way, the more lipophilic compounds are poorly attracted to the stationary phase and elute quickly, whereas the more polar compounds are retained and only eluted when the polar water concentration is increased. Compounds are eluted in order of increasing hydrophilicity (chromatographic polarity relative to water). Compared to metabolomics methods conducted with RP columns, where most of the separations are conducted

under acid conditions, a much wider pH range is used in HILIC columns. Mobile phase additives such as ammonium acetate, ammonium formate, and ammonium hydroxide are used to increase the pH [61].

After the separation, the ionization is the following step in LC-MS-based metabolomics analysis. Electrospray ionization (ESI) followed by atmospheric pressure chemical ionization (APCI) are the ionization techniques most used in LC-MS for metabolomics applications. ESI technique ionizes a wide range of medium polar and polar metabolites [49]. APCI is preferred for more non-polar metabolites and has been used in a smaller number of metabolomics works [49]. In order to expand the coverage of the metabolome, MS detection must be conducted in positive and negative mode.

The majority of non-targeted metabolomics studies are currently performed using a combination of UHPLC with TOF MS. Such systems combine the high chromatographic resolution and speed provided by UHPLC with the high mass accuracy (typically <5ppm), excellent sensitivity and rapid data acquisition provided by TOF analyzers [57]. However, other mass analyzers (working in tandem or hybrid configuration) can also be used in LC-MS-based metabolomics. Some these are Orbitrap, IT, FT-ICR, and different combinations such quadrupole-time-of-flight (Q/TOF), quadrupole-ion trap (Q/IT), linear trap quadrupole Orbitrap (LTQ-Orbitrap) or linear trap quadrupole FT-ICR (LTQ FT-ICR) [62,63]. High resolution MS (HRMS), such as FT-ICR, Orbitrap MS, and TOF MS can provide very accurate mass measurements to facilitate reliable metabolite identification. Furthermore, the acquisition of accurate-mass MS/MS spectra provides additional structural information for metabolite identification [63]. Coupling LC with ion mobility MS (IM-MS) has also been exploited in metabolomics. Using IM-MS, gas-phase ions are separated based on their mobility (usually linked to the ions collision cross section, which is related to their shape and

size), charge and mass. The increase of selectivity, background noise reduction and the possibility to separate isomers are some contributions from this technique [64].

Metabolomics approaches are in continuous evolution in food safety, food quality and traceability, as well as in food bioactivity. In this respect, metabolomics is considered a fundamental tool in Foodomics field.

Lipidomics

Lipidomics is focused on the comprehensive study of lipids in a biological system [65]. Lipids can be classified into eight categories: fatty acyls (FAs), glycerolipids (GLs), glycerophospholipids (GPs), sphingolipids (SPs), sterol lipids, phenol lipids, saccharolipids, and polyketides [66], and each group of lipids contains a different combination of acyl chains. Due to this chemical diversity, the simultaneous analysis of the entire lipidome is considered an important challenge in the field of analytical chemistry.

Lipidome analysis typically starts with the extraction of the lipids from the sample. Samples can be solid in nature (e.g., tissues) or highly complex biofluids (e.g., plasma, serum, urine, cyst fluid). Several sample preparation methods are described in the literature, although, usually the best results are obtained by using mixtures of solvents. In this sense, most lipidomics studies use some modified version of a procedure developed by Folch et al. in 1957 [67] and successively modified by Bligh and Dyer in 1959 [68]. Apart from these regular methods, alternative immiscible organic solvent systems were introduced by Matyash et al. (2008) [69] and Löfgren et al. (2012) [70].

In lipidomics, MS-based techniques are the best choice based on their higher sensitivity, molecular specificity, and the capability to obtain structural information. MS is often combined with LC or GC. Both approaches have their own advantages and limitations. Among them, LC hyphenated

with MS has become a very popular and widely used technique [71,72]. Besides of RP and HILIC separation modes, normal-phase (NP) is also frequently applied in lipids separation. In RP separation, lipid species with smaller chain are eluted earlier than those containing large chain, and polyunsaturated acyl structures are eluted earlier than saturated analogs [73]. HILIC and NP distinguish lipid species according to their hydrophilicity separating lipids in their respective classes according to their polarity [74]. Other chromatographic techniques used for lipid separation include supercritical fluid chromatography (SFC) [75], non-aqueous RP-LC [76], chiral LC [77], and silver-ion RP-LC [78]. Furthermore, for complete separation of complex lipids, a combination of different phase chromatography methods can be applied [79].

ESI and APCI are the preferred ionization modes when using the LC-MS coupling for lipidomics applications [72]. ESI is effective to ionize a wide range of lipids, meanwhile APCI is preferred for analyses of weak polar lipids such as fatty acids. Damen et al. [80] used RP-UHPLC together with IM-MS for the analysis of different lipid molecular species and lipid isomers. Intact lipid ions were separated based on their collision cross section values (CCS), mass, and charge. The fragment ion derived in the transfer cell was aligned with the precursors lipid ions, not only by retention time but also because the ion mobility. Such method cleans up the spectrum, showing only the fragment ions of that specific drift time [80].

Glycomics

Glycomics is essentially the study of the complete set of glycans (the glycome) produced in a given cell or organism. Glycans may be present either as free oligosaccharides or as glycoconjugates such as glycoproteins and glycolipids. Protein-bound glycans include N-linked glycans, linked to an asparagine on the protein backbone, O-linked glycans, linked to either threonine or serine, or

glycosaminoglycans, highly anionic and polymeric oligosaccharides linked to serine or threonine [81].

The complexity of glycan structures and their versatility makes Glycomics very challenging. Complex mixtures of glycans are usually separated by LC or CE and detected by fluorescence detector (FLD) or MS [82]. Fluorescence detection requires fluorescently tagged glycans, and gives limited structural information, while MS can be applied on both native and derivatized oligosaccharides and provides structural information of glycans. LC-MS coupling is currently considered the technique of choice for glycomics due to the high sensitivity and capability to analyze complex biological samples [83-86].

Sample preparation for Glycomics usually requires to remove proteins and salts that might interfere with derivatization and detection. A clean-up step, such as liquid-liquid extraction (LLE) or solid-phase extraction (SPE), is required to remove excess salts, which can interfere with MS analysis. Derivatization methods, such as hydrazone formation [86] and permethylation [87] can be applied to improve the efficiency of chromatographic separation and to enhanced MS ionization and detection. Glycolipids are generally isolated by extraction using chloroform and MeOH and glycans are released from the lipid backbone with either enzymes or chemical cleavage agents [86]. The stepwise removal of terminal monosaccharides through the use of exoglycosidases provides an alternate method for obtaining structural information [85]. In the case of glycoproteins, sample preparation is designed to first release the glycans from the proteinaceous structure. There are several methods to release glycans, the most used to release N-glycans from the protein backbone is by peptide-N-Glycosidase F [82,84-85]. In contrast, no enzyme has so far been characterized that enable efficient release of all types of O-linked glycan, thus, O-linked glycome is released via a reductive β-elimination reaction [82,85].

HILIC and more recently porous graphitized carbon (PGC) are typically used for glycan analysis. In HILIC, glycans interact with the stationary phase, applying often a gradient that consist of an aqueous part with some salt and/or acid and a less polar organic solvent, generally acetonitrile, with a gradual increase of the aqueous fraction (normally up to 50%) the elution of the glycans species is promoted [88]. The HILIC separation is predominantly based on the number of polar groups and size of the glycan species [89]. Meanwhile, in the PGC columns the mechanisms of separation are more complex and may be based on adsorption through hydrophobic, hydrophilic, and polar interactions [90]. Among several parameters, the ionic strength of the mobile phase and temperature plays an important role in the glycan retention in PGC stationary phase [90]. RP-LC [91] and anion-exchange chromatography [92] are also typically applied. Furthermore, others LC techniques such as microfluidic chip-LC [93] and nanoLC [94] have also contributed to the expansion of the glycome coverage.

ESI is one the most widely used ionization method in glycomics analysis [90,91,93]. This ionization mode is particularly applied in glycomics studies due to its capability to generate multiple charged species without excessive fragmentation [95].

LC-based Foodomics applications

As mentioned above, Foodomics involves the integration of several omics technologies for the study of a wide range of food aspects including bioactivity, safety, quality, authenticity and traceability. Considering the complexity of foods, integrated by a wide array of components with different chemical properties and different concentrations, and the novelty of the Foodomics approach, it is not surprising the scarce literature found on this topic. The number of works published is even lower when we look for the integration of several omics' platforms following a

global Foodomics approach, which implies not only handling multiple advanced analytical technologies but also using different bioinformatics and statistical tools. Some of the most recent applications of LC-based omics techniques to food bioactivity, safety, quality, authenticity and traceability are described below and summarized in **Table 10.1**.

<TABLE 10.1. HERE >

Food bioactivity

One of the main goals of Foodomics is to expand our knowledge about the effect of diet on the prevention of some diseases. **Figure 10.1** shows a scheme of an ideal Foodomics strategy to investigate the health benefits from dietary constituents. To this aim, the integration of the information at the three levels of expression, namely genes, proteins and metabolites, is crucial. However, as mentioned above, only few works have addressed the integration of several omics platforms for the study of the effects of dietary components in human health. Thus, a nutritional intervention study investigated the effect of a mixture of selected dietary ingredients (fish oil, green tea extract, resveratrol, vitamin E, vitamin C, and tomato extract) on overweight men suffering low-grade chronic inflammation [96]. Blood, urine and fat tissue samples were analyzed. Lipidomics analysis was performed by HPLC-MS using a C18 column and a ternary gradient [97], while metabolomics studies were carried out by GC-MS [97]. The results obtained were combined with those from large-scale profiling of genes and proteins, concluding that the mixture of ingredients tested induced several subtle changes indicative of modulated inflammation of adipose tissue, improved endothelial function, affected oxidative stress, and increased liver fatty acid oxidation.

<FIGURE 10.1. HERE>

A global Foodomics strategy was developed and applied by Ibáñez et al. [98] to evaluate the bioactive effect of a polyphenol-enriched supercritical fluid extract (SFE) from rosemary on human HT29 colon cancer cells [98]. Metabolic profiling of control and rosemary-treated colon cancer cells was performed by UHPLC-Q/TOF MS using both RP and HILIC separation mechanisms, which enabled a wide coverage of hydrophobic and hydrophilic compounds. This coverage was extended by the additional use of capillary electrophoresis coupled to TOF MS (CE-TOF MS). Data integration of metabolomics, transcriptomic and proteomics platforms suggested that polyphenolic extract of rosemary exhibited antioxidant activity inside the colon cancer cells, together with the induction of apoptosis and cell cycle arrest; these three mechanisms can explain the antiproliferative (and therefore potential chemopreventive) effect of the extract. A follow up study was designed using different rosemary extract concentrations and treatment times, in order to identify changes in amplitude and kinetics of proteins altered over the time [99]. In that work [99], a comprehensive proteomic study based on nanoLC coupled to an Orbitrap MS together with stable isotope DML labeling concluded that rosemary polyphenols induced time- and dose-dependent proteomic changes that were related to the attenuation of aggresome formation and activation of autophagy to alleviate cellular stress. Most of the altered proteins were implicated in the activation of Nrf2 transcription factor and the unfolded protein response, which corroborates the results obtained in the transcriptomic study [100]. **Figure 10.2** shows the correlation between both Omics in terms of the direction and amplitude of the statistically significant mRNA and protein changes. With the aim of shedding light into the molecular mechanisms behind the chemopreventive effect of the polyphenol-enriched rosemary extract [101], the antiproliferative effect of the major compounds present in this extract, namely carnosic acid (CA) and carnosol (CS) [102], was evaluated. Metabolomic profiles obtained by HILIC/UHPLC-TOF MS and CE-MS were integrated with

transcriptomic results of control and treated colon cancer cells revealing that the observed antiproliferative effect was also linked to the alteration of the polyamine metabolism.

<FIGURE 10.2. HERE>

A more recent global Foodomics study including quantitative proteomics analysis using iTRAQ labeling and nanoLC-MS/MS was performed by Jia et al. [103]. The effect of supplementing parsley to C57BL/6J mice with dextran sodium sulphate-induced colitis, was evaluated. A global transcriptome, proteome and metabolome analyses using colon and liver tissues and plasma, was conducted. Down-regulation of inflammatory cytokines and cancer markers was observed, together with up-regulation of fatty-acid synthesis genes (thereby improving body weight loss). An up-regulation of molecules involved in the citric acid cycle and urea cycle suggested improved impaired glycolysis and oxidative stress. The authors proposed parsley as a novel nutraceutical in inflammatory bowel disease (IBD) management.

There are many works in literature dealing with the study of nutritional biomarkers by a single omic platform, being of especial interest the functional study of bioactive compounds, as can be deduced from the many works reviewing the use of metabolomic, transcriptomic and proteomic approaches for the identification of diet-related biomarkers upon intervention studies [104-105]. In the following, some representative examples in which the employment of an HPLC-based omic approach combined with biological assays to reveal a particular bioactive effect will be shown. For instance, Fujimura et al. [106] investigated the ability of aqueous extracts from 43 Japanese green tea cultivars to inhibit thrombin-induced phosphorylation of myosin regulatory light chain (MRLC) in human umbilical vein endothelial cells (HUVECs). MRLC phosphorylation is a potential hallmark of vascular endothelial dysfunction, an early step in the development of atherosclerosis, which is associated with cardiovascular risk factors. Metabolomic profiling was performed in a C18/HPLC-

IT/TOF MS instrument. Sunrouge cultivar strongly inhibited thrombin-induced MRLC phosphorylation that could be associated to its metabolic profile [106]. Suh et al. [107] developed a UHPLC-Q/TOF MS method using C18 as stationary phase and a gradient water/acetonitrile (both containing 0.1% formic acid) to study the metabolic profile of a mixture of *Cudrania tricuspidata*, *Lonicera caerulea*, and *Glycine hispida* (soybean), before and after fermentation, and its effect on high-fat diet (HFD)-fed mice [107]. The differences between antiobesity effects of fermented and non-fermented mixture could be partially explained by the differences in lysophosphatidylcholines with C20:4, C16:0, C18:2 and C22:6 found in plasma samples [107].

Kunisawa et al. [108] applied a LC-MS/MS target lipidomics approach to identify 17,18-epoxyeicostetraenoic acid as a major ω-3 eicosapentaenoic acid (EPA)-derived metabolite generated from dietary α-linolenic acid in the gut. 17,18-epoxyeicostetraenoic acid exhibited anti-allergic function when administered *in vivo* to egg white ovalbumin-induced allergic mice [108]. The proposed method separated PUFAs' (polyunsaturated fatty acids) metabolites in a C18 column, using a binary gradient of water/acetate (100:0.1, v/v) and acetonitrile/methanol (4:1, v/v) [109]. Non-targeted plasma lipid profiling by UHPLC-IT/TOF MS was employed, instead, to evaluate the effect of the intragastric administration of the Chinese medicine *Allium macrostemon* in a rat model of depression [110]. Moreover, target MRM analysis by UHPLC-QqQ MS was performed for acylcarnitines. The concentration of several lysophosphatidylcholines as well as most medium- and long-chain acylcarnitines increased, while the concentration of some phosphatidylcholines and triglycerides decreased in the plasma of depressed rats. These changes indicated that depressed rats were associated with inflammatory conditions and an incomplete β-oxidation of fatty acids. Most of these dysregulated metabolites were returned to their normal levels after treatment with *A. macrostemon* [110]. Further lipidomics applications in food bioactivity can be found in reviews from Hyötyläinen et al. [111] and Zhao et al. [112].

Structure elucidation of glycans in Glycomics requires the employment of several analytical techniques, including HPLC, MS and NMR. Establishing a relationship between glycan structure and its biological function is an even more arduous issue to address; therefore, it is not surprising the very few studies on bioactivity of natural occurring glycans in food [113]. A very interesting comparison among different HPLC separation modes used in glycomics, including HILIC, RP, PGC and HPAEC, was reported by Brolk et al. [114] for the analysis of complex mixtures of neutral oligosaccharides [114]. HILIC mode proved to efficiently analyze oligosaccharides of different degree of polymerization, whereas PGC gave the best separation of samples composed of isomeric oligosaccharides with the same molecular weight (isobaric compounds).

One of the main interests in glycomics is the study of milk oligosaccharides as potential bioactive molecules, as can be seen for instance in the work by Totten et al. [115] in which they developed a rapid throughput method for the analysis of unconjugated oligosaccharides in breast milk by nanoLC chip-TOF MS. A SPE protocol in 96-well plates allowed the processing of different samples simultaneously, which can be very attractive for its use in intervention studies. Over 250 compounds were monitored, nearly 100 of which were assigned fully annotated structures [115]. Milk and dairy products are also an interesting source of bioactive peptides, which can be released during digestion or in exogenous processes as fermentation by certain lactic acid bacteria or by enzymatic proteolysis [116]. Other food sources of bioactive peptides are fish, eggs, meat, soybean, rice, sunflower and cereals [117]. LC-MS and MALDI-MS are techniques widely used in peptidomics analysis, occasionally combined with bioavailability assays (e.g., resistance of peptides to gastric digestion and subsequent intestinal absorption through the blood stream). Antioxidant activity and angiotensin converting-enzyme (ACE) inhibition (a measurement of potential antihypertensive effect) are among the most investigated peptide bioactivities. An example is the use of RP/HPLC-IT MS for the identification of antihypertensive peptides from a

bovine lactoferrin pepsin hydrolysate [118]; bioactivity of the hydrolysate against hypertension was evaluated in both *in vitro* and *in vivo* models [118]. NanoLC-LTQ-Orbitrap MS/MS was used for the identification of sarcoplasmic and myofibrillar fish peptides with potential antimicrobial activity [119]. In that work, 44 and 18 potential antimicrobial peptides were identified for sarcoplasmic and myofibrillar extracts, respectively [119].

In proteomics applications, SDS-PAGE fractionation prior to LC-MS/MS analysis (GeLC-MS/MS) [120] is sometimes used to achieve a better coverage of the proteome, which is essential to detect minimal changes with statistical significance. A GeLC-MS/MS approach was used by Yap et al. [121] to study the proteome of tiger milk mushroom (*Lignosus rhinocerotis*) sclerotium and the proteins related to its antiproliferative activity against human breast adenocarcinoma cells (MCF7); the bioactive protein was identified as a serine protease [121]. Quantitative proteomics using iTRAQ labeling combined with phosphopeptide enrichment and LC-QTRAP MS/MS analysis was proposed for the study of the bioactive effect of *Artemisia dracunculus* L. extract against insulin resistance [122]. Results showed that *A. dracunculus* extract increased phosphorylation levels of specific amino acids in proteins in the insulin-resistant state that are normally phosphorylated by insulin, thus, exerting insulin-sensitizing effects in skeletal muscle [122].

Food safety

Food safety is a field of utmost importance in food science and analytical chemistry. Food production and distribution occurs in a global market and consumers worldwide are demanding high standards of food quality and safety, which has promoted the development of stringent regulations by governments [123-125] and international organizations [126]. As an example, the establishment of restrictive maximum residue levels (MRLs) in foodstuffs for certain contaminant

compounds has made necessary the validation of sensitive, accurate and fast analytical methods, many of them based on LC-MS [127-128]. The use of the state-of-the-art instrumentation in combination with –omics approaches represents a powerful tool to face the challenge of detecting potentially harmful chemical compounds and microorganisms present in food at trace levels.

Chemical contaminants

Current analytical methods aim the simultaneous determination of several families of contaminants or residues (multi-residue methods) in foods, increasing sample throughput and the capabilities of routine laboratories. Residues of pesticides and pharmaceuticals are the most investigated contaminants in food of plant and animal origin, respectively [129-130]. Target metabolomics approaches based on LC-QqQ MS/MS methods operating in MRM mode have been widely employed to simultaneously monitor more than 100 compounds, as they offer high selectivity and sensitivity. Usually RP methods using C18 fast columns and linear gradients water-methanol or water-acetonitrile are able to separate a wide number of analytes in short analysis times, around 10 or 15 min. For instance, 104 pesticides were analyzed in olives samples in 15 min [131], or 238 pesticides were analyzed in Chinese cabbage and cucumber in 10 min [132]. A representative chromatogram of a Chinese cabbage sample spiked at low μg kg^{-1} level with 238 pesticides is shown in **Figure 10.3**. A screening method developed by Robert et al. [133] allowed the analysis of 160 veterinary drugs in food of animal origin (egg, honey, milk and muscle samples) in 12 min [133].

<FIGURE 10.3. HERE (Adapted)>

Despite the possibility of analyzing hundreds of compounds simultaneously and in short runs, the main disadvantage of target LC-MS/MS analysis is the previous knowledge required to set-up the

acquisition method: retention time and optimized MS/MS transitions for each contaminant monitored (which is done using commercial standards in most cases). HRMS detection can overcome this issue, allowing non-targeted analysis by accurate-mass acquisition. In addition, retrospective analysis of the samples can be done further on, in order to search for unknown contaminants or degradation products. Furthermore, non-targeted analysis can be aided by home-made accurate-mass databases, which have been reported as useful tools for HPLC-HRMS multi-residue applications in fruits and vegetables [134]. Other applications for large-scale multi-residue analysis include the use of target LC-MS/MS analysis using HRMS. For instance, Wang et al. monitored 451 pesticides in fruits and vegetables by UHPLC-Q-Orbitrap MS/MS [135].

The use of multi-residue methods covering a large number of chemical contaminants is desired, especially for routine analysis. However, there are some polar compounds that are not properly retained in RP columns and elute with the dead volume at the beginning of the chromatogram. These analytes require the development of particular HPLC methods that employs mixed-mode or HILIC columns [136]. In a very recent work, Inoue et al. [137] proposed the suitability of both RP and HILIC modes for the detection of unexpected contaminations in infant formulas. Processing HPLC-TOF MS results with PCA allowed classification of the samples for preliminary evaluation of contaminations with melamine, pesticides and heavy metals [137].

Independently of the separation and detection mode, sample preparation is a key point in the development of any multi-residue method. SPE and QuEChERS (Quick, Easy, Cheap, Effective, Rugged and Safe) are the most common methodologies for the analysis of contaminants in liquid and solid samples, respectively. In both cases, sorbent selection depends strongly not only on the target compounds but also on the food sample under study; in this sense, fatty foods are particularly challenging, occasioning strong matrix effects in LC-MS methods. Therefore,

dedicated works have been published regarding the improvement of sample preparation methods to reduce matrix effects when analyzing chemical contaminants in this kind of foods [138-139].

Pathogens and Toxins

Foodomics approaches have demonstrated to be useful tools to assess microbiological safety of food, through the detection of pathogens, toxins, and sub-products in food spoiled by microorganisms. Many efforts have been done to elucidate the proteome and secretome of food pathogens, whose knowledge constitutes a solid basis for applied studies on food spoilage and pathogens resistance. An example of the application of proteomics to the identification of microorganisms in food is the use of a proteomic method for the detection of *Enterococcus faecalis* spiked into milk, by MALDI-TOF MS and LC-IT MS/MS, using a zirconium hydroxide immobilization approach for pathogen isolation [140]. Besides, the combination of proteomics with other omics techniques can give a deep insight into the resistance and survival of pathogens to food processing conditions. In order to monitor changes during food processing, omics investigations of model microorganisms under stress conditions, such as temperature shock, osmotic pressure, high pressure and other factors such as the use of antimicrobials, have been performed to follow pathogens' adaptation and reaction to extreme conditions [141].

Another aspect related to microbiological safety of food is the study of toxins generated by pathogens. Bacteria, fungi and microalgae may produce toxins in foods while leaving the food appearance, odor or flavor unaltered. Foodomics approaches have been shown to be very useful for the detection of toxins in food [142]. Mycotoxins or fungal toxins are secondary metabolites highly investigated due to their harmful effects and persistence (they remain unaltered after food processing). LC-MS metabolomic approaches are prone to the development of multi-residue

methods, sometimes together with pesticides and other chemical contaminants. For instance, an UHPLC-MS/MS method was developed for the analysis of 56 mycotoxins and mycotoxins metabolites in 12 feeding matrices (feeding cereals, complex compound feeds, extracted oilcakes, fermented silages, malt sprouts or dried distillers' grains with solubles), with an overall run time of 15 min [143]. On the other hand, proteomics methods have been demonstrated to be a good choice for the investigation of bacterial toxins, such as the method developed by Sospedra et al. [144] for the identification of staphylococcal enterotoxins A and B in milk and fruit juices [144]. Separation of enterotoxin proteins was carried out in a gradient water-acetonitrile (both with 0.5% acetic acid) in a C4 RP column in 13 min [144].

Algal toxins can be accumulated in fish and seafood, occasioning harmful effects to the consumers. Paralytic shellfish poisoning (PSP) toxins are a group of neurotoxins produced from dinoflagellates whose level has been regulated in mollusks to ensure food safety. Some official methods include HPLC with fluorescence detection, requiring a derivatization step, but some methods based on HPLC-MS have been proposed as alternative. For example, a chromatographic method was developed for monitoring PSP toxins in shellfish combining UHPLC separation of analytes in HILIC mode together with MRM tandem mass spectrometry detection [145].

Food Allergens

Food allergies arise from an anomalous interaction between certain food components and the immune system. The eight food matrices that trigger the majority of food allergies are egg, fish, milk, tree nuts, peanuts, shellfish, soy and wheat. Most of the food allergies are caused by protein components and their degradation products; therefore, proteomics methods are used together with genomics and immunological methods such as ELISA (enzyme-linked immunosorbent assay)

for the detection of allergens in food. Comprehensive reviews on LC-MS methods for the proteomic analysis of allergen in food (the so-called “allergenomics”) have been performed, for instance, by Faeste et al. [146] and Koeberl et al. [147]. Monaci et al. [148]reported the use of UHPLC-HRMS for the quantification of casein allergens potentially present in white wines as a result of wine fining by caseinate [148]. This label-free quantitative approach consisted on the monitoring of representative tryptic peptides. In a different work, non-targeted nanoLC-Q/TOF MS/MS method was used to identify the representative peptides of gluten [149]. The developed method was finally applied to gluten containing cereals (wheat, rye, barley and oats) and non-gluten containing flours (corn, soy and rice).

Food quality, authenticity and traceability

Food integrity relies on food safety, quality, and authenticity. Food integrity has to be guaranteed by an appropriate traceability, which means the ability to track any food, feed, food-producing animal or substance that will be used for consumption, through all stages of production, processing and distribution. High-throughput methodologies employed in Foodomics provide valuable information on the precise composition of food products that can be directly correlated to their quality and to the different manufacture steps to which a particular food has been submitted. For instance, Hughey et al. [150] proposed a non-targeted metabolomics approach for the differential analysis of beer produced in two different years. The RP UHPLC-Q/TOF MS method consisted on a linear gradient water/acetonitrile (both containing 0.1% formic acid) that allowed the separation of the metabolites in 18 min. The developed method provided evidence of beer oxidation during storage by the detection of nonvolatile molecular indicators of oxidation in samples stored at room temperature prior analysis [150].

Metabolomics studies have also a high importance in the determination of geographical origin of food. The use of metabolomics approaches based on LC-MS combined with statistical analysis allows the selection of appropriate markers to carry out geographical product certifications, such as protected designation of origin (PDO) or protected geographical indication (PGI). For example, metabolic profiling by UHPLC-Q/TOF MS permitted a successful discrimination of geographical origin of Goji berries, mainly because of the different flavonoid composition of the fruits from different Asian locations [151]. However, the identification of the markers of origin is a challenging task due to the wide variety of metabolite classes, similarities among samples and the presence of isobaric compounds. For instance, metabolomic fingerprinting of saffron by RP chromatography using a partially-porous column and Q/TOF MS detection enabled the identification of authenticity markers, while geographical markers could not be identified [152]. In this regard, multidimensional approaches offer an enhanced peak capacity, which in the practice means a better separation of compounds with similar retention behavior. Comprehensive two-dimensional liquid chromatography (LC × LC) using a HILIC × RP-LC separation combined with IT MS/MS detection has been applied for an in-depth characterization of the polyphenol and saponin profile of licorice with the aim of searching for potential markers of authenticity and geographical origin [153].

Food fraud is another critical issue that has successfully been addressed by omics technologies. The high selectivity and sensitivity provided by the state-of-the-art instrumentation is capable of detecting food adulterants even at trace levels. For instance, an integrated metabolite profiling (GC-TOF MS) and lipidomics approach (UHPLC-LTQ/Orbitrap MS) was developed for the detection of the adulteration of beef with pork [154]. Different grades of beef mince and pork mince mixed at different percentage ratios were analyzed. The combination of metabolomic and lipidomic analyses with multivariate statistical processing revealed differential metabolites for the

identification of the two meat types. Those related to pork increased in line with the levels of adulteration of beef mince with pork. Additionally, there was a subset of metabolites which appeared to be directly correlated to the level of fat content in meat [154]. Proteomic methods have been also used for the authentication of food products [155]. A high-throughput proteomics method combined with non-targeted data acquisition and spectral library was developed for the authentication of fish [156]. MicroLC-MS/MS using two mass analyzers (IT and Q-Orbitrap) was used for the separation of the tryptic digests in 45 min. The method was found to be robust in different laboratories, and 94−97% of the analyzed flatfish samples were correctly identified, including processed samples [156].Proteomic profiling and metabolomic profiling have been also used to differentiate conventional food from organic [157] and transgenic foods [158], demonstrating the huge potential of Foodomics to solve new problems in the Food Science domain.

Acknowledgements

This work was supported by the project AGL2014-53609-P (Ministerio de Economía y Competitividad, Spain). B.G.L. thanks MINECO for her *Juan de la Cierv*a postdoctoral research contract (ref. JCI-2012-12972).

References

[1] García-Cañas V, Simó C, Herrero M, Ibáñez E, Cifuentes A. Present and future challenges in food analysis. Foodomics. Anal Chem 2012;84:10150–9.
[2] Gallo M, Ferranti P. The evolution of analytical chemistry methods in foodomics. J Chromatogr A 2016;1428:3-15.
[3] Nuñez O, Gallart-Ayala H, Martins CPB, Lucci P. New trends in fast liquid chromatography for food and environmental analysis. J Chromatogr A 2012;1228:298-323.

[4] Fekete S, Schappler J, Veuthey J-L, Guillarme D, Current and future trends in UHPLC. TrAC – Trends Anal Chem 2014;63:2-13.
[5] Wahab, MF, Dasgupta PK, Kadjo AF, Armstrong DW. Sampling frequency, response times and embedded signal filtration in fast, high efficiency liquid chromatography: A tutorial. Anal Chim Acta 2016;907:31-44.
[6] Wasinger VC, Cordwell SJ, Cerpa-Poljak A, Yan JX, Gooley AA, Wilkins MR, et al. Progress with gene-product mapping of the Mollicutes: Mycoplasma genitalium. Electrophoresis 1995;16:1090-4.
[7] McLafferty FW, Fridriksson EK, Horn DM, Lewis MA, Zubarev RA. Techview: biochemistry. Biomolecule mass spectrometry. Science 1999;284(5418):1289-90.
[8] Camerini S, Mauri P. The role of protein and peptide separation before mass spectrometry analysis in clinical proteomics. J Chromatogr A 2015;1381:1-12.
[9] Yates III JR. The revolution and evolution of shotgun proteomics for large-scale proteome analysis. J Am Chem Soc 2013;135(5):1629-40.
[10] Nagaraj N, Kulak NA, Cox J, Neuhauser N, Mayr K, Hoerning O, et al. System-wide perturbation analysis with nearly complete coverage of the yeast proteome by single-shot ultra HPLC runs on a bench top Orbitrap. Mol Cell Proteomics 2012;11:M111. 013722.
[11] Zurbriggen K, Schmugge M, Schmid M, Durka S, Kleinert P, Kuster T, et al. Analysis of minor hemoglobins by matrix-assisted laser desorption/ionization time-of-flight mass spectrometry. Clin Chem 2005;51(6):989-96.
[12] Han G, Ye M, Zhou H, Jiang X, Feng S, Jiang X, et al. Large-scale phosphoproteome analysis of human liver tissue by enrichment and fractionation of phosphopeptides with strong anion exchange chromatography. Proteomics 2008;8(7):1346-61.
[13] McNulty DE, Annan RS. Hydrophilic interaction chromatography reduces the complexity of the phosphoproteome and improves global phosphopeptide isolation and detection. Mol Cell Proteomics 2008;7(5):971-80.
[14] Perkins DN, Pappin DJ, Creasy DM, Cottrell JS. Probability-based protein identification by searching sequence databases using mass spectrometry data. Electrophoresis 1999;20(18):3551-67.
[15] Eng JK, McCormack AL, Yates III JR. An approach to correlate tandem mass spectral data of peptides with amino acid sequences in a protein database. J Am Soc Mass Spectrom 1994;5(11):976-89.
[16] Cox J, Neuhauser N, Michalski A, Scheltema RA, Olsen JV, Mann M. Andromeda: a peptide search engine integrated into the MaxQuant environment. J Proteome Res 2011;10(4):1794-805.
[17] Craig R, Beavis RC. A method for reducing the time required to match protein sequences with tandem mass spectra. Rapid Commun Mass Spectrom 2003;17(20):2310-6.
[18] Grigorov MG, van Bladeren PJ. Functional peptides by genome reverse engineering. Curr Opin Drug Discov Devel 2007;10(3):341-6.
[19] Wasinger VC, Zeng M, Yau Y. Current status and advances in quantitative proteomic mass spectrometry. Int J Proteomics 2013;2013:1-12.
[20] Ross PL, Huang YN, Marchese JN, Williamson B, Parker K, Hattan S, et al. Multiplexed protein quantitation in Saccharomyces cerevisiae using amine-reactive isobaric tagging reagents. Mol Cell Proteomics 2004;3(12):1154–69.
[21] Hsu JL, Huang SY, Chow NH, Chen SH. Stable-isotope dimethyl labeling for quantitative proteomics. Anal Chem 2003;75(24):6843-52.

[22] Ong SE, Blagoev B, Kratchmarova I, Kristensen DB, Steen H, Pandey A, et al. Stable isotope labeling by amino acids in cell culture, SILAC, as a simple and accurate approach to expression proteomics. Mol Cell Proteomics 2002;1(5):376-86.
[23] Boonen K, Landuyt B, Baggerman G, Husson SJ, Huybrechts J, Schoofs L. Peptidomics: the integrated approach of MS, hyphenated techniques and bioinformatics for neuropeptide analysis. J Sep Sci 2008;31(3):427-45.
[24] Schulz-Knappe P, Zucht HD, Heine G, Jürgens M, Hess R, Schrader M. Peptidomics: the comprehensive analysis of peptides in complex biological mixtures. Comb Chem High Throughput Screen 2001;4(2):207-17.
[25] Hruby VJ, Balse PM. Conformational and topographical considerations in designing agonist peptidomimetics from peptide leads. Curr Med Chem 2000;7(9):945-70.
[26]Liotta LA, Petricoin EF. Serum peptidome for cancer detection: spinning biologic trash into diagnostic gold. J Clin Invest 2006;116:26-30.
[27] Korhonen H, Pihlanto A. Bioactive peptides: production and functionality. Int Dairy J 2006;16(9):945-60.
[28] Kamau SM, Lu RR, Chen W, Liu XM., Tian FW, Shen Y, et al. Functional significance of bioactive peptides derived from milk proteins. Food Rev Int 2010;26(4):386-401.
[29] Hebert EM, Saavedra L, Ferranti P. Bioactive peptides derived from casein and whey proteins. In: Mozzi F, Raya RR, Vignolo GM, editors. Biotechnology of lactic acid bacteria: Novel applications. 1st ed. Ames: Wiley-Blackwell; 2010. p. 233-49.
[30] Ytterberg AJ, Dunsmore J, Lomeli SH, Thevis M, Xie Y, Loo RRO, et al. The Role of Mass Spectrometry for Peptide, Protein, and Proteome Characterization. In: Cole, IB, editor. Electrospray and MALDI Mass Spectrometry: Fundamentals, Instrumentation, Practicalities, and Biological Applications. 2nd ed. Hoboken: John Wiley & Sons; 2010. p. 683-721.
[31] Williams JD, Burinsky DJ. Mass spectrometric analysis of complex mixtures then and now: the impact of linking liquid chromatography and mass spectrometry. Int J Mass Spectrom 2001;212:111-33.
[32] Wilm M, Mann M. Analytical properties of the nanoelectrospray ion source. Anal Chem 1996;68:1-8.
[33] Bjellaas T, Holm A, Molander P, Tørnes JA, Greibrokk T, Lundanes E. Trace determination of peptides in water samples using packed capillary liquid chromatography with UV and MS detection and characterization of peptide oxidation products by MS. Anal Bioanal Chem 2004;378(4):1021-30.
[34] Secher A, Kelstrup CD, Conde-Frieboes KW, Pyke C, Raun K, Wulff BS, et al. Analytic framework for peptidomics applied to large-scale neuropeptide identification. Nat Commun 2016;7:11436. doi:10.1038/ncomms11436
[35] Paul M, Somkuti GA. Degradation of milk-based bioactive peptides by yogurt fermentation bacteria. Lett Appl Microbiol 2009;49(3):345-50.
[36] Gu B, Chen Z, Thulin CD, Lee ML. Efficient polymer monolith for strong cation-exchange capillary liquid chromatography of peptides. Anal Chem 2006;78(11):3509-18.
[37] Moya VJ, Flores M, Aristoy MC, Toldrá F. Pork meat quality affects peptide and amino acid profiles during the ageing process. Meat Sci 2001;58(2):197-06.
[38] Gómez-Ruiz JA, Ramos M, Recio I. Angiotensin converting enzyme-inhibitory peptides in Manchego cheeses manufactured with different starter cultures Int. Dairy J 2002;12(8):697-06.

[39] Hao Z, Lu CY, Xiao B, Weng N, Parker B, Knapp M, et al. Separation of amino acids, peptides and corresponding Amadori compounds on a silica column at elevated temperature. J Chromatogr A 2007;1147(2):165-71.
[40] Cutillas PR, Norden AG, Cramer R, Burlingame AL, Unwin RJ. Detection and analysis of urinary peptides by on-line liquid chromatography and mass spectrometry: application to patients with renal Fanconi syndrome. Clin Sci 2003;104(5):483-90.
[41] Lee K, Kim S. SSGE an DEE, new peptides isolated from a soy protein hydrolysate that inhibit platelet aggregation. Food Chem 2005;90(3):389-93.
[42] Clarke NJ, Crow FW, Younkin S, Naylor S. Analysis of in vivo-derived amyloid-beta polypeptides by on-line two-dimensional chromatography-mass spectrometry. Anal Biochem 2001;298:32-9.
[43] Issaq HJ, Chan KC, Janini GM, Conrads TP, Veenstra TD. Multidimensional separation of peptides for effective proteomic analysis. J Chromatogr B 2005;817:35-47.
[44] Oosterkamp AJ, Carrascal M, Closa D, Escolar G, Gelpi E, Abian J. On-line preconcentration microliquid chromatography tandem mass spectrometric method for bradykinin analysis in plasma. J Microcol Sep 2001;13(7):265-74.
[45] Cirulli C, Chiappetta G, Marino G, Mauri P, Amoresano A. Identification of free phosphopeptides in different biological fluids by a mass spectrometry approach. Anal Bioanal Chem 2008;392(1-2):147-59.
[46] Hawkridge AM, Heublein DM, Bergen HR, Cataliotti A, Burnett JCJr, Muddiman DC. Quantitative mass spectral evidence for the absence of circulating brain natriuretic peptide (BNP-32) in severe human heart failure. Proc Natl Acad Sci USA 2005;102(48):17442-7.
[47] Romanova EV, Dowd SE, Sweedler JV. Quantitation of endogenous peptides using mass spectrometry based methods. Curr Opin Chem Biol 2013;17(5):801-8.
[48] Dallas DC, Guerrero A, Parker EA, Robinson RC, Gan J, German JB, et al. Current peptidomics: applications, purification, identification, quantification, and functional analysis. Proteomics 2015;15(5-6):1026-38.
[49] Theodoridis GA, Gika HG, Want EJ, Wilson ID. Liquid chromatography–mass spectrometry based global metabolite profiling: A review. Anal Chim Acta 2012;711:7-16.
[50] Fiehn O. Combining genomics, metabolome analysis, and biochemical modelling to understand metabolic networks. Comp Funct Genomics 2001;2(3):155-68.
[51] Godzien J, Ciborowski M, Whiley L, Legido-Quigley C, Ruperez FJ, Barbas C. In-vial dual extraction liquid chromatography coupled to mass spectrometry applied to streptozotocin-treated diabetic rats. Tips and pitfalls of the method. J Chromatogr A 2013;1304:52-60.
[52] Raterink RJ, Lindenburg PW, Vreeken RJ, Ramautar R, Hankemeier T. Recent developments in sample-pretreatment techniques for mass spectrometry-based metabolomics. TrAC – Trends Anal Chem 2014;61:157-67.
[53] Cajka T, Fiehn O. Comprehensive analysis of lipids in biological systems by liquid chromatography-mass spectrometry. TrAC – Trends Anal Chem 2014;61:192-06.
[54] Dettmer K, Aronov PA, Hammock BD. Mass spectrometry-based metabolomics. Mass Spectrom Rev 2007;26:51-78.
[55] Wolfender JL, Marti G, Thomas A, Bertrand S. Current approaches and challenges for the metabolite profiling of complex natural extracts. J Chromatogr A 2015;1382:136-64.
[56] Wilson ID, Nicholson JK, Castro-Perez J, Granger JH, Johnson KA, Smith BW, et al. High resolution “ultra performance” liquid chromatography coupled to oa-TOF mass

spectrometry as a tool for differential metabolic pathway profiling in functional genomic studies. J Proteome Res 2005; 4(2):591-8.
[57] Gika HG, Theodoridis GA, Plumb RS, Wilson ID. Current practice of liquid chromatography–mass spectrometry in metabolomics and metabonomics. J Pharm Biomed Anal 2014;87:12-25.
[58] Zhang X, Clausen MR, Zhao X, Zheng H, Bertram HC. Enhancing the power of liquid chromatography–mass spectrometry-based urine metabolomics in negative ion mode by optimization of the additive. Anal Chem 2012;84(18):7785-92.
[59] Zhang R, Watson DG, Wang L, Westrop GD, Coombs GH, Zhang T. Evaluation of mobile phase characteristics on three zwitterionic columns in hydrophilic interaction liquid chromatography mode for liquid chromatography-high resolution mass spectrometry based untargeted metabolite profiling of Leishmania parasites. J Chromatogr A 2014;1362:168-79.
[60] Gama MR, da Costa Silva RG, Collins CH, Bottoli CB. Hydrophilic interaction chromatography. TrAC – Trends Anal Chem 2012;37:48-60.
[61] Contrepois K, Jiang L, Snyder M. Optimized Analytical Procedures for the Untargeted Metabolomic Profiling of Human Urine and Plasma by Combining Hydrophilic Interaction (HILIC) and Reverse-Phase Liquid Chromatography (RPLC)–Mass Spectrometry. Mol Cell Proteomics 2015;14(6):1684-95.
[62] Xiao JF, Zhou B, Ressom HW. Metabolite identification and quantitation in LC-MS/MS-based metabolomics. TrAC – Trends Anal Chem 2012;32:1-14.
[63] Zhou B, Xiao JF, Tuli L, Ressom HW. LC-MS-based metabolomics. Mol Biosyst 2012;8(2):470-81.
[64] Shah V, Castro-Perez JM, McLaren DG, Herath KB, Previs SF, Roddy TP. Enhanced data-independent analysis of lipids using ion mobility-TOFMSE to unravel quantitative and qualitative information in human plasma. Rapid Comm Mass Spectrom 2013;27(19):2195-200.
[65] Yang L, Li M, Shan Y, Shen S, Bai Y, Liu H. Recent advances in lipidomics for disease research. J Sep Sci 2016; 39:38-50.
[66] Fahy E, Subramaniam S, Murphy RC, Nishijima M, Raetz CR, Shimizu T, et al. Update of the LIPID MAPS comprehensive classification system for lipids. J Lipid Res 2009;50(Suppl 1): S9-14.
[67] Folch J, Lees M, Sloane-Stanley GH. A simple method for the isolation and purification of total lipids from animal tissues. J Biol Chem 1957;226:497-509.
[68] Bligh EG, Dyer WJ. A rapid method of total lipid extraction and purification. Can J Biochem Physiol 1959;37(8):911-17.
[69] Matyash V, Liebisch G, Kurzchalia TV, Shevchenko A, Schwudke D. Lipid extraction by methyl-tert-butyl ether for high-throughput lipidomics. J Lipid Res 2008;49(5):1137-46.
[70] Löfgren L, Ståhlman M, Forsberg GB, Saarinen S, Nilsson R, Hansson GI. The BUME method: a novel automated chloroform-free 96-well total lipid extraction method for blood plasma. J Lipid Res 2012;53(8):1690-700.
[71] Teo CC, Chong WPK, Tan E, Basri NB, Low ZJ, Ho YS. Advances in sample preparation and analytical techniques for lipidomics study of clinical samples. TrAC – Trends Anal Chem 2015;66:1-18.
[72] Li M, Zhou Z, Nie H, Bai Y, Liu H. Recent advances of chromatography and mass spectrometry in lipidomics. Anal Bioanal Chem 2011;399:243-9.

[73] Sandra K, dos Santos Pereira A, Vanhoenacker G, David F, Sandra P. Comprehensive blood plasma lipidomics by liquid chromatography/quadrupole time-of-flight mass spectrometry. J Chromatogr A 2010;1217(25):4087-99.
[74] Sandra K, Sandra P. Lipidomics from an analytical perspective. Curr Opin Chem Biol 2013;17(5):847-53.
[75] Lísa M, Holčapek M. High-Throughput and Comprehensive Lipidomic Analysis Using Ultrahigh-Performance Supercritical Fluid Chromatography–Mass Spectrometry. Anal Chem 2015;87(14):7187 95.
[76] Deng P, Zhong D, Wang X, Dai Y, Zhou L, Leng Y, et al. Analysis of diacylglycerols by ultra performance liquid chromatography-quadrupole time-of-flight mass spectrometry: Double bond location and isomers separation. Anal Chim Acta 2016;925:23-33.
[77] Lísa M, Holčapek M. Characterization of triacylglycerol enantiomers using chiral HPLC/APCI-MS and synthesis of enantiomeric triacylglycerols. Anal Chem 2013;85(3):1852-9.
[78] Lísa M, Velínská H, Holcapek M. Regioisomeric characterization of triacylglycerols using silver-ion HPLC/MS and randomization synthesis of standards. Anal Chem 2009;81(10):3903-910.
[79] Bang DY, Myeong HM. On-line two-dimensional capillary strong anion exchange/reversed phase liquid chromatography–tandem mass spectrometry for comprehensive lipid analysis. J Chromatogr A 2013;1310:82-90.
[80] Damen CW, Isaac G, Langridge J, Hankemeier T, Vreeken RJ. Enhanced lipid isomer separation in human plasma using reversed-phase UPLC with ion-mobility/high-resolution MS detection. J Lipid Res 2014;55(8):1772-83.
[81] Lebrilla CB, An HJ. The prospects of glycan biomarkers for the diagnosis of diseases. Mol Biosyst 2009;5:17-20.
[82] Mereiter S, Balmaña M, Gomes J, Magalhães A, Reis CA. Glycomic Approaches for the Discovery of Targets in Gastrointestinal Cancer. Front Onc 2016;6:55. doi: 10.3389/fonc.2016.00055.
[83] Hu Y, Zhou S, Yu CY, Tang H, Mechref Y. Automated Annotation and Quantitation of Glycan by LC-ESI-MS analysis using MultiGlycan-ESI Computational Tool. Rapid Commun Mass Spectrom 2015;29:135-42
[84] Hu Y, Zhou S, Khalil SI, Renteria CL, Mechref Y. Glycomic profiling of tissue sections by LC-MS. Anal Chem 2013;85(8):4074-9.
[85] Rakus JF, Mahal LK. New technologies for glycomic analysis: toward a systematic understanding of the glycome. Annu Rev Anal Chem 2011;4:367-92.
[86] Walker SH, Lilley LM, Enamorado MF, Comins DL, Muddiman DC. Hydrophobic derivatization of N-linked glycans for increased ion abundance in electrospray ionization mass spectrometry. J Am Soc Mass Spectrom 2011;22(8):1309-17
[87] Mechref Y, Kang P, Novotny MV. Solid-phase permethylation for glycomic analysis. In: Packer NH, Karlsson NG, editors. Glycomics: Methods and Protocols. 1st ed. NewYork: Humana Pr; 2009. p. 53-64.
[88] Zauner G, Deelder AM, Wuhrer M. Recent advances in hydrophilic interaction liquid chromatography (HILIC) for structural glycomics. Electrophoresis 2011;32(24):3456-66.
[89] Pabst M, Friedrich A. Glycan analysis by modern instrumental methods. Proteomics 2011;11(4): 631-43.
[90] Pabst M, Altmann F. Influence of electrosorption, solvent, temperature, and ion polarity on the performance of LC-ESI-MS using graphitic carbon for acidic oligosaccharides. Anal Chem 2008; 80(19):7534-42.

[91] Hu Y, Mechref Y. Comparing MALDI-MS, RP-LC-MALDI-MS and RP-LC-ESI-MS glycomic profiles of permethylated N-glycans derived from model glycoproteins and human blood serum. Electrophoresis 2012;33(12):1768-1777.
[92] Chataigné G, Couderc F, Poinsot V. Polysaccharides analysis of sinorhizobial capside by on-line anion exchange chromatography with pulsed amperometric detection and mass spectrometry coupling. J Chromatogr A 2008;1185(2):241-50.
[93] Gao WN, Yau LF, Liu L, Zeng X, Chen DC, Jiang M, et al. Microfluidic Chip-LC/MS-based Glycomic Analysis Revealed Distinct N-glycan Profile of Rat Serum. Sci Rep 2015;5:12844.doi: 10.1038/srep12844.
[94] Bereman MS, Williams TI, Muddiman DC. Development of a nanoLC LTQ orbitrap mass spectrometric method for profiling glycans derived from plasma from healthy, benign tumor control, and epithelial ovarian cancer patients. Anal Chem 2008;81(3):1130-6.
[95] Sethi MK, Kim H, Park CK, Baker MS, Paik YK, Packer NH, et al. In-depth N-glycome profiling of paired colorectal cancer and non-tumorigenic tissues reveals cancer-, stage- and EGFR-specific protein N-glycosylation. Glycobiology 2015;25(10):1064-78.
[96] Bakker GCM, van Erk MJ, Pellis L, Wopereis S, Rubingh CM, Cnubben NH, et al. An anti-inflammatory dietary mix modulates inflammation and oxidative and metabolic stress in overweight men. Am J Clin Nutr 2010; 91:1044-1059.
[97] Verhoeckx KCM, Bijlsma S, Jespersen S, Ramaker R, Verheij ER, Witkamp RF, van der Greef J, Rodenburg RJT. Characterization of anti-inflammatory compounds using transcriptomics, proteomics, and metabolomics in combination with multivariate data analysis. Int Immunopharmacol 2004;4:1499–1514.
[98] Ibáñez C, Valdés A, García-Cañas V, Simó C, Celebier M, Rocamora L, et al. Global foodomics strategy to investigate the health benefits of dietary constituents. J Chromatogr A 2012;1248:139-53.
[99] Valdés A, Artemenko KA, Bergquist J, García-Cañas V, Cifuentes A. Comprehensive proteomic study of the antiproliferative activity of a polyphenol-enriched rosemary extract on colon cancer cells using nanoliquid chromatography−orbitrap MS/MS. J Proteome Res 2016;15:1971-1985.
[100] Valdés A, Sullini G, Ibáñez E, Cifuentes A, García-Cañas V. Rosemary polyphenols induce unfolded protein response and changes in cholesterol metabolism in colon cancer cells. J Funct Foods 2015;15:429-439.
[101] Valdés A, García-Cañas V, Simó C, Ibáñez C, Micol V, Ferragut JA, Cifuentes A. Comprehensive Foodomics study on the mechanisms operating at various molecular levels in cancer cells in response to individual rosemary polyphenols. Anal Chem 2014;86:9807−9815.
[102] Herrero M, Plaza M, Cifuentes A, Ibáñez E. Green processes for the extraction of bioactives from Rosemary: Chemical and functional characterization via ultra-performance liquid chromatography-tandem mass spectrometry and in-vitro assays. J Chromatogr A 2010;1217:2512-2520.
[103] Jia H, Aw W, Hanate M, Takahashi S, Saito K, Tanaka H, Tomita M, Kato H. Multi-faceted integrated omics analysis revealed parsley (Petroselinum crispum) as a novel dietary intervention in dextran sodium sulphate induced colitic mice. J Funct Foods 2014;11:438-448.
[104] Ibáñez C, Simó C. MS-based metabolomics in nutrition and health research. In: Cifuentes A, editor. Foodomics: Advances Mass Spectrometry in Modern Food Science and Nutrition. New Jersey: John Wiley & Sons, Inc; 2013. p. 245-270.

[105] Odriozola L, Corrales FJ. Discovery of nutritional biomarkers: future directions based on omics technologies. Int J Food Sci Nutr 2015;66(Suppl 1):S31–S40.
[106] Fujimura Y, Kurihara K, Ida M, Kosaka R, Miura D, Wariishi H, Maeda-Yamamoto M, Nesumi A, Saito T, Kanda T, Yamada K, Tachibana H. Metabolomics-driven nutraceutical evaluation of diverse green tea cultivars. PLoS ONE 2011;6(8):e23426.
[107] Suh DH, Jung ES, Park HM, Kim SH, Lee S, Jo YH, Lee MK, Jung G, Do S-G, Lee CH. Comparison of metabolites variation and antiobesity effects of fermented versus nonfermented mixtures of *Cudrania tricuspidata*, *Lonicera caerulea*, and soybean according to fermentation in vitro and in vivo. PLoS ONE 2016;11(2):e0149022.
[108] Kunisawa J, Arita M, Hayasaka T, Harada T, Iwamoto R, Nagasawa R, Shikata S, Nagatake T, Suzuki H, Hashimoto E, Kurashima Y, Suzuki Y, Arai H, Setou M, Kiyono H. Dietary ω3 fatty acid exerts anti-allergic effect through the conversion to 17,18-epoxyeicosatetraenoic acid in the gut. Sci Rep 2015;5:9750.
[109] Isobe Y, Arita M, Matsueda S, Iwamoto R, Fujihara T, Nakanishi H, Taguchi R, Masuda K, Sasaki K, Urabe D, Inoue M, Arai H. Identification and structure determination of novel anti-inflammatory mediator Resolvin E3, 17,18-dihydroxyeicosapentaenoic acid. J Biol Chem 2012;287(13):10525–10534.
[110] Chen S, Wei C, Gao P, Kong H, Jia Z, Hu C, Dai W, Wu Y, Xu G. Effect of Allium macrostemon on a rat model of depression studied by using plasma lipid and acylcarnitine profiles from liquid chromatography/mass spectrometry. J Pharm Biomed Anal 2014;89:122-129.
[111] Hyötyläinen T, Bondia-Pons I, Orešič. Lipidomics in nutrition and food research. Mol Nutr Food Res 2013;57:1306–1318.
[112] Zhao Y-Y, Wu S-P, Liu S, Zhang Y, Lin R-C. Ultra-performance liquid chromatography–mass spectrometry as a sensitive and powerful technology in lipidomic applications. Chem Biol Interact 2014;220:181-192.
[113] Lane JA, Hickey RM. Analysis of bioactive food-sourced oligosaccharides by high-performance liquid chromatography. In: Moreno FJ, Sanz ML, editors. Food Oligosaccharides: Production, Analysis and Bioactivity. JohnWiley & Sons; 2014. p. 399-420.
[114] Brolk M, Hernández-Hernández O, Soria AC, Sanz ML. Evaluation of different operation modes of high performance liquid chromatography for the analysis of complex mixtures of neutral oligosaccharides. J Chromatogr A 2011;1218:7697-7703.
[115] Totten SM, Wu LD, Parker EA, Davis JCC, Hua S, Stroble C, Ruhaak LR, Smilowitz JT, German JB, Lebrilla CB. Rapid-throughput glycomics applied to human milk oligosaccharide profiling for large human studies. Anal Bioanal Chem 2014;406:7925–7935.
[116] Sánchez-Rivera L, Martínez-Maqueda D, Cruz-Huerta E, Miralles B, Recio I. Peptidomics for discovery, bioavailability and monitoring of dairy bioactive peptides. Food Res Int 2014;63:170-181.
[117] Saadi S, Saari N, Anwar F, Hamid AA, Ghazali HM. Recent advances in food biopeptides: Production, biological functionalities and therapeutic applications. Biotechnol Adv 2015;33(1):80-116.
[118] Ruiz-Giménez P, Salom JB, Marcos JF, Vallés S, Martínez-Maqueda D, Recio I, Torregrosa G, Alborch E, Manzanares P. Antihypertensive effect of a bovine lactoferrin pepsin hydrolysate: Identification of novel active peptides. Food Chem 2012;131:266-273.
[119] Capriotti AL, Cavaliere C, Foglia P, Piovesana S, Samperi R, Zenezini Chiozzi R, Laganà A. Development of an analytical strategy for the identification of potential bioactive

peptides generated by in vitro tryptic digestion of fish muscle proteins. Anal Bioanal Chem 2015; 407:845–854.
[120] Dzieciatkowska M, Hill R, Hansen KC. GeLC-MS/MS analysis of complex protein mixtures. Meth Mol Biol 2014;1156:53-66.
[121] Yap H-YY, Fung S-Y, Ng S-T, Tan C-S, Tan N-H. Shotgun proteomic analysis of tige rmilk mushroom (Lignosus rhinocerotis) and the isolation of a cytotoxic fungal serine protease from its sclerotium. J Ethnopharmacol 2015;174:437-451.
[122] Kheterpal I, Scherp P, Kelley L, Wang Z, Johnson W, Ribnicky D, Cefalu WT. Bioactives from Artemisia dracunculus L. enhance insulin sensitivity via modulation of skeletal muscle protein phosphorylation. Nutrition 2014;30:S43-S51.
[123] European Commission (2004) Regulation (EC) No 1935/2004 of the European Parliament and of the Council of 27 October 2004 on materials and articles intended to come into contact with food and repealing Directives 80/590/EEC and 89/109/EEC. Off J Eur Union L338:4-17, and subsequent updates.
[124] European Commission (2005) EC Regulation No. 396/2005, of 23 February 2005, on maximum residue levels of pesticides in or on food and feed of plant and animal origin and amending Council Directive 91/414/EEC, Off J Eur Commun L70:1–16, and subsequent updates.
[125] US Food Drug Administration; FDA (2011) Tolerances for residues on new animal drugs in food. Code of Federal Regulations. Food and Drugs, Part 556, Title 21; U.S. Food Drug Administration. Office of the Federal Register, National Archives and Records Administration: Washington, DC, April. Available on: http://www.gpo.gov/fdsys/pkg/CFR-2011-title21-vol6/pdf/CFR-2011-title21-vol6.pdf
[126] Codex Alimentarius (2015) General Standard for Food Additives (GSFA) Online Database. Available on: http://www.fao.org/fao-who-codexalimentarius/standards/gsfa/en/
[127] European Commission (2002) Comission Decision 2002/657/EC of 12 August 2002 implementing Council Directive 96/23/EC concerning the performance of analytical methods and the interpretation of results. Off J Eur Union L221:8-36.
[128] European Commission (2015) Guidance document on analytical quality control and method validation procedures for pesticides residues analysis in food and feed. SANTE/11945/2015.
[129] García-Reyes JF, Gilbert-López B, Ramos-Martos N, Molina-Díaz A. Herbicides and fungicides. In: Nollet LML, Toldra F, editors. Food Analysis by HPLC, 3rd ed. Boca Raton: CRC Press; 2012. p. 699-716.
[130] Garrido-Frenich A, Romero-González R, Aguilera-Luiz MM. Comprehensive analysis of toxics (pesticides, veterinary drugs and mycotoxins) in food by UHPLC-MS. TrAC – Trends Anal Chem 2014;63:158-169.
[131] Gilbert-Lopez B, García-Reyes JF, Lozano A, Fernández-Alba AR, Molina-Díaz A. Large-scale pesticide testing in olives by liquid chromatography–electrospray tandem mass spectrometry using two sample preparation methods based on matrix solid-phase dispersion and QuEChERS. J Chromatogr A 2010;1217:6022-35.
[132] Zhao M-A, Feng Y-N, Zhu Y-Z, Kim J-H. Multi-residue method for determination of 238 pesticides in Chinese cabbage and cucumber by liquid chromatography−tandem mass spectrometry: comparison of different purification procedures. J Agric Food Chem 2014;62:11449−56.
[133] Robert C, Gillard N, Brasseur P-Y, Pierret G, Ralet N, Dubois M, Delahaut Ph. Rapid multi-residue and multi-class qualitative screening for veterinary drugs in foods of animal origin by UHPLC-MS/MS. Food Addit Contam A 2013;30(3):443-57.

[134] Mezcua M, Malato O, García-Reyes JF, Molina-Díaz A, Fernández-Alba A.R. Accurate-mass databases for comprehensive screening of pesticide residues in food by fast liquid chromatography time-of-flight mass spectrometry. Anal Chem 2009;81:913–29.
[135] Wang J, Chow W, Chang J, Wong JW. Ultrahigh-performance liquid chromatography electrospray ionization Q‐Orbitrap mass spectrometry for the analysis of 451 pesticide residues in fruits and vegetables: Method development and validation. J Agric Food Chem 2014;62:10375−91.
[136] Vass A, Robles-Molina J, Pérez-Ortega P, Gilbert-López B, Dernovics M, Molina-Díaz A, García-Reyes JF. Study of different HILIC, mixed-mode, and other aqueous normal-phase approaches for the liquid chromatography/mass spectrometry-based determination of challenging polar pesticides. Anal Bioanal Chem 2016;408:4857–69.
[137] Inoue K, Tanada C, Hosoya T, Yoshida S, Akiba T, Min JZ, et al. Principal component analysis of molecularly based signals frominfant formula contaminations using LC-MS and NMR in foodomics. J Sci Food Agric 2016;96(11):3876-81.
[138] Barcellos Hoff R, Barreto F, Melo J, Targa Martins M, Pizzolato TM, Ruaro Peralba MC. Scope extension validation protocol: inclusion of analytes and matrices in an LC-MS/MS sulfonamide residues method. Food Addit Contam A 2014;31(1):39-47.
[139] López-Blanco R, Nortes-Méndez R, Robles-Molina J, Moreno-González D, Gilbert-López B, García-Reyes JF, Molina-Díaz A. Evaluation of different cleanup sorbents for multiresidue pesticide analysis in fatty vegetable matrices by liquid chromatography tandem mass spectrometry. J Chromatogr A 2016;1456:89-104.
[140] Chen C-T, Reddy PM, Ma Y-R, Ho Y-P. Mass spectrometric identification of pathogens in foods using a zirconium hydroxide immobilization approach. Int J Mass Spectrom 2012;312:45-52.
[141] Giacometti J, Josic D. Foodomics in microbial safety. TrAC – Trends Anal Chem 2013;52:16-22.
[142] Rešetar D, Kraljević Pavelić S, Josić D. Foodomics for investigations of food toxins. Curr Opin Food Sci 2015;4:86-91.
[143] Dzuman Z, Zachariasova M, Lacina O, Veprikova Z, Slavikova P, Hajslova J. A rugged high-throughput analytical approach for the determination and quantification of multiple mycotoxins in complex feed matrices. Talanta 2014;121:263-72.
[144] Sospedra I, Soler C, Mañes J, Soriano JM. Rapid whole protein quantitation of staphylococcal enterotoxins A and B by liquid chromatography/mass spectrometry. J Chromatogr A 2012;1238:54-9.
[145] Boundy MJ, Selwood AI, Harwood DT, McNabb PS, Turner AD. Development of a sensitive and selective liquid chromatography–mass spectrometry method for high throughput analysis of paralytic shellfish toxins using graphitized carbon solid phase extraction. J Chromatogr A 2015;1387:1-12.
[146] Faeste CK, Rønning HT, Christians U, Granum PE. Liquid chromatography and mass spectrometry in food allergen detection. J Food Protect 2011;74:316-45.
[147] Koeberl M, Clarke D, Lopata AL. Next generation of food allergen quantification using mass spectrometric systems. J Proteome Res 2014;13:3499-3509.
[148] Monaci L, Losito I, Palmisano F, Godula M, Visconti A. Towards the quantification of residual milk allergens in caseinate-fined white wines using HPLC coupled with single-stage Orbitrap mass spectrometry. Food Addit Contam A 2011;28(10):1304-14.
[149] Martínez-Esteso MJ, Nørgaard J, Brohée M, Haraszi R, Maquet A, O'Connor G. Defining the wheat gluten peptide fingerprint via a discovery and targeted proteomics approach. J Prot 2016; http://dx.doi.org/10.1016/j.jprot.2016.03.015

[150] Hughey CA, McMinn CM, Phung J. Beeromics: from quality control to identification of differentially expressed compounds in beer. Metabolomics 2016;12:11.
[151] Bondia-Pons I, Savolainen O, Törrönen R, Martinez JA, Poutanen K, Hanhineva K. Metabolic profiling of Goji berry extracts for discrimination of geographical origin by non-targeted liquid chromatography coupled to quadrupole time-of-flight mass spectrometry. Food Res Int 2014;63:132-38.
[152] Guijarro-Díez M, Nozal L, Marina ML, Crego AL. Metabolomic fingerprinting of saffron by LC/MS: novel authenticity markers. Anal Bioanal Chem 2015;407:7197–213.
[153] Montero L, Ibáñez E, Russo M, di Sanzo R, Rastrelli L, Piccinelli AL, Cifuentes A, Herrero M. Metabolite profiling of licorice (Glycyrrhiza glabra) from different locations using comprehensive two-dimensional liquid chromatography coupled to diode array and tandem mass spectrometry detection. Anal Chim Acta 2016;913:145-59.
[154] Trivedi DK, Hollywood KA, Rattray NJW, Ward H, Trivedi DK, Greenwood J, Ellis DI, Goodacre R. Meat, the metabolites: an integrated metabolite profiling and lipidomics approach for the detection of the adulteration of beef with pork. Analyst 2016;141:2155-64.
[155] Gallardo JM, Carrera M, Ortea I. Proteomics in Food Science. In: Cifuentes A, editor. Foodomics: Advances Mass Spectrometry in Modern Food Science and Nutrition. New Jersey: John Wiley & Sons, Inc; 2013. p. 125-65.
[156] Nessen MA, van der Zwaan DJ, Grevers S, Dalebout H, Staats M, Kok E, Palmblad M. Authentication of closely related fish and derived fish products using tandem mass spectrometry and spectral library matching. J Agric Food Chem 2016;64:3669−77.
[157] Vallverdú-Queralt A, Lamuela-Raventós RM. Foodomics: A new tool to differentiate between organic and conventional foods. Electrophoresis 2016;37:1784–94.
[158] Valdés A, Simó C, Ibáñez C, García-Cañas V. Foodomics strategies for the analysis of transgenic foods. TrAC – Trends Anal Chem 2013;52:2-15.

Table 10.1. Some representative Foodomics applications based on LC methods.

Food or ingredient under study	Foodomics application	Omic approach	Reference
Food Bioactivity			
Mixture of selected dietary ingredients: fish oil, green tea extract, resveratrol, vitamin E, vitamin C, and tomato extract	Bioactivity in low-grade chronic inflammation of overweight subjects	Global Foodomics: transcriptomics, metabolomics, lipidomics and proteomics	[96]
Rosemary phenolic extract	Chemopreventive effect against human HT29 colon cancer cells	Global Foodomics: transcriptomic, metabolomics, and proteomics	[98]
Rosemary phenolic extract	Antiproliferative effect against human HT29 colon cancer cells	Proteomics	[99]
Carnosic acid and carnosol	Chemopreventive effect against human HT29 colon cancer cells	Transcriptomic and metabolomics	[101]
Parsley	Bioactivity in a dextran sodium sulphate - induced colitic murine model	Global Foodomics: transcriptomic, metabolomics, and proteomics	[103]
Water extract of green tea from 43 Japanese cultivars	Bioactivity on HUVECs (inhibition of thrombin-induced MRLC phosphorylation)	Metabolomics	[106]
Fermented and non-fermented mixture of *Cudrania tricuspidata, Lonicera caerulea,* and *Glycine hispida* (soybean)	Antiobesity effects in HFD-diet mice	Metabolomics	[107]
Dietary oil rich in w-3 fatty acids	Anti-allergy effect against egg white ovalbumin-induced allergy in mice	Lipidomics	[108]
Allium macrostemon	Anti-depressive effect in a rat model	Lipidomics	[110]
Human breast milk	Bioactive unconjugated oligosaccharides	Glycomics	[115]
Bovine lactoferrin pepsin hydrolysate	Antihypertensive peptides	Peptidomics	[118]
Fish muscle	Antimicrobial peptides	Peptidomics	[119]
Tiger milk mushroom sclerotium	Antiproliferative activity against human breast adenocarcinoma MCF7 cells	Proteomics	[121]

Artemisia dracunculus L. extract	Bioactive insulin-sensitizing effects in skeletal muscle	Proteomics	[122]
	Food safety		
104 pesticides in olives	Food safety	Metabolomics	[131]
238 pesticides residues in Chinese cabbage and cucumber	Food safety	Metabolomics	[132]
Screening of 160 veterinary drugs residues in egg, honey, milk and muscle samples	Food safety	Metabolomics	[133]
Screening of pesticides in fruit and vegetable samples	Food safety	Metabolomics	[134]
451 pesticide residues in fruit and vegetable samples	Food safety	Metabolomics	[135]
24 highly polar pesticides in oranges	Food safety	Metabolomics	[136]
melamine, pesticides and heavy metals in infant formulas	Food safety	Metabolomics	[137]
Enterococcus faecalis in nonfat dry milk	Food safety	Proteomics	[140]
56 Mycotoxins and mycotoxins metabolites in 12 animal feeding matrices	Food safety	Metabolomics	[143]
Staphylococcal enterotoxins A and B in milk and fruit juices	Food safety	Proteomics	[144]
PSP toxins in shellfish	Food safety	Metabolomics	[145]
Casein allergens in white wines	Food safety	Proteomics	[148]
Gluten in cereals (wheat, rye, barley and oats) and flours (corn, soy and rice)	Food safety	Proteomics	[149]
	Food quality, authenticity and traceability		
Beer	Food quality	Metabolomics	[150]
Goji berry	Food authenticity and traceability	Metabolomics	[151]
Saffron	Food authenticity and traceability	Metabolomics	[152]
Licorice	Food authenticity and traceability	Metabolomics	[153]
Adulteration of beef with pork	Food quality and authenticity	Metabolomics and lipidomics	[154]
Flatfish	Food authenticity	Proteomics	[156]

Figure captions

Figure 10.1. Scheme of an ideal Foodomics strategy to investigate the health benefits from dietary constituents, including methodologies and expected outcomes. Reprinted with permission from [98]. Copyright 2012 Elsevier.

Figure 10.2. (A) Scatter plot of mRNA versus protein expression ratios (log_2) of HT-29 cells exposed to TGI concentration of SC-RE for 24h. (B) Principal component analysis of HT-29 cells incubated with GI50, TGI, and LC50 concentrations of SC-RE for 2, 6, and 24 h. Reprinted with permission from [99]. Copyright 2016 American Chemical Society.

Figure 10.3. Chromatogram of 238 pesticides at a spiked level of 8 μg kg^{-1} in Chinese cabbage samples. Reprinted (adapted) with permission from [132]. Copyright 2014 American Chemical Society.

Figures

Figure 10.1

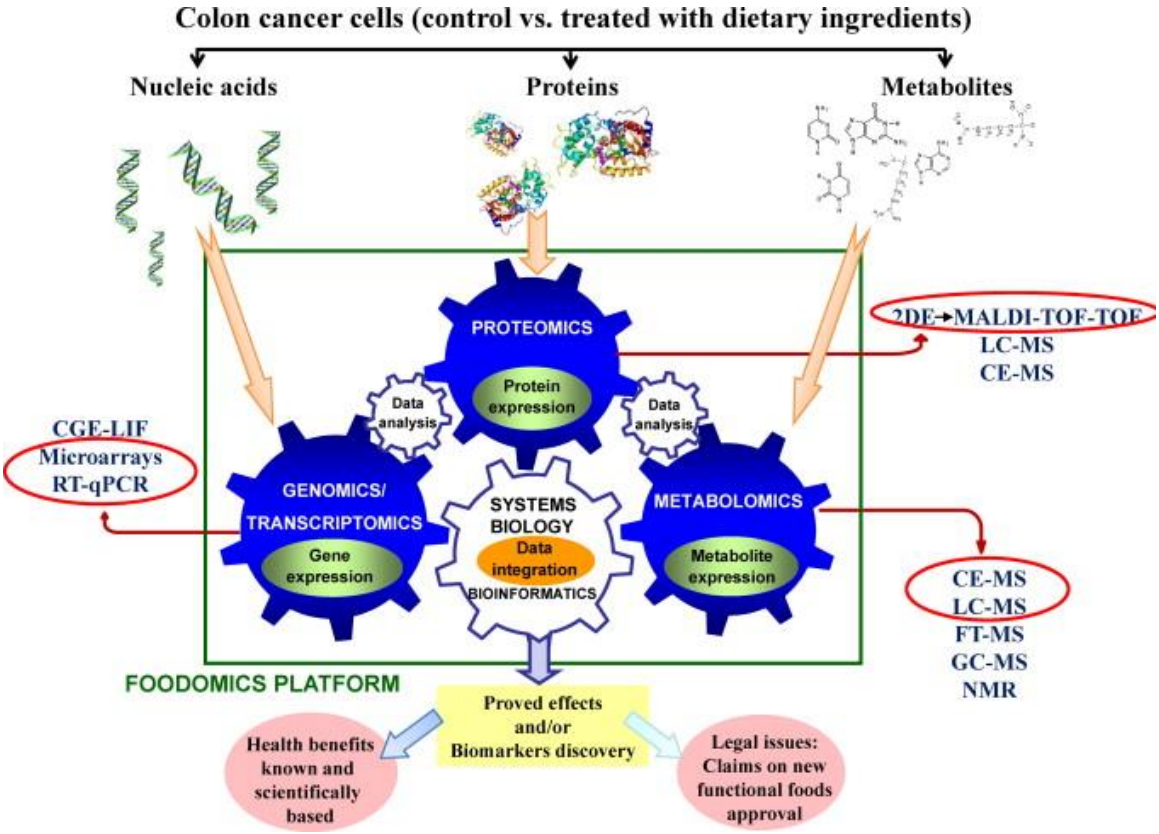

Figure 10.2

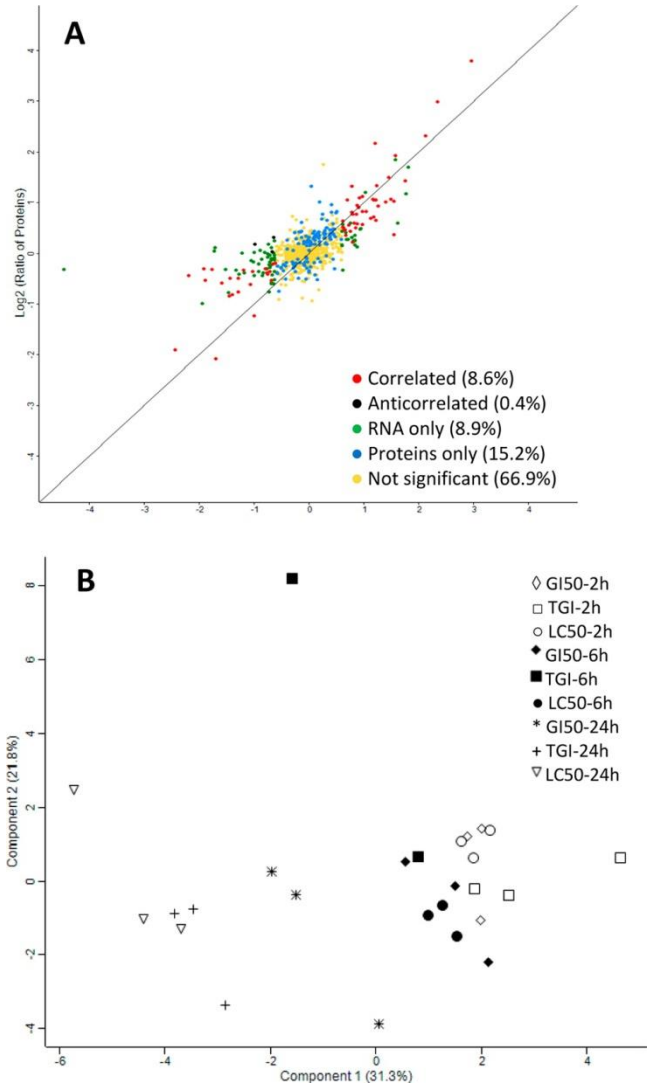
A
Log2 (Ratio of Protein)
Correlated (8.6%)
Anticorrelated (0.4%)
RNA only (8.9%)
Proteins only (15.2%)
Not significant (66.9%)
B
GI50-2h
TGI-2h
LC50-2h
GI50-6h
TGI-6h
LC50-6h
GI50-24h
TGI-24h
LC50-24h
Component 2 (21.8%)
Component 1 (31.3%)

Figure 10.3

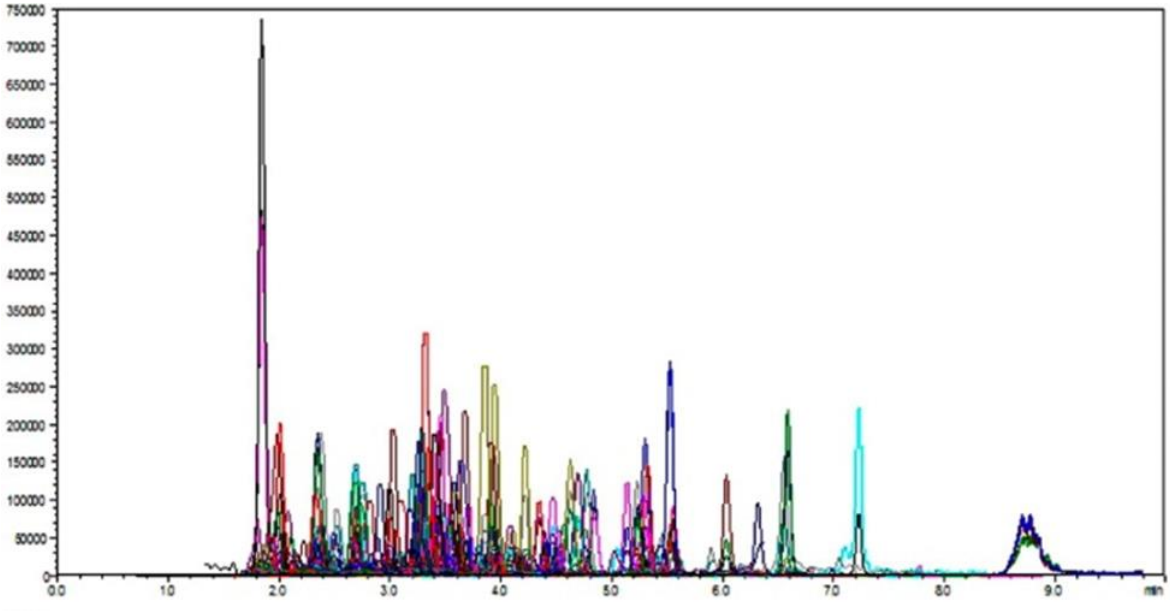
750000
700000
650000
600000
550000
500000
450000
400000
350000
300000
250000
200000
150000
100000
50000
0
0.0
1.0
2.0
3.0
4.0
5.0
6.0
7.0
8.0
9.0
min

1.3.3. Recent advances in the application of capillary electromigration methods for food analysis and Foodomics

Acunha, T., Ibáñez, C., García-Cañas, V., Simó, C., Cifuentes, A.

Electrophoresis **37,** 111–141 (2016).
DOI 10.1002/elps.20150029.

Tanize Acunha[1,2]
Clara Ibáñez[1]
Virginia García-Cañas[1]
Carolina Simó[1]
Alejandro Cifuentes[1]

[1]Laboratory of Foodomics, CIAL, CSIC, Madrid, Spain
[2]CAPES Foundation, Ministry of Education of Brazil, Brasília, DF, Brazil

Received June 23, 2015
Revised July 22, 2015
Accepted July 23, 2015

Review

Recent advances in the application of capillary electromigration methods for food analysis and Foodomics

This review work presents and discusses the main applications of capillary electromigration methods in food analysis and Foodomics. Papers that were published during the period February 2013–February 2015 are included following the previous review by Garcia-Cañas et al. (*Electrophoresis*, 2014, 35, 147–169). Analysis by CE of a large variety of food-related molecules with different chemical properties, including amino acids, hazardous amines, peptides, proteins, phenols, polyphenols, lipids, carbohydrates, DNAs, vitamins, toxins, contaminants, pesticides, residues, food additives, as well as small organic and inorganic compounds. This work includes recent results on food quality and safety, nutritional value, storage, bioactivity, as well as applications of CE for monitoring food processing. The use, among other CE developments, of microchips, CE-MS, and chiral CE in food analysis and Foodomics is also discussed.

Keywords:
Beverage analysis / CE / Food analysis / Foodomics
DOI 10.1002/elps.201500291

Correspondence: Professor Alejandro Cifuentes, Laboratory of Foodomics, CIAL, CSIC, Nicolas Cabrera 9, 28049 Madrid, Spain
E-mail: a.cifuentes@csic.es
Fax: +34-91-0017905

Abbreviations: AA, amino acid; **AD**, amperometric detection; **BA**, biogenic amine; **BPA**, bisphenol A; **β-CD**, β-cyclodextrin; **β-LG**, β-lactoglobulin; **CA**, carnosic acid; **CAs**, carrier ampholytes; **CEIA**, CE-based immunoassay; **cIEF**, capillary isoelectric focusing; **cITP-cITP**, column coupling capillary isotachophoresis; **CL**, chemoluminescence; **CLE**, chiral ligand exchange; **CN**, caseins; **CSEI**, cation-selective exhaustive injection; **DFMO**, difluoromethylornithine; **DLLME**, dispersive liquid–liquid microextraction; **DSP**, diarrheic shellfish poisoning; **ECL**, electrochemiluminescence; **ED**, electrochemical detection; **EDC**, endocrine disrupting compound; **FA**, fatty acid; **FASI**, field-amplified sample injection; **FASS**, field-amplified sample stacking; **FESI**, field-enhanced sample injection; **FID**, flame ionization detector; **FITC**, fluorescein isothiocyanate; **FLD**, fluorescence detection; **GABA**, gamma-aminobutyric acid; **GC-FID**, gas chromatography coupled with flame ionization detection; **GM**, genetically modified; **HMF**, 5-hydroxymethylfurfural; **HMW-SS**, high-molecular-weight secalin subunits; **HRMS**, high resolution MS; **IF**, infant milk formula; **LLE**, liquid–liquid extraction; **LVSS**, large volume sample stacking; **MeI**, methylimidazole; **MIP**, molecularly imprinted polymer; **MRL**, maximum residue limit; **MSS**, micelle to solvent stacking; **MWCO**, molecular weight cutoff; **NACE**, nonaqueous capillary electrophoresis; **NGS**, next-generation sequencing; **NSAID**, nonsteroidal anti-inflammatory drug; **OG-SE**, oregon green™ 488 carboxylic acid-succinimidyl ester; **OPA-AA**, o-phthalaldehyde labeled AA; **OS**, oligosaccharides; **OT**, open-tubular; **PCA**, principal component analysis; **PMP**, 1-phenyl-3-methyl-5-pyrazolone; **QD**, quantum dot; **RP**, ractopamine hydrochloride; **SPME**, solid-phase microextraction; **SRMM**, stacking in reverse migrating micelles; **UF**, ultrafiltration

1 Introduction

The development of new analytical methods and tools is crucial to assess food safety, the first step for food analysis. Detection of exogenous compounds (agrochemicals, environmental contaminants, veterinary drugs, etc.) is a major concern in food safety. Apart of the negative impact on human health, food contamination has also major economic costs. Quality and safety assessment as well as the evaluation of other biological properties of foods imply the use of robust, efficient, sensitive, and cost-effective analytical methodologies. These new analytical methods are also demanded by research laboratoires, regulatory agencies, and food companies, to corroborate the effect of diet on health. In this sense, regulatory authorities are requiring fully substantiated health claims linked to the so-called functional foods and nutraceuticals.

CE is a versatile technique that has found a huge number of applications in food analysis and Foodomics [1–5], as can be also corroborated from the information given in Table 1 [6–29]. Thus, due to its high separation efficiency, extremely small sample and reagents volume requirements, and rapid analysis, CE has demonstrated to be a very useful analytical tool in food science. In a rough classification, CE tools can be employed in two main approaches. The first one, the most common, is the use of CE for targeted analysis, which is mainly carried out for quality and safety assessments. The second approach is the use of CE for

Colour Online: See the article online to view Figs. 1–3 and 5 in colour.

Table 1. Some representative review papers on food analysis and Foodomics involving capillary electromigration methods published in the period covered by this work (February 2013–February 2015)

Subject	Publication year	Reference
Recent advances of CE-MS	2015	[6]
CE-MS for metabolomics	2015	[7]
Contactless conductivity detection in CE	2015	[8]
GMOs	2014	[9]
Biotoxin in food and environment via microchip	2014	[10]
Transgenic cultivars by CE and microchip-CE	2014	[11]
CE and herbicide analysis	2014	[12]
CE-MS applications	2014	[13]
On-line sample preconcentration techniques in CE	2014	[14]
Glycerophospho- and sphingolipids by CE	2014	[15]
Penicillins in milk of animal origin by CE	2014	[16]
Chiral CE-MS applications	2014	[17]
CE analysis of antibiotics and its use as chiral selectors	2014	[18]
Amino acid analysis by CE	2014	[19]
Analysis of natural products by CE	2014	[20]
CE and CEC in phytochemical analysis	2014	[21]
Foodomics strategies for the analysis of transgenic foods	2013	[22]
MS-based metabolomics for Foodomics	2013	[23]
MS-based approaches in food metabolomics	2013	[24]
Chiral separations in food analysis	2013	[25]
Biogenic amines in food samples	2013	[26]
CE-MS metabolomics, peptidomics and proteomics in Foodomics	2013	[27]
Metabolomics of fermented and functional foods	2013	[28]
Microchip electrophoresis for amino acid analysis	2013	[29]

GMO, genetically modified organism.

profiling and/or for nontargeted analysis, which presents the potential to improve the number of analytes that can be assessed simultaneously in a single analysis. Within this context, the use of CE in Foodomics offers enormous opportunities to obtain valuable detailed information that can be directly correlated to food quality, safety, bioactivity, and other features related to food processing, storage, authenticity assessment, etc. Table 1 summarizes the main review papers published within the period covered by this work on the state of the art of capillary electrodriven techniques with regard to new developments and applications in food analysis and Foodomics [1, 6–29]. As can be seen, recent advances and applications of CE-MS [6], including chiral CE-MS [17], and CE-MS for metabolomics [7], as well as detection schemes for CE [8], concentration procedures [14], and miniaturized CE systems [10,11,29] have been recently reviewed. The application of CE to the analysis of biotoxins [10], herbicides [12], glycerophospho- and sphingolipids [15], antibiotics [16, 18], amino acids [19], chiral compounds [25], biogenic amines [26], in different food products has been also reviewed. Also, several review papers have been published in the mentioned period focusing on the application of CE to the analysis of natural products and phytochemicals [20, 21]. It is also noteworthy the high number of review papers dealing with the application of CE in metabolomics [9, 23, 24, 28], including the use of metabolomic approaches to study genetically modified (GM) crops [9] and fermented and functional foods [28]. Besides, new results from the application of CE in the field of Foodomics have been also reviewed in the period covered by this work [1, 22–24].

The present work describes in the following sections the different CE approaches used to detect compounds of relevance in food analysis including amino acids, biogenic, and other hazardous amines, peptides and proteins, phenols, polyphenols, lipids, carbohydrates, DNAs, vitamins, small organic and inorganic ions, toxins, contaminants, pesticides and other residues, chiral compounds and also compounds related to food processing. Moreover, in this review work, an overview of the last developments and applications of CE in Foodomics and microchip CE in food analysis and Foodomics is provided.

2 Amino acids, biogenic amines, and other hazardous amines

Amino acids (AAs) play important roles in the organoleptic and nutritional characteristics of foodstuffs. A series of works have reviewed the analysis of AAs in foods using CE. Mandrioli et al. covered the role of chromatography and electromigration techniques for the analysis of AAs in fruit and fruit-derived foods [30]. In another work published in 2013, methodological developments involving on-line concentration for the separation of AAs and their enantiomers using CE were reviewed including their analysis in food [31]. Dąbrowska and Starek [32] have dedicated a review work to the analysis of carnitine, a vitamin-like AAs derivative, in biological materials, foods, and dietary supplements, using a variety of analytical techniques, including chromatographic, electrophoretic, as well as MS-based approaches.

Heating/cooking and/or fermentation processes can modify the quantity of existing AAs and introduce new AAs in the product. The applicability of CE for bioprocess monitoring has also been demonstrated [33]. Recently, Turkia et al. presented a MEKC method to monitoring the amino acid uptake of *Saccharomyces cerevisiae* during beer fermentation [34]. SDS and 18-crown-6-ether were added to the BGE to enhance the separation between AAs. LIF detection was used to improve the sensitivity of AAs that were derivatized with Oregon green™ 488 carboxylic acid, succinimidyl ester (OG-SE). The quantification limit was as low as 62.5 pM, and the

OG-SE-AAs (Arg, Lys, Leu/Ile, His, Gln, Val, Phe, Thr/Asn, Pro, Ser, Gly, Glu, and Asp) were analyzed in 45 min. After the analysis of AAs in beer fermentation for both samples it was observed that the yeast utilized all AAs to some extent, and that the AAs consumption halted at the same time as glucose was consumed from the fermentation media. MEKC with two fluorescence detection systems (LED induced and laser induced) were also used for the quantification of AAs in vegetable milk obtained from of *Cucurbitaceae* seeds of Sub-Saharan Africa [35]. Fluorescein isothiocyanate (FITC) was chosen in this work as a derivatizing agent. Eleven AAs (Phe, Trp, Ala, Asp, Val, Phe, Thr, Val, Trp, Ile, and Leu) were detected in the selected lyophilized milks from *Cucumeropsis mannii* Naudin and *Citrullus lanatus*. In a different work, analysis of tryptophan was used to discriminate pure fermented soy sauces, adulterated soy sauces and chemical soy sauces [36]. In that case, CE-ultra violet (UV) technique was only employed to validate the results obtained by fluorescence resonance energy transfer in a flow-injection system for the analysis of tryptophan in soy sauce. A method involving the use of ionic liquid as additive in the buffer was used for CE analysis of *o*-phthalaldehyde labeled AAs (OPA-AAs) [37]. Together with the ionic liquid 1-butyl-3-methylimidazolium tetrafluoroborate ([BMIm]BF4), other additives including SDS, β-cyclodextrin (β-CD), and ACN, were included in the running buffer to increase the separation resolution. The multiple additive strategy showed good performance for either CE separation or in-capillary derivatization. In-capillary derivatization of AAs was performed by a sandwich injection of OPA reagent solution, sample, and a second injection of OPA reagent solution. The method allowed simultaneous quantification of 17 OPA-AAs with LOD down to 10 μM. Finally, the proposed CE-UV method was applied to determine trace-amounts of OPA-AAs (His, Ala, Gly, Tyr, Val, Arg, Ile, Phe, Trp, Glu, and Lys) in less than 24 min in seven beer samples. In another work, analysis of 20 FITC-derivatized AAs was carried by MEEKC with LIF detection [38]. Running buffer was composed by phosphate buffer at pH 6, SDS, 1-butanol, cyclohexane, and ACN. Analysis was carried out in less than 25 min, and detection limits were in the range of 0.32–2.2 nM. The feasibility of the MEEKC-LIF method was demonstrated through the analysis of beverage and food samples. In a diferent work, CE-MS/MS was employed for the analysis of underivatized AAs to assess the quality of commercial royal jelly products (tablet, liquid drink, and raw material) as well as of honey [39]. Typical BGE containing 1 M formic acid at pH 1.8 was used for the separation of 16 AAs (Ala, Arg, Asp, Glu, Gly, His, Leu, Lys, Met, Phe, Pro, Ser, Thr, Tyr, Val, and gamma-aminobutyric acid (GABA)) in 20 min. LODs were lower than 10.5 μg/g. the CE-MS/MS method permitted discriminating between the different royal jelly products, and among the latter ones and honey.

Methionine and cysteine content were also analyzed by CE-MS in different inactive dry yeast preparations (normal and glutathione enriched) typically used in the wine industry due to their potential applications in winemaking [40]. The capabilities of CE-MS permitted also the identification for the first time of 14 sulfur-containing metabolites in the glutathione-enriched dry yeast that could be linked to the better properties of this yeast preparation.

Biogenic amines (BAs) are important nitrogen compounds that have aliphatic (putrescine, cadaverine, spermine, spermidine), aromatic (tyramine, phenylethylamine), or heterocyclic (histamine, tryptamine) structures. BAs are present in a wide range of food products and they can cause severe health problems to sensitive individuals. The presence of BAs above a certain level can be considered as indicative of undesired microbial spoilage. Moreover, BAs can also be related to fermentation processes. CE is considered as a good alternative to HPLC for the analysis of BAs in food samples [26]. However, one of the main problems that hinders the widespread application of CE is its low concentration sensitivity with some detection modes. Besides, analysis of BAs faces problems derived from the low concentration of these analytes in real food samples. In order to overcome this problem, a method based on CE with electrochemiluminescence (ECL) detection was optimized to separate and detect BAs (putrescine, histamine, tyramine, phenylethylamine, and spermidine) in oysters [41]. ECL detection was based on the luminophore tris(2,2'-bipyridyl)ruthenium(II) ($Ru(bpy)_3^{2+}$). Similar to electrochemical detection (ED), a certain potential is needed to oxidize $Ru(bpy)_3^{2+}$ to $Ru(bpy)_3^{3+}$, which reacts with analytes and then produces ECL emission. The analysis of these BAs in oysters by CE-ECL was proposed as an indicator of freshness [41]. Tyramine, histamine, and phenylethylamine levels increased slightly and did not change much throughout 8 days of storage, and their levels remained below from the maximum level established by the European Union (EU) (100 mg/kg) or (Food and Drug Administration) FDA (50 mg/kg). On the other hand, the increase in the putrescine and spermidine content was considerably higher. Putrescine concentration increased from 19 mg/kg to 137 mg/kg after 8 days of storage at 4°C. Spermidine increased to 120 mg/kg under the same storage contidions.

The content of short-chain aliphatic amines is also associated to freshness of food. Recently, Xie et al. applied a MEKC method for the quantification of methylamine, ethylamine, dimethylamine, and diethylamine in a variety of aquatic products (cuttlefish, squid, shrimps, hairtail, etc.) [42]. Amines were extracted by ultrasound-assisted dispersive liquid–liquid microextraction with trichloromethane. Before MEKC-UV analysis, the aliphatic amines were derivatized with 9-fluorenyl methyl chloroformate to improve their detection sensitivity, providing LODs in the range of 0.028–0.16 mg/kg.

3 Peptides and proteins

The interest on the use of CE for the analysis of peptides and proteins has continued in the last years [43–48]. Most of the methodological developments in CE for the analysis of peptides and proteins are directed to prevent their adsorption on the inner capillary wall, and to increase

their sensitivity. Peptides and proteins play a major role in determining nutritional and functional properties of food products. Research on structural and physico-chemical characteristics of food peptides/proteins aimed at elucidating their function is of utmost interest and much research in this field is needed to understand their functionality in foods. Proteolysis represents one of the most important biochemical processes occurring in food processes such as cheese ripening. CE-UV has been applied to determine caseins (CNs) and peptide profiles in different cheeses (*Brie, Caprino, Cheddar, Emmental, Fontina, Gorgonzola, Gouda, Grana, Padano, Maasdam, Provolone, Taleggio*) [49]. It was observed that the extent of proteolysis varied greatly among cheeses and led to different degrees of CN breakdown and diverse peptide profiles in the CZE patterns. The role of peptides/proteins as physiologically active components in the diet is being increasingly acknowledged [50]. They have potential beneficial health effects such as antihypertensive, antioxidative, antiobesity, immunomodulatory, antidiabetic, hypocholesterolemic, and anticancer activities. Small peptides with biofunctional properties can be produced during gastrointestinal digestion, food processing, and microbial proteolysis of various animals and plant proteins. Milk proteins are considered one of the most important sources of bioactive peptides and there is continuous interest in the identification of bioactive peptides from milk protein hydrolysates and fermented dairy products. For instance, the presence of bioactive peptides in several commercial hypoallergenic infant milk formulas (IFs) prepared from bovine milk protein hydrolysates has been recently studied by CE-MS [51]. High resolution TOF-MS was used for molecular mass measurement and identification. Each studied IF presented a characteristic electrophoretic profile. Most identified bioactive peptides were reported as inhibitors of angiotensin-converting enzyme, however, it was observed the presence of peptide sequences with other biological activities such as antithrombotic, hypocholesterolemic, antioxidant, or antimicrobial, to mention a few.

Peptides can also contain disease-specific information, and thus changes in their expression on certain peptides or peptide patterns may be disease specific. Following this idea, CE-MS methodology has also been applied to identify peptide biomarkers of bovine mastitis [52]. This disease affects the quality of the milk through changes in its composition, and has important economic consequences for the dairy industry. Thus, after the analysis by CE-MS, the peptides in milk from healthy dairy cows were compared to those detected in milk from cows with mastitis to determine if peptide biomarkers in milk could be identified. Comparison of the peptidome between healthy and mastitic milk identified 154 peptides for a biomarker panel, which in a model for diagnosis of mastitis showed 100% sensitivity and specificity. It was observed that β-CN and αs1 CN provided the majority of peptides identified in this model. The effect of the pathogen *Staphylococcus aureus* during mastitis on economically important bovine milk proteins has been studied by CE-UV [53]. To accomplish this, milk content of CN αS1, αS2, κ, βA1, and βA2 and whey proteins α-lactalbumin and β-lactoglobulin were analyzed and compared with the bacteria-free control milk. It was observed that *S. aureus* significantly lowered concentration of α(S1)-CN, β(A1)-CN, and β(A2)-CN. Moreover, *S. aureus* also hydrolyzed κ-CN into para-κ-CN, with significant reduction of κ-CN.

Technological properties of milk are determined by a variety of factors. Among them, protein (α-CN, β-CN, κ-CN, and β-LG) genetic variants influence cheese-yielding capacity, coagulation properties, etc. In this sense, Meza-Nieto et al. studied the effect of the addition to skim milk of different levels of variants A and B of β-lactoglobulin (β-LG) on cheese yield [54]. For that purpose, CE-UV was applied for determining β-LG A or B recovery in the curd during rennet-induced coagulation. The presence of β-LG variant B resulted in a significantly higher actual and dried mass cheese yield than when A or A-B were present at levels ≤0.675% of whey protein addition.

Apart of the functional properties of proteins in food processing, they have important impact on the nutritional quality. In this sense, storage proteins in cereal seeds will influence the utilization of the grain in food processing and will have direct impact on the nutritional quality of cereals. CE-UV has been proposed as an efficient alternative to SDS-PAGE for fast and more accurate characterization of storage proteins of rye [55]. These storage proteins of rye, usually termed secalins, have a high nutritional quality and their accurate characterization will enable the development of new genotypes with desirable properties. In particular, high-molecular-weight secalin subunits (HMW-SS) were characterized by CE-UV. The HMW-SS fraction was characterized in an uncoated fused-silica capillary using an isoelectric iminodiacetic buffer in combination with poly(ethylene oxide), lauryl sulfobetaine, and ACN as the separation buffer. Under these conditions, all rye HMW-SS isoforms were separated, and considerable variations in the subunit patterns were observed in the different rye cultivars analyzed. In a different work, glutelin, the major seed storage protein of rice, was analyzed by CE, which allowed the separation of multiple polymeric and monomeric subunits [56].

Capillary isoelectric focusing (cIEF) is also an interesting alternative to CZE for peptide/protein separation [57]. In any event, cIEF is characterized by high resolution, peak capacity, and concentration capacity. The generation of the pH gradients is usually carried out with carrier ampholytes (CAs), however, the main drawback of cIEF with CAs is its inability to form a stable pH gradient. Profiling and comparison of various commercial ovalbumin products with potential allergenicity was accomplished in two-step cIEF [58]. Lysozyme is another potential allergenic agent, and thus, it has to be declared according to the allergen labeling instructions of EU and FDA. Recently, a CE-MS method has been developed for detecting preservative lysozyme in cheese [59]. Polyacrylamide-coated fused silica capillary was used to prevent electrostatic and hydrophobic interactions of the proteins with the capillary wall. The method was suitable for the quantification of lysozyme in cheese in less than 15 min., reaching a LOD of 3.6 mg of lysozyme per 1 kg of cheese. The

concentration range of the lysozyme determined in four different cheese samples (*Edam*, *Parmesan*, *Gouda* and a "*mixture of natural cheeses*") was from 0.5 to 3.3 g of lysozyme per kg. Analysis of other allergens such as β-lactoglobulin in food products for infants has also been accomplished by CE-LIF [60].

Analyses of protein profiles by CZE-UV have been used to predict the cultivar of olive leaves and pulps [61]. Each protein profile was acquired in less than 15 min. with good reproducibilities; and the normalized protein peak areas were employed as predictors to construct linear discriminant analysis models (Fig. 1**)**. Both olive leaf and pulp samples belonging to nine cultivars from different Spanish regions were correctly classified, indicating that protein profiles are characteristic of each cultivar.

4 Phenols and polyphenols

At present, numerous natural dietary constituents are under scrutiny such as phenolic compounds, due to their promising anticancer, antimicrobial, and free-radical scavenging and antiinflamatory properties [62]. From a broad point of view, the family of phenolic compounds encompasses phenols, benzoic acid, cinnamic acid, coumarins, tannins, lignins, lignans, and flavonoids. Vegetables, spices, and fruits are natural sources of phenolic compounds. These chemical species have been associated with the beneficial effects derived from several foodstuffs, with special emphasis on foods from the Mediterranean diet such as wine, olive oil, fruits, etc. For instance, moderate consumption of wine has been associated with health benefits related in part to the presence of phenolic compounds [63]. Wine has been deeply investigated in several works due to previously reported beneficial effects on cardiovascular diseases, diabetes, osteoporosis, maybe neurological diseases, and longevity [64]. However, wine is a complex matrix influenced by a number of factors, such as grape variety, ripeness of the grapes, environmental conditions, winemaking process, among others. Thus, scientific community is increasingly interested in the knowledge of precise chemical characterization of wines. For that purpose, CE has emerged as a very powerful tool for characterization of wines [65]. Most of wine benefits on health have been associated with its antioxidant activity, which is mainly ascribed to its phenolic content [66]. For this reason, phenolic compounds are subject of intense research. In this line, polyphenol profiles of Spanish wines were obtained using CZE-DAD [67]. The developed analytical method was able to determine 20 polyphenols in wine in less than 25 min using 30 mM sodium tretraborate buffer solution at pH 9.2 with 5% isopropanol as BGE. That methodology was applied for the analysis of 102 wines and data were submitted to statistical analysis. Differences in phenolic content depending on the region were found and characteristic compounds were associated with the regions studied. Namely tyrosol and gallic acid were at higher levels in Catalunya wines, p-coumaric, and caffeic acids were characteristic from La Rioja wines, and protocatechuic was more specific of Castilla La Mancha wines. Also, a CZE-DAD method was used for Brazilian wines characterization [68], optimizing the method for the analysis of syringic acid, kaempferol, myricetin, quercetin, caffeic acid, and gallic acid in six red wines. For that purpose, wines were submitted to liquid–liquid extraction (LLE) and filtration before analysis. Concentrations for target compounds were in agreement with data previously reported.

CE detection often relies on UV spectroscopy using diode array devices, but other techniques, such as amperometric detection (AD), have also been found to be very useful for the analysis of wines [69]. For ED, 1 mm diameter glassy carbon electrodes were used. A total of 14 white wines made of *verdejo* or *airén* grapes from four different origin denominations were analyzed using 200 mM borate buffer at pH 9.4 with 10% v/v methanol as BGE at 27.5 kV. After principal component analysis (PCA), major differences were found in six compounds mainly attributed to grape variety.

Other typical foodstuff from the Mediterranean diet that has generated much interest due to its beneficial effects on health is virgin olive oil. Virgin olive oil is obtained exclusively by mechanical extraction of olive fruit (*Olea europea*) and the beneficial effects on human health are well known. Although phenolic acids are present in minor quantity in olive oil compared to fatty acids, they are particularly involved in the antioxidant properties of this oil. In this line, a liquid–liquid microextraction combined with CZE was used for the determination of caffeic acid, gallic acid, vanillic acid, syringic acid, cinnamic acid, p-coumaric acid, oleuropein, apigenin, luteolin, 3-hydroxytyrosol, and tyrosol, in virgin olive oil [70]. A dispersive liquid–liquid microextraction (DLLME) was used to enhance sensitivity. For that purpose, boric acid was used for extraction of analytes from olive oil and carbon tetrachloride was added as dispersive solvent. Before sample injection, a plug of water was injected for on-line preconcentration as stacking step and compounds were separated using 30 mM boric acid at pH 9.5. The methodology permitted the selective determination of phenolic compounds in virgin olive oil with adequate RSD and suitable sensitivities with respect to their levels present in olive oil. Later, the same research group aimed to correlate the phenolic profile with the antioxidant capacity of monovarietal olive oils, namely, *Arauco*, *Arbequina*, *Farga*, and *Empeltre* [71]. Fifteen compounds were simultaneously determined including tyrosol, vinylphenol, oleuropein, hydroxytyrosol, rutin, catechin, naringenin, cinnamic acid, chlorogenic acid, syringic acid, luteolin, apigenin, vanillin acid, quercetin, and caffeic acid. In that work, single molecules and classes of molecules were quantified by SPE-CZE. Those results were compared with the corresponding Folin–Ciocalteu results, and antioxidant capacity using three different tests. As a conclusion, *Arauco* olive oil was observed to possess the highest antioxidant activity related to its free-radical scavenging properties and potentially related to its higher phenolic compounds levels. In another work, a CE-DAD was optimized for the determination of phenolic compounds but only four out of 17 could be quantified in the 17 oil samples [72]. Namely,

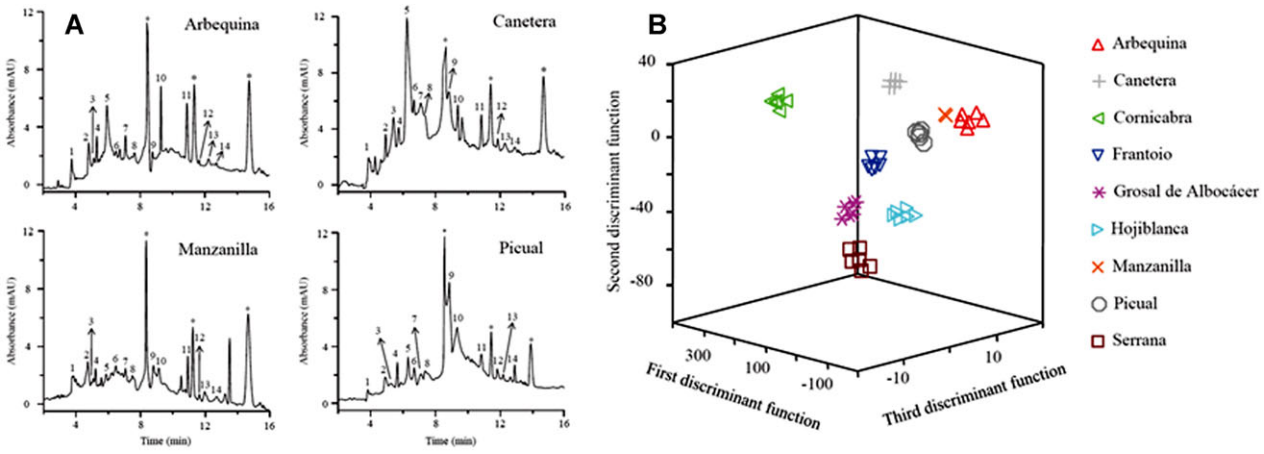

Figure 1. (A) Representative protein profiles by CE-UV Arbequina, Canetera, Manzanilla, and Picual cultivar olive pulp samples. CE-UV conditions: BGE, 50 mM sodium tetraborate, 50 mM sodium phosphate, 0.1% PVA at pH 9; hydrodynamic injection, 50 mbar for 3 s; separation voltage, +10 kV; capillary temperature, 25°C; detection, 214 nm. Numbered indicate common peaks between different samples. Peaks marked with an asterisk corresponded to lipase enzyme peaks. (B) Score plot on an oblique plane of the three-dimensional space defined by the three first discriminant functions of the linear discriminant analysis model constructed to classify olive pulps according to their cultivar. Redrawn from [61] with permission from Wiley-VCH.

quantification of tyrosol, (+)-pinoresinol, hydroxytyrosol and luteolin in virgin olive oil from Brazil was carried out using 101.3 mM boric acid (pH 9.15) as BGE at 30 kV. The phenolic compounds showed high variation depending on the different varieties and crop years. However, olive oils and other nonaqueous matrix present the limitation of tedious, complex, and time consuming procedures for the extraction of the phenolic compounds (generally including SPE and LLE procedures). In this regard, the pretreatment of the sample can be significantly simplified if nonaqueous CE is used. In this sense, nonaqueous capillary electrophoresis (NACE)-UV has been used for the determination of phenolic compounds in extra virgin olive oil [73]. NACE was combined with a second-order chemometric method to enhance the resolution and separation of the analytes, namely a multivariate curve resolution-alternating least-squares algorithm. Using 18 mM KOH and 25 mM boric acid in 1-propanol-methanol (74:26, v/v) as BGE, all the analytes were negatively charged and migrated against the EOF toward the anode in a maximum time of 12 min. Thus coumaric acid, caffeic acid, ferulic acid, 3,4-dihydroxyphenylacetic acid, vanillic acid, and 4-hydroxyphenylacetic acid in olive oil could be analyzed in a short-analysis time. Also, a NACE method was developed for the separation of phenolic compounds in other olive oil samples [74, 75]. For that purpose, UV-visible and fluorescence detection were used. All analytes passed firstly through the UV detector and then through the fluorescence detector in a maximum time of 25 min. The developed method permitted the detection of cinnamic acid, vanillic acid, *o*-coumaric acid, and tyrosol, among other phenolic compounds, in extra virgin olive oil samples.

One of the main pathogens that infect olive trees is included in genus *Phytophthora* and is responsible of significant losses in olives and oil production. Polyphenol composition of four different plant extracts from *Thymus vulgaris*, *Origanum vulgare*, *Matricaria recutita*, and *Larrea divaricate* was studied in order to correlate their composition with the inhibition of the disease and to determine the antimicrobial capacity of each individual phenolic compound against *Phytophthora spp*. [76]. Thus, a SPE followed by a CZE method using 30 mM boric acid buffer at pH 9.50 was applied to all extracts. Under optimal conditions, the determination of catechin, naringenin, cinnamic acid, syringic acid, chlorogenic acid, apigenin, vanillic acid, luteolin, quercetin, and caffeic acid was achieved in the plant extracts. As a result, *Larrea divaricate* and *Origanum vulgare* extracts were the most effective extracts against the pathogen. In addition cinnamic acid and naringenin were the two compounds that showed more antimicrobial effect by a solid agar bioassay. Extracts from *Rosmarinus officinalis* and *Melissa officinalis* have been later characterized by using a CE-MS method [77]. In that work, the two major components observed in the rosemary extract were carnosic acid (CA) and rosmarinic acid while for *Melissa officinalis* extracts the major compound was rosmarinic acid. A total of 15 and 13 phenolic compounds could be determined by CE-MS in rosemary and *Melissa* extracts, respectively.

Salvia miltiorrhiza is a shade-growing flowering plant from the genus *Salvia*. The root of this plant has been authorized to be food supplement by the European Comission. Namely, the dried root and rhizome of *Salvia miltiorrhiza,* also known as *Danshen*, has reported beneficial effects on cardiovascular and cerebrovascular diseases [78]. In this regard Cao et al. [79] developed a CE method using as BGE 20 mM sodium tetraborate adjusted to pH 9.0 with 12 mM β-CD as modifier for the separation of seven phenolic acids in *Danshen*. Good repeatability and high separation efficiency were achieved for the phenolic acids determined. To validate the analytical method developed, seven Salvia plants from four different origins were analyzed. Concentration of

protocatechuic aldehyde, savianolic acid (A, B, and C), rosmarinic acid, danshensu, and protocatechuic acid were determined showing differences in the phenolic acid content among plants analyzed.

As stated before for the wine composition, plant growth, environment, and other factors are critical for phenolic compounds content in plants. Given the potential benefits to health of phenolic compounds, the determination of the maximum content of these species is of major interest. In this regard, results from CE and LC-based analytical methods were combined to determine the optimum growth period for accumulating the most abundant functional phenols in germinated buckwheat that were soaked in darkness and buckwheat sprouts cultivated by hydroponic culture [80]. In that work, CE-UV analysis was conducted using 50 mM boric acid buffer containing 0.1 M SDS (pH 9.0) as BGE and monitoring the signal at 280 nm. The highest amounts of isoorientin, orientin, isovitexin, and vitexin were measured at day 3, with the exception of rutin that rapidly increased to 109.0 mg/100 g fresh mass until day 6. According to the obtained results, buckwheat sprouts cultivated by hydroponic culture for 6 days could be a good dietary source of phenols.

Polyphenol profiles have also been applied for the evaluation of antioxidant potential and authentication of fruit products [81]. Authentication of fruit products was carried out combining CZE and LC techniques. Samples under study included fruits (cranberry, blueberry, grapes, and raisins), fruit-based products (grape-juice and cranberry-juice), and commercial cranberry-based products (pharmaceutical natural extracts, powder capsules, syrup, and sachets) [82]. After data analysis using Matlab, the resultant PCA showed a clear clustering according to the fruit origin as can be observed in Fig. 2. Moreover, one sample was suspected to be an adulteration using the proposed LC and CE methods. Confirmation of that adulteration was performed via high resolution mass spectrometry (HRMS) analysis where a lack of A-type proanthocyanidin compounds was observed, confirming that the suspicious sample was not mainly cranberry-based extract as it was labeled.

In addition, phenolic profiles can be useful not only for authentication or adulteration issues but to distinguish among varieties within the same fruit specie. In line with this, phenolic acids were determined and quantified in 13 varieties of avocado fruits at two ripening stages [83]. CE-UV using 40 mM sodium tetraborate at pH 9.4 as BGE permitted the quantification from 8 to 14 compounds in avocado samples depending on the variety. Phenolic profiles were found to be characteristic from each variety. For instance, gallic acid was only found in *Sir Prize* variety and trans-cinnamic, m-coumaric, benzoic, γ-resorcylic, p-coumaric, and protocatechuic acids were detected in the ten genetically related samples out of the total 13 varieties analyzed.

Isoflavones are phenolic compounds with potential antioxidant activity and investigation on their health benefits is of interest. In this regard, a CE-MS method has been also developed for the analysis of isoflavones in soy drink [84]. Apigenin was added as internal standard during sample preparation through ethanol extraction and then an exhaustive CE-MS method optimization was carried out for the separation and analysis of six isoflavones, i.e. daidzin, genistin, biochanin A, formononetin, daidzein, and genistein. The phenolic compounds were separated as anions in positive CE mode and ionized in the positive ion mode. Finally, the developed method was successfully applied to four soy drinks.

Although LLE and SPE are by far the most common techniques for sample preparation of phenolic compounds prior to CE analysis, alternative procedures have also been employed. For example, a combination of CE-DAD preceded by a bar adsorptive microextraction coated with a mixed-mode anion exchange/reverse phase followed by liquid desorption, was used to determine phenolic compounds in food matrices [85]. The CE separation was performed following a voltage gradient varying from 25 kV to 13 kV showing acceptable reproducibility (RSD $< 15\%$) and suitable LODs (18.0–85.0 μg/L). To validate the methodology it was effectively applied to green tea, red fruit juice, and honey. Authors claimed that the new methodology is easy to implement, reliable, and sensitive.

Even in minor quantities, phenolic compounds have been reported as one of the groups of substances whose composition in flower nectar is crucial for insect preferences [86]. To deepen in that intriguing issue, CZE-UV method has been developed for the analysis of 4-vinylphenol, catechin, naringenin, rutin, cinnamic acid, syringic acid, chlorogenic acid, apigenin, vanillic acid, luteolin, quercetin, and caffeic acid in onion nectar [87]. Onion nectar was obtained in blossom from an open pollinated onion cultivar and three male sterile lines. The phenolic fraction was isolated by means of SPE and the methanol-based eluted fraction was directly injected in CE. Phenolic compounds could be baseline separated at 25 kV using 30 mM boric acid (pH 9.5) as BGE within 8 min. Marked differences in phenolic profiles of male sterile and open pollinated lines were observed pointing out a potential factor that affect onion pollination.

Among all the bioactive constituents present in plants, flavonoids play an important role in human health and are one of the main group of compounds responsible for the antioxidant activity of berries. Among flavonoids, catechins have been poorly reported in berries and the quantitative determination of catechins monomer levels may help to establish a relationship between secondary metabolites and their effects on human health. In this regard, Piovezan et al. [88] developed a MEKC method to determine and characterize-free catechins in fresh fruits of blackberry (*Rubus fruticosus*) during the annual production period [88]. After a methanol-based solid–liquid extraction of the raw sample content, flavonoids were purified by means of hydrochloric acid and diethyl ether addition. Then, the CE method was developed for the separation of catechins that are present in minor quantities in the fruits. An optimum BGE composition of 30 mM phosphoric acid, 40 mM SDS, and 0.1% triethylamine at pH 2.3 was used for the analysis operating in reverse polarity (–15 kV). Epicatechins were successfully determined in blackberry for the first time applying the methodology

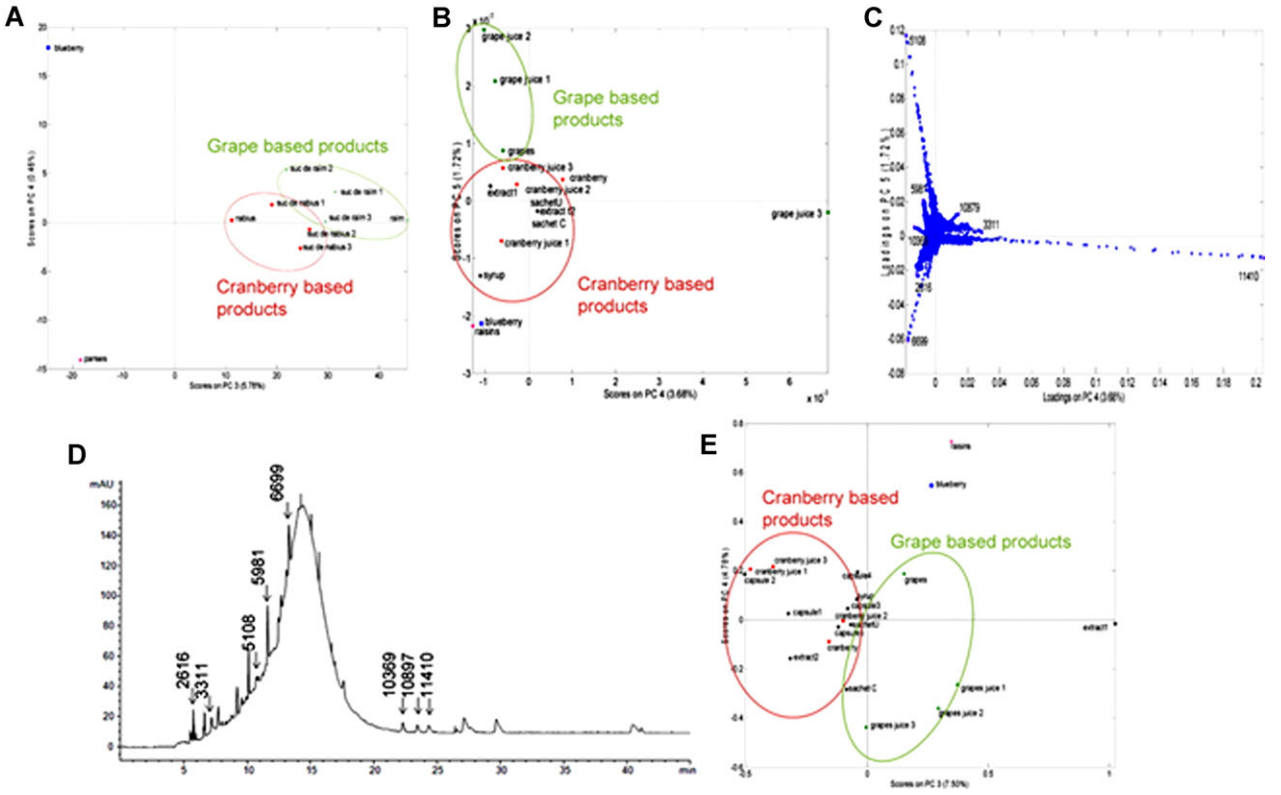

Figure 2. (A) PCA result (PC3 versus PC4 score plot) using electrophoretic polyphenolic profiles obtained for fruits and juice samples; (B) PCA results (PC4 versus PC5 score plot) using electrophoretic polyphenolic profiles for all samples except pharmaceutical capsules. (C) Loading plot using peak signal areas. (D) Electropherogram obtained for a cranberry commercial capsule. Discriminant peak signals are indicated with an arrow. (E) PCA result (PC3 versus PC4 score plot) using eight discriminant peak signal areas. Redrawn from [82] with permission from American Chemical Society.

developed in that work. In addition, the annual average temperature was observed as strong factor of influence on the epicatechin levels in blackberries. Flavonoids have been also investigated in food supplements [89]. For that purpose, the tablets or the contents of the capsules were weighed, homogenized, and subjected to extraction with DMSO in ultrasonic bath for 15 min. Citric flavonoids (hesperidin, diosmin, rutin, and troxerutin) together with ascorbic acid were determined by CZE adding cinnamic acid as internal standard. The method applied showed RSD values lower than 4.5% for all analyzed molecules. More recently, flavonoids of the *Chrysanthemum morifolium Ramat* plant were under scrutiny [90]. This plant possesses antimicrobial, antibacterial, antifungal, antiviral, and anti-inflammatory activities partially due to its flavonoid content. With the aim to extract the flavonoid content of *Chrysanthemum*, a matrix solid-phase dispersion procedure was carried out before CZE analysis. A complex BGE was used for the separation of flavonoids consisting of potassium dihydrogenphosphate, borate, hydroxypropyl-β-cyclodextrin, and ACN. As a result, eight flavonoids could be determined, namely, kaempferol, apigenin, naringenin, (+)-catechin hydrate, rutin hydrate, quercetin, luteolin, and ferulic acid. Flavonoids were also investigated in *Brassica oleracea* (broccoli) by CE-UV [91]. Kaempferol and quercetin are the main flavonols in broccoli, and they were extracted from the raw plant and concentrated via large volume sample stacking (LVSS) before CE analysis. Results were compared with those obtained by HPLC showing a good agreement in kaempferol and quercetin relative concentrations.

As can be observed, due to their high hydrocarbon content, organic solvent extraction has been the main method to extract phenolic compounds [92]. However, in order to evaluate the actual properties of the ingestion of tea water infusion, Liu et al. [93] developed a MEKC-UV method for the determination of seven catechins and one xanthine (caffeine) in water infusion of green tea. Two infusion temperatures (95º and 80º) during different times as well as several types of water of infusion (tap water, deionized water, spring water, reverse osmosis water, and distilled water) were tested in order to see the extent of these factors on catechin profiles variation. A solution consisting of 10 mM sodium tetraborate, 4 mM sodium phosphate and 25 mM SDS (pH 7) used as BGE permitted the separation of the major tea infusion compounds within 15 min. Infusion at 95°C for 10 min presented upper values of catechins than infusion at 80°C. In addition, other differences were also found depending on the water of infusion. Thus, epimerization of

catechins was more frequently observed in infusion brewed in tap water than in other types of water probably due to its higher ions content compared with the other water types tested.

5 Lipids

Lipids are hydrophobic or amphiphilic molecules with vital functions to human health such as energy provision and storage, structural components of cellular membranes and cell signaling. Lipid categories include fatty acids, steroids, glycerophospholipids, and sphingolipids among others. NACE-ESI-IT/MS has been applied for the determination of glycerophopholipid profiles in olive fruit and olive oil [94]. Olive fruit samples analyzed in that work were Arbequina (from two Spanish regions), Empeltre, and Lechín de Sevilla. In addition a monovarietal extra virgin olive oil from Arbequina variety was also included in the study. Best separation efficiency within less than 14 min analysis time was achieved using 100 mM ammonium acetate in 60:40 v/v methanol/ACN with 0.5% acetic acid as BGE, applying 25 kV. As a result phosphatidylcholine, phosphatidylethanolamine, lysophosphatidylethanolamine, phosphatidylinositol, phosphatidic acid, lysophosphatidic acid, and phosphatidylglycerol were detected in olive fruit. Differences in the relative abundance of the glycerophospholipid profiles were observed depending on the botanical and geographical origin of the olive fruits analyzed. In olive oil, five glycerophospholipids were observed, namely lysophosphatidic acid, phosphatidylcholine, phosphatidylethanolamine, lysophosphatidylethanolamine, and phosphatidylglycerol.

Steroid hydrosolubility is even lower than for glycerophospholipids and in addition they are hardly ionized. For these reasons, modification of the target molecules or the electrolyte solutions is required when using CE methods for the analysis of steroids. Particularly, MEKC technique has been successfully applied in steroid studies. In this regard, a MEKC method was developed for the analysis of steroids in vegetable oils [95]. For that purpose, microemulsion phases of colza oil, olive oil, linseed oil, and walnut oil were prepared by adding ~90% of 10 mM sodium tetraborate (pH 9.2), 3.3% SDS, and 6% of 1-butanol to oils. Steroids were separated based on their hydrophobicity being the hydrocortisone the fastest compound in the microemulsion. Applying the methodology developed, hydrocortisone, androstenedione, 17-α-hydroxyprogesterone, testosterone, 17-α-methyltestosterone, and progesterone could be separated in oil samples.

Fatty acids (FAs) are important lipid molecules used for energy production through β-oxidation or deposited in lipid droplets in the form of triglycerides as energy reservoir. The traditional method more widely used for the analysis of FAs is gas chromatography coupled with flame ionization detection (GC-FID). However, CE has already demonstrated to be a very useful analytical technique for the screening and quantification of FAs in food matrices [96]. In fact, CE presents inherent advantages over GC-FID as low cost, short-analysis time, high throughput, and simple sample preparation. In addition, contrarily to GC-FID, CE permits the separation of cis-trans isomers without the use of specific columns. FAs content in oils is of particular importance because it affects the flavor quality of the oil. On the other hand, due to FA instability a high concentration of FA can cause oil rancidity and formation of peroxides, which are noxious to human health. In this context, a CE method for FA determination in soybean oil, sunflower seed oil, and maize oil was developed [97]. Another innovative analytical approach for the analysis of FAs was developed by Buglione et al. [98]. A total of 12 FAs could be separated using a NACE method with LOD of 0.5 μM for all FAs determined. Optimal conditions included a polyvinyl alcohol-coated capillary for suppression of the EOF and to increase reproducibility together with the use of 10 mM deoxycholic acid in methanol as BGE. Validation of the method was achieved through the analysis of commercial sunflower oil, a commercial olive oil, and a homemade olive oil. More recently, several vegetable oils were also evaluated in terms of their FAs content [99]. That approach could be suitable to detect possible fraudulent extra virgin olive oils related to the different acidity expressed in relation with their oleic acid content.

Although oleic acid is the major component of olive oil it is present in other oils such as soybean oil. A fast and direct quantification method for the determination of that monounsaturated omega-9 fatty acid in soybean oil was developed [100]. For that purpose, a NACE method with capacitively coupled contactless conductivity detection was applied using methanol-propanol (1:6, v/v) with 0.04 M KOH and 10% ethylene glycol as BGE. That method enabled oleic acid determination without any sample treatment and authors state its usefulness for fraud detection.

Oleic acid is the major FA of pequi fruit (*Caryocar brasiliense Camb.*), a popular Brazilian fruit with high lipid content. FA profiles of pequi fruit have been investigated by CE [101]. Following the developed method, stearic (C18:0), oleic (C18:19c), palmitic (C16:0), linoleic (C18:2cc), and linolenic (C18:3) acids were separated and their levels were compared with the official GC method for these FAs determination. As a quality indicator of the method, no significant differences were observed between CE and GC methods; and CE method permitted the analysis of the samples without derivatization and lipid fractionation, which are required in the classical GC method.

Polyunsaturated FAs omega-3 and omega-6 are involved in regulation of blood pressure and inflammatory responses among other physiological functions and have been largely investigated for their potential benefits against diseases such as diabetes or cancer. Interestingly the ratio between omega-3 and omega-6 seems to be critical related to various disorders. In fact several chronic diseases decrease with lower omega-6 FAs intake and higher omega-3 FAs intake being the optimum omega-6/omega-3 ratio from 1:1 to 4:1 depending on the disease under consideration [102]. Given their importance, their analysis in foodstuff is of great relevance. In this

sense, omega-3 and omega-6 FAs have been determined in flax seed and oils (e.g. in a combination of flax seed oil, sunflower seed oil, sesame seed oil, rice oil, oat germ oil, coconut oil, and primrose oil) and a selection of grass-fed and grain-fed beef muscle samples by CZE-UV [103]. Using 40 mM borate buffer (pH 9.5) with 50 mM SDS, 10 mM β-CD, and 10% ACN separation of 15 polyunsaturated omega-3 and -6 FAs including α-linolenic acid, γ-linolenic acid, eicosapentaenoic acid, docosapentaenoic acid, and arachidonic acid among others, could be separated. Authors state that this method is comparable to the standard GC method for the analysis of omega-3 and-6 FAs.

Different isomers for the double bonds of FAs from the same hydrocarbon chain conform the cis and trans fatty acids. Depending on that fact, FAs may have very different effects on human health. Although some trans FAs are associated with industrial processes and are considered harmful to health, others are formed by biohydrogenation in ruminants such as vaccecin and conjugated linolenic acids, with reported beneficial effects (i.e. tumor growth regulation) [104]. Methods for the determination of cis- and trans-FAs are an increasing demand due to the above-mentioned health concerns and because of the requirements of the governmental health agencies. In this line, a quantitative method for the analysis of C18:0, C18:1 9t, C18:19c, C16:0, C18:2cc, and 18:3 ccc that constitute the most common cis–trans long chain FA has been developed by means of CE [105]. Optimum BGE consisted of 15 mM of NaH_2PO_4/Na_2HPO_4 (pH 6.86), 4 mM sodium dodecylbenzenesulfonate, 8.3 mM Brij 35 and 45% v/v of ACN, and 2.1% v/v of 1-octanol. The method parameters were validated in real samples of olive oil, soy oil, hydrogenated vegetable fat, butter, margarine, filled cookie, and bovine liver. Finally, levels of FAs were compared to the ones obtained by the official GC method and no significant differences were detected, confirming the suitability of the new methodology. Another CE method has been developed for the analysis of cis/trans long chain FAs [106]. Namely, lauric, myristic, tridecanoic (internal standard), pentadecanoic, palmitic, stearic, oleic, elaidic, linoleic, linolenic, and arachidic acids were separated showing values for intra- and interday RSD for migration times and peak areas lower than 9.7%. The method was further validated in margarine samples.

Vitamins included in lipid family are A, D, E, and K. They present an isoprene-based structure and are essential nutrients for humans found in a variety of foods such as carrots (rich in vitamin A), oily fish (vitamin D), spinach (vitamin E), and basil (vitamin K) to show some examples. Tocopherol (α, β, γ, and δ- tocopherols) or vitamin E presents antioxidant properties and edible oils are one of the natural sources where it can be found. For this reason, a NACE method using fluorescence detection was developed for the analysis of tocopherol in olive oil, sunflower oil, and maize-germ oil [107]. Prior to their analysis, samples were submitted to SPE with a silica cartridge. Optimum BGE composition was 12 mM borate buffer (3 mM sodium tetraborate), 60 mM sodium cholate, and 12 mM sodium hydroxide in methanol. Tocopherols levels in oil samples were compared with those obtained with the common LC method showing comparable results.

Some of the most important natural plant pigments to confer attractive colors to food ingredients include carotenoids, anthocyanins, and betalains. Pigments can be classified by their origin as natural or synthetic (synthetic pigments are included in "Food Additives" section). Among the natural pigments crocins are found in saffron. Crocins are hydrosoluble carotenoids composed of glycosides of aglycon crocetin. These compounds together with other typical saffron compounds have been analyzed by means of MEKC method in order to develop a simple procedure of quality screening [108]. The optimized BGE (20 mM disodium phosphate, 5 mM sodium tetraborate, and 100 mM SDS at pH 9.5) permitted the determination in saffron of two crocins, namely, picrocin that confers bitter taste to saffron, and safranal that is responsible of color.

6 Carbohydrates

Human diet is rich in carbohydrates because these molecules are the main source of energy and carbon of the body, providing from 40 to 80% of the total energy requirements. Attending to their molecular subunits there are four groups of carbohydrates, namely monosaccharides, disaccharides, oligosaccharides, and polysaccharides. CE has proven to be a powerful separation technique for the separation and analysis from small mono- and disaccharides to complex oligo- and polysaccharides [109]. Analysis of sucrose, D-lactose, D-fructose, D-ribose, and D-glucose was performed using a 10 cm long quartz capillary (10 μm i.d.) with an effective length of 4 cm and 75 mM NaOH as BGE in a homemade instrument [110]. All the carbohydrates were analyzed in less than 1 min. The developed method was then applied to four energy drinks and levels of sugars were compared to their declared content in sugar. Methods like the one previously described, are important to control food quality because saccharide contents in drinks and foodstuff are regulated and have to be declared. Since maple syrup is prone to adulteration with less expensive sugars (i.e. corn syrup), saccharide content from maple syrup was investigated through CE-UV with borate complexation [111]. After derivatization with 1-phenyl-3-methyl-5-pyrazolone (PMP), nine monosaccharides, and five disaccharides were separated using 200 mM borate buffer at pH 10.5 as BGE. Among all saccharides, it was observed that the main components of maple syrup and maple sugar were sucrose, glucose, and mannose. Due to economic value of fruit juices, they are also prone to adulteration by dilution with water and addition of sugars or of pulp wash, or even through mixture with cheaper fruit juices. In this regard, a CZE-UV method was developed for the differentiation of juices and blends based on their saccharides content [112]. More than 50 samples including juices from apple, grape, mandarin, orange, pineapple, and nectar from orange, pineapple as well as multifruit juices were

studied in that work. In addition, mixtures with different percentages of pineapple-grape and orange-grape juices were also analyzed to detect possible blends of fruit juices. Analytes were separated using 10 mM 2,6-pyridine dicarboxylic acid and 0.5 mM cetyltrimethylammonium bromide at pH 12.1. Juices and blends could be correctly classified based on their saccharides content and adulteration could be predicted by means of linear discriminant analysis and multiple linear regression. In addition to the importance to detect adulterations, sugar content has a relevant influence on organoleptic quality of foodstuffs. To deepen in this aspect, levels of fructose, glucose, and sucrose of seven vegetables and fruits were analyzed by CZE [113]. Namely, tomato (*Solanum lycopersicon L.*), pepper (*Capsicum annuum L.*), muskmelon (*Cucumis melo L.*), watermelon (*Citrullus lanatus (Thunb.) Matsum. & Nakai*), winter squash (Cucurbita moschata Duschene), and orange (*Citrus sinensis (L.) Osbeck*) were selected for their importance in the agricultural market. Analytes were separated using a BGE composed of 20 mM 2,6-pyridine dicarboxylic acid (pH 12.1) and 0.1% hexadimethrine bromide. It was observed that SDS rinsing avoided the loss of reproducibility after several injections. As a result, levels of the three saccharides were quantified in all samples. Same saccharides were determined in seven honey samples [114]. The quantitative results revealed that fructose was the major sugar in honey samples (33.65–45.46 g /100 g) followed by glucose (22.34–35.39 g/100 g). This method also allowed the determination of sucrose, which is useful in the detection of possible adulterations by the addition of syrups. Quantitative determination of saccharides was also performed in 13 commercial breakfast cereals [115]. A disodium hydrogen phosphate-based buffer permitted the determination of sucrose, maltose, glucose, and fructose by CZE with direct UV detection. It was observed that sucrose was the principal sugar of all samples analyzed. Another CE-DAD method was developed for the analysis of fructose, glucose, lactose, and sucrose in red wine and apple juice [116]. Levels of 335 mM fructose, 98 mM glucose, and 53 mM sucrose were found in apple juice in agreement with the bottle label. In addition, fructose and glucose were detected at 2.1 and 1.4 mM respectively, in the red wine samples. Similarly a CE-UV analytical approach was employed for the analysis of sorghum juices from 109 varieties [117]. Correlation between different saccharides and total saccharide content with brix values was carried out. As a result, it was observed that brix value was proportional to the total saccharide content corroborating its previous acceptance as indicator of total sugar content. In addition, sucrose was near 75% of the total sugar content in varieties with high brix values. Saccharides in milk and beer have also been analyzed applying CZE [118]. A CZE method was developed for the separation of 13 free monosaccharides and disaccharides, including a set of stereoisomers of aldopentose and aldohexose. For that purpose, derivatization with PMP was performed prior analysis. CZE-UV separation was achieved using 175 mM borate (pH 11.0) with 4% methanol as BGE. Maltose and glucose could be quantified in beer samples while maltose, lactose and glucose were determined in milk. Same analytical approach was carried out to determine the monosaccharide composition of fucoidan from *Saccharina japonica*, an important food from Japan [119]. After sample hydrolysis and prior analysis by CZE, derivatization with PMP was performed. It was observed that all of the fucoidans consisted of xylose, rhamnose, fucose, mannose, galactose, and glucuronic acid.

Milk is a very complex matrix and contains approximately 4.9% of carbohydrates, predominantly the disaccharide lactose. Especial attention has been paid to oligosaccharides found in milk, particularly, due to their bioactive effects on the gastrointestinal and immune systems including prebiotic and anti-infective functions [120, 121]. Caprine milk has a high level of oligosaccharides with similar profiles to human milk and has been reported to contain up to five times more oligosaccharides than bovine milk. A CE method has been applied to caprine whey as it has been postulated as a potential source of oligosaccharides [122]. A two-stage separation process for the caprine whey was carried out prior analysis. Separation was performed in a 75 mM borate electrolyte solution at 10 kV. The results showed that the whey separation process between lactose and oligosaccharides was effective achieving near 90% of carbohydrates recovered. Investigation of human milk composition, and especially characterization of some oligosaccharides probed as important dietary factors during the early life, is also being investigated. For this reason, different groups have developed CE methods for the analysis of oligosaccharides in human milk [123, 124]. In this line, a capillary gel electrophoresis (CGE method with LIF detection was developed aiming to correlate lactation time course and oligosaccharides content [124]. First, samples were treated and fluorescent labeled using reductive amination. Then, a method for the analysis of oligosaccharides was developed. Optimum separation was performed for 130 min at 15 kV. Moreover a database containing migration times and oligosaccharides found in human milk was generated. Finally, the method was applied to real samples and the oligosaccharides were identified. As a result, the individual changes within the oligosaccharide composition could be examined during the lactation time course [124]. In a more recent work, oligosaccharides from human milk have been also investigated [123, 124]. In that work, 17 neutral and acidic human milk oligosaccharides derivatized with 2-aminoacridone were analyzed using high-voltage CE separation with UV detection and 300 mM sodium borate at pH 10.5 containing 20% methanol as BGE. As a result, saccharides composition of the milk samples obtained using CE were found to be in agreement with previously published data achieved using HPLC-MS and anion-exchange chromatography-pulsed amperometry detector.

Polysaccharide molecules are complex linear or branched chains composed of monosaccharide units. Their compositional analysis generally encompasses a prior hydrolysis into their monosaccharide units. Determination of polysaccharides in asparagus (*Asparagus officinalis Linn.*) was done by CE-AD after their hydrolysis with 1 M sulfuric acid in boiling water [125]. As a result, fucose, galactose, glucose, rhamnose, arabinose, fructose, and xylose were determined in the

asparagus samples. More recently, hydrolysis of polysaccharides of edible mushrooms (*Termitomyces albuminosus* and *Panus giganteus*) was performed with 2 M TFA [126]. After hydrolysis with TFA, PMP derivatization was carried out and xylose, arabinose, glucose, mannose, and glucuronic acid were quantified in the two species of mushrooms analyzed by CZE [126].

7 DNAs

Over the last few years, novel DNA-sequencing approaches, known as next-generation sequencing (NGS), are emerging with cutting-edge applications in food science [127]. Despite the high-throughput capabilities of the NGS instruments for nucleic acids analysis, the technology is still evolving and remains inaccessible to many laboratories. In consequence, CE is still the method of choice in many food applications for DNA analysis. It is interesting to note that, in the period covered by the present review, most of de published CE methods for DNA analysis have been aimed at assessing food authenticity [128–134] and traceability [135].

In this area, the use of commercial microfluidic CE instruments to the analysis of genetic markers has notably increased. Commercial miniaturized CGE solutions offer many advantages such as simplicity and speed of analysis. For instance, Garino et al. [128] developed a method to distinguish seven pure Italian rice varieties from imported blends. In this case, the genetic markers of choice were classical short-tandem repeats polymorphisms that were amplified by PCR and separated and detected using the Agilent Lab-on-a-chip® technology with a new postanalysis statistical processing method. This procedure allowed the generation of genetic distances between the samples under study, clustering the locally cultivated Italian rice varieties separately from other foreign cultivars. In addition to the authentication of pure rice samples, the proposed method enabled the identification of artificial blends, which suggests the good possibilities of the method for rice testing. In a different approach, Spaniolas et al. [129] compared the performance of the Lab-on-a-chip® microfluidic system applied to the detection of PCR-RFLP in coffee varieties with two SNP-based diagnostic assays, namely, single-base primer extension coupled to CGE-LIF analysis and pyrosequencing. The results of the study indicated that single-base primer extension-CGE-LIF provided the best sensitivity, whereas pyrosequencing revealed the best linearity. In contrast to the other two methods, based on SNPs, authors stated that although the PCR-RFLP-Lab-on-a-chip® method performed well, the application of this strategy is limited to the presence/absence of a restriction site. Using commercial QIAGEN QIAxcell CGE microfluidic system, Barakat et al. [130] developed a procedure for detection of pork adulteration in sausages. Authors optimized various porcine- and pork-specific PCR systems based on amplifications of mitochondrial D-loop and cytochrome b genes, and used 18S ribosomal gene sequence as internal control for amplification. Then, the specificity of amplified products was assayed using the miniaturized CGE system. The method was robust and suitable for detecting 0.1% pork adulteration in raw and cooked sausages. QIAxcell system has gained popularity and other interesting applications can be found in recent scientific literature. For instance, a new method based on PCR-RFLP and QIAxcell separation technology was developed for the discrimination of oils from 17 Turkish olive cultivars [132]. To discriminate the varietal origin of the samples, five PCR-RFLP systems were necessary. The procedure was also applied to oil mixtures containing oil from more than one variety, allowing the identification of varieties in binary mixtures. Another authenticity issues related with fish products that have recently raised several concerns include occurrence of allergies, abuse of endangered species and use of cheap or toxic species. In line with this, *Cyprinidae* fish species are high-priced food in Taiwan is frequently subject of substitution with other fish that remain undetectable by consumers. To address this problem, Chen et al. [131] developed a PCR-RFLP system that combined with QIAxcell microfluidics system for the identification of ten *Cyprinidae* fish species in processed products. The applicability of the method was demonstrated by the identification of the species in 24 commercial *Cyprinidae*-related products, showing the potential of the procedure for routine food authentication. Also related with fish authenticity, Rolli et al. [135] evaluated the suitability of microsatellites as DNA markers for the traceability of European perch (*Perca fluviatilis*), an economically relevant freshwater species in Europe. Microsatellites, which are short tandemly repetitive DNA sequences, are considered good genetic markers for traceability because of their abundance and high polymorphism. Authors combined specific methods for microsatellite markers generation with fluorescent labeling and CGE separation using a conventional CE apparatus coupled to a laser module to increase sensitivity and precision of genotyping. Using this approach, three polymorphic microsatellites and their combinations allowed correctly assigning or excluding 60 out of 62 Swiss perch samples into their origin population. Rodríguez-Ramírez et al. [134] have recently published an article that exemplifies another CGE application to the detection of adulteration of fish-related products. In their method, a PCR method to amplify specific DNA sequences of soy in canned tuna samples was developed. As a positive amplification control, authors used a Cytb gene sequence specific for tuna. After amplification step, PCR products were unequivocally identified by CGE with LIF detection. The method was applied to the analysis of real adulterated canned tuna samples providing evidences of commercial fraud. In addition to the fraudulent practices detected for the mentioned fish species, some *Gadus* species are frequently subjected to fraudulent or unintentional mislabeling when are commercialized as fillets. Thus, Dalmasso et al. [133] proposed a novel molecular method for species identification of salted and dried products derived from species belonging to Gadiformes. The method involves the generation of PCR fragments in a multiplex minisequencing reaction based on single-base primer extension. After purification of the extension products, samples were analyzed using a conventional

capillary sequencer. Authors demonstrated the applicability of this methodology to the analysis of commercial samples, confirming the species indicated in the label for all samples.

In the past decade, following the pioneering works from our group [136], several CE-based methods have been developed for the detection of genetically modified organisms in food samples. For instance, Basak et al. [137] developed strategies for detection of insect-resistant cotton (MON531) and herbicide-tolerant soybean (GTS40-3-2). More precisely, two multiplex PCR methods were developed to specifically detect trace amounts of the GM cotton and soybean, respectively. Optimal conditions for multiplex reactions were established using primer pairs, in which the forward primer was fluorescently labeled with one of the two fluorophores (6-carboxyfluorescein and hexacloro-6-carboxyfluorescein) used in the study. This strategy allowed the generation of several fluorescent PCR products with similar size, but different fluorescent features, which also provided additional discriminatory information about the amplified DNA sequence when analyzed by CGE equipped with a charge-coupled device detector and set of appropriate filters.

The analysis of DNA markers for detecting the presence of microorganisms is an interesting topic in food safety. Recently, Ruan et al. [138] proposed a novel methodology based on the use of duplex PCR in combination with CGE-LIF for the detection of *Cronobacter* spp., an emerging opportunistic pathogen with high mortality rate in infants resulting from the consumption of contaminated food. The method involved the amplification of gene sequences of 16S-23S rDNA internal transcribed spacer and the outer membrane protein A of *Cronobacter* spp. Using linear polyacrylamide coated capillaries and a sieving matrix containing 0.9% methylcellulose and SYBR Green I, separations of duplex PCR products were resolved in 12 min. The method proved to be suitable for the analysis of artificially inoculated food samples, including milk powder, instant noodles, fermented bread, beef, and egg cakes. Moreover, the method was applied to the analysis of infant formula products collected in different food factories from nine provinces of China revealing that small amounts of domestic commercial baby formula milk powder were contaminated by the pathogen. The detection of other two relevant foodborne pathogens, *Listeria monocytogenes* and *Escherichia coli* O157:H7, is also of major importance. To this regard, there is much interest in the development of new methods allowing the rapid, sensitive, and simultaneous detection of food-borne pathogenic species. Wang et al. [139] developed a novel strategy that involved the use of polydopamine functionalized magnetic nanoparticles to efficiently capture bacterial DNA in samples. After magnetic separation and elution, DNA can be used as templates for polymerase chain reaction followed by CGE-UV analysis. This analytical strategy was successfully applied to the detection of both food-borne pathogens in milk. The study of food spoiling microorganisms is still a relevant research area in food microbiology. Recently, Alberice et al. [140] performed a comparative study of two procedures for *Alicyclobacillus acidoterrestris* quantification in orange juice. The study indicated that reverse transcription-PCR combined with Lab-on-a-chip® technology was more rapid and sensitive for the detection of cell viability than conventional plating methods.

8 Vitamins

Vitamins are organic biological compounds that are necessary for our organism and, due to the incapacity of the human organism to synthesize the majority of them, their administration by a balanced diet is indispensable. Vitamins differ in their structure, biological, and chemical properties and according to their solubility can be divided into two groups: water- and fat-soluble vitamins.

The separation and determination analysis in dietary supplements of ten water-soluble vitamins, including PP (nicotinamide), B12 (cyanocobalamin), B2 (riboflavin), B6 (pyridoxine), B8 (biotin), C (ascorbic acid), B5 (pantothenic acid), B3 (nicotinic acid), B1 (thiamine), and B9 (folic acid) have been evaluated by MEKC-UV [141]. Under the optimized conditions, all vitamins could be separated within 18 min with %RSDs values lower than 6% for sample analysis.

A MEKC method for the simultaneous analysis of some vitamins belonging to the B group (thiamine, riboflavine, nicotinic acid, and nicotinamide) and vitamin C in multivitamin preparations and in artichokes (*Cynara cardunculus subsp. scolymus (L.) Hegi*) has been developed [142]. The total analysis time was less than 20 min. and the LODs were 5 μg/mL for all vitamins. The accuracy of the analytical procedure was confirmed by the analysis of certified and labeled commercial multivitamin dietary supplements.

An experimental design and artificial neural network to optimize CE separation of nicotinic acid and nicotinamide in food (russula alutacea, instant dry yeast, functional drinks, and vitamin water) was developed by Mu et al. [143]. Experimental variables, such as SDS concentration and voltage, were optimized using a statistical model. Under optimal conditions, the LOD values were lower than 0.16 μg/mL and the total analysis time was less than 5 min. This CE method was reported as an environmental friendly alternative to HPLC routine analysis of these compounds.

Cereal grains are also an important source of B-group vitamins. Recently, Parveen et al. reported the simultaneous determination of phenolic compounds and vitamins B1 and B6 in eight wheat varieties by MEKC [144]. Optimum separation was achieved with a BGE at pH 9 containing sodium tetraborate, SDS, and propanol at a wavelength of 225 nm. Using this methodology, LODs were 0.03 and 0.05 mg/L for vitamin B1 and B6, respectively.

The development of a simple, sensitive, and reliable method for the routine determination of riboflavin in cereal grains by CE-LIF was studied by Chen et al. [145]. Two on-line concentration techniques including stacking in reverse migrating micelles (SRMM) and sweeping were investigated and compared. The optimal conditions of separation were achieved with 20 mM phosphoric acid, 140 mM SDS, and SRMM on-line concentration method. Under these

conditions, the LOD of the riboflavin was 0.29 ng/mL. The method was applied to the evaluation of the 18 samples of nine types of cereal grains (wheat bran, wheat, rice, black rice, oats, corn, millet, buckwheat, and rye).

CZE with UV detection method has been used for the determination of nicotinic acid and vitamin C content in black bean [146] Recoveries between 87–119% ($n = 4$) and 88–108% ($n = 4$) for nicotinic acid and vitamin C, respectively, were reported. Falkova et al. developed an automated procedure for analyses of the solid samples based on multicommutated stepwise injection analysis with subsequent determination by CE-UV [147]. The applicability of the method was demonstrated by determination of ascorbic acid in *Sorbus aucuparia* (fruits), kiwi, apple, sweet pepper, and applesauce. LOD was 0.03 mg/g for ascorbic acid and satisfactory repeatability was reported with RSD values ranging from 5 to 7% from ten replicate measurements of the ascorbic acid content in real samples.

Capillary electrophoresis coupled with chemoluminescence (CL) detection was proposed for analysis of nicotinamide in yogurt [148]. The methodology was based on the inhibitory effect of nicotinamide to CL reaction of luminol-$K_3Fe(CN)_6$ in alkaline aqueous solution.Authors reported an RSD value lower than 2.2%, recoveries between 98 and 104%, and a LOD of 3.0 nM.

Novel CE-ESI-triple quadrupole MS/MS methodology has been developed for the analysis of different vitamins B in dietary supplements [149]. Simultaneous separation of thiamine, riboflavin, nicotinamide, nicotinic acid, pantothenic acid, pyridoxine, biotin, folic acid, and cyanocobalamine could be achieved within 16 min. The LODs of the method ranged from 0.0419 to 0.2252 μg/mL, and RSD values were less than 0.7 and 4.5%, for migration time and peak area, respectively.

9 Small organic and inorganic compounds

Small organic and inorganic compounds are naturally present or added to food and beverages. Recently, Azevedo et al. developed and validated a simple and rapid (<10 min) CZE method with indirect UV detection for the simultaneous analysis of ten short-chain aliphatic organic acids in commercial Brazilian sugarcane spirits [150]. The separations were performed using a semipermanent capillary coating comprised of 2-hydroxypropyltrimethyl-ammonium chloride chitosan, and a 21 mmol/L β-alanine and 10 mmol/L3.5 dinitrobenzoic acid buffer (pH 3.6) as BGE. The LOD and LOQ ranged from 0.69 to 2.70 mg/L and 2.76 to 8.11 mg/L, respectively, intraday and interday precision for the whole procedure was lower than 9% RSDs, and the recoveries percentage ranged from 74–112%.

A simple CE method has also been partially validated for the simultaneous quantification of nine aliphatic (formic, oxalic, succinic, malic, tartaric, acetic, citric, lactic, and butyric) and three aromatic (benzoic, phenyllactic, and hydroxyphenyllactic) organic acids in 15 min in fermentation products of lactic acid bacteria [151]. The optimum BGE composition was 0.5 M H_3PO_4 and 0.5 mM CTAB (pH 6.24) with 15% v/v methanol. The investigated method showed LODs values ranging from 0.001 to 1.43 μg/mL, LOQs ranged from 0.004 to 4.72 μg/mL and RSDs values for intraday and interday reproducibility were lower than 5%.

Reversed-phase HPLC and CE methods have been validated and compared for the determination of (latic, acetic, propionic, and butyric) organic acids in cassava starch fermentation wastewaters by de Sena Aquino et al. [152]. The LODs for HPLC and CE ranged from 1.0 to 3.7 mg/L and 2.0 to 3.0 mg/L, and the LOQs from 3.1 to 12.2, and 8.0 to 12.5 mg/L for HPLC and CE, respectively. With regard to the compounds analyzed, no significant differences were found between the methods in terms of analytical performance. However, some benefits of CE compared with HPLC were lower cost, lower waste generation, and shorter analysis time (less than 2 min and 14 min, respectively).

A novel CZE method for simultaneous nitrate and nitrite determination in less than 0.5 min has been proposed by Betta et al. [153]. The influence of different parameters on the separation was studied and a solution of 10 mmol/L perchloric acid and 40 mmol/L β-alanine (pH 3.96) was used as BGE. An experimental design was also applied to establish the appropriate extraction procedure. The method was validated and applied to the analysis of 14 baby food samples. Authors reported %RSDs values of 0.21 and 0.89 for migration time and LODs of 0.09 and 0.15 mg/L for nitrate and nitrite, respectively. The possibility of applying the CZE method for routine determination of nitrate and nitrite in food was highlighted [153].

Simultaneous determination of inorganic iodine species and iodinated AAs by CE was reported by Sun et al. [154]. In this work, the feasibility of an ion-pairing reagent for resolution improvement for iodine speciation analysis by a pressure-driven CE with UV detection was demonstrated. The methodology was based on an electrostatic interaction between tetrabutyl ammonium hydroxide and the negatively charged iodine species. Baseline separation of iodine species was achieved within 7 min, the LODs were below 0.06 mg/L and %RSDs values for peak heights and areas were lower than 3%. The application of the studied method was demonstrated by speciation analysis of iodine in seaweed samples. However, it suffered from high detection limits, which hindered its application the analyses of real samples containing ultra-trace iodine species.

Another interesting approach to elemental speciation includes the coupling of CE with inductively coupled plasma MS (ICP-MS). CE-ICP MS has been studied to combine the efficient separation capacity with the ultrasensitive detection ability for high resolution studies. In this context, Qu et al. developed and optimized a system consisting of a CE system instrument interfaced with ICP-MS for speciation and characterization of metallic nanoparticles (e.g. gold, platinum, and palladium) in dietary supplements [155].

The on-line combination of cITP and cITP (column coupling capillary isotachophoresis, cITP-cITP) has also been

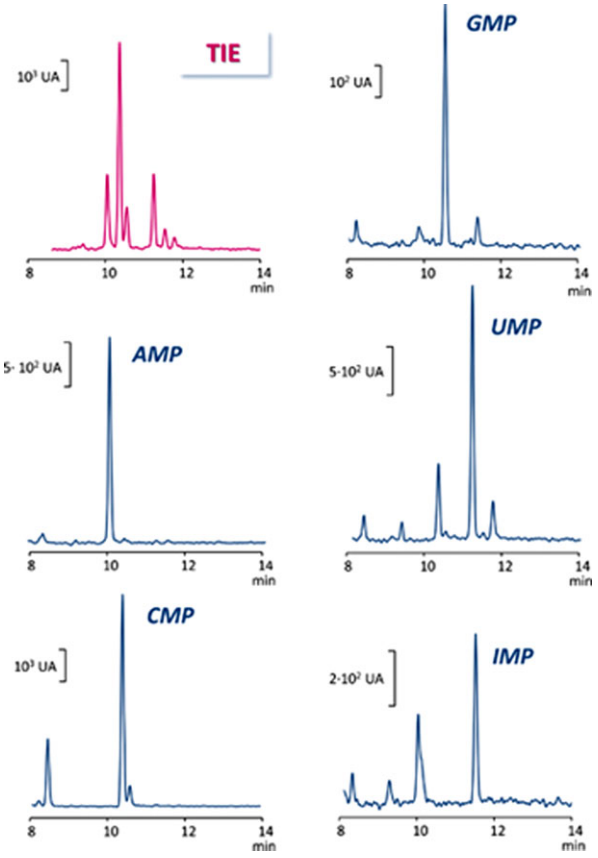

Figure 3. Total ion electropherogram (TIE) and extracted ion electropherograms. (EIEs) of a sample of powdered infant formula. CE-MS conditions: BGE, 30 mM ammonium formate-ammonia medium (pH 9.6); separation voltage, +30 kV; capillary temperature, 25°C; sheath liquid, 50:50, v/v isopropanol:UHQ water mixture; flow rate,1.00 mL/min, and negative ion ESI-MS mode. Redrawn from [158] with permission from Wiley-VCH.

applied to the simultaneous determination of macro- and micro-nutrients at low concentration levels. cITP-cITP procedure has been developed by Chmiel et al. for the simultaneous determination of K^+, Na^+, Ca^{2+}, Mg^{2+}, and ammonium in berries in related products [156]. Detection limits for the method ranged from 0.030 to 0.097 mg/L with RSDs values lower than 4.5%. Capillary ITP has also been applied for the analysis of glucosamine [157]. The validation of the method demonstrated recovery values of 98.8%, LOD of 2.4 mg/L, and a good precision (RSD = 1.82%). The method was applied to the evaluation of the glucosamine in 35 samples of dietary supplements.

CE-ESI-MS has been proposed by Rodríguez-Gonzalo et al. [158] for the determination and simultaneous quantification of five ribonucleotide 5′-monophosphates (adenosine 5′-monophosphate, cytidine 5′-monophosphate, guanosine 5′-monophosphate, uridine 5′-monophosphate, and inosine 5′-monophosphate) in infant formulas (see Fig. 3). In their study, authors optimized the separation and quantification of the analytes, and studied the compatibility of several sample treatments with CE separation and ESI ionization. A simple method based on centrifugal ultrafiltration was applied as sample treatment. The method proposed was validated according to European Legislation. The LOD values ranged from 0.8 to1.8 μg/g, and the recoveries percentage from 90–106%. This CE-ESI-MS method was reported as an alternative to other chromatographic methods for the analysis of nucleotides and related compounds.

10 Toxins, contaminants, pesticides, and residues

The occurrence of toxins in food represents a serious concern worldwide due to their harmful effect on human health. Although the maximum acceptable levels of many toxins in foods have already been established, the imposition of regulatory limits for new toxins in foods is expected to continue as new toxins are being identified as well as their potential risk to public health. To guarantee the food safety, and to minimize the potential risk to human health, it is necessary to develop fast, sensitive, and reliable methods to detect toxins. Mycotoxins are a group of secondary metabolites produced by organisms of the *fungus* kingdom that can enter human food chain affecting a large variety of food products. The last developments in mycotoxin analysis, including those based on capillary electromigration methods, were recently reviewed by Berthiller et al. [159]. Mycotoxins have been object of investigation by CE in recent years. For instance, the electrophoretic analysis of patulin, an important mutagenic mycotoxin, produced by filamentous fungi of the genera *Penicillium*, *Aspergillus*, and *Byssochlamys*, has been attempted by Güray et al. [160]. Authors developed a CZE method with UV detection for the analysis of patulin without any interference from hydroxymethyl furfural, a typical and important interference in patulin detection by HPLC-UV in certain food samples. In that work, different buffer types, pH, organic modifiers, detection wavelength, injecting mode, and timewere studied to achieve optimal sensitivity. Optimized separation conditions included a BGE containing 25 mM of sodium tetraborate and 10% ACN at pH 10. The validation of the method demonstrated good linearity in the range from 0.250 to 4.99 μg/mL of patulin. In addition, the reported LOD and LOQ values for patulin were 5.9 and 17.9 ng/mL, respectively, demonstrating the good sensitivity of the method. Also, Guray et al. [161] optimized a CZE-DAD method for the detection of zearalenone in feed and cereals. In this approach, CZE-DAD procedure involved the use of 20 mM sodium tetraborate at pH 9.0 with 15% ACN and the addition of phenobarbital as internal standard. Using these conditions, LOD and LOQ values of 8.25 and 25 μg/L were achieved, respectively. The application of the method to the analysis of commercial samples revealed the presence of zearalenone in 5 out of 15 samples indicating the suitability of the proposed method for detecting the mycotoxin in complex food samples.

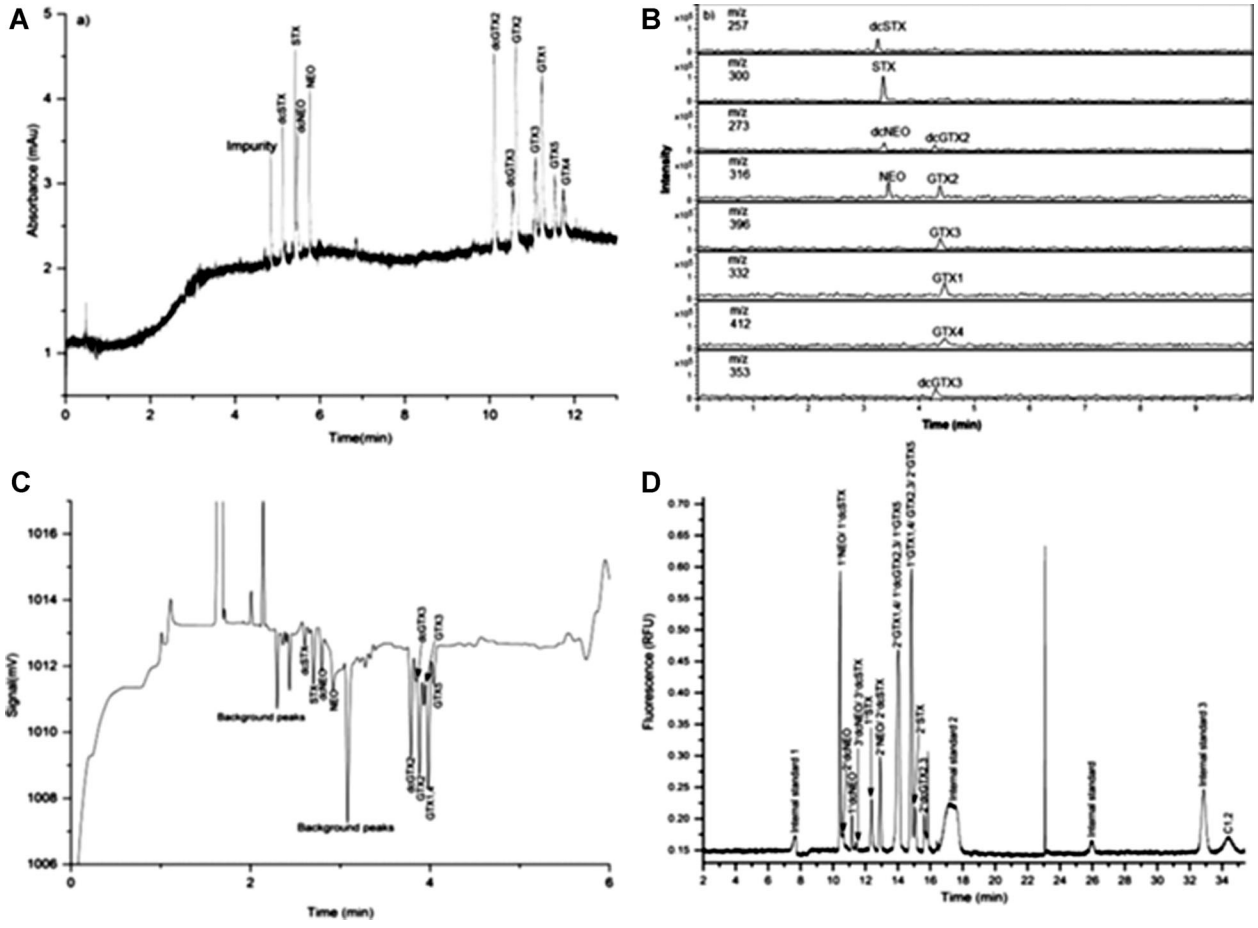

Figure 4. Separation of paralytic shellfish toxins mixture using four different CE methods. (A) Electropherogram of CZE-UV using 30 mM phosphate buffer pH 2.5, sample injected at 5 kV for 10 s. (B) Extracted ion electropherogram) of CZE-MS at selected *m/z* using 35 mM morpholine pH 5.0, sample injected at 5 kV for 10 s. (C) Electropherogram of CZE-C^4D using 25 mM sodium acetate buffer pH 4.22, sample injected at 5 kV for 10 s. (D) Electropherogram of MEKC-FLD using 30 mM phosphate buffer at pH 8.5 containing 80 mM SDS, sample injected at 0.7 psi for 10 s. Redrawn from [163] with permission from Wiley-VCH.

A relevant number of marine microalgae (including dinoflagellates, cyanobacteria, and diatoms) and bacteria are also responsible for the production of toxins that can accumulate in certain herbivorous fish, zooplankton, and filter-feeding shellfish becoming toxic for humans. CE presents potential to separate a wide spectrum of these compounds, which is being exploited for the accurate determination of major marine toxin groups involved in paralytic shellfish poisoning, diarrheic shellfish poisoning (DSP), and ciguatera disease. Sassolas et al. [162] have reviewed current CE approaches, among others, for the analysis of okadaic acid, a DSP toxin that contaminates bivalves and originates severe public health problems and economic damages to shellfish farming. Recently, Abdul Keyton et al. [163] explored the potential of using CZE-UV, CZE-capacitively coupled contactless conductivity detection (C^4D), CZE-MS, and MEKC-fluorescence detection (FLD) techniques for the analysis of 12 paralytic shellfish toxins (see Fig. 4). A comparative study of the four methods showed that CZE-UV and CZE-MS failed to meet the required LODs imposed by legislation, but CZE-C^4D and MEKC-FLD showed LOD values below or close to regulatory limits. Although CZE was not suitable for the separation of neutral C1 and C2 toxins, when it was coupled to C^4D detector, the method allowed for identification of ten of the 11 charged toxins within a few minutes. By contrast, MEKC-FLD method was suitable for fast screening of contaminated mussel samples with the 12 toxins although with less sensitivity than the one provided typically by the most common HPLC-FLD technique for shellfish toxin screening. Further work by the same research group focused on the development of a transient isotachophoresis-CZE with UV and C^4D detection for the analysis of paralytic shellfish toxins in mussel samples [164]. In this approach, counter-flow transient isotachophoresis was used to improve the sensitivity and reduce sample matrix effects. Under optimized conditions, separations of ten different paralytic shellfish toxins were completed in 30 min. The method provided quantitative results comparable to those obtained with HPLC-FLD in contaminated mussel samples. Following a different strategy, Zhang et al. [165] developed a novel CE-based

immunoassay (CEIA) method using ED for the simultaneous detection of four shellfish toxins, saxitoxin, brevetoxin, domoic acid, and okadaic acid in shellfish samples. Authors developed a competitive model in which a horseradish peroxidase-labeled antigen was first mixed with different concentrations of nonlabeled antigen (standard solution or sample extract) that competed for binding with the limited and fixed amount of antibody to form immunological complexes that are subsequently separated by CE. The main novelty of the method was the use of conjugated gold nanoparticles in the capillary to improve the resolution by altering the mobility of analytes. In addition to this, the presence of gold nanoparticles improved the sensitivity since the bound enzyme-labeled complex allows the amplification of electrochemical signal. The enhanced CE method with gold nanoparticle labels was successfully applied for the simultaneous determination of four shellfish toxins in shellfish samples achieving LOD values ranging from 3.1 to 36.7 ng/L. In a separate report, Zhang et al. [166] have recently applied the same concept to the detection of ciguatoxin CTX1B in fish samples. The parameters studied during the method development stage included the amount of enzyme and antibody absorbed onto the nanoparticles, incubation time on immunocomplex formation, and other parameters affecting electrophoretic separation. Under optimal CZE-UV conditions, a LOD value of 0.045 ng/mL was achieved, which is over 38-fold lower than that of HPLC-MS for the same toxin. A novel and interesting design for postcolumn reaction in CE systems has been recently reported by Abdul Keyton et al. [167]. In their work, authors devised a micro cross for positioning a salt bridge-electrode opposite the separation capillary outlet to keep the electrical connection during the electrophoretic separation. Using this strategy, it was possible to use droplets of water-in-oil with a size of approximately 14 nL containing reagents for in-capillary oxidation and subsequent LIF detection of paralytic shellfish toxins. The method was validated for neosaxitoxin and decarbamoylgonyautoxin 2 that were detected in 10 min, showing good performance in terms of sensitivity, precision, and linear range.

The extensive use of pesticides in agriculture has attracted much attention since the persistence of residues in food represents a risk for human health. Regarding the new developments of CE-based methods for the analysis of this chemically diverse group of compounds, the bulk of published papers have been focused on herbicides. On this topic, a comprehensive overview of the current CE developments for herbicide analysis [12] and a more general article reviewing the analysis of orphan and difficult pesticides [168] have been recently published. Improvements in sampling and sample preparation methods used to detect herbicides in food products continue to be a high priority in this analytical area. For instance, Puzio et al. [169] synthesized three molecularly imprinted polymers (MIPs) to bind efficiently glyphosate in water. Authors used CE-UV for the optimization of sample preparation conditions. Then, a comparative study on the efficiency and selectivity of the developed materials with those of nonimprinted polymer by SPE demonstrated the superior capabilities of MIPs over the more traditional SPE materials for glyphosate herbicide. Also, the direct analysis of glyphosate, glufosinate-ammonium, and aminomethylphosphonic acid in apple skin has been approached using liquid extraction surface analysis in-line coupled with CE by Sung et al. [170]. The herbicides were directly extracted into a liquid microjunction formed by dispensing the extractant from the inlet tip of a separation capillary. After extraction, pesticides were derivatized in-capillary with 4-fluoro-7-nitro-2,1,3-benzoxadiazole and analyzed with CE-LIF. Optimization of derivatizing agent concentration, mixing time, and standby time allowed to improve the sensitivity of the method, achieving LOD values between 1 and 10 ppb, which are about 20-fold lower than the tolerance limits established by regulatory authorities. In another application, Kukusamude et al. [171] successfully attained the detection of paraquat and diquat, two cationic quaternary ammonium herbicides in cow milk, using a combination of field enhanced sample injection (FESI) and micelle to solvent stacking (MSS) with CZE-UV. In this methodology, a sample clean-up step by cloud point separation using Triton X-114 was included previous to electrophoretic analysis to remove unwanted milk proteins. A detailed study during optimization of the methodology involved the investigation of parameters affecting the clean-up process such as the equilibrium temperature and time, as well as the conditions affecting stacking by FESI-MSS, including hydrodynamic micellar solution injection and electrokinetic sample injection times. Using this procedure on milk samples, good linearity, and LODs were obtained for both paraquat (0.004 μg/mL) and diquat (0.018 μg/mL) improving from 1.5 to 2 orders of magnitude in detection sensitivity over the nonstaking CZE method.

The use of nanomaterials in CE methods also offers good potential for the analysis of herbicides. This has been exemplified in a recent study on the combined use of dispersed carbon nanotubes with ionic liquid for CE separations of sulfonylureas in wheat and sorghum [172]. In that study, a clean-up preconcentration procedure was done prior CE analysis. Then, nicosulfuron, ethoxysulfuron, sulfometuron methyl, and chlorsulfuron herbicides were separated in 16 min without using organic solvents. The herbicides were detected at levels below the maximum residue limits (MRLs) imposed for each analyte, demonstrating the suitability of the method for the analysis of sulfonylureas in cereals. More recently, the determination of halosulfuron-methyl, another sulfonylurea herbicide, has also been approached using CE-MS/MS [173]. Authors extracted the herbicide from sugarcane juice and tomato samples using a procedure based on quick, easy, cheap, effective, rugged, and safe followed by electrophoretic separation in NH_4HCO_3 electrolyte at pH 8.5, and detection by electrospray-MS/MS. The reported recovery values for spiked samples ranged from 96 to 105%, and the LOD for the herbicide in juice and tomato was 2 ppb. In a separate report, the application of CE-ECL was investigated to the analysis of yam samples for the detection of three phenylurea herbicides, namely monuron, monolinuron, and diuron [174]. Separations were performed using

25 mM phosphate buffer at pH 8.0 as BGE and a CE instrument coupled with an ECL detector. Initially, the optimum Pt electrode potential for the detection of the three herbicides was established in the detection system. Then, several variables affecting the separation, including buffer composition and pH, and separation voltage were investigated using a standard mixture of the three herbicides. In order to validate the feasibility of the procedure for the analysis of the three phenylureas, the performance of the method was evaluated with spiked yam samples. CE-ECL analysis provided separations without interfering signals, and LOD values were lower than 0.01 μg/kg.

Besides the great interest on herbicide analysis, there are also examples of the application of novel capillary electromigration developments for the determination of fungicides and insecticides in food samples. A work by Soliman and Donkor demonstrated the good possibilities of using MEKC-UV for the determination of a group of three fungicides (i.e. thiabendazole, carbendazim, and fuberidazole) in water [175]. During method development, several experimental variables were investigated to provide optimal conditions suitable for the analysis. The study revealed that phosphate/SDS buffer provided better resolution and sensitivity, than acetate/cholate buffer making it more suitable for quantitative analysis. After optimization of separation and detection parameters, the reported LODs were about 0.7 mg/L. The use of MIPs in SPE coupled to CE was also useful for the detection of trichlorfon insecticide in cucumber, lettuce, and radish samples [176]. In that study, extraction conditions including the eluent composition and volume, and the sample loading flow rate and time, were optimized to achieve highest sensitivity. Optimal separation conditions were achieved using sodium borate–boric acid at pH 9.3 as buffer system. The whole procedure showed good selectivity and the use of MIP improved sensitivity by 160-fold. The recovery of the method was high with low variation indicating the there was little matrix effect in the analysis of real samples.

The persistence of antibiotic residues in food is becoming a serious concern and in consequence, the presence of these drugs in food is regulated in many countries by specific legislations imposing strict MRLs. The enforcement of these regulations implies that sufficiently sensitive analytical tools must be available to provide reliable determinations of multiple antibiotics in food products. To this aim, several CE-based methodologies have demonstrated excellent potential allowing the separation of a wide spectrum of these compounds in different food matrices. Excellent reviews covering advances in CE analysis of antibiotics have been lately published [16, 18]. Recent developments for the determination of quinolones have been directed to improve sensitivity with different innovative materials for sample preparation. This was exemplified in a work by Spirnger et al. [177], where the determination of ciprofloxacin, norfloxacin, and ofloxacin was successfully achieved in bovine milk using CE-UV and a pipette-tip SPE step based on multiwalled carbon nanotubes prior CE separation. The mount of sorbent material, pH of sample solution, sample volume, extraction temperature, and the number of rinsing sets necessary for quinolones extraction were studied and optimized. During optimization of the separation conditions, the addition of CTAB to a BGE containing 20 mM amomonium dihydrogenphosphate at pH 3.0 provided the best resolution in the separation of the three quinolones. The simplicity of the method as well as the achieved sensitivity were enough to meet the requirements imposed by legislation, suggesting the good possibilities of this method for routine testing. In a separate report, Tian et al. [178] approached the analysis of quinolones using polyamidoamine dendrimers, which are highly branched and symmetrical macromolecules. Their uniform surface charge density and structural homogeneity provided better separation performance than other pseudostationary phases. In that study, dendrimers were used as binding agent in sample solution and in running buffer as pseudostationary phase to achieve the resolution of six quinolones in chicken samples. As for the case of other food contaminants, a MIP has been exploited in combination with CE-MS for the selective analysis of eight quinolones in bovine milk samples [179]. In this case, a MIP was used as sorbent for the construction of an in-line SPE analyte concentrator in CE-MS. The reported recoveries were higher than 70% and LODs values ranged from 1.0 to 1.4 μg/kg, which are below MRLs established in the EU regulation. Following a different strategy, Springer et al. [180] also combined CE and MS for the determination of fluoroquinolones in bovine milk. More precisely, ciprofloxacin, norfloxacin, and ofloxacin were analyzed by CE and off-line CE-MALDI-TOF spectrometry coupling. Such off-line coupling allowed the individual deposition of analytes in small size spots and provided direct information of the mass of the molecules. The chemical composition of BGE and the capillary coating were optimized to minimize suppression of the MS signal after spot deposition. Deng et al. [181] combined FESI-based CE with the use of a bubble cell capillary to enhance the sensitivity detection of five fluoroquinolones (ciprofloxacin, enrofloxacin, lomefloxacin, fleroxacin, and ofloxacin) in bovine milk. In that work, authors investigated the effect of BGE composition, injection parameters, and injection water plug on the separation. Under the optimized conditions, the analysis of fluoroquinolones provided LODs between 0.4 and 1.3 ng/mL, which are much lower (from 460 to 1500 times) than those obtained by a conventional CE in a standard capillary without bubble cell. Xu et al. [182] explored the application of another simple online preconcentration method that combines field-amplified sample stacking (FASS) with sweeping technique for the determination of enrofloxacin and ciprofloxacin in a variety of food samples. The analysis of real samples was performed using 120 mM sodium deoxycholate in the BGE and adding gamma-cyclodextran to the sample matrix to improve the efficiency of sweeping process. Authors attained LODs that were lower than the MRLs of the tested compounds in milk, chicken, pork, swine liver, and kidney samples showing interesting perspectives the application of this approach for routine analysis. Besides UV and MS, other detection schemes such as LIF detection have been recently exploited for the

determination of quinolones in food samples. For instance, Meng et al. [183] optimized a new MEKC method using quantum dot indirect LIF to detect five quinolone in animal-derived food products. Quantum dots (QDs) are the semiconductor nanoparticles made up of the II–VI and III–V group elements in the periodic table, which have interesting spectral properties, such as stable and intense fluorescence emission. In addition, the emission wavelength of QDs can be controlled by engineering their particle size in the process of synthesis. Thus, in that work, authors synthetized cadmium telluride QDs that could be used as fluorescent background substance in MEKC-indirect LIF detection of quinolones. Using an optimized running buffer containing 20 mM SDS, 7.2 mg/L QDs, and 10 mM borate at pH 8.8, the separation of five quinolones was achieved within 8 min with LODs values between 3 and 8 μg/kg. Recently, a novel CEIA method with LIF detection was developed for norfloxacin residue analysis in food products [184]. This novel development involved labeling of norfloxacin with fluorescein isothiocyanate to perform competitive immunoassay between the labeled and nonlabeled forms of quinolone with a limited amount of antinorfloxacine. Then, the intensities of labeled norfloxacin and labeled immonocomplex were related to the original concentration of free norfloxacin in chicken, pork, fish, and milk samples. The proposed CEIA-LIF method demonstrated to be more sensitive than ELISA method (LODs, 0.05 versus 0.016 μg/L), avoiding the multiple steps and reducing errors and deviations.

Sulphonamides are another relevant group of antibiotics whose residues in food of animal origin have caused much concern because of their harmful effects on human health and the potential development of resistance to pathogens. Last developments based on CE techniques have been focused on the investigation of novel strategies for sample preparation, with particular attention in nanomaterials. For instance, graphene, a new class of carbon nanomaterial, has been used as SPE adsorbent for CZE determination of four sulfonamides in meat samples [185]. In another approach, Polo-Luque et al. [186] explored the sorption capabilities of single walled carbon nanotubes and multiwalled carbon nanotubes dispersed in the ionic liquid 1-hexyl-2-methylimidazolium hexafluorophosphate to preconcentrate sulphonamides from milk samples. The dispersed nanomaterials were retained on a C18 stationary phase to obtain a hybrid material with excellent sorption capabilities. Other novel approaches for sulfonamide detection include the application of efficient techniques such as combined accelerated solvent extraction, which has demonstrated its potential to obtain sulfonamides and their N^4-acetylated metabolites from shrimp samples for subsequent analysis by CZE-UV [187]. The proposed method reduced the volume of solvent required compared to conventional extraction techniques. The whole process provided rapid separations with satisfactory repeatability and good sensitivity.

The traditional addition of 5-nitroimidazoles, a specific class of antibiotics, to animal feed as growth promoters involves the need of carrying out exhaustive controls with the aim of detecting this illegal practice. The determination of these antibiotics in milk was investigated using SPE and MEKC-UV by Hernández-Mesa et al. [188]. Using mixed cation exchange SPE cartridges, an off-line concentration factor of 18 was achieved whereas in capillary sweeping effects enabled further concentration of all the analytes, providing LODs lower than 1.8 μg/L.

In addition to the aforementioned methods for determination of specific categories of antibiotics in food, other CE-based methods have been developed to simultaneously detect different classes of antibiotics. For instance, Zhai et al. [189] have recently published a report on the determination of chloramphenicol, ciprofloxacin, and nitrofuran antibiotics and their metabolites in fishery products by CE-UV. As nitrofuran metabolites lack UV chromophores, a derivatization step was implemented for their detection by UV. The optimized separation buffer, containing 2 mM sodium dihydrogen phosphate, 20 mM disodium hydrogen phosphate, 80 mM sodium deoxycholate, and 10 % methanol v/v, pH 9.0, and a running voltage of 20 kV allowed the separation of the three antibiotics and their metabolites.

Endocrine disrupting compounds (EDCs) are other class of food contaminants whose determination has been also approached by CE. The occurrence of most of these xenobiotics in foodstuffs is due to the use of synthetic chemical products for packaging. Among EDCs, bisphenol A (BPA) have attracted particular attention and, in last years, its analysis has been approached using various extraction procedures in combination with CE. For instance, Alenazi et al. [190] successfully developed a MIP using ethylene glycol dimethacrylate and methacrylic acid to specifically bind BPA in water and milk samples. After MIP preparation, nonspecific-binding sites were blocked by site-selective chemical modification with dizomethane. In this study, CE-UV method was used to evaluate the selectivity of the treated MIP toward BPA in the presence of other spiked compounds. The reported results of the study suggested that the treated MIP provided more selectivity than commercial MIPs. DLLME combined with CZE-UV has also been applied to the analysis of BPA in beverages [191]. A major advantage of DLLME over other extraction methods such as SPE and solid-phase microextraction (SPME) was the lower consumption of organic solvents (microliters), shorter extraction time (few seconds), and simplicity of operation. The application of DLLME with CZE-UV allowed the analysis BPA in real samples, with little matrix interference. In addition to these improvements in sample preparation of BPA, a new CZE-AD method proved to be a good alternative for the analysis of this EDC in drinking water [192]. In this procedure, samples were prepared using an off-line SPE method and a boron-doped diamond electrode was used as an electrochemical detector that provided a favorable analytical performance for detecting BPA and other three EDCs (bisphenol F, 4-ethylphenol, and bisphenol A diglycidylether). The main advantages were the achievement of lower noise levels, higher peak resolution with enhanced sensitivity, and improved resistance against electrode

passivation. The LODs for the four compounds ranged from 0.01 to 0.06 μM, and the methodology enabled the detection of 0.03 μM BPA in plastic bottle water container exposed to sunlight for 7 days.

The consumption of meat containing residual ractopamine hydrochloride (RP) presents serious concerns in public health. This veterinary drug is a β-adrenergic agonist, frequently used for enhancing feeding efficiency in animals, and its presence in meat may cause side effects in humans upon consumption. Matrix interferences are often the major problem encountered in most of the analytical solutions developed for the determination of RP in meat samples. The quantitative determination of RP and its homologue dehydroxyractopamine has been recently approached using cation-selective exhaustive injection (CSEI) sweeping-MEKC [193]. Using CSEI-sweeping-MEKC, samples are dissolved in a low-conductivity matrix and are electrokinetically injected in to a higher conductivity buffer zone for a long time. Then, the analytes can be swept and separated by MEKC. In that work, authors used a fractional factorial design and response surface methodology to facilitate the optimization of the different parameters affecting the analysis. The sensitivity improvement was about 900-fold in the case of LODs of the proposed method compared to the normal CZE. The method was validated and applied to the analysis of several porcine meat samples demonstrating the good possibilities of the method as a simple and fast procedure for routine analysis of RP. Another veterinary medicine that has attracted attention is amprolium. This drug is often used to prevent and treat coccidiosis in poultry and, in case of abusive intake or withdrawal periods are not fully accomplished, it may arrive to consumers. The application of field-amplified sample injection (FASI)-CZE equipped with diode array detection system has recently showed to be suitable for the analysis of amprolium in eggs [194]. The methodology involved a previous step of sample treatment using SPE, followed by in-line preconcentration using FASI in order to achieve higher sensitivity. During method validation stage using egg samples, authors observed an interfering compound comigrating with amprolium. The analysis of this compound using CE-MS allowed its identification as thiamine. The reoptimized method allowed separation of the amprolium and thiamine and the quantification of the former in eggs at concentrations below the MRL imposed by regulatory authorities.

Nonsteroidal anti-inflammatory drugs (NSAIDs) are other type of contaminants that represents a risk to the consumer if their residues enter the food chain. Etodolac, naproxen, ketoprofen, flurbiprofen, and ciclofenac belong to NSAIDs class and are frequently used in veterinary medicine. In consequence, the use of NSAIDs in food-producing animals might create public health problems, especially in the international trade of milk and dairy products. FASS-CZE determination of five NSAIDs has been approached using DLLME for sample preparation [195]. DLLME parameters including type and volume of extraction and disperser solvents, ionic strength, and extraction time were key for optimal extraction of the five drugs. The performance of the DLLME-FASS-CE method was evaluated with spiked milk, yogurt, and white cheese samples. The study revealed LOD values between 3 and 12.1 μg/kg and LOQs ranging from 10 to 43.7 μg/kg, with good reproducibility (%RSD<6.2% for interday analysis). Finally, the applicability of the whole procedure was demonstrated in real samples and compared to other SPME-, SPE-, and LLE-based methods coupled to different high-resolution separation techniques.

Recently, the increasing occurrence of drug-facilitated crimes based on the drug-spiking on drinks has raised some concerns and challenges in forensic science. Benzodiazepines constitute one of the groups of drugs more commonly sued to perform such crimes, in which the analysis of the drinks used to perpetrate drug-facilitated crimes is necessary, as they might be the only lasting evidence. Sáiz et al. [196] have used CE-C^4D technique in combination with chemometric multivariate techniques, including PCA and soft independent modeling of class analogies classification. This novel strategy, based on the comparison of electrophoretic profiles obtained from 63 different club drinks spiked with benzodiazepine, allowed the determination of this drug in drinks without the use of drug standards.

11 Food additives

Many food additives are currently used in the preparation of processed foods. In general, these additives can be obtained from nature or manufactured by the chemical industry. The main food additives analyzed by CE in the period covered by this review (2013–2015) were sweeteners [197–201], preservatives [202–210], and colorants [211–213].

Sweeteners are compounds that are added to foodstuffs in order to confer a sweet taste, for economic reasons or for health reasons where glucose has to be reduced (blood glucose regulation or caloric control). The vast majority of sweeteners approved for food are syntheticwith some exceptions as for instance sorbitol and xylitol, which are natural sweeteners found in berries, fruit, vegetables, and mushrooms. Most artificial sweeteners approved by US and EU food agencies are stevia, aspartame, sucralose, neotame, acesulfame potassium, saccharin, and advantame. A very recent CE method using indirect UV detection with a short-end injection procedure has been developed for the determination of aspartame, cyclamate, acesulfame-K, and saccharin [197]. Samples and standards were injected hydrodynamically and separated using 45 mM 2-amino-2-(hydroxymethyl)-1,3-propanediol and 15 mM benzoic acid (pH 8.4), in less than 1 min. The CZE-UV method permitted the quantification of the analytes in five sweeteners (two liquid and three solids), four soft drinks, two ice teas, and four pharmaceutical preparations. The same artificial sweeteners were determined by a CZE-UV method in a lemon tea sachet [198]. Separation was carried out using 20 mM sodium tetraborate, 15 mM Tris and 7.5 mM benzoic acid (pH 9.15) as BGE followed by simultaneous indirect and direct UV detection. As a result, baseline resolution was achieved in 6 min. In addition, no significant

differences were found in the label of lemon tea sachet when compared to the experimental levels of sweeteners obtained using that method. A CE method with contactless conductivity detection was developed for the analysis of the same four sweeteners [199]. In this later, case the BGE consisted of 150 mM 2-(cyclohexylamino) ethanesulfonic acid and 400 mM tris(hydroxymethyl)aminomethane at pH 9.1. Validation of the method was achieved by the analysis of a tabletop sweetener tablet, two confectionaries and three low calorie soft drinks.

Neotame is a new artificial sweetener already approved as a food additive by the US Food and Drug Administration. Although up to date HPLC is considered the standard method for neotame analysis, there is an increasing demand of less expensive methods for the determination of this sweetener. For instance, a CZE-UV method has been developed for the analysis of neotame in cola drink and yoghurt [200]. Due to the low concentration of neotame in samples, SPE was performed prior analysis. Optimal analysis conditions included borate buffer at 20 mM (pH 8). The developed method was suitable for neotame analysis in a short-analysis time (less than 5 min). Recently, neotame and other sweeteners, i.e. aspartame, sodium cyclamate, sodium saccharin, and acesulfame have been analyzed by CE-UV using 0.2 M borate (pH 8.29) as electrophoresis buffer at +23 kV separation voltage [201]. Good linear regression equation correlation and low RSD values (below 7%) were obtained for all sweeteners showing good potential for its application to food samples.

Preservatives are food additives typically added to food to control the growth of undesirable microorganisms and to maintain the freshness of foodstuffs. However, at excessive quantities they can be harmful to health. The development of suitable and rapid analytical methods to determine preservatives is imperative to ensure food safety without health risk. Among food preservatives, organic acids and their salts are common preservatives due to their ability to inhibit a wide variety of pathogens and may also act as acidity regulators in food and beverages. Ten preservatives (i.e. dehydroacetic acid, sorbic acid, benzoic acid, methyl paraben, ethyl paraben, isopropyl paraben, propyl paraben, isobutyl paraben, butyl paraben, isopentyl paraben) were analyzed by MEKC in different sauces (soy, oyster, abalone, tomato, jam, and chili sauces) and pickle, jam, beverages, candied fruit, cheese, pastries, cake, and jelly samples. [202]. Sample treatment prior analysis was dependent on the nature of each sample. The ten preservatives were spiked at different concentrations (from 1.5 to 200 mg/L) within all samples in order to construct calibration curves using MEKC. Six samples (two kinds of pickles, pastries, and cheese) were detected to have sorbic acid and benzoic levels above the permitted levels (levels established in China). In addition, the results showed that the current method could meet the needs for routine analysis for these preservatives.

Given the low concentration of preservatives in food samples different approaches have been employed to increase sensitivity. For instance, an online dynamic pH junction-sweeping method was coupled to CE for the analysis of benzoic acid and sorbic acid [203]. Dynamic pH junction together with sweeping demonstrated to significantly enhance sensitivity during CE analysis. As a result, nanomolar concentrations of preservatives could be detected. The developed method was applied to real food samples of juice, two soft drinks, two soy sauces, and a wine sample. Another strategy applied to increase sensitivity for preservatives detection was a two dimensional isotachophoretic cITP-cITP method [204]. Preservatives were detected by two methods of detection, namely conductometric and UV-Vis. Benzoates, sorbates, citrates, and orthophosphates were detected in five juice samples and seven soft drinks.

Recently, ionic liquids were incorporated in a CE method for the quantitative determination of 8 preservatives (i.e. butyl p-hydroxybenzoate, propyl p-hydroxybenzoate, ethyl p-hydroxybenzoate, methyl p-hydroxybenzoate, m-amino benzoic acid, sorbic acid, benzoic acid, p-hydroxybenzoic acid) [205]. The method was used for the determination of preservatives in four soft drinks. It was observed that sorbic acid was present in the three fruit juices (lemon, grape, and haw juices) while benzoic acid was detected in the vitamin beverage.

Parabens are a group of compounds widely used in foods as preservatives due to their antimicrobial activity. Parabens are alkyl esters of p-hydroxybenzoic acid and their antimicrobial activity is directly related to the hydrocarbon chain length [206]. However, their water solubility also decreases with the hydrocarbon chain length and thus, the use of parabens with longer alkyl chains is limited. Some important members of this family are methylparaben, ethylparaben, n-propylparaben, iso-propylparaben, n-butylparaben, isobutylparaben, and benzylparaben. Parabens are generally found in low concentration and thus different approaches of sensitive enhancement have been applied for their analysis. For instance, DLLME followed by CE has been recently applied for parabens analysis [207]. Applying that method, methyl-, ethyl-, propyl-, and butyl- parabens were analyzed in samples of breast milk, tomato paste, pickle, mixed fruit juice, and ice cream. Another approach to increase paraben sensitivity is to use on-column preconcentration strategies prior to CE separation. In this line LVSS, FASI, sweeping, and in-line SPE-CE, were investigated for the simultaneous separation and preconcentration of a group of parabens [208]. Methods were optimized for the determination of methylparaben, ethylparaben, propylparaben, isopropylparaben, butylparaben, and benzylparaben and were validated in water samples. Although sensitive was still not enough to detect parabens in water, the in-line SPE-CE method offered the most sensitive results among the four preconcentration strategies.

Another research work was focused on the determination not only of parabens but also of organic acids in food by CE with laser induced fluorescence detection [209]. For that purpose, cadmium telluride QDs were used as fluorescent background. After optimization of analysis conditions five preservatives, namely propylpareben, sodium dehydroacetate, sorbic acid, benzoic acid, and sodium propionate were analyzed in 8.5 min with %RSD values lower than 4%. Using that methodology, two beverages, cake and biscuit samples

were further analyzed showing low %RSD values for preservatives (less than 5%).

Other additives present in a wide range of foods and used as food preservatives are nitrates and nitrites. These compounds in addition to conferring bacteriostasis also help to develop color of food. Zhan et al. developed an open-tubular (OT) CEC for the analysis of nitrites and nitrates in hams and sausages [210]. Authors highlighted the high stability of the OT-CEC system as well as the suitability of the method for its application in the analysis of trace nitrites and nitrates in food samples.

Pigments and colorants are chemical substances that can provide good-looking colors to food ingredients. Main reason to use pigments for foods is that there is a great influence of color of food in the flavor perceived. Pigments can be classified by their origin as natural or synthetic or by their composition as dyes or lakes. Among dyes and lakes, main difference is that lakes are composed of a dye mixed with precipitants and salts conferring higher stability to the formula. Recently, two aluminum-based lakes were evaluated through CZE [211]. The analytical methods developed for the analysis of both lakes were similar except for the voltage applied and the concentration of the BGE. As a result limits of detection of 0.26 and 0.27 mg/L were obtained for tartrazine lake and sunset yellow lake respectively highlighting the potential use of these methods for the analysis of color lakes in foods [211]. More recently a dispersive solid-phase microextraction was developed for the determination of four very common food colorants, carminic acid, tartrazine, sunset yellow, and brilliant blue [212]. Separation of all these colorants was achieved in less than 8 min. When the method was applied to juice beverages, effects of coexisting species such as citric, ascorbic, benzoic or malic acid among others, was studied and no interferences were found. In addition, authors highlighted the great sensitivity obtained using this method compared to the direct CZE analysis, being LOD 60-fold lower for the new method. Other colorants that have been widely used as food additives are Sudan dyes. Sudan dyes have demonstrated to present dangerous effects on human health being their use forbidden in the European Union. However, due to the global market, Sudan dyes have been detected in imported food revealing the importance of fast and sensitive analytical methods for their detection. In order to give respond to this issue, a MEKC-MS/MS method was developed for the detection of Sudan dyes I, II, III, and IV [213]. For that purpose, analytes were separated using a BGE composed of 40 mM ammonium bicarbonate, 25 mM SDS, and 32.5% ACN v/v. Since UV detection was not suitable for the determination of these dyes, parameters for MEKC coupling with MS in the positive ion mode were optimized. That strategy permitted the MS fragmentation of each dye contributing to their identification. Finally, the method was successfully validated in chilli powder samples.

In addition to the above-mentioned methods for determination of specific categories of preservatives in food, additional CE-based methods have been designed to detect different classes of preservatives at the same time. For instance, a group of 16 food additives, namely, ten colorants and six preservatives, could be effectively separated using a CE method developed by Long et al. 2012 [214]. Colorants including acid red 92, patent blue V, uranine, acid red 1, indigo carmine, black BN, ponceau 6R, quinoline, amaranth, lemon yellow colorants, and preservatives such as benzoic acid, sorbic acid, methyl paraben, ethyl paraben, propyl paraben, and butyl paraben were analyzed in beverages using as BGE 70 mM boric acid with 4% ACN at 30 kV and 220 nm as wavelength.

12 Food processing

Food processing is a crucial issue in food science since the chemical composition of food components can be modified during the different processing steps, they include, e.g. heating, roasting, storage, ripening, etc. The difficulty to evaluate these changes is high considering that there are many parameters that can contribute to the chemical changes of food compounds during processing, such as temperature, pH of the system, oxygen availability, the presence of metal ions as well as other compounds that can interact to each other [215].

HMF (5-hydroxymethylfurfural) is an important marker of food processing and storage widely recognized as an important parameter of food freshness and quality. Its amount depends on the composition of a food product and on the thermal treatments to which the food is subjected. An innovative CE-MS/MS method was developed for the quantification of HMF in food products exploiting selected product ion monitoring as acquisition mode. The method was applied to the analysis of different kind of samples: cereal-based baby foods, coffee, soft beverages, and vinegars. In order to show the reliability of the proposed method, results were compared with those obtained by HPLC-UV, and a good accordance between the two sets of data was found [216].

Membrane processing offers several advantages over conventional methods for separation, fractionation, and recovery of bioactive components from food by-products. In a recent work, CE was used to monitorize the isolation of natural lactose-derived oligosaccharides (OS) from caprine whey using membrane processing. The final use of the OS was the development of functional foods for clinical and infant nutrition. CE allowed to determine the most efficient process consisiting in the combination of a pretreatment to eliminate proteins and fat, using an ultrafiltration (UF) membrane of 25-kDa molecular weight cutoff (MWCO), followed by a tighter UF membrane with 1-kDa MWCO. *Circa* 90% of the carbohydrates recovered in the final retentate were OS [122]. Also CE was used to monitor whey demineralization, which is mandatory for further processing and food applications of this dairy byproduct. CE was applied to determine the main whey cations (K^+, Na^+, Ca^{2+}, Mg^{2+}) and a lab-scale electrodialysis unit was used to remove these ions from ten model solutions of fresh or reconstituted whey with increased dry matter and sodium content. The results demonstrated that mineral salts could effectively be removed from whey with this procedure even if it was concentrated and highly salted [217].

Determination of changes in the metabolic profile of avocado fruits (*Persea americana*) during ripening was carried out by using two CE-MS approaches (targeted and nontargeted). To do this, CE with two different MS detection conditions (multiple reaction monitoring and full scan) was applied to determine qualitative and quantitative changes in the metabolic profile of avocado fruits. The two MS approaches were used to quantify ten metabolites (phenolic acids, flavonoids, a carbohydrate, an organic acid, a vitamin, and a phytohormone) in 18 samples of avocado at different ripening states, and the achieved results were compared. Perseitol, quinic, chlorogenic, trans-cinnamic, pantothenic, and abscisic acids, as well as epicatechin and catechin decreased during the ripening process, whereas ferulic and p-coumaric acids showed the opposite trend. Moreover, some other unknown compounds whose concentration changed largely during ripening were also studied by MS/MS and quadrupole TOF-MS to get a tentative identification [218].

Caramel color is one of the most usual additives used in beverages, desserts, and breads worldwide. However, during its fabrication process, 2- and 4-methylimidazole (MeI), highly carcinogenic compounds, are generated. A CE method was developed for the separation and determination of 2- and 4-MeI in caramel colors, overcoming the limitations of LC- and GC-MS for the analysis of these compounds. Thus, the CE method allowed the determination of 2- and 4-MeI improving the analysis speed, decreasing the amount of organic solvent needed as well as the pretreatment steps [219].

13 Chiral analysis of food compounds

The analysis of chiral compounds is finding interesting applications in food science. The detection of chiral compounds in food is needed to assess the factors that influence their origin, formation, biological function, safety, and function, since they can originally be found in foods, can be formed during food processing or can also be originated from microbiological sources. Since enantiomers have identical electrophoretic mobility, chiral complexing reagents (chiral selectors) are usually added to the separation buffer to form diastereomeric complexes in dynamic equilibra that allow their separation. Following this CE direct enantioseparation approach, cyclodextrins (CDs) are the most widely used chiral selectors [220]. Some reviews have been published during the period covered by this review, on chiral separations in food analysis by CE [220].

The presence of free D-AAs in foodstuff may be an indication of microbial contamination, or adulteration, making these compounds good indicators of food quality and authenticity. Tezcan at al. developed a chiral MEKC-LIF method, using sodium dodecylbenzene sulphonate as surfactant and β-CD as chiral selector, for the determination of chiral AAs (L-Arg, D-Leu, L-Trp, L-Leu, L-Pro, D-Pro, L-Asn, L-Ser, L-Ala, L-Glu, and L-Asp) in fresh and commercial pomegranate juices [221]. L-Asn was also proposed as a marker for the adulteration of pomegranate juices with apple juices. However, a marker for the adulteration of pomegranate juice with grape juice, one of the most common adulterants of pomegranate juice, was not found. Analysis of α-hydroxy acids and their enantiomers by chiral ligand exchange CE (CLE-CE) was used to distinguish authentic and adulterated fruit juices (apple, grape, orange, pineapple, grapefruit). Enantiomers of D/L-malic, D/L-tartaric, and D/L-isocitric acids, and citric acid were detected by CLE-CE-UV using D-quinic acid as the selector ligand. Sun et al. developed also a CLE-CE method with Zn (II)-L-alanine as the chiral selector in the presence of β-CD for enantioseparation of dansylated-AAs [222]. CLE-CE-UV method was used to explore the inhibitory effect of kojic acid and soy sauce on the enzyme tyrosinase. Tyrosinase is a copper-containing enzyme that can cause enzymatic browning in raw fruits, vegetables, and beverages. Since L-Tyr is the specific substrate for tyrosinase, authors proposed the measurement of the activity of tyrosinase through the determination of L-Tyr concentration variation after being incubated with the enzyme. Thus, the inhibitory activity of kojic acid and soy sauce against tyrosinase was investigated through monitoring the concentration variation of Dns-L-Tyr and Dns-D-Tyr by CLE-CE-UV. Analysis of Dns-D/L-Tyr was achieved in 32 min. and the LOD was 15.52 μM. Another chiral CE method was reported for the chiral separation of neotame [223]. Neotame is an artificial sweetener with two chiral centers in its structure, hence, it can form four diastereomers being its sweetness attributed to the presence of L,L-diastereomer. Chiral separation of neotame diastereomers (L,L and D,D) was accomplished by adding heptakis 2,3,6 tri-o-ethylbetacyclodextrin to the BGE. The developed method was applied to the analysis of different neotame-spiked fruit juices and drinks.

14 Microchip CE (MCE) technology in food analysis

MCE has continued demonstrating its potential for in situ analysis and fast multiparameter analysis. In the last years, novel developments and application of MCE have kept growing and several reviews have been published focusing on the application of this technology to the field of nutrition [224], food analysis [225], as well as to other specific food issues such as the analysis of transgenic food [11]. In addition, the use of multidimensional carbon allotropes as electrochemical detectors in MCE has been recently reviewed by Martín et al. [226]. As it has been discussed in the section devoted to DNA analysis, a growing number of applications of commercial instruments based on microfluidic CE have been reported in last years. In the present section, however, the attention will be focused on the technical advances in MCE, including new materials, designs, and detection systems.

Achieving good sensitivity has been a major challenge in MCE due to the small sample volumes used in microchip

devices. Since the beginning of this technology, LIF detection has been widely exploited owing to its easy focusing and inherent sensitivity. Recently, interesting developments have been published on the use of LIF detection in MCE. For instance, Barrios-Romero et al. [227] developed a SDS-gel electrophoresis method on SU8 microchips for the separation of three whey proteins (α-lactalbumin, β-lactoglobulin, and BSA). Authors used a commercial coating to control the EOF and a low-viscosity solution of dextran as a sieving polymer. In that work, proteins were first derivatized with the fluorogenic reagent Chromeo P540, and then separated and detected by flurescence using a laser with emission at 532 nm. In a separate report, Wei et al. [228] used disposable cyclic olefin copolymer microchips and a low-cost LIF detector system for the detection of glyphosate and glufosinate herbicides. The method involved analyte derivatization and the use of a sieving buffer containing 10 mM borax and 2.0% *m/v* hydroxypropyl cellulose at pH 9.0. The method, tested in spiked water, soybean, and broccoli samples, showed good sensitivity and recovery values without any preconcentration involved, indicating its good applicability to real samples.

Electrochemical detection has also gained relevance in the last years, and different MCE systems have been implemented using amperometry and conductometry approaches. Among the main advantages of electrochemical systems are the easy to miniaturize without loss of performance, high compatibility with microfabrication techniques and good sensitivity. These advantages have been achieved with the microfabrication of a portable lab-on-a-chip device with C^4D detection for on-site analysis of ten commonly found organic and inorganic acids in apple juice [229]. The microchip device allowed the quantification of anions that matched closely to what was stated on the beverage packaging. The RSD values for migration time and peak area were lower than 3 and 5%, respectively, showing an acceptable reproducibility. Contactless conductivity detection has been also integrated in a MCE device that allows sample extraction, injection, separation and detection to be automatically performed in sequence [230]. The system consisted of a glass microfluidic chip with a PDMS substrate embedded with an SPE monolithic column with MIP for analyte extraction. This novel microchip was successfully applied to analyze auramine O in shrimp. An excellent demonstration of the suitability of MCE technology for real-life applications has been provided by Castañeda et al. [231]. In their report, authors present a novel SU-8/pyrex-based microchip with integrated ED for evaluating the antioxidant capacity of polyphenol-enriched herbal extracts. Using a running buffer containing 25 mM 2-(*N*-morpholino)ethanesulfonic acid at pH 5.0, total flavonoids, and total phenolic acids migrated into two separated peaks, respectively, allowing a class-selective electrochemical index determination of total indexes for each structure classes (flavonoids and acids). A simplified calibration protocol using hesperidin and chlorogenic acid was used to calculate total flavonoid and total acid contents in real samples. The proposed MCE approach provided results that were in agreement with those obtained by HPLC, but comparatively with shorter analysis time and avoiding the use of toxic solvents. Another interesting application by García and Escarpa [232] was the AD monossacharides in honey samples using MCE and copper nanowires. This approach presented reduced analysis times (4 min) and LODs that were between 5 and 22 times lower than other approaches opening new perspectives for emerging applications of this technology in food analysis. In addition to the good potential offered by fluorescence and electrochemical detection for MCE coupling, other alternatives have been explored in the food analysis field. For instance, ICP-MS has been coupled to a MCE device for the determination of bromate and bromide in bread samples [233]. This bromide speciation method operated with separations conditions for FASI technique providing analysis in 35 s with enrichment factors higher than 12.

15 Foodomics and other future trends of CE in food analysis

Foodomics involves the development, use and integration of omics approaches (mainly, transcriptomics, proteomics, and metabolomics) to investigate food science and nutrition aiming to improve consumer's well-being, health, and knowledge (see Fig. 5). Foodomics applies these advanced tools to boost food science investigations, including those related to speed up the resolution of food safety issues, to improve food quality and food traceability and, to understand the bioactivity of food and food ingredients in our body at molecular level. In this context, the important role that CE- and CE-MS-based methods can play in Foodomics has already been identified [234–238]. Besides the review papers on Foodomics that have come out in the period covered by this work and described in Table 1, several book chapters have been also devoted to discuss this topic [239–242]. The use of CE-MS for metabolomics has corroborated the great possibilities of this technique in Foodomics [243]. Thus, the optimization of an effective CE-MS protocol for cell metabolomics was demonstrated by our group [244]. The feasibility of the whole method for cell metabolomics was proved via a fast and sensitive profiling of the intracellular metabolites of HT-29 colon cancer cells. The suitability of this methodology was further corroborated through the examination of the metabolic changes in the polyamines pathway produced in HT-29 colon cancer cells by difluoromethylornithine (DFMO), a known potent ornithine decarboxylase inhibitor. The selection of the optimum extraction conditions allowed a higher sample volume injection that led to an increase in CE-MS sensitivity. Following a nontargeted metabolomics approach, ten metabolites (namely, putrescine, ornithine, GABA, oxidized, and reduced glutathione, 5'-deoxy-5'-(methylthio)adenosine, N-acetylputrescine, cysteinyl-glycine, spermidine, and an unknown compound) were found to be significantly altered by DFMO ($p < 0.05$) in HT-29 cells. In addition to the effect of DFMO on polyamine metabolism, minor modifications of other metabolic pathways (e.g. related to intracellular thiol redox state) were observed [244].

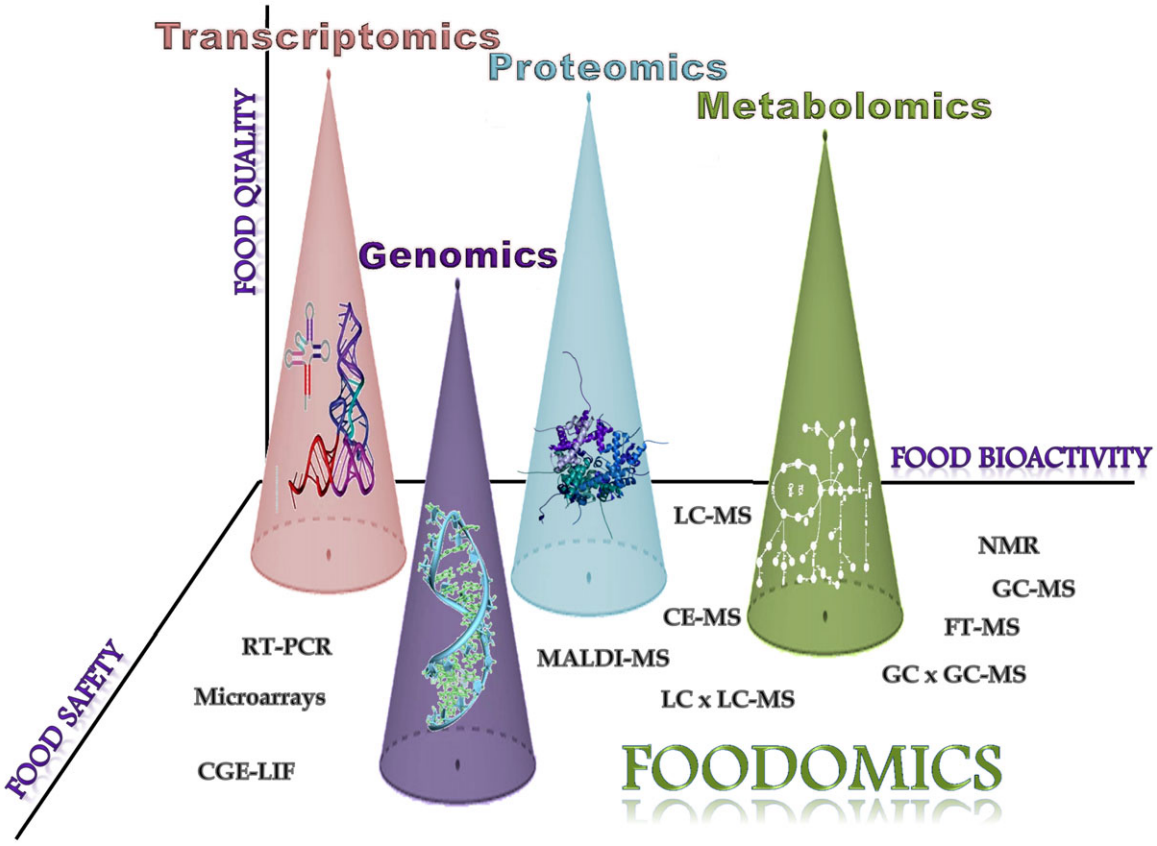

Figure 5. Scheme of Foodomics including the main tools employed and fields of application.

Following the pioneering works on the use of CE-MS for metabolomics of wild and transgenic maize and soybean [245–247], more recently, seed metabolomic and ionomic diversity was investigated in a soybean lineage representing 35 years of breeding (launch years 1972–2008). Six conventional and three GM glyphosate-tolerant lines were selected and investigated using several hyphenated techniques including CE-MS [248]. According to these authors, metabolomics successfully differentiated between the newer and older soybean. Correlation analysis also revealed associations between yield data and specific metabolites. However, their results did not show clear metabolic differences between the conventional and GM lines [248], contrarily with what has already been observed by other authors for transgenice maize and soybean [246–248].

Several of the Foodomics works recently published have involved the use of NMR [249–251] or other liquid techniques (e.g. UHPLC, nano-LC) hyphenated to HRMS [252–254]. Interestingly, several of the analytical steps necessary to carry out a metabolomic analysis are common among these hyphenated techniques, including the data treatment. In this regard, the development of new data analysis strategies is also mandatory. Thus, classical two dimensional representations of CE-MS, LC-MS, or GC-MS data (e.g. base peak electropherogram/chromatogram or total ion electropherogram/chromatogram), usually hide a large number of features that if correctly assessed will show the presence of comigrating species and/or the low abundant ones. The development of new peak picking algorithms able to detect and measure as many peaks as possible from a dataset allows extracting much more information. A good example of these new approaches is a new algorithm called centergram, which squeezes data from CE-MS (LC-MS or GC-MS) and allows detecting a number of peaks threefold higher compared to the standard procedures [255].

In a recent Foodomics work from our group, the variations of genes and metabolites were simultaneously investigated and integrated in order to understand (and to explain at molecular level) the effect of CA and carnosol, two major compounds present in rosemary, against colon cancer HT-29 cells proliferation. The Foodomics study revealed that CA induced transcriptional activation of genes that encode detoxifying enzymes and altered the expression of genes linked to transport and biosynthesis of terpenoids in the colon cancer cell line. Functional analysis highlighted the activation of the reactive oxygen species metabolism and alteration of several genes involved in pathways describing oxidative degradation of relevant endogenous metabolites, providing new evidences about the transcriptional change induced by CA in HT-29 cells. Metabolomics analysis carried out using LC-MS and CE-MS, showed that the treatment with CA affected the intracellular levels of glutathione. Elevated levels of glutathione

provided additional evidences to transcriptomic results regarding chemopreventive response of cells to CA treatment. Moreover, the Foodomics approach was useful to establish the links between decreased levels of N-acetylputrescine and its degradation pathway at the gene level. The findings from this work and the predictions based on microarray data will help exploring novel metabolic processes and potential signaling pathways to further elucidate de effect of CA in colon cancer cells [256].

The works presented in this review demonstrate the relevant role of CE in food analysis and Foodomics over the last two years. It is expected that the number of new CE developments applicable to food analysis will keep growing to overcome the still existing limitations of this technique, mainly, its limited sensitivity and low reproducibility. On the other hand, the limitations generated by the current bioinformatic tools, the lack of information in the databases (e.g. on the identity of many metabolites), our poor knowledge on many molecular processes taking place in cells, or the difficulty to combine the huge data generated by transcriptomics, proteomics, and metabolomics approaches (e.g. via systems biology) are still critical issues for Foodomics as well as for any holistic approach that encompass the integration of big data from several levels of expression. In spite of these limitations, the global outlook that Foodomics proposes is a good response to solve many of the complex issues and challenges in current and future food science.

As a proof of its usefulness, since the first definition of Foodomics in 2009 in a SCI journal, the use of omic approaches in food science and nutrition has quantitatively evolved and grown as can be easily checked in any database or search-engine. The Foodomics concept has also become more and more popular, because it is the ideal frame and distinctive stamp of any work in which an omic approach is used to investigate safety, quality, traceability, or bioactivity of food.

This work was supported by the project AGL2014-53609-P (Ministerio de Economía y Competitividad, Spain). T. A. thanks the CAPES Foundation, Ministry of Education of Brazil for her pre-doctoral Scholarship - Proc. N° 1532/13-8.

The authors have declared no conflict of interest.

16 References

[1] García-Cañas, V., Simó, C., Castro-Puyana, M., Cifuentes, A., *Electrophoresis* 2014, *35*, 147–169.

[2] Castro-Puyana, M., García-Cañas, V., Simó, C., Cifuentes, A., *Electrophoresis* 2012, *33*, 147–167.

[3] Herrero, M., García-Cañas, V., Simó, C., Cifuentes, A., *Electrophoresis* 2010, *31*, 205–228.

[4] García-Cañas, V., Cifuentes, A., *Electrophoresis* 2008, *29*, 294–309.

[5] Cifuentes, A., *J. Chromatogr. A* 2009, *1216*, 7109–7110.

[6] Kleparnik, K., *Electrophoresis* 2015, *36*, 159–178.

[7] Ramautar, R., Somsen, G.W., deJong, G. J., *Electrophoresis* 2015, *36*, 212–224.

[8] Kuban, P., Hauser, P. C., *Electrophoresis* 2015, *36*, 195–211.

[9] Simó, C., Ibáñez, A., Valdés, A, Cifuentes, A., García-Cañas, V., *Int. J. Mol. Sci.* 2014, *15*, 18941–18966.

[10] Zhang, Z., Yu, L., Xu, L., Hu, X., Li, P., Zhang, Q., Ding, X., Feng, X., *Electrophoresis* 2014, *35*, 1547–1559.

[11] Vega, E. D., Marina, M. L., *Int. J. Mol. Sci.* 2014, *15*, 23851–23877.

[12] Rojano-Delgado, A. M., Luque de Castro, M. D., *Electrophoresis* 2014, *35*, 2509–2519.

[13] Rodriguez Robledo, V., Smyth, W. F., *Electrophoresis* 2014, *35*, 2292–2308.

[14] Kitagawa, F., Otsuka, K., *J. Chromatogr. A* 2014, *1335*, 43–60.

[15] Montealegre, C., Verardo, V., Marina, M. L., Caboni, M. F., *Electrophoresis* 2014, *35*, 779–792.

[16] Piñero, M. Y., Bauza, R., Arce, L., Valcárcel, M., *Talanta* 2014, *119*, 75–82.

[17] Wuethrich, A., Haddad, P. R., Quirino, J. P., *Electrophoresis* 2014, *35*, 2–11.

[18] Domínguez-Vega, E., Pérez-Fernández, V., Crego, A. L., García, M. A., Marina, M. L., *Electrophoresis* 2014, *35*, 28–49.

[19] Poinsot, V., Ong-Meang, V., Gavard, P., Couderc, F., *Electrophoresis* 2014, *35*, 50–68.

[20] Tubaon, R. M. S., Rabanes, H., Haddad, P. R., Quirino, J. P., *Electrophoresis* 2014, *35*, 190–204.

[21] Zhao, J., Hu, D. J., Lao, K., Yang, Z. M., Li, S. P., *Electrophoresis* 2014, *35*, 205–224.

[22] Valdés, A., Simó, C., Ibáñez, C., García-Cañas, V., *Trac-Trend. Anal. Chem.* 2013, *52*, 2–15.

[23] Hu, C., Xu, G., *Trac-Trend. Anal. Chem.* 2013, *52*, 36–46.

[24] Ibáñez, C., García-Cañas, V., Valdés, A., Simó, C., *Trac-Trend. Anal. Chem.* 2013, *52*, 100–111.

[25] Rocco, A., Aturki, Z., Fanali, S., *Trac-Trend. Anal. Chem.* 2013, *52*, 206–225.

[26] Erim, F. B., *Trac-Trend. Anal. Chem.* 2013, *52*, 239–247.

[27] Ibáñez, C., Simó, C., García-Cañas, V., Cifuentes, A., Castro-Puyana, M., *Anal. Chim. Acta*, 2013, *802*, 1–13.

[28] Mozzi, F., Ortiz, M. E., Bleckwedel, J., De Vuyst, L., Pescuma, M., *Food Res. Int.* 2013, *54*, 1152–1161.

[29] Ou, G., Feng, X., Du, W., Liu, X., Liu, B. F., *Anal. Bioanal. Chem.* 2013, *405*, 7907–7918.

[30] Mandrioli, R., Mercolini, L., Raggi, M. A., *Anal. Bioanal. Chem.* 2013, *405*, 7941–7956.

[31] Chiu, T-C., *Anal. Bioanal. Chem.* 2013, *405*, 7919–7930.

[32] Dąbrowska, M., Starek, M., *Food. Chem.* 2014, *142*, 220–232.

[33] Alhusban, A. A., Breadmore, M. C., Guijt, R. M., *Electrophoresis* 2013, *34*, 1465–1482.

[34] Turkia, H., Sirén, H., Penttilä, M., Pitkänen, J. P., *Talanta* 2015, *131*, 366–371.

[35] Enzonga, J., Ong-Meang, V., Couderc, F., Boutonnet, A., Poinsot, V., Tsieri, M. M., Silou, T., Bouajila, J., *Electrophoresis* 2013, *34*, 2632–2638.

[36] Gao, Y. S., Hsieh, B. C., Cheng, T. J., Chen, R. L., *Food Chem.* 2015, *178*, 122–127.

[37] Tian, M., Zhang, J., Mohamed, A. C., Han, Y., Guo, L., Yang, L., *Electrophoresis* 2014, *35*, 577–584.

[38] Lin, W-C., Liu, W-L., Tang, W-Y., Huang, C-P., Huang, H-Y., Chin, T-Y., *Electrophoresis* 2014, *35*, 1751–1755.

[39] Akamatsu, S., Mitsuhashi, T., *J. Food Comp. Anal.* 2013, *30*, 47–51.

[40] Rodríguez-Bencomo, J. J., Andújar-Ortiz, I., Moreno-Arribas, M. V., Simó, C., González, J., Chana, A., Dávalos, J., Pozo-Bayón, M. A., *J. Agric. Food Chem.* 2014, *62*, 1373–1383.

[41] An, D., Chen, Z., Zheng, J., Chen, S., Wang, L., Huang, Z., Weng L., *Food Chem.* 2015, *168*, 1–6.

[42] Xie, J., Li, Y., Zhang, J., Zeng, L., Lu, D., Liu, Y., Yang, Y., Sun, C., *Anal. Methods* 2014, *6*, 5140–5146.

[43] Kašička V., *Electrophoresis* 2014, *35*, 69–95.

[44] Mesbah, K., Verpillot, R., de L'escaille, F., Falmagne, J. B., Taverna, M., *Methods Mol. Biol.* 2013, *984*, 167–190.

[45] Righetti, P. G., Sebastiano, R., Citterio, A., *Proteomics* 2013, *13*, 325–34.

[46] Ali, I., Al-Othman, Z. A., Al-Warthan, A., Asnin, L., Chudinov, A., *J. Sep. Sci.* 2014, *37*, 2447–2466.

[47] Zhao, S. S., Chen, D. D., *Electrophoresis* 2014, *35*, 96–108.

[48] Puangpila, C., Mayadunne, E., El Rassi, Z., *Electrophoresis* 2015, *36*, 238–252.

[49] Stuknytė, M., Cattaneo, S., Masotti, F., De Noni, I., *Food Chem.* 2015, *168*, 27–33.

[50] Korhonen, H., Pihlanto, A., *Int. Dairy J.* 2006, *16*, 945–960.

[51] Català-Clariana, S., Benavente, F., Giménez, E., Barbosa, J., Sanz-Nebot, V., *Electrophoresis* 2013, *34*, 1886–1894.

[52] Mansor, R., Mullen, W., Albalat, A., Zerefos, P., Mischak, H., Barrett, D. C., Biggs, A., Eckersall, P. D., *J. Proteomics* 2013, *85*, 89–98.

[53] Johansson, M., Åkerstedt, M., Li, S., Zamaratskaia, G., Sternesjö Lundh, Å., *J. Food Prot.* 2013, *76*, 1638–1642.

[54] Meza-Nieto, M. A., González-Córdova, A. F., Piloni-Martini, J., Vallejo-Cordoba, B., *J. Dairy Sci.* 2013, *96*, 6777–6681.

[55] Salmanowicz, B. P., Langner, M., Kubicka-Matusiewicz, H., *J. Agric. Food Chem.* 2014, *62*, 10535–10541.

[56] Katsube-Tanaka, T., *Methods Mol. Biol.* 2013, *984*, 253–261.

[57] Millioni, R., Franchin, C., Tessari, P., Polati, R., Cecconi, D., Arrigoni, G., *J. Chromatogr. A* 2013, *1293*, 1–9.

[58] Kristl, T., Stutz, H., *J. Sep. Sci.* 2015, *38*, 148–156.

[59] Kondeková, M., Maier, V., Ginterová, P., Marák, J., Sevčík, J., *Food Chem.* 2014, *153*, 398–404.

[60] Garrido-Medina, R., Puerta, A., Pelaez,-Lorenzo, C., Rivera-Monroy, Z., Guttman, A., Diez-Masa, J. C., de Frutos, M., *Methods Mol. Biol.* 2013, *984*, 207–225.

[61] Vergara-Barberán, M., Lerma-García, M. J., Herrero-Martínez, J. M., Simó-Alfonso, E. F., *Electrophoresis* 2014, *35*, 1652–1659.

[62] Montero, L., Herrero, M., Ibáñez, E., Cifuentes, A. *J. Chromatogr. A* 2013, *1313*, 275–283.

[63] Jiménez-Girón, A., Ibáñez, C., Cifuentes, A., Simó, C., Muñoz-González, I., Martín-Álvarez, P. J., Bartolomé, B., Moreno-Arribas, M. V., *J. Proteome Res.* 2015, *14*, 897–905.

[64] Artero, A., Artero, A., Tarín, J. J., Cano, A., *Maturitas* 2015, *80*, 3–13.

[65] Gomez, F. J., Monasterio, R. P., Vargas, V. C., Silva, M. F., *Electrophoresis* 2012, *33*, 2240–2252.

[66] Carluccio, M. A., Siculella, L., Ancora, M. A., Massaro, M., Scoditti, E., Storelli, C., Visioli, F., Distante, A., De Caterina, R., *Arterioscler. Thromb. Vasc. Biol.* 2003, *23*, 622–629.

[67] Franquet-Griell, H., Checa, A., Núñez, O., Saurina, J., Hernández-Cassou, S., Puignou, L., *J. Agric. Food Chem.* 2012, *60*, 8340–8349.

[68] Dias, F. D., Klassen, A., Tavares, M. F. M., David, J. M., *Chromatographia* 2013, *76*, 559–563.

[69] Arribas, A. S., Martínez-Fernández, M., Moreno, M., Bermejo, E., Zapardiel, A., Chicharro, M., *Electrophoresis* 2014, *35*, 1693–1700.

[70] Monasterio, R. P., de Los Angeles Fernández, M., Silva, M. F., *Electrophoresis* 2013, *34*, 1836–1843.

[71] de Fernandez, M. D., SotoVargas, V. C., Silva, M. F., *J. Am. Oil Chem. Soc.* 2014, *91*, 2021–2033.

[72] Ballus, C. A., Meinhart, A. D., Campos, F. A. D., da Silva, L. F. D., de Oliveira, A. F., Godoy, H. T., *Food Res. Int.* 2014, *62*, 74–83.

[73] Godoy-Caballero, M. P, Culzoni, M. J., Galeano-Díaz, T., Acedo-Valenzuela, M. I., *Anal. Chim. Acta* 2013, *763*, 11–19.

[74] Godoy-Caballero, M. P., Acedo-Valenzuela, M. I., Durán-Merás, I., Galeano-Díaz, T., *Anal. Bioanal. Chem.* 2012, *403*, 279–90.

[75] Godoy-Caballero, M. P., Galeano-Díaz, T., Acedo-Valenzuela, M. I., *J. Sep. Sci.* 2012, *35*, 3529–3539.

[76] Boiteux, J., Soto Vargas, C., Pizzuolo, P., Lucero, G., Silva, M. F., *Electrophoresis* 2014, *35*, 1709–1718.

[77] Maringer, L., Ibáñez, E., Buchberger, W., Klampfl, C. W., Causon, T. J., *Electrophoresis* 2015, *36*, 348–354.

[78] Cheng, T. O., *Int. J. Cardiol.* 2007, *121*, 9–22.

[79] Cao, J. L., Wei, J. C., Tian, K., Su, H. X., Wan, J. B., Li, P., *J. Sep. Sci.* 2014, *37*, 3738–3744.

[80] Koyama, M., Nakamura, C., Nakamura, K., *J. Food Sci.Technol.* 2013, *50*, 86–93.

[81] Rocco, A., Fanali, C., Dugo, L., Mondello, L., *Electrophoresis* 2014, *35*, 1701–1708.

[82] Navarro, M., Núñez, O., Saurina, J., Hernández-Cassou, S., Puignou, L., *J. Agric. Food Chem.* 2014, *62*, 1038–1046.

[83] Hurtado-Fernández, E., Contreras-Gutiérrez, P. K., Cuadros-Rodríguez, L., Carrasco-Pancorbo, A., Fernández-Gutiérrez, A., *Food Chem.* 2013, *141*, 3492–3503.

[84] Bustamante-Rangel, M., Delgado-Zamarreño, M. M., Carabias-Martínez, R., Domínguez-Álvarez, J., *Anal. Chim. Acta.* 2012, *709*, 113–119.

[85] da Rosa Neng, N., Sequeiros, R. C., Florêncio-Nogueira, J. M., *Electrophoresis* 2014, *35*, 2488–2494.

[86] González-Teuber, M., Heil, M., *Plant. Signal Behav.* 2009, *4*, 809–813.

[87] Soto, V. C., Fernandez, M. A., Galmarini, C. R., Silva, M. F., *Anal. Methods* 2014, *6*, 4878–4884.

[88] Piovezan, M., García-Seco, D., Micke, G. A., Gutiérrez-Mañero, J., Ramos-Solano, B., *Electrophoresis* 2013, *34*, 2251–2258.

[89] Siroka, J., Martincova, A., Pospisilova, M., Polasek, M., *Food Anal.Method* 2013, *6*, 1561–1567.

[90] Zhang, H. J., Kang, M. Q., Zhang, H. Q., Yu, Y., *Anal. Methods* 2014, *6*, 766–773.

[91] Lee, I. S. L., Boyce M. C., Breadmore M. C., *Food Chem.* 2012, *133*, 205–211.

[92] Khoddami, A., Wilkes, M. A., Roberts, T. H., *Molecules* 2013, *18*, 2328–2375.

[93] Liu, C. M., Chen, C. Y., Lin, Y. W., *Food Chem*. 2014, *150*, 145–150.

[94] Montealegre, C., Sánchez-Hernández, L., Crego, A. L., Marina, M. L., *J. Agric. Food Chem.* 2013, *61*, 1823–1832.

[95] Sirén, H., Vesanen, S., Suomi, J., *J. Chromatogr. B Analyt. Technol. Biomed. Life Sci.* 2014, *945*, 199–206.

[96] de Oliveira, M. A., Porto, B.L., Faria, I. D., de Oliveira, P. L., de Castro Barra, P. M., de Jesus Coelho Castro, R., Sato, R.T. *Molecules* 2014, *19*, 14094–14113.

[97] Wu, J., Ge, Y., Qin, W., *J. Agric. Food Chem.* 2014, *62*, 4104–4111.

[98] Buglione, L., See, H. H., Hauser, P.C., *Electrophoresis* 2013, *34*, 2072–2077.

[99] Sato, R. T., de Jesus Coelho Castro, R., de Castro Barra, P. M., de Oliveira, M. A. *Phytochem. Anal.* 2014, *25*, 241–246.

[100] Bockel, W. J., da Silva, Y. P., Mendonca, C. R. B., Simó-Alfonso, E. F., Ramis-Ramos, G., Piatnicki, C. M. S., *J. Brazil Chem Soc.* 2014, *25*, 1662–1666.

[101] Barra, P. M. D., de Oliveira, M. A. L., Nery-Enes, B., Cardoso, L. D., Cesario, C. D., Moreira, A. V. B., Pinheiro-Sant'Ana, H. M., Peluzio, M. D. G., *Quím. Nova* 2013, *36*, 1430–1433.

[102] Simopoulos, A. P. *Biomed. Pharmacother*. 2002, *56*, 365–379.

[103] Soliman, L. C., Donkor, K. K., Church, J. S., Cinel, B., Prema, D., Dugan, M. E., *J. Sep. Sci.* 2013, *36*, 3440–3448.

[104] Gebauer, S. K., Chardigny, J. M., Jakobsen, M. U., Lamarche, B., Lock, A.L., Proctor, S. D., Baer, D. J., *Adv. Nutr.* 2011, *2*, 332–354.

[105] Barra, P. M. D., Castro, R. D. C., de Oliveira, P. L., Aued-Pimentel, S., da Silva, S. A., de Oliveira, M. A. L., *Food Res. Int*. 2013, *52*, 33–41.

[106] Wong, Y. F., Saad, B., Makahleh, A., *J. Chromatogr. A* 2013, *1290*, 82–90.

[107] Galeano-Diaz, T., Acedo-Valenzuela, M. I., Silva-Rodriguez, A., *J. Food Compos. Anal.* 2012, *25*, 24–30.

[108] Gonda, S., Parizsa, P., Surányi, G., Gyémánt, G., Vasas, G., *J. Pharm. Biomed. Anal*. 2012, *66*, 68–74.

[109] El Rassi, Z., *Carbohydrate Analysis by Modern Chromatography and Electrophoresis*. Elservier, USA 2002.

[110] Vochyanova, B., Opekar, F., Tuma, P., Stulik, K., *Anal. Bioanal. Chem.* 2012, *404*, 1549–1554.

[111] Taga, A., Kodama, S., *Chromatographia* 2012, *75*, 17–18.

[112] Navarro-Pascual-Ahuir, M., Lerma-García, M. J., Simó-Alfonso, E. F., Herrero-Martínez, J. M., *J. Agric. Food Chem.* 2015, *63*, 2639–2646.

[113] Cebolla-Cornejo, J., Valcárcel, M., Herrero-Martínez, J. M., Roselló, S., Nuez, F., *Electrophoresis* 2012, *33*, 2416–2423.

[114] Rizelio, V. M., Tenfen, L., da Silveira, R., Gonzaga, L.V., Costa, A. C., Fett, R., *Talanta* 2012, *93*, 62–66.

[115] Toutounji, M. R., Van Leeuwen, M. P., Oliver, J. D., Shrestha, A. K., Castignolles, P., Gaborieau, M., *Carbohydr. Res.* 2015, *408*, 134–141.

[116] Sarazin, C., Delaunay, N., Costanza, C., Eudes, V., Gareil, P., *Talanta* 2012, *99*, 202–206.

[117] Kawahigashi, H., Kasuga, S., Okuizumi, H., Hiradate, S., Yonemaru, J., *Grassland Sci.* 2013, *59*, 11–19.

[118] Wang, T., Yang, X., Wang, D., Jiao, Y., Wang, Y., Zhao, Y., *Carbohyd. Polym.* 2012, *88*, 754–762.

[119] Guo, H. Z., Liu, F. L., Jia, G.Y., Zhang, W.Q., Wu, F., *J. Appl. Phycol*. 2013, *25*, 1903–1908.

[120] Moreno, F. J., Montilla, A., Villamiel, M., Corzo, N., Olano, A., *Electrophoresis* 2014, *35*, 1519–1534.

[121] Lee, H., Garrido, D., Mills, D. A., Barile, D., *Electrophoresis* 2014, *35*, 1742–1750.

[122] Oliveira, D. L., Wilbey, R. A., Grandison, A. S., Roseiro, L. B., *Food Bioprocess. Tech.* 2014, *7*, 915–920.

[123] Galeotti, F., Coppa, G.V., Zampini, L., Maccari, F., Galeazzi, T., Padella, L., Santoro, L., Gabrielli, O., Volpi, N., *Electrophoresis* 2014, *35*, 811–818.

[124] Kottler, R., Mank, M., Hennig, R., Müller-Werner, B., Stahl, B., Reichl, U., Rapp, E., *Electrophoresis* 2013, *34*, 2323–2336.

[125] Yang, Z. Y., Wang, H., Zhang, W., Wang, Q. J., He, P. G., Fang, Y. Z., *Chromatographia* 2012, *75*, 297–304.

[126] Hu, Y., Wang, T., Yang, X., Zhao, Y., *Carbohydr. Polym.* 2014, *102*, 481–488.

[127] Valdés, A., Ibáñez, C., Simó, C., García-Cañas, V., *Trends Anal. Chem.* 2013, *52*, 142–154.

[128] Garino, C, Rinaldi, M., de Paolis, A., Travaglia, F., Coïsson, J. D., Arlorio, M., *Food Res. Int.* 2014, *64*, 790–798.

[129] Spaniolas, S., Bazakos, C., Tucker, G. A., Bennett, M. J., *J. AOAC Int.* 2014, *97*, 1114–1120.

[130] Barakat, H., El-Garhy, H., Moustafa, M. M., *Appl. Microbiol. Biotechnol.* 2014, *98*, 9805–9816.

[131] Chen, C. H., Hsieh, C. H., Hwang, D. F., *Food Control.* 2013, *33*, 477–483.

[132] Uncu, A. T., Frary, A., Soganlar, S., *J. Agric. Food Chem.* 2015, *63*, 2284–2295.

[133] Dalmasso, A., Chiesa, F., Civera, T., Bottero, M. T., *Food Control* 2013, *34*, 296–299.

[134] Rodríguez-Ramírez, R., Valejo-Córdoba, B., Mazorra-Manzano, M. A., González-Córdova, A. F., *Anal. Methods* 2015, *7*, 530–537.

[135] Rolli, J., Girardet, S., Monachon, C., Richard, C., *Chimia* 2014, *68*, 726–731.

[136] García-Cañas, V., González, R., Cifuentes, A., *J. Sep. Sci.* 2002, *25*, 577–583.

[137] Basak, S., Ehtesham, N. Z., Sesikeran, B., Ghosh, S., *J. AOAC Int.* 2014, *97*, 159–165

[138] Ruan, J., Li, M., Liu, Y. P., Li, Y. Q., Li, Y. X., *J. Chromatogr. B* 2013, *921*, 15–20.

[139] Wang, Y., Ma, X., Ding, C., Jia, L., *Anal. Chim. Acta* 2015, *862*, 33–40.

[140] Alberice, J. V., Funes-Huacca, M. E., Carrilho, E., *J. Braz. Chem. Soc.* 2014, *25*, 91–97.

[141] da Silva, D. C., Visentainer, J. V., de Souza, N. E., Oliveira, C. C., *Food Anal.* 2013, *6*, 1592–1606.

[142] Serni, E., Audino, V., Del Carlo, S., Manera, C., Saccomanni, G., Macchia, M., *Nat. Prod. Res.* 2013, *3*, 2212–2215.

[143] Mu, G., Luan, F., Liu, H., Gao, Y., *Food Anal. Methods* 2013, *6*, 191–200.

[144] Parveen, S., Siyal, A. N., Memon, N., Memon, S. Q., Khuhawar, M. Y., *J. Liq. Chromatogr. Relat. Technol.* 2015, *38*, 143–152.

[145] Chen, J., Sun, J., Parveen, S., *Anal. Lett.* 2013, *46*, 887–899.

[146] Liu, A. X., Xu, Y., Hong, L., Yan, Y–M, Ye Wang, L. T., Cao, H., *J. Chem. Pharm. Res.* 2014, *5*, 1327–1330.

[147] Falkova, M. T., Bulatov, A. V., Pushina, M. O., Ekimov, A. A., Alekseeva, G. M., Moskvin, L. N., *Talanta* 2015, *133*, 82–87.

[148] Han, S., Wu, K., *J. Chin. Chem. Soc.* 2015, *62*, 73–78.

[149] Maráková, K., Piešťanský, J., Havránek, E., Mikuš, P., *Die Pharm. Int. J. Pharm. Sci.* 2014 *69*, 663–668.

[150] Azevedo, M. S., Pirassol, G., Fett, R., Micke, G. A., Vitali, L., Costa, A. C. O., *Food Res. Int.* 2014, *60*, 123–130.

[151] Gatea, F., Teodor, E. D., Paun, G., Matei, A. O., Radu, G. L., *Food Anal. Methods* 2015, *8*, 1335–1340.

[152] de Sena Aquino, A. C. M., Azevedo, M. S., Ribeiro, D. H. B., Costa, A. C. O., Amante, E. R., *Food Chem.* 2015, *172*, 725–730.

[153] Betta, F. D., Vitali, L., Fett, R. Costa, C. O., *Talanta* 2014, *122*, 23–29.

[154] Sun, J., Wang, D., Cheng, H., Liu, J., Wang, Y., Xu, Z., *J. Chromatogr. A* 2015, *1379*, 112–117.

[155] Qu, H., Mudalige, T. K., Linder, S. W., *Anal. Chem.* 2014, *86*, 11620–11627.

[156] Chmiel, T., Abogado, D., Wardencki, W., *Anal. Bioanal. Chem.* 2014, *20*, 4965–4986.

[157] Václavíková, E., Kvasnička, F., *Czech. J. Food Sci.* 2013, *1*, 55–65.

[158] Rodríguez-Gonzalo, E., Domínguez-Álvarez, J., Mateos-Vivas, M., García-Gómez, D., Carabias-Martínez, R., *Electrophoresis* 2014, *35*, 1677–1684.

[159] Berthiller, F., Burdaspal, P. A., Crews, C., Iha, M. H., Krska, R., Lattanzio, V. M. T., MacDonald, S., Malone, R. J., Maragos, C., Solfrizzo, M., Stroka, J., Whitaker, T. B., *World Mycotoxin. J.* 2014, *7*, 3–33.

[160] Güray, T., Tuncel, M., Uysal, U. D., *J. Chromatogr. Sci.* 2013, *51*, 310–317.

[161] Güray, T., Tuncel, M., Uysal, U. D., Oncu-Kaya, E.M., *J. Liq. Chromatogr. Related Technol.* 2013, *36*, 1366–1378.

[162] Sassolas, A., Hayat, A., Catanante, G., Marty, J. L., *Talanta* 2013, *105*, 306–316.

[163] Abdul Keyton, A. S. A., Guijt, R. M., Gaspar, A., Kazarian, A. A., Nesterenko, P. N., Bolch, C. J., Breadmore, M. C., *Electrophoresis* 2014, *35*, 1496–1503.

[164] Keyton, A. S. A, Guijt, R. M., Bolch, C. J. S., Breadmore, M. C., *J. Chromatogr. A* 2014, *1364*, 295–302.

[165] Zhang, Z., Li, X., Ge, A., Zhang, F., Sun, X., Li, X., *Biosens. Bioelectron.* 2013, *41*, 452–458.

[166] Zhang, Z., Liu, Y., Zhang, C., Luan, W., *Toxicon* 2015, *96*, 89–95

[167] Keyton, A. S. A., Guijt, M. R., Bolch, C. J., Breadmore, M. C., *Anal. Chem.* 2014, *86*, 11811–11818.

[168] Raina-Fulton, R., *J. AOAC Int.* 2014, *97*, 965–977.

[169] Puzio, K., Claude, B., Amalric, L., Berho, C., Grellet, E., Bayoudh, S., Nehmé, R., Morin, P., *J. Chromatogr. A* 2014, *1361*, 1–8

[170] Sung, I. H., Lee, Y. W., Chung, D. S., *Anal. Chim. Acta* 2014, *838*, 45–50.

[171] Kukusamude, C., Srijaranai, S., Kato, M., Quirino, J. P., *J. Chromatogr. A* 2014, *1351*, 110–114.

[172] Springer, V. H., Aprile, F., Lista, A.G., *Food Chem.* 2014, *143*, 348–353.

[173] Daniel, D., dos Santos, V. B., Rajh Vidal, D. T., do Lago, C. L., *Food Chem.* 2015, *175*, 82–84.

[174] Hu, Y., *J. Chromatogr. B* 2015, *986*, 143–148.

[175] Soliman, L. C., Donkor, K. K., *J. Environm. Sci. Health* 2014, *49*, 153–158.

[176] Zhao, T., Gao, H., Wang, X., Zhang, L., Qiao, X., Xu, Z., *Food Anal. Methods* 2014, *7*, 1159–1165.

[177] Springer, V., Jacksén, J., Ek, P., Lista, A. G., Emmer, A., *J. Sep. Sci.* 2014, *37*, 158–164.

[178] Tian, J., Hu, J., Yang, F., Tang, T., Guo, J., Qin, W., *Food Chem.* 2014, *157*, 498–503.

[179] Moreno-González, D., Lara, F. J., Gámiz-Gracia, L., García-Campaña, A. M., *J. Chromatogr. A* 2014, *1360*, 1–18

[180] Springer, V., Jacksén, J., Ek, P., Lista, A.G., Emmer, A., *Chromatographia* 2015, *78*, 285–290

[181] Deng, Y., Gasilova, N., Qiao, L., Zhou, Y. L., Zhang, X. X., Girault, H. H., *Electrophoresis* 2014, *35*, 3355–3362.

[182] Xu, X., Liu, L., Jia, Z., Shu, Y., *Food Chem.* 2015, *176*, 219–225.

[183] Meng, H. L., Chen, G. H., Guo, X., Chen, P., Cai, Q. H., Tian, Y. F., *Anal. Bioanal. Chem.* 2014, *406*, 3201–3208.

[184] Liu, C., Feng, X., Qian, H., Fang, G., Wang, S., *Food Anal. Methods* 2015, *8*, 596–603.

[185] Ye, N., Shi, P., Wang, Q., Li, J., *Chromatography* 2013, *76*, 553–557.

[186] Polo-Luque, M. L., Simonet, B. M., Valcáercel, M., *Analyst* 2013, *138*, 3786–3791.

[187] Sun, H., Haijing, Q., Li, H., *Food Anal. Methods* 2013, *6*, 1049–1055.

[188] Hernández-Mesa, M., García-Campaña, A. M., Cruces-Blanco, C., *Food Chem.* 2014, *145*, 161–167.

[189] Zhai, H., Zhang, L., Pan, Y., Yuan, K., Huang, L., Yu, X., *Chromatogr.* 2015, *78*, 551–556.

[190] Alenazi, N. A., Manthorpe, J. M., Lai, E. P. C., *Food Control* 2015, *50*, 778–783.

[191] Wang, H., Zhang, A., Wang, W., Zhang, M., Liu, H., Wang, X., *J. AOAC Int.* 2013, *96*, 459–465.

[192] Browne, D. J., Zhou, L., Luong, J. H. T., Glennon, J. D., *Electrophoresis* 2013, *34*, 2025–2032.

[193] Wang, C. C., Lu, C. C., Chen, Y. L., Cheng, H. L., Wu, S. M., *J. Agric. Food Chem.*, 2013, *61*, 5914–5920.

[194] Martínez-Villalba, A., Núñez, O., Moyano, E., Galcerán, M. T., *Electrophoresis* 2013, *34*, 870–876.

[195] Alshana, U., Göger, N.G., Ertas, N., *Food Chem.* 2013, *138*, 890–897.

[196] Sáiz, J., Ortega-Ojeda, F., López-Melero, L., Montalvo, G., García-Ruiz, C., *Electrophoresis* 2014, *35*, 3250–3257.

[197] Vistuba, J. P., Dolzan, M. D., Vitali, L., de Oliveira, M. A., Micke, G. A., *J. Chromatogr. A* 2015, *1396*, 148–52.

[198] Fernandes, V. N. O., Fernandes, L. B., Vasconcellos, J. P., Jager, A.V., Tonin, F. G., de Oliveira, M. A. L., *Anal. Method.* 2013, *5*, 1524–1532.

[199] Stojkovic, M., Mai, T. D., Hauser, P. C., *Anal. Chim. Acta* 2013, *787*, 254–259.

[200] Hu, F., Xu, L., Luan, F., Liu, H., Gao, Y., *J. Sci. Food Agric.* 2013, *93*, 3334–3338.

[201] Xue, H., Zhang, H., Liang, L., Yang, J., Shen, L., Tao, Z., *J. Food Sci. Biotechnol.* 2014, *33*, 315–320.

[202] Ding, X. J., Xie, N., Zhao, S., Wu, Y. C., Li, J., Wang, Z., *Food Chem.* 2015, *181*, 207–214.

[203] Hsu, S. H., Hu, C. C., Chiu, T. C., *Anal. Bioanal. Chem.* 2014, *406*, 635–641.

[204] Jastrzebska, A., Kurzawa, M., Hrynczyszyn, P., Szlyk, E., *J. Anal. Chem.* 2012, *67*, 172–178.

[205] Sun, B., Qi, L., Wang, M., *J. Sep. Sci.* 2014, *37*, 2248–2252.

[206] Soni, M. G., Taylor, S. L., *Food Chem Toxicol.* 2002, *40*, 1335–1373.

[207] Alshana, U., Ertaş, N., Göğer, N. G., *Food Chem.* 2015, *181*, 1–8.

[208] Maijó, I., Borrull, F., Aguilar, C., Calull, M., *Electrophoresis* 2013, *34*, 363–373.

[209] Guo, D. S., Chen, G. H., Tong, M. Z., Wu, C. Q., Fang, R., Yi, L. X., *Chinese J. Anal. Chem.* 2012, *40*, 1379–1384.

[210] Zhang, Y., Tian, X., Guo, Y., Li, H., Yu, A., Deng, Z., Sun, B. B., Zhang, S., *J. Agric. Food Chem.* 2014, *62*, 3400–3404.

[211] Zhang, Y., Chang, C., Guo, Q., Cao, H., Bai, Y., Liu, H., *Se. Pu.* 2014, *32*, 438–442.

[212] Liu, F. J., Liu, C. T., Li, W., Tang, A. N., *Talanta* 2015, *132*, 366–372.

[213] Fukuji, T. S., Castro-Puyana, M., Tavares, M. F. M., Cifuentes, A., *Electrophoresis* 2012, *33*, 705–712.

[214] Long, W., Cen, Y., Wang, X., Bai, Y., Liu, H., *Se. Pu.* 2012, *30*, 747–751.

[215] Ananingsih, V. K., Sharma, A., Weibiao Z., *Food Res. Int.* 2013, *50*, 469–479.

[216] Bignardi, C., Cavazza, A., Corradini, C., *Food Cont.* 2014, *46*, 41–48.

[217] Diblikova, L., Curda, L., Kincl, J. T., *Int. Dairy J.* 2013, *31*, 29–33.

[218] Contreras-Gutierrez, P. K., Hurtado-Fernandez, E., Gomez-Romero, M., Hormaza, J. I., Carrasco-Pancorbo, A., Fernandez-Gutierrez, A., *Electrophoresis* 2013, *34*, 2928–2942.

[219] da Silveira Petruci, J. F., Pereira, E. A., Cardoso, A. A., *J. Agric. Food Chem.* 2013, *61*, 2263–2267.

[220] Stavrou, I. J., Mavroudi, M. C., Kapnissi-Christodoulou, C. P., *Electrophoresis* 2015, *36*, 101–123.

[221] Tezcan, F., Uzaşçı, S., Uyar, G., Öztekin, N., Erim, F. B., *Food Chem.* 2013, *141*, 1187–1191.

[222] Sun, B. B., Qi, L., Mu, X. Y., Qiao, J., Wang, M. L., *Talanta* 2013, *116*, 1121–1125.

[223] Bathinapatla, A., Kanchi, S., Singh, P., Sabela, M. I., Bisetty, K., *Anal. Lett.* 2014, *47*, 2795–2812.

[224] Li, S., Kiehne, J., Sinoway, L. I., Cameron, C. E., Huang, T. J., *Lab Chip* 2013, *13*, 3933–4003.

[225] Escarpa, A., *Lab Chip* 2014, *14*, 3213–3224.

[226] Martín, A., López, M. A., González, M. C., Escarpa, A., *Electrophoresis* 2015, *36*, 179–194.

[227] Barrios-Romero, M. M., Crevillén, A. G., Diez-Masa, J. C., *J. Sep. Sci.* 2013, *36*, 2530–2537.

[228] Wei, X., Gao, X., Zhao, L., Peng, X., Zhou, L., Wang, J., Pu, Q., *J. Chromatogr. A* 2013, *1281*, 148–154.

[229] Ansari, K., Shu Ying, J. Y., Hauser, P. C., de Rooij, N. F., Rodriguez, I., *Electrophoresis* 2013, *34*, 1390–1399.

[230] Zhai, H., Li, J., Chen, Z., Su, Z., Liu, Z., Yu, X., *Microchem. J.* 2014, *114*, 223–228.

[231] Castañeda, R., Vilela, D., González, M. C., Mendoza, S., Escarpa, A., *Electrophoresis* 2013, *34*, 2129–2135.

[232] García, M., Escarpa, A., *Electrophoresis* 2014, *35*, 425–432.

[233] Cheng, H., Han, C., Xu, Z., Liu, J., Wang, Y., *Food Anal. Methods* 2014, *7*, 2153–2162.

[234] García-Cañas, V., Simó, C., Herrero, M., Ibáñez, E., Cifuentes, A., *Anal. Chem.* 2012, *84*, 10150–10159.

[235] Herrero, M., Simó, C., García-Cañas, V., Ibáñez, E., Cifuentes, A., *Mass Spectrom. Rev.* 2012, *31*, 49–69.

[236] Ibáñez, C., Valdés, A., García-Cañas, V., Simó, C., Celebier, M., Rocamora, L., Gómez, A., Herrero, M., Castro, M., Segura-Carretero, A., Ibáñez, E., Ferragut, J., Cifuentes, A., *J. Chrom. A* 2012, *1248*, 139–153.

[237] Valdés, A., Simó, A., Ibáñez, A., Rocamora, A., Ferragut, A., García-Cañas, V., Cifuentes, A., *Electrophoresis* 2012, *33*, 2314–2327.

[238] Cifuentes, A., *Electrophoresis* 2014, *35*, 1517–1518.

[239] Simó, C., Cifuentes, A., Kasicka, V., in: Volpi, N., Maccari, F. (Eds.), *Capillary Electrophoresis of Biomolecules, Methods and Protocols*. Humana Press, New York 2013, pp. 139–151.

[240] Cifuentes, A., in: Cifuentes, A. (Ed.), *Foodomics: Advanced Mass Spectrometry in Modern Food Science and Nutrition*, John Wiley & Sons, Hoboken 2013, pp. 1–13.

[241] Valdés, A., Cifuentes, A., García-Cañas, V., in: Benkeblia, N. (Ed.), *Omics Technologies and Crop Improvement*, CRC Press, Boca Raton 2014, pp. 15–43.

[242] Ibáñez, E., Cifuentes, A., in: Garcia-Cañas, V., Cifuentes, A., Simó, C. (Eds), *Applications of Advanced Omics Technologies: From Genes to Metabolites*, Elsevier, Amsterdam 2014, pp. 395–440.

[243] Hirayama, A., Wakayama, M., Soga, T., *TrAC-Trends Anal. Chem.* 2014, *61*, 215–222.

[244] Ibáñez, C., Simó, C., Valdés, A., Campone, L., Piccinelli, A. L., García-Cañas, V., Cifuentes, A., *J. Pharmaceut. Biomed.* 2015, *110*, 83–92.

[245] García-Villalba, R., León, C., Dinelli, G., Segura, A., Fernández, A., Garcia-Cañas, V., Cifuentes; A., *J. Chromatogr. A* 2008, *1195*, 164–173.

[246] Levandi, T., Leon, C., Kaljurand, M., Garcia-Cañas, V., Cifuentes. A., *Anal. Chem.* 2008, *80*, 6329–6335.

[247] Leon, C., Rodriguez, I., Lucio, M., Garcia-Cañas, V., Ibañez, E., Schmitt-Kopplin, P., Cifuentes, A., *J. Chromatogr. A* 2009, *1216*, 7314–7323.

[248] Kusano, M., Baxter, I., Fukushima, A., Oikawa, A., Okazaki, Y., Nakabayashi, R., Bouvrette, D. J., Achard, F., Jakubowski, A. R., Ballam, J. M., *Metabolomics* 2015, *11*, 261–270.

[249] Melis, R., Anedda, R., *Electrophoresis* 2014, *35*, 1590–1598.

[250] Bordoni, A., Laghi, L., Babini, E., Di Nunzio, M., Picone, G., Ciampa, A., Valli, V., Danesi, F., Capozzi, F., *Electrophoresis* 2014, *35*, 1607–1614.

[251] Capitani, D., Sobolev, A. P., Delfini, M., Vista, S., Antiochia, R., Proietti, N., Bubici, S., Carradori, S., De Salvador, F. R., Mannina, L., *Electrophoresis* 2014, *35*, 1615–1626.

[252] Abu-Reidah, I. M., del Mar Contreras, M., Arraez-Roman, D., Fernandez-Gutierrez, A., Segura-Carretero, A., *Electrophoresis* 2014, *35*, 1571–1581.

[253] LeParc, A., Dallas, D. C., Duaut, S., Leonil, J., Martin, P., Barile, D., *Electrophoresis* 2014, *35*, 1560–1570.

[254] Sanchez-Rivera, L., Diezhandino, I., Gomez-Ruiz, J. A., Fresno, J. M., Miralles, B., Recio, I., *Electrophoresis* 2014, *35*, 1627–1636.

[255] Erny, G. L., Simó, C., Cifuentes, A., Esteves; V. I., *J. Chromatogr. A* 2014, *1330*, 89–96.

[256] Valdés, A., García-Cañas, V., Simó, C., Ibáñez, C., Ferragut, J. A., Micol, V., Cifuentes, A., *Anal. Chem.* 2014, *86*, 9807–9815.

CAPÍTULO 2

Objetivos

2. OBJETIVOS

La presente Tesis Doctoral profundiza en los desarrollos metodológicos y aplicaciones en el campo de la metabolómica para el estudio de compuestos bioactivos de la dieta y sus efectos sobre la salud.

Los principales objetivos de este trabajo son:

- Desarrollar nuevas metodologías mediante CE-MS para aplicaciones Alimentómicas.

- Emplear la metabolómica como herramienta para obtener información del efecto de compuestos bioactivos de romero en células hepáticas HepaRG a nivel molecular.

Los objetivos parciales, el plan de trabajo para lograr dichos objetivos y los resultados obtenidos están descritos detalladamente en los Capítulos 3 y 4 de esta Tesis Doctoral. En concreto, el Capítulo 3 contiene cuatro trabajos, en los cuales se demuestra el potencial del acoplamiento CE-MS en el análisis de alimentos y Alimentómica, y en los que se han desarrollado nuevas estrategias analíticas basadas en CE-MS para aplicaciones en este campo. El Capítulo 4 comprende un trabajo acerca del uso de estrategias metabolómicas empleando múltiples plataformas analíticas para obtener información a nivel molecular detallada sobre el efecto de ácido carnósico, carnosol y rosmanol, compuestos bioactivos del romero (*Rosmarinus officinallis* L.), en células hepáticas HepaRG.

CAPÍTULO 3

Nuevos desarrollos metodológicos mediante CE-MS para el análisis de proteínas, péptidos y metabolitos polares

3.1. INTRODUCCIÓN

3.1.1. El papel de la CE-MS en aplicaciones *alimentómicas*

La electroforesis capilar (CE) engloba un conjunto de técnicas de separación basadas en la diferente movilidad electroforética de las especies a analizar en disolución bajo la acción de un campo eléctrico en el interior de un tubo capilar (Ewing y col., 1989). Por lo general, en CE los tiempos de análisis son cortos ya que el empleo de capilares, en los que la elevada relación superficie externa/volumen interno permite una gran disipación del calor generado por efecto Joule, hace posible la aplicación de elevados voltajes de separación. Además, la CE requiere volúmenes muy pequeños de muestra (del orden de nanolitros) así como de electrolitos de separación (del orden de mililitros).

El acoplamiento de la CE como técnica analítica de separación y de la MS como sistema de detección ha despertado un gran interés en la comunidad científica debido a que el acoplamiento CE-MS combina la rapidez del análisis, el alto poder de resolución, y el consumo muy pequeño de muestra y disolventes proporcionados por CE, con la selectividad del análisis y la información estructural que proporciona MS. Para llevar a cabo el acoplamiento de la CE que trabaja en fase líquida con la MS que trabaja en fase gaseosa, es necesaria una interfase adecuada así como el empleo de tampones de separación volátiles para evitar interferencias en la detección mediante MS (Huhn y col., 2010; Hommerson y col., 2011; Albalat y col., 2014). A pesar de la variedad de interfases desarrolladas para el acoplamiento CE-MS, la más utilizada actualmente es la interfase de tipo ionización por electrospray (ESI) (Hommerson y col., 2011). El cierre del circuito eléctrico a la salida del capilar en CE-ESI-MS se suele llevar a cabo mediante un componente conductor, como por ejemplo un recubrimiento externo metálico o mediante la adición de un líquido adicional conductor (Huhn y col., 2010), siendo esta última la opción más utilizada en la actualidad. Las funciones principales de este líquido adicional son principalmente la del cierre del circuito eléctrico en el capilar de separación y la estabilización del electrospray aplicando un flujo de líquido adecuado (del orden de µL/min). La interfase ESI con flujo adicional es el acoplamiento que se ha empleado en esta tesis doctoral y se encuentra representada en la **Figura 3.1**.

Esta interfase está formada por tres tubos concéntricos, el primero de ellos es el propio capilar de separación que se encuentra rodeado por un tubo de acero inoxidable por el que se hace fluir el líquido adicional conductor, y por un tercer tubo en el que se introduce un gas nebulizador que favorece la formación del electrospray. Se trata de una interfase que aún presenta algunas limitaciones, como por ejemplo la disminución de la sensibilidad resultante de la dilución de los analitos que eluyen del capilar por el líquido adicional.

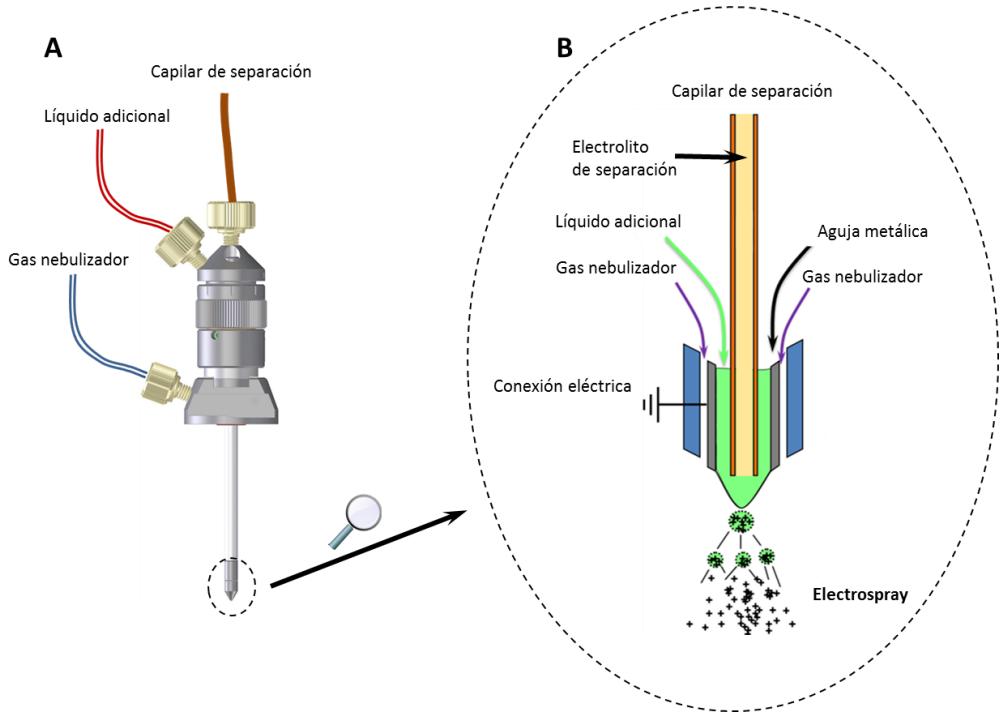

Figura 3.1. (A) Interfase ESI comercial con líquido adicional (Agilent Technologies). (B) Zona ampliada del extremo final de la interfase, donde se produce el cierre del circuito eléctrico.

En el área de la Ciencia y Tecnología de los Alimentos y Nutrición, la técnica CE-MS tiene una gran importancia como se recoge en los dos capítulos de libro que se incluyen en esta sección titulados "*Capillary Electrophoresis in Food and Foodomics*" de Ibañez y col. (**Trabajo 3.3.1**) y "*CE-MS in Food Analysis y Foodomics*" de Acunha y col. (**Trabajo 3.3.2**). En el primero de los trabajos se presenta un resumen de diferentes desarrollos metodológicos basados en CE para aplicaciones importantes en el área de ciencias de los alimentos y alimentómica, así como una detallada descripción experimental y metodológica del uso de CE-MS para el análisis metabolómico. En el segundo trabajo se expone una visión global de las contribuciones más representativas del empleo del acoplamiento CE-MS en muestras de interés alimentario en diversos campos relacionados con la seguridad de los alimentos, la detección de adulteraciones, residuos de medicamentos, residuos de herbicidas y contaminantes naturales. También se repasa el uso de la CE-MS para el análisis de aditivos, metales y alérgenos en alimentos. Además, entre las aplicaciones ómicas más relevantes que se describen destacan las aplicaciones en proteómica, peptidómica y metabolómica, dirigidas a la caracterización exhaustiva de los alimentos y del efecto de los alimentos en la salud. En el campo de las aplicaciones ómicas el acoplamiento CE-MS, por sus características, se utiliza fundamentalmente en estudios proteómicos, peptidómicos y metabolómicos (Ibáñez y col., 2013).

3.1.2. Proteómica y peptidómica mediante CE-MS

La proteómica es el estudio del conjunto completo de las proteínas expresadas en un determinado sistema biológico en un momento dado (Wasinger y col., 1995), mientras que la peptidómica se refiere al análisis completo de los péptidos endógenos generados por un determinado organismo (Schrader y Schulz-Knappe, 2001). Los péptidos y las proteínas representan una clase importante de biomoléculas y desempeñan un papel esencial en la regulación y control de muchos de los procesos biológicos en el organismo. En el campo de la Ciencia de los Alimentos, los péptidos y las proteínas desempeñan una función trascendente en las propiedades organolépticas, nutricionales y funcionales de los productos alimentarios (Català-Clariana y col., 2013), así como en la seguridad y calidad alimentaria (Kondekonvá y col., 2014; Mansor y col., 2013).

El análisis de mezclas complejas de proteínas y péptidos mediante CE-MS se considera de gran importancia debido a la complementariedad que aporta frente a otras técnicas como LC-MS (Simó y col., 2010; Stalmach y col., 2013; Albalat y col., 2014). Recientes estudios han demostrado que la técnica CE-MS tiene la suficiente robustez para llevar a cabo el mapeo de péptidos en múltiples laboratorios (Wenz y col., 2015). Sin embargo, un problema típico que presenta esta técnica es la adsorción de las proteínas y péptidos (con carga positiva) a la pared interna del capilar (con los silanoles cargados negativamente). Esta adsorción, que afecta negativamente a la separación de estos biopolímeros al originar ensanchamiento de las bandas electroforéticas, es especialmente significativa en proteínas y péptidos de carácter básico. Esto se produce principalmente a través de la interacción electrostática, pero el efecto negativo puede aumentar rápidamente mediante el despliegue de las proteínas adsorbidas que a su vez pueden participar, a través de un efecto cooperativo, en la adsorción con otras proteínas, envolviendo varios tipos de interacciones moleculares (hidrófobas, dipolares, enlaces de hidrógeno, etc.) (Lucy y col., 2008; Doherty y col., 2003). La adsorción de péptidos y proteínas provoca además alteraciones en el flujo electroosmótico (EOF), originando pérdida de eficacia y de resolución en la separación, así como una baja reproducibilidad de los tiempos de migración.

Con la finalidad de minimizar estos efectos de adsorción se pueden adoptar diferentes estrategias. Una de ellas es aumentar la fuerza iónica del electrolito de separación (BGE), que tiene como objetivo la disminución de la interacción electrostática de las proteínas con la pared interna del capilar, ya que los cationes del BGE actúan como competidores de las proteínas por interaccionar con los silanoles de la pared interna del capilar cargados negativamente. Sin embargo, en CE-MS, altas concentraciones de sales en el electrolito de separación causan la pérdida de sensibilidad en el análisis por MS. Además, una alta concentración de sales en el BGE provoca el calentamiento del capilar debido al aumento de la corriente eléctrica (efecto Joule). El empleo de pares de iones (*ion pairing*) o tensoactivos puede ser una estrategia alternativa, sin embargo, el uso de estos aditivos no volátiles puede llevar a la supresión de la ionización de las moléculas por lo que su uso no es frecuente (Huhn y col., 2010; Albalat y col., 2014). Otra alternativa es el empleo de electrólitos de separación altamente ácidos o altamente alcalinos (Huhn y col.,

2010; Haselberg y col., 2013). Con un electrolito de separación con un pH muy bajo los grupos silanoles de la superficie del capilar estarán protonados y la posibilidad de interaccionar electrostáticamente con las proteínas se reduce. Lo mismo sucede con el uso de BGEs con un alto pH, en los que las proteínas y los grupos silanoles presentan carga global negativa lo que conduce a una disminución de la interacción electrostática. No obstante, el uso de electrolitos de separación con pHs extremos puede generar problemas de estabilidad y solubilidad de proteínas y péptidos, produciendo en algunos casos desnaturalización y/o precipitación de los mismos.

Una estrategia que ha demostrado ser una opción efectiva para evitar la adsorción de las proteínas a la pared interna del capilar y mejorar la eficacia de la separación por CE es el recubrimiento interno del capilar de sílice fundida (Lucy y col., 2008; Halseberg y col., 2013; Huhn y col., 2010; Dolník y col., 2008). Los métodos empleados para el recubrimiento del capilar en CE se basan en estrategias de recubrimiento dinámico o estático. En el recubrimiento dinámico, los agentes empleados se añaden al electrólito de separación, mientras que los agentes de recubrimiento estáticos se unen a la superficie del capilar mediante adsorción física (recubrimiento semi-permanente) o por unión covalente (recubrimiento permanente) (Huhn y col., 2010). Sin embargo, los aditivos que se suelen añadir al electrólito de separación para un recubrimiento dinámico pueden causar la supresión de iones en la fuente de ionización ESI y pueden conducir a la contaminación del espectrómetro de masas y/o aumento del ruido de fondo (Huhn y col., 2010). Por lo tanto, para un acoplamiento eficaz CE-ESI-MS es recomendable el uso de recubrimientos estáticos estables. Una estrategia atractiva y simple para la creación de recubrimientos estáticos es el empleo de polímeros cargados (positiva o negativamente) adsorbidos físicamente a la pared interna del capilar. En esta Tesis Doctoral se presentan los resultados obtenidos en el estudio de una nueva familia de polímeros como recubrimientos capilares adsorbidos físicamente para el análisis de péptidos y proteínas básicas por CE-UV y CE-MS. Los resultados de este estudio están recogidos en el **Trabajo 3.3.3**, correspondiente a la publicación "*Potential of prodendronic polyamines with modulated segmental charge density as novel coating for fast and efficient analysis of peptides and basic proteins by CE and CE-MS*" de Acunha y col., publicado en Electrophoresis, 36 (2015) 1564–1571.

3.1.3. Metabolómica mediante CE-MS

La técnica CE-MS ha demostrado ser una poderosa herramienta para el análisis de especies cargadas y ha demostrado su utilidad en numerosos estudios metabolómicos de una gran variedad de muestras (plantas, alimentos, tejidos, células, fluidos biológicos, etc.) (Ramautar y col, 2013; Ramautar y col., 2017). Sin embargo, la mayoría de los estudios en metabolómica mediante CE-MS se han centrado en el análisis de metabolitos catiónicos como se explica a continuación. Tal y como se muestra en la **Figura 3.2A**, la separación en CE-MS se lleva a cabo típicamente en capilares de sílice fundida sin recubrimiento interno y empleando un electrolito de separación volátil a bajo pH, como por ejemplo ácido fórmico o ácido acético. En estas condiciones y con el equipo CE trabajando en polaridad normal (ánodo en el extremo de

inyección del capilar y cátodo en el extremo de salida del capilar) se genera un pequeño flujo electroosmótico en dirección hacia el cátodo. Este pequeño flujo electroosmótico permite mantener estable el circuito eléctrico necesario para llevar a cabo la separación electroforética. En estas condiciones, el análisis de metabolitos catiónicos por CE-MS es rápido y presenta una buena estabilidad.

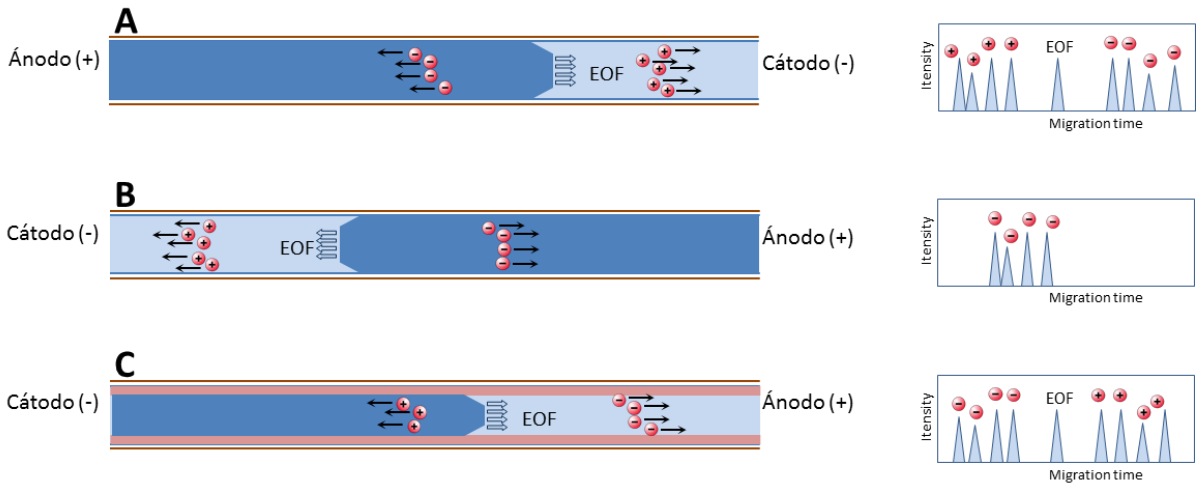

Figura 3.2. Representación esquemática del interior de un capilar de sílice fundida (A) sin recubrimiento interno y polaridad normal, (B) sin recubrimiento interno y polaridad inversa y (C) con recubrimiento interno y polaridad inversa. A la derecha se representan los electroferogramas representativos de metabolitos catiónicos y aniónicos en cada una de las condiciones.

No obstante, una buena parte de los metabolitos intermediarios de las rutas metabólicas esenciales para el mantenimiento de las actividades biológicas son compuestos aniónicos que poseen grupos ácido y que son susceptibles de cargarse negativamente. En estas condiciones, el análisis de metabolitos aniónicos es todo un desafío para la técnica CE-MS. Tal y como se puede ver en la **Figura 3.2A**, empleando las mismas condiciones de separación aplicadas para el análisis de metabolitos catiónicos, los tiempos de análisis son mucho más largos para los compuestos aniónicos, lo que en muchos casos hace inviable el empleo de la CE-MS en aplicaciones metabolómicas ya que muchos de estos aniones no llegan al espectrómetro de masas al ser su movilidad electroforética opuesta y mayor que la movilidad del flujo electroosmótico.

Una posible estrategia para el análisis de metabolitos aniónicos por CE-MS podría ser la inversión de la polaridad (cátodo en el extremo de inyección del capilar y ánodo en el extremo de salida del capilar), sin embargo, en estas condiciones, el EOF se dirige hacia al cátodo, lo que resulta en una gran inestabilidad de la conexión eléctrica haciendo imposible la separación electroforética (**Figura 3.2B**). Una alternativa para llevar a cabo el análisis rápido y robusto de compuestos aniónicos mediante CE-MS es el empleo de recubrimientos de la pared interna del capilar. En este sentido, el uso de recubrimientos con polímeros catiónicos resulta ser una estrategia muy interesante para invertir el flujo electroosmótico, acelerar la

separación de aniones y evitar la inestabilidad de la corriente en CE-MS (**Figura 3.2C**). Puesto que la pared interna del capilar una vez recubierto está cargada positivamente, el EOF queda invertido hacia el ánodo, permitiendo así el análisis de compuestos aniónicos sin la inestabilidad eléctrica del sistema. Siguiendo este enfoque, se decidió investigar el potencial del copolímero poli-Metacrilato de 2-(3-(bis(2-(dietilamino)etil)amino)propanamido)etilo - Metacrilamida de *N*-(2-hidroxipropilo) (TEDETAMA-HPMA) 50:50 como recubrimiento catiónico del capilar para el análisis del perfil metabólico de aniones por CE-MS. Los resultados obtenidos en este estudio se recogen en el **Trabajo 3.3.4**, correspondiente a la publicación "*Anionic metabolite profiling by capillary electrophoresis–mass spectrometry using a noncovalent polymeric coating. Orange juice and wine as case studies*" de Acunha y col., publicado en Journal Chromatography A 1428 (2016) 326–335.

3.2. OBJETIVOS Y PLAN DE TRABAJO

Los objetivos de este Capítulo son:

- Evaluación de una nueva familia de polímeros como recubrimientos capilares adsorbidos físicamente para el análisis de péptidos y proteínas básicas por CE-UV y CE-MS.
- Desarrollo de un nuevo método rápido y robusto mediante CE-MS para la obtención del perfil de metabolitos aniónicos.

Para conseguir dichos objetivos, se siguió el siguiente plan de trabajo:

a. Estudio del efecto del recubrimiento del capilar con diferentes polímeros de TEDETAMA en el flujo electroosmótico empleando distintos valores de pH del electrolito de separación.

b. Evaluación de diferentes polímeros de TEDETAMA como recubrimientos para el análisis de proteínas básicas y péptidos por CE-UV y CE-MS.

c. Aplicación del capilar recubierto para el análisis de lisozima en queso por CE-MS, con la finalidad de demostrar su utilidad en muestras reales de alimentos.

d. Estudio del efecto del recubrimiento polimérico sobre la separación de los metabolitos aniónicos empleando electrolitos de separación a diferentes pHs y selección de las mejores condiciones.

e. Evaluación de los parámetros de calidad del método en las condiciones seleccionadas.

f. Aplicación del método de CE-MS para el análisis del perfil de metabolitos aniónicos en muestras reales de alimentos, tales como zumo de naranja y vino tinto.

3.3. PUBLICACIONES RELACIONADAS

3.3.1. Capillary Electrophoresis in Food and Foodomics

Ibañez, C., Acunha, T., Valdés, A, García-Cañas, V., Cifuentes, A., Simó, C.

In Capillary Electrophoresis: Methods and Protocols, Methods in Molecular Biology,
Edited by Schmitt-Kopplin, P., 1483, 471–507 (2016) Springer, New York.
DOI: 10.1007/978-1-4939-6403-1_22.

Capillary Electrophoresis

Methods and Protocols

Second Edition

Edited by

Philippe Schmitt-Kopplin

Helmholtz Zentrum Munchen, Neuherberg, Germany

Humana Press

Editor
Philippe Schmitt-Kopplin
Helmholtz Zentrum Munchen
Neuherberg, Germany

ISSN 1064-3745 ISSN 1940-6029 (electronic)
Methods in Molecular Biology
ISBN 978-1-4939-6401-7 ISBN 978-1-4939-6403-1 (eBook)
DOI 10.1007/978-1-4939-6403-1

Library of Congress Control Number: 2016952998

Cover Illustration: Capillary Electrophoresis, from small to macromolecules.

Printed on acid-free paper

This Humana Press imprint is published by Springer Nature
The registered company is Springer Science+Business Media LLC New York

Chapter 22

Capillary Electrophoresis in Food and Foodomics

Clara Ibáñez, Tanize Acunha, Alberto Valdés, Virginia García-Cañas, Alejandro Cifuentes, and Carolina Simó

Abstract

Quality and safety assessment as well as the evaluation of other nutritional and functional properties of foods imply the use of robust, efficient, sensitive, and cost-effective analytical methodologies. Among analytical technologies used in the fields of food analysis and foodomics, capillary electrophoresis (CE) has generated great interest for the analyses of a large number of compounds due to its high separation efficiency, extremely small sample and reagent requirements, and rapid analysis. The introductory section of this chapter provides an overview of the recent applications of capillary electrophoresis (CE) in food analysis and foodomics. Relevant reviews and research articles on these topics are tabulated including papers published in the period 2011–2014. In addition, to illustrate the great capabilities of CE in foodomics the chapter describes the main experimental points to be taken into consideration for a metabolomic study of the antiproliferative effect of carnosic acid (a natural diterpene found in rosemary) against HT-29 human colon cancer cells.

Key words Capillary electrophoresis, CE-MS, Food bioactivity, Food safety, Food traceability, Foodomics, Food quality, Metabolomics

1 Introduction

Food safety assessment and food quality control are major concerns of modern society. There is also a growing interest to improve health and general well-being of consumers through diet beyond the provision of the basic nutritional requirements. In this sense, regulatory authorities are requiring fully substantiated health claims linked to the so-called functional foods. Analysis of exogenous compounds (agrochemicals, environmental contaminants, veterinary drugs, etc.) is also a major concern in food safety. Apart from the negative impact on human health, food contamination has also major economic costs. Quality and safety assessment as well as the evaluation of other nutritional and functional properties of foods imply the use of robust, efficient, sensitive, and cost-effective analytical methodologies.

Philippe Schmitt-Kopplin (ed.), *Capillary Electrophoresis*: Methods and Protocols, Methods in Molecular Biology, vol. 1483,
DOI 10.1007/978-1-4939-6403-1_22,

Foods are very complex matrices; moreover, many food components undergo numerous reactions in the course of food processing and storage. Hence, the use of advanced analytical instrumentation for food analysis is needed. Comparison of different analytical platforms employed in food analysis has been described before [1–6]. Among them, capillary electrophoresis (CE) is a versatile technique that has generated great interest due to its high separation efficiency, extremely small sample and reagent requirements, and rapid analysis. CE has demonstrated to be a very useful and complementary analytical tool, especially when (highly) polar and charged metabolites are analyzed and sample volume is limited. Targeted analysis is currently carried out for quality and safety assessments, involving a combination of procedures of sample preparation and the subsequent CE analysis of a given number of compounds (DNA, proteins, small molecules) from a complex mixture [7–9]. As an alternative strategy to target analysis, the development and use of profiling technologies present the potential to improve the number of analytes that can be assessed simultaneously in a single analysis. In this context, foodomics, defined as a new discipline that studies the food and nutrition domains through the application and integration of advanced omics technologies in order to improve consumers' well-being and confidence [3, 7, 10], can be regarded as a useful analytical approach in food science and nutrition research. As it has been shown in various published reports, the use of CE in foodomics offers enormous opportunities to obtain valuable detailed information that can be directly correlated to food quality, safety, and other features related to food processing, storage, authenticity assessment, etc. The main applications of CE in food analysis and foodomics in the period 2011–2014 are presented in this work. Recent results on food quality and safety, nutritional value, storage, bioactivity, as well as applications of CE for monitoring food interactions and food processing have been reviewed. These applications regarding the analysis of foods and food components using capillary electromigration methods are tabulated (*see* Table 1).

Since the introduction of foodomics, capillary electrophoresis-mass spectrometry (CE-MS) has found great application in the study of the health effects of food ingredients, e.g., on the proliferation of various cancer cells, where CE-MS has demonstrated to be as valuable as other high-performance analytical techniques [148–153]. Next, the experimental and methodological description on the use of CE-MS for metabolomics is provided in detail. In this study CE-MS is used to investigate the changes induced in the metabolite fingerprinting of human colon cancer cells (i.e., HT-29 cells) after the treatment with a bioactive compound with antiproliferative activity and potential use as functional food ingredient. Time-of-flight (TOF) mass analyzer is used for the CE-MS

Table 1
Summary of CE-based methods developed to analyze compounds relevant to food science and foodomics in the period 2011–2014

	Sample	Sample preparation	Topic of interest	Analytical platform	Ref.
Amino acids, biogenic amines, other hazardous amines					
Cypromazine, melamine	Dairy products	Extraction with trichloroacetic acid, water, and chloroform	FS	MEKC-UV	[11]
Melamine	Milk powder, gluten, chicken feed, cookies	Centrifugation, SPE	FS	MEKC-UV	[12]
Melamine	Milk	Ultrasonic-assisted extraction	FS	CE-UV	[13]
Ala, Arg, Asp, Cys, Glu, Lys, Met, Pro, Thr, Ser	Wine	DTAF/microwave-assisted derivatization	FQ, FS, FT	CE-LIF	[14]
Ornithine, alanine, GABA, alloisoleucine, citrulline, pyroglutamic acid	Olive oil	Butanol derivatization	FQ, FS	CE-Q/IT MS/MS	[15]
Arg, Val, Thr	Health drink	FITC derivatization	FQ	CE-LIF	[16]
Phe, Tyr, cadaverine, histamine, tryptamine, spermidine, putrescine	Wine, fruit molasses	FITC derivatization	FS	MEKC-LIF	[17]
Histamine, 2-phenylethylamine, tyramine	Wines	Filtration	FQ	ITP-CZE-UV	[18]
Putrescine, cadaverine, histamine, tyramine, spermine, spermidine	Meat (pork, beef, poultry)	Extraction with trichloroacetic acid	FQ	ITP-conductivity detection	[19]
Melamine and related by-products	Milk powder	Ultrasonic-assisted extraction	FS	CEC-UV CEC-TOF MS	[20]
Methylamine, ethylamine, *n*-propylamine, *n*-butylamine, *n* pentylamine, *n*-hexylamine	Wine	MeCy5-OSu derivatization	FS	CE-LIF	[21]

(continued)

Table 1
(continued)

	Sample	Sample preparation	Topic of interest	Analytical platform	Ref.
Spermine, spermidine, histamine, Cad, phenylethylamine, tyramine, tryptamine	Tap water	SPE, filtration	FQ, FS	CZE-amperometric detection	[22]
Ala, Arg, Asp, GABA, Glu, Gly, His, Leu, Ile, Lys, Met, Phe, Pro, Ser, Thr, Tyr, Val, Cys	Royal jelly products	Extraction with ethanol	FQ	CE-Q MS/MS	[23]
Histidine	Meat, meat products, fish, and fish products	Extraction with methanol	FQ	CITP-conductivity detector	[24]
Lys, Arg, Val, Thr, Ala, Phe, Glu, Trp, Asp	Gourd seed milks	Extraction with water and FITC derivatization	FQ	CE-LIF; CE-LED-induced fluorescence	[25]
Peptides					
Phosphopeptides	Milk powder	Digestion with trypsin	Foodomics	t-ITP-CE-TOF MS	[26]
Profiling of tryptic digests of water-soluble proteins	*Bacillus thuringiensis* (Bt)-transgenic, native nontransgenic maize varieties	Extraction with water and digestion with bovine pancreatic trypsin immobilized on agarose gel	FS, FT	CZE-UV	[27]
Bioactive peptides	Hypoallergenic infant milk formulas	Dilution with water, centrifugation, SPE	FB, FS	CZE-TOF MS	[28]
Proteins					
Glutelin protein fraction	Rice	Extraction with NaOH	FQ	CE-UV	[29]

Protein profiling	Maize, and soybeans	Extraction with ACN:water mixture with 0.3% acetic acid	FS, FT	CE-UV	[30]
β-Lactoglobulin, β-lactalbumin	Milk, skimmed milk powder	Dilution, centrifugation, precipitation of casein	FQ, FS	Immunoaffinity CE-UV, and immunoaffinity CE-MALDI-TOF MS	[31]
Lysozyme, conalbumin, ovalbumin β-Lactoglobulin A, β -lactoglobulin B, β-lactalbumin	Hen egg white, milk powder	Filtration Centrifugation, filtration	FQ, FS	CE-UV	[32]
Two proteins (MW of 70.2 and 85.4 kDa) and one ribosomal protein (MW of 16.3 kDa)	*Listeria monocytogenes* and *Staphylococcus aureus*	Cell disruption, filtration	FS	CE-UV	[33]
Casein fractions and derived peptides	Goat milk, goat milk cheese	Solubilization with urea buffer	FQ	CE-UV	[34]
Protein profiling	Soybean, olive seeds	Extraction with water:ACN (4:1, v/v) Extraction with Tris-HCl buffer	FQ, FT	EKC-UV	[35]
Protein profiling	Olive	Extraction with chloroform:methanol, precipitation, and solubilization with Tris-HCl buffer	FQ, FT	CGE-UV	[36]
β-Lactoglobulin	Infant foods	On-capillary derivatization	FQ, FS	CE-LIF	[37]
Protein profiling	Genetic modified maize	Extraction with water Extraction with urea and DTT Extraction with Tris, NaCl, and CHAPS	FQ, FS	CGE (chip)-LIF	[38]
Histamine	Tuna fish	Extraction with ethanol	FQ, FS	CZE-UV	[39]

(continued)

Table 1
(continued)

	Sample	Sample preparation	Topic of interest	Analytical platform	Ref.
Phenols, polyphenols, pigments, and lipids					
Tyrosol, hydroxytyrosol, oleuropein glycoside, ferulic acid, *p*-coumaric acid, cinnamic acid, *p*-hydroxybenzoic acid, gallic acid, caffeic acid, luteolin, apigenin, vanillic acid, 3,4-dihydroxybenzoic acid	Extra-virgin olive oil	Online pre-concentration (stacking)	FQ, FT, FB	CE-UV	[40]
Ferulic acid, caffeic acid, gallic acid, and (+) -catechin	White wine	Filtration	FQ, FB	CZE-amperometric detection	[41]
Sinapic acid, ferulic acid, *p*-coumaric acid, caffeic acid	Broccoli, broccolini, Brussels sprouts, cabbage, cauliflower	SPE	FB	CZE-UV	[42]
Caffeic acid hexose, catechin glucoside, catechin, (Epi)afzelechin-(epi)catechin isomer A and B, procyanidin B_2, 2-hydroxy-3-O-β-d-glucopyranosyl-benzoic acid, (epi)afzelechin (epi)catechin-O-di methyl gallate, epicatechin-O-3,4-dimethylgallate, swertiamacroside isomer A and B, rutin, hyperin, dihydroxy-trimethoxyisoflavan, and 5,7,4′-trimethoxyflavan	Buckwheat	Extraction with ethanol:water (4:1, v/v), sonication	FB	CE-TOF MS	[43]
Hydroxytyrosol, tyrosol, vanillic acid	Olive oil	Dilution with propanol	FQ, FT, FB	NACE-UV-FL	[44]
Hydroxytyrosol, tyrosol, vanillic acid, cinnamic acid, caffeic acid	Olive oil	LLE with ethanol	FQ, FT, FB	NACE-UV-FL	[45]

Epicatechin gallate, epigallocatechin gallate, epicatechin, epigallocatechin, gallic acid, gallocatechin gallate, caffeine	Tea	Extraction with water	FB	MEKC-UV	[46]
2-(4-Hydroxyphenyl) ethanol, resveratrol, epicatechin, catechin, veratric acid, homovanillic acid, vanillin, cinnamic acid, sinapic acid, quercetin, homogentisic acid, syringic acid, ferulic acid, fisetin, *p*-coumaric acid, quercetin, caffeic acid, 4-hydroxybenzoic acid, gallic acid, and 3,4-dihydroxybenzoic acid	Wine	Filtration	FQ, FT, FB	CE-UV	[47]
Kaempferol and quercetin	Broccoli	SPE	FB	LVSS-CZE-UV	[48]
Daidzin, genistin, daidzein, genistein, formononetin, biochanin A, glycitein	Soy drink	LLE with ethanol	FB	CZE-UV; CZE-Q MS	[49]
Crocetin (β-d-glycosyl)-(β-d-gentiobiosyl) ester, crocetin di-(β-d-gentiobiosyl) ester, picrocrocin, safranal	Saffron (*Crocus sativus*)	Extraction with BGE (disodium phosphate, sodium tetraborate, and SDS)	FB, FT	MEKC-UV	[50]
Lysophosphatidic acid, phosphatidylcholine, lysophosphatidylethanolamine, phosphatidylethanolamine, phosphatidylinositol, phosphatidic acid and phosphatidylglycerol	Olive fruit, olive oil	Extraction with chloroform:methanol:water Dilution with hexane, extraction with ethanol, and water	FB, FT	NACE-Q/IT MS/MS	[51]
Rutin	Buckwheat sprouts	Extraction with water:acetone (1:1, v/v), filtration, evaporation	FB	CE-PDA	[52]

(continued)

Table 1
(continued)

	Sample	Sample preparation	Topic of interest	Analytical platform	Ref.
Citrus flavonoids, troxerutin, and ascorbic acid	Food supplements and pharmaceuticals	Extraction with DMSO	FB	CZE-DAD	[53]
Omega-3 and omega-6	Oil and beef muscle	Extraction with chloroform:methanol (1:1, v/v) and saponification with KOH	FQ	CZE-UV/DAD	[54]
Isoflavone	Soy-based foods	Extraction with hexane and QuEChERS	FB	CE-Q MS	[55]
p-Coumaric, caffeic, ferulic, 3,4-dihydroxyphenylacetic, vanillic, and 4-hydroxyphenilacetic acids	Virgin olive oil	Extraction with ethanol	FB, FQ	NACE-DAD	[56]
DNAs					
Genetically modified yeasts	Yeasts from wine	DNA extraction, amplification with *Multiplex* PCR	FS, FT	CGE-LIF	[57]
DNA fragments	*Listeria monocytogenes, Salmonella enterica Escherichia coli* O157	DNA extraction and amplification with *Multiplex* PCR	FS	NGS-CE-UV	[58]
Target DNA sequences	GM maize lines	DNA extraction, denaturation	FS, FT	(qc)-PCR-CGE-LIF	[59]
Genomic DNA	GM soybean seed	DNA extraction, amplification	FS, FT	CGE-UV	[60]
Specific DNA sequences (cow, sheep, goat, buffalo)	Dairy products	DNA extraction, and amplification with *Multiplex* PCR	FQ, FS, FT	CGE	[61]
Specific DNA sequences (chicken, turkey, pork)	Heat-treated meat mixtures	DNA extraction, amplification	FQ, FS, FT	CGE-LIF	[62]
Specific DNA fragments	Maize, barley, soybean, rape, sunflower, alfalfa	DNA extraction, and amplification by TBP strategy	FS, FT	CGE-LIF	[63]

Specific DNA fragments *Salmonella enterica*, *Listeria monocytogenes*, *Campylobacter jejuni*, *Staphylococcus aureus*, *Bacillus cereus*, *Clostridium perfringens*, *Escherichia coli* O157:H7, *Yersinia enterocolitica*, *Vibrio parahaemolyticus*, *Enterobacter sakazakii*	Ten foodborne pathogenic bacteria	DNA extraction, amplification	FS	CE-single strand conformation polymorphism	[64]
Species-specific sequences *Yersinia enterocolitica*, *Vibrio parahaemolyticus*, *Escherichia coli* O157:H7, *Staphylococcus aureus*, *Shigella flexneri*, *Listeria monocytogenes*, *Campylobacter jejuni*, *Clostridium perfringens*, *Bacillus cereus*, *Salmonella enterica*	Inoculated milk	DNA isolation, and amplification by multiplex displacement amplification (MDA)	FS	CE-single strand conformation polymorphism	[65]
Genotyping of the wine spoilage yeast *Dekkera/Brettanomyces bruxellensis*	Wine spoilage yeast *Dekkera/Brettanomyces bruxellensis*	DNA extraction, and amplification by intron splice site PCR amplification	FQ	CGE-LIF	[66]
Polymorphic tandem repeat regions of *L. monocytogenes*	*L. monocytogenes*	Amplification of tandem repeat regions	FS	CGE-LIF	[67]
Specific DNA fragments	Colon cancer SW480 cells, blood lymphocytes	RNA isolation, transcription to cDNA, amplification	FS, FT	CGE-LIF	[68]
Cyprinidae-related products	Cyprinidae fish species	PCR-RFLP	FT, FQ	CGE (chip)	[69]
Cronobacter spp.	Milk powder, instant noodles, fermented bread, beef and egg cakes	DNA extraction and amplification	FS	CE-LIF	[70]
Vitamins					

(continued)

Table 1
(continued)

	Sample	Sample preparation	Topic of interest	Analytical platform	Ref.
Thiamine hydrochloride (B1), riboflavin (B2), nicotinic acid (B3), pyridoxine hydrochloride (B6), and cyanocobalamine (B12), and vitamin C (ascorbic acid)	Cornflour and fortified corn flakes	Extraction with methanol	FQ	MEKC-UV	[71]
Vitamin C	Tomato	Extraction with phosphoric acid	FQ	CZE-UV	[72]
Riboflavin, folic acid, niacinamide	Health drink	Dilution and filtration; Dilution, filtration, and FITC derivatization	FQ	CE-LIF	[16]
Thiamine, nicotinamide, pyridoxine, riboflavin, folic acid	Bacterial growth media, *Ilex paraguariensis* leaves	Filtration, online preconcentration Extraction with water, dilution with NaH_2PO_4, online preconcentration	FQ	MEKC-UV	[73]
Tocopherols	Vegetable oils	SPE	FQ	NACE-UV-FL	[74]
Vitamins B3, C, B1, B2, B5, B6, B8, B9, B12, PP	Energy drinks, vitamin tablets, and fluit pulp powders	Extraction with ethanol	FQ	MECK-UV	[75]
Riboflavin	Cereal grains	SRMM or sweeping	FB	CE-LIF	[76]
Nicotinic acid and nicotinamide	Vitamin functional drinks, vitamins,water, russula alutacea, and instant dry yeast	Extraction with HCl	FQ	CZE-UV	[77]
Carbohydrates					
Saccharose, lactose, lactulose, epilactose, maltotriose, maltose, galactose, glucose, arabinose, mannose, fructose, xylose, ribose	Orange juice, red wine; rice brand, condensed milk coffee, and breakfast cereals	Dilution of the juice with water Extraction with acid solution	FQ	MEKC-UV	[78]
Glucose, lactose, sucrose, fructose	Glucose, lactose, sucrose, fructose standards	Dilution with water	FQ	CE-DAD	[79]

Glucose, fructose, galactose, mannose, ribose, sucrose, lactose	Fruit juices, cola drinks, milk, red and white wines, yoghurts, honey, foodstuff additive	Dilution with water:ACN (1:1, v/v)	FQ, FS	CE-C^4D	[80]
Fructose, glucose, sucrose	Multifloral honey	Dilution with water	FQ, FS	CE-DAD	[81]
Fructose, glucose, sucrose	Tomato, pepper, muskmelon, winter squash, orange	Dilution of the juice with water	FQ	CE-DAD	[82]
D-Mannose, D-ribose, D-glucose, L-rhamnose, D-glucuronic acid, D-galacturonic acid, glucosamine, D-xylose, D-galactose, larabinose, D-fucose, maltose, lactose	Herbal (*Lycipus lucidus Turcz*), chinese jujube (*Zizyphus jujuba*), beer, milk	Extraction or dilution with water, and PMP derivatization	FQ	CZE-UV	[83]
Galactose, glucose, mannose, ribose, lyxose, xylose, arabinose, maltose, N-acetylgalactosamine, N-acetylglucosamine, gentiobiose, melibiose, cellobiose, lactose	Maple syrup and maple sugar	PMP derivatization	FQ	CE-DAD	[84]
Fructose, glucose, lactose, sucrose, ribose, xylose, maltose, mannose, galactose	Fructose, glucose, ribose, xylose, mannose, lactose, galactose, maltose, sucrose stantards	Dilution with water	FQ	CE-pulsed amperometric detection	[85]
Fructose, glucose, lactose, sucrose	Red wine, apple juice	Dilution with water	FQ	CE-UV	[86]
Sucrose, lactose, glucose, fructose, ribose	High-energy drinks	Dilution with water, sonication	FQ	CZE-C^4D	[87]
Small organic and inorganic compounds					
Orthophosphates, pyrophosphates, tripolyphosphates, nitrites, and nitrates	Meat, seafood products	Extraction with water	FS	cITP-conductivity detector	[88]
Quinine	Beverages	Sonication and dilution in H_2SO_4	FS	CITP-CZE-DAD	[89]

(continued)

Table 1
(continued)

	Sample	Sample preparation	Topic of interest	Analytical platform	Ref.
Glycine betaine, trigonelline, proline betaine, total content of carnitines	Seed oils and extra virgin olive oils	Extraction with methanol:chloroform (2:1, v/v), wash with methanol:chloroform:water (2:1:0.8, v/v/v), aqueous-phase derivatization with butanol	FQ, FT	CE-Q/IT MS/MS	[90]
Formaldehyde, acetaldehyde, propanal, butanal, pentanal, hexanal, glutaradehyde, 2,3-butanedione, methylgloxal	Wines, oils, water-soaked products	Filtration, TBA derivatization	FQ, FS	CE-AD	[91]
Formaldehyde, acetaldehyde	Wines, waterishlogged products	Filtration, TBA derivatization	FQ, FS	mini-CE-AD	[92]
Namely, sinapaldehyde, syringaldehyde, coniferaldehyde, vanillin	Whiskey	Online preconcentration	FQ	CE-UV	[93]
Sodium	Milk, milk products	Extraction with water and acidification with oxalic acid	FS	CZE-UV	[94]
Co, Zn, Cu, Ni, and Cd	Juices	Extraction with carboxylic group functionalized magnetic nanoparticles and re-extraction with acid solution	FS	CE-UV	[95]
Perchlorate	Cow's milk, water, red wine	Electrokinetic injection of analytes across a disposable supported liquid membrane	FS	CE-C^4D	[96]
Lactic acid, malic acid, tartaric acid, citric acid	Fruits, juices, nectars, wines, beer	Injection direct	FQ	CE-UV	[97]

Nitrate, nitrite, oxalate	Kale (*B. oleracea* var. *acephala*), sultana pea (*Pisum sativum* var. saccharatum)	Extraction with water Extraction with HCl	FS	CE-DAD	[98]
Glucosamine	Nutritional supplements	Extraction with water, and in-capillary derivatization with *o*-phthalaldehyde	FQ	CE-PDA	[99]
Caffeine	Energy drinks	Centrifugation and dilution with buffer	FS	MEEKC-DAD	[100]
4-Bromophenol, 2,4,6-triBromophenol, 2,4 diBromophenol, 2-Bromophenol, 2,6-diBromophenol	Seafood	Homogenization with H_2SO_4, distillation extraction, concentration	FQ	CZE-pulsed amperometric detection	[101]
Sotolon	Maple-flavored food additive	Extraction with water	FQ	CZE-pulsed amperometric detection	[102]
Glucosamine and chondroitin sulfate	Dietary supplements	Extraction with water	FQ	CITP-conductivity detector	[103]
Melamine, ammelide, ammeline, and cyanuric acid	Milk products	Protein precipitation with HCl and SPE	FS	MECK-UV	[104]
Toxins, contaminants, pesticides, and residues					
Sulfadiazine, sulfamerazine, sulfapyridine, sulfamethazine, sulfisoxazole, sulfadimethoxine, sulfaquinoxaline, sulfamonomethoxine, sulfathiazole	Porcine liver and kidney	SPE, online concentration	FS	CEC-TOF MS	[105]
Sulfamethazine, sulfamerazine, sulfathiazole, sulfacarbamide, sulfachloropyridazine, sulfamethoxazole, sulfaguanidine	Poultry tissue	Deproteinization with ACN, centrifugation, SPE	FS	MEKC-UV	[106]

(continued)

Table 1
(continued)

	Sample	Sample preparation	Topic of interest	Analytical platform	Ref.
Oxacillin, penicillin V, penicillin G, nafcillin, ampicillin, amoxicillin	Porcine liver, kidney	Extraction with ACN, SPE	FS	NSM-W/O--MEEKC- 3D UV-vis	[107]
Colchicine	Milk	Deproteinization with HCl, LLE with dichloromethane:isopropanol (95:5, v/v), evaporation, dilution with phosphate buffer	FS	CZE, NACE, MEKC-UV	[108]
Marbofloxacin, CIP, danofloxacin, ENR, sarafloxacin, difloxacin, oxolinic acid, flumequine	Bovin, porcine plasm	SPE	FS	CE-UV	[109]
Isoproturon, linuron, iduron	Green vegetable, rice	Matrix solid-phase dispersion extraction	FS	CE-ECL	[110]
Saxitoxin, decarbamoylsaxitoxin	Shellfish	Extraction with acetic acid solution, filtration, immunoreaction	FS	Immunoaffinity CE-EC	[111]
Quinolone enrofloxacin, ciprofloxacin	Milk	Deproteinization with HCl solution, centrifugation, SPE	FS	CE-UV	[112]
Tetracycline, oxytetracycline, doxycycline	Milk	Extraction with matrix solid-phase dispersion	FS	CZE-UV	[113]
Albendazole, fenbendazole, mebendazole, thiabendazole, albendazole sulfoxide, albendazole sulfone, oxfendazole, fenbendazole sulfone, 2-amino-albendazole sulfone, 5-hydroxy thiabendazole	Swine tissue	Extraction with ACN, magnetic solid-phase extraction	FS	FASS-CZE-DAD	[114]

Methomyl, propoxur, carbofuran, carbaryl, isoprocarb, promecarb	Fruit juices	Filtration	FS	REPSM-MEKC-PDA	[115]
Metolcarb	Rice, cucumber	Homogenization with methanol and filtration	FS	Immunoaffinity CE-LIF	[116]
2,4-Dichlorophenol, 2,4,5-trichlorophenol, 4 tert-butyl-phenol, pentachlorophenol, bisphenol-A, 4-tert-butyl benzoic acid	Honey	LLE with hexane, QuEChERS	FS	PNP-CE-Q MS	[117]
Brevetoxin B	Shellfish	Extraction with methanol, filtration, immunoreaction	FS	Immunoaffinity CE-EC	[118]
Citrinin, a nephrotoxic, hepatotoxic mycotoxin	Red yeast rice, monascus color	Selective extraction and cleanup by immunoaffinity column	FS	CZE-UV	[119]
Ochratoxin A	Mould strains	Extraction with chloroform, filtration, evaporation	FS	MEKC-UV	[120]
Sulfonamides and their acetylated metabolites	Shrimp, sardine, and anchovy	Accelerated solvent extraction with ACN	FS	CZE-DAD	[121]
Polycyclic aromatic hydrocarbons	Isio 4®oil	SPE	FS	CZE-LIF	[122]
Polycyclic aromatic hydrocarbons	Bovine milk	Hydrolisis with b-glucuronidase, extraction with ACN, SPE	FS	CZE-UV	[123]
Patulin	Apple juices	Dispersive liquid-liquid microextraction	FS	MECK-DAD	[124]
Patulin	Apple juices	Extraction with ethyl acetate	FS	CZE-UV	[125]
Zearalenone	Poultry feed and cereals	Extraction with methanol and dicholoromethane, SPE	FS	CZE-UV	[126]
Glyphosate and glufosinate	Water, soybean, and broccoli	Extraction with water, FITC derivatization	FS	CE-LIF (chip)	[127]
Amprolium	Eggs	Extraction with water, SPE, and FASI preconcentration	FQ, FS	CE-Q/IT MS/MS	[128]

(continued)

Table 1
(continued)

	Sample	Sample preparation	Topic of interest	Analytical platform	Ref.
Anthelmintic benzimidazoles	Eggs	Extraction with ethyl acetate, hexane and SPE; extraction with water and SPE; QuEChERS and SPE	FS	CE-Q MS	[129]
Brevetoxin-B	Shellfish	Extraction with methanol	FS	CE-immunoassay	[118]
Arsenic compounds: As (III), As (V), DMA, MMA, AsB, AsC, 3-NHPAA, 4-NPAA,o-ASA (o-arsanilic acid) and p-UPAA	Herbal plants and chicken meat	Extraction with water	FS	CE-ICP MS	[130]
Sulfonamide residues: Sulfamethazine, sulfadiazine, and sulfathiazole	Milk	Protein precipitation with HCl, and SPE	FQ, FS	CE-UV/DAD	[131]
Food additives					
Citrate, tartrate, malate, succinate, adipate, acetate, propionate, lactate, benzoate, sorbate, dehydroacetate, ascorbate, gluconate	Wine, health drink, yogurt, pickled ginger	Dilution with water, filtration	FQ, FS	CZE-DAD	[132]
Methyl, ethyl, propyl, and butyl parabens	Sweetener	Filtration	FS	CEC-UV	[133]
Benzoic acid, sorbic acid	Beverages, vinegar, fruit jam	Dilution with buffer, filtration	FS	CZE-UV-Vis	[134]

Sudan I (1-(phenylazo)-2-naphthalenol) Sudan II (1-[(2,4-dimethylphenyl) azo]-2-naphthalenol) Sudan III (1-[[4-(phenylazo)phenyl] azo]-2-naphthalenol) Sudan IV (1-[[2-methyl-4-[(2-methylphenyl)-azo]phenyl] azo]-2-naphthalenol)	Chilli tomato sauces	Extraction with acetone:dichloromethane:methanol (3:2:1, v/v/v), evaporation	FS	MEKC-UV MEKC-Q/IT MS/MS	[135]
Sudan I (1-(phenylazo)-2-naphthalenol) Sudan II (1-[(2,4-dimethylphenyl) azo]-2-naphthalenol) Sudan III (1-[[4-(phenylazo)phenyl] azo]-2-naphthalenol) Sudan IV (1-[[2-methyl-4-[(2-methylphenyl)-azo]phenyl] azo]-2-naphthalenol)	Chilli tomato sauces, chilli powder	Extraction with acetone:dichloromethane:methanol (3:2:1, v/v/v), evaporation	FS	MEKC-Q/IT MS/MS	[136]
Benzoyl peroxide, benzoic acid	Wheat flour	Dilution with methanol, reduction with potassium iodide solution, filtration	FS	CZE-UV	[137]
Hydroxyproline	Meat products	Digestion, filtration, reaction with fluorescamine reagent, evaporation	FQ	CE-UV	[138]
Hydroxyproline	Milk powder, liquid milk, milk drink, soymilk powder	Hydrolysis, dilution, in-capillary derivatization	FQ	MEKC-LIF	[139]
Neotame	Nonalcoholic beverage	Dilution with water or extraction with formic acid:triethylamine:water (4:125:5000, v/v/v), and SPE	FQ	CZE-UV	[140]
2-Methylimidazole and 4-Methylimidazole	Color caramel	Dilution with water	FS	CZE-UV	[141]

(continued)

Table 1
(continued)

	Sample	Sample preparation	Topic of interest	Analytical platform	Ref.
Aspartame, cyclamate, saccharin, and acesulfame K	Tabletop sweetener tablet, confectionary sweets, soft drink samples	Dilution with water	FQ	CE-conductivity detector	[142]
Aspartame, cyclamate, saccharin, and acesulfame-K	Lemon tea sachet	Dilution with water	FQ	CZE-UV	[143]
Chiral compounds					
Amino acid enantiomers	Food supplements	FMOC derivatization	FQ	Chiral selector CEC-UV	[144]
Thirteen α-amino acid enantiomeric pairs	Amino acids	FITC derivatization	FQ	Chiral selectors CE-DAD	[145]
Enantiomers of lipoic acid	Food supplements	Extraction with ethanol	FQ	Chiral selector CE-UV	[146]
A-hydroxy acids and their enantiomers	Fruit juices	Dilution with water, SPE	FQ	Ligand exchange CE-UV	[147]
Foodomics					
Metabolite profiling	GM tomato varieties and traditional tomato cultivars	Extraction with methanol:chloroform:water (3:1:1, v/v/v), centrifugation	FS, FT	CE-TOF MS	[148]
Metabolite profiling	Dietary polyphenol-treated HT-29 cells	SPE, ultrafiltration, and methanol deproteinization	FB	CE-TOF MS	[149, 150]

Metabolite profiling	Dietary polyphenol-treated HT-29 cells	Ultrafiltration	FB	CE-TOF MS	[151, 152]
Metabolite profiling	Dietary polyphenol-treated K562 cells	Ultrafiltration		CE-TOF MS	[153]
Metabolite profiling	Avocado fruits	Extraction with methanol	FT	CZE-IT MS	[154]

FB food bioactivity, *FS* food safety, *FT* food traceability, *FQ* food quality, *LVSS* large-volume sample stacking, *NSM* normal stacking mode, *FASS* field-amplified sample stacking, *REPSM* reversed electrode polarity stacking mode, *PMP* 1-phenyl-3-methyl-5-pyrazolone, *SRMM* stacking in reverse migrating micelles, *DTAF* 5-(4,6-dichlorotriazinyl)amino-fluorescein, *FASI*: field-amplified sample injection, *t-ITP* transient-isotachophoresis
Topics of interest: food bioactivity, food safety (FS), food quality (FQ), food traceability (FT), foodomics

coupling due to its high scan speed and high mass resolution and accuracy, what perfectly fits with the narrow and fast peaks provided by CE and the needs of a metabolomic study.

2 Materials

2.1 Reagents

2.1.1 Reagents for Sample Preparation

1. Human colon adenocarcinoma HT-29 cell line (American Type Culture Collection, LGC Promochem, UK).
2. Dimethyl sulfoxide (DMSO) (Sigma-Aldrich, St. Louis, MO, USA).
3. McCoy's 5A cell culture media (Lonza, Barcelona, Spain).
4. Penicillin-streptomycin mixture (5000 IU/mL penicillin G, 5 mg/mL streptomycin) (Lonza).
5. Heat-inactivated fetal calf serum (Biowest, Nuaillé, France).
6. Carnosic acid as pure standard (Sigma-Aldrich).
7. Phosphate-buffered saline (PBS) solution: 138 mM Sodium chloride, 2.7 mM potassium chloride, and 10 mM sodium hydrogen phosphate, at pH 7.4 (Lonza).
8. Trypsin-Versene (Lonza).
9. Trypan blue (0.4%, w/v) 0.81% sodium chloride, 0.06% potassium phosphate (Sigma-Aldrich).
10. Liquid nitrogen (Carburos Metalicos-Air Products Group, Barcelona, Spain).
11. Metabolite internal standards (IDs): Tyramine, DL-methionine sulfone (Sigma-Aldrich).
12. Water from Milli-Q system (Millipore, Bedford, MA, USA).

2.1.2 Reagents for CE-ESI-TOF MS Analysis

1. MS-grade water (Scharlau, Barcelona, Spain).
2. MS-grade formic acid (Sigma-Aldrich).
3. MS-grade 2-propanol (Labscan, Gliwice, Poland).
4. Sodium hydroxide (NaOH) (Panreac, Barcelona, Spain).
5. Metabolite commercial standards (Sigma-Aldrich) for quality control (QC) mixture: Spermine, spermidine, putrescine, cadaverine, *N*-acetylspermine, ornithine, lysine, arginine, S-adenosylmethionine, adenine, tyramine, *N*-acetyl-putrescine, S-adenosylhomocysteine, homocysteine, cysteine, *N*-acetyl-ornithine, cytidine, methionine, adenosine, methyl-thio-adenosine, DL-methionine sulfone, glutathione, oxidized glutathione.

2.1.3 Preparation of Solutions

1. Culture media solution: Add 50 mL heat-inactivated fetal calf serum and 5 mL penicillin-streptomycin mixture to 450 mL McCoy's 5A media in a cell culture flask.

2. Carnosic acid (CA) (100 mM): Dissolve CA in DMSO to obtain a final concentration of 33.22 (mg/mL) (*see* **Note 1**).
3. Metabolite extraction solvent with IDs at 125 μM concentration: Prepare 0.91 mg/mL tyramine and 0.62 mg/mL DL-methionine sulfone solution in Milli-Q water.
4. QC mixture: Mix 56 μL MS-grade water and 2 μL 5 mM solutions of putrescine, cadaverine, *N*-acetylspermine, ornithine, lysine, arginine, S-adenosyl-methionine, adenine, tyramine, *N*-acetyl-putrescine, S-adenosyl-homocysteine, cysteine, *N*-acetyl-ornithine, cytidine, methionine, adenosine, methyl-thio-adenosine, and DL-methionine sulfone. Finally add 4 μL 2.5 mM solutions of glutathione, oxidized glutathione, spermine, spermidine, and homocysteine.
5. Sodium hydroxide (1 M): Dissolve 4 g of sodium hydroxide in 95 mL of Milli-Q water. Then reach a final volume of 100 mL using a volumetric flask.
6. Sodium hydroxide (0.1 M): Dilute 1 mL 1 M NaOH in 9 mL Milli-Q water
7. Sodium formate (10 mM) for MS calibration: Mix 200 μL 1 M NaOH and 39.8 μL formic acid and make up volume to 10 mL with 2-propanol:water (50:50, v/v).
8. Formic acid (3 M): Mix 200 mL MS-grade water with 11.31 mL formic acid in a volumetric flask and reach a final volume of 250 mL with water.
9. Sheath liquid (2-propanol-water (50:50, v/v): Mix 5 mL of MS-grade 2-propanol with 5 mL MS-grade water.

2.2 Consumables and Equipment

2.2.1 Consumables and Equipment for Sample Preparation

1. Light microscope (ID3, Carl Zeiss, Jena, Germany).
2. Tissue culture flasks 100 mL volume (Sarstedt, Barcelona, Spain).
3. P150 tissue culture plates (Sarstedt).
4. Neubauer counting chamber (Brand, Wertheim, Germany).
5. Vortex (JP Selecta, Barcelona, Spain) to prepare commercial standard solutions.
6. Rotina 380R centrifuge (Hettich, MA, USA).
7. Ultrasonic bath (JP Selecta, Barcelona, Spain).
8. Ball mill MM 400 (Retsch, Haan, Germany).
9. Glass beads (212–300 μm) (Sigma-Aldrich).
10. 2 mL Microcentrifuge screw tubes.
11. PTFE adapter rack for ten reaction vials 1.5 and 2.0 mL (Ref: 22.008.0008) (Retsch).
12. Amicon Ultra 3 kDa 0.5 mL centrifugal devices from Millipore (Billerica).

2.2.2 Consumables and Equipment for CE-ESI-TOF MS Analysis

1. Uncoated fused silica capillary (80 cm length, 50 μm i.d.) (Composite Metal Services, Worcester, England).
2. High-performance capillary electrophoresis (CE) system model P/ACE 5500 (Beckman, Fullerton, CA, USA) controlled by a PC equipped with System Gold software (Beckman).
3. TOF MS instrument (micrOTOF model) (Bruker Daltonics, Bremen, Germany).
4. Cole Palmer syringe pump (model 74900-00-05) (Vernon Hills, IL, USA).
5. Glass syringe (2.5 mL volume) (SGE, Milton Keynes, UK).
6. Orthogonal electrospray ionization (ESI) interface (model G1607A) (Agilent Technologies, Palo Alto, CA, USA).

2.2.3 Software and Bioinformatic Tools

1. DataAnalysis 4.0 software (Bruker Daltoniks).
2. Data file format converter: Trapper (free available at http://tools.proteomecenter.org/wiki/index.php?title=Software:trapper).
3. Free access databases used for identification [155–157].
4. Software for statistical analysis: STATISTICA v.7 (Statsoft, Tulsa, OK, USA).

3 Methods

3.1 Cell Culture Preparation Protocol

1. Grow colon adenocarcinoma HT-29 cells in 10 mL culture media inside a culture flask at 37 °C in humidified atmosphere and 5% CO_2.
2. When cells reach ~50% confluence (cells fill ~50% flask), discard culture media and place cells in a 15 mL Falcon tube with 4 mL trypsin and 4 mL cell culture media solution.
3. Centrifuge at 500 × *g* for 3 min, discard the supernatant, and suspend the cell pellet in 4 mL culture media solution.
4. Seed cells at 10,000 cells/cm^2 onto six independent P150 tissue culture dishes: Take 0.5 mL cell suspension, add 19.5 mL cell culture media, and incubate overnight at 37 °C (*see* **Note 2**).
5. Add 5.96 μL 100 mM CA solution to three of the culture dishes to obtain 9.9 μg/mL final concentration of CA in the cell plates and incubate all six cell cultures (CA-treated and non-treated) for 48 h at 37 °C.

3.2 Obtainment of Ten Million Cells from Cell Culture Dishes

1. Aspire growth medium from culture plates, add 2 mL trypsin solution, and rapidly aspire it.
2. Dispense 5 mL trypsin solution covering the monolayer of cells and incubate cells at 37 °C for 15 min.

3. Transfer cells suspended in trypsin to 15 mL Falcon tubes. Add 3 mL trypsin more to culture dish to collect maximum number of cells and transfer these 3 mL to the same 15 mL Falcon tube (*see* **Note 3**).
4. Centrifuge at 300 × *g* for 5 min, discard the supernatants, and add 1 mL PBS to each pellet ($n = 6$) to suspend the cells (*see* **Note 4**).
5. Cell counting: Dilute 5 μL of cell suspension (obtained in the previous step) in 15 μL PBS and add 20 μL trypan blue commercial solution. Mix well by gentle pipetting within the pellet using a micropipette and place the suspension on Neubauer counting chamber. Count the cells in the central square and in the four squares at the corners using a light microscope. Count separately viable (opaque) and nonviable (blue-stained) cells (*see* **Note 5**). Repeat this procedure to obtain the average number of cells from at least three different squares of Neubauer chamber (*see* **Note 6**) and calculate the number of cells/mL and the volume of cell suspension to have 10×10^6 cells (*see* **Note 7**).
6. Transfer the volume required to have 10×10^6 cells from the PBS cell suspension previously obtained (Subheading 3.2, **step 4**) to 2 mL microcentrifuge screw tubes to obtain six independent tubes (three non-treated and three CA-treated cells) containing 10×10^6 cells each.
7. Centrifuge for 10 min at 500 × *g* to obtain the cell pellets containing 10×10^6 cells.

3.3 Metabolite Extraction Procedure

1. Add 0.3 g glass beads and 300 μL metabolite extraction solvent containing the IDs to each screw tube ($n = 6$).
2. Perform three cycles of metabolite quenching and cell disruption applying the three following steps: First submerge a rack with the six cell suspension tubes in liquid nitrogen (*see* **Note 8**) for 3 min. Then carefully take the rack with the tubes and thaw on ultrasonic bath at 50 Hz for 5 min. The third step consists of placing the tubes inside the PTFE adapter racks and applying 30 Hz frequency for 3 min using a ball mill. Repeat three times these steps.
3. Centrifuge the tubes at 24,000 × *g* for 10 min at 4 °C.
4. Filter 200 μL supernatant (cellular content) from each tube by using 3 kDa molecular weight filters programming the centrifuge at 14,000 × *g* for 40 min at 20 °C.
5. Store fraction less than 3 kDa (metabolic fraction) in screw tubes at −80 °C until CE-MS analysis.

3.4 CE-ESI-TOF MS Methodology

1. Condition all new capillaries by flushing with 0.1 M NaOH for 20 min, followed by MS-grade water for 20 min and background electrolyte (BGE) (3 M formic acid) for 5 min (*see* **Note 9**).
2. Introduce the capillary through the interface (ESI) and set the sheath-flow configuration to establish the electrical contact at the ESI tip. Program 0.24 mL/min sheath liquid flow rate in the syringe pump menu.
3. Create an analysis method with the following CE-TOF MS parameters: CE voltage set at +27 kV, CE temperature at 25 °C, positive ionization mode MS, MS capillary voltage set at 4 kV, acquisition *m/z* range from 50 to 600 *m/z*, dry nitrogen gas heated at 200 °C delivered at 4 L/min and maintained at 0.4 bar.
4. Perform TOF MS external calibration by introducing 10 mM sodium formate before each injection. For internal calibration record signal obtained using the same solution at the end of each sample file for 2 min. Ions used for calibration are 90.9766, 158.9641, 226.9515, 294.9389, 362.9263, 430.9138, 498.9012, and 566.8886 *m/z* (Fig. 1).

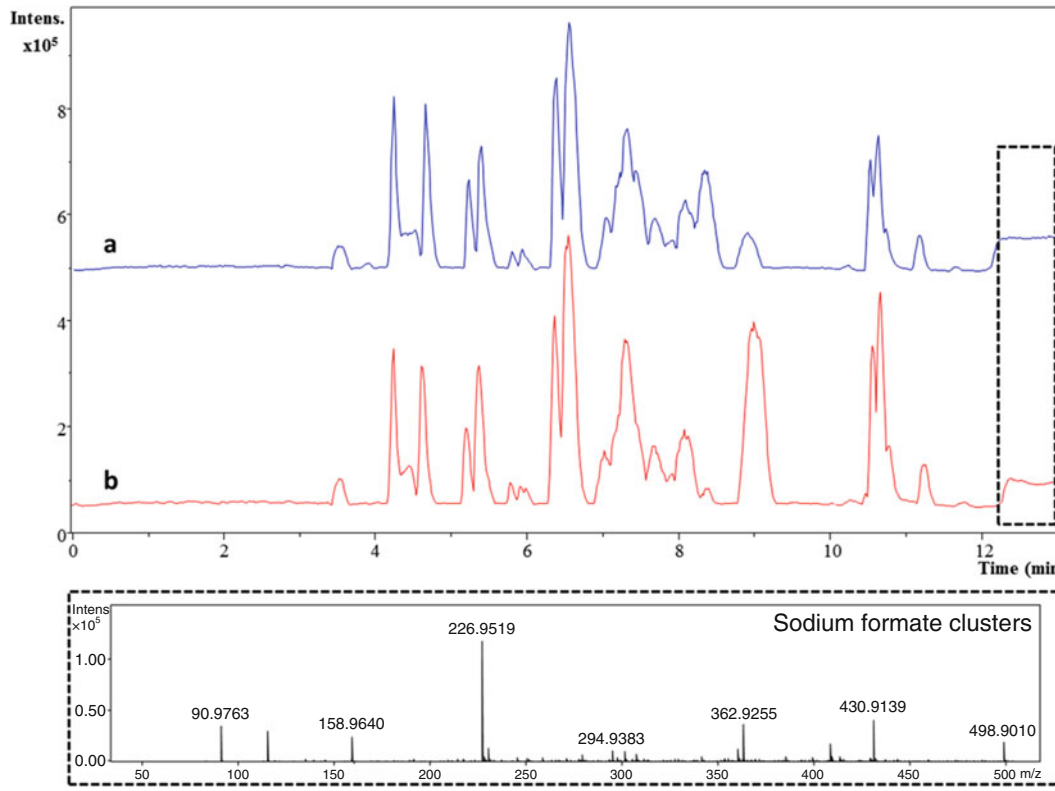

Fig. 1 CE-ESI-TOF MS base peak electropherograms (BPE) of the cytosolic fraction from (**a**) control HT-29 colon cancer cells and (**b**) treated with carnosic acid. Calibrant acquisition is framed at the end of the two electropherograms using a dashed line rectangle. (**c**) An example of MS spectra from the framed area showing the experimental clusters used for calibration

5. Inject the sample for 80 s at 0.5 psi (34.5 mbar) and apply the CE-MS method described above. Obtain the metabolic profiles of control and CA-treated cells (Fig. 1).
6. Inject each sample to obtain three CE-MS replicates. Check the suitability of the results using DataAnalysis 4.0 software.
7. Each three injections change BGE vial and inject QC mixture (Fig. 2).
8. After each injection and the subsequent external calibration, condition the capillary for 5 min with BGE.

3.5 Data Processing

1. Use DataAnalysis 4.0 software to check the suitability of your data by extracting known ions such as internal standards and ions from the QC (Fig. 2) to calculate deviation intra and inter day.
2. Export ".d" CE-MS data to the MS exchange format "mzXML" using Trapper bioinformatic tool. Select the pathways where sample data files are stored in the PC, select "peak

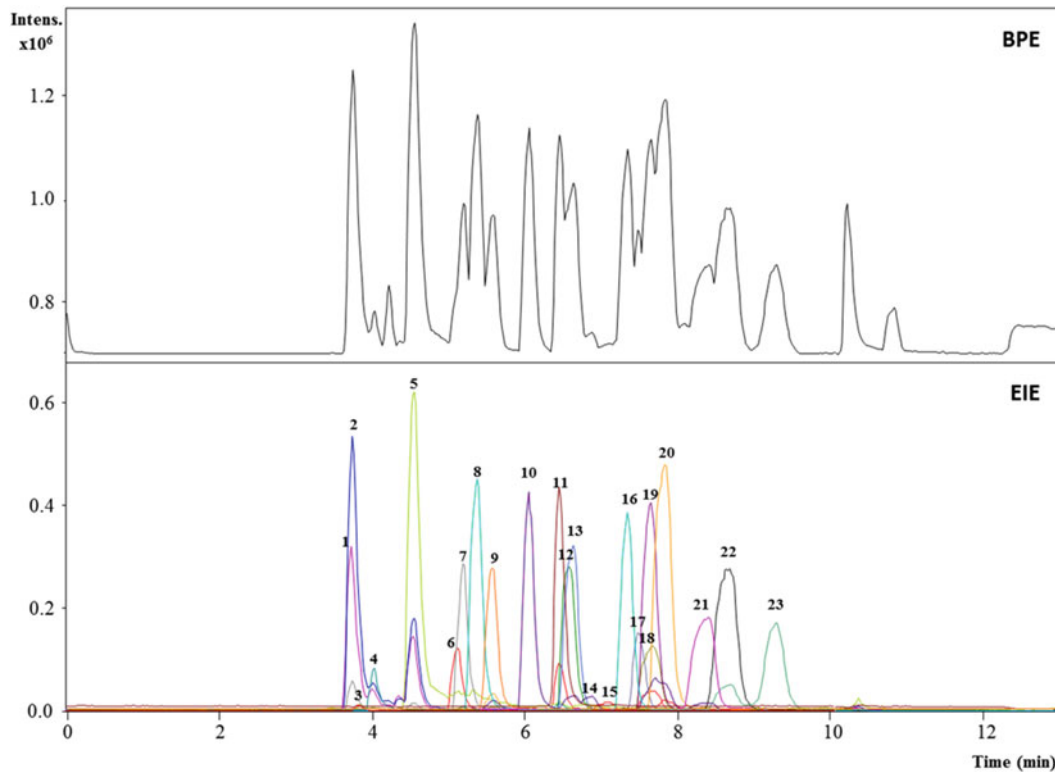

Fig. 2 CE-ESI-TOF MS base peak chromatogram (BPE) of quality control mixture and extracted ion chromatograms (EIE) of the 23 metabolite standards: 1, spermine; 2, spermidine; 3, putrescine; 4, cadaverine; 5, *N*-acetyl-spermine; 6, ornithine; 7, lysine; 8, arginine; 9, S-adenosyl-methionine; 10, adenine; 11, tyramine; 12, *N*-acetyl-putrescine; 13, S-adenosyl-homocysteine; 14, homocysteine; 15, cysteine; 16, *N*-acetyl-ornithine; 17, cytidine; 18, methionine; 19, adenosine; 20, methyl-thio-adenosine; 21, ethionine sulfone; 22, oxidized glutathione; 23, glutathione

picking" option to centroid your data, and click start to begin with the conversion.

3. Process exported centroided mzXML data with MZmine program (*see* **Note 10**). Set the threshold of electropherograms (*see* **Note 11**). Use wavelet transform algorithm to detect the masses with a wavelet window size set at 50% and normalize migration time between replicates setting minimum standard intensity at 5×10^4 a.u.. For deconvolution use "baselina cut-off" algorithm setting the minimum peak height at 3×10^2 a.u. Then align the replicates and samples applying the "Join aligner" algorithm with m/z tolerance set at 0.01 and weight for m/z set at 90. Finally perform adduct and complex search within your detected peaks and export the resulting data table to csv format.
4. Import the csv table in Excel and remove the metabolic signals showing high variability within the same group of samples (i.e., control and treated cells) from CE-MS data set. Transpose the data table to get samples arranged in rows and high-confident metabolic signals in columns.
5. Open the transposed data table using STATISTICA program.
6. Inspect your data variability by means of principal component analysis (PCA). If necessary remove high-variable metabolic signals and/or outlier samples.
7. Detect significantly different molecular features due to CA treatment applying an analysis of variance method (i.e., ANOVA, *t*-test, Kruskal-Wallis) and setting p-value at 0.05.

3.6 Identification of Potential Biomarkers

1. Match the experimental m/z value of the metabolites showing significant differences ($p < 0.05$) with m/z values contained in different databases: Human Metabolome Database, METLIN, and KEGG, with a mass accuracy window of 10 ppm (Table 2).
2. Use Generate-Molecular Formula editor (DataAnalysis 4.0) to compare the isotopic pattern of the theoretical formulas obtained from the databases with the experimental isotopic pattern of each of the metabolites differentially expressed.
3. Inject metabolite standards to corroborate tentative identifications, in the same analytical conditions and spiked (if possible) in cell culture samples (*see* **Note 12**).
4. Associate metabolite expression (up or down expression) to CA treatment and study the most affected cellular pathways (Fig. 3).

Table 2
Tentative identification of metabolites differentially expressed in HT-29 cells after CA treatment sorted according to their migration time

Metabolite ID	*m/z*	Ion	Formula	Error (ppm)	Identification	Standard coinjection	HMDB identifier	Expression
1	131.118	M+H	$C_6H_{14}N_2O$	-2.9	*N*-acetyl-putrescine	YES	HMDB02064	DOWN
2	104.070	M+H	$C_4H_9NO_2$	-6.7	γ-Aminobutyric acid	YES	HMDB00650	DOWN
3	298.096	M+H	$C_{11}H_{15}N_5O_3S$	-3.8	Methyl-thio-adenosine	YES	HMDB01173	DOWN
4	179.049	M+H	$C_5H_{10}N_2O_3S$	4.5	Cysteinyl-glycine[a]	NO	HMDB28775	UP
5	307.086	M+2H	$C_{20}H_{32}N_6O_{12}S_2$	8.5	Oxidized glutathione	YES	HMDB03337	DOWN
6	308.092	M+H	$C_{10}H_{17}N_3O_6S$	1.8	Reduced glutathione	YES	HMDB00125	UP
7	244.094	M+H	$C_9H_{13}N_3O_5$	5.5	Cytidine	YES	HMDB00089	DOWN

[a]Cysteine-glycine was tentatively identified due to the lack of standard

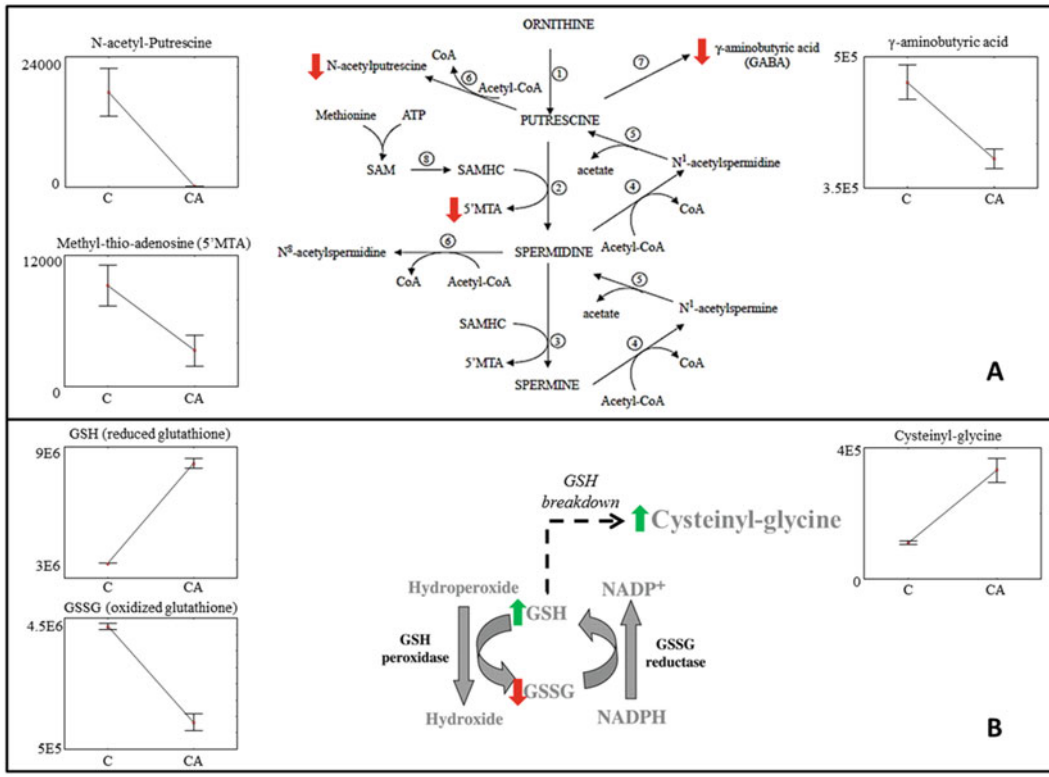

Fig. 3 Main pathways within HT29 metabolome altered after the CA treatment. CA brings about modifications on polyamine pathway (**a**) by the down-expression of N-acetylputrescine, methyl-thio-adenosine, and γ-aminobutyric acid. CA also alters glutathione metabolism (**b**) by a down-expression of oxidized glutathione that gives rise to increased levels of reduced glutathione and cysteinyl-glycine. Down- and up-expressed metabolites are marked with *red* and *green* arrows, respectively. Whisker plots of average metabolite areas (±SD) in control- (**c**) and carnosic acid-treated (CA) cells are also shown for significantly different metabolites involved in A and B pathways. Enzymes involved in polyamine pathway are ornithine decarboxylase (1), spermidine synthase (2), spermine synthase (3), acetyl-CoA: spermidine/spermine N 1-acetyltransferase (4), polyamine oxidase (5), spermidine N 8-acetyltransferase (6), amine oxidase plus aldehyde dehydrogenase (7), S-adenosylmethionine decarboxylase (8)

4 Notes

1. CA molecule is easily degradable and photosensitive. For this reason avoid light and high temperature when preparing CA solution. Divide the resulting solution in several aliquots and store them at −80 °C.
2. Volume of 0.5 mL cell suspension is estimated with the microscope to obtain a final density of cells up to 10,000 cells/cm^2. Thus, this volume has to be estimated in each study.
3. A final volume of 8 mL trypsin is added to the culture dish to collect cells and can be added in one step before incubation (Subheading 3.2). However to divide trypsin addition in two

steps (add 5 mL trypsin, then incubate, and add 3 mL trypsin) is more advisable to obtain the maximum recovery of cells from the culture dish.

4. PBS volume is estimated in order to obtain a 10×10^6 cell suspension.
5. In order to follow a routine on how to count the cells, it is important to establish a procedure to not count more than one time each cell. To do so, one possibility is to count the cells touching the midline of the triple line, on the top and left of each square (of the Neubauer chamber). Do not count cells touching the midline of the triple line, on the bottom or right side of the square.
6. The total count of cells must be around 100. If not, adjust the dilution of cell suspension by modifying PBS volume. It is important to note that a half of the total volume of the final solution to count cells has to consist of trypan blue (commercially available at 0.4%). Namely 0.2% final trypan blue concentration is necessary to count cells.
7. The formulas for calculation are the following ones:

   Cells/mL = average number of cell counted × 104 × dilution factor [8] (dilution factor can change depending on the result obtained from cell counting (*see* **Note 2**).

   Total cells = cells/mL × vol. of original suspension.

   Another relevant parameter if for example proliferation under given conditions is under scrutiny is the viability of cells described below:

   % Viability = (number of viable cells counted/total number of cells counted) × 100.
8. Liquid nitrogen must be carefully used because contact may produce burns. Always use security glasses and gloves to work with it. The use of a rack or container with a handle or handgrip is recommended to submerge the tubes.
9. Low-pH BGE promotes positive charge of analytes and is recommended to avoid analyte adsorption onto the inner capillary wall.
10. Every parameter in data processing must be carefully optimized for each experiment and instrument. MZmine has the advantage to present a very visual interface which is very recommendable for CE-MS data processing due to higher migration time deviations compared to LC- or GC-MS and moreover data processing experience is not necessary to visually check the results.
11. There are many ways to estimate the minimum intensity from which peaks are detected in data process. One of the most common estimations of the threshold is to divide the lower signal intensity (low-abundant species) by 3.

12. Migration time or intensity of standards could be different from the values obtained in the samples if standards are injected alone. Salts, viscosity, and other matrix properties contribute to migration time and intensity values of metabolites.

Acknowledgments

This work was supported by an AGL2011-29857-C03-01 project (Ministerio de Educacion y Ciencia, Spain). A.V. thanks the Ministerio de Economía y Competitividad for his FPI predoctoral fellowship. T.A. thanks the Capes Foundation, Ministry of Education of Brazil, for her predoctoral fellowship (proc. nº: BEX 1532/13-8).

References

1. LeDoux M (2011) Analytical methods applied to the determination of pesticide residues in foods of animal origin. A review of the past two decades. J Chromatogr A 1218:1021–1036
2. García-Cañas V, Simó C, Herrero M, Ibáñez E, Cifuentes A (2012) Present and future challenges in food analysis: foodomics. Anal Chem 84:10150–10159
3. Herrero M, Simó C, García-Cañas V, Ibáñez E, Cifuentes A (2012) Foodomics: MS-based strategies in modern food science and nutrition. Mass Spectrom Rev 31:49–69
4. Ellis DI, Brewster VL, Dunn WB, Allwood JW, Golovanovc AP, Goodacre R (2012) Fingerprinting food: current technologies for the detection of food adulteration and contamination. Chem Soc Rev 41:5706–5727
5. Monakhova YB, Kuballa T, Lachenmeier DW (2013) Chemometric methods in NMR spectroscopic analysis of food products. J Anal Chem 68:755–766
6. Ibáñez C, García-Cañas V, Valdés A, Simó C (2013) Novel MS-based approaches and applications in food metabolomics. TrAC 52:100–111
7. Herrero M, García-Canñas V, Simó C, Cifuentes A (2010) Recent advances in the application of capillary electromigration methods for food analysis and foodomics. Electrophoresis 31:205–228
8. Castro-Puyana M, García-Canñas V, Simó C, Cifuentes A (2012) Recent advances in the application of capillary electromigration methods for food analysis and Foodomics. Electrophoresis 33:147–167
9. García-Cañas V, Simó C, Castro-Puyana M, Cifuentes A (2014) Recent advances in the application of capillary electromigration methods for food analysis and foodomics. Electrophoresis 35:147–169
10. Cifuentes A (2009) Food analysis and foodomics. J Chromatogr A 1216:7109–7110
11. Li X, Hu J, Han H (2011) Determination of cypromazine and its metabolite melamine in milk by cationselective exhaustive injection and sweepingcapillary micellar electrokinetic chromatography. J Sep Sci 34:323–330
12. Wu W-C, Tsai I-L, Sun S-W, Kuo C-H (2011) Using sweeping-micellar electrokinetic chromatography to determine melamine in food. Food Chem 128:783–789
13. Lv Y-K, Sun Y-N, Wang L-M, Jia C-L, Sun H-W (2011) A simple and high-throughput method of ultrasonic extraction-capillary electrophoresis for determination of melamine in milk. Anal Meth 3:2557–2561
14. Mandrioli R, Morganti E, Mercolini L, Kenndler E, Raggi MA (2011) Fast analysis of amino acids in wine by capillary electrophoresis with laser-induced fluorescence detection. Electrophoresis 32:2809–2815
15. Sánchez-Hernández L, Marina ML, Crego AL (2011) A capillary electrophoresis-tandem mass spectrometry methodology for the determination of non-protein amino acids in vegetable oils as novel markers for the detection of adulterations in olive oils. J Chromatogr A 1218:4944–4951
16. Zhao D, Lu M, Cai Z (2012) Separation and determination of B vitamins and essential

amino acids in health drinks by CE-LIF with simultaneous derivatization. Electrophoresis 33:2424–2432

17. Uzaşçı S, Başkan S, Erim FB (2012) Biogenic amines in wines and pomegranate molasses-A non-ionic micellar electrokinetic chromatography assay with laser-induced fluorescence detection. Food Anal Meth 5:104–108
18. Ginterová P, Marák J, Staňová A, Maier V, Ševčík J, Kaniansky D (2012) Determination of selected biogenic amines in red wines by automated on-line combination of capillary isotachophoresis-capillary zone electrophoresis. J Chromatogr B 904:135–139
19. Jastrzębska A (2012) A comparative study for determination of biogenic amines in meat samples by capillary isotachophoresis with two electrolyte systems. Eur Food Res Technol 235:563–572
20. Huang H-Y, Lin C-L, Jiang S-H, Singco B, Cheng Y-J (2012) Capillary electro chromatography-mass spectrometry determination of melamine and related triazine by-products using poly(divinyl benzene-alkene-vinylbenzyl trimethylammonium chloride) monolithic stationary phases. Anal Chim Acta 719:96–103
21. Fu N-N, Zhang H-S, Wang H (2012) Analysis of short-chain aliphatic amines in food and water samples using a near infrared cyanine 1-(ε-succinimydyl-hexanoate)-1′-methyl-3,3,3′,3′-tetramethyl-indocarbocyanine-5,5′-disulfonate potassium with CE-LIF detection. Electrophoresis 33:3002–3007
22. Li W-L, Ge J-Y, Pan Y-L, Chu Q-C, Ye J-N (2012) Direct analysis of biogenic amines in water matrix by modified capillary zone electrophoresis with 18-crown-6. Microchim Acta 177:75–80
23. Akamatsu S, Mitsuhashi T (2013) Development of a simple analytical method using capillary electrophoresis tandem mass spectrometry for product identification and simultaneous determination of free amino acids in dietary supplements containing royal jelly. J Food Compost Anal 30:47–51
24. Jastrzębska A, Piasta A, Filipiak-Szok A, Szłyk E (2013) Optimization of capillary isotachophoretic method for histidine determination in protein matrices. Anal Lett 46:1364–1378
25. Enzonga J, Ong-Meang V, Couderc F, Boutonnet A, Poinsot V, Tsieri MM, Silou T, Bouajila J (2013) Determination of free amino acids in African gourd seed milks by capillary electrophoresis with light-emitting diode induced fluorescence and laser-induced fluorescence detection. Electrophoresis 34:2632–2638
26. Heemskerk AA, Busnel JM, Schoenmaker B, Derks RJ, Klychnikov O, Hensbergen PJ, Deelder AM, Mayboroda OA (2012) Ultra-low flow electrospray ionization-mass spectrometry for improved ionization efficiency in phosphoproteomics. Anal Chem 84:4552–4559
27. Sázelova P, Kašička V, Leon C, Ibáñez E, Cifuentes A (2012) Capillary electrophoretic profiling of tryptic digests of water soluble proteins from Bacillus thuringiensis-transgenic and non-transgenic maize species. Food Chem 134:1607–1615
28. Català-Clariana S, Benavente F, Giménez E, Barbosa J, Sanz-Nebot V (2013) Identification of bioactive peptides in hypoallergenic infant milk formulas by CE-TOF-MS assisted by semiempirical model of electromigration behavior. Electrophoresis 34:1886–1894
29. Baxter G, Zhao J, Blanchard C (2011) Salinity alters the protein composition of rice endosperm and the physicochemical properties of rice flour. J Sci Food Agric 91:2292–2297
30. Latoszek A, García-Ruiz C, Marina ML, de la Mata FJ, Gómez R, Rasines B, Cifuentes A, Poboży E, Trojanowicz M (2011) Modification of resolution in capillary electrophoresis for protein profiling in identification of genetic modification in foods. Croat Chem Acta 84:375–382
31. Gasilova N, Gassner AL, Girault HH (2012) Analysis of major milk whey proteins by immunoaffinity capillary electrophoresis coupled with MALDI-MS. Electrophoresis 33:2390–2398
32. Chen L, Zeng R, Xiang L, Luo Z, Wang Y (2012) Polydopamine-*graft*-PEG antifouling coating for quantitative analysis of food proteins by CE. Anal Meth 4:2852–2859
33. Trudeau K, Vu KD, Shareck F, Lacroix M (2012) Capillary electrophoresis separation of protein composition of γ-irradiated food pathogens *Listeria monocytogenes* and *Staphylococcus aureus*. PLoS One 7:e32488
34. Masotti F, Battelli G, De Noni I (2012) The evolution of chemical and microbiological properties of fresh goat milk cheese during its shelf life. J Dairy Sci 95:4760–4767
35. Montealegre C, Rasines B, Gómez R, de la Mata FJ, García-Ruiz C, Marina ML (2012) Characterization of carboxylate-terminated carbosilane dendrimers and their evaluation as nanoadditives in capillary electrophoresis for vegetable protein profiling. J Chromatogr A 1234:16–21
36. Montealegre C, García MC, del Río C, Marina ML, García-Ruiz C (2012) Separation of olive proteins by capillary gel electrophoresis. Talanta 97:420–424b

37. Garrido-Medina R, Puerta A, Pelaez-Lorenzo C, Rivera-Monroy Z, Guttman A, Diez-Masa JC, de Frutos M (2013) Capillary electrophoresis with laser-induced fluorescence detection of proteins from two types of complex sample matrices: food and biological fluids. Meth Protocols 984:207–225
38. Pobozy E, Filaber M, Koc A, Garcia-Reyes JF (2013) Application of capillary electrophoretic chips in protein profiling of plant extracts for identification of genetic modifications of maize. Electrophoresis 34:2740–2753
39. Vitali L, Valese AC, Azevedo MS, Gonzaga LV, Costa AC, Piovezan M, Vistuba JP, Micke GA (2013) Development of a fast and selective separation method to determine histamine in tuna fish samples using capillary zone electrophoresis. Talanta 106:181–185
40. Ballus CA, Meinhart AD, Bruns RE, Godoy HT (2011) Use of multivariate statistical techniques to optimize the simultaneous separation of 13 phenolic compounds from extra-virgin olive oil by capillary electrophoresis. Talanta 83:1181–1187
41. Moreno M, Sanchez Arribas A, Bermejo E, Zapardiel A, Chicharro M (2011) Analysis of polyphenols in white wine by CZE with amperometric detection using carbon nanotube-modified electrodes. Electrophoresis 32:877–883
42. Lee ISL, Boyce MC, Breadmore MC (2011) A rapid quantitative determination of phenolic acids in Brassica oleracea by capillary zone electrophoresis. Food Chem 127:797–801
43. Verardo V, Gomez-Caravaca AM, Segura-Carretero A, Caboni MF, Fernandez-Gutierrez A (2011) Development of a CE-ESI-microTOF-MS method for a rapid identification of phenolic compounds in buckwheat. Electrophoresis 32:669–673
44. Godoy-Caballero MP, Acedo-Valenzuela MI, Duran-Meras I, Galeano-Diaz T (2012) Development of a non-aqueous capillary electrophoresis method with UV-visible and fluorescence detection for phenolics compounds in olive oil. Anal Bioanal Chem 403:279–290
45. Godoy-Caballero MP, Galeano-Diaz T, Acedo-Valenzuela MI (2012) Simple and fast determination of phenolic compounds from different varieties of olive oil by nonaqueous capillary electrophoresis with UV-visible and fluorescence detection. J Sep Sci 35:3529–3539
46. Papieva IS, Kirsanov DO, Legin AV, Kartsova LA, Alekseeva AV, Vlasov YG, Bhattacharyya N, Sarkar S, Bandyopadkhyay R (2011) Analysis of tea samples with a multisensor system and capillary electrophoresis. Rus J Appl Chem 84:964–971
47. Franquet-Griell H, Checa A, Núñez O, Saurina J, Hernandez-Cassou S, Puignou L (2012) Determination of polyphenols in Spanish wines by capillary zone electrophoresis. Application to wine characterization by using chemometrics. J Agric Food Chem 60:8340–8349
48. Lee ISL, Boyce MC, Breadmore MC (2012) Extraction and on-line concentration of flavonoids in *Brassica oleracea* by capillary electrophoresis using large volume sample stacking. Food Chem 133:205–211
49. Bustamante-Rangel M, Delgado-Zamarreno MM, Carabias-Martinez R, Dominguez-Alvarez J (2012) Analysis of isoflavones in soy drink by capillary zone electrophoresis coupled with electrospray ionization mass spectrometry. Anal Chim Acta 709:113–119
50. Gonda S, Parizsa P, Surányi G, Gýmánt G, Vasas G (2012) Quantification of main bioactive metabolites from saffron (Crocus sativus) stigmas by a micellar electrokinetic chromatographic (MEKC) method. J Pharm Biomed Anal 66:68–74
51. Montealegre C, Sánchez-Hernández L, Crego A, Marina ML (2013) Determination and characterization of glycerophospholipids in olive fruit and oil by nonaqueous capillary electrophoresis with electrospray-mass spectrometric detection. J Agric Food Chem 61:1823–1832
52. Koyama M, Nakamura C, Nakamura K (2013) Changes in phenols contents from buckwheat sprouts during growth stage. J Food Sci Technol 50:86–93
53. Široká J, Martincová A, Pospíšilová M, Polášek M (2013) Assay of citrus flavonoids, Troxerutin, and ascorbic acid in food supplements and pharmaceuticals by capillary zone electrophoresis. Food Anal Methods 6:1561–1567
54. Soliman LC, Donkor KK, Church JS, Cinel B, Prema D, Dugan MER (2013) Separation of dietary omega-3 and omega-6 fatty acids in food by capillary electrophoresis. J Sep Sci 36:3440–3448
55. Bustamante-Rangel M, Delgado-Zamarreño MM, Pérez-Martín L, Carabias-Martínez R (2013) QuEChERS method for the extraction of isoflavones from soy-based foods before determination by capillary electrophoresis-electrospray ionization-mass spectrometry. Microchem J 108:203–209
56. Godoy-Caballero MP, Culzoni MJ, Galeano-Díaz T, Acedo-Valenzuela MI (2013) Novel combination of non-aqueous capillary electrophoresis and multivariate curve resolution-alternating least squares to determine phenolic

acids in virgin olive oil. Anal Chim Acta 763:11–19

57. León C, García-Cañas V, González R, Morales P, Cifuentes A (2011) Fast and sensitive detection of genetically modified yeasts in wine. J Chromatogr A 1218:7550–7556
58. Zhang S, Jiang C, Jia L (2011) Tetrabutylammonium phosphate-assisted separation of multiplex polymerase chain reaction products in non-gel sieving capillary electrophoresis. Anal Biochem 408:284–288
59. Holck AL, Pedersen BO (2011) Simple, sensitive, accurate multiplex quantitative competitive PCR with capillary electrophoresis detection for the determination of genetically modified maize. Eur Food Res Technol 233:951–991
60. Jiang C, Xu S, Zhang S, Jia L (2012) Chitosan functionalized magnetic particle-assisted detection of genetically modified soybeans based on polymerase chain reaction and capillary electrophoresis. Anal Biochem 420:20–25
61. Gonçalves J, Pereira F, Amorim A, van Asch B (2012) New method for the simultaneous identification of cow, sheep, goat, and water buffalo in dairy products by analysis of short species-specific mitochondrial DNA targets. J Agric Food Chem 60:10480–10485
62. Hernández-Chávez JF, González-Córdova AF, Rodríguez-Ramírez R, Vallejo-Cordoba B (2011) Development of a polymerase chain reaction and capillary gel electrophoresis method for the detection of chicken or turkey meat in heat-treated pork meat mixtures. Anal Chim Acta 708:149–154
63. Gavazzi F, Casazza AP, Depedro C, Mastromauro F, Breviario D (2012) Technical improvement of the TBP (tubulin-based polymorphism) method for plant species detection, based on capillary electrophoresis. Electrophoresis 33:2840–2851
64. Oh MH, Hwang HW, Chung B, Paik HD, Han S, Kang SM, Ham JS, Kim HW, Seol KH, Jang A, Jung GY (2012) Simultaneous detection of 10 foodborne pathogens using capillary electrophoresis-based single strand conformation polymorphism. Korean J Food Sci Ani Resour 32:241–246
65. Chung B, Shin GW, Na J, Oh MH, Jung GY (2012) Multiplex quantitative foodborne pathogen detection using high resolution CE-SSCP coupled stuffer-free multiplex ligation-dependent probe amplification. Electrophoresis 33:1477–1481
66. Vigentini I, De Lonrenzis G, Picozzi C, Imazio S, Merico A, Galafassi S, Piskur J, Poschino R (2012) Intraspecific variations of Dekkera/Brettanomyces bruxellensis genome studied by capillary electrophoresis separation of the intron splice site profiles. Int J Food Microbiol 157:6–15
67. Miya S, Takahashi H, Kamimura C, Nakagawa M, Kuda T, Kimura B (2012) Highly discriminatory typing method for Listeria monocytogenes using polymorphic tandem repeat regions. J Microbiol Methods 90:285–291
68. Valdés A, García-Cañas V, Cifuentes A (2013) CGE-laser induced fluorescence of double-stranded DNA fragments using GelGreen dye. Electrophoresis 34:1555–1562
69. Chen CH, Hsieh CH, Hwang DF (2013) PCR-RFLP analysis using capillary electrophoresis for species identification of Cyprinidae-related products. Food Control 33:477–483
70. Ruan J, Li M, Liu YP, Li YQ, Li YX (2013) Rapid and sensitive detection of Cronobacter spp. (previously Enterobacter sakazakii) in food by duplex PCR combined with capillary electrophoresis-laser-induced fluorescence detector. J Chromatogr B Anal Technol Biomed Life Sci 921–922:15–20
71. Truica GI, Teodor E, Dumitru E, Radu GL (2012) Quantification of ascorbic acid and B-complex vitamins in corn flour and corn flakes. Rev Chim 63:445–450
72. Tortajada-Genaro LA (2012) Determination of L-ascorbic acid in tomato by capillary electrophoresis. J Chem Educ 89:1194–1197
73. Dziomba S, Kowalski P, Baczek T (2012) Field-amplified sample stacking-sweeping of vitamins B determination in capillary electrophoresis. J Chromatogr A 1267:224–230
74. Galeano-Diaz T, Acedo-Valenzuela MI, Silva-Rodriguez AJ (2012) Determination of tocopherols in vegetable oil samples by non-aqueous capillary electrophoresis (NACE) with fluorimetric detection. Food Compos Anal 25:24–30
75. Da Silva DC, Visentainer JV, de Souza NE, Oliveira CC (2013) Micellar electrokinetic chromatography method for determination of the ten water-soluble vitamins in food supplements. Food Anal Meth 6:1592–1606
76. Chen J, Sun J, Liu S (2013) Determination of riboflavin in cereal grains by capillary electrophoresis with laser-induced fluorescence detection with on-line concentration. Anal Lett 46:887–899
77. Mu G, Luan F, Liu H, Gao Y (2013) Use of experimental design and artificial neural network in optimization of capillary electrophoresis for the determination of nicotinic acid and nicotinamide in food compared with high-performance liquid chromatography. Food Anal Meth 6:191–200

78. Meinhart AD, Ballus CA, Bruns RE, Lima Pallone JA, Godoy HT (2011) Chemometrics optimization of carbohydrate separations in six food matrices by micellar electrokinetic chromatography with anionic surfactant. Talanta 85:237–244
79. Sarazin C, Delaunay N, Costanza C, Eudes V, Mallet JM, Gareil P (2011) New avenue for mid-UV-range detection of underivatized carbohydrates and amino acids in capillary electrophoresis. Anal Chem 83:7381–7387
80. Tuma P, Malkova K, Samcova E, Stulik K (2011) Rapid monitoring of mono- and disaccharides in drinks, foodstuffs and foodstuff additives by capillary electrophoresis with contactless conductivity detection. Anal Chim Acta 698:1–5
81. Rizelio VM, Tenfen L, da Silveira R, Gonzaga LV, Oliveira Costa AC, Fett R (2012) Development of a fast capillary electrophoresis method for determination of carbohydrates in honey samples. Talanta 93:62–66
82. Cebolla-Cornejo J, Valcarcel M, Herrero-Martinez JM, Rosello S, Nuez F (2012) High efficiency joint CZE determination of sugars and acids in vegetables and fruit. Electrophoresis 33:2416–2423
83. Wang T, Yang X, Wang D, Jiao Y, Wang Y, Zhao Y (2012) Analysis of compositional carbohydrates in polysaccharides and foods by capillary zone electrophoresis. Carbohydr Polym 88:754–762
84. Taga A, Kodama S (2012) Analysis of reducing carbohydrates and fructosyl saccharides in maple syrup and maple sugar by CE. Chromatographia 75:1009–1016
85. Sarazin C, Delaunay N, Costanza C, Eudes V, Gareil P, Vial J (2012) On the use of response surface strategy to elucidate the electrophoretic migration of carbohydrates and optimize their separation. J Sep Sci 35:1351–1358
86. Sarazin C, Delaunay N, Costanza C, Eudes V, Gareil P (2012) Application of a new capillary electrophoretic method for the determination of carbohydrates in forensic, pharmaceutical, and beverage samples. Talanta 99:202–206
87. Vochyánová B, Opekar F, Tůma P, Štulík K (2012) Rapid determinations of saccharides in high-energy drinks by short-capillary electrophoresis with contactless conductivity detection. Anal Bioanal Chem 404:1549–1554
88. Jastrzebska A (2011) Capillary isotachophoresis as rapid method for determination of orthophosphates, pyrophosphates, tripolyphosphates and nitrites in food samples. J Food Comp Anal 24:1049–1056
89. Mikus P, Marakova K, Veizerova L, Piestansky J (2011) Determination of quinine in beverages by online coupling capillary isotachophoresis to capillary zone electrophoresis with UV spectrophotometric detection. J Sep Sci 34:3392–3398
90. Sanchez-Hernandez L, Castro-Puyana M, Marina ML, Crego AL (2011) Determination of betaines in vegetable oils by capillary electrophoresis tandem mass spectrometry—application to the detection of olive oil adulteration with seed oils. Electrophoresis 32:1394–1401
91. Zhang JB, Li MJ, Li WL, Chu QC, Ye JJ (2011) A novel capillary electrophoretic method for determining aliphatic aldehydes in food samples using 2-thiobarbituric acid derivatization. Electrophoresis 32:705–711
92. Zhang D, Zhang J, Li M, Li W, Aimaiti G, Tuersun G, Ye J, Chu Q (2011) A novel miniaturised electrophoretic method for determining formaldehyde and acetaldehyde in food using 2-thiobarbituric acid derivatisation. Food Chem 129:206–212
93. Heller M, Vitali L, Leal O, Marcone A, Costa AC, Micke GA (2011) A Rapid sample screening method for authenticity control of whiskey using capillary electrophoresis with online preconcentration. Agric Food Chem 59:6882–6888
94. Masotti F, Erba D, De Noni I, Pellegrino L (2012) Rapid determination of sodium in milk and milk products by capillary zone electrophoresis. J Dairy Sci 95:2872–2881
95. Carpio A, Mercader-Trejo F, Arce L, Valcarcel M (2012) Use of carboxylic group functionalized magnetic nanoparticles for the preconcentration of metals in juice samples prior to the determination by capillary electrophoresis. Electrophoresis 33:2446–2453
96. Kuban P, Kiplagat IK, Bocek P (2012) Electrokinetic injection across supported liquid membranes: New sample pretreatment technique for online coupling to capillary electrophoresis. Direct analysis of perchlorate in biological samples. Electrophoresis 33:2695–2702
97. Golubenko AM, Nikonorov VV, Nikitina TG (2012) Determination of hydroxycarboxylic acids in food products by capillary electrophoresis. J Anal Chem 67:778–782
98. Erdogan BY, Onar AN (2012) Determination of nitrates, nitrites and oxalates in kale and sultana pea by capillary electrophoresis. J Food Drug Anal 20:532–538
99. Akamatsu S, Mitsuhashi T (2012) Development of a simple capillary electrophoretic determination of glucosamine in nutritional supplements using in-capillary derivatisation with o-phthalaldehyde. Food Chem 130:1137–1141

100. Liotta E, Gottardo R, Seri C, Rimondo C, Miksik I, Serpelloni G, Tagliaro F (2012) Rapid analysis of caffeine in "smart drugs" and "energy drinks" by microemulsion electrokinetic chromatography (MEEKC). Forensic Sci Int 220:279–283
101. Yue ME, Xu J, Li QQ, Hou WG (2012) Separation and determination of bromophenols in *Trachypenaeus curvirostris* and *Lepidotrigla microptera* by capillary zone electrophoresis. J Food Drug Anal 20:88–93
102. Taga A, Sato A, Suzuki K, Takeda M, Kodama S (2012) Simple determination of a strongly aromatic compound, sotolon, by capillary electrophoresis. J Oleo Sci 61:45–48
103. Václavíková E, Kvasnička F (2013) Isotachophoretic determination of glucosamine and chondroitin sulphate in dietary supplements. Czech J Food Sci 1:55–65
104. Vachirapatama N, Maitresorasun S (2013) Simultaneous determination of melamine, ammelide, ammeline and cyanuric acid in milk products by micellar electrokinetic chromatography. J Food Drug Anal 21:66–72
105. Cheng YJ, Huang SH, Singco B, Huang HY (2011) Analyses of sulfonamide antibiotics in meat samples by on-line concentration capillary electrochromatography-mass spectrometry. J Chromatogr A 1218:7640–7647
106. Kowalski P, Plenis A, Oledzka I, Konieczna L (2011) Optimization and validation of the micellar electrokinetic capillary chromatographic method for simultaneous determination of sulfonamide and amphenicol-type drugs in poultry tissue. J Pharm Biomed Anal 54:160–167
107. Huang HY, Liu WL, Hsieh SH, Shih YH (2011) On-line concentration sample stacking coupled with water-in-oil microemulsion electrokinetic chromatography. J Chromatogr A 1218:7663–7669
108. Bodoki E, Iacob BC, Oprean R (2011) Capillary electromigration techniques for the quantitative analysis of colchicine. Croat Chem Acta 84:383–391
109. Hermo MP, Nemutlu E, Barbosa J, Barrón D (2011) Multiresidue determination of quinolones regulated by the European Union in bovine and porcine plasma. Application of chromatographic and capillary electrophoretic methodologies. Biomed Chromatogr 25:555–569
110. Wang Y, Xiao L, Cheng M (2011) Determination of phenylureas herbicides in food stuffs based on matrix solid-phase dispersion extraction and capillary electrophoresis with electrochemiluminescence detection. J Chromatogr A 1218:9115–9119
111. Zhang X, Zhang Z (2012) Capillary electrophoresis-based immunoassay with electrochemical detection as rapid method for determination of saxitoxin and decarbamoylsaxitoxin in shellfish samples. J Food Compos Anal 28:61–68
112. Piñeiro MY, Garrido-Delgado R, Bauza R, Arce L, Valcarcel M (2012) Easy sample treatment for the determination of enrofloxacin and ciprofloxacin residues in raw bovine milk by capillary electrophoresis. Electrophoresis 33:2978–2986
113. Mu G, Liu H, Xu L, Tian L, Luan F (2012) Matrix solid-phase dispersion extraction and capillary electrophoresis determination of tetracycline residues in milk. Food Anal Meth 5:148–153
114. Hu XZ, Chen ML, Gao Q, Yu QW, Feng YQ (2012) Determination of benzimidazole residues in animal tissue samples by combination of magnetic solid-phase extraction with capillary zone electrophoresis. Talanta 89:335–341
115. Santalad A, Srijaranai S, Burakham R (2012) Reversed electrode polarity stacking sample preconcentration combined with micellar electrokinetic chromatography for the analysis of carbamate insecticide residues in fruit juices. Food Anal Meth 5:96–103
116. Liu C, Fang G, Deng Q, Zhang Y, Feng J, Wang S (2012) Determination of metolcarb in food by capillary electrophoresis immunoassay with a laser-induced fluorescence detector. Electrophoresis 33:1471–1476
117. Domínguez-Álvarez J, Rodríguez-Gonzalo E, Hernández-Méndez J, Carabias-Martínez R (2012) Programed nebulizing-gas pressure mode for quantitative capillary electrophoresis-mass spectrometry analysis of endocrine disruptors in honey. Electrophoresis 33:2374–2381
118. Zhang X, Zhang Z (2013) Capillary electrophoresis-based immunoassay for the determination of brevetoxin-B in shellfish using electrochemical detection. J Chromatogr Sci 51:107–111
119. Zhu D, Zhang H, Bing X (2013) Preparation of an immunoaffinity column for the clean-up of fermented food samples contaminated with citrinin. Food Add Cont 20:389–394
120. Luque MI, Córdoba JJ, Rodríguez A, Núñez F, Andrade MJ (2013) Development of a PCR protocol to detect ochratoxin A producing moulds in food products. Food Control 29:270–278
121. Sun H, Qi H, Li H (2013) Development of capillary electrophoretic method combined with accelerated solvent extraction for simultaneous

determination of residual sulfonamides and their acetylated metabolites in aquatic products. Food Anal Meth 6:1049–1055

122. Ferey L, Delaunay N, Rutledge DN, Huertas A, Raoul Y, Gareil P, Vial J (2013) Use of response surface methodology to optimize the simultaneous separation of eight polycyclic aromatic hydrocarbons by capillary zone electrophoresis with laser-induced fluorescence detection. J Chromatogr A 1302:181–190
123. Knobel G, Campiglia AD (2013) Determination of polycyclic aromatic hydrocarbon metabolites in milk by a quick, easy, cheap, effective, rugged and safe extraction and capillary electrophoresis. J Sep Sci 36:2291–2298
124. Víctor-Ortega MD, Lara FJ, García-Campaña AM, Olmo-Iruela M (2013) Evaluation of dispersive liquideliquid microextraction for the determination of patulin in apple juices using micellar electrokinetic capillary chromatography. Food Control 31:353–358
125. Güray T, Tuncel M, Uysal UD (2013) A rapid determination of patulin using capillary zone electrophoresis and its application to analysis of apple juices. J Chromatogr Sci 51:310–317
126. Güray T, Tuncel M, Uysal UD, Oncu-Kaya EM (2013) Determination of zearalenone by the capillary zone electrophoresis-UV detection and its application to poultry feed and cereals. J Liq Chromatogr Relat Technol 36:1366–1378
127. Wei X, Gao X, Zhao L, Peng X, Zhou L, Wang J, Pu Q (2013) Fast and interference-free determination of glyphosate and glufosinate residues through electrophoresis in disposable microfluidic chips. J Chromatogr A 1281:148–154
128. Martínez-Villalba A, Núñez O, Moyano E, Galceran MT (2013) Field amplified sample injection-capillary zone electrophoresis for the analysis of amprolium in eggs. Electrophoresis 34:870–876
129. Domínguez-Álvarez J, Mateos-Vivas M, García-Gómez D, Rodríguez-Gonzalo E, Carabias-Martínez R (2013) Capillary electrophoresis coupled to mass spectrometry for the determination of anthelmintic benzimidazoles in eggs using a QuEChERS with preconcentration as sample treatment. J Chromatogr A 1278:166–174
130. Liu L, He B, Yun Z, Sun J, Jiang G (2013) Speciation analysis of arsenic compounds by capillary electrophoresis on-line coupled with inductively coupled plasma mass spectrometry using a novel interface. J Chromatogr A 1304:227–233
131. Polo-Luque ML, Simonet BM, Valcárcel M (2013) Solid phase extraction-capillary electrophoresis determination of sulphonamide residues in milk samples by use of C18-carbon nanotubes as hybrid sorbent materials. Analyst 138:3786–3791
132. Yoshikawa K, Saito S, Sakuragawa A (2012) Simultaneous analysis of acidulants and preservatives in food samples by using capillary zone electrophoresis with indirect UV detection. Food Chem 127:1385–1390
133. Bottoli CBG, Gutierrez-Ponce MJS, Aguiar VS, de Aquino WM (2011) Determination of parabens in sweeteners by capillary electrochromatography. J Pharm Sci 47:779–785
134. Zhang X, Xu S, Sun Y, Wang Y, Wang C (2011) Simultaneous determination of benzoic acid and sorbic acid in food products by CE after on-line preconcentration by dynamic pH junction. Chromatographia 73:1217–1221
135. Fukuji TS, Castro-Puyana M, Tavares MFM, Cifuentes A (2011) Fast determination of Sudan dyes in chilli tomato sauces using partial filling micellar electrokinetic chromatography. J Agric Food Chem 59:11903–11909
136. Fukuji TS, Castro-Puyana M, Tavares MFM, Cifuentes A (2012) Sensitive and fast determination of Sudan dyes in chilli powder by partial-filling micellar electrokinetic chromatography- tandem mass spectrometry. Electrophoresis 33:705–712
137. Mu G, Liu H, Gao Y, Luan F (2011) Determination of benzoyl peroxide, as benzoic acid, in wheat flour by capillary electrophoresis compared with HPLC. J Sci Food Agric 4:960–964
138. Mazorra-Manzano A, Torres-Llanez M, Gonzalez-Córdova MJ, González-Córdova AF, Vallejo-Cordoba B (2012) A capillary electrophoresis method for the determination of hydroxyproline as a collagen content index in meat products. Food Anal Method 5:46–470
139. Dong YL, Yan N, Li X, Zhou XM, Zhou L, Zhang HJ, Chen XG (2012) Rapid and sensitive determination of hydroxyproline in dairy products using micellar electrokinetic chromatography with laser-induced fluorescence detection. J Chromatogr A 1233:156–160
140. Hu F, Xu L, Luan F, Liu H, Gao Y (2013) Determination of neotame in non-alcoholic beverage by capillary zone electrophoresis. J Sci Food Agric 93:3334–3338
141. Petruci JF, Pereira EA, Cardoso AA (2013) Determination of 2-methylimidazole and 4-methylimidazole in caramel colors by capillary electrophoresis. J Agric Food Chem 61:2263–2267

142. Stojkovic M, Mai TD, Hauser PC (2013) Determination of artificial sweeteners by capillary electrophoresis with contactless conductivity detection optimized by hydrodynamic pumping. Anal Chim Acta 787:254–259
143. Fernandes VNO, Fernandes LB, Vasconcellos JP, Jager AV, Tonin FG, de Oliveira MAL (2013) Simultaneous analysis of aspartame, cyclamate, saccharin and acesulfame-K by CZE under UV detection. Anal Methods 5:1524–1532
144. Dominguez-Vega E, Crego AL, Lomsadze K, Chankvetadze B, Marina ML (2011) Enantiomeric separation of FMOC-amino acids by nano-LC and CEC using a new chiral stationary phase, cellulose tris(3-chloro-4-methylphenylcarbamate. Electrophoresis 32:2700–2707
145. Giuffrida A, Caruso R, Messina M, Maccarrone G, Contino A, Cifuentes A, Cucinotta V (2012) Chiral separation of amino acids derivatised with fluorescein isothiocyanate by single isomer derivatives 3-monodeoxy-3-monoamino-β- and -γ-cyclodextrins: the effect of the cavity size. J Chromatogr A 1269:360–365
146. Kodama S, Taga A, Aizawa S-I, Kemmei T, Honda Y, Suzuki K, Yamamoto A (2012) Direct enantioseparation of lipoic acid in dietary supplements by capillary electrophoresis using trimethyl-β-cyclodextrin as a chiral selector. Electrophoresis 33:2441–2445
147. Kodama S, Aizawa S, Taga A, Yamamoto A, Honda Y, Suzuki K, Kemmei T, Hayakawa K (2013) Determination of α-hydroxy acids and their enantiomers in fruit juices by ligand exchange CE with a dual central metal ion system. Electrophoresis 34:1327–1333
148. Kusano M, Redestig H, Hirai T, Oikawa A, Matsuda F, Fukushima A, Arita M, Watanabe S, Yano M, Hiwasa-Tanase K, Ezura H, Saito K (2011) Covering chemical diversity of genetically-modified tomatoes using metabolomics for objective substantial equivalence assessment. PLoS One 6:e16989
149. Simó C, Ibáñez C, Gómez-Martínez A, Ferragut JA, Cifuentes A (2011) Is metabolomics reachable? Different purification strategies of human colon cancer cells provide different CE-MS metabolite profiles. Electrophoresis 32:1765–1777
150. Celebier M, Ibañez C, Simó C, Cifuentes A (2012) A Foodomics approach: CE-MS for comparative metabolomics of colon cancer cells treated with dietary polyphenols. Methods Mol Biol 869:185–195
151. Ibáñez C, Simó C, García-Cañas V, Ferragut JA, Cifuentes A (2012) CE/LC-MS multiplatform for broad metabolomic analysis of dietary polyphenols effect on colon cancer cells proliferation. Electrophoresis 33:2328–2336
152. Ibáñez C, Valdés A, García-Cañas V, Simó C, Celebier M, Rocamora L, Gómez A, Herrero M, Castro M, Segura-Carretero A, Ibáñez E, Ferragut JA, Cifuentes A (2012) Global foodomics strategy to investigate the health benefits of dietary constituents. J Chromatogr A 1248:139–153
153. Valdés A, Simó C, Ibáñez C, Rocamora L, Ferragut JA, García-Cañas V, Cifuentes A (2012) Effect of dietary polyphenols on K562 leukemia cells: a foodomics approach. Electrophoresis 33:2314–2327
154. Contreras-Gutiérrez PK, Hurtado-Fernández E, Gómez-Romero M, Hormaza JI, Carrasco-Pancorbo A, Fernández-Gutiérrez A (2013) Determination of changes in the metabolic profile of avocado fruits (Persea americana) by two CE-MS approaches (targeted and non-targeted). Electrophoresis 34:2928–2942
155. Wishart DS, Knox C, Guo AC, Eisner R, Young N, Gautam B, Hau DD, Psychogios N, Dong E, Bouatra S, Mandal R, Sinelnikov I, Xia J, Jia L, Cruz JA, Lim E, Sobsey CA, Shrivastava S, Huang P, Liu P, Fang L, Peng J, Fradette R, Cheng D, Tzur D, Clements M, Lewis A, De Souza A, Zuniga A, Dawe M, Xiong Y, Clive D, Greiner R, Nazyrova A, Shaykhutdinov R, Li L, Vogel HJ, Forsythe I (2009) HMDB: a knowledgebase for the human metabolome. Nucleic Acids Res 37:D603–D610
156. Smith CA, O'Maille G, Want EJ, Qin C, Trauger SA, Brandon TR, Custodio DE, Abagyan R, Siuzdak G (2005) METLIN: a metabolite mass spectral database. Ther Drug Monit 27:747–751
157. Kanehisa M, Goto S (2000) KEGG: Kyoto encyclopedia of genes and genomes. Nucleic Acids Res 28:27–30

3.3.2. CE-MS in food analysis and Foodomics

Acunha, T., Ibañez, C., García-Cañas, V., Cifuentes, A., Simó, C.

In Capillary Electrophoresis–Mass Spectrometry (CE-MS): Principles and Applications, Edited by De Jong, G., 193–215 (2016) Wiley-VCH, Weinheim.

DOI: 10.1002/9783527693801.ch8.

Edited by
Gerhardus de Jong

Capillary Electrophoresis – Mass Spectrometry (CE-MS)

Principles and Applications

WILEY-VCH
Verlag GmbH & Co. KGaA

Editor

Prof. Gerhardus de Jong
Utrecht University
Department of Pharmaceutical Sciences
David de Wiedgebouw
Universiteitsweg 99
3584 CG Utrecht
The Netherlands

Library of Congress Card No.: applied for

British Library Cataloguing-in-Publication Data
A catalogue record for this book is available from the British Library.

Bibliographic information published by the Deutsche Nationalbibliothek
The Deutsche Nationalbibliothek lists this publication in the Deutsche Nationalbibliografie; detailed bibliographic data are available on the Internet at <http://dnb.d-nb.de>.

Print ISBN: 978-3-527-33924-2
ePDF ISBN: 978-3-527-69383-2
ePub ISBN: 978-3-527-69381-8
Mobi ISBN: 978-3-527-69382-5
oBook ISBN: 978-3-527-69380-1

Cover Design Formgeber, Mannheim, Germany
Typesetting SPi Global, Chennai, India
Printing and Binding

Printed on acid-free paper

8
CE-MS in Food Analysis and Foodomics

Tanize Acunha, Clara Ibáñez, Virginia García-Cañas, Alejandro Cifuentes, and Carolina Simó

8.1
Introduction: CE-MS, Food Analysis, and Foodomics

As a result of globalization in food trade, the distance between the producers of food and food ingredients and the consumers has increased enormously. Consequently, maintaining safety and quality along the food chain has become a difficult challenge nowadays. Moreover, food safety and quality are crucial not only due to their impact on consumers' health but also because food industry is a mainstay of the economy of many countries. To ensure consumption of safe and high-quality foodstuffs, it is essential to improve traceability. The EU defines traceability as the ability to trace and follow a food, feed, food-producing animal or substance intended to be or expected to be incorporated into a food or feed, through all stages of production, processing, and distribution [1]. Effective traceability systems are useful for the prevention of fraudulent practices, which, in most cases, focus on illicit economic gain. Such practices may include adulteration, mislabeling, false use of geographical indications, and deliberate fraudulent practices (production, processing, and distribution), among others. Not only is traceability a way to improve food safety, but it can also be seen as a strategic tool to improve the quality of foods and a way to increase the trust of costumers, and therefore, companies can use traceability as a source of competitive advantages [2].

Foodomics has been defined as a discipline that studies the food and nutrition domains through the application and integration of advanced omics technologies to improve consumer's well-being, health, and confidence [3, 4]. Thus, Foodomics is intended to be a global discipline that includes all of the emerging working areas in which food (including nutrition), advanced analytical techniques (mainly omics tools), and bioinformatics are combined [3]. For both conventional food analysis and Foodomics, advanced analytical strategies are applied [4], and among them, mass spectrometry (MS) plays a crucial role [5]. However, due to the complexity of the food matrices, the use of MS is often not enough to unravel their composition. To overcome this important limitation, hyphenated mass spectrometry techniques such as gas chromatography–mass spectrometry (GC-MS), liquid chromatography–mass spectrometry (LC-MS), and capillary

Capillary Electrophoresis–Mass Spectrometry (CE-MS): Principles and Applications,
First Edition. Edited by Gerhardus de Jong.

electrophoresis–mass spectrometry (CE-MS) have achieved great success in food analysis applications [6]. LC-MS is applicable to the analysis of a wide range of semipolar compounds with a wide range of molecule sizes. GC-MS is particularly appropriate for the analysis of volatile organic compounds. CE-MS, on the other hand, is particularly suited for the rapid separation of ionic, weakly ionic, and/or highly polar compounds with very high resolution. Main advantages include minimum sample and reagent consumption and fast separation speed. It is also environmentally friendly due to its low solvent consumption. On the other hand, poor sensitivity is one of the main drawbacks of CE, which can be improved by combining CE with MS detection [7]. Moreover, the use of preconcentration strategies can give further sensitivity gain. It is worth mentioning that CE-MS is not as robust and stable as GC-MS or LC-MS, due to the need to complete the CE electrical circuit for separation and simultaneously provide an electrical potential to the spray tip. Typically, this is accomplished with a sheath-liquid ESI interface due to its higher robustness compared to other ESI interface approaches. Sheath liquid compromises sensitivity, and thus, continuous efforts are still being made for the development of robust sheathless interfaces with the aim to improve stability and sensitivity. The use of high-resolution mass spectrometry also greatly improves the analytical performance of CE-MS and offers a good combination of selectivity and sensitivity. When working with CE-MS, the combination of migration time, accurately measured mass, and, when possible, MS/MS fragmentation spectra can support compound identification. Within this context, the use of CE-MS in food analysis and Foodomics offers numerous opportunities to obtain valuable information that can directly be correlated to food quality, safety, bioactivity, and other features related to food processing, storage, authenticity assessment, and so on.

This chapter presents an overview on the advantages and drawbacks of the application of CE-MS in food safety and quality, as well as in other aspects related to food traceability and bioactivity following classical food analysis as well as novel Foodomics approaches.

8.1.1 CE-MS and Food Safety

Food safety is still a global health objective. Although the safety of food has dramatically improved, foodborne diseases from microbial contamination, chemicals, and toxins are a major cause of illness and death worldwide. Food safety assessment involves the examination of food for the presence of hazards induced by pathogen agents such as bacteria, viruses, parasites, toxigenic molds, microalgae and also for the presence of noxious chemical compounds such as agrochemicals, toxins, industrial/environmental contaminants, veterinary drugs, and allergens. On the other hand, adulteration and other deliberate fraudulent practices (production, processing, packing, distribution) might also have implications in food safety. Analytical information, including the following data for both recognized and new hazardous compounds, is therefore essential to advance in this important area of research.

Economically motivated food adulteration is an emerging health risk in a growing globalized food trade. In most cases, fraudsters are focused on economic gain and do not have the resources/knowledge to assess whether such a manipulation poses any toxicological or hygienic risk to the purchaser or the consumer [8]. A clear example is the adulteration of milk and milk products with melamine to falsely increase the apparent protein levels [9]. This dangerous fact promoted analytical method development worldwide focused on the detection of that contaminant [10]. LC and GC coupled with MS have demonstrated to be powerful techniques to analyze melamine and related compounds [11]. CE/capillary electrochromatography (CEC)-MS have also been shown to be attractive alternative methods for fast and minimum sample and reagent consumption approaches [12, 13]. As an example, a CEC-MS method was proposed by Huang *et al*. as an alternative to LC-MS, employing poly(divinyl benzene-alkene-vinylbenzyl trimethylammonium chloride) monoliths as stationary phase for the analysis of melamine and its three by-products (ammeline, ammelide, and cyanuric acid) [13]. MS detection permitted the reduction of the LODs by three orders of magnitude relative to UV detection reaching values of $2.2-19.4\,\mu g\,l^{-1}$.

Determination of veterinary drug residues in food products from treated animals is an issue of major concern on food analysis due to its implications on human health. Animals may be treated with drugs for prevention or cure of diseases or to promote their growth. As a result, undesirable antibiotic residues can remain on meat, milk, eggs, and so on. The presence of these drug residues in food is strictly regulated by specific legislation in many countries through the imposition of maximum residue limit (MRL) values. Thus, an efficient analysis of veterinary drugs residues in foodstuffs, and also in environmental samples, is a constant challenge for researchers. Excellent review works on CE analysis of antibiotics have been published in which interested readers on this issue can find more detailed information [14, 15]. The problem of the low sensitivity of CE for drug residue analysis has been addressed by a variety of preconcentration techniques. For example, field-amplified sample injection (FASI)-CE permitted the quantification of amprolium in eggs at concentrations down to $75\,\mu g\,kg^{-1}$ [16]. In that work, CE-MS permitted the identification of one interference from the matrix (thiamine) eluting at the same migration time as amprolium and the subsequent method optimization. Domínguez-Álvarez *et al*. developed and validated a combination of QuEChERS (quick, easy, cheap, effective, rugged, and safe) methodology with CE-MS for the determination of trace levels of benzimidazoles (2-aminobenzimidazole, carbendazim, albendazole-2-aminosulfone, 5-hydroxy-thiabendazole, oxibendazole, albendazole, fenbendazole, oxfendazole, albendazole-sulfone, fenbendazole-sulfone) in eggs [17]. Following this approach, the LODs for these residues in egg samples were between 3 and $51\,\mu g\,l^{-1}$. Molecularly imprinted polymers (MIPs) have been evaluated as sorbents for in-line solid-phase extraction (SPE) and sample cleanup in CE-MS for antibacterial drugs [18]. This in-line MISPE-CE-MS system permitted direct milk injection for the determination of eight veterinary quinolones and related metabolites (danofloxacin, sarafloxacin, difloxacin, enrofloxacin, ciprofloxacin, flumequine,

marbofloxacin, and oxolinic acid) with LOD values from 1.0 to 1.4 $\mu g\,kg^{-1}$, which are below the MRLs established by the EU regulation. A group of fluoroquinolones were analyzed by CE-UV and off-line combination of CE and matrix-assisted laser desorption/ionization–time-of-flight mass spectrometry (MALDI-TOF) [19]. Although the advantages of this off-line approach are not clear, it permitted the separation and identification of ciprofloxacin, norfloxacin, and ofloxacin in bovine milk samples.

Analysis of pesticide residues is of the outmost importance in environmental and food samples. Within this field, a comprehensive overview of the current CE developments for herbicide analysis was published in 2014 [20]. There are also examples of the application of novel CE developments for the determination of fungicides and insecticides in food samples [21, 22]. Regarding the use of CE-MS, Daniel *et al*. showed the applicability of this technique for the determination of halosulfuron-methyl herbicide residues in samples of sugarcane juice and tomato [23]. The samples were submitted to a QuEChERS extraction procedure prior to CE-MS/MS analysis to accomplish with the sensitivity and specificity values indicated by the international legislation about halosulfuron-methyl in sugarcane and tomato. The reported recovery values for spiked samples ranged from 96% to 105%, and the LOD for the herbicide in juice and tomato was 2 ppb.

In addition to the analysis of drug/pesticide residues, there is a wide range of **contaminants** that can be found in food/feed. According to the *Codex Alimentarius* [24], a contaminant is "any substance not intentionally added to food, which is present in such food as a result of the production, manufacture, processing, preparation, treatment, packing, packaging, transport or holding of such food or as a result of environmental contamination." A variety of industrial chemicals have been reported as persistent organic pollutants or environmental contaminants, which may enter at several stages of food/feed production. Food-packaging-derived chemicals may also contaminate foodstuffs, and some of them can alter functions of the endocrine system and consequently cause adverse health effects. The feasibility of CE-MS for the analysis of several endocrine disruptors has also been demonstrated [25]. CE-MS was applied to the analysis of 2,4-dichlorophenol, 2,4,5-trichlorophenol, pentachlorophenol, bisphenol-A, 4-*tert*-butyl-phenol, and 4-*tert*-butyl benzoic acid in spiked honey samples. Prior to CE-MS, a liquid–liquid extraction procedure was applied and LODs were in the 1–4 $ng\,g^{-1}$ range. Naturally occurring toxins (produced by algae, fungi, and plants), which are not intentionally added to food and feed, can also get into the food chain [26]. Phycotoxin-producing algae can be accumulated in edible shellfish, crustaceans, and fish, causing possible poisoning when inadvertently consumed. Poisoning due to marine toxins occurs worldwide and can produce acute effects, or chronic health effects, but also economic damages to shellfish farming. Sassolas *et al*. have reviewed current capillary electromigration approaches, among others, for the analysis of okadaic acid, a toxin that contaminates bivalves and causes severe public health problems and economic damages to shellfish farming [27]. Keyon *et al*. compared four CE methods with different detection methods, for the analysis of paralytic shellfish toxins (PSTs) in terms

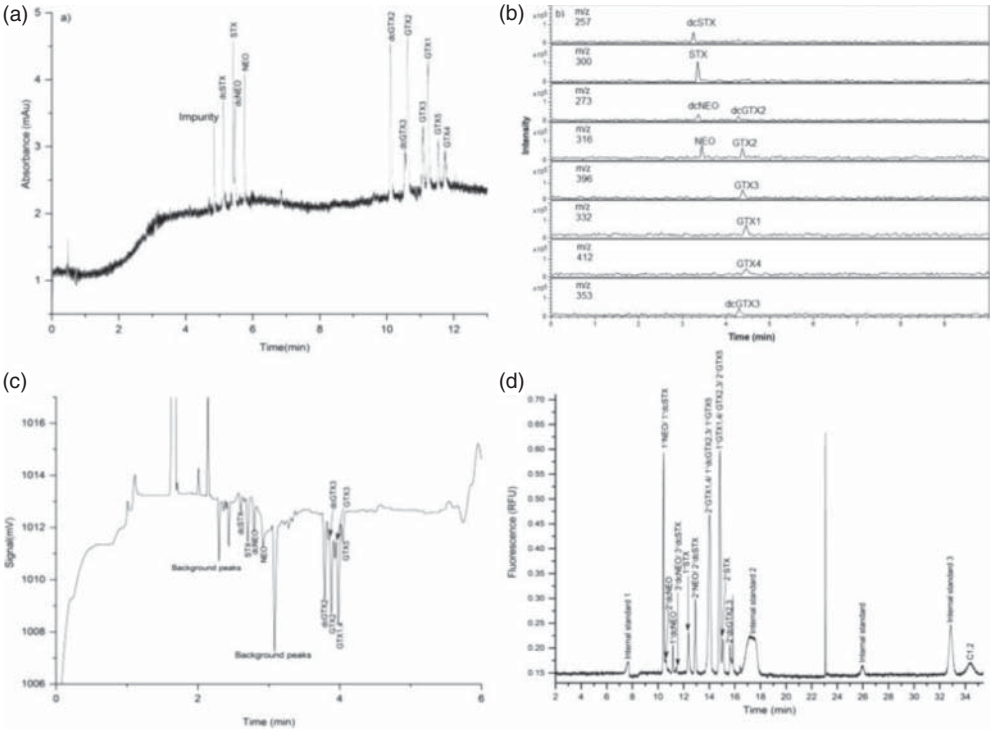

Figure 8.1 Separation of PST mixture using four different CE methods. (a) Electropherogram of CZE-UV using 30 mM phosphate buffer pH 2.5, sample injected at 5 kV for 10 s. (b) Extracted ion electropherogram) of CZE-MS at selected *m/z* using 35 mM morpholine pH 5.0, sample injected at 5 kV for 10 s. (c) Electropherogram of CZE-C4D using 25 mM sodium acetate buffer pH 4.22, sample injected at 5 kV for 10 s. (d) Electropherogram of MEKC-FLD using 30 mM phosphate buffer at pH 8.5 containing 80 mM SDS, sample injected at 0.7 psi for 10 s. (Reproduced from [28] with permission from Wiley.)

of resolution, selectivity, separation efficiency, and sensitivity [28]. A standard mixture of PSTs (saxitoxin, decarbamoylsaxitoxin, neosaxitoxin, decarbamoylneosaxitoxin, gonyautoxin 1 to gonyautoxin 5, decarbamoylgonyautoxin 2, decarbamoylgonyautoxin 3, and C toxins) was used for that purpose (Figure 8.1). The developed capillary zone electrophoresis–ultraviolet detection (CZE-UV) and CZE capacitively coupled contactless conductivity detection (C4D) methods provide overall better resolution, selectivity, and separation efficiency compared to CZE-MS and micellar electrokinetic chromatography–fluorescence detection (MEKC-FLD). On the other hand, the sensitivity of the CZE-C4D and MEKC-FLD methods was superior to that of UV and MS. Although the CZE-MS method only separates saxitoxin, decarbamoylsaxitoxin, decarbamoylneosaxitoxin, and neosaxitoxin from the gonyautoxins (1–5), differences in mass and fragmentation pattern allow for specific quantification of at least 10 of the 11 charged PSTs. When applied to real shellfish samples, the CZE-C4D method suffered from

significant interferences from matrix, while MEKC-FLD was successfully used for PST screening. Mycotoxins can appear in the food chain because of fungal infection of crops, either by being consumed directly by humans or by being used as livestock feed [29]. The last developments in mycotoxin analysis, including those based on capillary electromigration methods, were recently reviewed by Berthiller *et al*. [30]. Acute poisoning is also seen to be related to the consumption of wild mushrooms. In this regard, Ginterová *et al*. proposed a CE-MS/MS method for the screening of mushroom intoxication [31]. For that purpose, mushroom toxins, ibotenic acid, muscimol and muscarine were analyzed in a spiked urine sample. The LOD values were in the range of 0.05–0.73 ng ml^{-1}. The presence of biogenic amines (BAs) above a certain level can be considered as indicative of undesired microbial activity. Biogenic amines (BAs) are nitrogen compounds (e.g., putrescine, cadaverine, spermine, spermidine, tyramine, phenylethylamine, histamine, tryptamine), which are present in a wide range of food products [32], especially in fish products and fermented foods [33]. They can cause severe health problems, particularly to sensitive individuals. CE is considered as a good alternative to high-performance liquid chromatography (HPLC) for the analysis of BAs in food samples [34]. Putrescine, cadaverine, histamine, phenylethylamine, tyramine, and other less common BAs (ethanolamine, isoamylamine, tryptamine, spermine, and spermidine) are BAs frequently found in wines; they have been analyzed in less than 8 min by CE-MS [35].

During food processing, certain substances not present or present at much lower concentrations in the raw material might be produced. Some of these substances might be undesirable either because they have an adverse effect on product quality or because they are potentially harmful. Evaluation of chemical changes during food processing is a difficult task, considering the complexity of food matrices and the large number of parameters that can contribute to those changes during processing, such as temperature, pH of the system, pressure, oxygen availability [36]. Particular attention has been given to detect known contaminants and suspected carcinogenic food processing contaminants such as acrylamide, furan, 5-hydroxymethylfurfural (HMF), furosine, heterocyclic amines, and polycyclic aromatic hydrocarbons [37–39]. In this field, a new CE-MS/MS method was developed for the analysis of furosine in foods. The formation of furosine is directly related to the heat applied to many foods. Flour samples of different origin (wheat, chestnut, lupin, einkorn, chickpeas), as well as processed foods such as pasta, milk, and bread, were analyzed. LOD and LOQ values determined by CE-MS/MS were 0.07 and 0.25 mg l^{-1}, respectively. CE-MS/MS results were compared with those obtained by reversed-phase HPLC-UV, achieving a good agreement between the results provided by both techniques. A similar CE-MS/MS approach was applied for the quantification of hydroxy-methyl-furfural (HMF) in food products [40]. Although it is not present in fresh or untreated foods, it rapidly accumulates during the heat treatment. Thus, HMF is widely recognized as a marker of food deterioration due to excessive heating or inadequate storage conditions. The CE-MS/MS method was applied to the analysis of cereal-based baby foods, coffee, soft beverages, and

vinegars. When compared to RP-HPLC-UV, good agreement between the two methodologies was also observed [41].

A variety of hazardous compounds used as additives in food products in some countries are currently illegal and prohibited for use as food additives by other countries, because of their carcinogenicity to humans. As an example, Sudan dyes have been extensively used in some countries as additives in foods (i.e., chilli powder, paprika, sauces, etc.), and they are prohibited in the EU. In order to give response to this issue, a MEKC-MS/MS method was developed for the detection of Sudan dyes I–IV in chilli powder samples [42]. Since UV detection was not suitable for the determination of these dyes, MS detection in the positive ion was employed and MS/MS spectra of each dye permitted their identification.

Foodstuffs may also be a major source of toxic metals causing health hazards to the consumers. The toxicity, environmental mobility, and accumulation of certain elements in living organisms depend on the form in which they occur. Thus, elemental speciation is an important discipline within food safety. In the recent years, CE with inductively coupled plasma MS (ICP-MS) has become one of the preferred techniques for speciation analysis [43], and the number of reports on its use in food safety has continued to grow. An interesting example is the arsenic speciation. As occurred with other elements such as mercury [44]. The effects of arsenic in certain foods are less dependent on its total concentration, but more on the concentration of its various species [45]. Marine food contains a great variety and relatively high concentrations of arsenic compounds. This is because in seawater, arsenic occurs predominantly as inorganic species, namely, arsenate and arsenite. Marine organisms exhibit mechanisms of biotransformation and detoxification, and they produce a large variety of organoarsenic species with very different toxic effects. Thus, there is a clear interest to separate, identify, and quantify every arsenic species individually. CE-ICP-MS has been applied to identify and quantify the arsenic species arsenobetaine (AsB), arsenite (As^{III}), arsenate (As^{V}), and dimethylarsinic acid (DMA) in fish samples. LODs obtained were 1×10^{-7} M for AsB, 5×10^{-7} M for DMA, and 1×10^{-6} M for As^{III} and As^{V} [46]. Rice products are also of particular interest since rice plants have higher accumulation rates of arsenic when compared to other crops [47]. Quantification of common arsenic species in rice and rice cereal using CE-ICP-MS has also been reported [48]. In that work, an enzyme (i.e., α-amylase)-assisted water-phase microwave extraction procedure was used to extract four common arsenic species, including dimethylarsinic acid (DMA), monomethylarsonic acid (MMA), arsenite (As^{III}), and arsenate (As^{V}), from the rice matrices (Figure 8.2). Nanoparticles are currently used as additives to food and drinks, since they can prevent caking, help to deliver nutrients, and prevent bacterial growth. But as nanoparticles increase in use, so do concerns over their health and environmental effects. CE-ICP-MS has also been applied for rapid and high-resolution speciation and characterization of metals (e.g., gold, platinum, and palladium) [49]. In this sense, it was observed that the diameters of the nanoparticles followed a linear relationship with their relative electrophoretic

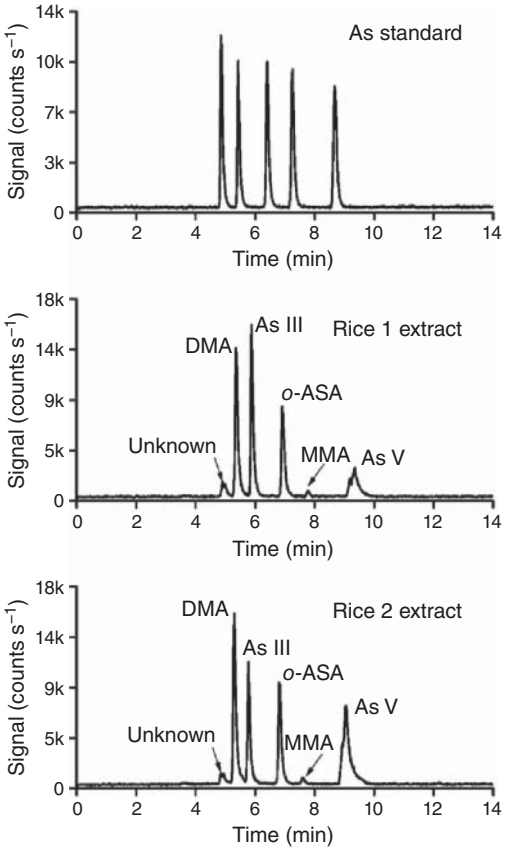

Figure 8.2 CE-MS electropherograms of arsenic standards and rice extracts with post-extraction addition of the internal standard *o*-arsanilic acid (*o*-ASA). DMA, dimethylarsinic acid; As III, arsenite; MMA, monomethylarsonic acid; As V, arsenate. CE conditions: sodium carbonate at pH 11 as separation buffer. Injection: 15 mbar for 8 s. Running voltage: +30 kV. (Reproduced from [48] with permission from American Chemical Society.)

mobility, and size information on unknown nanoparticle samples could be extrapolated from a standard curve. The CE-ICP-MS method was successfully applied to the analysis of commercially available metallic nanoparticle-based dietary supplements.

Food allergies represent an important health problem [50]. Most cases of food allergy are associated with a limited range of products, such as molluscs, eggs, fish, peanuts, tree nuts, soybeans, milk, celery, mustard, sesame, cereals containing gluten, crustaceans, lupin, and sulfur dioxide [51]. The extent to which allergy is associated with particular foods varies with dietary habits and preferences, as well as the introduction of new foods, but also in the way in which foods are processed and prepared [52]. Sensitive and selective determination methods are therefore in continuous development to guarantee food safety for sensitive

individuals. Milk whey proteins are among the main allergens and can cause allergy even at a very low concentration. Among them, β-lactoglobulin and α-lactalbumin are the main allergens in milk. They have been successfully detected by immunoaffinity capillary electrophoresis (IACE) off-line coupled to MALDI-TOF MS. Sensitive quantitative analysis of β-lactoglobulin and α-lactalbumin was achieved in different milk samples including fortified soy milk [53] as well as total IgE quantification in blood serum of milk-allergic patients [54]. Lysozyme is another potential allergenic agent, and thus, it has to be declared according to the labeling requirements in each country. CE-MS method has been applied for preservative lysozyme in cheese [55, 56]. To prevent protein adsorption onto the fused-silica capillary inner surface, a novel copolymer carrying pendant dendronic triamines has recently been synthesized and used as effective capillary coating for the determination of the basic protein lysozyme in complex food samples [57]. The coating showed full compatibility with MS detection. As can be seen in Figure 8.3, the method was demonstrated to be effective for the analysis of lysozyme in commercial cheese samples, as well as some remaining whey proteins as α-lactalbumin and β-lactoglobulins were identified in the cheese. Moreover, a variety of peaks with lower molecular masses (550 – 1200 Da) were detected in the same analysis, most probably from polypeptides derived from the proteolysis that occurred during the ripening process.

8.1.2 CE-MS in Food Quality and Authenticity

As mentioned earlier, food chain integrity includes not only safety concerns but also origin fraud and quality concern. Food quality is intrinsically linked to food safety and is determined to a large extent by the biological and genetic variability of the raw constituents and also by the treatment of food during production, processing, and storage [58]. Food traceability can be employed to know the composition and origin of a particular food product during the whole manufacturing process [59]. In this context, the profiling of free amino acids (AAs) has been frequently used to discriminate the origin of a substance and its shelf life [60]. Apart from the nutritional properties of amino acids in foodstuffs, they have important impact on the quality. CE-MS offers a selective, sensitive approach for amino acid analysis in complex samples [61]. CE-MS/MS has been employed for the analysis of AAs to assess the quality of several commercial royal jelly products as well as of honey [62]. Thus, 16 AAs (Ala, Arg, Asp, GABA, Glu, Gly, His, Leu, Lys, Met, Phe, Pro, Ser, Thr, Tyr, and Val) were analyzed in less than 20 min with LODs lower than 10.5 $\mu g\, g^{-1}$. The CE-MS/MS method permitted discrimination between the different royal jelly products (tablet, liquid drink, and raw material) and among the royal jelly raw materials and honey. Chemical characterization of different inactive dry yeast preparations (normal and glutathione-enriched) typically used within the wine industry has been recently presented [63]. The capabilities of CE-MS permitted the detection, for the first time, of 14 sulfur-containing compounds in the glutathione-enriched dry yeast (g-IDY) that could have direct effect on the

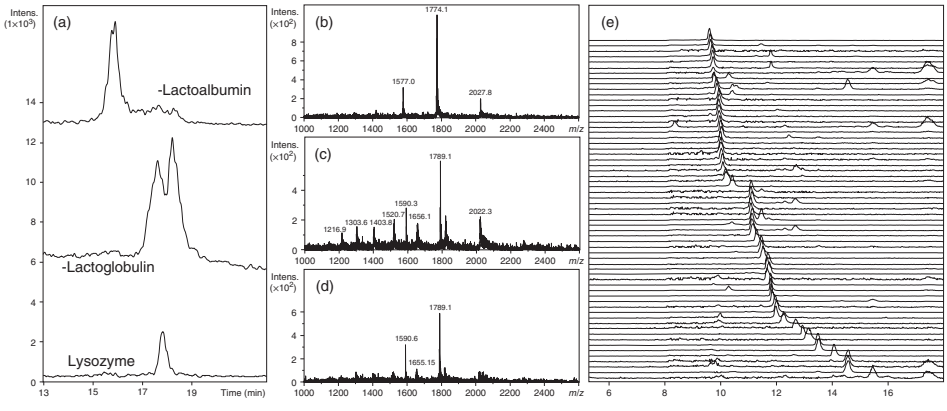

Figure 8.3 (a) CE-MS extracted ion electropherograms of detected proteins in a cheese extract. Mass spectra from (b) α-lactoalbumin, (c) β-lactoglobulin, and (d) lysozyme. (e) CE-MS extracted ion electropherograms of low-molecular-mass compounds. Capillary coated with poly-(TEDETAMA-co-HPMA) 50 : 50 copolymer. CE conditions: 35 mM ammonium acetate at pH 4.8 as separation buffer. Injection: 0.5 psi for 10 s. Running voltage: −30 kV. (Reproduced from [57] with permission from Wiley.)

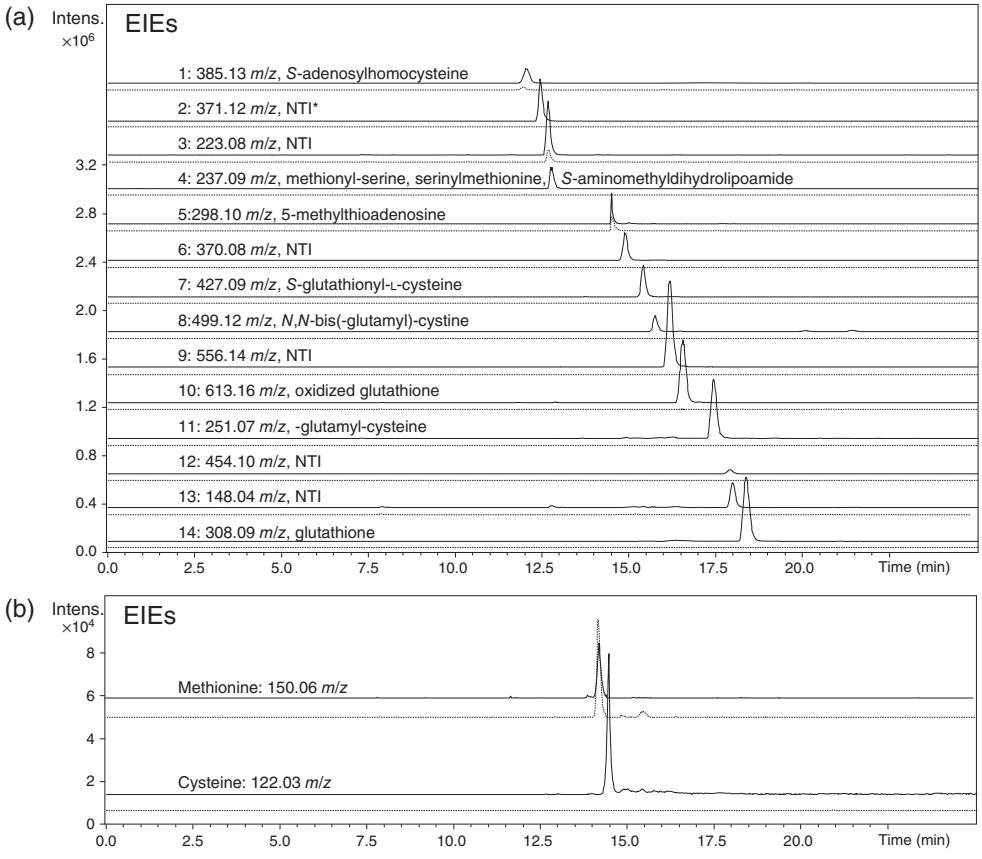

Figure 8.4 CE-TOF MS extracted ion electropherograms (EIEs) of (a) the 14 most abundant sulfur-containing compounds and (b) methionine and cysteine from inactive dry yeast (n-IDY) and GSH-enriched inactive dry yeast (g-IDY). A continuous line for g-IDY permeate and a dotted line for n-IDY permeate are used. CE conditions: 3 M formic acid as separation buffer. Running voltage: +25 kV. Injection: 0.5 psi for 80 s. (Reproduced from [63] with permission from American Chemical Society.)

better properties of this yeast preparation (Figure 8.4a). Moreover, other interesting sulfur-containing amino acids (methionine and cysteine) that might have useful properties for wine preservation were also detected (Figure 8.4b). Enantioselective separations of amino acid by CE-MS have been successfully applied for identifying adulterated foods and beverages and for controlling and monitoring the fermentation processes and products [64, 65]. CE-MS has also been employed by [66] for the analysis of vitamins B. The group of vitamins B involves thiamine (B1), riboflavin (B2), nicotinic acid/nicotinamide (B3), pantothenic acid (B5), pyridoxine (B6), biotin (B7), folic acid (B9), and cyanocobalamine (B12), and they are water-soluble and provide (individually or simultaneously) many important biological actions in organism. The simultaneous and highly reliable determination

and identification of vitamins B are very important for the quality control of vitamin-fortified food products, food supplements, and pharmaceuticals. On the other hand, their determination is problematic due to the very different chemical structures and low stability of these vitamins [66]. CE-MS is also a promising technique to guarantee authentication and origin of agro-products, through the study of their chemical composition. Analysis of amino acids [65], phenolic compounds [67], proteins [68], peptides [69], and so on by CE-MS can be applied as a valid procedure to obtain information about the origin of foods. As an example, CE has scarcely been employed to analyze phospholipids due to the low hydrosolubility of these compounds; in this sense, the electrophoretic modes more frequently used have been MEKC and nonaqueous capillary electrophoresis (NACE). A NACE-MS method was developed by Montealegre *et al*. for the determination of glycerophospholipid profiles in olive oil and olive fruit of different varieties and geographical origins [70]. Namely, three different olives varieties (i.e., Arbequina (collected in two Spanish regions), Empeltre, and Lechín) and a monovarietal extra virgin olive oil from Arbequina variety were analyzed in that work. Lysophosphatidic acid (lyso-PA), phosphatidylcholine (PC), lysophosphatidylethanolamine (lyso-PE), phosphatidylethanolamine (PE), phosphatidylinositol (PI), phosphatidic acid (PA), phosphatidylglycerol (PG) were detected in olive fruit (Figure 8.5). Apparently, differences in the relative abundance of the glycerophospholipid profiles were observed as a function of the different geographical origins and variety of the olive fruits analyzed.

8.1.3 CE-MS and Foodomics

The progress of novel, high-throughput omics technologies has opened new frontiers in the research of food safety, food quality, food traceability, and dietary components and their effects on health. Among omics technologies, Genomics, Transcriptomics, Proteomics, Peptidomics, and Metabolomics aim to detect the complete set of genes, transcripts, proteins, peptides, and metabolites in a biological system, respectively. These technologies allow for generating and integrating huge amounts of information. Recent advances in omics technologies present the potential to expand the coverage of analytes that can be simultaneously determined in a single analysis. Thus, omics technologies significantly improve the simplistic and reductionist experimental models used by classical target approaches that offer only a temporal snapshot of the huge complexity and dynamic nature of biological networks. Omics development and progress have led to an increasing demand on the knowledge about the possible effects and interactions between diet and individual gene expression, as well as the different individual responses to nutrients depending on gene polymorphisms. However, health and disease status are affected not only by genetic elements but also by behavioral and environmental factors, among others. In this scenario, there is a need for expanding our knowledge about the processes occurring at molecular level due to dietary components and their consequences on gene, protein, and metabolite expression addressed by

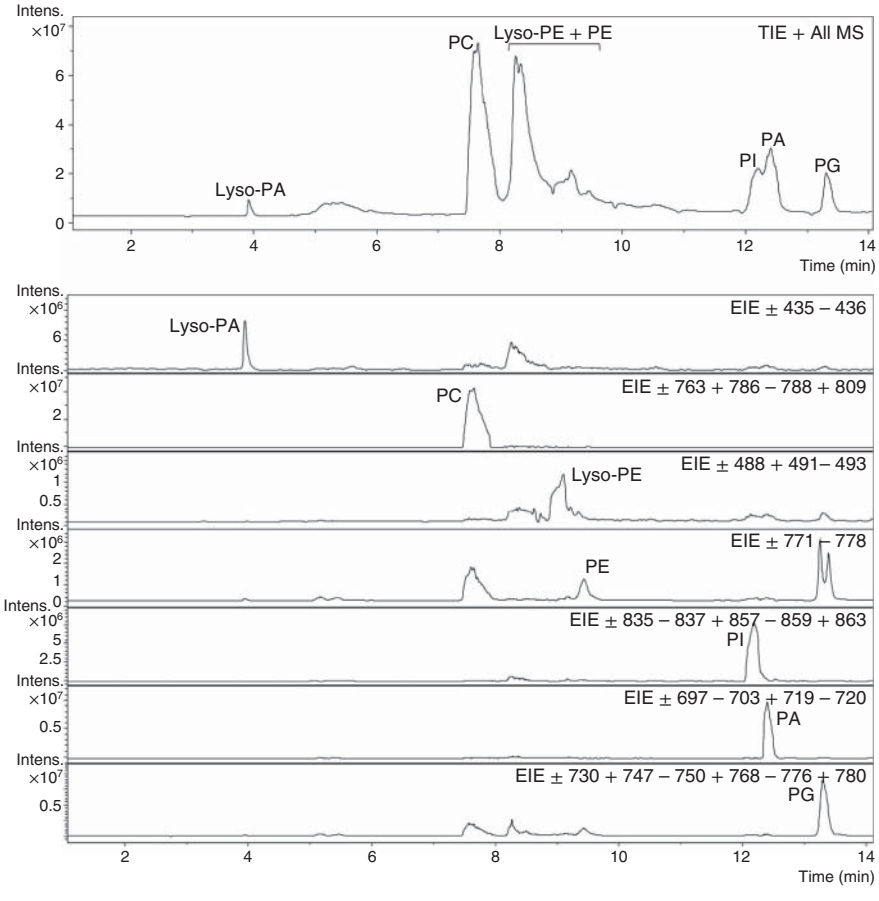

Figure 8.5 Total ion electropherograms (TIE) of glycerophospholipid profile and EIEs for each phospholipid from Arbequina olive oil samples analyzed. Conditions were as shown in Figure 8.2. Peaks: lyso-PA, lysophosphatidic acid; PC, phosphatidylcholine; lyso-PE, lysophosphatidylethanolamine; PE, phosphatidylethanolamine; PI, phosphatidylinositol; PA, phosphatidic acid; PG, phosphatidylglycerol. CE conditions: 100 mM ammonium acetate in 60 : 40 (v/v) methanol/ACN with 0.5% acetic acid as separation buffer. Running voltage: +25 kV. Injection: 50 mbar during 5 s. (Reproduced from [70] with permission from American Chemical Society.)

omics technologies. As a long-term goal, different individual responses to dietary compounds could be determined, leading to a personalized diet and/or tailored dietary preventive interventions. In this complex framework, Foodomics discipline has emerged to integrate information from omics technologies concerning food science and nutrition in order to improve human nutrition and consumers' well-being and confidence [3, 71]. CE-MS has proven to be a powerful analytical technique in Foodomics, allowing for the analysis of a wide range of analytes, from ions to macromolecules, with high efficiency and selectivity. Within

the global Foodomics field, CE-MS has been shown to be especially suitable for metabolomics and peptidomics applications.

Metabolomics is conceived as the ultimate response of a biological system to genetic, physiological, environmental, and dietary factors and aims for the analysis of the maximal possible coverage of low-molecular weight compounds in a biological system. However, a single biological system is complex because it contains a great variety of metabolites with a very heterogeneous nature (lipids, carbohydrates, and many other small compounds such as amino acids, organic acids, nucleic acids, fatty acids, phytochemicals, minerals) and in a wide range of concentrations (from pmol or lower to mmol) [72]. This fact hampers the analysis of the global metabolome using a single analytical methodology, which is firstly limited by the selected sample treatment. The selection of the most suitable metabolite purification protocol for metabolomics of adherent mammalian cell culture by CE-MS has been investigated by comparing different metabolite extraction strategies [73], and by using different extraction solvents [74].

Elucidation of composition and characterization of foods and food ingredients is the starting point for the study of their potential beneficial effects on health. Going further, foods are generally complex matrices that can be modified through, for example, alteration of environmental conditions, food manipulation, transport, storage, or fermentation, which alter the composition and thus can have impact on human health. In this regard, CE–time-of-flight mass spectrometry (CE-TOF MS) has been combined with LC-MS/MS to evaluate the effects of time and temperature of storage on pasteurized and unpasteurized Japanese sake [75]. Thus, pasteurization and storage modified both metabolic and peptide profiles of sake. For instance, amino acid content was significantly altered with storage time and pasteurization and peptides increased during storage. However, it was observed that the type of sake and storage temperature did not meaningfully modify sake composition. In another work, the effect of absence of light during plant development on tea leaves has been characterized by a metabolomics multiplatform including CE-MS, GC-MS, and LC-MS analysis [76]. Cationic and anionic metabolites were acquired in the positive and negative MS ionization modes, respectively. As a result, more than 200 metabolites could be detected, among which altered concentrations of volatile compounds and amino acids were highlighted. More recently, the same metabolomics multiplatform has been employed for the investigation of mesocarp metabolites in different ripening stages of high- and low-yielding oil palm populations [77]. Lipid biosynthesis was the metabolic pathway most severely affected when high- and low-yielding populations were compared. Other important metabolic features included changes in lipids, glycolysis, citric cycle organic acids, amino acids, and nucleosides at different ripening stages of fruit [77]. Ripening time has also been demonstrated to change the metabolic profiles of avocado fruits [78]. In that work, quantification of 10 compounds including flavonoids and phenolic acids in 18 avocado samples at different ripening states by CE-MS was carried out using two MS modes, multiple reaction monitoring (MRM) and full scan [78]. After comparison of the levels of the compounds in the function of ripening

time, perseitol, quinic acid, chlorogenic acid, *trans*-cinnamic acid, pantothenic acid, abscisic acid, epicatechin, and catechin decreased throughout the fruit development, while ferulic and *p*-coumaric acids increased in the same period of ripening.

Metabolomics has also been employed for the investigation of soybean fermentation for the production of a traditional Korean food (cheonggukjang) whose health benefits are mainly attributed to its content in vitamins, minerals, isoflavonoids, and saponins [79]. For that purpose, CE-TOF MS and GC-TOF MS analytical platforms were used for the evaluation of the metabolic profiles using different fermentation microorganisms and fermentation times. After multivariate data analysis, it was observed that samples were mainly differentiated as a function of fermentation time. Some of the most relevant metabolites altered during fermentation time were hypoxanthine, guanine, and xanthine. Apart from bacterial fermentation processes, pathogen bacteria are included among the main factors that led to an alteration of foodstuff. For instance, bacteria producing bovine mastitis affect milk quality and quantity of production, leading to important economic consequences. To elucidate the causes of those effects at a molecular level, Mansor *et al*. [80] compared milk peptidic profiles obtained from cows diagnosed with mastitis versus healthy cows. Data analysis and statistical results led to a diagnosis method with 100% sensitivity and specificity enabling differentiation of cows. Furthermore, cows under study suffering mastitis caused by either of the two pathological agents (i.e., *Staphylococcus aureus* and *Escherichia coli*) could be differentiated with 75% sensitivity with a set of 47 peptides.

The role of bioactive peptides from milk is being increasingly investigated. To going further into this topic, a peptidomic approach was conducted to evaluate three hypoallergenic infant milk formulas by CE-TOF MS [81]. To purify the peptidic fraction, two different SPE cartridges (i.e., C18 and StrataX™ (STX)) were used in parallel in order to widen the analytes coverage. After CE-MS analysis, a number of bioactive peptides ranging from 64 to 116 could be identified in milk formulas depending on the sample. This CE-MS method was substantially faster than the more spread method based on LC-MS offering complementary information on peptide composition. Another CE-MS method was developed for the analysis of phosphopeptides in tryptic digests of bovine milk, which showed unprecedented sensitivity for those analytes [82]. To achieve this good sensitivity, a transient-isotachophoresis (t-ITP) step as the sole sample concentration stage followed by a sheathless CE-MS method was applied to milk samples using a neutrally coated capillary.

Foodomics discipline is especially concerned with diet ingredients evaluation and their effect on humans health, including the prevention of chronic diseases such as cancer. A number of investigations have been devoted to this topic using CE-MS-based metabolomics strategies to study cancer cell cultures following a Foodomics approach [74, 83–89]. Investigations have been carried out, given the potential antiproliferative effects of certain food ingredients such as olive oil [83], dietary polyphenols [89], or rosemary [85] on colon-cancer cells. Thus, differences at the molecular level were determined to explain the reduction on

colon-cancer cell proliferation macroscopically observed after the treatment with polyphenol-rich extracts obtained from rosemary [85]. Metabolic fingerprints from the cytosolic content of HT29 colon-cancer cells treated and nontreated with the rosemary extract were achieved using three complementary analytical platforms. Thus, information from CE-TOF MS, HILIC/UPLC-TOF MS, and RP/UPLC-TOF MS was integrated. As a result, an increase in the ratio between reduced and oxidized glutathione in the treated cells was observed together with a significant alteration in the polyamine content and its catabolites. In order to clarify those effects at a cellular level, other omics technologies were applied to the same samples [86]. Integration of the results obtained from Metabolomics with Transcriptomics and Proteomics information was performed following a global Foodomics approach for the first time [86] (Figure 8.6). Thus, 1308 genes, 17 proteins, and 65 metabolites were observed to be significantly altered. Using the "Ingenuity Pathway Analysis" software, differences observed in the metabolomic and transcriptomic data could be integrated, revealing alteration in nitrogen metabolism, glutamate, glutathione, arginine, and proline and in the urea cycle and metabolism of amino groups. The same software was used for the integration of Metabolomic and Transcriptomic information for the investigation of rosemary extract effects on two lines of K562 leukemia cell

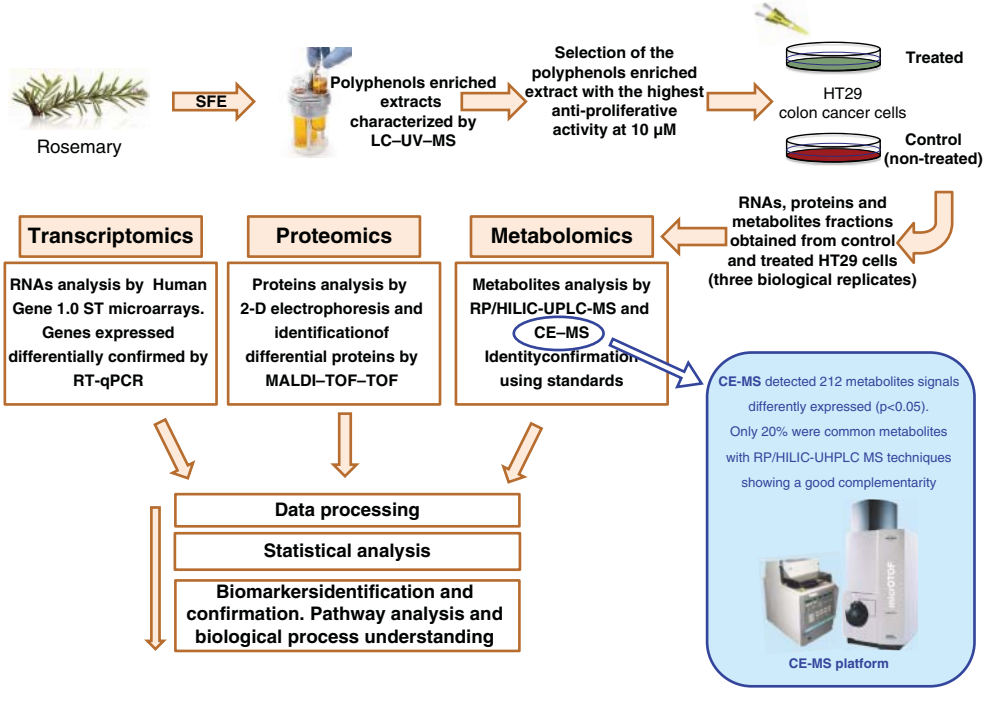

Figure 8.6 Global Foodomics strategy used by Ibáñez *et al.* [85] to investigate the activity of rosemary polyphenols against colon-cancer HT29 cells at molecular level. Contribution of CE-MS on this workflow is highlighted. (Reproduced from [85] with permission from Wiley.)

proliferation [87]. Namely, a human erythroleukemia K562 and daunomycin (DNM)-resistant K562/R cell lines were under scrutiny. Metabolic extracts obtained after ultrafiltration were analyzed via CE-MS and RP/UHPLC-MS. After integration with Transcriptomics, the behaviors of both cell lines after rosemary extract treatment were observed to be slightly different (e.g., glutathione metabolism, urea cycle, and metabolism of amino groups). The special relevance is also the investigation of cell lines from intestinal epithelium in order to unravel physiological mechanisms of absorption and metabolism of dietary ingredients before they are absorbed. Shimoda *et al*. evaluated the effects of *Cistus monspeliensis* leaf extract, mainly focusing on the energy metabolism effects in Caco-2 cells by CE-TOF MS [88]. The extract under study was shown to induce ATP production in human intestinal cells and was postulated as a possible antiaging agent probably associated to its phenolic compounds content (e.g., quercetin, kaempferol, aesculin, myricetin, and flavan-3-ols).

8.2 Concluding Remarks

CE-MS has shown to play a relevant role in food analysis and Foodomics. Representative applications of CE-MS in the field of food safety, food quality, food authenticity, and food bioactivity as discussed in this book chapter clearly demonstrate its value. CE-MS can help in different applications, including monitoring of food fermentation, detection of the undesirable compounds formed during food processing/cooking, determination of industrial/environmental contaminants, detection of unexpected natural toxins, quantification of veterinary drugs and pesticide residues, allergen detection, assessment of the quality of foods through components determination. Moreover, the capabilities of CE-MS in Foodomics have already demonstrated the full potential of this technique in this new field of research.

CE-MS complies with essential requirements in food analysis such as short analysis time, high efficiency and resolution and environmental friendliness. However, there is a variety of challenges that still need to be addressed, including sensitivity and reproducibility of this technique, and that will remain to be investigated. In spite of these needed improvements, the global outlook that CE-MS proposes is a good response to solve complex issues and challenges in the current and future food science and Foodomics.

Acknowledgments

This work was supported by the project AGL2014-53609-P (Ministerio de Economía y Competitividad, Spain). T. A. thanks the CAPES Foundation, Ministry of Education of Brazil, for her predoctoral Scholarship – Proc. No. 1532/13-8.

References

1. Regulation, C. (2002) No 178/2002 of the European Parliament and of the Council of 28 January 2002: Laying down the general principles and requirements of food law, establishing the European Food Safety Authority and laying down procedures in matters of food safety. *Off. J. Eur. Communities*, **31** (1.2), 1–24.
2. Alfaro, J.A. and Rábade, L.A. (2009) Traceability as a strategic tool to improve inventory management: A case study in the food industry. *Ìnt J Prod Econ*, **118** (1), 104–110.
3. Cifuentes, A. (2009) Food analysis and foodomics. *J. Chromatogr. A*, **1216** (43), 7109.
4. García-Cañas, V., Simó, C., Herrero, M., Ibáñez, E., and Cifuentes, A. (2012) Present and future challenges in food analysis: Foodomics. *Anal. Chem.*, **84** (23), 10150–10159.
5. Herrero, M., Simó, C., García-Cañas, V., Ibáñez, E., and Cifuentes, A. (2012) Foodomics: MS-based strategies in modern food science and nutrition. *Mass Spectrom. Rev.*, **31** (1), 49–69.
6. Kaufmann, A. (2011) The current role of high-resolution mass spectrometry in food analysis. *Anal. Bioanal. Chem.*, **403** (5), 1233–1249.
7. Zhao, S.S., Zhong, X., Tie, C., and Chen, D.D. (2012) Capillary electrophoresis–mass spectrometry for analysis of complex samples. *Proteomics*, **12** (19–20), 2991–3012.
8. Moore, J.C., Spink, J., and Lipp, M. (2012) Development and application of a database of food ingredient fraud and economically motivated adulteration from 1980 to 2010. *J. Food Sci.*, **77** (4), R118–R126.
9. Ingelfinger, J.R. (2008) Melamine and the global implications of food contamination. *N. Engl. J. Med.*, **359** (26), 2745–2748.
10. Wu, Y. and Zhang, Y. (2013) Analytical chemistry, toxicology, epidemiology and health impact assessment of melamine in infant formula: Recent progress and developments. *Food Chem. Toxicol.*, **56** (1), 325–335.
11. Sun, F., Ma, W., Xu, L., Zhu, Y., Liu, L., Peng, C., Wang, L., Kuang, H., and Xu, C. (2010) Analytical methods and recent developments in the detection of melamine. *TrAC*, **29** (11), 1239–1249.
12. Himmelsbach, M. and Thanh, V.T.D. (2014) Determination of melamine impurities by capillary zone electrophoresis with UV- and quadrupole time-of-flight mass spectrometric detection. *Electrophoresis*, **35** (9), 1362–7136.
13. Huang, H.Y., Lin, C.L., Jiang, S.H., Singco, B., and Cheng, Y.J. (2012) Capillary electrochromatography–mass spectrometry determination of melamine and related triazine by-products using poly(divinyl benzene-alkene-vinylbenzyl trimethylammonium chloride) monolithic stationary phases. *Anal. Chim. Acta*, **719** (16), 96–103.
14. Piñero, M.Y., Bauza, R., Arce, L., and Valcárcel, M. (2014) Determination of penicillins in milk of animal origin by capillary electrophoresis: Is sample treatment the bottleneck for routine laboratories? *Talanta*, **119** (15), 75–82.
15. Domínguez-Vega, E. and Marina, M.L. (2014) Characterization and study of transgenic cultivars by capillary and microchip electrophoresis. *Int. J. Mol. Sci.*, **15** (12), 23851–23877.
16. Martínez-Villalba, A., Núñez, O., Moyano, E., and Galceran, M.T. (2013) Field amplified sample injection-capillary zone electrophoresis for the analysis of amprolium in eggs. *Electrophoresis*, **34** (6), 870–876.
17. Domínguez-Álvarez, J., Mateos-Vivas, M., García-Gómez, D., Rodríguez-Gonzalo, E., and Carabias-Martínez, R. (2013) Capillary electrophoresis coupled to mass spectrometry for the determination of anthelmintic benzimidazoles in eggs using a QuEChERS with preconcentration as sample treatment. *J. Chromatogr. A*, **1278** (1), 166–174.
18. Moreno-González, D., Lara, F.J., Gámiz-Gracia, L., and García-Campaña, A.M. (2014) Molecularly imprinted polymer as in-line concentrator in capillary electrophoresis coupled with mass

spectrometry for the determination of quinolones in bovine milk samples. *J. Chromatogr. A*, **1360** (1), 1–8.

19. Springer, V., Jacksén, J., Patrik, E.K., Lista, A.G., and Emmer, A. (2015) Capillary electrophoretic determination of fluoroquinolones in bovine milk followed by off-line MALDI-TOF-MS analysis. *Chromatographia*, **78** (3–4), 285–290.
20. Rojano-Delgado, A.M. and Luque de Castro, M.D. (2014) Capillary electrophoresis and herbicide analysis: Present and future perspectives. *Electrophoresis*, **35** (17), 2509–2519.
21. Soliman, L.C. and Donkor, K.K. (2014) Micellar electrokinetic chromatography method development for simultaneous determination of thiabendazole, carbendazim, and fuberidazole. *J. Environ. Sci. Health*, **49** (3), 153–158.
22. Zhao, J., Hu, D.J., Lao, K., Yang, Z.M., and Li, S.P. (2014) Advance of CE and CEC in phytochemical analysis (2012–2013). *Electrophoresis*, **35** (1), 205–224.
23. Daniel, D., Dos Santos, V.B., Vidal, D.T., and Do Lago, C.L. (2015) Determination of halosulfuron-methyl herbicide in sugarcane juice and tomato by capillary electrophoresis-tandem mass spectrometry. *Food Chem.*, **175** (1), 82–84.
24. CODEX-STAN 193-1995 (1995) *Codex General Standard for Contaminants and Toxins in Food and Feed*, WHO Tech. Rep. Ser., Food and Agriculture Organization of the United Nations/World Health Organization, Switzerland.
25. Domínguez-Álvarez, J., Rodríguez-Gonzalo, E., Hernández-Méndez, J., and Carabias-Martínez, R. (2012) Programed nebulizing-gas pressure mode for quantitative capillary electrophoresis–mass spectrometry analysis of endocrine disruptors in honey. *Electrophoresis*, **33** (15), 2374–2381.
26. Dolan, L.C., Matulka, R.A., and Burdock, G.A. (2010) Naturally occurring food toxins. *Toxins*, **2** (9), 2289–2332.
27. Sassolas, A., Hayat, A., Catanante, G., and Marty, J.L. (2013) Detection of the marine toxin okadaic acid: Assessing seafood safety. *Talanta*, **105** (1), 306–316.
28. Keyon, A.S., Guijt, R.M., Gaspar, A., Kazarian, A.A., Nesterenko, P.N., Bolch, C.J., and Breadmore, M.C. (2014) Capillary electrophoresis for the analysis of paralytic shellfish poisoning toxins in shellfish: Comparison of detection methods. *Electrophoresis*, **35** (10), 1496–1503.
29. Marin, S., Ramos, A.J., Cano-Sancho, G., and Sanchis, V. (2013) Mycotoxins: Occurrence, toxicology, and exposure assessment. *Food Chem. Toxicol.*, **60** (1), 218–237.
30. Berthiller, F., Burdaspal, P.A., Crews, C., Iha, M.H., Krska, R., Lattanzio, V.M.T., MacDonald, S., Malone, R.J., Maragos, C., Solfrizzo, M., Stroka, J., and Whitaker, T.B. (2014) Developments in mycotoxin analysis: An update for 2012–2013. *World Mycotoxin J.*, **7** (1), 3–33.
31. Ginterová, P., Sokolová, B., Ondra, P., Znaleziona, J., Petr, J., Ševčík, M., and Maier, V. (2014) Determination of mushroom toxins ibotenic acid, muscimol and muscarine by capillary electrophoresis coupled with electrospray tandem mass spectrometry. *Talanta*, **125** (1), 242–247.
32. Shalaby, A.R. (1996) Significance of biogenic amines to food safety and human health. *Food Res. Int.*, **29** (1), 675–690.
33. Linares, D.M., Martín, M.C., Ladero, V., Alvarez, M.A., and Fernández, M. (2011) Biogenic amines in dairy products. *Crit. Rev. Food Sci. Nutr.*, **51** (7), 691–703.
34. Erim, F.B. (2013) Recent analytical approaches to the analysis of biogenic amines in food samples. *TrAC*, **52** (1), 239–247.
35. Simó, C., Moreno-Arribas, M.V., and Cifuentes, A. (2008) Ion-trap versus time-of-flight mass spectrometry coupled to capillary electrophoresis to analyze biogenic amines in wine. *J. Chromatogr. A*, **1195** (1-2), 150–156.
36. Van der Plancken, I., Verbeyst, L., De Vleeschouwer, K., Grauwet, T., Heiniö, R.L., Husband, F.A., Lille, M., Mackie, A.R., Van Loey, A., Viljanen, K., and Hendrickx, M. (2012) (Bio)chemical reactions during high pressure/high

temperature processing affect safety and quality of plant-based foods. *Trends Food Sci. Tech.*, **23** (1), 28–38.

37. Purcaro, G., More, T.S., and Conte, L.S. (2013) Overview on polycyclic aromatic hydrocarbons: Occurrence, legislation and innovative determination in foods. *Talanta*, **105** (1), 292–305.
38. Wenzl, T., Lachenmeier, D.W., and Gökmen, V. (2007) Analysis of heat-induced contaminants (acrylamide, chloropropanols and furan) in carbohydrate-rich food. *Anal. Bioanal. Chem.*, **389** (1), 119–137.
39. Anese, M., Manzocco, L., Calligaris, S., and Nicoli, M.C. (2013) Industrially applicable strategies for mitigating acrylamide, furan, and 5-hydroxymethylfurfural in food. *J. Agric. Food Chem.*, **61** (43), 10209–10214.
40. Bignardi, C., Cavazza, A., and Corradini, C. (2012) Determination of furosine in food products by capillary zone electrophoresis–tandem mass spectrometry. *Electrophoresis*, **33** (15), 2382–2389.
41. Bignardi, C., Cavazza, A., and Corradini, C. (2014) Selected product ion monitoring for quantification of 5-hydroxymethylfurfural in food products by capillary zone electrophoresis–tandem ion trap mass spectrometry. *Food Control*, **46** (1), 41–48.
42. Fukuji, T.S., Castro-Puyana, M., Tavares, M.F.M., and Cifuentes, A. (2012) Sensitive and fast determination of Sudan dyes in chilli powder by partial-filling micellar electrokinetic chromatography–tandem mass spectrometry. *Electrophoresis*, **33** (4), 705–712.
43. Álvarez-Llamas, G., Fernández de la Campa, M.D.R., and Sanz-Medel, A. (2005) ICP-MS for specific detection in capillary electrophoresis. *TrAC*, **24** (1), 28–36.
44. Vallant, B., Kadnarb, R., and Goessler, W. (2007) Development of a new HPLC method for the determination of inorganic and methylmercury in biological samples with ICP-MS detection. *J. Anal. At. Spectrom.*, **22** (1), 322–325.
45. European Food Safety Authority (EFSA) (2009) Scientific opinion on arsenic in food. EFSA Panel on Contaminants in the Food Chain (CONTAM). *EFSA J.*, **7** (10), 1531–1550.
46. Meermann, B., Bartel, M., Scheffer, A., Trümpler, S., and Karst, U. (2008) Capillary electrophoresis with inductively coupled plasma-mass spectrometric and electrospray time of flight mass spectrometric detection for the determination of arsenic species in fish samples. *Electrophoresis*, **29** (12), 2731–2737.
47. Williams, P.N., Villada, A., Deacon, C., Raab, A., Figuerola, J., Green, A.J., Feldmann, J., and Meharg, A.A. (2007) Greatly enhanced arsenic shoot assimilation in rice leads to elevated grain levels compared to wheat and barley. *Environ. Sci. Technol.*, **41** (19), 6854–6859.
48. Qu, H., Mudalige, T.K., and Linder, S.W. (2015) Arsenic speciation in rice by capillary electrophoresis/inductively coupled plasma mass spectrometry: Enzyme-assisted water-phase microwave digestion. *J. Agric. Food Chem.*, **63** (12), 3153–3160.
49. Qu, H., Mudalige, T.K., and Linder, S.W. (2014) Capillary electrophoresis/inductively-coupled plasma-mass spectrometry: Development and optimization of a high resolution analytical tool for the size-based characterization of nanomaterials in dietary supplements. *Anal. Chem.*, **86** (23), 11620–11627.
50. Sicherer, S.H. and Sampson, H.A. (2010) Food allergy. *J. Allergy Clin. Immunol.*, **125** (2 Suppl 2), S116–S125.
51. European Commission (2006) Commission Directive 2006/142/EC of 22 December 2006 amending Annex IIIa of Directive 2000/13/EC of the European Parliament and of the Council listing the ingredients which must under all circumstances appear on the labeling of foodstuffs. *Off. J. Eur. Union*, **368** (1), 110–111.
52. Verhoeckx, K.C., Vissers, Y.M., Baumert, J.L., Faludi, R., Feys, M., Flanagan, S., Herouet-Guicheney, C., Holzhauser, T., Shimojo, R., Van der Bolt, N., Wichers, H., and Kimber, I. (2015) Food processing and allergenicity. *Food Chem. Toxicol.*, **80** (1), 223–240.

53. Gasilova, N., Gassner, A.L., and Girault, H.H. (2012) Analysis of major milk whey proteins by immunoaffinity capillary electrophoresis coupled with MALDI-MS. *Electrophoresis*, **33** (15), 2390–2398.
54. Gasilova, N. and Girault, H.H. (2014) Component-resolved diagnostic of cow's milk allergy by immunoaffinity capillary electrophoresis-matrix assisted laser desorption/ionization mass spectrometry. *Anal. Chem.*, **86** (13), 6337–6345.
55. Kondeková, M., Maier, V., Ginterová, P., Marák, J., and Sevčík, J. (2014) Analysis of lysozyme in cheese samples by on-line combination of capillary zone electrophoresis and mass spectrometry. *Food Chem.*, **153** (1), 398–404.
56. Acunha, T., Ibáñez, C., Pascual Reguera, M.I., Sarò, M., Navarro, R., Alfonso-Redondo, J., Reinecke, H., Gallardo, A., Simó, C., and Cifuentes, A. (2015) Potential of prodendronic polyamines with modulated segmental charge density as novel coating for fast and efficient analysis of peptides and basic proteins by CE and CE–MS. *Electrophoresis*, **36** (14), 1564–1571.
57. Simó, C., Elvira, C., González, N., San Román, J., Barbas, C., and Cifuentes, A. (2004) Capillary electrophoresis–mass spectrometry of basic proteins using a new physically adsorbed polymer coating. Some applications in food analysis. *Electrophoresis*, **25** (13), 2056–2064.
58. Gallardo, J.M., Carrera, M., and Ortea, I. (2013) Proteomics in food science, in *Foodomics: Advanced Mass Spectrometry in Modern Food Science and Nutrition*, 1st edn (ed A. Cifuentes), John Wiley & Sons Ltd, Hoboken, pp. 125–165.
59. Castro-Puyana, M., Mendiola, J., Ibáñez, E., and Herrero, M. (2013) MS-based metabolomics approaches for food safety, quality, and traceability, in *Foodomics: Advanced Mass Spectrometry in Modern Food Science and Nutrition*, 1st edn (ed A. Cifuentes), John Wiley & Sons Ltd, Hoboken, pp. 453–470.
60. Shen, F., Yibin, Y., Li, B., Zheng, Y., and Zhuge, Q. (2011) Multivariate classification of rice wines according to ageing time and brand based on amino acid profiles. *Food Chem.*, **129** (2), 565–569.
61. Britz-McKibbin, P. (2012) New advances in amino acid profiling by capillary electrophoresis–electrospray ionization-mass spectrometry. *Methods Mol. Biol.*, **828** (1), 83–99.
62. Akamatsu, S. and Mitsuhashi, T. (2013) Development of a simple analytical method using capillary electrophoresis–tandem mass spectrometry for product identification and simultaneous determination of free amino acids in dietary supplements containing royal jelly. *J. Food Compos. Anal.*, **30** (1), 47–51.
63. Rodríguez-Bencomo, J.J., Andújar-Ortiz, I., Moreno-Arribas, M.V., Simó, C., González, J., Chana, A., Dávalos, J., and Pozo-Bayón, M.A. (2014) Impact of glutathione-enriched inactive dry yeast preparations on the stability of terpenes during model wine aging. *J. Agric. Food Chem.*, **62** (6), 1373–1383.
64. Herrero, M., Simó, C., García-Cañas, V., Fanali, S., and Cifuentes, A. (2010) Chiral capillary electrophoresis in food analysis. *Electrophoresis*, **31** (13), 2106–2114.
65. Simó, C., Rizzi, A., Barbas, C., and Cifuentes, A. (2005) Chiral capillary electrophoresis–mass spectrometry of amino acids in foods. *Electrophoresis*, **26** (7–8), 1432–1441.
66. Maráková, K., Piešťanský, J., Havránek, E., and Mikuš, P. (2014) Simultaneous analysis of vitamins B in pharmaceuticals and dietary supplements by capillary electrophoresis hyphenated with triple quadrupole mass spectrometry. *Pharmazie*, **69** (9), 663–668.
67. Carrasco-Pancorbo, A., Neusüss, C., Pelzing, M., Segura-Carretero, A., and Fernández-Gutiérrez, A. (2007) CE- and HPLC-TOF-MS for the characterization of phenolic compounds in olive oil. *Electrophoresis*, **28** (5), 806–821.
68. Erny, G.L., Marina, M.L., and Cifuentes, A. (2007) CE–MS of zein proteins from conventional and transgenic maize. *Electrophoresis*, **28** (22), 4192–4201.
69. Simó, C., Domínguez-Vega, E., Marina, M.L., García, M.C., Dinelli, G., and

Cifuentes, A. (2010) CE-TOF MS analysis of complex protein hydrolyzates from genetically modified soybeans: A tool for foodomics. *Electrophoresis*, **31** (7), 1175–1183.

70. Montealegre, C., Sánchez-Hernández, L., Crego, A.L., and Marina, M.L. (2013) Determination and characterization of glycerophospholipids in olive fruit and oil by nonaqueous capillary electrophoresis with electrospray–mass spectrometric detection. *J. Agric. Food Chem.*, **61** (8), 1823–1832.

71. Herrero, M., García-Canñas, V., Simó, C., and Cifuentes, A. (2010) Recent advances in the application of capillary electromigration methods for food analysis and Foodomics. *Electrophoresis*, **31** (1), 205–228.

72. Dunn, W.B. and Ellis, D.I. (2005) Metabolomics: Current analytical platforms and methodologies. *TrAC*, **24** (4), 285–294.

73. Simó, C., Ibáñez, C., Gómez-Martínez, A., Ferragut, J.A., and Cifuentes, A. (2011) Is metabolomics reachable? Different purification strategies of human colon cancer cells provide different CE–MS metabolite profiles. *Electrophoresis*, **32** (13), 1765–1777.

74. Ibáñez, C., Simó, C., Valdés, A., Campone, L., Piccinelli, A.L., García-Cañas, V., and Cifuentes, A. (2015) Metabolomics of adherent mammalian cells by capillary electrophoresis–mass spectrometry: HT-29 cells as case study. *J. Pharm. Biomed. Anal.*, **110** (1), 83–92.

75. Sugimoto, M., Kaneko, M., Onuma, H., Sakaguchi, Y., Mori, M., Abe, S., Soga, T., and Tomita, M. (2012) Changes in the charged metabolite and sugar profiles of pasteurized and unpasteurized Japanese sake with storage. *J. Agric. Food Chem.*, **60** (10), 2586–2593.

76. Yang, Z., Kobayashi, E., Katsuno, T., Asanuma, T., Fujimori, T., Ishikawa, T., Tomomura, M., Mochizuki, K., Watase, T., Nakamura, Y., and Watanabe, N. (2012) Characterisation of volatile and non-volatile metabolites in etiolated leaves of tea (*Camellia sinensis*) plants in the dark. *Food Chem.*, **135** (4), 2268–2276.

77. Teh, H.F., Neoh, B.K., Hong, M.P., Low, J.Y., Ng, T.L., Ithnin, N., Thang, Y.M., Mohamed, M., Chew, F.T., Yusof, H.M., Kulaveerasingam, H., and Appleton, D.R. (2013) Differential metabolite profiles during fruit development in high-yielding oil palm mesocarp. *PLoS One*, **8** (4), e61344.

78. Contreras-Gutierrez, P.K., Hurtado-Fernandez, E., Gomez-Romero, M., Hormaza, J.I., Carrasco-Pancorbo, A., and Fernandez-Gutierrez, A. (2013) Determination of changes in the metabolic profile of avocado fruits (*Persea americana*) by two CE–MS approaches (targeted and non-targeted). *Electrophoresis*, **34** (19), 2928–2942.

79. Kim, J., Choi, J.N., John, K.M., Kusano, M., Oikawa, A., Saito, K., and Lee, C.H. (2012) GC-TOF-MS- and CE-TOF-MS-based metabolic profiling of cheonggukjang (fast-fermented bean paste) during fermentation and its correlation with metabolic pathways. *J. Agric. Food Chem.*, **60** (38), 9746–9753.

80. Mansor, R., Mullen, W., Albalat, A., Zerefos, P., Mischak, H., Barrett, D.C., Biggs, A., and Eckersall, P.D. (2013) A peptidomic approach to biomarker discovery for bovine mastitis. *J. Proteomics*, **85** (1), 89–98.

81. Català-Clariana, S., Benavente, F., Giménez, E., Barbosa, J., and Sanz-Nebot, V. (2013) Identification of bioactive peptides in hypoallergenic infant milk formulas by CE-TOF-MS assisted by semiempirical model of electromigration behavior. *Electrophoresis*, **34** (13), 1886–1894.

82. Heemskerk, A.A., Busnel, J.M., Schoenmaker, B., Derks, R.J., Klychnikov, O., Hensbergen, P.J., Deelder, A.M., and Mayboroda, O.A. (2012) Ultra-low flow electrospray ionization–mass spectrometry for improved ionization efficiency in phosphoproteomics. *Anal. Chem.*, **84** (10), 4552–4559.

83. Fernández-Arroyo, S., Gómez-Martínez, A., Rocamora-Reverte, L., Quirantes-Piné, R., Segura-Carretero, A., Fernández-Gutiérrez, A., and Ferragut, J.A. (2012) Application of nano LC-ESI-TOF-MS for the metabolomic analysis of

phenolic compounds from extra-virgin olive oil in treated colon-cancer cells. *J. Pharm. Biomed. Anal.*, **63** (1), 128–134.

84. Celebier, M., Ibañez, C., Simó, C., and Cifuentes, A. (2012) A Foodomics approach: CE–MS for comparative metabolomics of colon cancer cells treated with dietary polyphenols. *Methods Mol. Biol.*, **869** (1), 185–195.
85. Ibáñez, C., Simó, C., García-Cañas, V., Gómez-Martínez, A., Ferragut, J.A., and Cifuentes, A. (2012) CE/LC-MS multiplatform for broad metabolomic analysis of dietary polyphenols effect on colon cancer cells proliferation. *Electrophoresis*, **33** (15), 2328–2336.
86. Ibáñez, C., Valdés, A., García-Cañas, V., Simó, C., Celebier, M., Rocamora, L., Gómez, A., Herrero, M., Castro, M., Segura-Carretero, A., Ibáñez, E., Ferragut, J.A., and Cifuentes, A. (2012) Global foodomics strategy to investigate the health benefits of dietary constituents. *J. Chromatogr. A*, **1248** (1), 139–153.
87. Valdés, A., Simó, A., Ibáñez, A., Rocamora, A., Ferragut, A., García-Cañas, V., and Cifuentes, A. (2012) Effect of dietary polyphenols on K562 leukemia cells: A Foodomics approach. *Electrophoresis*, **33** (15), 2314–2327.
88. Shimoda, Y., Han, J., Kawada, K., Smaoui, A., and Isoda, H. (2012) Metabolomics analysis of *Cistus monspeliensis* leaf extract on energy metabolism activation in human intestinal cells. *J. Biomed. Biotechnol.*, **2012** (1), 1–7.
89. Valdés, A., García-Cañas, V., Simó, C., Ibáñez, C., Ferragut, J.A., Micol, V., and Cifuentes, A. (2014) Comprehensive foodomics study on the mechanisms operating at various molecular levels in cancer cells in response to individual rosemary polyphenols. *Anal. Chem.*, **86** (19), 9807–9815.

3.3.3. Potential of prodendronic polyamines with modulated segmental charge density as novel coating for fast and efficient analysis of peptides and basic proteins by CE and CE-MS

Acunha, T., Ibáñez, C., Reguera, M. I.P., Sarò, M. Navarro, R., Redondo, J. A., Reinecke, H., Gallardo, A., Simó, C., Cifuentes, A.

Electrophoresis **36,** 1564–1571 (2015).
DOI: 10.1002/elps.201400576.

Tanize Acunha[1,2]
Clara Ibáñez[1]
María Isabel Pascual Reguera[3]
Mariagiovanna Sarò[4]
Rodrigo Navarro[5]
Juan Alfonso Redondo[5]
Helmut Reinecke[5]
Alberto Gallardo[5]
Carolina Simó[1]
Alejandro Cifuentes[1]

[1]Laboratory of Foodomics, Institute of Food Science Research (CIAL), CSIC, Campus de Cantoblanco, Madrid, Spain
[2]CAPES Foundation, Ministry of Education of Brazil, Brasília, DF, Brazil
[3]Departamento de Química Física y Analítica, University of Jaen, Spain
[4]Dipartimento di Scienze del Farmaco e dei Prodotti per la Salute, Facoltà di Farmacia, Università degli Studi di Messina, Messina, Italy
[5]Instituto de Ciencia y Tecnología de Polímeros, ICTP-CSIC, Madrid

Received December 4, 2014
Revised March 12, 2015
Accepted March 12, 2015

Research Article

Potential of prodendronic polyamines with modulated segmental charge density as novel coating for fast and efficient analysis of peptides and basic proteins by CE and CE-MS

In this work, the suitability of a new polymer family has been investigated as capillary coatings for the analysis of peptides and basic proteins by CE. This polymer family has been designed to minimize or completely prevent protein–capillary wall interactions and to modify the EOF. These coating materials are linear polymeric chains bearing as side cationizable moiety a dentronic triamine derived from *N,N,N′,N′*-tetraethyldiethylenetriamine (TEDETA), which is linked to the backbone through a spacer (unit labeled as TEDETAMA). Four different polymers have been prepared and evaluated: a homopolymer which comprised only of those cationizable repetitive units of TEDETAMA, and three copolymers that randomly incorporate TEDETAMA together with neutral hydrosoluble units of N-(2-hydroxypropyl) methacrylamide (HPMA) at different molar percentages (25:75, 50:50 and 75:25). It has been demonstrated that the composition of the copolymers influences the EOF and therefore the separation of the investigated biopolymers. Among the novel polymers studied, poly-(TEDETAMA-*co*-HPMA) 50:50 copolymer was successfully applied as coating material of the inner capillary surface in CE-UV and CE-MS, providing EOF reversing together with fast and efficient baseline separation of peptides and basic proteins. Finally, the feasibility of the polymer-coated capillary was shown through the analysis of lysozyme in a cheese sample.

Keywords:
Basic proteins / CE-MS / *N,N,N′,N′*-tetraethyldiethylenetriamine / *N*-(2-hydroxypropyl) methacrylamide / Peptides

DOI 10.1002/elps.201400576

Additional supporting information may be found in the online version of this article at the publisher's web-site

1 Introduction

CE is a powerful technique well suited for the separation of peptides and proteins, and is especially interesting as the analysis can be performed without causing conformational changes in these biopolymers. However, it is well known that anionic and hydrophobic nature of the fused-silica capillary inner surface causes undesirable interactions with analytes such as proteins, and particularly with cationic proteins. The simplest strategies to avoid adsorption processes comprise (i) the use of extreme acidic electrolyte solutions with the aim to suppress silanol dissociation on the capillary wall, (ii) increase the ionic strength of the BGE to minimize protein–wall interaction as co-ions in the BGE compete with the surface binding sites, or (iii) the employment of BGE pH values higher than the protein p*I* for conditioning both the proteins and the capillary wall to a negatively charged state to provoke electrostatic repulsions. Extreme pH values are not suitable because those conditions may denature proteins, thus, to prevent protein adsorption as well as denaturation reactions, modification of the inner capillary wall is generally carried out. In a series of works from Haselberg *et al.* [1–3] and Dolník [4, 5], capillary coatings have been

Correspondence: Dr. Carolina Simó
E-mail: c.simo@csic.es

Abbreviations: HPMA, *N*-(2-hydroxypropyl) methacrylamide; **PB**, hexadimethrine bromide or Polybrene; **TEDETA**, *N,N,N′,N′*-tetraethyldiethylenetriamine; **TEDETAMA**, 2-(3-(Bis (2(diethylamino)ethyl)amino) propanamido)ethyl methacrylate

reviewed for their use in the analysis of proteins by CE and CE-MS. Covalently bonded polymers are frequently used as wall coatings to avoid undesirable interactions between the proteins and the active sites on the inner wall of the fused silica capillary. However, laborious capillary preparation and limited pH range are often major concerns when working with covalent coatings; moreover, many of them are neutral coatings and thus, unstable electrospray might take place in CE-MS coupling. Alternatively, noncovalent capillary coatings have several advantages relative to covalent coatings, such as, the simplicity of coating procedure and the possibility of coating regeneration; moreover, the CE separation performance can be tailored by selecting the coating material properties [6]. Dynamic coating in which coating material (such as, Polybrene or PolyE-323) is present in the BGE has been demonstrated for the analysis of intact proteins by CE-MS [7, 8]. However, although the main advantage of the self-coating BGEs is their ease of use, this approach is not often used for the analysis of intact proteins by CE-MS due to contamination of the ion source and MS instrument. Particularly attractive are the "static" adsorbed coatings since the coating material is not in the BGE. Following this idea, our research group has synthesized and evaluated a variety of interesting polymers with different properties for their use in CE-UV and CE-MS. By using these self-made copolymers, the possibility to adapt the magnitude and direction of the EOF (anodal or cathodal EOF) depending on the working pH was successfully implemented. In all cases, typical dependence on the BGE pH was found: anodal EOF at low pH values, a nearly zero EOF at pH 6–7, and cathodal EOF at higher pHs [9–13]. Nevertheless, compatibility with CE-MS was only demonstrated for EPyM-DMA coating [10]. When working with MS detection, additional requirements to the CE system, such as the direction and magnitude of the EOF and the need to obtain robust electrospray conditions have to be considered [14]. Thus, constant and sufficient EOF is preferred to achieve stable and reproducible interfacing conditions. Self-made cationic capillary coatings such as OHNOON and EPyM-DMA have been used in CE-MS to analyze peptides BSA digest [15], basic proteins in food [16], and glycoprofiling in human serum [17] samples; however, in some cases electrospray stability was limited due to the low flux of liquid out of the capillary generated by the anodal EOF [15]. Anodal EOF was also generated in PolyE-323-coated capillaries [18]; net positive charge of this coating was constant from pH 4–8, giving a stable EOF over this pH range. PolyE-323-coated capillaries were able to generate an EOF high enough to sustain a stable electrospray in CE-MS coupling [19]. This coating showed good efficiency for the CE-MS analysis of standard proteins (RNAse, cyt c, lysozyme, and β-lactoglobulin), but when applied to human plasma samples, poor mass spectra were obtained [19]. Other commercially available coating materials inducing the EOF to be reversed toward the anode such as the polycationic polymer Polybrene (PB), generates stronger EOF. On the other hand, it has been demonstrated that noncovalent coatings involving PB are more stable when applying successive multiple layers. Thus, a triple-layer coating of successive layers of PB, dextran sulfate (DS) and PB, initially introduced by Katayama [20] was demonstrated to be a stable coating, exhibiting a pH independent and reproducible anodic EOF [21, 22]. The potential of this approach was demonstrated for baseline separation of four model intact basic proteins [23], and for the analysis of basic proteins for purity and stability purposes of biopharmaceuticals [24, 25].

The development of new coating materials for the analysis of basic proteins and peptides by CE-UV and CE-MS remains as an active area of research, and it opens the field of potential applications. In the present work, we introduce the use of novel coatings for CE-UV and CE-MS, based on linear polymeric chains bearing as side cationizable moiety a triamine derived from *N,N,N',N'*-tetraethyldiethylenetriamine (TEDETA). This cationic moiety is linked to the polymeric backbone through a spacer, forming a unit labeled as TEDETAMA (see Fig. 1A). There are two remarkable structural issues regarding this polymeric family. On the one hand, unlike the previously reported polymeric coatings described above that are based on cationizable monomers carrying single tertiary amines, the cationizable pendant moiety of TEDETAMA is a voluminous dendronic triamine, a branched tetradentate structure derived from TEDETA that resembles an inner block of hyperbranched PEI. Supported TEDETA has recently been used to adsorb different proteins [26, 27]. TEDETA is also a ligand that possesses well-known applications in certain chemical reactions such as atom transfer radical polymerization [28, 29]. On the other hand, it has been recently described by our group that the statistical incorporation of neutral and hydrophilic HPMA to TEDETAMA-based polymers has a strong influence on the electrostatic interactions of the TEDETAMA units with DNA [30]. It was found that the polymer/DNA interaction was dependent on the HPMA content. Even the copolymers with low molar content of TEDETAMA (25%) were able to condense DNA in an effective way [30], unlike analogous copolymers with a similar molar content of single amine [31]. This interesting feature is related to the dendronic nature of TEDETAMA (with three cationizable amines) that makes the local charge density around the TEDETAMA unit to be high enough to interact with DNA despite of a high surrounding content of HPMA. In any case, the higher the HPMA content in TEDETAMA-based polymers the weaker the interaction is, because neutral HPMA shields the electrostatic interaction. In other words, and unlike other commercial polymeric amines, modulation of charge density on polymers derived from TEDETAMA may be easily achieved just by the statistical incorporation of neutral HPMA at the appropriate ratio. Taking advantage of these properties it is therefore hypothesized in this work that the dendronic nature of the cationizable unit as well as the composition of the copolymer will play a key role on the behavior of the coating of the inner capillary surface in CE for proteomics applications. In addition to homopolymer poly-TEDETAMA, different poly-(TEDETAMA-*co*-HPMA) copolymers with three nominal molar percentages of TEDETAMA (25, 50 and 75%) are studied as CE coatings.

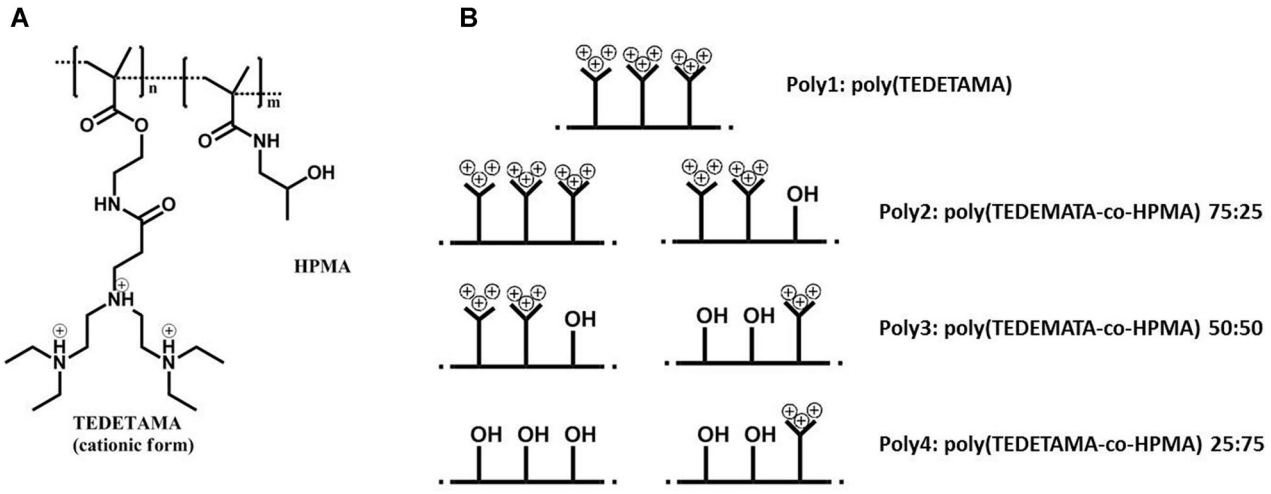

Figure 1. **(A)** Generic structure of the polymeric family studied in this work (TEDETAMA has been represented in its aqueous cationic form, below p*Ka* of the amines). **(B)** Scheme of the more populated triads for the polymers studied in this work, according to Supporting Information Table 1.

Effectiveness of the coatings is confirmed through basic proteins and peptides analysis by CE-UV and CE-MS platforms.

2 Materials and methods

2.1 Chemicals and samples

Formic acid, acetic acid, ammonium hydroxide, ammonium formate, ammonium bicarbonate, and 2,2′-azobisisobutyronitrile (AIBN) were purchased from Merck (Darmstad, Germany). DMF, HCl, bovine trypsin, PB, cytochrome c (cyt c) from horse, bovine cyt c, and lysozyme from chicken egg-white were purchased from Sigma (St. Louis, MO, USA). Sodium hydroxide (NaOH) and sodium chloride (NaCl) were purchased from Panreac Quimica S.A. (Barcelona, Spain). 2-(3-(Bis(2(diethylamino)ethyl)amino) propanamido)ethyl methacrylate (TEDETAMA) and *N*-(2-hydroxypropyl) methacrylamide (HPMA) were synthesized according to procedures described elsewhere [30, 32, 33].

Basic proteins (theoretical p*I* values > 9.4) lysozyme, bovine cyt c, and equine cyt c were dissolved in Milli-Q-water at 0.11, 0.14, and 0.07 mg/mL, respectively. Peptide mixture was obtained from Equine cyt c (2 mg/mL) digested with trypsin [34]. Cured sheep cheese was purchased from a local supermarket (Madrid, Spain) and subjected to lysozyme extraction [35] (Supporting Information).

2.2 Synthesis and characterization of polymers

The homo and copolymerizations were carried out by conventional free radical polymerization [30]. Briefly, the reaction was performed at 60°C, using AIBN ($[I] = 1.5 \times 10^{-2}$ mol/L) as the radical initiator and a monomer concentration of 1 M using DMF as solvent. All solutions were carefully degassed through dried nitrogen flow to remove all the oxygen traces. After 24 h, the obtained polymers were dialyzed in distilled water, using dialysis membranes Spectra/Por® (Spectrum Laboratories, Inc., Rancho Dominguez, CA, USA) with a molecular weight cut off of 3.5 kDa, and freeze dried. The composition and molecular weight of the polymers were determined respectively by ^{1}H-NMR spectroscopy and size exclusion chromatography [30].

2.3 CE-UV and CE-MS instrumentation

A capillary electrophoresis P/ACE 2100 system from Beckman (Fullerton, CA, USA) was used. Bare fused-silica capillaries of 50 μm id were purchased from Composite Metal Services (Worcester, UK). Electrophoretic separation was achieved using different running voltages (+20, −20, and −30 kV) at a constant temperature of 25°C with different BGEs (indicated in each case). Detection wavelength was 254/214 nm for CE-UV.

CE was coupled to a micrOTOF MS (Bruker Daltonics, Bremen, Germany) through an orthogonal ESI interface model G1607A from Agilent Technologies (Palo Alto, CA, USA). Electrical contact at the ESI needle tip was established via a sheath liquid. The nebulizer (N_2) and drying gas (N_2) were delivered at 0.4 bar and 4 L/min, respectively. The ESI chamber was maintained at 200°C. Spectra were acquired in the 800–2400 and 50–2400 m/z range in the positive ion mode for protein and peptide analysis, respectively.

2.4 Capillary coating

Four polymers were studied: poly-(TEDETAMA) (*Poly1*), poly-(TEDETAMA-*co*-HPMA) 75:25 (*Poly2*), poly-(TEDETAMA-*co*-HPMA) 50:50 (*Poly3*), and poly-(TEDETAMA-*co*-HPMA)

25:75 (*Poly4*). Before polymer coating, silica capillary was flushed with 1 M NaOH (20 min), water (10 min) and 0.1 mg/mL polymer (20 min). After this, polymer was left to stand overnight inside the capillary. Between injections, 37-cm capillaries were treated with polymer (2 min) and buffer (2 min) in CE-UV, and 80-cm capillaries with polymer (4 min) and buffer (4 min).

2.5 EOF measurement

BGE-water-acetone (20:70:10, v/v/v) was employed as marker to measure the EOF. It was injected using N_2 pressure at 0.5 psi for 3 s and detected 254 nm. The voltage applied was 20 kV. BGEs for EOF evaluation by CE-UV are described in Supporting Information.

2.6 Statistical determination of triads

The molar fractions of triads were obtained by using the Copol software [36] using monomers reactivity ratios from literature for methacrylate/methacrylamide couple, $r_{TEDETAMA} = 0.66$, $r_{HPMA} = 0.84$ [37]. The terminal model describes instantaneously the molar fractions of any sequence, using conditional probabilities. The conditional probabilities p_{ii} and p_{ij} for the i or j monomer addition to a growing chain end $\sim M_i$ (i,j = 1,2), is given by the propagation rates ratio (Eq. (1) and (2):

$$p_{ii} = \frac{R_{ii}}{R_{ii} + R_{ij}} = \frac{k_{ii}[M_i]}{k_{ii}[M_i] + k_{ij}[M_j]} = \frac{r_i}{r_i + [M_j]/M_i} \quad (1)$$

$$p_{ij} = 1 - p_{ii} \quad (2)$$

where $[M_i]$ and $[M_j]$ are the monomer feed concentrations. Thus, the instantaneous molar fraction of any sequence is equal to the probability of existence of the first unit (f, the copolymer molar fraction) multiplied by the corresponding conditional probabilities. For instance, the *iii*-triad molar fraction will be:

$$F_{iii} = f_i\, p_{ii}\, p_{ii} \quad (3)$$

The sequence molar fraction is related to the sequence population and therefore to the microstructure (sequence distribution). The Copol software approximates the cumulative molar fraction at 100% conversion (data used in this work) by performing a simple numerical integration of the instantaneous data obtained as explained before.

3 Results and discussion

3.1 Description of the polymers

Chemical structure and compositional characteristics of the polymers studied in this work are shown in Fig. 1A and Supporting Information Table 1, respectively. ^{1}H-NMR analysis demonstrated that all systems showed good monomer incorporation during the copolymerization, as the molar fractions in the final copolymers are quite similar to the nominal feed molar fractions. Polymers showed relatively low molecular weight typical for standard radical processes [30].

We have described the microstructure of the poly(TEDETAMA-*co*-HPMA) statistical copolymers as a function of the composition, that is the distribution of monomer units along the macromolecular chains, by the theoretical determination of the triad molar fractions (Supporting Information Table 1) using the Copol software and assuming that the copolymerization fits to the terminal model. This model can be used for the description of these systems considering that it is a good approximation to the reality [38, 39]. This theoretical description of triads may be related to the segmental charge density. This issue has been illustrated by representing the more populated triads for each polymer (Fig. 1B). The dendronic nature (and the three charges) of the TEDETAMA unit and the influence of the composition is also shown. It can clearly be seen that an increase of the HPMA content decreases the segmental charge density.

3.2 Effects of BGE pH and polymeric coatings on EOF

The properties of the coated capillaries were first studied by measuring the EOF and studying its dependence on the BGE pH. The four polymers described in Section 3.1 were evaluated: one homopolymer containing cationizable repetitive units of TEDETAMA (*Poly1*) and three copolymers of TEDETAMA with neutral hydrosoluble units of HPMA at different molar percentages (25%: *Poly 2*, 50%: *Poly 3* and 75%: *Poly4*). Bare silica and PB-coated capillary were also included in the study for comparison purposes.

The amine groups belonging to the unit labeled as TEDETAMA (which is common to all four synthesized polymers) will provide cationic character that will depend on the pH, being the p*K*a of the tertiary aliphatic amines in an interval centered at 8.5 [32]. It is also expected that different molar percentages of HPMA units will provide to the poly(TEDETAMA-*co*-HPMA) copolymer different behavior due to the extent of the shielding on the electrostatic interactions and the modulation of the charge density, as indicated in Fig. 1B.

The EOF values of bare fused-silica and coated capillaries were measured using the BGEs described in Supporting Information ranging from pH 1.9–10. The results obtained from this experiment are shown in Fig. 2. As can be seen, the EOF obtained for the bare fused silica displays a typical behavior depending on the pH: EOF close to zero at very low pH, an increase of EOF at higher pHs until pH 8, and nearly a constant EOF value at pH values higher than 8. Focusing on polymer-coated capillaries, overall, they showed an anodal EOF in all the pH range studied. In all cases, all TEDETAMA-based-coated capillaries showed an anodal EOF at low pHs and a nearly zero EOF at pHs between 9 and 10.

This behavior was different to that observed previously with other synthesized copolymers [9–13] in which both

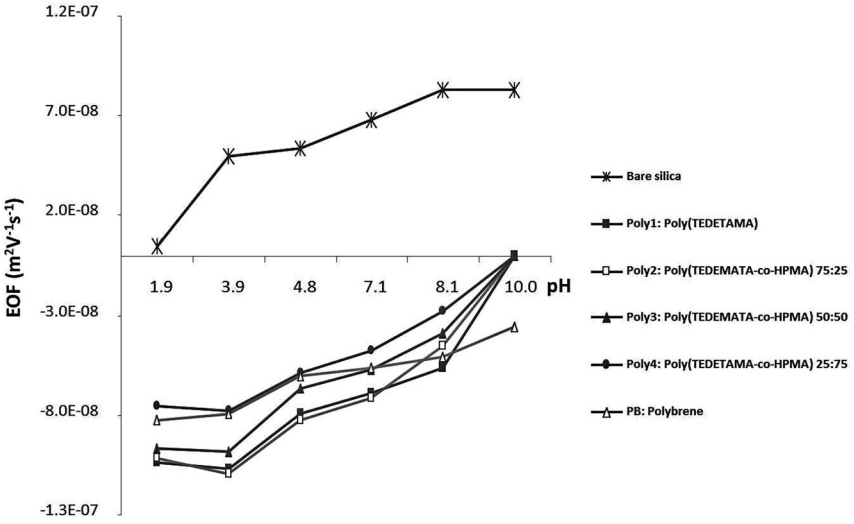

Figure 2. Electroosmotic mobility as function of pH and type of capillary coating. See Sections 2.3–2.5 for detailed experimental conditions.

Table 1. Percent RSD ($n = 3$) values of the EOFs obtained for bare fused silica and five different coated capillaries at six different pH values

BGE pH	Bare silica	*Poly 1*	*Poly 2*	*Poly 3*	*Poly 4*	PB
1.9	0.29	0.11	1.59	0.12	0.75	0.36
3.9	0.63	0.40	0.34	0.15	0.87	0.86
4.8	0.99	0.47	0.86	0.11	0.13	0.42
7.1	1.67	0.58	0.51	0.97	1.44	0.09
8.1	0.05	0.43	1.45	2.37	1.26	1.70
10.0	0.13	-	-	-	-	7.37

anodic and cathodic EOF were observed depending on the pH, most probably due to the involvement of both the amine groups of the polymers (positive charge) and the remaining silanol groups onto the silica wall (negative charge). By using poly-(TEDETAMA) and poly-(TEDETAMA-*co*-HPMA) the measured EOF was anodal when pH was below 8.1, and tends toward zero at higher pHs, which is related to the deprotonation of the amines (as mentioned above, the p*K*a has been described to be close to 8.5 [32]). In addition to this general behavior, more detailed comparison between different polymer coatings was carried out at each pH. It was observed that when decreasing the molar percentage of HPMA the EOF value was increased, as the positive charge density of the poly-(TEDETAMA-*co*-HPMA) is higher. This effect is more clearly observed at pH 8.1 as can be seen in Fig. 2. Also the differences of poly-(TEDETAMA) and poly-(TEDETAMA-*co*-HPMA) family compared to the commercial PB are notable. At pH above 5, PB shows a lower pH dependency than the TEDETAMA-based polymers, probably due to the permanent character of the PB's charges compared to the protonable character of the amines of TEDETAMA (p*K*a 8.5). Besides, the anodic EOF observed for *Poly1-3* at low pHs is higher (up to pH 7.1), that may be related to the intrinsic dendronic nature and the higher segmental charge density which is higher than in PB and *Poly4*. The reproducibility provided by these polymeric coatings was studied and % RSD values were calculated for the EOFs obtained after triplicated CE runs carried out at six different pHs (between 1.9 and 10). Table 1 shows the percent RSD values obtained as a function of the capillary type and pH. These results indicate that the coatings were stable over a wide pH range.

3.3 Analysis of basic proteins and peptides

To prevent basic protein adsorption, *Poly1-4* capillary coatings were evaluated with the purpose to allow efficient, fast, and reproducible CE separations of proteins and further application to CE-MS. To examine the protein separation using each coated capillary, a mixture of standard basic proteins were selected: bovine cyt c, equine cyt c, and poultry lysozyme. Among the BGEs described in Supporting Information, best separation was achieved at pH 4.8 (Fig. 3). It was observed that as HPMA molar percentage increased, both resolution and migration times increased too. These results show that the effect on EOF due to content on neutral HPMA play an important role on protein separation. As occurred with EOF, *Poly1* and *Poly2* showed a similar behavior, also in terms of peak selectivity and migration time: in both cases, equine cyt c and lyzozyme could not be baseline resolved. This similar behavior of *Poly1* and *Poly2* may be related to conformational issues, to be precise, some copolymers may compensate the lower segmental charge with a higher mobility of TEDETAMA units and a better orientation

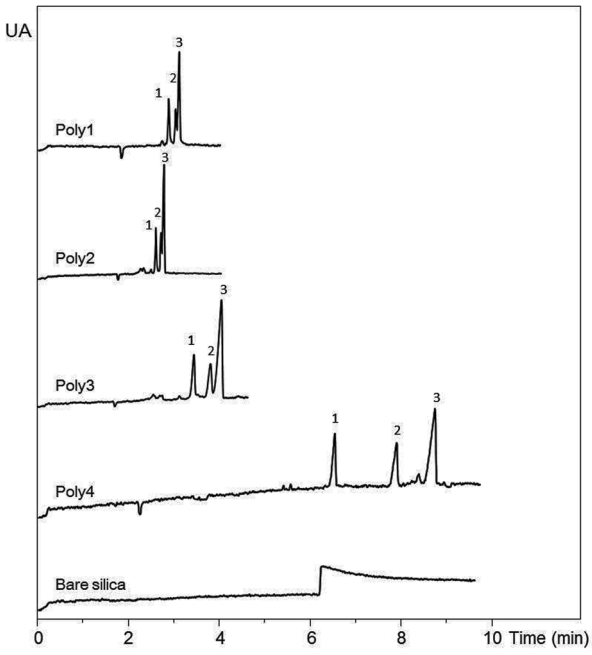

Figure 3. CE-UV electropherogram of basic proteins mixture: bovine cyt c (i), equine cyt c (ii), and poultry lysozyme (iii). Poly-(TEDETAMA) and Poly-(TEDETAMA-*co*-HPMA)-coated capillaries with 50 μm id, and 30/37 cm of detection/total length. Running buffer: 35 mM ammonium acetate at pH 4.8. Injection: 0.5 psi for 5 s. Running voltage: −20 kV. Temperature: 25°C.

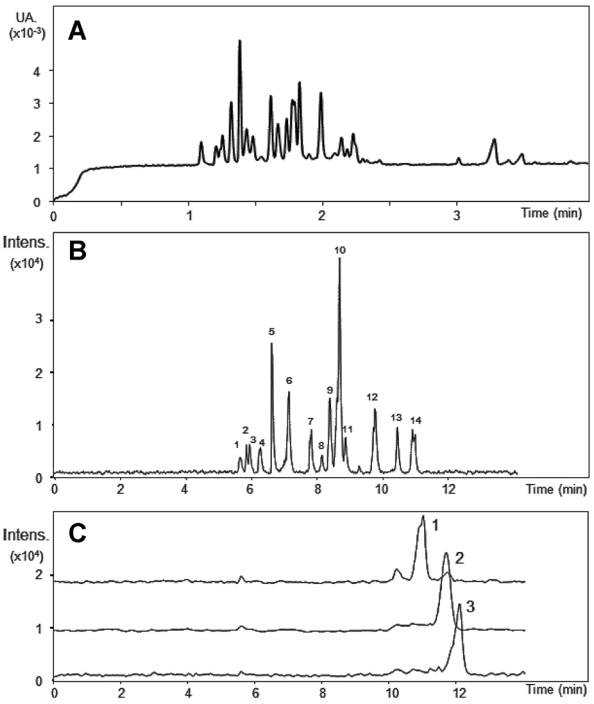

Figure 4. (A) CE-UV analysis of cytochrome c digest. Same analytical conditions as in Fig. 3. **(B)** CE-MS base peak electropherogram of cytochrome c tryptic digest; for peptides identification see peak numbers in Supporting Information Table 3, and **(C)** CE-MS extracted ion electropherograms of basic proteins mixture comprising bovine cyt c (i), equine cyt c (ii), and poultry lysozyme (iii). 80 cm of detection/total capillary length. Injection: 0.5 psi for 10 s. Running voltage: −30 kV. Temperature: 25°C. Other analytical conditions as in Fig. 3.

respect to the negative charges of the wall due to the presence of adjacent HPMA units. It has to be noted that substituted vinyl polymers obtained by radical polymerization are mainly syndiotactic, and a possible steric hindrance of the syndiotactic sequences are maximized in the homopolymers, as it has been described in the literature for other polyelectrolytes [40]. Baseline separation was obtained using *Poly3*- and *Poly4*-coated capillaries. Moreover, no significant differences in effective mobilities of the three proteins using *Poly3*- and *Poly4*-coated capillaries, were observed. Namely, calculated effective mobilities for the *Poly3*-coated capillary were: $2.7{\cdot}10^{-4}$, $2.9{\cdot}10^{-4}$, and $3.0{\cdot}10^{-4}$ cm^2/sV, for peak 1, 2, and 3, respectively; while for the *Poly4*-coated capillary these values were practically the same (namely, $2.7{\cdot}10^{-4}$, $3.0{\cdot}10^{-4}$, and $3.1{\cdot}10^{-4}$ cm^2/sV). Thus, protein interaction with *Poly3* and *Poly4* coatings did not contribute to the separation. As can be seen in Fig. 3, an optimal compromise between analysis time and resolution was obtained with poly-(TEDETAMA-*co*-HPMA) 50:50 copolymer-coated capillary (*Poly3*). Under these conditions, good migration time repeatability was obtained: namely, 0.5, 0.6, and 0.6% RSD ($n = 5$), for bovine cyt c, equine cyt c, and poultry lysozyme, respectively. RSD values for peak areas ($n = 5$) were 1.2, 1.3, and 1.9% for bovine cyt c, equine cyt c, and poultry lysozyme, respectively. Moreover, three different capillaries were submitted to polymer coating with *Poly3* and acceptable repeatability for migration time (Supporting Information Table 2) was obtained, with percent RSD values of 4.4, 4.9, and 5.3 for three different capillaries and three different days. Plate numbers for the mentioned basic proteins were up to 280 000 and up to 125 000, using the Poly3 and Poly4 coating, respectively. Also, plate numbers for each protein peak did not significantly change in successive runs, indicating a stable coating.

CE has also become a recognized complementary technique to frequently used reversed-phase LC for peptide analysis, especially in clinical research [41]. Analysis of peptides is also of great importance since both the structure and function of many proteins are identified *via* their peptidic fragments. In this important line of research, coated capillaries can also be used to control the efficiency and speed of the CE separation of peptides. In this work, a first attempt to analyze a peptide mixture obtained after tryptic digestion of cytochrome c was carried out using the *Poly3*-coated capillary. As can be seen in Fig. 4A, good separation of the peptides was achieved in less than 4 min. However, absorbance detection provides little structural information, and therefore, on-line coupling with MS detection can provide peptide identification and increased selectivity. Thus, the usefulness and compatibility of *Poly3* coating was also tested in a CE-MS platform, and good separation performance for both peptides mixture (Fig. 4B and Supporting Information Table 3) and basic proteins mixture (Fig. 4C) was obtained with no signal

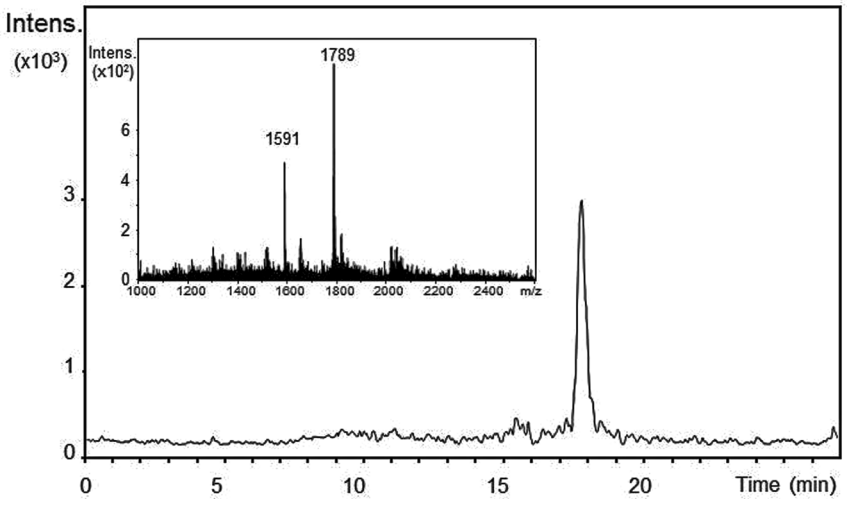

Figure 5. CE-MS analysis of lysozyme in cheese: extracted ion electropherogram from lysozyme and mass spectra are given. Analytical conditions are indicated in Fig. 4 and text.

suppression or contamination of the ion source (Supporting Information Fig. 1).

3.4 CE-MS analysis of lysozyme in food samples

One of the most important applications of lysozyme in food industry is the prevention of late blowing of cheeses by inhibiting growth of *Clostridium tyrobutyricum*, as well as a preservative in wine to control malolactic fermentation. Lysozyme is a potential allergenic agent, and thus, it has to be declared according to the allergen labeling instructions of EU and FDA. The methods to detect lysozyme in foods are mostly based on ELISA performed with various formats. When compared to HPLC with fluorescence detection, it was observed that ELISA was prone to cheese matrix interferences during the immunological reactions [42] giving rise to underestimation of the lysozyme concentration. Specificity and sensitivity of the analysis of lysozyme in cheese was improved by using by SELDI-TOF-MS with weak cationic exchanger chips [43] and by using immunocapture purification before MALDI-TOF-MS analysis [35], in both cases at expenses of cost per analysis. Recently, an LC-MS/MS method has been developed for preservatives determination, including lysozyme, in cheeses [44]. CE-MS has several advantages over the LC-MS, in particular with regard to requirements of sample and reagent volumes and separation efficiencies. Moreover, CE allows fast separation and is generally not affected by many compounds that interfere with LC. Feasibility of the use of poly-(TEDETAMA-*co*-HPMA) 50:50 copolymer-coating and CE-MS for the analysis of lysozyme in cheese is shown in Fig. 5. As expected, migration time shift of the lysozyme peak was observed due to a higher ionic strength of the sample as a result of the high salt content of the cheese extract (i.e. 1 M NaCl, 1 M NaOH, and 1 M HCl were used for extraction). Additionally, the CE-MS method leads to other information from cheese. Thus, some remaining whey proteins as α-lactalbumin and β-lactoglobulins were identified in the cheese. Moreover, a variety of peaks with lower molecular masses (550–1200 Da) were detected, most probably from polypeptides derived from the proteolysis during the ripening process (Supporting Information Fig. 2).

4 Concluding remarks

A series of polymers and copolymers carrying pendant dendronic triamines (TEDETAMA) have been synthesized and used as effective capillary coating for the first time for the separation of basic proteins. All these polymer coatings could effectively reversed the EOF over a pH range of 2–10. Statistical incorporation of HPMA modulates the interaction with the silica wall, reducing the anodal EOF. The separation performance can be tailored by adjusting the copolymer composition. A statistical copolymer that incorporates both components TEDETAMA and neutral HPMA at 50:50 molar ratio gave best overall results in terms of protein separation and analysis time for basic protein analysis, with high plate numbers. The coating showed full compatibility with MS detection, and standard mixture of basic proteins and peptides was efficiently separated by using the capillary coated with poly-(TEDETAMA-*co*-HPMA) 50:50 copolymer by CE-MS. Although more in-depth evaluation of the applicability of CE-MS using poly-(TEDETAMA-*co*-HPMA) 50:50 copolymer coating is needed, the feasibility of the current approach was shown by the analysis of lysozyme in commercial cheese samples.

This work was supported by an AGL2011-29857-C03-01, MAT2010-10001, and MAT2013-42957-R projects (Ministerio de Educacion y Ciencia, Spain). J.A.R. and R.N. acknowledge funding from the Spanish Research Council (CSIC) and European Social Fund (ESF) through the JAE program.

The authors have declared no conflict of interest.

5 References

[1] Haselberg, R., de Jong, G. J., Somsen, G. W., *J. Chromatogr. A* 2007, *1159*, 81–109.

[2] Haselberg, R., de Jong, G. J., Somsen, G. W., *Electrophoresis* 2011, *32*, 66–82.

[3] Haselberg, R., de Jong, G. J., Somsen, G. W., *Electrophoresis* 2013, *34*, 99–112.

[4] Dolník, V., *Electrophoresis* 2006, *27*, 126–141.

[5] Dolník, V., *Electrophoresis* 2008, *29*, 143–156.

[6] Lucy, C. A., MacDonald, A. M., Gulcev, M. D., *J. Chromatography A*, 2008, *1184*, 81–105.

[7] Garza, S., Chang, S., Moini, M., *J. Chromatogr. A*, 2007, *1159*, 14–21

[8] Nguyen, A., Moini, M., *Anal. Chem.* 2008, *80*, 7169–7173

[9] González, N., Elvira, C., San Román, J., Cifuentes, A., *J. Chromatogr. A* 2003, *1012*, 95–101.

[10] Simó, C., Rizzi, A., Barbas, C., Cifuentes, A., *Electrophoresis* 2005, *26*, 1432–1441.

[11] Bernal, J., Rodríguez-Meizoso, I., Elvira, C., Ibáñez, E., Cifuentes, A., *J. Chromatogr. A* 2008, *1204*, 104–109.

[12] Bernal, J., Sánchez-Hernández, L., Elvira, C., Velasco, D., Ibáñez, E., Cifuentes, A., *J. Sep. Sci.* 2009, *32*, 605–612.

[13] Herrero, M., Bernal, J., Velasco, D., Elvira, C., Cifuentes, A., *J. Chromatogr A.* 2010, *1217*, 7586–7592.

[14] Huhn, C., Ramautar, R., Wuhrer, M., Somsen, G. W., *Anal. Bioanal. Chem.* 2010, *396*, 297–314

[15] Pattky, M., Huhn, C., *Anal. Bioanal. Chem.* 2013, *405*, 225–237.

[16] Simó, C., Elvira, C., González, N., San Román, J., Barbas, C., Cifuentes, A., *Electrophoresis* 2004, *25*, 2056–2064

[17] Ongay, S., Neusüβ, C., *Anal. Bioanal. Chem.* 2010, *398*, 845–855.

[18] Hardenborg, E., Zuberovic, A., Ullsten, S., Söderberg, L., Heldin, E., Markides, K. E., *J. Chromatography A*, 2003, *1003*, 217–221.

[19] Ullsten, S., Zuberovic, A., Wetterhall, M., Hardenborg, E., Markides, K. E., Bergquist, J., *Electrophoresis* 2004, *25*, 2090.

[20] Katayama, H., Ishihama, Y., Asakawa, N., *Anal. Chem.* 1998, *70*, 5272–5277.

[21] Haselberg, R., de Jong, G. J., Somsen, G. W., *J. Sep. Sci.* 2009, *32*, 2408–2415.

[22] Haselberg, R., van der Sneppen, L., Ariese, F., Ubachs, W., Gooijer, C., de Jong, G. J., Somsen, G. W., *Anal. Chem.* 2009, *81*, 10172–10178.

[23] Haselberg, R., de Jong, G. J., Somsen, G. W., *Anal. Chim. Acta* 2010, *678*, 128–134.

[24] Haselberg, R., de Jong, G. J., Somsen, G. W., *J. Sep. Sci.* 2009, *32*, 2408–2415

[25] Haselberg, R., Brinks, V., Hawe, A., de Jong, G. J., Somsen, G. W., *Anal. Bioanal. Chem.* 2011, *400*, 295–303.

[26] Bayramoglu, G., Karagoz, B., Altintas, B., Arica, M. Y., Bicak, N., *Bioprocess Biosyst. Eng.* 2011, *34*, 735–746.

[27] Bayramoglu, G., Karagoz, B., Yilmaz, M., Bicak, N., Arica, M. Y., *Bioresour. Technol.* 2011, *102*, 3653–3661.

[28] Shen, Y., Tang, H., Ding, S., *Progress Polymer Sci.* 2004, *29*, 1053–1078.

[29] Matyjaszewski, K., Xia, J., *Chem. Rev.* 2001, *101*, 2921–2990.

[30] Redondo, J. A., Martínez-Campos, E., Navarro, R., Reinecke, H., Elvira, C. , López-Lacomba, J. L., Gallardo, A., *Eur. J. Pharm. Biopharm.* 2015, *93*, 303–310.

[31] Redondo, J. A., Velasco, D., Pérez-Perrino, D., Reinecke, H., Gallardo, A., Pandit, A. Elvira, C., *Eur. J Pharm. Biopharm.* 2015, *90*, 38–43.

[32] Redondo, J. F., Navarro, R., Martínez-Campos, E., Pérez-Perrino, M., París, R., López-Lacomba, J. L., Elvira, C., Reinecke, H., Gallardo, A., *J. Polym. Sci. Polym. Chem.* 2014, *52*, 2297–2305.

[33] Ulbrich, K., Strohalm, J., Plocova, D., Jelinkova, M., Rihova, B., *J. Control. Release* 2000, *64*, 63–69.

[34] Simó, C., Cifuentes, A., *Electrophoresis* 2003, *24*, 834–842.

[35] Schneider, N., Becker, C-M., Pischetsrieder, M., *J. Chromatogr. B*, 2010, *878*, 201–206.

[36] Gallardo, A., Aguilar, M. R., Abraham, G., San Román, J., *J. Chem. Educ.* 2004, *81*, 1210–1215.

[37] Kopecek, J., Bazilova, H. *Eur. Poly. J.* 1973, *9*, 7–14.

[38] Coote, M., Davis, T. P., *Prog. Polym. Sci.* 1999, *24*, 1217–1251.

[39] Matyjaszewski, K., Davis, T. P., Wiley, J., *Handbook of Radical Polymerization*. Wiley-Interscience, Hoboken 2002.

[40] Tardajos, M. G., García-Fernández, L., Reinecke, H., Aguilar, M. R., Gallardo, A., San Román, J., *J. Bioact. Comp. Polym.* 2012, *25*, 453–466.

[41] Stalmach, A., Albalat, A., Mullen, W., Mischak, H., *Electrophoresis* 2013, *34*, 1452–1464.

[42] Kerkaert, B., Mestdagh, F., Meulenaer, B., *Food Chem.* 2010, *120*, 580–584.

[43] Dragoni, I., Balzaretti, C., Rossini, S., Rossi, L., Dell'Orto, V., Baldi, A., *Food Anal. Methods* 2011, *4*, 233–239.

[44] Fuselli, F., Guarino, C., La Mantia, A., Longo, L., Faberi, A., Marianella, R. M., *J. Chromatogr. B* 2012, *906*, 9–18.

Supplementary information

POTENTIAL OF PRO-DENDRONIC POLYAMINES WITH MODULATED SEGMENTAL CHARGE DENSITY AS NOVEL COATING FOR FAST AND EFFICIENT ANALYSIS OF PEPTIDES AND BASIC PROTEINS BY CAPILLARY ELECTROPHORESIS AND CAPILLARY ELECTROPHORESIS-MASS SPECTROMETRY

Tanize Acunha, Clara Ibáñez, María Isabel Pascual Reguera, Mariagiovanna Sarò, Rodrigo Navarro, Juan Alfonso Redondo, Helmut Reinecke, Alberto Gallardo, Carolina Simó*, Alejandro Cifuentes

Materials and Methods

BGEs for EOF evaluation by CE-UV were: 1 M formic acid (adjusted to pH 1.9 with ammonium hydroxide), 100 mM acetic acid (adjusted to pH 3.9 with ammonium hydroxide), 35 mM ammonium acetate (adjusted to pH 4.8 with acetic acid), 25 mM ammonium formate (adjusted to pH 7.1 with ammonium hydroxide), 40 mM ammonium acetate (adjusted to pH 8.1 with ammonium hydroxide), and 50 mM boric acid (adjusted to pH 10 with ammonium hydroxide). The pH was set to the desired value with either acetic acid or ammonia, while ionic strength was 40-45 mM.

Lysozyme extraction from cheese: Cured sheep cheese was purchased from a local supermarket (Madrid, Spain) and subjected to lysozyme extraction [35]. Briefly, two grams of grounded cheese (using a CryoMill from Retsch GmbH, Haan, Germany) were mixed with 20 mL NaCl 1M (10 min at 30 Hz). Resulting solution was adjusted to pH 6.0 with NaOH 1M, and then maintained at 40°C for 30 minutes. After that, pH was adjusted to pH 4.3 with HCl 1M and filtered through a filter paper first and then through a 0.22 µm pore size filter (Symta, Spain).

Table S1. Compositional and microstructural characteristics, and molecular weight of the four novel polymers evaluated in this study. $F_{TEDETAMA}$=nominal feed molar fraction of the copolymers. $f_{TEDETAMA}$= real copolymer molar fraction of the copolymers determined experimentally. Mn= average number molecular weight (Da). Microstructure is described by the theoretical cumulative molar fraction of triads along the macromolecular chains. T=TEDETAMA, H=HPMA. TTH* =TTH+HTT. HHT*=HHT+THH.

Polymer name	Abbreviated name	$F_{TEDETAMA}$	$f_{TEDETAMA}$	Mn	Theoretical molar fractions of triads					
					f_{TTT}	f_{TTH^*}	f_{HTH}	f_{HHH}	f_{HHT^*}	f_{THT}
Poly-(TEDETAMA)	Poly1	1.00	1.00	23900	1.00	-	-	-	-	-
Poly-(TEDETAMA-*co*-HPMA) 75:25	Poly2	0.75	0.71	20700	0.40	0.29	0.06	<0.01	0.07	0.17
Poly-(TEDETAMA-*co*-HPMA) 50:50	Poly3	0.50	0.47	16100	0.08	0.22	0.16	0.12	0.27	0.15
Poly-(TEDETAMA-*co*-HPMA) 25:75	Poly4	0.25	0.25	17900	<0.01	0.07	0.17	0.39	0.30	0.06

Table S2. Repeatability for three different capillaries coated with Poly3 and three different days.

Capillary 1, day 1			
	Migration time (min)		
Run	Bovine Cyt C	Equine Cyt C	Lysozyme
No. 1	3.52	3.75	3.88
No. 2	3.56	3.81	3.95
No. 3	3.54	3.78	3.92
No. 4	3.54	3.78	3.92
No. 5	3.53	3.78	3.92
Mean	**3.53**	**3.78**	**3.92**
SD	**0.02**	**0.02**	**0.02**
% RSD	**0.47**	**0.56**	**0.64**

Capillary 2,day 2			
	Migration time (min)		
Run	Bovine Cyt C	Equine Cyt C	Lysozyme
No. 1	3.28	3.46	3.56
No. 2	3.23	3.41	3.51
No. 3	3.22	3.43	3.50
No. 4	3.23	3.42	3.52
No. 5	3.20	3.38	3.48
Mean	**3.23**	**3.42**	**3.52**
SD	**0.03**	**0.03**	**0.03**
% RSD	**0.92**	**0.81**	**0.87**

Capillary 3, day 3			
	Migration time (min)		
Run	Bovine Cyt C	Equine Cyt C	Lysozyme
No. 1	3.51	3.76	3.90
No. 2	3.51	3.75	3.89
No. 3	3.54	3.79	3.93
No. 4	3.57	3.83	3.98
No. 5	3.57	3.83	3.97
Mean	**3.54**	**3.79**	**3.93**
SD	**0.03**	**0.04**	**0.04**
% RSD	**0.83**	**0.95**	**1.05**

Inter-capillary/day			
	Migration time (min)		
	Bovine Cyt C	Equine Cyt C	Lysozyme
Mean	**3.44**	**3.66**	**3.79**
SD	**0.15**	**0.18**	**0.20**
% RSD	**4.41**	**4.91**	**5.35**

Table S3. Sequence assignment of the peaks shown in Figure 4B.

Peak No.	Assignment	Experimental m/z	Sequence	Missed Cleavages
1	$[M+H]^+$	748.4	(K)EETLMEYLENPK(K)	0
2	$[M+H]^+$	964.5	(R)EDLIAYLK(K)	0
3	$[M+2H]^+$	812.4	(K)EETLMEYLENPKK(Y)	1
4	$[M+2H]^{2+}$, $[M+3H]^{3+}$	1041.0, 694.4	(K)GITWKEETLMEYLENPK(K)	1
5	$[M+2H]^{2+}$, $[M+3H]^{3+}$	1105.1, 737.0	(K)GITWKEETLMEYLENPKK(Y)	2
6	$[M+2H]^{2+}$	739.9	(K)TEREDLIAYLKK(A) (K)KTEREDLIAYLK(K)	2
7	$[M+2H]^{2+}$	799.9	(R)KTGQAPGFTYTDANK(N)	1
8	$[M+2H]^{2+}$	478.3	Not identified	-
9	$[M+H]^+$	779.5	MIFAGIK	0
10	$[M+H]^+$	634.4	(K)IFVQK(C)	0
11	$[M+H]^+$	604.4	(K)GITWK(E)	0
12	$[M+H]^+$	584.8	(K)TGPNLHGLFGR(K)	0
13	$[M+2H]^{2+}$	453.3	Acetyl-MGDVEKGK(K)	1
14	$[M+2H]^{2+}$	403.7	(K)KYIPGTK(M)	1

Figure S1. CE-MS electropherograms obtained using an uncoated and a Poly3-coated capillary. Electrophoretic separations were achieved using +20 kV (uncoated capillary) or -20 kV (Poly3-coated capillary). Spectra were acquired in the 800-2400 m/z range in the positive ion mode. Other CE-MS conditions are indicated in Section 2.3. TIEs are indicated in panel A. Representative mass spectra are indicated in panels B, C and D.

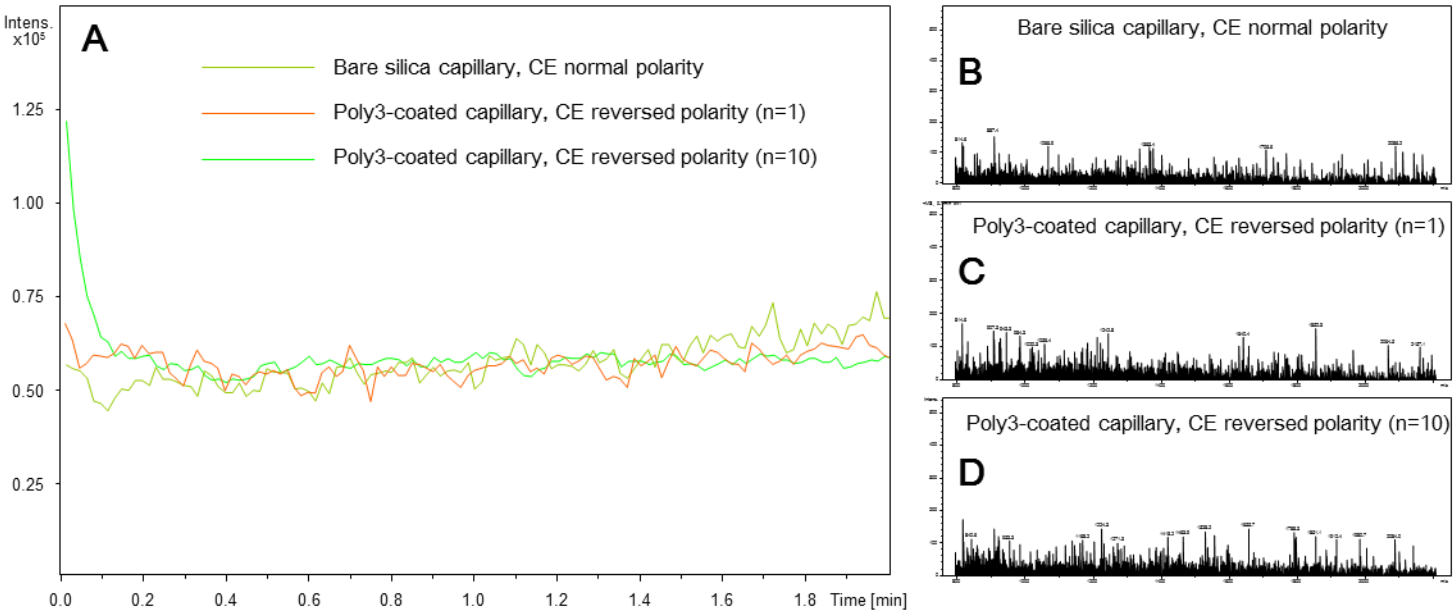

Figure S2. CE-MS extracted ion electropherograms (A) of low molecular mass compounds and (B) of detected proteins in a cheese extract. Mass spectra from (C) α-Lactoalbumin, (D) β-Lactoglobulin, and (E) lysozyme.

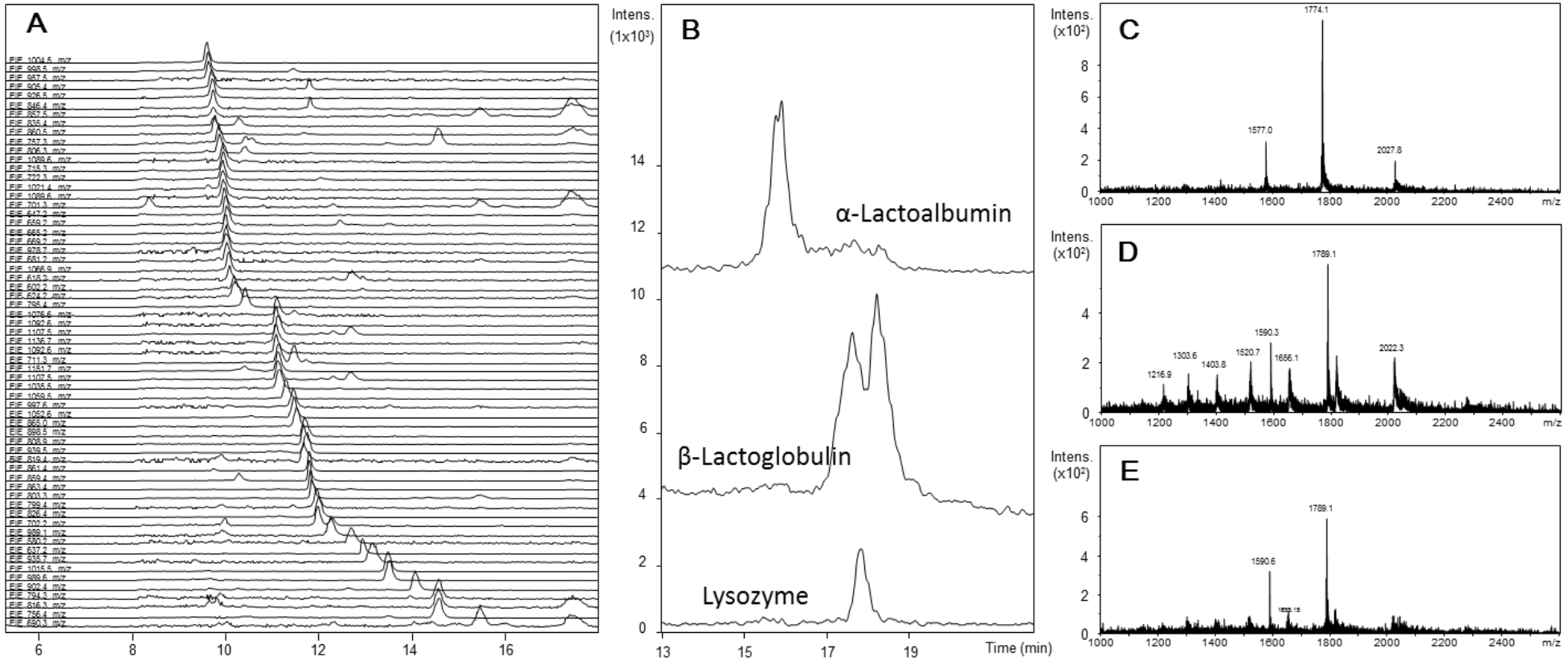

3.3.4. Anionic metabolite profiling by capillary electrophoresis–mass spectrometry using a noncovalent polymeric coating. Orange juice and wine as case studies

Acunha, T., Simó, C., Ibáñez, C., Gallardo, A., Cifuentes, A.

Journal Chromatography A **1428,** 326–335 (2016).
DOI: 10.1016/j.chroma.2015.08.00.

Journal of Chromatography A, 1428 (2016) 326–335

Contents lists available at ScienceDirect

Journal of Chromatography A

journal homepage: www.elsevier.com/locate/chroma

Anionic metabolite profiling by capillary electrophoresis–mass spectrometry using a noncovalent polymeric coating. Orange juice and wine as case studies

Tanize Acunha[a,b], Carolina Simó[a,*], Clara Ibáñez[a], Alberto Gallardo[c], Alejandro Cifuentes[a]

[a] Laboratory of Foodomics, CIAL, CSIC, Nicolas Cabrera 9, 28049 Madrid, Spain
[b] CAPES Foundation, Ministry of Education of Brazil, 70040-020 Brasília, DF, Brazil
[c] Instituto de Ciencia y Tecnología de Polímeros, ICTP-CSIC, Juan de la Cierva 3, 28006 Madrid, Brazil

ARTICLE INFO

Article history:
Received 11 June 2015
Received in revised form 21 July 2015
Accepted 1 August 2015
Available online 5 August 2015

Keywords:
Anionic metabolite
Capillary electrophoresis–mass spectrometry
Food analysis
Foodomics
Metabolomics
Orange juice
Wine

ABSTRACT

In several metabolomic studies, it has already been demonstrated that capillary electrophoresis hyphenated to mass spectrometry (CE–MS) can detect an important group of highly polar and ionized metabolites that are overseen by techniques such as NMR, LC–MS and GC–MS, providing complementary information. In this work, we present a strategy for anionic metabolite profiling by CE–MS using a cationic capillary coating. The polymer, abbreviated as PTH, is composed of a poly-(N,N,N',N'-tetraethyldiethylenetriamine, N-(2-hydroxypropyl) methacrylamide, TEDETAMA-co-HPMA (50:50) copolymer. A CE–MS method based on PTH-coating was optimized for the analysis of a group of 16 standard anionic metabolites. Separation was achieved within 12 min, with high separation efficiency (up to 92,000 theoretical plates per meter), and good repeatability, namely, relative standard deviation values for migration times and peak areas were below 0.2 and 2.1%, respectively. The optimized method allowed the detection of 87 metabolites in orange juice and 142 metabolites in red wine, demonstrating the good possibilities of this strategy for metabolomic applications.

1. Introduction

Among the different mass spectrometry (MS)-based approaches used in metabolomics, those that combine a physical/chemical separation/fractionation prior to MS analysis are the most widely used. Thus, although at the expenses of less high-throughput performance, hyphenation of high-resolution separation techniques and MS is usually carried out in order to avoid sample matrix effects while revealing the metabolome of a biological system as much as possible. The majority of applications in the field of metabolomics over the last years have used liquid chromatography–mass spectrometry (LC–MS) and gas chromatography–mass spectrometry (GC–MS). However, ionized, highly polar and hydrophilic compounds are poorly retained in reversed-phase (RP) LC–MS. Hydrophilic interaction chromatography–MS (HILIC–MS) allows profiling of polar compounds, providing complementary metabolic information to RPLC, as has been previously demonstrated [1]. It should be mentioned that re-equilibration of HILIC columns is slow particularly with gradient elution of mobile phases containing buffers while resolution in HILIC is not as high as in RPLC. Capillary electrophoresis–mass spectrometry (CE–MS) is considered a powerful analytical tool for the analysis of charged and highly polar metabolite species [2,3] that provides complementary information to RPLC–MS and HILIC–MS [4–6]. Up to date, the number of applications involving the analysis of cationic metabolites and CE–MS in positive ionization mode far exceeds the number of works involving anionic metabolite profiling [7]. This is mainly due to the fact that in CE–MS the outlet of the capillary is not immersed in the vial electrolyte, thus, by using a fused silica capillary and normal polarity, the electroosmotic flow (EOF) moves from the anode to the cathode (where the MS detector is located), and the CE electrical current is stabilized. Additionally, rapid analysis with good resolution is obtained since both EOF and the electrophoretic mobility of cationic metabolites are toward the cathode (MS detector). In contrast, by using a fused silica capillary and reversed polarity for anionic compounds analysis, the direction of the EOF is opposing to the MS detector, and thus, unstable electrical connection between the tip of the capillary and the grounded electrospray needle, is

* Corresponding author.
E-mail address: c.simo@csic.es (C. Simó).

http://dx.doi.org/10.1016/j.chroma.2015.08.001
0021-9673/

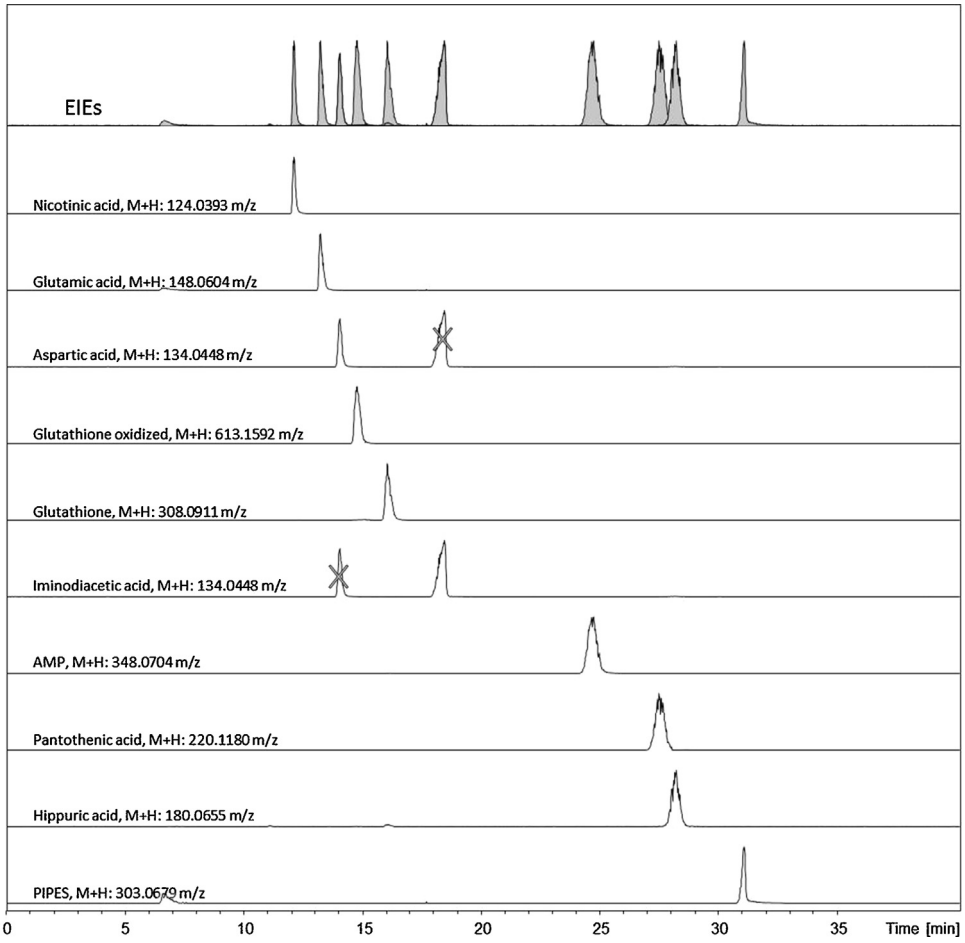

Fig. 1. CE–ESI–TOF MS extracted ion electropherograms (EIEs) of metabolites in mix of anionic metabolites (ARM) separated using 1 M formic acid as BGE at normal CE polarity (+20 kV) in a bare silica capillary and positive ion ESI–MS mode. Sheath liquid: 2-propanol–water (50:50, v/v) at 0.24 mL/h. Other analytical conditions are described in Section 2.4.

typically observed [8]. However, obtaining metabolome information as complete as possible requires the combination of several methodologies, inherent to the highly diverse chemical structure of metabolites. For anionic metabolites, CE under alkaline background electrolyte (BGE) conditions has been demonstrated to be a useful approach when no MS detection is carried out. When alkaline BGEs are used, low signals were observed for anionic test mixtures [9]. Profiling of anionic compounds for metabolomic applications has been achieved by pressure assisted CE using fused-silica [10], inert polymer capillaries [8] or non-charged polymer inner surface coating [11]. On the other hand, since the very first work by Tsuda [12] who described the use of the cationic surfactant cetyltrimethylammonium bromide (CTAB) added to the separation buffer to reverse the EOF, a variety of cationic surfactant additives have been developed. However, this procedure should generally be avoided when working with MS detection since these surfactants suppress sample ionization and contaminate the ion source. An interesting strategy in CE to reverse the EOF toward the anode (the MS direction when working in reversed polarity), to prevent current drops, is the use of physically adsorbed coating materials. Following this strategy, just by rinsing the capillary with a solution containing the coating agent, the coated capillary can be easily prepared. In this work a polymer bearing a dendronic triamine derived from N,N,N',N'-tetraethyldiethylenetriamine (TEDETA) moiety, which is linked to a unit through a spacer, (unit labeled as TEDETAMA), was copolymerized together with neutral hydrosoluble units of hydroxypropylmethacrylamide (HPMA) at a 50:50 molar percentage. This copolymer is tested for the first time as a robust coating to reverse EOF for anionic metabolite profiling by CE–MS. The feasibility of the polymer-coated capillary approach was corroborated via the analysis of anionic metabolites of complex samples such as orange juice and red wine.

2. Materials and methods

2.1. Chemicals

All chemicals were of analytical reagent grade and used as received. Standard metabolites were from Sigma–Aldrich (St. Louis, MO, USA). All reagents and solvents employed in the preparation of CE electrolytes and sheath liquids were of MS grade: methanol and 2-propanol were from Sigma–Aldrich (St. Louis, MO, USA). Ammonium hydroxide, formic acid and acetic acid were from Fluka (Buchs, Switzerland). Ammonium acetate, ammonium formate and boric acid were purchased from Merck (Darmstad, Germany). The distilled water was deionized using a Milli-Q system from Millipore (Bedford, MA, USA). An aqueous solution containing 0.1 M of sodium hydroxide, from Panreac Quimica S.A. (Barcelona, Spain) was used to rinse the capillary.

2.2. Metabolite test mixtures and sample preparation

Cationic metabolite-rich mixture (CRM) was composed of 0.5 mM of: L-carnosine, L-anserine, L-ornithine,

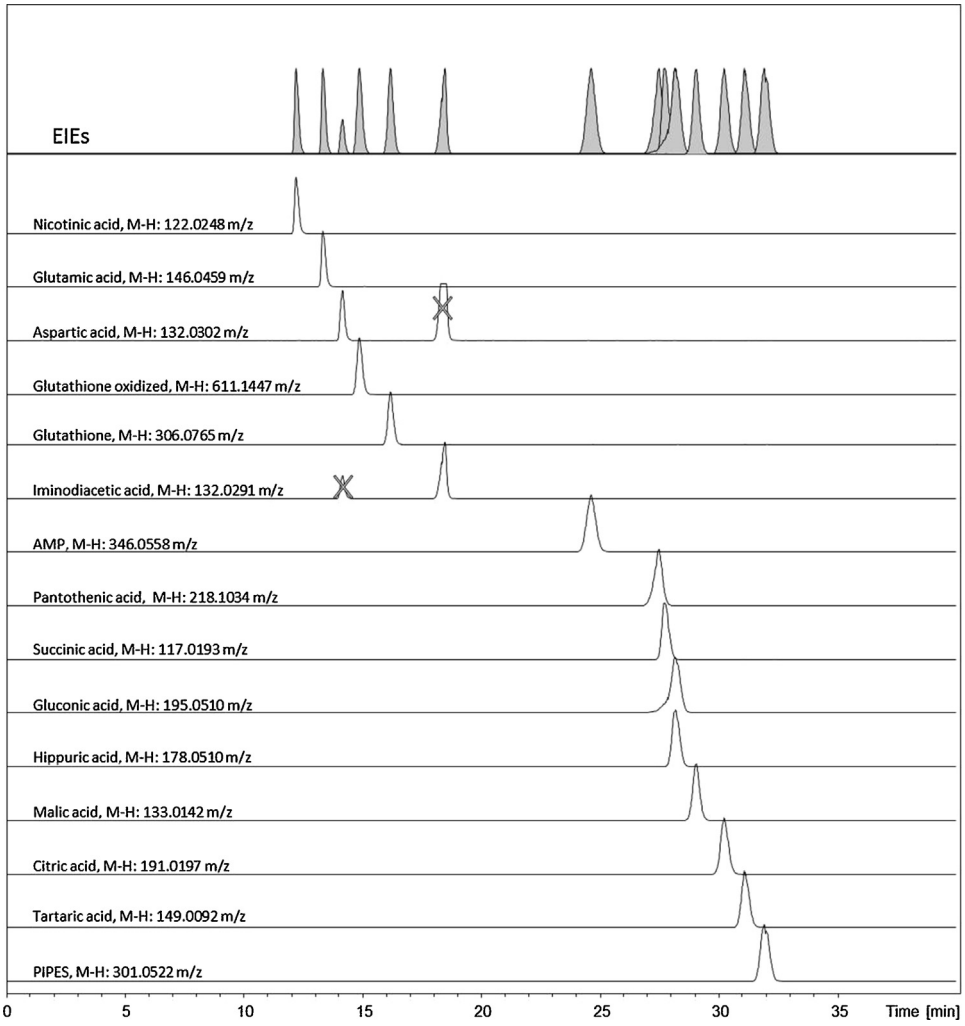

Fig. 2. CE–ESI–TOF MS EIEs of ARM analyzed in negative ion ESI–MS mode. Other CE–MS conditions as in Fig. 1.

L-lysine, L-creatinine, alanine, β-alanine, sarcosine, L-arginine, δ-hydroxylysine, L-histidine, 1-methyl-L-histidine, 3-methyl-L-histidine, γ-amino-n-butyric acid, β-aminoisobutyric acid, α-amino-n-butyric acid, homocystine, valine, serine, cystathionine, leucine, isoleucine, threonine, methionine, proline, tryptophan, glutamic acid, citrulline, phenylalanine, cystine, tyrosine, aspartic acid and hydroxy-L-proline. The anionic metabolite-rich mixture (ARM) consisted of the following compounds: 0.3 mM adenosine triphosphate (ATP), 7.8 mM nicotinic acid, 0.5 mM glutamic acid, 1.0 mM aspartic acid, 0.3 mM glutathione oxidized, 0.6 mM glutathione reduced, 2.7 mM iminodiacetic acid, 0.2 mM adenosine monophosphate (AMP), 0.2 mM panthotenic acid, 1.4 mM succinic acid, 0.1 mM gluconic acid, 0.4 mM hippuric acid, 0.3 mM malic acid, 0.2 mM citric acid, 0.2 mM tartaric acid, and 2.8 mM 1,4 piperazinediethanesulfonic acid (PIPES). Orange juice was prepared in the laboratory from fresh oranges (*C. sinensis*) and filtered through 0.2 μm polyethersulfone filter before CE–MS injection to remove possible particles from the liquid matrix. A young red wine (Pinot Noir, vintage 2010) was similarly filtered before CE–MS analysis.

2.3. Polymer synthesis and capillary coating

The coating material used in this work is based in linear polymeric chains bearing as side cationizable moiety a dendronic triamine derived from N,N,N',N'-tetraethyldiethylenetriamine (TEDETA), which is linked to the backbone through a spacer (unit labeled as TEDETAMA). The copolymer, abbreviated as PTH, randomly incorporates TEDETAMA together with neutral hydrosoluble units of N-(2-hydroxypropyl) methacrylamide (HPMA) at a molar percentage of 50%. The copolymerizations were carried out by conventional free radical polymerization as described elsewhere [13]. Briefly, the reaction was performed at 60 °C, using AIBN ($[I] = 1.5 \times 10^{-2}$ M) as the radical initiator and a monomer concentration of 1 M using DMF as solvent. All solutions were carefully degassed using dried nitrogen flow to remove all the oxygen traces. After 24 h, the obtained polymers were dialyzed in distilled water, using dialysis membranes Spectra/Por® (Spectrum Laboratories Inc., Rancho Dominguez, CA, USA) with a molecular weight cut off of 3.5 kDa, and freeze dried. The composition and molecular weight of the polymers were determined respectively by ^{1}H NMR spectroscopy and size exclusion chromatography [13]. Coating procedure consisted of flushing the fused-silica capillary with 1 mg/mL of PTH solution for 20 min. Silica capillary was washed between runs with 0.1 mg/mL PTH solution for 4 min and separation buffer for 3 min.

2.4. CE–ESI–TOF MS conditions

CE analyses were carried out in a P/ACE 5500 CE apparatus from Beckman Instruments (Fullerton, CA, USA). Bare fused-silica capillaries of 50 μm id were purchased from Composite Metal Services (Worcester, UK). Between runs, silica capillary was washed

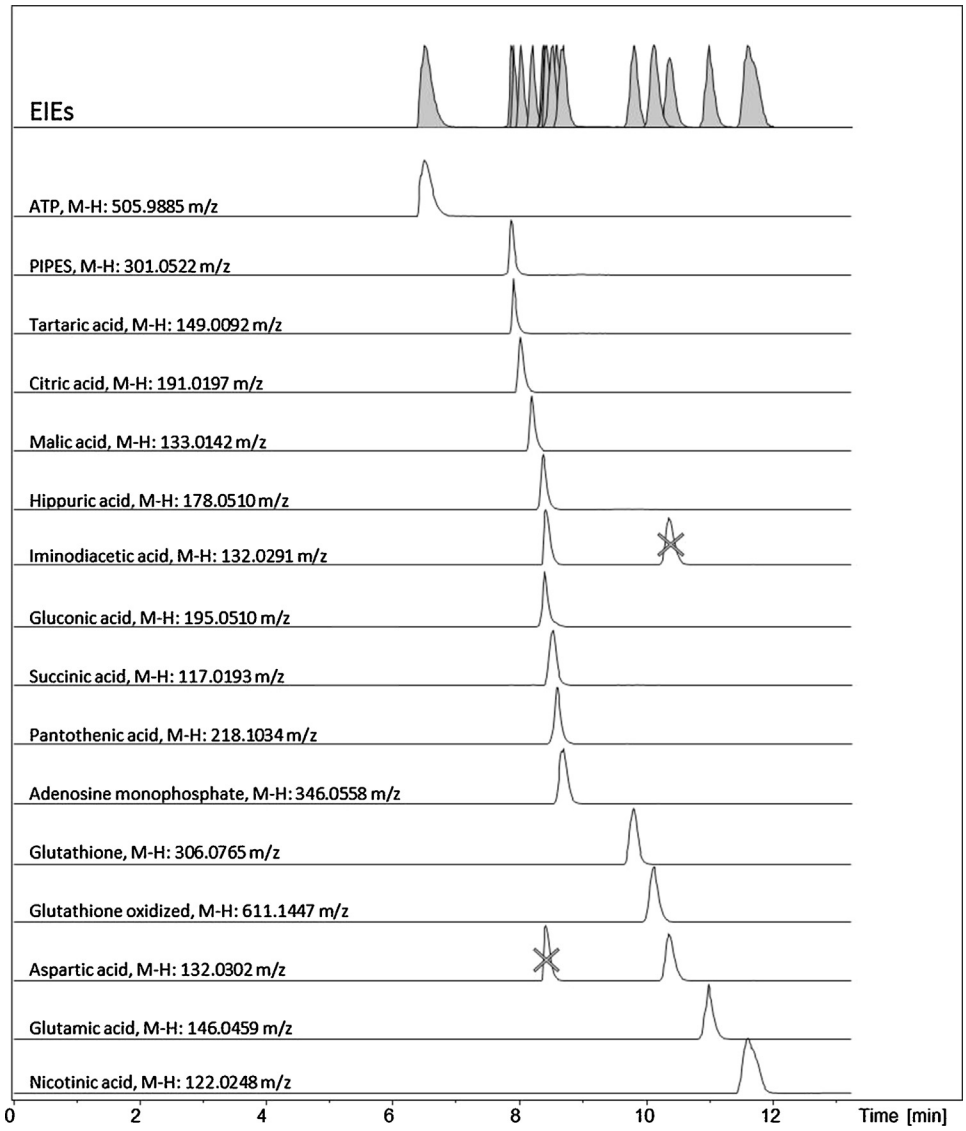

Fig. 3. CE–ESI–TOF MS EIEs of ARM analyzed at reverse CE polarity (−20 kV), PTH-coated capillary and negative ion ESI–MS mode. Other CE–MS conditions as in Fig. 2.

with 0.1 mg/mL PTH for 4 min and separation buffer for 3 min. Injections were made using N_2 pressure at 0.5 psi (34.5 mbar) for 80 s. The electrophoretic separation was achieved using different running voltages (+20 or −20 kV) at a constant temperature of 25 °C with different background electrolytes (BGEs). Acidic BGEs were prepared from 1 M formic acid (pH 1.8). When required, pH was increased to pH 2.0, 2.2, 2.4 and 2.6 with ammonium hydroxide. On the other hand, BGEs with higher pH were prepared as follows: 35 mM ammonium acetate (adjusted to pH 5.0 with acetic acid), 25 mM ammonium formate (adjusted to pH 7.0 with ammonium hydroxide), 40 mM ammonium acetate (adjusted to pH 8.0 with ammonium hydroxide), and 50 mM boric acid (adjusted to pH 10 with ammonium hydroxide).

The instrument was controlled by a PC running the System Gold software from Beckman. The capillaries were coupled on-line to the TOF MS instrument through an orthogonal ESI interface model G1607 A from Agilent Technologies (Palo Alto, CA, USA). Electrical contact at the electrospray needle tip was established via a sheath liquid delivered at a flow rate of 0.24 mL/h by a 74900-00-05 Cole Palmer syringe pump (Vernon Hills, IL, USA). A TOF–MS instrument (micrOTOF) from Bruker Daltonics (Bremen, Germany) was employed. The mass spectrometer operated with the ESI source working in the positive or negative ionization mode. The nebulizer and drying gas conditions were 0.4 bar N_2 and 4 L/min N_2, respectively, maintaining the ESI chamber at 200 °C. The micrOTOF was operated to acquire spectra in the m/z range of 50–650 every 90 ms. External and internal calibration of the TOF MS instrument was performed by introducing a 5 mM sodium formate solution through the separation capillary. Masses for the calibration of the TOF MS instrument were next: 90.9766, 158.9641, 226.9515, 294.9389, 362.9263, 430.9138, 498.9012 and 566.8886 m/z in positive ion mode and 180.973, 248.9594, 316.9479, 384.9353, 452.9227, 520.9102 m/z in negative ion mode. The instrument was controlled by a PC running the micrOTOF control software from Bruker Daltonics.

3. Results and discussion

3.1. Selecting CE–MS conditions for metabolic profiling

The combination of CE–MS with acidic buffers and ESI–MS in positive ionization mode has been demonstrated to exhibit excellent performance for the analysis of cationic metabolites [6,14]. One of the benefits of using CE–MS for cationic metabolites (e.g., amino/derived compounds) is the possibility to carry out a direct and sensitive analysis of these compounds without any

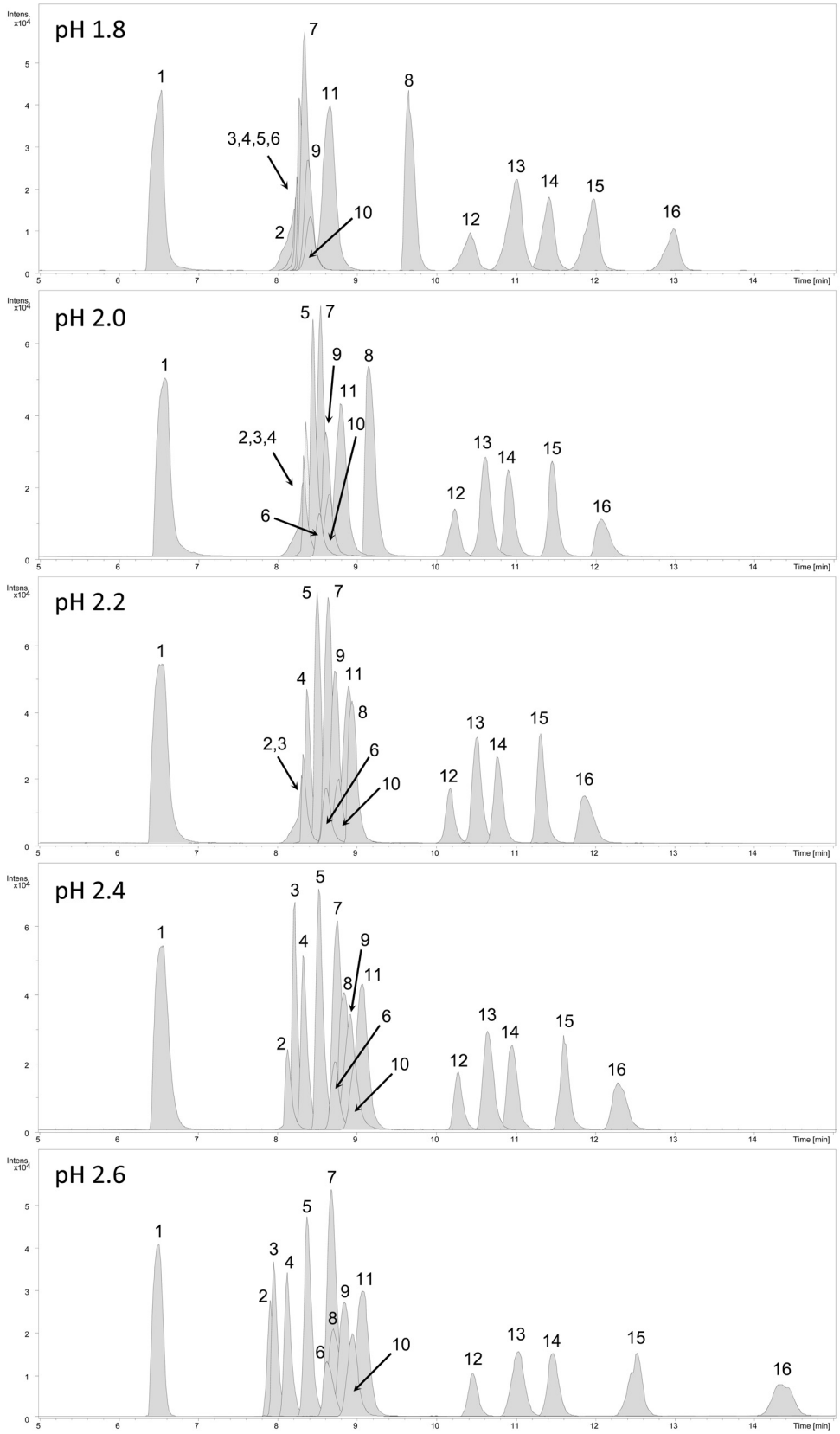

Fig. 4. CE–ESI–TOF MS EIEs of ARM separated using 1 M formic acid (pH 1.8, 2.0, 2.2, 2.4, 2.6) as BGEs at reverse CE polarity (−20 kV) in PTH-coated capillary and negative ion ESI–MS mode. Other analytical conditions as in Fig. 3. Peaks: (1) ATP, (2) PIPES, (3) tartaric acid, (4) citric acid, (5) malic acid, (6) hippuric acid, (7) gluconic acid, (8) iminodiacetic acid, (9) succinic acid, (10) pantothenic acid, (11) adenosine monophosphate, (12) glutathione, (13) glutathione oxidized, (14) aspartic acid, (15) glutamic acid and (16) nicotinic acid.

derivatization step. As can be seen in Fig. S1 (supplementary material), good selectivity in less than 12 min was obtained for the cationic metabolite-rich mixture (CRM) under these conditions. To evaluate the capability of this method for anions analysis, typical CE–MS separation conditions for cationic metabolites were used and a test mix of 16 anionic metabolite-rich mixture (ARM) was injected. The obtained electropherograms are shown in Fig. 1. 10 out of 16 metabolites from ARM were observed. Although anionic compounds tend to migrate toward the inlet capillary tip (anode), it was possible to detect them as they were pushed toward the capillary outlet (cathode) by the small EOF generated together with some additional low siphoning typically taking place in the ESI interface [15]. As expected, compounds having only acidic groups in their structure (namely, succinic acid, gluconic acid, malic acid, citric acid and tartaric acid) were not detected by using MS in positive ion mode. Although the method was initially optimized for the separation of cationic metabolites, it allowed the detection of acidic metabolites by changing to negative ESI MS polarity (Fig. 2). Under these conditions ARM analysis was achieved in ca. 35 min. As can be observed, 15 out of 16 metabolites from ARM were detected. It is important to emphasize that with this method it is impossible to detect all anionic metabolites because faster migrating anionic metabolites with electrophoretic mobilities opposite and larger than the EOF do not reach the MS. Indeed, under these conditions, ATP was not detected in less than 40 min. It is expected that in a real sample with hundreds of anionic metabolites, this unfavorable situation is amplified. To reduce excessively long analysis times, pressure from the capillary inlet can be applied, but this can cause peak broadening because of the generated parabolic profile from the hydrodynamic flow. On the other hand, it is already well-known that analysis of anionic metabolites by CE–MS reversing the CE polarity (negative mode), where the inlet of the separation capillary is at the cathode and the outlet at the anode, creates electrical current instability at the capillary exit due to the EOF movement toward the cathode. With the aim to detect as many anionic metabolites as possible and to reduce overall analysis time of anionic metabolites, reversing the direction of the EOF from cathode to anode with a cationic polymer coating was next investigated.

3.2. PTH-coated capillary for anionic metabolite profiling

The compatibility of poly-(TEDETAMA-co-HPMA) with different nominal molar percentages of TEDETAMA with CE–UV and CE–MS for the analysis of basic proteins has been previously studied by our group [16], and it exhibited durability and good chemical stability without ESI source contamination. In a previous work [16], 0.1 mg/mL polymer solution was left to stand overnight inside the capillary and reproducible anodic EOF was achieved. However, in order to reduce to overall coating procedure, this step was slightly modified in the present work. Thus, flushing the capillary with 1 mg/mL of PTH solution for 20 min gave identical results in terms of reproducibility and stability of the coating. According to the molecular structure of the PTH copolymer (Fig. S2), the EOF obtained for the bare fused-silica showed a dependence on the BGE pH (Fig. S3). The PTH-coated capillary showed an anodal EOF at low and intermediate pH values, while a nearly zero EOF was observed at running buffers above 9. At pH values higher than 9, the global electrical charge onto the capillary wall is zero, bringing no EOF. Consequently, when using CE–MS in reversed polarity (the inlet of the capillary is at the cathode and the outlet at the anode), at low and intermediate pH values an EOF toward the MS detector is generated. Taking advantage of the stronger anodal EOF at low and intermediate pH values, anionic metabolites test mix (ARM) was analyzed by using a BGE with low pH, reversed polarity and with the ESI source in the negative ion mode (Fig. 3). When compared to previous analysis conditions using a bare silica capillary (Fig. 2), the

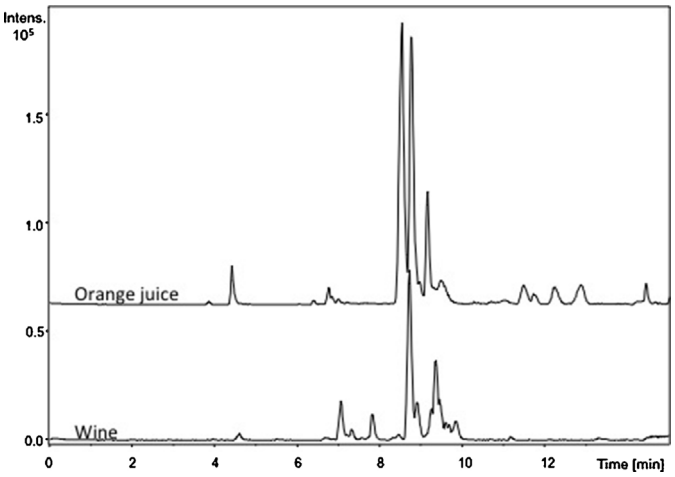

Fig. 5. CE–ESI–TOF MS base peak electropherogram (BPE) of metabolites in orange juice and red wine. CE–ESI–TOF MS conditions as in Fig. 4.

use of PTH-coated capillary showed significant advantages in terms of time of analysis. ATP, which was not detected using an uncoated capillary (Fig. 2) was observed to be the fastest eluted metabolite using the cationic PTH coating (Fig. 3). It was also observed that no peak broadening was produced due to interactions of anionic compounds with the positively charged capillary wall.

Observing the EOF plot at different pHs when a PTH-coated capillary is employed (Fig. S3), optimization of the BGE pH appears particularly interesting for anionic metabolite analysis by CE–MS. Hence, the effect of the pH was studied over the range 1.8–10 (namely, 1.8, 5, 7, 8, and 10 pH values). Results showed that increasing pH did not improve metabolite separation (data not shown). However, when pH was studied in a narrower range (from pH 1.8 to 2.6) slight improvement in resolution of ARM was observed; even following small pH changes, mobilities of anionic compounds varied significantly. This result can easily be explained based on the proximity of pK_a values of the acidic groups to the pH of the BGE. In Fig. 4, it can be observed that a slightly better separation was obtained when the separation was carried out with 1 M formic acid at pH 2.4. Also, the overall peak intensities of all metabolites appear to be similar in the pH range studied. The composition of the BGE was also modified adding an organic modifier in order to investigate its effect on CE selectivity (through variations on BGE, dielectric constant, and viscosity). The addition of methanol to BGE (up to 20%) did not improve the separation of metabolites, and thus, it was discarded for further experiments.

The reproducibility was evaluated on the basis of the relative standard deviation (%RSD) of the migration time and peak area, obtained from three replicate analyses and for five representative compounds from ARM for the same day and three different days (Table S1). The intra-assay and inter-assay precision for peak migration times was <0.1% and 0.6%, respectively. The intra-assay and inter-assay precision for peak area was <0.5% and 7.3%, respectively. The theoretical LOD calculated by a 3-fold-signal-to-noise ratio for these metabolites ranged from 0.1 to 16.4 ppm and the LOQ was in the range of 0.3 to 54.6 ppm. On the other hand, plate numbers were up to 92,000 per meter. These results show that by using this coating a fast anionic metabolite analysis with good reproducibility can be obtained.

3.3. Anionic metabolite profiling of food samples by CE–MS

Food matrices are very complex matrices consisting of hundreds/thousands of compounds (nutrients and non-nutrients) in a wide dynamic range of concentrations. The application of metabolite profiling offers enormous opportunities to obtain precious

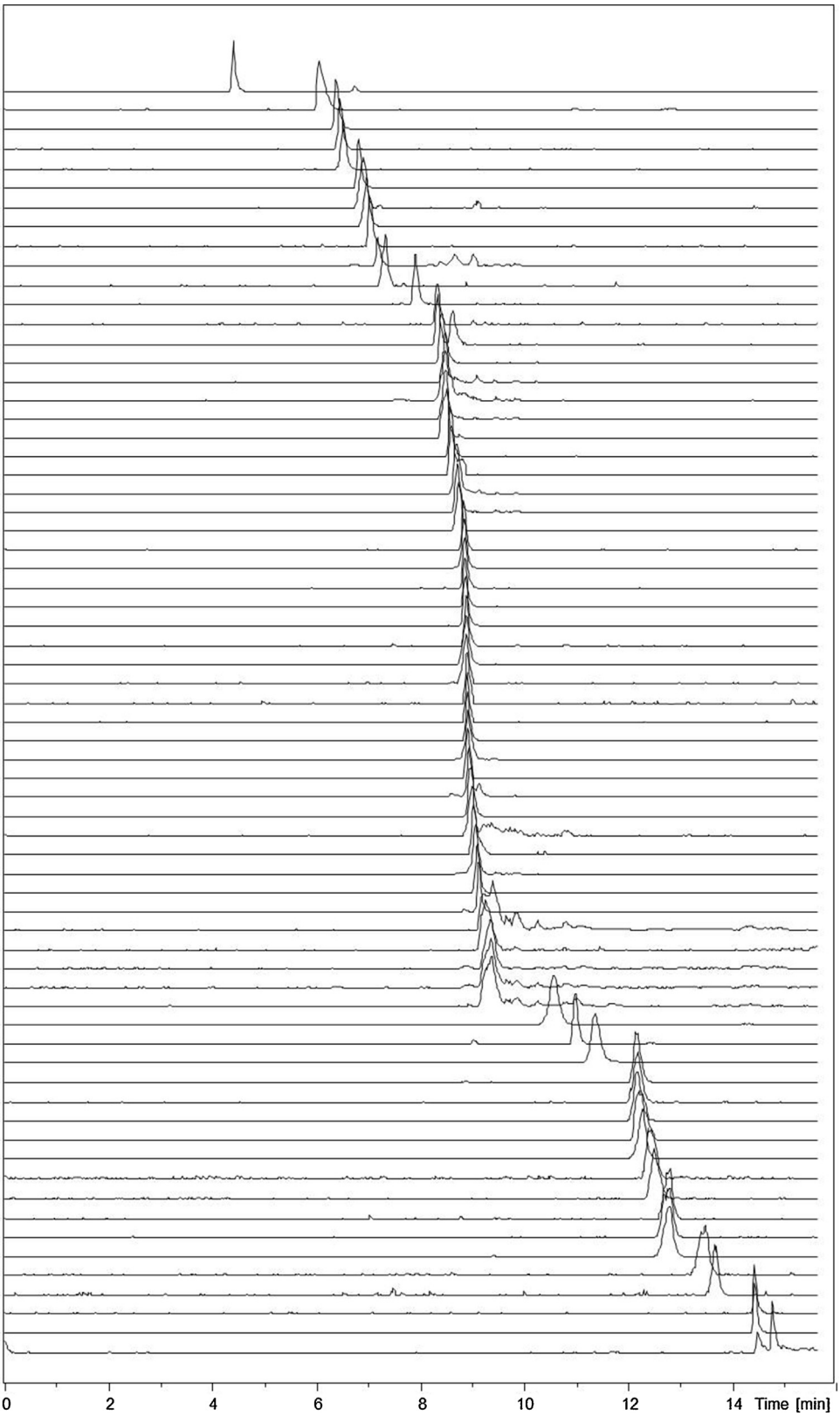

Fig. 6. CE–ESI–TOF MS EIEs of metabolites detected in orange juice using 1 M formic acid (pH 2.4) as BGE at reverse CE polarity (−20 kV) in coated capillary and negative ion ESI–MS mode. Other analytical conditions as in Fig. 5.

detailed information that can be directly correlated to food quality, safety, and other features related to food processing, storage, authenticity assessment, etc. [17,18]. The majority of applications in the field of food metabolomics over the past years have used LC–MS and GC–MS, and in a less extent, CE–MS approaches [19,20]. However CE–MS has demonstrated to be a very useful and complementary analytical tool in food metabolomics [2,19]. In this work, we have selected as case studies the untargeted analysis of orange

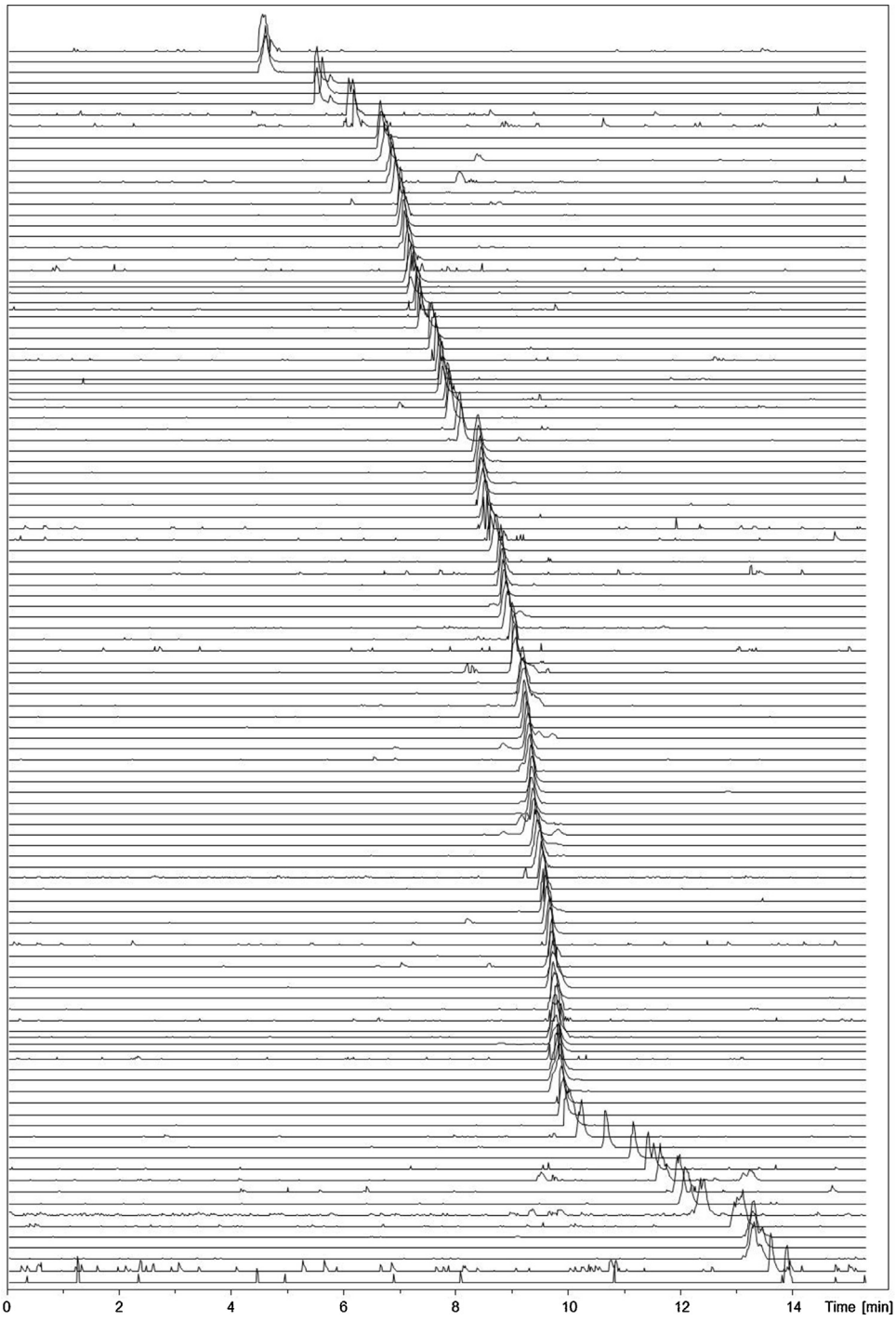

Fig. 7. CE–ESI–TOF MS EIEs of metabolites detected in wine. Same CE–MS conditions as in Fig. 5.

juice and wine metabolites to demonstrate the capabilities of this method for metabolite profiling. Samples were just filtered prior to their CE–MS analysis.

CE–MS anionic metabolite profile from orange juice is represented in Fig. 5. After peak detection, filtering and peak grouping, 87 metabolites were detected in orange juice. The extracted ion electropherograms (EIEs) of detected metabolites are represented in Fig. 6. The elemental formula estimation was carried out with the use of accurate single MS mass of parent ion and isotopic profile. Online chemical databases were queried by molecular formula or accurate mass to search for metabolites: the Human Metabolome Database (HMDB, www.hmdb.ca), Food Database (FooDB, www.foodb.ca), Metlin (http://metlin.scripps.edu/). Of the various compound hits obtained, those metabolites whose presence was probable in fruit juices were chosen. Data corresponding to the detected compounds are summarized in Table S2. Sugars, amino acids, organic acids, and other metabolites were found as can be seen in this table. Some identifications were corroborated by co-injection with standards. Main observed metabolite signals under these analytical conditions were organic acids. Organic acids in citrus are important compounds for fruit flavor, nutritional quality and freshness, and they are affected by factors including fruit size, juice content, organic acid synthesis, transport, storage, among others. To date, most published investigations on orange juice have

been focused on the analysis by LC–MS of most abundant organic acids in orange juices [21,22]. With the present CE–MS method it was observed that predominant organic acids were citric, malic and ascorbic acids (see Fig. S4). However, other organic acids, such as, phosphoglyceric acid, oxoglutaric acid, aconitic acid, tartaric acid, pyruvic acid, citramalic acid, lactic acid, ascorbalamic acid, 2-methylcitric acid, hydroxypyruvic acid, ribonic acid, gluconic acid, dehydroascorbic acid, succinic acid, pantothenic acid, methylglutaconic acid, glutaric acid and glucoheptenoic acid, were detected. Sugars were also important signals in the analyzed orange juice. Among them, sucrose, glucose and fructose were observed to be the most abundant signals. More than 20 amino acids were also observed. Major signals were from aspartic acid, glutamic acid, proline, asparagine and arginine. The amino acid composition of fresh orange juice changes by technological treatments, and thus, the study of the amino acid profile of the processed juice is a key element to confirm its nutritional value and freshness. Moreover, amino acids are precursors of aromatic substances, and consequently, they are important factors in flavor and taste.

CE–MS anionic metabolite profile from red wine is also represented in Fig. 5. After data processing, 142 metabolites were detected in wine. CE–MS EIEs of detected metabolites are represented in Fig. 7. As occurred with orange juice, an important group of organic acids were observed. The content of organic acids gives also a characteristic taste to wines [23]. They have a major role on the evolution of the acidity during the different steps of the wine-making process. Predominant signal was from tartaric acid, one of the major components of wines and the main acid responsible for wine acidity. An important group of organic acids was tentatively identified. Among them, citric acid, malic acid, galactaric acid, succinic acid, gluconic acid, citraconic acid, glutaconic acid, citramalic acid, and 2-hydroxyglutaric acid, among others (see Table S3 for more details), were detected. When compared to HILIC–MS [24] and C18/LC–MS [25], complementary information can be obtained with the presented CE–MS. Phenolic compounds are also very abundant metabolites in foods of plant origin [26]. They are of great importance in wine since they are also closely related to its quality and organoleptic properties [27]. Moreover, interest in phenolic compounds has been increasing due to compelling evidence of their promoting health effects through the prevention of several diseases [28]. Among phenolic acids, hydroxybenzoic acids, such as gallic acid, galacturonic acid, syringic acid, gentisic acid and *p*-hydroxybenzoic acid; and the hydroxycinnamic acids, *p*-coumaric acid, caffeic acid, caftaric acid, coutaric acid and fertaric acid were detected. In wine, these compounds are also precursors of volatile phenols that greatly influence its aroma. Proanthocyanidins catechin and gallocatechin were also detected under the current analytical conditions. Proanthocyanidin B-type dimers, which contain monomeric units of catechin and/or epicatechin, were detected too. Weaker signals from pigments, such as myricetin, quercetin, malvidin-3-glucoside, quercetin-3-glucoside, quercetin 3-O-glucuronide were also observed in good agreement with previous results obtained by LC–MS [29].

4. Conclusions

A new CE–MS method that employs a polymeric dynamic coating material has been presented in this work for simple, selective, and reproducible anionic metabolites profiling. The coating is generated in an automatic and straightforward procedure by simply flushing the capillary with PTH solution between runs, without its addition into the BGE. This polymeric coating has been applied for the first time for anionic metabolite profiling. The reproducibility of the method enables a reliable comparison of metabolite profiles and facilitates peak alignment when a large number of samples have to be analyzed. The feasibility of the CE–MS method was demonstrated by the analysis of anionic metabolites in orange juice and wine providing a more complete coverage of the complex composition of these products, which moreover is complementary to the information provided by other analytical techniques.

Acknowledgements

This work was supported by an AGL2014-53609-P project (Ministerio de Educación y Ciencia, Spain). T.A. thanks the CAPES Foundation, Ministry of Education of Brazil for her pre-doctoral Scholarship-Proc. N 1532/13-8.

Appendix A. Supplementary data

Supplementary data associated with this article can be found, in the online version, at http://dx.doi.org/10.1016/j.chroma.2015.08.001

References

[1] K. Spagou, H. Tsoukali, N. Raikos, H. Gika, I.D. Wilson, G. Theodoridis, Hydrophilic interaction chromatography coupled to MS for metabonomic/metabolomic studies, J. Sep. Sci. 33 (2010) 716–727.
[2] R. Ramautar, G.W. Somsen, G.J. de Jong, CE–MS for metabolomics: developments and applications in the period 2012–2014, Electrophoresis 36 (2015) 212–224.
[3] V.R. Robledo, W.F. Smyth, Review of the CE–MS platform as a powerful alternative to conventional couplings in bio-omics and target-based applications, Electrophoresis 35 (2014) 2292–2308.
[4] M.G.M. Kok, G.W. Somsen, G.J. de Jong, Comparison of capillary electrophoresis-mass spectrometry and hydrophilic interaction chromatography–mass spectrometry for anionic metabolic profiling of urine, Talanta 132 (2015) 1–7.
[5] C. Ibáñez, A. Valdés, V. García-Cañas, C. Simó, M. Celebier, L. Rocamora-Reverte, A. Gómez-Martínez, M. Herrero, M. Castro-Puyana, A. Segura-Carretero, E. Ibáñez, J.A. Ferragut, A. Cifuentes, Global Foodomics strategy to investigate the health benefits of dietary constituents, J. Chromatogr. A 1248 (2012) 139–153.
[6] C. Ibáñez, C. Simó, V. García-Cañas, Á. Gómez-Martínez, J.A. Ferragut, A. Cifuentes, CE/LC–MS multiplatform for broad metabolomic analysis of dietary polyphenols effect on colon cancer cells proliferation, Electrophoresis 33 (2012) 2328–2336.
[7] R. Ramautar, G.W. Somsen, G.J. de Jong, CE–MS for metabolomics: developments and applications in the period 2010–2012, Electrophoresis 34 (2013) 86–98.
[8] Y. Tanaka, T. Higashi, R. Rakwal, S.I. Wakida, H. Iwahashi, Development of a capillary electrophoresis mass spectrometry method using polymer capillaries for metabolomic analysis of yeast, Electrophoresis 29 (2008) 2016–2023.
[9] R. Ramautar, J.M. Busnel, A.M. Deelder, O.A. Mayboroda, Enhancing the coverage of the urinary metabolome by sheathless capillary electrophoresis–mass spectrometry, Anal. Chem. 84 (2012) 885–892.
[10] T. Soga, T. Ishikawa, S. Igarashi, K. Sugawara, Y. Kakazu, M. Tomita, Analysis of nucleotides by pressure-assisted capillary electrophoresis–mass spectrometry using silanol mask technique, J. Chromatogr. A 1159 (2007) 125–133.
[11] T. Soga, Y. Ueno, H. Naraoka, K. Matsuda, M. Tomita, T. Nishioka, Pressure-assisted capillary electrophoresis electrospray ionization mass spectrometry for analysis of multivalent anions, Anal. Chem. 74 (2002) 6224–6229.
[12] T.J. Tsuda, Modification of electroosmotic flow with cetyltrimethylammonium bromide in capillary zone electrophoresis, J. High Resolut. Chromatogr. 10 (1987) 622–624.
[13] J.A. Redondo, R. Navarro, E. Martínez-Campos, H. Reinecke, C. Elvira, J.L. López-Lacomba, A. Gallardo, Effect on in vitro cell response of the statistical insertion of N-(2-hydroxypropyl) methacrylamide on linear pro-dendronic polyamine's gene carriers, Eur. J. Pharm. Biopharm. 93 (2015) 303–310.
[14] C. Simó, C. Ibáñez, A. Gomez-Martinez, J.A. Ferragut, A. Cifuentes, Is metabolomics reachable? Different purification strategies of human colon cancer cells provide different CE–MS metabolite profiles, Electrophoresis 32 (2011) 1765–1777.
[15] C. Simó, A. Rizzi, C. Barbas, A. Cifuentes, Chiral capillary electrophoresis–mass spectrometry of amino acids in foods, Electrophoresis 26 (2005) 1432–1441.
[16] T. Acunha, C. Ibáñez, M.I. Reguera, M. Sarò, R. Navarro, J.A. Redondo, H. Reinecke, A. Gallardo, C. Simó, A. Cifuentes, Potential of pro-dendronic polyamines with modulated segmental charge density as novel coating for fast and efficient analysis of peptides and basic proteins by capillary electrophoresis and capillary electrophoresis–mass spectrometry, Electrophoresis (2015), http://dx.doi.org/10.1002/elps.201400576
[17] J.M. Cevallos-Cevallos, J.I. Reyes-De-Corcuera, E. Etxeberria, M.D. Danyluk, G.E. Rodrick, Metabolomic analysis in food science: a review, Trends Food Sci. Tech. 20 (2009) 557–566.

[18] C. Ibáñez, V. García-Cañas, A. Valdés, C. Simó, Novel MS-based approaches and applications in food metabolomics, TrAC 52 (2013) 100–111.
[19] V. García-Cañas, C. Simó, M. Castro-Puyana, A. Cifuentes, Recent advances in the application of capillary electromigration methods for food analysis and Foodomics, Electrophoresis 35 (2014) 147–169.
[20] M. Castro-Puyana, V. García-Cañas, C. Simó, A. Cifuentes, Recent advances in the application of capillary electromigration methods for food analysis and Foodomics, Electrophoresis 33 (2012) 147–167.
[21] G. Tyagi, D.K. Jangir, P. Singh, R. Mehrotra, R. Ganesan, E.S.R. Gopal, Rapid determination of main constituents of packed juices by reverse phase-high performance liquid chromatography: an insight in to commercial fruit drinks, J. Food Sci. Technol. 51 (2014) 476–484.
[22] S. Ehling, S. Cole, Analysis of organic acids in fruit juices by liquid chromatography–mass spectrometry: an enhanced tool for authenticity testing, J. Agric. Food Chem. 59 (2011) 2229–2234.
[23] J.C. Hufnage, T. Hofmann, Quantitative reconstruction of the nonvolatile sensometabolome of a red wine, J. Agric. Food Chem. 56 (2008) 9190–9199.
[24] M. Arbulu, M.C. Sampedro, A. Gómez-Caballero, M.A. Goicolea, R.J. Barrio, Untargeted metabolomic analysis using liquid chromatography quadrupole time-of-flight mass spectrometry for non-volatile profiling of wines, Anal. Chim. Acta 858 (2015) 32–41.
[25] K.L. Ross, T.T. Tu, S. Smith, J.J. Dalluge, Profiling of organic acids during fermentation by ultraperformance liquid chromatography–tandem mass spectrometry, Anal. Chem. 79 (2007) 4840–4844.
[26] P. Mattila, J. Hellström, R. Törrönen, Phenolic acids in berries, fruits, and beverages, J. Agric. Food Chem. 54 (2006) 7193–7199.
[27] J.A. Kennedy, C. Saucier, Y. Glories, Grape and wine phenolics: history and perspective, Am. J. Enol. Vitic. 57 (2006) 239–248.
[28] A. Crozier, I.B. Jaganath, M.N. Clifford, Dietary phenolics: chemistry, bioavailability and effects on health, Nat. Prod. Rep. 26 (2009) 1001–1043.
[29] A. Bimpilas, D. Tsimogiannis, K. Balta-Brouma, T. Lymperopoulou, V. Oreopoulou, Evolution of phenolic compounds and metal content of wine during alcoholic fermentation and storage, Food Chem. 178 (2015) 164–171.

SUPPLEMENTARY MATERIAL

ANIONIC METABOLITE PROFILING BY CAPILLARY ELECTROPHORESIS-MASS SPECTROMETRY USING A NOVEL NONCOVALENT POLYMERIC COATING. ORANGE JUICE AND WINE AS CASE STUDIES

Tanize Acunha[1,2], Carolina Simó[1,*], Clara Ibáñez[1], Alberto Gallardo[3], Alejandro Cifuentes[1]

[1]Laboratory of Foodomics, CIAL, CSIC, Nicolas Cabrera 9, 28049 Madrid, Spain.
[2]CAPES Foundation, Ministry of Education of Brazil, 70040-020 Brasília, DF, Brazil.
[3]Instituto de Ciencia y Tecnología de Polímeros, ICTP-CSIC, Juan de la Cierva 3, 28006 Madrid

Figure S1. CE-ESI-TOF MS EIEs of a cationic test mix (CTM) separated using 1 M formic acid (pH 1.8) as BGE at normal CE polarity (+20 kV) in a bare silica capillary and positive ion ESI-MS mode. Other analytical conditions are described in *Section 2*.

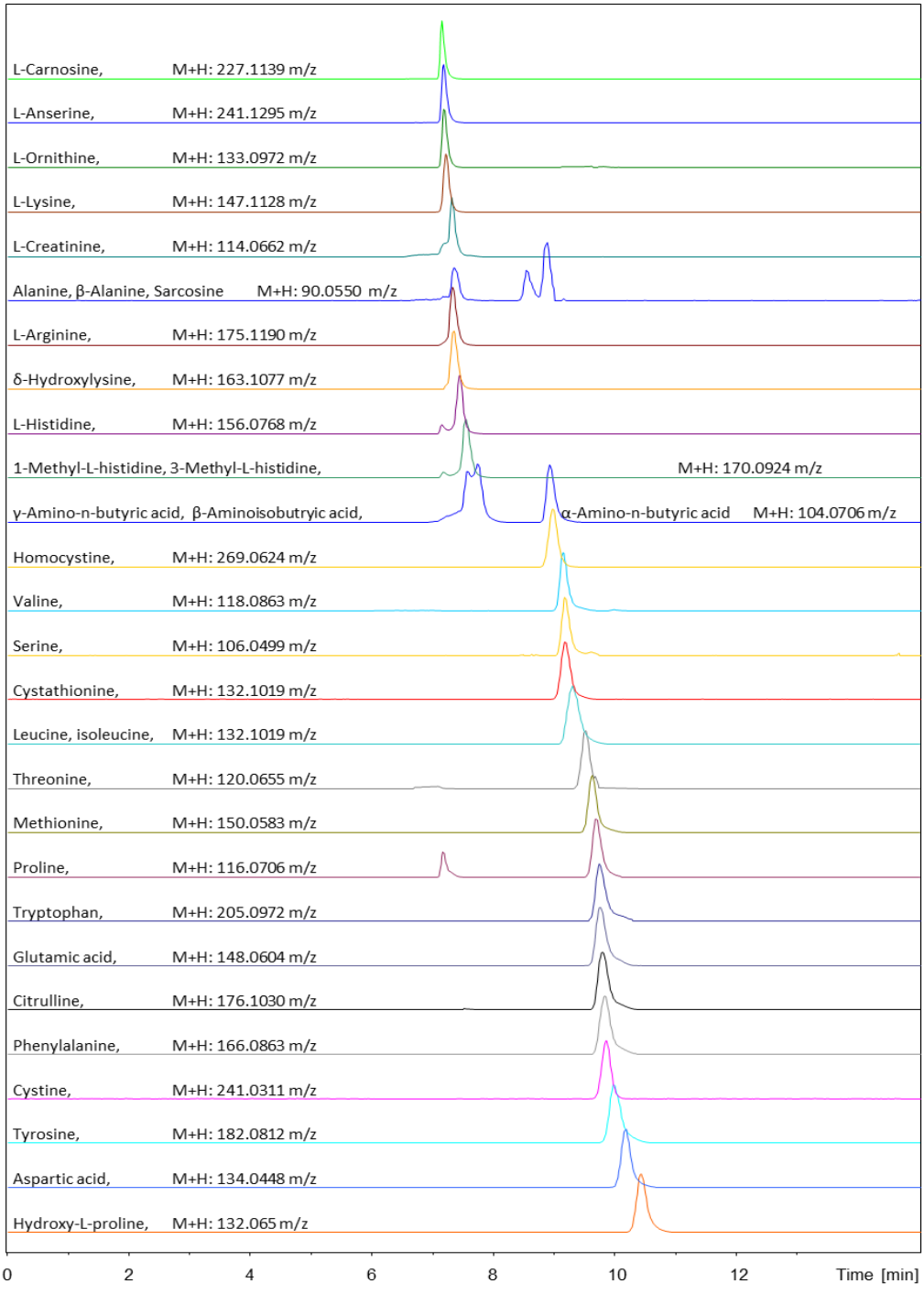

Figure S2. Generic structure of the polymeric family studied in this work (TEDETAMA has been represented in its aqueous cationic form).

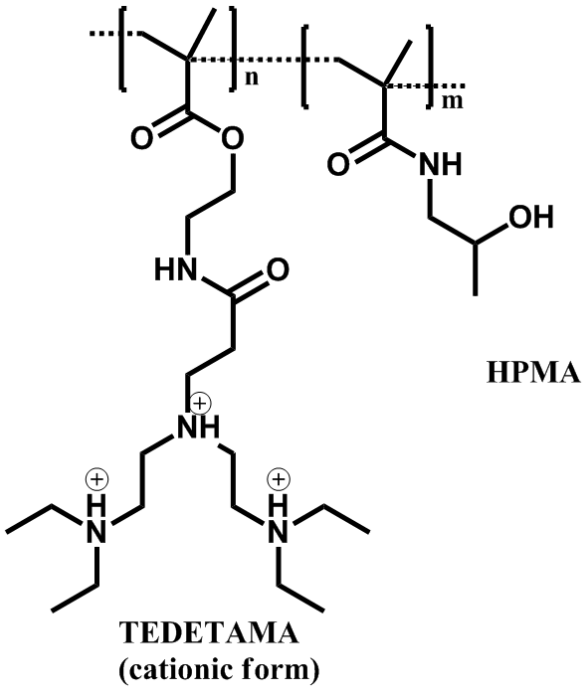

Figure S3. Electroosmotic mobility as function of pH using a bare silica capillary and a capillary coated with Poly (TEDETAMA-co-HPMA) 50:50. BGEs conditions: 1 M formic acid (adjusted to pH 1.9 with ammonium hydroxide), 100 mM acetic acid (adjusted to pH 3.9 with ammonium hydroxide), 35 mM ammonium acetate (adjusted to pH 4.8 with acetic acid), 25 mM ammonium formate (adjusted to pH 7.1 with ammonium hydroxide), 40 mM ammonium acetate (adjusted to pH 8.1 with ammonium hydroxide), and 50 mM boric acid (adjusted to pH 10 with ammonium hydroxide). CE-UV conditions: Silica capillaries of 50 µm ID, 30/37 cm of detection/total length, running voltages (+20, -20 kV), and detection wavelength of 254 nm. Figure redrawn from Acunha *et al*. [16].

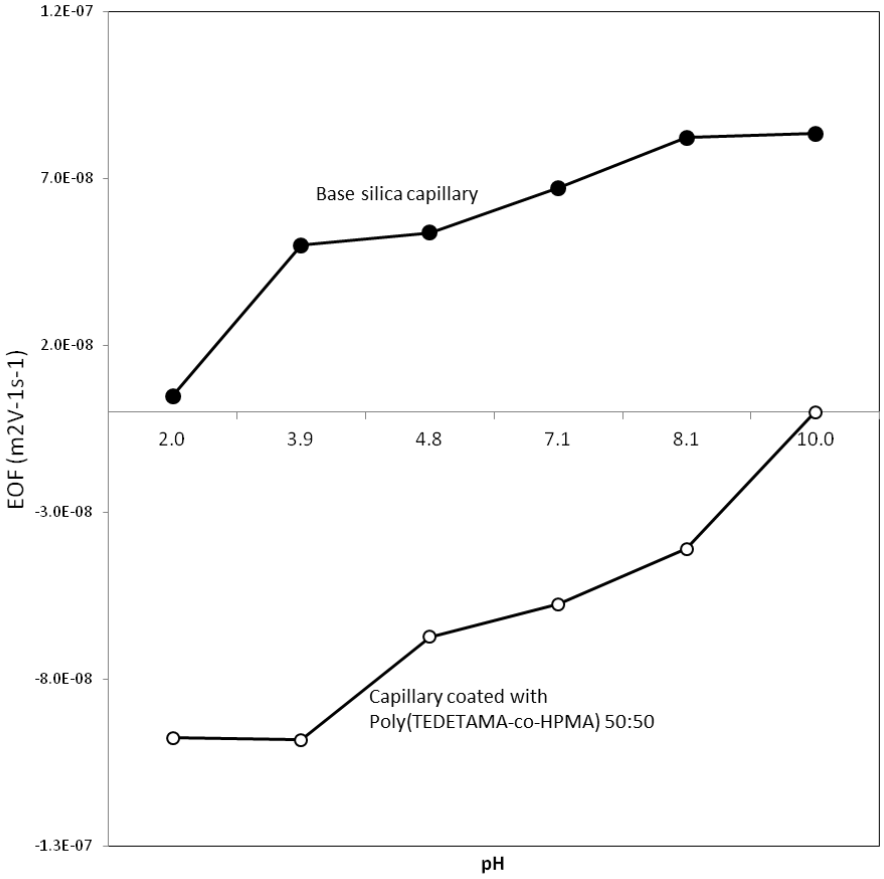

Figure S4. CE-ESI-TOF MS extracted ion electropherograms (EIEs) of organic acids identified in orange juice. CE-MS conditions as in Fig. 5.

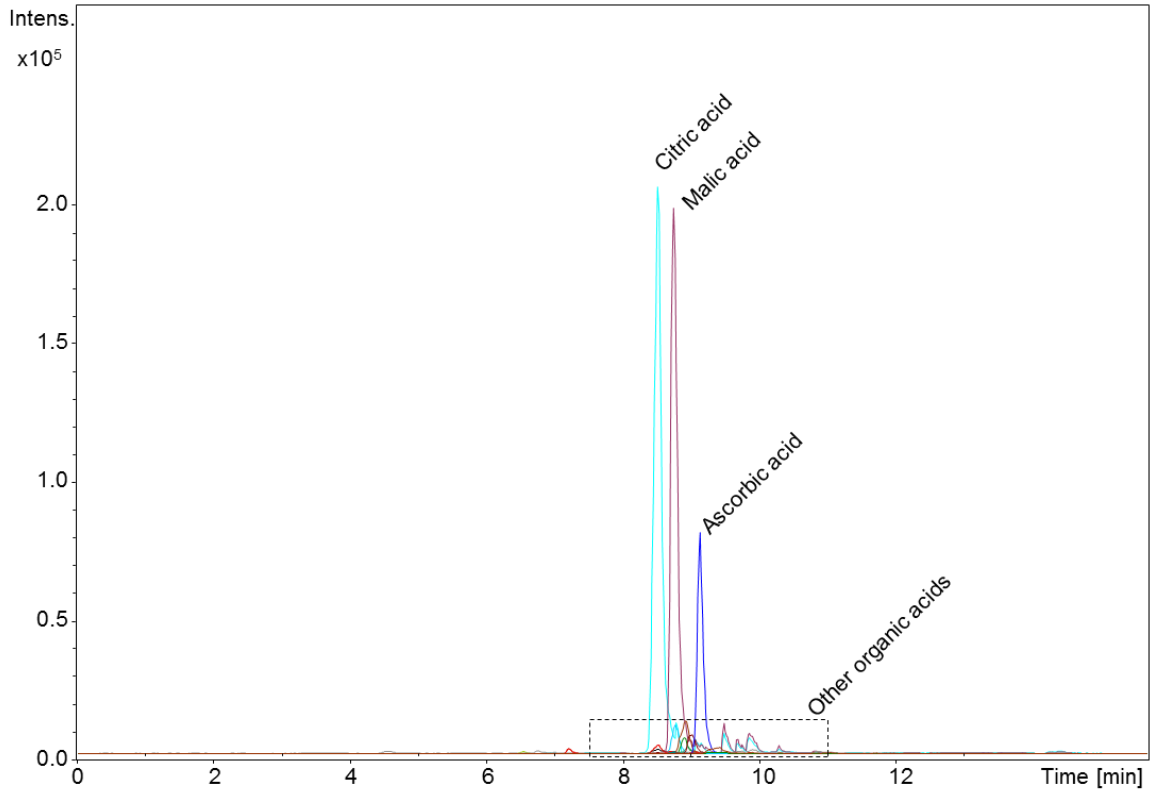

Table S1. % RSD values of the migration time and peak area intra- and inter-day, limit of detection (LOD) and limit of quantification (LOQ) of five selected compounds of the anionic metabolite-rich mixture.

	Pipes	**Citric acid**	**Gluconic acid**	**Adenosine monophosphate**	**Iminodiacetic acid**
%RSD Peak area Intra-day (n=3)	0.5	2.0	2.0	1.3	2.0
%RSD Peak area Inter-day (n=9)	5.3	7.3	6.5	4.7	4.4
%RSD Migration time intra-day (n=3)	0.1	0.1	0.1	0.1	0.1
%RSD Migration time inter-day (n=9)	0.4	0.5	0.6	0.6	0.6
LOD (ppm)	16.4	0.2	0.1	0.3	1.7
LOQ (ppm)	54.6	0.6	0.3	1.0	5.8

Table S2. Tentative identification of the metabolites found in the orange juice sample.

Metabolite ID	m/z	Migration time	Ion	Tentative Formula	Error (ppm)	Tentative Identification	Class of Metabolites	Other possibilities
1	**96.9594**	4.43	$[M-H]^-$	N/A		N/A		
2	**338.9894**	6.06	$[M-H]^-$	N/A		N/A		
3	**565.0485**	6.40	$[M-H]^-$	C15H24N2O17P2	1	UDP-glucose	Nucleotides	UDP-D-galactose; UDP-alpha-D-galacto-1,4-furanose
4	**606.0745**	6.47	$[M-H]^-$	C17H27N3O17P2	1	UDP-N-acetyl-D-galactosamine	Nucleotides	UDP-N-acetyl-D-mannosamine, Uridine diphosphate-N-acetylglucosamine
5	**184.9855**	6.53	$[M-H]^-$	C3H7O7P	0	2-Phospho-glyceric acid	Organic acids	2-Phospho-D-glyceric acid; (2R)-2-Hydroxy-3-(phosphonatooxy)propanoate
6	**317.0548**	6.83	$[M-H]^-$	C18H10N2O4	6	Melanin	Phenolic compounds	Prekinamycin
7	**145.0157**	6.93	$[M-H]^-$	C5H6O5	10	Oxoglutaric acid	Organic acids	Methyloxaloacetate; Oxaloacetate 4-methyl ester; Dehydro-D-arabinono-1,4-lactone; 5-Hydroxy-2,4-dioxopentanoate
8	**259.0215**	6.99	$[M-H]^-$	C6H13O9P	2	Glucose phosphate	Carbohydrates	Fructose 1-phosphate; D-myo-Inositol-1-phosphate; Galactose 1-phosphate; Mannose 1-phosphate; etc.
9	**333.0596**	7.06	$[M-H]^-$	C9H19O11P	1	1-(sn-Glycero-3-phospho)-1D-myo-inositol	Organic compounds	2-(beta-D-Glucosyl)-sn-glycerol 3-phosphate; alpha-D-Galactosyl-(1,1')-sn-glycerol 3-phosphate; 2-(alpha-D-Galactosyl)-sn-glycerol 3-phosphate
10	**173.0097**	7.21	$[M-H]^-$	C6H6O6	3	Aconitic acid	Organic acids	Dehydroascorbic acid
11	**421.0749**	7.34	$[M-H]^-$	C12H23O14P	0	N/A		
12	**203.0189**	7.94	$[M-H]^-$	C7H8O7	4	N/A		
13	**149.0099**	8.30	$[M-H]^-$	C4H6O6	4	Tartaric acid [a]	Organic acids	
14	**237.0607**	8.36	$[M-H]^-$	C8H14O8	3	N/A		
15	**313.0566**	8.36	$[M-H]^-$	C13H14O9	0	N/A		
16	**649.2505**	8.45	$[M-H]^-$	C32H42O14	0	Ichangin 4-glucoside	Organic compounds	Glucosyl-limonin
17	**87.0082**	8.50	$[M-H]^-$	C3H4O3	6	Pyruvic acid	Organic acids	Glucosereductone; 3-Hydroxypropenoate; Malonic semialdehyde
18	**147.0309**	8.51	$[M-H]^-$	C5H8O5	6	Citramalic acid	Organic acids	threo-3-Methylmalate; Arabinono-1,4-lactone; 2-Hydroxyglutarate; 3-Hydroxyglutaric acid; 2-Methylmalate; etc.
19	**191.0193**	8.52	$[M-H]^-$	C6H8O7	2	Citric acid [a]	Organic acids	
20	**627.9858**	8.54	$[M-H]^-$	N/A		N/A		
21	**651.2645**	8.62	$[M-H]^-$	C32H44O14	2	Dicrocin	Organic compounds	Crocin 3; beta-D-Gentiobiosyl crocetin
22	**128.0361**	8.64	$[M-H]^-$	C5H7NO3	6	Pyrroline hydroxycarboxylic acid	Organic acids	N-Acryloylglycine; (R)-(+)-2-Pyrrolidone-5-carboxylic acid; 4-Oxoproline; 1-Pyrroline-4-hydroxy-2-carboxylate; L-1-Pyrroline-3-hydroxy-5-carboxylate; Pyroglutamic acid

23	**385.0777**	8.64	$[M-H]^-$	C16H18O11	0	O-Feruloylgalactarate	Carbohydrates	
24	**313.0565**	8.67	$[M-H]^-$	C13H14O9	0	N/A		
25	**353.0727**	8.73	$[M-H]^-$	N/A		N/A		
26	**89.0225**	8.75	$[M-H]^-$	N/A		N/A		
27	**133.0153**	8.75	$[M-H]^-$	C4H6O5	7	Malic acid [a]	Organic acids	
28	**209.0293**	8.77	$[M-H]^-$	C6H10O8	4	Citric acid monohydrate	Organic acids	Galactaric acid; D-Glucarate
29	**447.0981**	8.86	$[M-H]^-$	N/A		N/A		
30	**223.0445**	8.87	$[M-H]^-$	N/A		N/A		
31	**158.0469**	8.89	$[M-H]^-$	C6H9NO4		N/A		
32	**525.1204**	8.89	$[M-H]^-$	N/A		N/A		
33	**262.0557**	8.90	$[M-H]^-$	C9H13NO8	4	Ascorbalamic acid	Amino acids	
34	**142.0514**	8.92	$[M-H]^-$	C6H9NO3	6	Vinylacetylglycine	Amino acids	
35	**205.0345**	8.92	$[M-H]^-$	C7H10O7	4	2-Methylcitrate	Organic acids	Homoisocitrate; (R)-2-Hydroxybutane-1,2,4-tricarboxylate; Methylisocitric acid
36	**399.0928**	8.93	$[M-H]^-$	N/A		N/A		
37	**290.9810**	8.94	$[M-H]^-$	N/A		N/A		
38	**397.0992**	8.94	$[M-H]^-$	N/A		N/A		
39	**383.1198**	8.95	$[M-H]^-$	C14H24O12	0	Acetyl-maltose	Carbohydrates	
40	**103.0040**	8.95	$[M-H]^-$	C3H4O4	3	Hydroxypyruvic acid	Organic acids	Malonic acid; Tartronate semialdehyde
41	**165.0409**	8.95	$[M-H]^-$	C5H10O6	2	Ribonic acid	Organic acids	Apionic acid; S-Propyl 1-propanesulfinothioate; L-Xylonate; D-Xylonate; L-Lyxonate; L-Arabinonic acid
42	**192.0560**	8.95	$[M-H]^-$	N/A		N/A		
43	**295.0684**	8.98	$[M-H]^-$	N/A		N/A		
44	**195.0505**	9.01	$[M-H]^-$	C6H12O7	2	Gluconic acid [a]	Organic acids	
45	**149.0462**	9.03	$[M-H]^-$	C5H10O5	4	Ribose	Carbohydrates	Ribulose; Xylose; Lyxose; Arabinose; etc.
46	**173.0102**	9.06	$[M-H]^-$	C6H6O6	5	Dehydroascorbic acid	Organic acids	Aconitic acid
47	**293.1247**	9.06	$[M-H]^-$	C12H22O8	1	N/A		
48	**515.1268**	9.11	$[M-H]^-$	N/A		N/A		
49	**117.0222**	9.12	$[M-H]^-$	C4H6O4	7	Succinic acid [a]	Organic acids	
50	**175.0248**	9.14	$[M-H]^-$	C6H8O6	0	Ascorbic acid	Organic acids	2-Dehydro-D-glucono-1,5-lactone; Propane-1,2,3-tricarboxylate
51	**517.1406**	9.16	$[M-H]^-$	N/A		N/A		
52	**387.1151**	9.42	$[M-H]^-$	C12H25N2O10P	5	Fructoselysine 6-phosphate	Carbohydrates	
53	**218.1012**	9.26	$[M-H]^-$	C9H17NO5	10	Pantothenic acid [a]	Organic acids	
54	**497.3338**	9.29	$[M-H]^-$	N/A		N/A		

55	**143.0357**	9.37	$[M-H]^-$	C6H8O4	5	Methylglutaconic acid	Organic acids	trans-2-Hexenedioic acid; 3-Hexenedioic acid; Ethyl hydrogen fumarate; Dimethyl fumarate; 3-Hydroxyadipic acid 3,6-lactone; Maleic acid homopolymer
56	**161.0457**	9.39	$[M-H]^-$	C6H10O5	0	N/A		
57	**269.0900**	9.39	$[M-H]^-$	C10H14N4O5	3	Histidinyl-Aspartate	Amino acids	Aspartyl-Histidine
58	**131.0360**	9.40	$[M-H]^-$	C5H8O4	7	Glutaric acid	Organic acids	3-hydroxy-3-methyl-2-oxo-Butyric acid; Methylsuccinic acid; mono-Ethyl malonate; Dimethylmalonic acid; 2-Acetolactic acid; etc.
59	**209.0654**	9.40	$[M-H]^-$	C7H14O7	3	N/A		
60	**225.0603**	9.41	$[M-H]^-$	C7H14O8	3	Glucoheptonic acid	Organic acids	
61	**179.0559**	9.41	$[M-H]^-$	C6H12O6	1	Fructose	Carbohydrates	Glusose; Mannose; Galactose; myo-Inositol; Allose; Sorbose; etc
62	**341.1096**	9.42	$[M-H]^-$	C12H22O11	1	Sucrose	Carbohydrates	Lactose; Isomaltose; Lactulose; Maltulose; 2-alpha-D-Glucosyl-D-glucose; etc.
63	**683.2242**	9.43	$[M-H]^-$	C37H36N2O11	0	Citbismine C	Organic compounds	
64	**306.0759**	10.65	$[M-H]^-$	C10H17N3O6S	2	Glutathione [a]	Amino acids	
65	**204.0871**	11.03	$[M-H]^-$	C8H15NO5	3	N/A		
66	**88.0390**	11.41	$[M-H]^-$	C3H7NO2	15	Alanine	Amino acids	Sarcosine; Nitropropane; Lactamide; Urethane
67	**132.0314**	11.43	$[M-H]^-$	C4H7NO4	10	Aspartic acid [a]	Amino acids	
68	**180.0651**	12.03	$[M-H]^-$	C9H11NO3	8	Tyrosine	Amino acids	L-Threo-3-Phenylserine; 4-Hydroxy-4-(3-pyridyl)-butanoic acid; 4,6,7-Trihydroxy-1,2,3,4-tetrahydroisoquinoline
69	**346.0115**	12.19	$[M-H]^-$	N/A		N/A		
70	**102.0560**	12.21	$[M-H]^-$	C4H9NO2	0	GABA	Amino acids	O-Acetylethanolamine; 3-Aminobutanoic acid; 2-Aminoisobutyric acid; Dimethylglycine; N-Methyl-L-alanine; etc.
71	**146.0473**	12.21	$[M-H]^-$	C5H9NO4		Glutamic acid [a]	Amino acids	
72	**114.0574**	12.26	$[M-H]^-$	C5H9NO2	7	Proline	Amino acids	4-Amino-2-methylenebutanoic acid; 3-Acetamidopropanal; 1-aminocyclobutane carboxylic acid
73	**164.0721**	12.31	$[M-H]^-$	C9H11NO2	3	Phenylalanine	Amino acids	N-(4-Hydroxyphenyl)propanamide, 2-amino-4'-hydroxy-Propiophenone, 2-Propylisonicotinic acid, 4-(3-Pyridyl)-butanoic acid, benzocaine, Methyl N-methylanthranilate, Ethyl 2-aminobenzoate
74	**203.0822**	12.47	$[M-H]^-$	C11H12N2O2	0	Tryptophan	Amino acids	3-Hydroxymethylantipyrine
75	**145.0633**	12.53	$[M-H]^-$	C5H10N2O3	9	Glutamine	Amino acids	Gly-Ala; Ala-Gly; Isoglutamine

76	**118.0516**	12.80	$[M-H]^-$	C4H9NO3	5	Threonine	Amino acids	Homoserine, Methylserine, Aminohydroxybutyric acid; (-)-erythro-(2R,3R)-Dihydroxybutylamide
77	**285.0822**	12.82	$[M-H]^-$	N/A		N/A		
78	**420.0229**	12.83	$[M-H]^-$	N/A		N/A		
79	**131.0456**	12.84	$[M-H]^-$	C4H8N2O3	4	Asparagine	Amino acids	3-Ureidopropionic acid; Gly-Gly; N-Nitroso-N-methylurethane; Methylazoxymethanol acetate; N-Carbamoylsarcosine
80	**104.0362**	13.50	$[M-H]^-$	C3H7NO3	8	Serine	Amino acids	2-Amino-3-hydroxypropanoic acid
81	**116.0706**	13.68	$[M-H]^-$	C5H11NO2	9	Valine	Amino acids	Betaine; Norvaline; 2-Amino-3-methylbutanoic acid; 5-Aminopentanoic acid; 4-amino-pentanoic acid; etc.
82	**283.2653**	14.17	$[M-H]^-$	C18H36O2	3	N/A		
83	**130.0626**	14.32	$[M-H]^-$	C4H9N3O2	2	Guanidinopropionic acid [a]	Amino acids	
84	**154.0637**	14.43	$[M-H]^-$	C6H9N3O2	7	Histidine	Amino acids	L-2-Amino-3-(1-pyrazolyl)propanoic acid; 3-(Pyrazol-1-yl)-L-alanine
85	**173.1052**	14.44	$[M-H]^-$	C6H14N4O2	4	Arginine	Amino acids	
86	**158.9801**	14.68	$[M-H]^-$	N/A		N/A		
87	**174.9568**	14.78	[M-H]-	N/A		N/A		

[a] Identification confirmed through co-injection of standards with the sample.

Table S3. Tentative identification of the metabolites found in the red wine sample.

Metabolite ID	m/z	Migration time	Ion	Tentative Formula	Error (ppm)	Tentative Identification	Class of Metabolites	Other possibilities
1	**216.9116**	4.56	$[M-H]^-$	N/A		N/A	N/A	
2	**96.9584**	4.59	$[M-H]^-$	N/A		N/A	N/A	
3	**247.8412**	4.61	$[M-H]^-$	N/A		N/A	N/A	
4	**116.9282**	4.63	$[M-H]^-$	N/A		N/A	N/A	
5	**124.9917**	5.51	$[M-H]^-$	C2H6O4S	2	Ethyl hydrogen sulfate	Organic acid	
6	**208.9790**	5.61	$[M-H]^-$	N/A		N/A	N/A	
7	**124.9909**	5.75	$[M-H]^-$	C2H6O4S	5	N/A	N/A	Ethyl hydrogen sulfate
8	**170.9953**	6.12	$[M-H]^-$	C6H4O6	10	N/A	N/A	
9	**152.9923**	6.17	$[M-H]^-$	N/A		N/A	N/A	
10	**125.0013**	6.65	$[M-H]^-$	C2H7O4P	3	N/A	N/A	
11	**259.0142**	6.68	$[M-H]^-$	C6H12O9S	5	Glucose 6-sulfate	Carbohydrate	Galactose 6-sulfate
12	**243.0195**	6.72	$[M-H]^-$	N/A		N/A	N/A	
13	**199.0405**	6.83	$[M-H]^-$	C12H8O3	2	N/A	N/A	
14	**171.0056**	6.87	$[M-H]^-$	C3H9O6P	5	Glycerol 3-phosphate	Organic acid	Glycerophosphoric acid
15	**271.0480**	6.92	$[M-H]^-$	C11H12O8	7	3,4-Dihydroxybenzyltartaric acid	Organic acid	
16	**153.0206**	6.98	$[M-H]^-$	C7H6O4	8	3,5-Dihydroxybenzoic acid	Organic acid	2,6-Dihydroxybenzoic acid
17	**245.0450**	6.99	$[M-H]^-$	N/A	6	N/A	N/A	
18	**343.0180**	7.00	$[M-H]^-$	N/A		N/A	N/A	
19	**412.8810**	7.03	$[M-H]^-$	N/A		N/A	N/A	
20	**196.9041**	7.04	$[M-H]^-$	N/A		N/A	N/A	
21	**292.9229**	7.05	$[M-H]^-$	N/A		N/A	N/A	
22	**317.0529**	7.06	$[M-H]^-$	N/A		N/A	N/A	
23	**189.0049**	7.07	$[M-H]^-$	C6H6O7	4	Oxalosuccinic acid	Organic acid	
24	**242.9927**	7.14	$[M-H]^-$	N/A		N/A	N/A	
25	**357.0767**	7.15	$[M-H]^-$	C22H14O5	1	5,7-Dihydroxyflavone 7-benzoate	Phenolic compound	
26	**287.0535**	7.18	$[M-H]^-$	C10H12N2O8	5	Orotidine	Nucleoside	
27	**145.0145**	7.19	$[M-H]^-$	C5H6O5	1	2-Ketoglutaric acid	Organic acid	5-Hydroxy-2,4-dioxopentanoate; Dehydro-D-arabinono-1,4-lactone; Oxaloacetate 4-methyl ester; Methyloxaloacetate
28	**199.9696**	7.2	$[M-H]^-$	C3H7NO5S2	1	Cysteine-S-sulfate	Amino Acid	
29	**419.0464**	7.24	$[M-H]^-$	N/A		N/A	N/A	
30	**230.0126**	7.29	$[M-H]^-$	C8H9NO5S	1	Benzeneacetamide-4-O-sulphate	Organic compound	
31	**333.0568**	7.3	$[M-H]^-$	C9H19O11P	8	1-(sn-Glycero-3-phospho)-1D-myo-inositol	Alcohols	
32	**359.0579**	7.34	$[M-H]^-$	N/A		N/A	N/A	

33	**369.0265**	7.37	$[M-H]^-$	N/A		N/A	N/A	
34	**397.0229**	7.55	$[M-H]^-$	N/A		N/A	N/A	
35	**427.0323**	7.6	$[M-H]^-$	N/A		N/A	N/A	
36	**495.1111**	7.62	$[M-H]^-$	C22H24O13	7	4'-Methyl-(-)-epigallocatechin 3'-glucuronide	Phenolic compound	
37	**561.0892**	7.7	$[M-H]^-$	C17H28N2O15P2	0	N/A	N/A	
38	**390.9956**	7.72	$[M-H]^-$	N/A		N/A	N/A	
39	**577.0853**	7.73	$[M-H]^-$	N/A		N/A	N/A	
40	**591.1006**	7.74	$[M-H]^-$	N/A		N/A	N/A	
41	**623.0873**	7.75	$[M-H]^-$	N/A		N/A	N/A	
42	**129.0201**	7.8	$[M-H]^-$	C5H6O4	5	Methyl hydrogen fumarate	Organic acid	2-Pentendioate; Citraconic acid; 2-Hydroxyglutaric acid lactone; Gamma-delta-Dioxovaleric acid; Itaconic acid; 2,5-Dioxopentanoate; Mesaconic acid; Glutaconic acid
43	**188.0569**	7.84	$[M-H]^-$	C7H11NO5	2	N-Acetyl-L-glutamic acid	Amino Acid	Glutarylglycine
44	**287.0332**	7.85	$[M-H]^-$	N/A		N/A	N/A	
45	**213.9877**	7.89	$[M-H]^-$	N/A		N/A	N/A	
46	**258.0396**	8.05	$[M-H]^-$	C6H14NO8P	4	Aminofructose 6-phosphate	Carbohydrate	Glucosamine phosphate
47	**187.0252**	8.09	$[M-H]^-$	C8H12OS2	3	cis-2-Methylaconitate	Organic acid	Furfuryl propyl disulfide
48	**207.0550**	8.22	$[M-H]^-$	N/A		N/A	N/A	
49	**203.0195**	8.3	$[M-H]^-$	C7H8O7	2	Oxaloglutarate	Organic acid	Daucic acid
50	**295.0444**	8.38	$[M-H]^-$	C13H12O8	5	cis-Coutaric acid	Phenolic compound	Caffeoylmalic acid
51	**221.0337**	8.39	$[M-H]^-$	N/A		N/A	N/A	
52	**533.0755**	8.42	$[M-H]^-$	N/A		N/A	N/A	
53	**179.0340**	8.44	$[M-H]^-$	C9H8O4	6	Caffeic acid	Phenolic compound	
54	**311.0387**	8.45	$[M-H]^-$	C13H12O9	7	Caftaric acid	Phenolic compound	Cis-Caffeoyl tartaric acid
55	**177.0196**	8.47	$[M-H]^-$	C9H6O4	1	7,8-Dihydroxycoumarin	Phenolic compound	Caffeoquinone; 5,7-Dihydroxy-4H-1-benzopyran-4-one; ESCULETIN; 4,7-Dihydroxy-2H-1-benzopyran-2-one
56	**147.0322**	8.49	$[M-H]^-$	C6H12S2	9	Methyl 3-methyl-1-butenyl disulfide	Organic compound	Propenyl propyl disulfide
57	**293.1025**	8.51	$[M-H]^-$	C15H18O6	2	N/A	N/A	
58	**219.1040**	8.52	$[M-H]^-$	C13H16O3	6	1-(5-Acetyl-2-hydroxyphenyl)-3-methyl-1-butanone	Phenolic compound	
59	**137.0248**	8.54	$[M-H]^-$	C7H6O3	2	3-Hydroxybenzoic acid	Phenolic compound	4-Hydroxybenzoic acid; Salicylic acid
60	**473.0910**	8.61	$[M-H]^-$	N/A		N/A	N/A	
61	**149.0089**	8.71	$[M-H]^-$	C4H6O6	2	Tartaric acid [a]	Organic acid	
62	**439.9867**	8.76	$[M-H]^-$	N/A		N/A	N/A	

63	**635.1461**	8.79	$[M-H]^-$	C32H28O14	8	Kaempferol 3-(4''-acetyl-6''-p-coumarylglucoside)	Phenolic compound	
64	**237.0636**	8.79	$[M-H]^-$	C8H14O8	8	3-Deoxy-D-manno-octulosonate	Carbohydrate	2-Keto-3-deoxyoctonate
65	**315.0683**	8.8	$[M-H]^-$	C20H12O4	6	N/A	N/A	cis-4-(7-Hydroxtpyren-8-yl)-2-oxobut-3-enoate; cis-4-(8-Hydroxypyren-7-yl)-2-oxobut-3-enoate
66	**351.0532**	8.81	$[M-H]^-$	C19H12O7	6	N/A	N/A	Daphnoretin; 12a-Hydroxydolineone; Coumestrol diacetate
67	**383.0438**	8.82	$[M-H]^-$	N/A	0	N/A	N/A	
68	**367.0497**	8.84	$[M-H]^-$	C19H12O8	10	N/A	N/A	
69	**191.0208**	8.89	$[M-H]^-$	C6H8O7	5	Citric acid [a]	Organic acid	Isocitric acid; 2,3-Diketo-L-gulonate; Diketogulonic acid; D-Glucaro-1,4-lactone
70	**156.0656**	8.91	$[M-H]^-$	C7H11NO3	7	Tiglylglycine	Amino Acid	3-Methylcrotonylglycine
71	**385.0622**	8.99	$[M-H]^-$	N/A		N/A	N/A	
72	**339.0872**	9.02	$[M-H]^-$	C19H16O6	1	N/A	N/A	
73	**403.1002**	9.03	$[M-H]^-$	C20H20O9	8	trans-Resveratrol 3-O-glucuronide	Phenolic compound	
74	**367.1216**	9.04	$[M-H]^-$	C21H20O6	8	8-(1,1-Dimethylallyl)kaempferide	Phenolic compound	3'-Angeloyloxy-2',4'-dihydroxy-6'-methoxychalcone; 4',5-Dihydroxy-8-hydroxymethyl-6",6"-dimethylpyrano[2",3":7,6]flavanone; etc.
75	**207.0536**	9.05	$[M-H]^-$	C8H16O2S2	8	Dihydrolipoate	Organic compound	
76	**219.0508**	9.06	[M-H]-	C8H12O7	1	3-Hydroxy-3-carboxymethyl-adipic acid	Organic acid	
77	**177.0414**	9.12	$[M-H]^-$	C7H14OS2	0	Methylthiomethyl 2-methylbutanethiolate	Organic compound	
78	**133.0148**	9.17	$[M-H]^-$	C4H6O5	4	Malic acid [a]	Organic acid	
79	**337.0749**	9.19	$[M-H]^-$	C19H14O6	9	N/A	N/A	O-Methylsterigmatocystin
80	**355.0854**	9.2	$[M-H]^-$	C12H20O12	8	Acaciabiuronic acid	Carbohydrate	
81	**565.1235**	9.21	$[M-H]^-$	C25H26O15	6	Quercetin 3-apiosyl-(1->2)-xyloside	Phenolic compound	Herbacetin 8-alpha-L-arabinopyranoside-4'-xyloside; Herbacetin 8,4'-dixyloside; Isoorientin 6''-O-alpha-L-arabinoside; etc.
82	**419.0659**	9.22	$[M-H]^-$	N/A		N/A	N/A	
83	**209.0303**	9.24	$[M-H]^-$	C6H10O8	0	Galactaric acid	Carbohydrate	Glucarate; Citric acid monohydrate
84	**175.0590**	9.26	$[M-H]^-$	N/A		N/A	N/A	
85	**311.0597**	9.27	$[M-H]^-$	N/A		N/A	N/A	
86	**256.9918**	9.29	$[M-H]^-$	N/A		N/A	N/A	
87	**223.0491**	9.3	$[M-H]^-$	C8H8N4O4	8	N/A	N/A	

88	**387.0758**	9.32	$[M-H]^-$	C19H16O9	9	Urolithin B 3-O-glucuronide	Carbohydrate	12a-Hydroxy-9-demethylmunduserone-8-carboxylic acid; 5,7,2',5'-Tetrahydroxy-3,4'-dimethoxyflavone 5'-acetate; 3,5-Dihydroxy-6,7,8-trimethoxy-3',4'-methylenedioxyflavone; Gossypetin 7,4'-dimethyl ether 8-acetate
89	**135.0312**	9.34	$[M-H]^-$	C5H4N4O	1	Hypoxhantine	Nitrogenous base	
90	**515.1248**	9.34	$[M-H]^-$	C25H24O12	10	Pyrano malvidin 3-glucoside	Phenolic compound	
91	**193.0362**	9.34	$[M-H]^-$	C7H6N4O3	3	6-(Hydroxymethyl)-2,4(1H,3H)-pteridinedione	Organic compound	
92	**165.0401**	9.36	$[M-H]^-$	C5H10O6	2	Arabinonic acid	Organic acid	Ribonic acid; Xylonate; Apionic acid; ; Lyxonate; S-Propyl 1-propanesulfinothioate
93	**147.0303**	9.38	$[M-H]^-$	C5H8O5	2	2-Hydroxyglutaric acid	Organic acid	Citramalic acid; Ribonolactone; D-Xylono-1,5-lactone; 3-Methylmalic acid
94	**195.0527**	9.41	$[M-H]^-$	C7H8N4O3	8	Gluconic acid [a]	Organic acid	
95	**605.1904**	9.44	$[M-H]^-$	C29H34O14	4	N/A	N/A	
96	**129.0200**	9.47	$[M-H]^-$	C5H6O4	5	Methylenebutanedioic acid	Organic acid	2-Pentendioate; Glutaconic acid; 2-Hydroxyglutaric acid lactone; Gamma-delta-Dioxovaleric acid; Itaconic acid; 2,5-Dioxopentanoate; Mesaconic acid; Methyl hydrogen fumarate
97	**237.0648**	9.48	$[M-H]^-$	C9H10N4O4	7	N/A	N/A	
98	**161.0460**	9.49	$[M-H]^-$	C6H10O5	3	1,5-Anhydrofructose	Carbohydrate	Fucono-1,5-lactone; Deoxy-scyllo-inosose; Diethyl pyrocarbonate; Dimethyl D-malate; 3-hydroxy-3-methyl-Glutaric acid; Methylpropyl 1-propenyl disulfide; etc.
99	**131.0674**	9.51	$[M-H]^-$	N/A		N/A	N/A	
100	**366.1176**	9.54	$[M-H]^-$	C13H25N3O5S2	3	Tripeptide (M,M,S)	Amino Acid	
101	**293.1223**	9.56	$[M-H]^-$	C12H22O8	7	Ethyl (S)-3-hydroxybutyrate glucoside	Carbohydrate	
102	**117.0199**	9.58	$[M-H]^-$	C4H6O4	4	Succinic acid [a]	Organic acid	Methylmalonic acid; Threonolactone; 2(3H)-Furanone, dihydro-3,4-dihydroxy; Erythrono-1,4-lactone; 4-Hydroxy-2-oxobutanoic acid; Methyl oxalate; xi-3-Hydroxy-2-oxobutanoic acid
103	**368.0981**	9.61	$[M-H]^-$	N/A		N/A	N/A	
104	**169.0132**	9.66	$[M-H]^-$	C7H6O5	7	Gallic acid	Phenolic compound	Trihydroxybenzoic acid; Benzyl methyl disulfide; Diethylthiophosphate
105	**218.1056**	9.67	$[M-H]^-$	C9H17NO5	10	Pantothenic acid [a]	Organic acid	
106	**137.0258**	9.68	$[M-H]^-$	C7H6O3	10	4-Hydroxybenzoic acid	Phenolic compound	3-Hydroxybenzoic acid; Salicylic acid
107	**487.1603**	9.69	$[M-H]^-$	C25H28O10	1	N/A	N/A	
108	**153.0235**	9.7	$[M-H]^-$	C4H10O4S	5	N/A	N/A	

109	**145.0499**	9.71	$[M-H]^-$	C6H10O4	5	Solerol	Organic compound	Adipic acid; Dimethylsuccinic acid; Methylglutaric acid
110	**577.1324**	9.72	$[M-H]^-$	C30H26O12	5	Procyanidin B2	Phenolic compound	Procyanidin B5; Procyanidin B8; 4-O-8',5'-5"-Dehydrotriferulic acid; Pelargonidin 3-(6-p-coumaroyl)glucoside; Kaempferol 3-(2"-(Z)-p-coumaroylrhamnoside), Epicatechin-(6'->8)-epicatechin; etc.
111	**167.0294**	9.73	$[M-H]^-$	N/A		N/A	N/A	
112	**287.0569**	9.74	$[M-H]^-$	C15H12O6	2	Dihydrokaempferol	Phenolic compound	Micromelin; 3,5-Dimethoxy-1,6-dihydroxyxanthone; 2,6,7,4'-Tetrahydroxyisoflavanone; Fustin; Carthamidin; etc.
113	**305.0678**	9.75	$[M-H]^-$	C15H14O7	3	Gallocatechin	Phenolic compound	
114	**197.0458**	9.76	$[M-H]^-$	C9H10O5	1	Syringic acid	Phenolic compound	3,4-O-Dimethylgallic acid Syringic acid; Vanillylmandelic acid; Ethyl gallate; 3-hydroxy-4-methoxymandelate; 3-(3,4-Dihydroxyphenyl)lactate; 2-Hydroxy-3,4-dimethoxybenzoic acid
115	**389.1213**	9.77	$[M-H]^-$	C20H22O8	8	(Z)-Resveratrol 4'-glucoside	Phenolic compound	(E)-2-Glucosyl-3,4',5-trihydroxystilbene; Piceid
116	**289.0704**	9.78	$[M-H]^-$	C15H14O6	5	Catechin	Phenolic compound	Epicatechin; Luteoforol; Marshrin; 3-Hydroxyphloretin; alpha-Cotonefuran; cis-3 and trans-2-Hexenyl propionate; etc.
117	**177.0381**	9.8	$[M-H]^-$	N/A		N/A	N/A	
118	**431.1600**	9.81	$[M-H]^-$	C19H28O11	9	Benzyl gentiobioside	Carbohydrate	Zizybeoside I
119	**181.0699**	9.82	$[M-H]^-$	C6H14O6	10	Galactitol	Carbohydrate	Mannitol; Sorbitol; Iditol
120	**341.1057**	9.83	$[M-H]^-$	C19H18O6	8	3,5,6,7-Tetramethoxyflavone	Phenolic compound	4-{2,6-Dihydroxy-3-[(2E)-3-(4-hydroxyphenyl)-2-propenoyl]phenyl}-3-hydroxy-2-butanone 4-{2,6-Dihydroxy-3-[(2E)-3-(4-hydroxyphenyl)-2-propenoyl]phenyl}-3-hydroxy-2-butanone; Tetramethylkaempferol; 8-Desmethylkalmiatin; Fisetin tetramethyl ether; etc.
121	**387.1119**	9.84	$[M-H]^-$	C20H20O8	9	5-Hydroxy-3,7,8,2',4'-pentamethoxyflavone	Phenolic compound	Gossypetin 3,7,8,3',4'-pentamethyl ether; Emmaosunin 5-Hydroxy-7,2',3',4',5'-pentamethoxyflavone; Gossypetin 3,5,8,3',4'-pentamethyl ether; Artemetin; Quercetagetin 5,6,7,3',4'-pentamethyl ether; etc.
122	**214.0512**	9.87	$[M-H]^-$	C12H9NO3	1	Robustine	Organic compound	
123	**302.0978**	9.91	$[M-H]^-$	C13H22NO3PS	3	N/A	N/A	
124	**151.0275**	9.99	$[M-H]^-$	C5H4N4O2	8	Xanthine	Organic compound	6,8-Dihydroxypurine
125	**202.0751**	10.23	$[M-H]^-$	C9H9N5O	8	(5-Phenyl-1,2,4-triazol-3-yl)urea	Organic compound	

126	**487.0646**	10.65	$[M-H]^-$	N/A		N/A	N/A	
127	**257.1160**	11.15	$[M-H]^-$	C11H18N2O5	6	gamma-L-Glutamyl-L-pipecolic acid	Amino Acid	(2S,2'S)-Pyrosaccharopine
128	**307.1113**	11.41	$[M-H]^-$	C18H16N2O3	8	Azacridone A	Organic compound	Tyrphostin B44 (-); Citrus Red No.2
129	**174.0755**	11.63	$[M-H]^-$	C7H13NO4	10	2-Aminoheptanedioic acid	Organic acid	Calystegin B2; Calystegine B5; N-Carboxyethyl-γ-aminobutyric acid
130	**229.0995**	11.97	$[M-H]^-$	C13H14N2O2	5	(1xi,3xi)-1,2,3,4-Tetrahydro-1-methyl-beta-carboline-3-carboxylic acid	Organic compound	
131	**302.1346**	12.07	$[M-H]^-$	C12H21N3O6	4	N5-Acetyl-N2-gamma-L-glutamyl-L-ornithine	Amino Acid	
132	**130.0504**	12.28	$[M-H]^-$	C5H9NO3	5	Hydroxyproline	Amino Acid	5-Amino-2-oxopentanoic acid; L-Glutamic gamma-semialdehyde; N-Acetyl-L-alanine; Propionylglycine; 4-Hydroxy-2-pyrrolidinecarboxylic acid
133	**132.0309**	12.37	$[M-H]^-$	C4H7NO4	4	Aspartic acid [a]	Amino Acid	Iminodiacetic acid
134	**180.0655**	13.07	$[M-H]^-$	C9H11NO3	7	Tyrosine	Amino Acid	L-Threo-3-Phenylserine; 4-Hydroxy-4-(3-pyridyl)-butanoic acid; 4,6,7-Trihydroxy-1,2,3,4-tetrahydroisoquinoline
135	**128.0358**	13.27	$[M-H]^-$	C5H7NO3	3	Pyroglutamic acid	Amino Acid	1-Pyrroline-4-hydroxy-2-carboxylate; N-Acryloylglycine; 5-Oxoprolinate
136	**146.0459**	13.28	$[M-H]^-$	C5H9NO4	0	Glutamic acid [a]	Amino Acid	
137	**114.0567**	13.29	$[M-H]^-$	C5H9NO2	5	Proline	Amino Acid	4-Amino-2-methylenebutanoic acid; 3-Acetamidopropanal; 1-aminocyclobutane carboxylic acid
138	**164.0707**	13.30		C9H11NO2	7	Phenylalanine	Amino Acid	N-(4-Hydroxyphenyl)propanamide; 2-amino-4'-hydroxy-Propiophenone; 2-Propylisonicotinic acid ;4-(3-Pyridyl)-butanoic acid; etc.
139	**118.0514**	13.60		C4H9NO3	3	Threonine	Amino Acid	Allothreonine; Homoserine; Methylserine; Minohydroxybutyric acid; (-)-erythro-(2R,3R)-Dihydroxybutylamide
140	**131.0459**	13.61		C4H8N2O3	3	Asparagine	Amino Acid	3-Ureidopropionic acid; Gly-Gly; N-Nitroso-N-methylurethane; Methylazoxymethanol acetate; N-Carbamoylsarcosine
141	**154.0634**	13.85		C6H9N3O2	7	Histidine	Amino Acid	L-2-Amino-3-(1-pyrazolyl)propanoic acid; 3-(Pyrazol-1-yl)-L-alanine
142	**145.0969**	13.89		C6H14N2O2	10	Lysine	Amino Acid	Diaminohexanoate; Carbachol

[a] Identification confirmed through co-injection of standards with the sample.

CAPÍTULO 4

Estudio metabolómico del efecto de compuestos bioactivos de romero en células hepáticas

4.1. INTRODUCCIÓN

4.1.1. El romero, fuente natural de compuestos bioactivos contra el cáncer

El romero (*Rosmarinus officinallis* L.) es una planta nativa de la región mediterránea que pertenece a la familia Lamiaceae. Aunque tradicionalmente se ha empleado con fines culinarios y aromáticos, desde la antigüedad se han atribuido a esta planta diversas propiedades medicinales (Avila-Sosa y col., 2011). Desde 2008 el extracto de romero está considerado como aditivo alimentario debido a su potencial antioxidante para los alimentos (Aguilar y col., 2008). Recientemente, se han ampliado los usos autorizados para el extracto de romero a través del Reglamento 2016/56, en concreto, como antioxidante en grasas para untar (EFSA Panel on Food Additives and Nutrient Sources added to Food, 2015). En los últimos años, se ha estudiado intensamente el potencial farmacológico del romero, además de su bien conocida actividad antioxidante (Moreno y col., 2006; Bozin y col., 2007), antimicrobiana (Moreno y col., 2006; Bozin y col., 2007) y antiinflamatoria (Peng y col., 2007), el romero es reconocido por su efecto contra enfermedades cardiovasculares (Afonso y col., 2013), diabetes (Sedighi y col., 2015), trastornos neurológicos (de Oliveira, 2016), entre otras (Al-Sereit y col., 1999; Habtemariam, 2016). Además, un gran número de evidencias *in vitro* (Tai y col., 2012; Valdés y col., 2012; Valdés y col., 2013; González-Vallinas y col., 2014a) e *in vivo* (Petiwala y col., 2014; Gonzáles-Vallinas y col., 2014b; Yan y col, 2015) han demostrado que el extracto de romero presenta efectos anticancerígenos.

La capacidad anticancerígena de los extractos de romero se ha investigado en modelos *in vitro*, utilizando distintas líneas de células tumorales, incluyendo leucemia (Valdés y col., 2012), cáncer de mama (González-Vallinas y col., 2014a), hígado (Vicente y col., 2013), ovario (Tai y col., 2012), colon (Valdés y col., 2013), próstata (Petiwala y col., 2013), cérvix (Berrington y Lall, 2012) y pulmón (Yesil-Celiktas y col., 2010). En estudios con distintos modelos *in vivo* también se ha demostrado la capacidad de los compuestos de romero de evitar el desarrollo y reducir el tamaño de tumores de próstata y de cáncer de colon en ratones xenoinjertados (Petiwala y col., 2014; Gonzáles-Vallinas y col., 2014b; Yan y col., 2015), así como en la reducción de tumores de cáncer de piel y oral inducidos en modelos animales (Sancheti y Goyal, 2006; Rajasekaran y col., 2012).

Varios trabajos han atribuido los efectos anticancerígenos de los compuestos de romero a su actividad quimioprotectora la cual está relacionada fundamentalmente a las propiedades antioxidantes de los diterpenos fenólicos de la planta, más específicamente a la capacidad de estos compuestos de secuestrar radicales libres del medio, lo que protege frente al daño oxidativo inducido por las especies reactivas del oxígeno (ROS) a lípidos, proteínas y DNA (Xiang y col., 2013; Gonzáles-Vallinas y col., 2015). Además de la capacidad de secuestrar radicales libres, los diterpenos fenólicos y los extractos de romero también podrían ejercer una actividad protectora indirecta mediante la inducción de la respuesta frente al estrés oxidativo modulada por el factor de transcripción nuclear eritroide-2 (NRF2), aumentando las defensas antioxidantes de la célula y mejorando su capacidad de detoxificación de xenobióticos (Satoh y col., 2008).

Entre los compuestos más importantes presentes en los extractos de romero se pueden destacar los compuestos volátiles (alcanfor, 1,8-cineol, cariofileno, borneol, terpineol, cadineno, etc.) (Fornari y col., 2012), flavonoides (apigenina, diosmetina, hispidulina, cirsimaritina, luteolina, hesperidina, homoplantaginina, diosmina, genkwanina, eriocitrina, luteolina, gallocatequina, nepetrina y luteolina glucurónidos, entre otros) (Bai y col., 2010; Del Baño y col., 2004; Borrás-Linares y col., 2014), ácidos fenólicos (ácido rosmarínico, ácido cafeico, ácido siríngico, ácido vainíllico, ácido cumárico, etc.) (Zgórka y Glowniak, 2001) y diterpenos fenólicos (ácido carnósico, carnosol, rosmanol, ácido metil-carnósico, etc.). Algunos de los diterpenos que se han podido identificar en romero se muestran en la **Figura 4.1**.

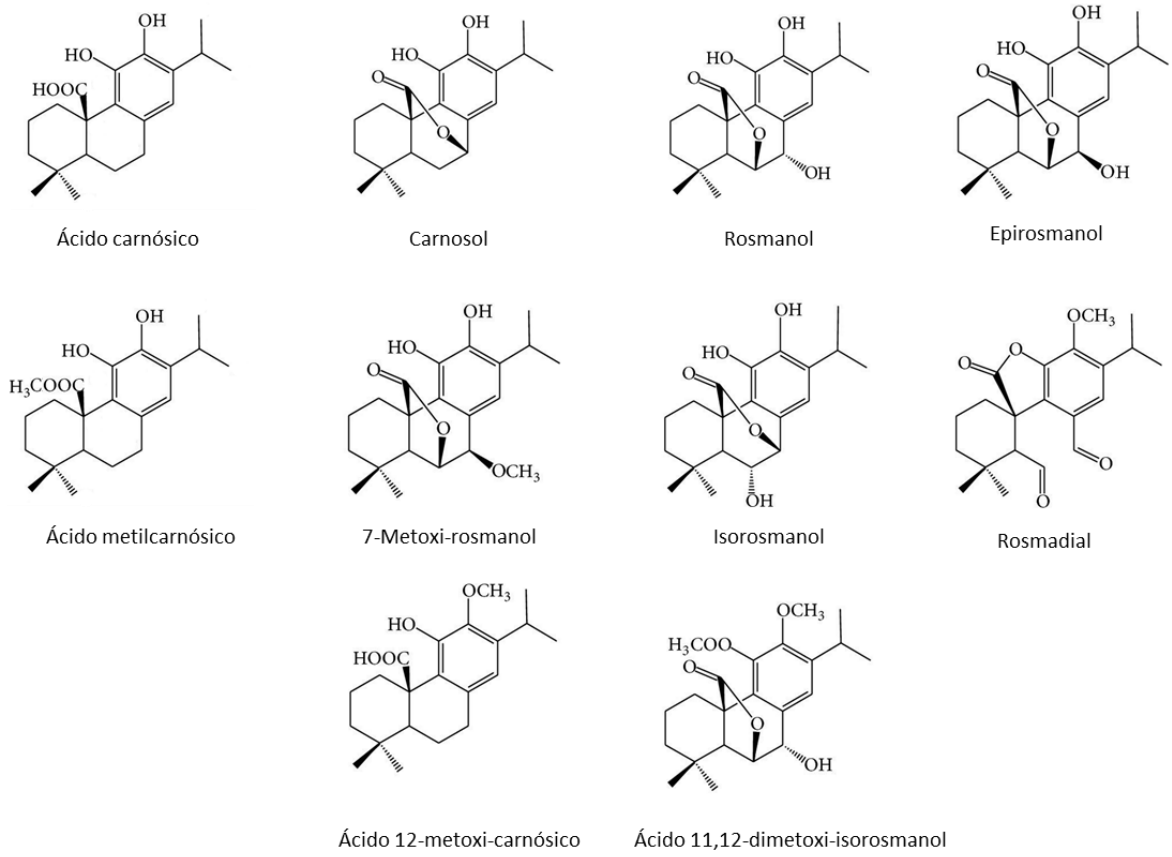

Figura 4.1. Estructuras químicas de los diterpenos fenólicos más importantes identificados en romero.

Entre los diterpenos fenólicos del romero, el ácido carnósico y el carnosol pueden llegar a representar hasta el 5% del peso seco de la hoja de romero y se estima que pueden ser responsables de más del 90% de la actividad antioxidante de los extractos de romero (Aruoma y col., 1992). El ácido carnósico es hasta la fecha el compuesto más estudiado del romero. Numerosos estudios *in vitro* indican la posible actividad anticancerígena de este compuesto en distintos modelos celulares de cáncer (Barni y col., 2012). Por ejemplo, se ha demostrado que el ácido carnósico provoca una disminución en la viabilidad celular, en el

modelo de cáncer de colon HCT116, mediada por un proceso de apoptosis debida a la producción de ROS (Kim y col., 2016). En los últimos años, el grupo de Alimentómica del CIAL ha trabajado intensamente en la actividad antitumoral de extractos de romero obtenidos mediante fluidos presurizados, ricos en los diterpenos ácido carnósico y carnosol. La capacidad de estos extractos de inhibir la proliferación de células cancerígenas se ha relacionado con alteraciones en el ciclo celular (Valdés y col., 2013; Ibañez y col., 2012a; Ibañez y col, 2012b), así como con un aumento del proceso de apoptosis celular (Ibañez y col, 2012b). Estudios previos también han demostrado que el efecto de los diterpenos del romero varía en función del modelo celular en estudio, de la concentración y del tipo de diterpeno y del tiempo de incubación (Valdés y col., 2012; Valdés y col, 2013; Valdés y col., 2016b; Valdés y col., 2017). En esta Tesis Doctoral se ha empleado una aproximación metabolómica no dirigida, con el fin de avanzar en el conocimiento acerca del posible efecto tóxico de los principales diterpenos del romero en un modelo *in vitro* de células hepáticas.

4.1.2. Flujo de trabajo en metabolómica

El esquema de trabajo convencional en un experimento metabolómico integra una serie de etapas relacionadas con la preparación de la muestra, la elección de una o más plataformas analíticas, el procesamiento de los datos, el análisis estadístico de los datos e interpretación biológica de los resultados obtenidos. Todas estas etapas están interrelacionadas y deben ser minuciosamente optimizadas eliminando el riesgo de cualquier desviación que pueda llevar a resultados erróneos. En la **Figura 4.2** se presentan de forma esquematizada las principales etapas de un estudio metabolómico.

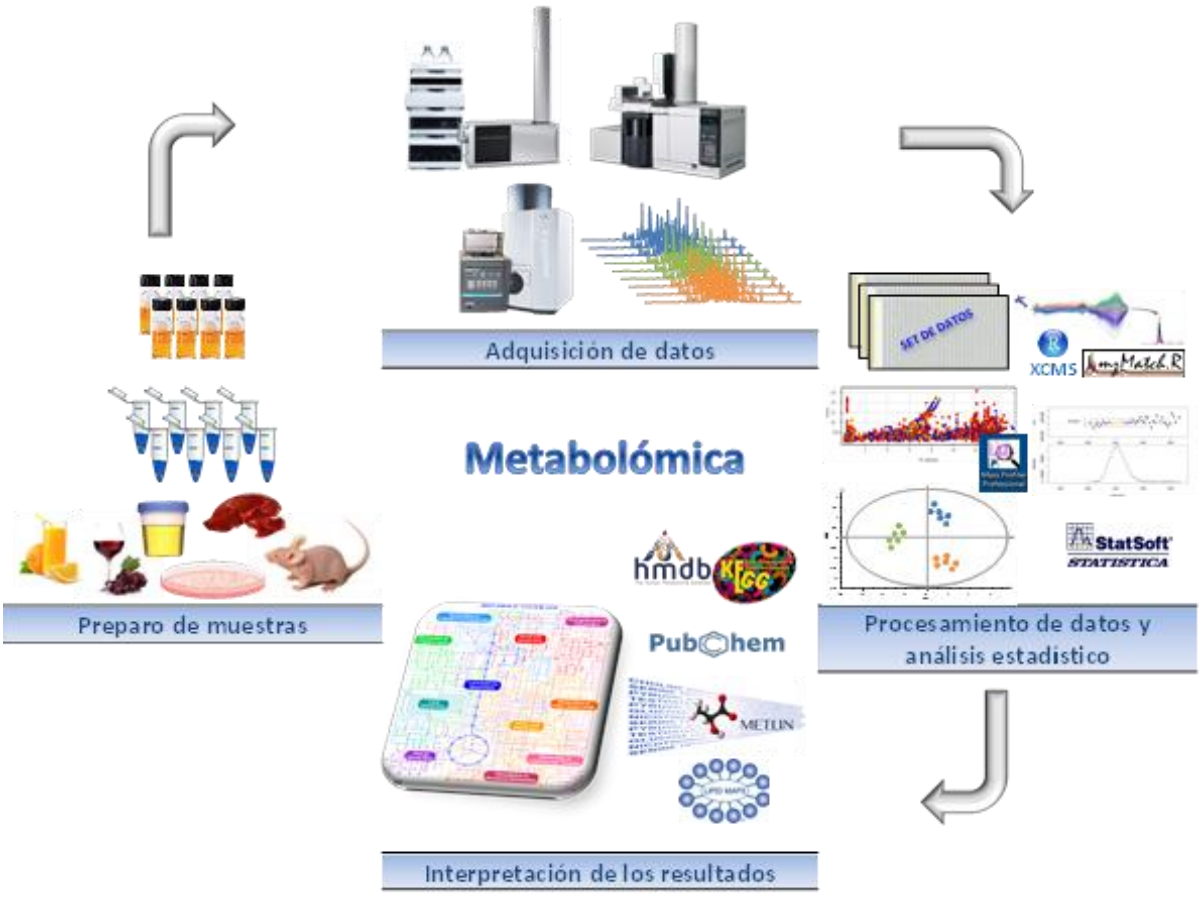

Figura 4.2. Flujo simplificado de trabajo de un estudio metabolómico.

La **preparación de la muestra** es una etapa de gran importancia en metabolómica ya que afecta directamente al contenido de los metabolitos de la muestra a analizar. El tratamiento de la muestra previo al análisis metabolómico dependerá fundamentalmente del tipo de muestra (orina, plasma, tejido, cultivo celular, etc.) y de la plataforma analítica elegida para su análisis. El método ideal de preparación de muestras en metabolómica debería ser: i) poco selectivo, para asegurar la mayor cobertura del metaboloma posible; ii) simple y rápido, para impedir la perdida de metabolitos durante el proceso; y iii) altamente reproducible (Vuckovic, 2012). En el momento de la recogida de la muestra es primordial llevar a cabo una rápida inactivación de la actividad enzimática y del bloqueo de las reacciones metabólicas ("*quenching"*) que puedan estar teniendo lugar. Este proceso se suele llevar a cabo mediante una disminución drástica de la temperatura, generalmente a través del empleo de nitrógeno líquido, o mediante el uso de disolventes orgánicos (Dettmer y col., 2007). En metabolómica, uno de los objetivos del tratamiento previo de la muestra es la eliminación de macromoléculas (DNA y proteínas, esencialmente) para evitar interferencias en el análisis químico y/o supresión de las señales analíticas de los metabolitos. Los métodos más comúnmente empleados para la preparación de muestras líquidas (suero, plasma, orina, etc.) se basan fundamentalmente en la desproteinización de la muestra por

precipitación mediante el uso de disolventes orgánicos, como metanol o acetonitrilo (Rico y col., 2014), o por ultrafiltración (Tiziani y col., 2008; Vuckovick, 2012). La extracción en fase sólida (SPE) también se emplea en metabolómica cuando el objetivo es extraer una familia determinada de metabolitos con unas características físico-químicas similares (Idborg-Björkman y col., 2003; Michopoulos y col., 2009). Al ser un método más selectivo, la SPE provoca la disminución de la cobertura del metaboloma en estudio (Rico y col., 2014) y hace que su uso sea menos frecuente en el análisis metabolómico no dirigido (Vuckovick, 2012). La extracción de metabolitos en muestras sólidas o semisólidas (células, tejidos, etc.) exige además del *quenching*, una etapa adicional de homogeneización y lisis celular de la muestra. El disolvente para la extracción se puede seleccionar según se desee obtener en el extracto metabólico, un predominio de metabolitos polares, apolares o bien utilizando ambos tipos de disolventes para crear un sistema bifásico y así analizar posteriormente por separado ambos extractos metabólicos (Wu y col., 2008; Lin y col., 2007; Bi y col., 2013; Southam y col., 2017).

Una vez llevada a cabo la preparación de la muestra, el siguiente paso es el análisis de los metabolitos a través de la plataforma analítica elegida. La elección de la técnica analítica y del método de análisis dependerá del objetivo del estudio y del tipo de estrategia analítica (análisis del perfil metabólico o de la huella metabólica). Tal y como ya se ha comentado en el primer Capítulo de esta Tesis Doctoral, las plataformas analíticas comúnmente empleadas en metabolómica son: NMR, MS, LC-MS, GC-MS y CE-MS. A diferencia de otras tecnologías ómicas, la metabolómica supone un gran reto analítico debido a la gran variedad de moléculas con distintas propiedades fisicoquímicas y estructuras, así como por el amplio intervalo de concentraciones de los metabolitos en cualquier muestra biológica. Aunque los avances técnicos en la instrumentación así como la hibridación de técnicas analíticas están aportando una información metabolómica cada vez más completa, a menudo es necesario en los estudios de metabolómica emplear diversas plataformas analíticas que aportan una información complementaria, necesaria a la hora de llevar a cabo un análisis del metaboloma lo más completo posible. Todavía hoy, buena parte de los esfuerzos en metabolómica están dirigidos tanto hacia el desarrollo instrumental como al metodológico.

El siguiente paso en un estudio metabolómico es el procesamiento de los datos obtenidos de las diferentes plataformas analíticas y su posterior análisis estadístico. El **procesado de datos** obtenidos mediante plataformas metabolómicas basadas en MS, como la GC-MS, LC-MS y CE-MS, consta de varias etapas (Katajamaa y Orešič, 2007; Sugimoto y col., 2012). Las principales etapas son la detección de "*features*", alineamiento y la normalización de las señales. Para la detección de *features* los datos deben ser filtrados para reducir el ruido del sistema y seleccionar solamente las señales espectrales provenientes de los metabolitos. El alineamiento se basa en la corrección de la diferencia de los tiempos de migración/retención de los *features* entre diferentes inyecciones y muestras. Por último, el objetivo de la normalización es la eliminación de fuentes de variación entre muestras, como por ejemplo alteraciones en la sensibilidad del MS o errores durante la manipulación/inyección/separación de la muestra, a fin de garantizar que los datos de todas las muestras sean comparables entre sí de forma fiable. Al final del

procesado se obtiene una matriz de datos con los valores de *m/z* extraídos, tiempos de migración/retención y la intensidad o área correspondiente a cada pico. En la actualidad existen varias herramientas para llevar a cabo el procesado de datos, tanto de acceso libre, como MZmine (Katajama y Orešič, 2005) o XCMS (Smith y col., 2006), como comercial, como MassLynx (Waters Corp.), Mass Profiler Profesional (MPP, Agilent Technologies), etc. Estos últimos, suelen ser menos flexibles respecto a la elección de parámetros que los softwares de acceso libre, si bien son de uso más sencillo. Por otro lado, además del procesado de los datos, los softwares comerciales generalmente permiten realizar el análisis estadístico univariante y/o multivariante.

El **análisis estadístico** de los datos obtenidos en un estudio metabolómico requiere el uso de herramientas quimiométricas avanzadas debido fundamentalmente al gran volumen y complejidad de los datos. Las matrices de datos obtenidas en la etapa previa de procesado, se someten al análisis estadístico univariante y/o multivariante. Para la detección de los metabolitos significativamente diferentes entre los diferentes grupos de muestras, se puede emplear pruebas paramétricas como el test *t de Student* (comparación de dos grupos de muestras) o el análisis de varianza (ANOVA) para la comparación de más de dos grupos de muestras; y pruebas no paramétricas (por ejemplo el test de Kruskal-Wallis y Mann-Whitney U) para conjuntos de datos que no presenten distribución normal. Existen distintos programas que pueden ser utilizados para llevar a cabo el análisis estadístico en metabolómica, entre ellos Statistica (http://statistica.io/) y SIMCA (http://umetrics.com/) son algunos de los más comúnmente empleados debido a la amplia variabilidad de técnicas estadísticas y representaciones gráficas disponibles. Los métodos de análisis estadísticos multivariantes se dividen en dos grandes grupos: "no supervisados" donde el modelo se construye sin el conocimiento previo de los grupos de clasificación de las muestras y los métodos "supervidados", los cuales tienen cuenta la existencia de las diferentes clases. El Análisis de Componentes Principales (PCA) es un método no supervisado comúnmente utilizado en metabolómica que permite detectar muestras atípicas (*outliers*) y observar las agrupaciones y tendencias entre los grupos de muestras en estudio. El PCA se utiliza generalmente como paso previo a la aplicación de métodos estadísticos supervisados, para evaluar la calidad de los datos (Boccard y col., 2010). Entre los métodos de clasificación supervisados empleados en metabolómica se encuentran el Análisis por Mínimos Cuadrados Parciales (PLS), Proyecciones Ortogonales a Estructuras Latentes (OPLS) que son una modificación del método PLS (Triba y col., 2015) y el Análisis Lineal Discriminante (LDA) (Lindon y Nicholson, 2001; Hewer y col., 2006). El LDA utiliza un procedimiento de pasos sucesivos (*Stepwise procedure*) para seleccionar los metabolitos que más contribuyen a la diferenciación de los grupos de muestras (potenciales biomarcadores) y generalmente utiliza el análisis canónico discriminante (CVA) para obtener una representación gráfica de los resultados de la clasificación. En los análisis por PLS-DA (Análisis Discriminante de Mínimos Cuadrados Parciales) y por OPLS-DA (Análisis Discriminante por Mínimos Cuadrados Parciales Ortogonal) las variables más relevantes en cada modelo estadístico son seleccionados a través de informaciones provenientes de una o más representaciones gráficas, como la importancia de la variable en la proyección (VIP), *loading plot* o *S-Plot* (forma de visualización del

OPLS-DA que combina la covarianza modelada y la correlación de las variables en un gráfico de dispersión), que de forma resumida expresan la influencia y la importancia de las variables sobre la proyección y la fiabilidad del resultado.

Tras el análisis estadístico y la selección de las variables (metabolitos) estadísticamente significativos entre los diferentes grupos de muestras, el siguiente paso es la **identificación de los metabolitos**. Cuando el análisis se lleva a cabo mediante GC-MS con interfase de impacto electrónico existen diversas bases de datos espectrales disponibles comercialmente o de acceso libre, tales como Golm Metabolome Database (GMD) (Kopka y col., 2005), MassBank database (Horai et al., 2010), NIST (Babushok y col, 2007) y Wiley (Roessner y col., 2000), que permiten realizar la identificación de los metabolitos mediante la comparación del espectro de fragmentación experimental con los espectros de fragmentación contenidos en estas librerías. Además del patrón de fragmentación espectral, algunas librerías ayudan a llevar a cabo esta identificación con el índice de retención (Kind y col., 2009). El proceso de identificación es más laborioso cuando el análisis se ejecuta mediante LC-MS o CE-MS y se lleva generalmente a cabo mediante la comparación de los valores de *m/z* experimental con valores de *m/z* teóricos de los metabolitos presentes en bases de datos como HMDB (Wishart y col., 2009), Metlin (Smith y col., 2005), PubChem (Bolton y col., 2008), KEGG (Kanehisa, 1997), LIPID MAPS (Sud y col., 2007), o mediante la comparación de los espectros de fragmentación MS/MS experimentales con los publicados en estas bases de datos. Además, se puede complementar la identificación tentativa de cada metabolito mediante la comparación del perfil isotópico del espectro experimental y del teórico. Para confirmar la identidad del metabolito normalmente es necesario realizar la co-inyección de estándares de metabolitos (si están disponibles comercialmente), en las mismas condiciones de análisis que las muestras reales. Por último, para relacionar cada metabolito identificado con sus respectivas rutas metabólicas, se pueden emplear herramientas bioinformáticas como MetaboAnalyst (http://www.metaboanalyst.ca/), Ingenuity Pathway Analysis (QIAGEN Bioinformatics), MBROLE (http://csbg.cnb.csic.es/mbrole2/), entre otras.

4.1.3. Estudio metabolómico del efecto de los diterpenos ácido carnósico, carnosol y rosmanol en un modelo *in vitro* de células de hígado humano

La evaluación de la toxicidad de los compuestos bioactivos del romero es un aspecto esencial a considerar para validar su uso seguro. En estudios previos, diversos extractos de romero, ricos en diterpenos fenólicos obtenidos mediante extracción con fluidos supercríticos (SFE) no mostraron efectos toxicológicamente negativos con una dosis aguda de 2000 mg extracto/kg peso corporal en ratas (Anadón y col., 2008). En otro estudio de toxicidad aguda llevado a cabo por Wang y col. (Wang y col., 2012), se estimó que la dosis letal de ácido carnósico en ratones era de 7100 mg de ácido carnósico/kg peso corporal; además los ratones tratados con una dosis diaria de ácido carnósico (600 mg/kg peso corporal) durante 30 días, mostraron algunos signos de toxicidad. El estudio histopatológico de los ratones reveló que a dosis tóxicas se producían daños en el hígado y en el corazón. Las investigaciones llevadas a cabo

hasta la fecha indican que los extractos de romero y el ácido carnósico tienen una toxicidad oral relativamente baja, sin embargo, no existe información acerca de la toxicidad de los compuestos bioactivos del romero en concentraciones a las cuales éstos presentan efecto antiproliferativo.

Recientemente, se ha desarrollado una nueva línea celular humana, la línea HepaRG, procedente de un paciente con carcinoma hepatocelular (Gripon y col., 2002). Cuando estas células se cultivan en determinadas condiciones, se diferencian en células similares a las de los hepatocitos primarios adultos y a células epiteliales biliares, imitando la estructura histológica del hígado *in vivo* (Guillouzo y col., 2007); estas células expresan más del 80% de los genes activos en hepatocitos humanos (Jossé y col., 2008; Mueller y col., 2015). A diferencia de otros modelos celulares hepáticos, las células HepaRG mantienen varias funciones metabólicas, secretoras y de actividad de desintoxicación de xenobióticos (Aninat y col., 2006). Entre otras características, las células HepaRG imitan a los hepatocitos humanos expresando múltiples receptores nucleares, así como el citocromo P450, una amplia familia de hemoproteínas responsables del metabolismo oxidativo de los xenobióticos. Entre los receptores nucleares destaca el receptor nuclear PXR (*pregnane X receptor*), que activa los genes de la subfamilia CYP3A del citocromo P450, en respuesta a fármacos y otros xenobióticos (Guillouzo y col., 2007). En virtud del Reglamento REACH (*European Regulation on Registration, Evaluation, Authorisation and Restriction of Chemicals*), existe una necesidad de mejorar la seguridad de los compuestos químicos, empleando para ello ensayos *in vitro* alternativos, a fin de evitar ensayos innecesarios con animales. Por este motivo, la línea HepaRG presenta una alternativa prometedora para estudios de toxicidad *in vitro* y del metabolismo de xenobióticos. Además, mediante aproximaciones metabolómicas no dirigidas vamos a poder estudiar los cambios metabólicos que un determinado tratamiento con xenobióticos produce en células como las HepaRG. De esta manera, se puede obtener información sobre las alteraciones en el metabolismo celular, y por lo tanto, de los mecanismos a través de los cuales un determinado compuesto con bioactividad ejerce un efecto concreto en la fisiología de la célula.

En el trabajo que se anexa a este Capítulo (**Trabajo 4.3.1**) titulado "*Metabolomics of early metabolic changes in hepatic HepaRG cells in response to rosemary diterpenes exposure*", se ha llevado a cabo un estudio metabolómico del efecto de los principales diterpenos del romero (ácido carnósico, carnosol y rosmanol) en células HepaRG. Este artículo se ha enviado recientemente para su publicación en la revista Analytica Chimica Acta.

4.2. OBJETIVO Y PLAN DE TRABAJO

El objetivo de este Capítulo es:

- Estudio metabolómico del efecto tóxico de los diterpenos mayoritarios en romero, ácido carnósico, carnosol y rosmanol, en un modelo *in vitro* de células HepaRG, que imitan las funciones de las células hepáticas humanas.

Para conseguir dicho objetivo, se llevó a cabo el siguiente plan de trabajo:

a. Análisis de la viabilidad celular de dos líneas celulares de cáncer de cólon (HCT116 y HT-29), tratadas con diferentes concentraciones de diterpenos del romero (ácido carnósico, carnosol y rosmanol).

b. Análisis de la viabilidad celular de células hepáticas HepaRG diferenciadas y no diferenciadas tratadas con diferentes concentraciones de ácido carnósico, carnosol y rosmanol, de acuerdo con los resultados obtenidos en el objetivo anterior.

c. Extracción de los metabolitos de las células hepáticas HepaRG tratadas con los diterpenos fenólicos de romero y células hepáticas HepaRG sin tratar (control).

d. Análisis de los perfiles metabólicos del contenido intracelular de las células HepaRG tratadas y control mediante GC-TOF MS y UHPLC-TOF MS.

e. Procesado de los datos obtenidos, análisis estadístico y estudio comparativo de los perfiles metabólicos de las células HepaRG control vs. tratadas con los diterpenos ácido carnósico, carnosol y rosmanol.

4.3. PUBLICACIÓN RELACIONADA

4.3.1. Metabolomics of early metabolic changes in hepatic HepaRG cells in response to rosemary diterpenes exposure

Acunha, T., García-Cañas, V., Valdés, A., Cifuentes, A., Simó, C.

Enviado para su publicación a la revista Analytica Chimica Acta.

Metabolomics of early metabolic changes in hepatic HepaRG cells in response to rosemary diterpenes exposure

Tanize Acunha[a,c], Virginia García[b,*], Alberto Valdés[c], Alejandro Cifuentes[c], Carolina Simó[b,*]

[a]CAPES Foundation, Ministry of Education of Brazil, 70040-020 Brasília, DF, Brazil.

[b]Molecular Nutrition and Metabolism, Institute of Food Science Research (CIAL, CSIC), Nicolas Cabrera 9, 28049 Madrid, Spain.

[c]Laboratory of Foodomics, Institute of Food Science Research (CIAL, CSIC), Nicolas Cabrera 9, 28049 Madrid, Spain.

*Corresponding Authors: c.simo@csic.es, virginia.garcia@csic.es Tel: +34-910017900, Fax: +34-910017905

Abstract

Rosemary diterpenes have demonstrated diverse biological activities, such as anti-cancer, antiinflammatory, as well as other beneficial effects against neurological and metabolic disorders. In particular, carnosic acid (CA), carnosol (CS) and rosmanol (RS) diterpenes have shown interesting results on anti-cancer activity. However, little is known about the toxic effects of rosemary diterpenes at the concentrations needed to exert their antiproliferative effect on cancer cells. In our study, CA, CS and RS exhibited a concentration-dependent effect on cell viability of two human colon cancer cell lines (HT-29 and HCT116) after 24 h. HT-29 cell line was more resistant to the inhibitory effect of the three diterpenes than HCT116 cell line. Among the three diterpenes, RS exerted the strongest effect in both cell lines. To investigate the hepatotoxicity of CA, CS and RS, undifferentiated and differentiated HepaRG cells were exposed to increasing concentrations of the diterpenes (from 10 to 100 μM). Differentiated cells were found to be more resistant to the toxic activity of the three diterpenes than undifferentiated HepaRG, probably related to a higher detoxifying function of differentiated HepaRG cells compared with the undifferentiated cells. The metabolic profiles of differentiated HepaRG cells in response to CA, CS and RS were examined to determine biochemical

alterations and deepen the study of the effects of rosemary phenolic diterpenes at molecular level. A multiplatform metabolomics study based on liquid- and gas- chromatography hyphenated to high resolution mass spectrometry revealed that rosemary diterpenes exerted different effects when HepaRG cells were treated with the same concentration of each diterpene. RS revealed a greater metabolome alteration followed by CS and CA, in agreement with their observed cytotoxicity. Metabolomics provided valuable information about early events in the metabolic profiles after the treatment with the investigated diterpenes from rosemary.

Keywords: Metabolomics, HepaRG, rosemary, diterpenes, carnosic acid, carnosol, rosmanol

1. Introduction

Accumulating evidence from epidemiological and dietary intervention studies indicates that naturally occurring phytochemicals from vegetables and fruits may play a useful role in preventing a number of diseases [1]. Rosemary (*Rosmarinus officinallis*) is an herb, member of the mint family *Lamiaceae*, native to the Mediterranean region that has traditionally been used as flavouring or preserving agents in foods. Rosemary extracts have been used as a therapeutic agent in the treatment of a diversity of disorders [2] and have been well known for their antiinflamatory [3] and antimicrobial properties [4, 5]. The health promoting properties of rosemary have been attributed in part to the antioxidant activity of some of the phenolic diterpenes present in the extracts. Rosemary leaves are abundant in phenolic diterpenes such as carnosic acid (CA), carnosol (CS), rosmanol (RS), methyl carnosic acid, epirosmanol, epirosmanol methyl ether, among others [6]. In rosemary, CA and CS represent approximately 5% of the dry weight of the leaves, and they are estimated to account for more than 90% of the antioxidant activity [7]. In recent years, rosemary diterpenes are receiving increasing interest for a variety of health promoting properties such as antimicrobial [8], anti-inflammatory [9], neuroprotective [10, 11], antioxidant [12], and anticancer properties [13, 14, 15]. CA and CS interfere with a range of different cellular processes related to cell proliferation, invasiveness, tumorigenesis, and survival of cancer cells. In fact, the wide range of reported pleiotropic cellular and molecular effects conferred to CA and CS supports the idea that the underlying mechanisms of action of these compounds are diverse and complex. Recently, Foodomics has proven to be a useful approach to identify a wide range of molecular changes induced by rosemary diterpenes in *in vitro* cell models. For instance, previous transcriptomic and metabolomics studies have demonstrated that a CA-enriched rosemary extract alters the intracellular redox status [16, 17], and triggers a strong Nrf2-mediated antioxidant response in addition to the unfolded protein response to alleviate endoplasmic reticulum stress in cancer cells [18, 19, 20]. Furthermore, recent applications of bottom-up proteomic strategies have revealed new molecular targets of CS and have provided new insights regarding the role of autophagy and proteostasis in the cellular response to rosemary phenolic compounds in *in vitro* colon cancer cells [21, 22].

Regarding the safety of rosemary bioactive compounds and extracts, a published study showed that a single oral gavage dosage of 2,000 mg rosemary extract/kg of body weight did not cause evidences of toxicity in Wistar rats for two weeks [23]. Furthermore, Wang et al. [24] reported that the oral lethal dose for mice was 7,100 mg CA/kg body weight in an acute toxicity study, and that high-dose of CA (600 mg/kg per day) taken for 30 days also had toxic effects. In that study, histopathological analysis of mice tissues revealed that toxic doses exerted both liver and heart injury in mice. These studies suggest that rosemary extract and CA have relatively low oral toxicity; however, limited information is available about the safety of these compounds at doses in which they exert antiproliferative effects. For this reason, in the present work, the toxicity of a range of CA, CS and RS concentrations that are demonstrated to induce antiproliferative effects on colon cancer cells have been tested on HepaRG cells. This cell line has emerged as a very promising *in vitro* model able to display features of liver progenitor cells [25, 26] and it has shown great potential in toxicological studies [27, 28, 29]. In addition, a multiplatform metabolomics study has been carried out using complementary analytical techniques. Namely, reversed-phase (RP)-ultra high performance liquid chromatography (UHPLC) coupled with time-of-flight (TOF) MS and gas chromatography (GC)-TOF MS have been applied to investigate metabolite changes in HepaRG cells in response to individual rosemary diterpenes, RS, CA, and CS. The objectives of this study were, therefore, to determine the changes in metabolite quantities altered in HepaRG cells after diterpene exposures compared to untreated controls, and to detect differences between the metabolite profiles obtained in RS-, CA- and CS-treated cells in order to shed light on the specific metabolic pathways altered by each diterpene in hepatocyte-like cells.

2. Materials and methods

2.1. Reagents

Carnosic acid (CA), carnosol (CS), rosmanol (RS), phenyl-β-D-glucopyranoside, and heptadecanoic acid were obtained from Sigma-Aldrich (St. Louis, MO), ergosterol from Acros Organics (Geel, Belgium), and N-benzoyl-L-tyrosine from Fluka (Buchs, Switzerland). Reagent and solvents employed in the preparation of the UHPLC mobile phases were of MS grade: formic acid from Fluka

(Buchs, Switzerland), methanol (MeOH) and acetonitrile (ACN) from Sigma-Aldrich (St. Louis, USA). Water was purified in a Milli-Q system from Millipore (Bedford, USA). Reagents for derivatization: pyridine and N-Methyl-N- trimethylsilyltrifluoroacetamide with 1% Trimethylchlorosilane (MSTFA + 1% TMCS), were purchased from Thermo Fisher Scientific (Rockford, IL) and *O*-methoxyamine hydrochloride was from Sigma-Aldrich (St. Louis, MO). FAMEs (Fatty Acid Methyl Ester, chain lengths from C8-C30) and d27-myristc acid was purchased in form of the Fiehn GC/MS Metabolomics Standards Kit from Agilent Technologies (Santa Clara, CA).

2.2. Cell culture

Colon adenocarcinoma HT-29 and HCT-116 cells, obtained from ATCC (American Type Culture Collection, LGC Promochem, UK), were grown in McCoy's 5A medium (Lonza, USA) supplemented with 10% (v/v) heat inactivated Fetal Bovine Serum (Biowest , France), 50 U/mL penicillin G and 50 U/mL streptomycin (both from Lonza, USA) at 37 °C in humidified atmosphere and 5% CO_2. Cryopreserved undifferentiated HepaRG® cells and recommended culture media (Growth Medium Supplement®, Differentiation Medium Supplement® and Basal Hepatic cell medium) were obtained from Biopredict International (Saint-Gregoire, France). HepaRG cells were cultured and differentiated following manufacturer's indications at 37 °C and 5 % CO_2 (Biopredic Int., France). Briefly, the HepaRG cells were seeded at a cell density of 2.8 x 10^4 cells cm^{-2} and cultured in 710 growth medium (Biopredic Int.), which was refreshed every two or three days. After two weeks, cells were cultured in 720 differentiation medium (Biopredic Int.) for two additional weeks, resulting in differentiated HepaRG cell cultures. At that time, the cultures showed hepatocyte-like and primitive biliary cells morphology and were ready for treatment with the rosemary diterpenes for the metabolomics study.

2.3. Cell viability assay on colon cancer and HepaRG cells

MTT (3-(4,5-dimethyl-2-thiazolyl)-2,5-diphenyl-2H-tetrazolium bromide bromide) assay was performed on HT-29 and HCT-116 cancer cell lines to determine the effect of the different rosemary

diterpenes (CA, CS and RS) on cell viability. Briefly, cultured cells at ~50% confluence were trypsinized, neutralized with culture medium, seeded at 10,000 cells cm^{-2}, and allowed to adhere overnight at 37 °C. Afterwards, cells were treated with the vehicle (0.1% DMSO, v/v) regarded as untreated controls or with different concentrations (10-100 µM) of the diterpenes, and incubated for 24 h. After treatments, cells were incubated with serum-free medium containing MTT (0.5 mg mL^{-1}) at 37 °C for 4 h. The medium was removed, and the purple formazan crystals were dissolved in DMSO. Then, the absorbance at 570 nm was measured in a microplate reader (Synergy HT).

MTT assays were also conducted to determine the cytotoxic effect of the rosemary diterpenes (CA, CS and RS) on both, undifferentiated and differentiated HepaRG cells. In both assays, confluent undifferentiated HepaRG cells were trypsinized, seeded in 96-well plates, and allowed to adhere overnight at 37 °C. For the assay on undifferentiated HepaRG cells, 24 h after seeding, cells were incubated with different concentrations (10-100 µM) of the diterpenes for 24 h at 37 °C and 5% CO_2. For the assay on differentiated HepaRG cells, the cells were cultured for 14 days and differentiated for other 14 days at 37 °C and 5% CO_2 following the same procedure as mentioned in the previous section. Differentiated cells were then treated with different concentrations (10-100 µM) of the diterpenes (dissolved in DMSO) and incubated for 24 h at 37 °C and 5% CO_2. After treatments, the cells were incubated with William's E medium (supplemented with 2 mM L-glutamine and 25 mM HEPES) containing MTT (0.5 mg mL^{-1}) at 37 °C for 4 h. The medium was removed, and the purple formazan crystals were dissolved in DMSO. Then, the absorbance at 570 nm was measured as described for colon cancer cells. The results from MTT assays are provided as the mean of the percentage of treated minus control samples ± standard error of the mean (SEM) of at least three replicates.

2.4. Sample preparation for the metabolomic study.

Differentiated HepaRG cells were exposed to 60 µM of CA, CS and RS in William's Medium E (Lonza, Belgium) supplemented with 2 mM L-glutamine and 25 mM HEPES (Sigma Aldrich, USA) for 10 h. In parallel, HepaRG cells were exposed to the vehicle (0.1% DMSO) and regarded as

controls. After treatment, HepaRG cells were trypsinized, washed with PBS solution and centrifuged. Supernatants were removed and cells were resuspended in PBS and subjected to trypan blue exclusion assay to determine the number of viable cells present in the cell suspensions. Aliquots containing $4x10^6$ of cells were used for the metabolite extraction. The metabolite extraction protocol was based on a biphasic fraction procedure. Metabolites were extracted using 760 µL of a precooled MeOH-Water mixture (1:0.9, v/v) containing N-Benzoyl-L-tyrosine and phenyl-β-D-glucopyranoside as internal standards (IS). Each extract was vortexed until complete dissolution of the pellet and 400 µL of ice cold chloroform containing ergosterol and heptadecanoic acid as IS, was added. Cells extracts were then homogenized with cell disrupter at 30Hz for 10 minutes and centrifuged at 2200 g for 5 minutes at 4 °C. After layer separation, 640 µL of the polar fraction and 300 µL of the nonpolar fraction were transferred to new precooled tubes. 300 µL aliquots from each fraction were then evaporated to dryness using a nitrogen flow and stored at -80 °C until analysis. Dried polar and apolar aliquots were then re-suspended with methanol-water (1:1, v/v) and methanol, respectively, for UHPLC-MS analysis or derivatized for GC-MS analysis.

2.5. LC-MS metabolic profiling analysis

UHPLC-TOF analysis was carried out using a 1290 system from Agilent (Agilent Technologies, Santa Clara, CA, USA) coupled to a quadrupole-time-of-flight mass spectrometer (Q/TOF MS) Agilent 6540 equipped with an orthogonal electrospray ionization (ESI) source (Agilent Jet Stream, AJS). The applied strategy comprises two liquid chromatography approaches: RP chromatography for the polar and nonpolar fraction analysis, using C8 and C18 columns, respectively. The RP metabolomic profiling analysis of polar fraction was performed on an Agilent ZORBAX C8, Rapid Resolution HD (2.1 × 100 mm, 1.8 µm) using phase A (water with 0.01% (v/v) formic acid) and phase B (acetonitrile with 0.1% (v/v) formic acid), and following gradient program: 0% B (1 min), 0-30% B in 1-7 min, 30-100% B in 7-9 min, and 100% B in 9-11 min. For the RP metabolomic profiling analysis of nonpolar fraction an Agilent Zorbax Eclipse Plus C18 (2.1 × 50 mm, 1.8 µm) column was applied, using phase A (water with 0.01% (v/v) formic acid) and phase B (acetonitrile

with 0.1% (v/v) formic acid), and following gradient program: 0% B (0.5 min), 0-100% B in 0.5-9 min, and 100% B in 9-11 min. Before each run, columns were re-equilibrated for 4 min using the initial solvent composition. The flow rate was set constant at 0.5 mL min^{-1} and the column temperature was maintained at 30 °C for all separations. Two microliters of samples solution were injected for each analysis, and each sample was analyzed in duplicate. RP metabolic profiling analyses were achieved in both positive and negative mode. MS operation conditions were as follows: capillary voltages were set at -4000 V in the positive mode or 4000 V in the negative mode; nebulizer pressure at 40 psi, drying gas flow rate at 10 L min^{-1}, gas temperature at 350 °C and skimmer voltage at 45 V. Full scan data were collected in the TOF scan mode from 50 to 1100 m/z at 1.5 spectra s^{-1} for both ionization modes.

2.6. GC-MS metabolic profiling analysis

For derivatization process, the dried extract of samples were first oximated by adding 10 µL of methoxyamine hydrochloride solution in pyridine (40 mg mL^{-1}), mixed in a vortex mixer and subsequently shaken for 90 min at 30 °C. Afterward, 90 µL of N-methyl-N-trimetylsilyltrifluoroacetamide (MSTFA) with 1% trimethylchlorosilane (TMCS) and 2 µL of the FAME/d27-myristic acid mixture were added and shaken at 37 °C for 30 min to form trimethylsilyl (TMS) derivatives. GC-TOF MS analysis was performed using a 7890B system (Agilent) coupled to a quadrupole time-of-fight (Q/TOF) 7200 (Agilent) equipped with an electron ionization (EI). 1 µL of the prepared samples were injected with a split ratio of 10:1 and a split flow of 8.4 mL min^{-1} with the injector at a temperature of 250 °C. The separation of metabolites was achieved using an Agilent Zorbax DB5- MS + 10m Duragard Capillary Column (30 m x 250 µm x 0.25 µm). Helium was used as carrier gas at a constant flow rate of 0.8 mL min^{-1} through the column. The column temperature was maintained at 60 °C for 1 min, then increased at a rate of 10 °C min^{-1} to 325 °C, and held at this temperature for 10 min, MS parameters: electron impact ionization at 70 eV, filament source temperature of 250 °C, quadrupole temperature of 150 °C, m/z scan range 50-600 at a rate of 5 spectra

198 s^{-1}. Mass spectral signals were recorded after a 5.9 min solvent delay to avoid derivatization
199 interferences.

200

201 **2.7. MS data processing, statistical analysis and metabolite identification**

202 Raw data from LC-MS were processed by using the Molecular Feature Extraction (MFE) tool in
203 MassHunter Qualitative Analysis Software (version B.07.00, Agilent Technologies). For GC-MS
204 data, corresponding peak integration and deconvolution were achieved by "Find by Chromatographic
205 Deconvolution" tool on Mass Hunter Qualitative Analysis. Alignment of drift (by retention time and
206 mass) and data filtering were performed with Mass Profiler Professional (version 14.5, Agilent
207 Technologies). Metabolites that did not exist in 75% of samples in one group were filtered. The
208 metabolomic LC-MS data generated was subjected to non-supervised principal component analysis
209 (PCA) in a search of discriminant metabolomic patterns contributing to either generic or mechanism-
210 specific effect. To deepen the knowledge on the alterations caused by each specific phenolic
211 compound, pairwise comparisons (each phenolic diterpene *vs*. control) were performed, which led to
212 the identification of specific metabolites related to each action mechanism. Differences between
213 control and treated HepaRG cells were evaluated for individual metabolites using univariate statistical
214 analysis by unpaired t-test. A Benjamin Hochberg FDR correction was also applied to adjust the p-
215 values. A p-value <0.05 was considered significant to select metabolites. Accurate masses of features
216 with significant differences by LC-MS were searched against HMDB (http://www.hmdb.ca/),
217 METLIN (https://metlin.scripps.edu/), and LIPID MAPS (http://www.lipidmaps.org/) databases.
218 Compound identification by GC-MS was performed by comparing obtained mass spectra with those
219 available in the National Institute of Standards and Technology mass spectra library (NIST MS, v.
220 2.2) and by using the target metabolite Fiehn GC/MS Metabolomics RTL (Retention Time Locked)
221 library (G1676AA, Agilent Technologies).

222

223 **3. Results**

In the present work, the toxicity of a range of CA, CS and RS concentrations that are demonstrated to induce antiproliferative effects on colon cancer cells have been evaluated on HepaRG cells. In addition, a multiplatform metabolomics study has been carried out using C8/C18-UHPLC-TOF MS and GC-TOF MS to investigate metabolite changes in HepaRG cells in response to the individual rosemary diterpenes. The workflow used in the current study is shown in **Figure 1** and the obtained results are presented as follows:

3.1. In vitro effect of CA, CS and RS on HT-29 and HCT116 colon cancer cells viability

The effects of the three diterpenes depending on their concentration were assayed in exponentially growing HT-29 and HCT116 cells. To attain this, HT-29 and HCT116 cells were incubated with increasing concentrations of diterpenes (from 10 to 100 μM) for 24 h and cell viability was analyzed by the MTT assay. All the diterpenes exhibited a concentration-dependent effect after 24 h (**Figure 2**). As it is shown in **Figure 2**, HT-29 and HCT116 cell lines showed different sensitivity to the diterpenes. Specifically, HCT116 cells were less refractory to the cytotoxic effect of the three diterpenes than HT-29 cells. For instance, CS exhibited a strong cytotoxic effect at 40 μM in HCT116 cells (85% cell viability reduction), whereas the cell viability decrease obtained with the same concentration in the assays with HT-29 cells was well below that value (11 %).

3.2. Cell viability of HepaRG cells treated with CA, CS and RS

To investigate the hepatotoxic potential of CA, CS and RS, undifferentiated and differentiated HepaRG cells were incubated with increasing concentrations of the diterpenes (from 10 to 100 μM) for 24 h and cell viability was analyzed by the MTT assay (**Figure 3**). In undifferentiated cells, concentration-dependent reduction of cell viability was observed starting from 40 μM for CA (**Figure 3A, dark grey bars**), whereas this dependence started from 10 μM of the other two diterpenes (CS and RS; **Figure 3B and C**). As a general trend, undifferentiated HepaRG cells were more sensitive to the treatment with diterpenes than differentiated cells. In differentiated cells, the three diterpenes caused null or mild toxic effects at concentrations that are typically toxic (20-40 μM) in colon cancer

cells. Interestingly, RS treatment was the most effective compounds, reducing ~19% cell viability at 60 μM in differentiated cells after 24 h, whereas the same concentration of the other two diterpenes showed not significant (p-value > 0.05) effects in cell viability.

3.3. Metabolite profiling of HepaRG cells treated with CA, CS and RS

In order to investigate the changes in the relative abundance of metabolites altered in HepaRG cells by each diterpene exposure, differentiated HepaRG cells were exposed to 60 μM of CA, CS or RS for 10 h. As mentioned above, this diterpene concentration is highly toxic in colon cancer cell but only exerts mild or null toxicity in HepaRG cells. Cells were treated and processed as described in experimental sections and subsequently analyzed following a multiplatform metabolomics strategy. Trypan blue exclusion assay performed in control and treated HepaRG cells confirmed the mild toxic effect (17% dead cells relative to control) of 60 μM RS treatment after 10 h exposure, as well as the lack of toxic effects in cells treated with the same concentration of CS and CA (data not shown). After peak detection, alignment and filtering, different data matrices were obtained from C8/LC-MS in positive ionization mode (ESI+), C8/LC-MS in negative ionization mode (ESI-), C18/LC-MS (ESI+), C18/LC-MS (ESI-) and GC-EI-MS analyses. Namely, 1144 entities were detected in C8/LC-MS (ESI+), 613 entities in C8/LC-MS (ESI-), 2487 entities in C18/LC-MS (ESI+), 1022 entities in C18/LC-MS (ESI-), and 322 entities in GC-MS.

Principal components were generated by PCA to represent the major latent variables. PCA was chosen as explorative to visualize how the different treatments of HepaRG cells were able to reveal differences in the scores and the accompanying loadings. Two dimensional plots of PC1 *vs*. PC2 were generated from the different data matrices obtained from each analytical platform (see **Supplementary Figure 1**). In addition, all the information provided by the different analytical platforms and conditions for a given sample was joined to a single matrix, and PCA was carried out (**Figure 4**). The PCA score plot showed good separation between control cells and those treated with CA, CS and RS. The plot showed that the projection onto the first principal component (PC1) was effective in separating non-treated from phenolic diterpenes-treated HepaRG cells as can be seen in

Figure 4. The second principal component (PC2) separated CA treatment from CS and RS-treated cells.

In addition to multivariate data analysis, univariate analysis (t-test with post hoc Benjamini Hochberg (FDR) correction and $p<0.05$) was carried out foreach diterpene treatment *vs.* control HepaRG cells. The univariate statistical analysis revealed individual significant metabolites after CA treatment, yielding 21 statistically significant features in C8/LC-MS (ESI+), 11 in C8/LC-MS (ESI-), 17 in C18/LC-MS (ESI+), 18 in C18/LC-MS (ESI-), and 25 in GC-MS (data collected in **Supplementary Table 1**). The summary of the entities revealed as statistically significant by t-test after CS treatment is given in the **Supplementary Table 2;** briefly, 32 statistically significant features in C8/LC-MS (ESI+), 21 in C8/LC-MS (ESI-), 49 in C18/LC-MS (ESI+), 39 in C18/LC-MS (ESI-), and 35 in GC-MS, were obtained. The univariate analysis of metabolomics results from RS-treated HepaRG cells differentiated 74 entities in C8/LC-MS (ESI+), 55 in C8/LC-MS (ESI-), 110 in C18/LC-MS (ESI+), 46 in C18/LC-MS (ESI-), and 40 in GC-MS (data collected in **Supplementary Table 3**). A summary of tentatively identified metabolites with a p-value<0.05 in HepaRG cells treated with CA, CS and RS, is given in **Table 1**. As it is shown in **Table 1**, a wide variety of metabolite classes and subclasses were altered by the three diterpenes. To note, regarding fatty acid metabolism a number of different acylcarnitines and fatty acids were altered by the three rosemary diterpenes. Although the three diterpenes appear to affect the same metabolite classes, only ten of them were commonly observed in the three experimental conditions. The analysis indicated that the direction of the change in the ten common metabolites was the same. On the other hand, changes in metabolite classes specific to a CS and RS were also found. Hence, it could be observed glycerolypids class exclusively decreased in CS-treated cells. Futhermore, decreased levels in fatty acyl CoA and glycerophospholipids (except phosphatidylcholine), together with accumulation of lysophospholipids were exclusively observed in RS-treated cells.

Besides the metabolites summarized in **Table 1**, for improved information we focused on other biologically relevant metabolites that were statistically significant (p-value <0.05) but did not pass the restrictive Benjamin Hochberg FDR correction. Thus, alterations in well-known low-molecular-

weight oxidative stress markers were detected. Specifically, a decrease in reduced glutathione (GSH, p-value<0.0456; fold change (FC), -4.8) concomitant to a marked increase of oxidized glutathione (GSSG, p-value< 0.0047; FC, 3.8) was observed in RS-treated cells. Interestingly, the levels of GSH were also decreased (GSH, p-value< 0.0379; FC, -5.5) in CS-treated cells relative to control cells; however, in this case the change in GSSG levels induced by CS was not statistically significant (GSSG, p-value<0.3357; FC, 1.7). The levels of other metabolites involved in glutathione metabolism, such as gamma-glutamyl glutamine and S-lactoylglutathione, were also altered in RS-treated cells.

4. Discussion

Several articles have demonstrated the *in vitro* chemoprotective activity of rosemary extracts and phenolic diterpenes, namely CA and CS, at low concentrations (<10 μM) [12, 30]. However, interesting results have been also reported in studies evaluating the potency of these compounds in inhibiting cell proliferation and viability of cancer cell lines, activities commonly observed at concentrations within the medium micromolar range (25-100 μM) [31, 32]. Although some studies suggest that diterpene-enriched rosemary extracts and CA have relatively low oral toxicity; little is known about the toxic effects of rosemary diterpenes at the concentrations needed to exert antiproliferative effects on cancer cells. In line with this, liver and heart injuries were evidenced after administration of high oral doses of CA in mice in an acute toxicity study [24]. Regarding the *in vitro* toxicity evaluation, HepaRG cells have been successfully used to assess the hepatotoxicity of various drugs as alternative for primary human hepatocytes, referred to as the gold standard in hepatotoxicity studies [27-29]. HepaRG cells are derived from a hepatocellular carcinoma and when differentiate toward hepatocyte-like cells the mRNAs encoding metabolizing enzymes reach levels of expression close to those found in primary human hepatocytes [25, 26]. Therefore, their metabolic capacity is nearly similar to normal hepatic function and allows the investigation of metabolites generated by all hepatic enzymatic metabolism [25]. In addition, HepaRG cells mimic human hepatocytes with the expressions of multiple nuclear receptors and cytochromes P450, including pregnane X receptor

(PXR) and *CYP3A4* gene [33]. Thus, the consistent differentiation status, high viability and stable phenotype of HepaRG cells suggest that they may provide a useful model system for investigation of toxic responses *in vitro*. On the other hand, metabolomics represent a promising tool for studying the metabolic changes induced by xenobiotics as it can provide instantaneous snapshots of alterations in the cellular metabolism, providing meaningful information regarding the mechanisms through which an exogenous compound causes a particular effect in cell physiology [34]. To the best of our knowledge, there are not metabolomic studies on the effects of rosemary diterpenes in HepaRG cells.

In our present work, the results on the antiproliferative effect of individual diterpenes on HT-29 and HCT116 cells are in agreement with previous published results regarding the activity of these compounds in colon cancer cells [18, 22, 35-38]. Our data also reveals that HT-29 cell line was more resistant to the inhibitory effect of the three diterpenes than HCT116 cell line. A similar observation has been reported in a recent study on the effect of different diterpene-enriched rosemary extracts on these two cell lines [39]. It is also interesting to note that RS exerted the strongest effect among the three diterpenes in both cell lines, an observation that is also in the same line with the study performed with CS and RS in COLO205 cells by Cheng et al. [40].

Our results with HepaRG cells indicate that differentiated cells are more resistant to the toxic activity of the three diterpenes than undifferentiated HepaRG and colon cancer cells. This observation is consistent with a higher detoxifying function of differentiated HepaRG cells compared with the undifferentiated cells and the assayed colon cancer cells. It also highlights the relevance of the metabolizing features acquired during HepaRG cell differentiation for the detoxification of exogenous compounds. In line with this, published results obtained foe the less metabolically efficient HepG2 cells, a cell line commonly used in cytotoxicity testing, indicated that 100 μM CA decreased the number of viable cells by approximately 92% [41], whereas according to our data the same concentration of CA only reduces viability of differentiated HepaRG cells by 24%. Our results, are also in agreement with those reported by Dickmann et al. [42] demonstrating that 100 μM CA decreased viability of cultured cryopreserved human hepatocytes from three donors to less than 10% of untreated control cells.

In the present work, we implemented a metabolomic strategy to investigate early changes in metabolites levels in differentiated HepaRG cells after treatment with each individual rosemary diterpenes, CA, CS and RS. The great physicochemical diversity in addition to a wide concentration range of intracellular metabolites makes the metabolites extraction and separation major challenges in metabolomics. In this study a combined extraction method of amphiphilic and lipophilic metabolites, together with advanced analytical techniques as UHPLC-TOF MS, with two chromatography approaches (namely, C8 and C18), and GC-TOF MS, have been used in complementarity to provide a more comprehensive metabolomic snapshot of the biological system under study. A diterpene concentration that has been shown to be toxic in both colon cell lines, HT-29 and HCT116, was selected to study different effects in HepaRG metabolism. As mentioned above, 60 µM RS induced a toxic effect in absence of massive cell death after 10 h of exposure. This strategy allows detecting the initial specific effects of the diterpene on cell metabolism while longer times or treatments at higher concentrations may lead to the appearance of adaptation responses not directly related to the primary toxic effect or non-specific damages. To the opposite, 60 µM CA or CS exposures showed non-significant effects on the viability of differentiated cells. In this regard, metabolomic data permitted separation by the use of non-supervised data analysis with a two-component PCA model between non treated cells with those treated with the different phenolic diterpenes. Metabolomics analysis also revealed differences among the three treatments, which were found to be partially separated. Indeed, RS-treated HepaRG cell group, the toxic experimental condition assayed, was more distant to the other treatments and control cells in our PCA model. According to the metabolites statistically significantly altered after treatments with CA, CS and RS, both common and diterpene-specific altered metabolites, were observed. In general, RS treatment induced a greater metabolome alteration than CS and CA exposures, which reflects more extensive metabolic disequilibrium, concordant with the observed cytotoxic effect exerted by the former diterpene. Indeed, a good correlation between the changes in endogenous oxidative markers and cell toxicity was observed in RS-treated cells. Particularly, the alterations induced by 60 µM RS in GSH and GSSG levels relative to control cells are indicative of altered cellular redox homeostasis, increasing the possibilities for damage by oxidative stress, a condition that potentially can trigger cell death. Regarding the effects of CS

exposure, this diterpene induced a similar decrease in GSH levels compared to RS effect, but did not significantly elevated GSSG levels. GSH depletion in CS- and RS-treated cells may be due to GSH oxidation to GSSG or to the GSH consumption in conjugation reactions. In either case, further experiments are needed to deepen in the causal relationship of CS and RS treatment on GSH depletion in HepaRG cells. The results obtained with CS are in the same line as those reported in a study on the prooxidant activity of rosemary diterpenes (~40 μM) in *in vitro* assays in HT-29 cells [20]. On the other hand, Chen et al. [30] reported a transient increase of GSH in HepG2 cells after 12 h of treatment with non-toxic CS concentrations (≤ 10 μM). It was suggested this effect protected against damage from oxidative stress and it was associated to the transcriptionally induction of genes coding enzymes involved in GSH synthesis, mediated by Nrf2 transcription factor. However, in a recent proteomic study in HT-29 cells, cytostatic and cytotoxic CS concentrations within the medium micromolar range (40-70 μM) also induced a generalized Nrf2-mediated antioxidant response that included the expression of genes for GSH synthesis, among others [22]. These contrasting results suggest CS induces Nrf2-mediated response regardless the cell type and concentration, whereas its ability to alter intracellular GSSG and GSH levels might be concentration-dependent, and this alteration in some cases might be related with its associated toxicity.

In addition to alterations of cellular redox status, the most marked metabolic changes in the present study were those involving lipid metabolism, specifically sphingolipids and glycerophospholipids. Sphingolipids are not just the structural components of cell membrane, but bioactive molecules that participate in diverse functions controlling fundamental cellular processes such as cell division, differentiation, and cell death [43]. In our study, sphingolipids were mainly increased after diterpene treatments. According to the tentatively identified metabolites, sphingomyelin SM(d18:1/14:0) was increased in the HepaRG cells treated with the three diterpenes. Phytosphingosine and (4E,8E,10E-d18:3)sphingosine were found to be increased in CS- and RS-treated cells, whereas, shingosine and sphinganine were increased in HepaRG cells exposed to RS and CA, respectively. Sphingolipid metabolites such as ceramides, sphingosines, sphingosine 1-phosphates, and phytosphingosine have emerged as key regulators of apoptosis in a variety of cells [44, 45] and for this reason have attracted

increasing interest. Although phytosphingosine is structurally similar to sphingosine, the physiological roles of phytosphingosine are still largely unknown. It has been reported that phytosphingosine induces apoptotic cell death in human cancer cells both by caspase-dependent and -independent pathways [46, 47]. In this regard, further research is needed to understand the mechanisms by which CA, CS and RS regulate sphingolipid metabolism.

In terms of energy metabolism, experimental evidence showed that a CA-enriched rosemary extract increased cell glucose consumption and glycolysis in HepG2 by activation of AMPK-ACC pathway and altered the expression of SIRT1, PGC1α, and G6Pase genes [48]. This regulatory effect of the energy metabolism suggests a role for some rosemary constituents in blocking fatty acid synthesis and increasing β-oxidation. Similarly, Wang et al. [49] demonstrated that CA activated AMPK and inhibited palmitate-induced lipid accumulation in HepG2 cells and CA feeding decreased the fat accumulation in hepatocytes of leptin-deficient ob/ob mice (a model of type 2 diabetes with relatively mild hyperglycemia and obesity). In agreement with the data reported in the literature, in our study, the levels of free unsaturated fatty acids decreased in HepaRG cells upon CA exposure. Moreover, three acylcarnitines were also found to be altered in CA-treated cells. The primary function of acylcarnitines is to transport long chain fatty acids into the mitochondria, where they are required for β-oxidation. Because acylcarnitines are broken down for β-oxidation, their accumulation has been suggested as markers of mitochondrial dysfunction [50]. However, in our study, the accumulated and depleted state of the detected acylcarnitines varied depending on the acylcarnitine type. Regarding glucose metabolism, reported data in the literature suggests that CA-enriched rosemary extracts increases glycolysis, while decreases gluconeogenesis and glycogen content in HepG2 cells [48] and glucose uptake in muscle cells [51]. Our results indicated intriguing changes in various metabolites related with glycolysis and TCA cycle intermediates. Interestingly, intracellular pyruvic acid, lactic acid and succinic acid were depleted in all diterpene treatments, whereas accumulation of glucose was only observed in RS-treated cells. This last observation suggests that RS treatment impairs glucose utilization in contrast to the effects induced by CA and CS. Related with glucose metabolism, other

intriguing change in RS-treated HepaRG cells was the accumulation of S-lactoylglutathione in RS-treated cells. This metabolite is an intermediate of the methylglyoxal detoxification. Methylglyoxal is normally considered as a toxic by-product of protein and fatty acid metabolism, but the glycolytic pathway represents the most important endogenous source of methylglyoxal. High levels of this potent glycating agent occur when the concentrations of their precursors are elevated such as in impaired glucose utilization condition making its accumulation highly toxic for the cell [52]. In addition to the detected endogenous metabolites, we also detected significant accumulation in diterpene metabolites as the result of diterpene oxidation. For instance, in CS-treated cells accumulated carnosol and rosmadial, the oxidation product of rosmanol, suggesting that 10 h were not enough to totally detoxify 60 µM CS and its oxidation products.

5. Conclusions

In this study, the diterpenes CA, CS and RS, naturally occurring bioactive compounds originating from rosemary, have been selected for a first investigation of the early metabolic changes in hepatic HepaRG cells by metabolomics. The capabilities of metabolomics to assess the HepaRG cell responses to external stimuli have been demonstrated. The chemical diversity of the metabolites together to a large dynamic concentration range evidenced that more than a unique high-throughput approach is necessary to obtain ample metabolite coverage. After MS-based metabolomics study of HepaRG cells, substantial alterations induced by CA, CS and RS were revealed. The information achieved delivers a preliminary set of metabolites, evidencing some alterations on the metabolome of HepaRG derived from rosemary phenolic diterpenes exposure. Indeed, our results demonstrate the sensitivity of this comparative metabolomic approach to identify novel metabolic differences between the cytotoxic mechanism of RS and the non-toxic effects of CA and CS. The relative abundance of metabolites involved in redox and detoxifying reactions, lipid and glucose metabolism, was differentially altered upon exposure to CA, CS and RS, pointing to modifications in energy metabolism and redox homeostasis, which are key biochemical processes to sustain cell function.

Acknowledgements

This work was supported by an AGL2014-53609-P project (*Ministerio de Educación y Ciencia, Spain*). T.A. thanks the CAPES Foundation, Ministry of Education of Brazil for her pre-doctoral Scholarship-Proc. N 1532/13-8. We thank Dr. Guguen-Guillouzo, Dr. Gripon and Dr. Trepo who made HepaRG cells available.

REFERENCES

[1] R.H. Liu, Health-Promoting Components of Fruits and Vegetables in the Diet, Adv. Nutr. 4 (2013) 384S–392S.

[2] M.R. Al-Sereiti, K.M. Abu-Amer, P. Sen, Pharmacology of rosemary (*Rosmarinus officinalis* Linn.) and its therapeutic potentials, Indian J. Exp. Biol. 37 (1999) 124–130.

[3] C.-H. Peng, J.-D. Su, C.-C. Chyau, T.-Y. Sung, S.-S. Ho, C.-C. Peng, R.Y. Peng, Supercritical Fluid Extracts of Rosemary Leaves Exhibit Potent Anti-Inflammation and Anti-Tumor Effects, Biosci. Biotechnol. Biochem. 71 (2014) 2223–2232.

[4] S. Moreno, T. Scheyer, C.S. Romano, A. A. Vojnov, Antioxidant and antimicrobial activities of rosemary extracts linked to their polyphenol composition, Free Radic. Res. 40 (2006) 223–231.

[5] B. Bozin, N. Mimica-Dukic, I. Samojlik, E. Jovin, Antimicrobial and antioxidant properties of Rosemary and Sage (*Rosmarinus officinalis* L. and *Salvia officinalis* L., Lamiaceae) essential oils, J. Agric. Food Chem. 55 (2007) 7879–7885.

[6] I. Borrás-Linares, Z. Stojanović, R. Quirantes-Piné, D. Arráez-Román, J. Švarc-Gajić, A. Fernández-Gutiérrez, A. Segura-Carretero, *Rosmarinus officinalis* leaves as a natural source of bioactive compounds, Int. J. Mol. Sci. 15 (2014) 20585–20606.

[7] O. I. Aruoma, B. Halliwell, R. Aeschbach, J. Loligers, J. Antioxidant and pro-oxidant properties of active rosemary constituents: carnosol and carnosic acid, Xenobiotica 22 (1992) 257–268.

[8] S. Weckesser, K. Engel, B. Simon-Haarhaus, A. Wittmer, K. Pelz, C.M. Schempp, Screening of plant extracts for antimicrobial activity against bacteria and yeasts with dermatological relevance, Phytomedicine 14 (2007) 508–516.

[9] D. Poeckel, C. Greiner, M. Verhoff, O. Rau, L. Tausch, C. Hörnig, D. Steinhilber, M. Schubert-Zsilavecz, O. Werz, Carnosic acid and carnosol potently inhibit human 5-lipoxygenase and suppress pro-inflammatory responses of stimulated human polymorphonuclear leukocytes, Biochem. Pharmacol. 76 (2008) 91–97.

[10] S.J. Kim, J.S. Kim, H.S. Cho, H.J. Lee, S.Y. Kim, S. Kim, S.Y. Lee, H.S. Chun. Carnosol, a component of rosemary (*Rosmarinus officinalis* L.) protects nigral dopaminergic neuronal cells. Neuro Report 17 (2006) 1729–1733.

[11] M.R. de Oliveira, The Dietary Components Carnosic Acid and Carnosol as Neuroprotective Agents: a Mechanistic View, Mol. Neurobiol. 53 (2016) 6155–6168.

[12] T. Satoh, K. Kosaka, K. Itoh, A. Kobayashi, M. Yamamoto, Y. Shimojo, C. Kitajima, J. Cui, J. Kamins, S.I. Okamoto, M. Izumi, T. Shirasawa, S.A. Lipton, Carnosic acid, a catechol-type electrophilic compound, protects neurons both *in vitro* and *in vivo* through activation of the Keap1/Nrf2 pathway via S-alkylation of targeted cysteines on Keap1, J. Neurochem. 104 (2008) 1116–1131.

[13] J.J. Johnson, D.N. Syed, Y. Suh, C.R. Heren, M. Saleem, I.A. Siddiqui, H. Mukhtar. Disruption of androgen and estrogen receptor activity in prostate cancer by a novel dietary diterpene carnosol: implications for chemoprevention. Cancer Prev. Res. (Phila) 3 (2010) 1112–1123.

[14] S.M. Petiwala, J.J. Johnson, Diterpenes from rosemary (*Rosmarinus officinalis*): Defining their potential for anti-cancer activity, Cancer Lett. 367 (2015) 93–102.

[15] A. Niedzwiecki, M.W. Roomi, T. Kalinovsky, M. Rath, Anticancer efficacy of polyphenols and their combinations, Nutrients. 8 (2016) 552.

[16] C. Ibáñez, C. Simó, V. García-Cañas, Á. Gómez-Martínez, J.A. Ferragut, A. Cifuentes, CE/LC-MS multiplatform for broad metabolomic analysis of dietary polyphenols effect on colon cancer cells proliferation, Electrophoresis. 33 (2012a) 2328–2336.

[17] C. Ibáñez, A. Valdés, V. García-Cañas, C. Simó, M. Celebier, L. Rocamora-Reverte, Á. Gómez-Martínez, M. Herrero, M. Castro-Puyana, A. Segura-Carretero, E. Ibáñez, J.A. Ferragut, A. Cifuentes, Global Foodomics strategy to investigate the health benefits of dietary constituents, J. Chromatogr. A. 1248 (2012b) 139–153.

[18] A.Valdés, V. García-Cañas, C. Simó, C. Ibáñez, V. Micol, J.A. Ferragut, A. Cifuentes, Comprehensive foodomics study on the mechanisms operating at various molecular levels in cancer cells in response to individual rosemary polyphenols, Anal. Chem. 86 (2014) 9807–9815.

[19] A.Valdés, G. Sullini, E. Ibáñez, A. Cifuentes, V. García-Cañas, Rosemary polyphenols induce unfolded protein response and changes in cholesterol metabolism in colon cancer cells, J. Funct. Foods. 15 (2015) 429–439.

[20] A.Valdés, V. García-Cañas, E. Koçak, C. Simó, A. Cifuentes, Foodomics study on the effects of extracellular production of hydrogen peroxide by rosemary polyphenols on the anti-proliferative activity of rosemary polyphenols against HT-29 cells, Electrophoresis. (2016) 1795–1804.

[21] A.Valdés, K.A. Artemenko, J. Bergquist, V. García-Cañas, A. Cifuentes, Comprehensive proteomic study of the antiproliferative activity of a polyphenol-enriched rosemary extract on colon cancer cells using nanoliquid chromatography-Orbitrap MS/MS, J. Proteome Res. 15 (2016) 1971–1985.

[22] A.Valdés, V. García-Cañas , K.A.Artemenko, C. Simó, J.Bergquist, A. Cifuentes, Nano-liquid chromatography-orbitrap MS-based quantitative proteomics reveals differences between the mechanisms of action of carnosic acid and carnosol in colon cancer cells. Mol Cell Proteomics*16* (2017) 8–22.

[23] A. Anadón, M.R. Martínez-Larrañaga, M. A. Martínez, I. Ares, M.R. García-Risco, F.J. Señoráns, G. Reglero, Acute oral safety study of rosemary extracts in rats., J. Food Prot. 71

548 (2008) 790–795.

549 [24] Q.L. Wang, H. Li, X.X. Li, C.Y. Cui, R. Wang, N.X. Yu, L.X. Chen, Acute and 30-day oral
550 toxicity studies of administered carnosic acid, Food Chem. Toxicol. 50 (2012) 4348–4355.

551 [25] T.B. Andersson, K.P. Kanebratt, J.G. Kenna, The HepaRG cell line: a unique in vitro tool for
552 understanding drug metabolism and toxicology in human., Expert Opin. Drug Metab.
553 Toxicol. 8 (2012) 909–920.

554 [26] A. Guillouzo, A. Corlu, C. Aninat, D. Glaise, F. Morel, C. Guguen-Guillouzo, The human
555 hepatoma HepaRG cells: A highly differentiated model for studies of liver metabolism and
556 toxicity of xenobiotics, Chem. Biol. Interact. 168 (2007) 66–73.

557 [27] N. Van den Eede, M. Cuykx, R.M. Rodrigues, K. Laukens, H. Neels, A. Covaci, T.
558 Vanhaecke, Metabolomics analysis of the toxicity pathways of triphenyl phosphate in
559 HepaRG cells and comparison to oxidative stress mechanisms caused by acetaminophen,
560 Toxicol. Vitr. 29 (2015) 2045–2054.

561 [28] S. Anthérieu, C. Chesné, R. Li, C. Guguen-Guillouzo, A. Guillouzo, Optimization of the
562 HepaRG cell model for drug metabolism and toxicity studies, Toxicol. Vitr. 26 (2012) 1278–
563 1285.

564 [29] M.R. McGill, H.-M. Yan, A. Ramachandran, G.J. Murray, D.E. Rollins, H. Jaeschke,
565 HepaRG cells: A human model to study mechanisms of acetaminophen hepatotoxicity,
566 Hepatology. 53 (2011) 974–982.

567 [30] H. Chen, H. Chen, C. Hsieh, Y. Yang, U. Wung, Upregulation of NF-E2-related factor-2-
568 dependent glutathione by carnosol provokes a cytoprotective response and enhances cell
569 survival., Acta Pharmacol. Sin. 32 (2011) 62–69.

570 [31] Y. I. Ishida, M. Yamasaki, C. Yukizaki, K. Nishiyama, H. Tsubouchi, A. Okayama, H.
571 Kataoka, Carnosol, rosemary ingredient, induces apoptosis in adult T-cell

leukemia/lymphoma cells via glutathione depletion: Proteomic approach using fluorescent two-dimensional differential gel electrophoresis, Hum. Cell. 27 (2014) 68–77.

[32] Y. Al Dhaheri, S. Attoub, G. Ramadan, K. Arafat, K. Bajbouj, N. Karuvantevida, S. AbuQamar, A. Eid, R. Iratni, Carnosol induces ROS-mediated beclin1-independent autophagy and apoptosis in triple negative breast cancer, PLoS One. 9 (2014) e109630.

[33] S. Anthérieu, C. Chesné, R. Li, S. Camus, A. Lahoz, L. Picazo, M. Turpeinen, A. Tolonen, J. Uusitalo, C. Guguen-Guillouzo, A. Guillouzo Stable expression, activity, and inducibility of cytochromes P450 in differentiated HepaRG cells, Drug Metab Dispos 38 (2010) 516–525.

[34] J.C. García- Cañaveras, J. V. Castell, M.T. Donato, A. Lahoz, A metabolomics cell-based approach for anticipating and investigating drug-induced liver injury, Sci. Rep. 6 (2016) 27239.

[35] M. V. Barni, M.J. Carlini, E.G. Cafferata, L. Puricelli, S. Moreno, Carnosic acid inhibits the proliferation and migration capacity of human colorectal cancer cells, Oncol. Rep. 27 (2012) 1041–1048.

[36] J.M. Visanji, D.G. Thompson, P.J. Padfield, Induction of G2/M phase cell cycle arrest by carnosol and carnosic acid is associated with alteration of cyclin A and cyclin B1 levels, Cancer Lett. 237 (2006) 130–136.

[37] J.E. Park, B. Park, I.G. Chae, D.H. Kim, J. Kundu, J.K. Kundu, K.S. Chun, Carnosic acid induces apoptosis through inactivation of Src/STAT3 signaling pathway in human renal carcinoma Caki cells, Oncol. Rep. 35 (2016) 2723–2732.

[38] M. Yan, G. Li, S.M. Petiwala, E. Householter, J.J. Johnson, Standardized rosemary (*Rosmarinus officinalis*) extract induces Nrf2/sestrin-2 pathway in colon cancer cells, J. Funct. Foods. 13 (2015) 137–147.

[39] A. Sánchez-Camargo, V. García-Cañas, M. Herrero, A. Cifuentes, E. Ibáñez, Comparative

Study of Green Sub- and Supercritical Processes to Obtain Carnosic Acid and Carnosol-Enriched Rosemary Extracts with in Vitro Anti-Proliferative Activity on Colon Cancer Cells, Int. J. Mol. Sci. 17 (2016) 2046.

[40] A.C. Cheng, M.F. Lee, M.L. Tsai, C.S. Lai, J.H. Lee, C.T. Ho, M.H. Pan, Rosmanol potently induces apoptosis through both the mitochondrial apoptotic pathway and death receptor pathway in human colon adenocarcinoma COLO 205 cells, Food Chem. Toxicol. 49 (2011) 485–493.

[41] Q. Xiang, Y. Ma, J. Dong, R. Shen, Carnosic acid induces apoptosis associated with mitochondrial dysfunction and Akt inactivation in HepG2 cells., Int. J. Food Sci. Nutr. 66 (2015) 76–84.

[42] L.J. Dickmann, B.M. Vandenbrink, Y.S. Lin, In vitro hepatotoxicity and cytochrome P450 induction and inhibition characteristics of carnosic acid, a dietary supplement with antiadipogenic properties, Drug Metab. Dispos. 40 (2012) 1263–1267.

[43] Y.A. Hannun, L.M. Obeid, Principles of bioactive lipid signalling: lessons from sphingolipids., Nat. Rev. Mol. Cell Biol. 9 (2008) 139–150.

[44] W.C. Hung, H.C. Chang, L.Y. Chuang, Activation of caspase-3-like proteases in apoptosis induced by sphingosine and other long-chain bases in Hep3B hepatoma cells., Biochem. J. 338 (1999) 161–166.

[45] Huang, C. Freter, Lipid metabolism, apoptosis and cancer therapy, Int. J. Mol. Sci. 16 (2015) 924–949.

[46] M. Park, J.A. Kang, J. Choi, C. Kang, T. Kim, S. Bae, Phytosphingosine Induces Apoptotic Cell Death via Caspase 8 Activation and Bax Translocation in Human Cancer Cells Phytosphingosine Induces Apoptotic Cell Death via Caspase 8 Activation and Bax Translocation in Human Cancer Cells 1, Clin. Cancer Res. 9 (2003) 878–885.

[47] Y. Nagahara, T. Shinomiya, S. Kuroda, N. Kaneko, R. Nishio, M. Ikekita, Phytosphingosine induced mitochondria-involved apoptosis, Cancer Sci. 96 (2005) 83–92.

[48] Z. Tu, T. Moss-Pierce, P. Ford, T.A. Jiang, Rosemary (*Rosmarinus officinalis* L.) extract regulates glucose and lipid metabolism by activating AMPK and PPAR pathways in HepG2 cells, J. Agric. Food Chem. 61 (2013) 2803–2810.

[49] T. Wang, Y. Takikawa, T. Tabuchi, T. Satoh, K. Kosaka, K. Suzuki, Carnosic acid (CA) prevents lipid accumulation in hepatocytes through the EGFR/MAPK pathway, J. Gastroenterol. 47 (2012) 805–813.

[50] M.R. McGill, F. Li, M.R. Sharpe, C.D. Williams, S.C. Curry, X. Ma, H. Jaeschke, Circulating acylcarnitines as biomarkers of mitochondrial dysfunction after acetaminophen overdose in mice and humans, Arch. Toxicol. 88 (2014) 391–401.

[51] M. Naimi, T. Tsakiridis, T.C. Stamatatos, D.I. Alexandropoulos, E. Tsiani, Increased skeletal muscle glucose uptake by rosemary extract through AMPK activation., Appl. Physiol. Nutr. Metab. 40 (2015) 407–413.

[52] I. Allaman, M. Bélanger, P.J. Magistretti, Methylglyoxal, the dark side of glycolysis, Front. Neurosci. 9 (2015) 1–12.

Table 1. Compounds statistically significant (by t test and FDR correction with p-value<0.05) identified by UHPLC-MS and GC-MS for HepaRG cells exposed to CA, CS and RS.

Class, *subclass*	***Metabolite***	**ID[a]** ***(HMDB , LMSD or Metlin)***	**Molecular formula**	***Treatment***		
				CA	***CS***	***RS***
Fatty acids and derivatives						
FA (straight chain)	Palmitic acid	HMDB00220	C16H32O2	NS[b]	up	up
FA (unsaturated)	Octadecadienoic acid	HMDB00673	C18H32O2	down	down	down
FA (straight chain)	Nonadecanoic acid	HMDB00772	C19H38O2	NS	up	NS
FA (unsaturated)	9Z-hexadecenoic acid	HMDB03229	C16H30O2	down	NS	NS
FA (unsaturated)	13Z-Octadecenoic acid	HMDB62218	C18H34O2	down	down	down
N-acylamide	N-stearoyl valine	75504	C23H45NO3	NS	NS	down
N-acylamide	N-palmitoyl alanine	75505	C19H37NO3	down	NS	NS
Carnitine metabolites						
Acylcarnitine	Decanoylcarnitine	HMDB00651	C17H33NO4	NS	down	down
Acylcarnitine	Dodecanoylcarnitine	HMDB02250	C19H37NO4	NS	up	up
Acylcarnitine	Arachidylcarnitine	HMDB06460	C27H53NO4	NS	NS	down
Acylcarnitine	9-Decenoylcarnitine	HMDB13205	C17H31NO4	up	up	up
Acylcarnitine	trans-2-Dodecenoylcarnitine	HMDB13326	C19H35NO4	up	up	up
Acylcarnitine	Pivaloylcarnitine, Valerylcarnitine, 2-Methylbutyroylcarnitine, Isovalerylcarnitine	HMDB41993[c]	C12H23NO4	down	NS	NS
Acylcarnitine	3-hydroxypentadecanoyl carnitine	HMDB61641	C22H43NO5	NS	up	NS
Fatty esters (Fatty acyl CoA)						
Fatty acyl CoA	S3-Hydroxytetradecanoyl-CoA	HMDB03934	C35H62N7O18P3S	NS	NS	down
Sterols						
Sterol	Cholesterol	HMDB00067	C27H46O	up	NS	NS
Bile acid	Taurocholic acid	HMDB00036	C26H45NO7S	NS	down	down
Bile salt	Lithocholyltaurine	HMDB00722	C26H45NO5S	NS	NS	up
Steroid	6-Dehydrotestosterone glucuronide	HMDB10337	C25H34O8	up	NS	NS
Glycerolipids						
DAG	DG(15:0/0:0/16:1n7)	HMDB55988	C34H64O5	NS	down	NS
TAG	2,3-Diacetoxypropyl stearate	HMDB59931	C25H46O6	NS	down	NS
Glycerophospholipids						
diacylglycerophosphoglycerol	PG(16:0/16:0)	HMDB10570	C38H75O10P	NS	NS	down
glycerophosphocholine	PC(0-12:0/0-1:0)	40186	C21H46NO6P	NS	up	NS
glycerophosphate	PA(P-18:0/20:4(5Z,8Z,11Z,14Z))	82331	C41H73O7P	NS	NS	down
glycerophosphoserine	PS(16:1(9Z)/14:1(9Z))	77868	C35H69O10P	NS	NS	down
glycerophosphoserine	PS(O-18:0/13:0)	78666	C37H74NO9P	NS	NS	down
monoacylglycerophosphate	PA(17:1/0:0)	3887	C20H39O7P	NS	NS	down
phosphatidylcholine	PC(14:0/P-18:1(11Z))	HMDB07897	C40H78NO7P	NS	NS	up
Lysophospholipid						

	LysoPC, LysoPE	HMDB10381, HMDB11129	C23H48NO7P	NS	NS	up
	LysoPE(0:0/16:0)	HMDB11473	C21H44NO7P	NS	NS	up
Sphingolipids						
Ceramide	CerP(d18:1/18:0)	HMDB10701	C36H72NO6P	NS	NS	down
Sphingoid base homolog	C16 Sphinganine	LMSP01040001	C16H35NO2	NS	down	NS
Sphingoid base homolog	6-hydroxysphingosine	LMSP01080003	C18H37NO3	down	NS	NS
Sphingoid base homolog	(4E,8E,10E-d18:3)sphingosine	LMSP01080013	C18H33NO2	NS	up	up
Sphingoid base	Sphingosine	HMDB00252	C18H37NO2	NS	NS	up
Sphingoid base	Sphinganine	HMDB00269	C18H39NO2	up		
Sphingoid base	Phytosphingosine	HMDB04610	C18H39NO3	NS	up	up
Sphingomyelin	SM(d18:1/14:0)	HMDB12097	C37H75N2O6P	up	up	up
AA and derivatives						
AA	Glutamic acid	HMDB00148	C5H9NO4	NS	down	down
AA	Alanine	HMDB00161	C3H7NO2	down	down	down
AA	Lysine	HMDB00182	C6H14N2O2	NS	down	NS
AA	Serine	HMDB00187	C3H7NO3	NS	NS	down
AA	N-Acetylserine	HMDB02931	C5H9NO4	NS	down	down
AA	Valine, Betaine	HMDB00883, HMDB00043	C5H11NO2	up	NS	NS
n-acyl-alpha AA	N-Phenylacetyl-L-glutamine	HMDB06344	C13H16N2O4	NS	NS	up
n-acyl-alpha AA	N-heptanoylglycine	HMDB13010	C9H17NO3	down	NS	NS
Nucleosides and nucleotides						
Nucleoside	Adenosine	HMDB04401	C10H13N5O4	NS	NS	up
Nucleotide	Inosinic acid	HMDB00175	C10H13N4O8P	NS	up	NS
Nucleotide	Uracil	HMDB00300	C4H4N2O2	down	NS	down
Peptides						
	Asparaginyl-Tyrosine	HMDB28743	C13H17N3O5	NS	up	NS
	Tetrapeptide (Phe, Val, Met, Phe)	243563/241283[c]	C28H38N4O5S	NS	NS	down
	Dipeptide (Asn, Cys)	85684/85643[c]	C7H13N3O4S	NS	NS	up
	Tetrapeptide (Asn, Asn, Asn, Ser)	228110/197710[c]	C15H25N7O9	NS	NS	up
	Tetrapeptide (Trp Phe Ser Thr)	253803/253575[c]	C27H33N5O7	NS	NS	up
	Peptide (Leu/Ile, Ala, Gly, Arg)	181084/181179[c]	C17H33N7O5	NS	down	NS
Polyamines						
	N1-Acetylspermidine, N8-Acetylspermidine	HMDB01276, HMDB02189	C9H21N3O	NS	up	NS
Vitamins and related metabolites						
Niacin precursor	L-Kynurenine	HMDB00183	C10H12N2O3	NS	NS	up
Nicotinamide metabolite	1-methylnicotinamide	HMDB00699	C7H9N2O	down	NS	NS
Vitamin B5	Pantothenic acid	HMDB00210	C9H17NO5	NS	NS	up
Carboxylic acids						
dicarboxylic	Methylmalonic acid	HMDB00202	C4H6O4	NS	down	NS
dicarboxylic	Oxalic acid	HMDB02329	C2H2O4	down	down	down
dicarboxylic	Succinic acid	HMDB00254	C4H6O4	down	down	down
tricarboxylic	Citric acid	HMDB00094	C6H8O7	up	NS	NS
Other metabolites						
	Glucose	HMDB00122	C6H12O6	NS	NS	up

Pyruvic acid	HMDB00243	C3H4O3	down	down	down
3-hydroxybutyrate	HMDB00357	C4H8O3	NS	down	down
S-Lactoylglutathione	HMDB01066	C13H21N3O8S	NS	NS	up
Carnosol	HMDB02121	C20H26O4	NS	up	NS
Rosmadial	HMDB38219	C20H24O5	NS	up	NS
Isorosmanol/Epirosmanol	HMDB36661/ HMDB35812	C20H26O5	NS	NS	up
Uric acid	HMDB00289	C5H4N4O3	NS	NS	down
Lactic acid	HMDB03328	C3H6O3	down	down	down
Hydroxyvaleric acid	HMDB01863	C5H10O3	NS	down	down

a) ID from the Human Metabolome Database (HMDB) is given. Alternatively, ID from LIPID MAPS Database (LMSD) or METLIN database are given.
b) NS: This metabolite was not statistically significant in treated HepaRG cells with regard to non-treated cells
c) More than one identifier

Figure captions

Figure 1. Workflow of the study.

Figure 2. Viability HT-29 (dark grey) and HCT116 (light grey) colon cancer cells exposed to different concentrations (10-100 µM) of CA (A), CS (B) and RS (C) for 24h. (* indicates significant differences between the treated and control samples as determined by t-test, $P < 0.05$). Error bars represent standard error of the mean (SEM).

Figure 3. Viability of undifferentiated (dark grey) and differentiated (light grey) HepaRG cells exposed to different concentrations (10-100 µM) of CA (A), CS (B) and RS (C) for 24h. (* indicates significant differences between the treated and control samples as determined by t-test, $P < 0.05$). Error bars represent standard error of the mean (SEM).

Figure 4. Score plot for PCA model built with the whole dataset obtained from the different analytical platforms, for control HepaRG cells (black), and HepaRG cells exposed to CA (dark grey), CS (light grey) and RS (white). R2=0.515, Q2=0.02.

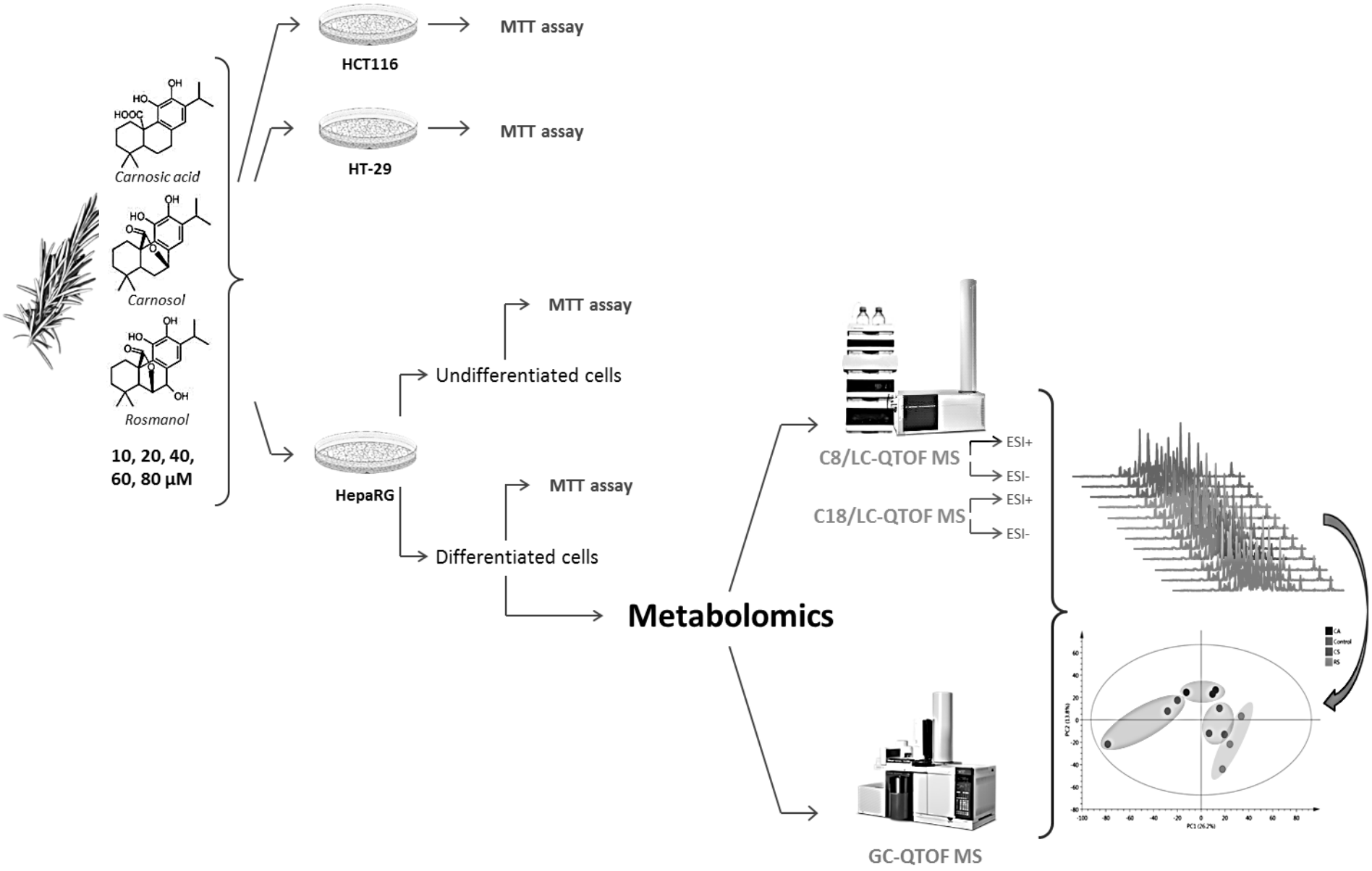
HCT116
MTT assay
HT-29
MTT assay
Carnosic acid
Carnosol
Rosmanol
10, 20, 40, 60, 80 µM
HepaRG
Undifferentiated cells
MTT assay
Differentiated cells
MTT assay
Metabolomics
C8/LC-QTOF MS
ESI+
ESI-
C18/LC-QTOF MS
ESI+
ESI-
GC-QTOF MS
CA
Control
CS
RS

Figure 1

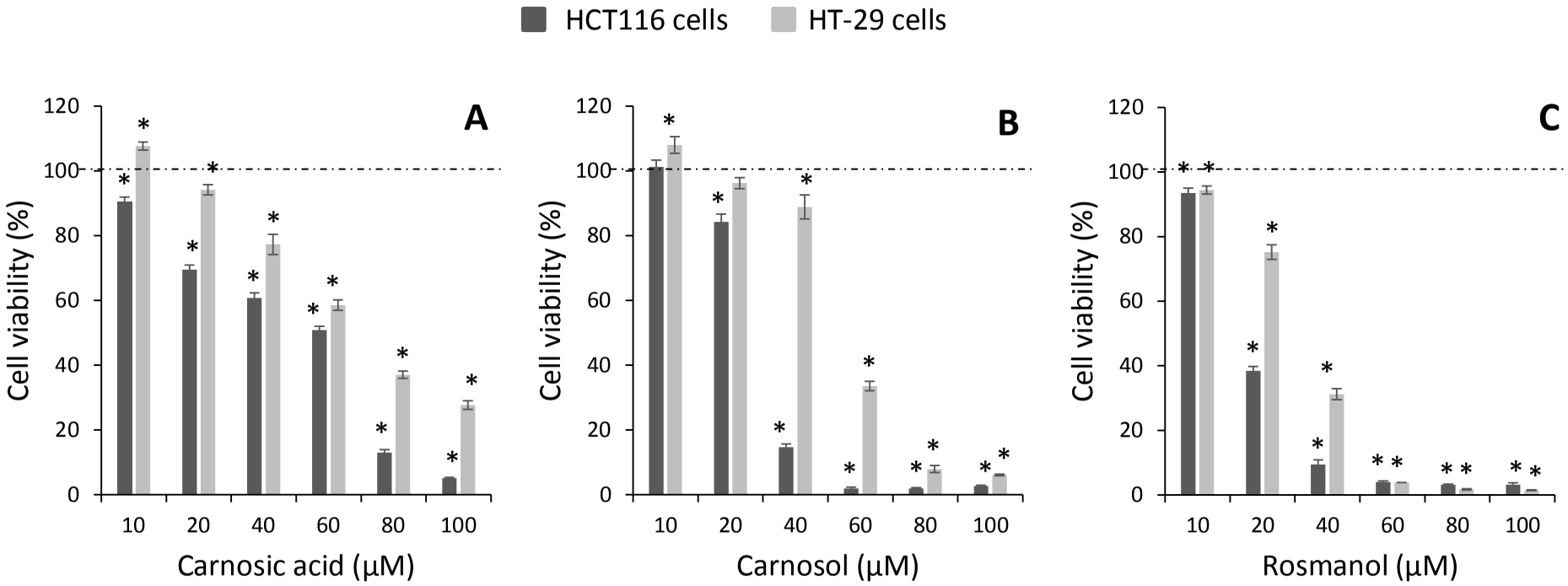
HCT116 cells
HT-29 cells
A
B
C
Cell viability (%)
120
100
80
60
40
20
0
10
20
40
60
80
100
Carnosic acid (μM)
Carnosol (μM)
Rosmanol (μM)

Figure 2

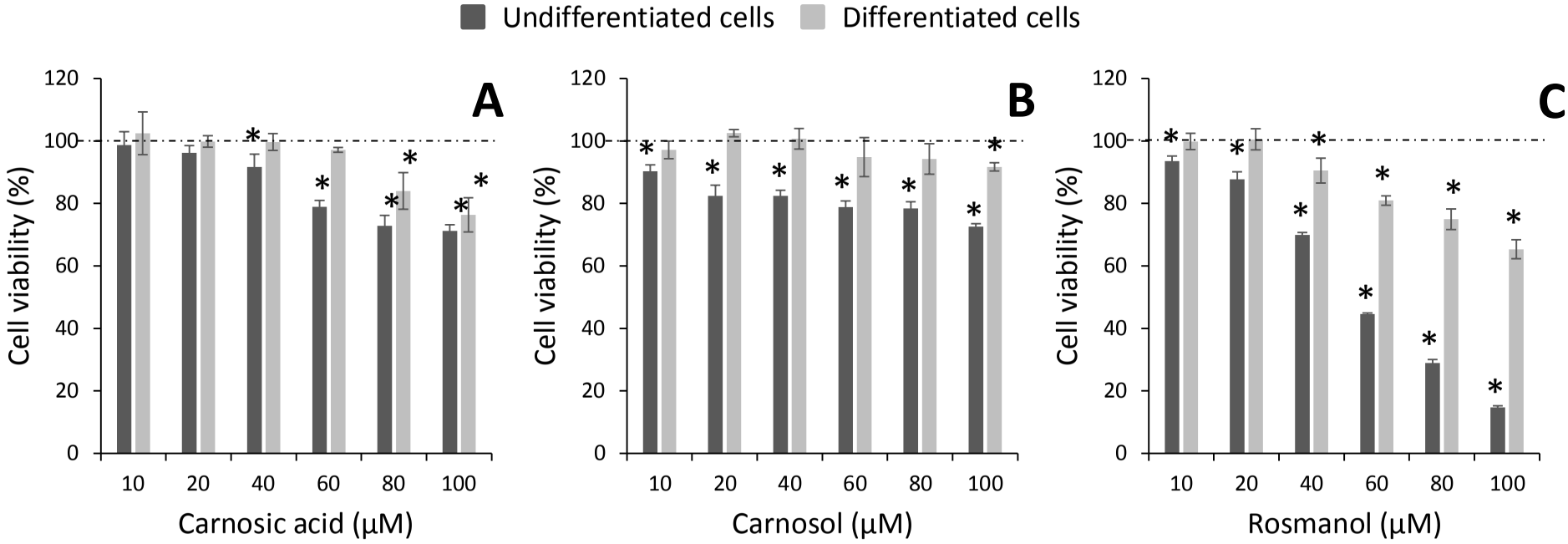
Undifferentiated cells
Differentiated cells
A
B
C
Cell viability (%)
120
100
80
60
40
20
0
10
20
40
60
80
100
Carnosic acid (µM)
Carnosol (µM)
Rosmanol (µM)
*

Figure 3

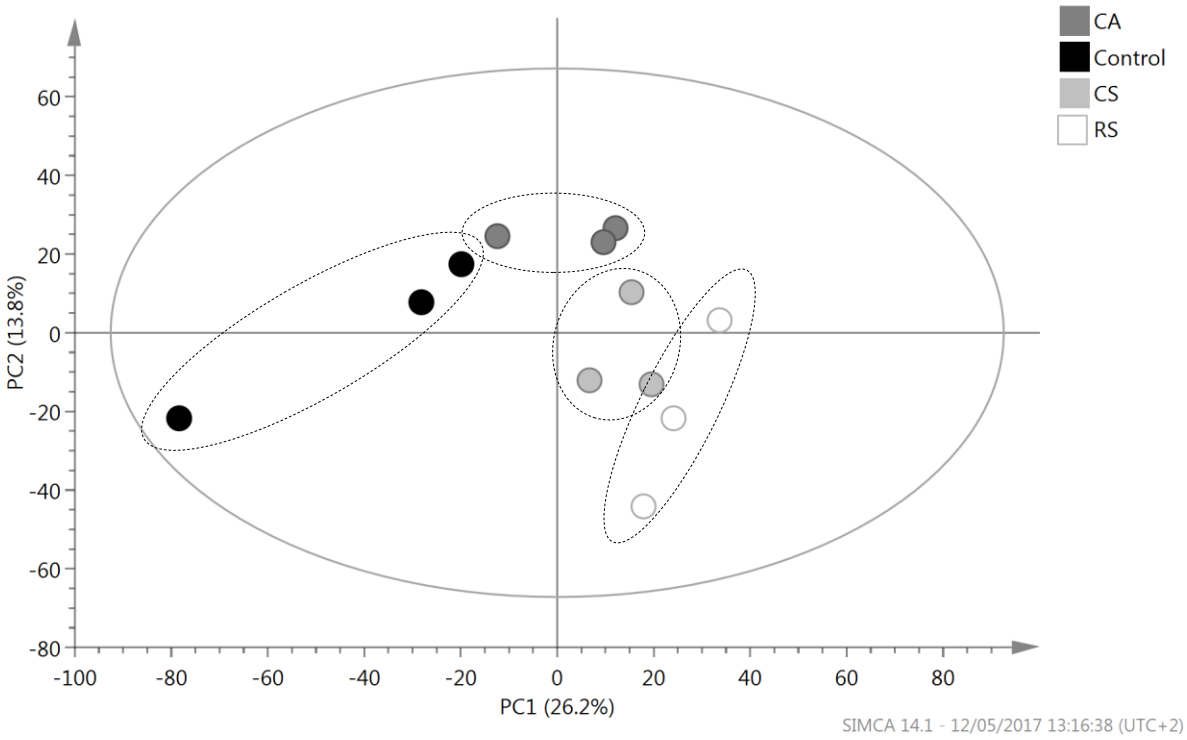
CA
Control
CS
RS
PC2 (13.8%)
PC1 (26.2%)
60
40
20
0
-20
-40
-60
-80
-100
-80
-60
-40
-20
0
20
40
60
80
SIMCA 14.1 - 12/05/2017 13:16:38 (UTC+2)

Figure 4

Supplementary Figure 1

PCA score plots of control (blue), CA-treated (green), CS-treated (red), and RS-treated (yellow) HepaRG cells. (A) C8/LC-MS, ESI+ (R^2 = 0.524, Q^2 = 0.075), (B) C8/LC-MS, ESI- (R^2 = 0.502, Q^2 = 0.044), (C) C18/LC-MS, ESI+ (R^2 = 0.623, Q^2 = 0.080), (D) C18/LC-MS, ESI- (R^2 = 0.587, Q^2 = 0.086), and (E) GC-MS (R^2 = 0.665, Q^2 = 0.177).

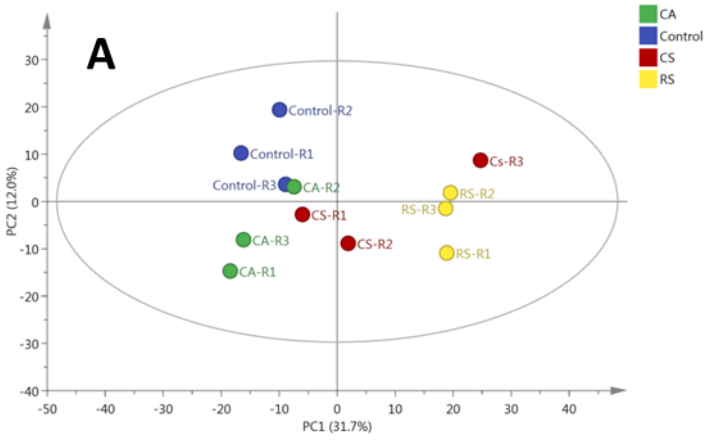

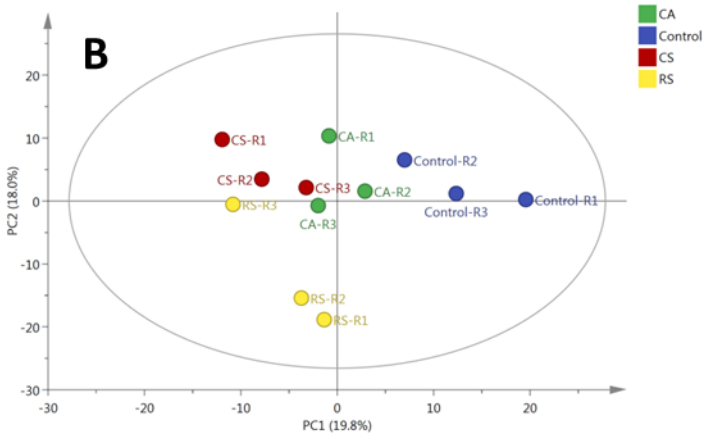

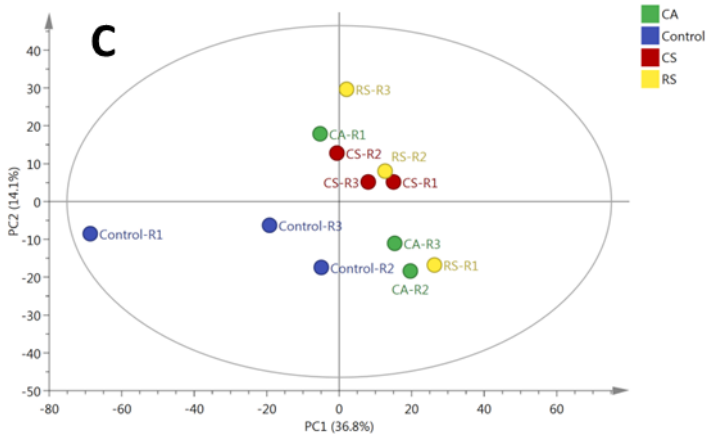
C
CA
Control
CS
RS
RS-R3
CA-R1
CS-R2
RS-R2
CS-R3
CS-R1
Control-R1
Control-R3
CA-R3
Control-R2
RS-R1
CA-R2
PC2 (14.1%)
PC1 (36.8%)

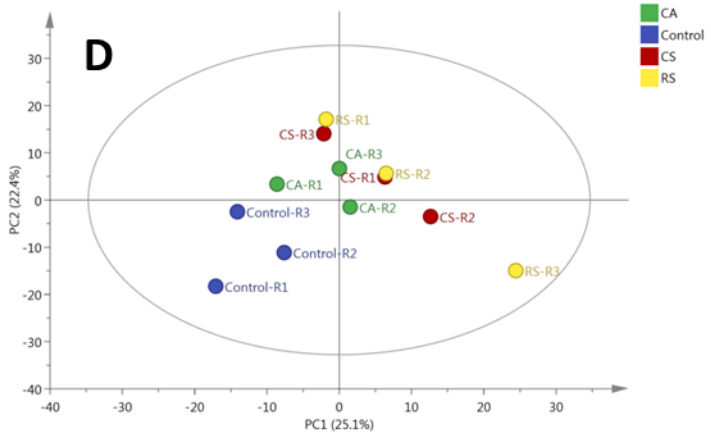
D
CA
Control
CS
RS
RS-R1
CS-R3
CA-R3
CS-R1
RS-R2
CA-R1
Control-R3
CA-R2
CS-R2
Control-R2
RS-R3
Control-R1
PC2 (22.4%)
PC1 (25.1%)

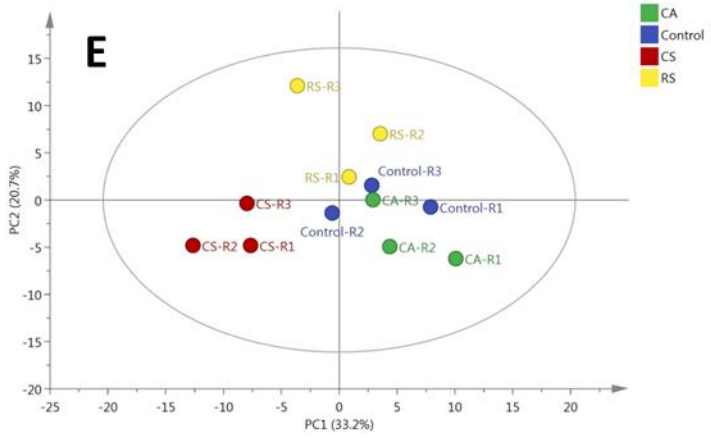
E
CA
Control
CS
RS
RS-R3
RS-R2
RS-R1
Control-R3
CS-R3
CA-R3
Control-R1
Control-R2
CS-R2
CS-R1
CA-R2
CA-R1
PC2 (20.7%)
PC1 (33.2%)

Supplementary Table 1. Differentiating metabolites between carnosic acid-treated cells and control cells.

Results from C8/LC-MS with ESI in positive mode

No.	*Mass*	*Retention Time*	*p (Corr)*	*Regulation*
CA-C8pos-001	234.1582	0.612	4.79231E-02	up
CA-C8pos-002	117.0792	0.617	1.97028E-02	up
CA-C8pos-003	245.1631	4.579	1.17149E-02	down
CA-C8pos-004	187.1212	5.402	4.27920E-02	down
CA-C8pos-005	434.1602	8.412	2.69920E-02	down
CA-C8pos-006	541.8991	8.510	1.47755E-02	down
CA-C8pos-007	157.1471	8.652	1.17149E-02	up
CA-C8pos-008	462.2261	8.780	1.78000E-11	up
CA-C8pos-009	530.2137	8.780	7.08000E-11	up
CA-C8pos-010	525.258	8.781	1.58000E-11	up
CA-C8pos-011	313.2253	8.849	1.17149E-02	up
CA-C8pos-012	313.2263	8.849	1.17149E-02	up
CA-C8pos-013	335.2081	8.850	1.17149E-02	up
CA-C8pos-014	542.2553	9.028	1.17149E-02	down
CA-C8pos-015	208.1467	9.031	3.22487E-02	down
CA-C8pos-016	341.2583	9.112	1.40716E-02	up
CA-C8pos-017	315.2785	9.256	3.48417E-02	down
CA-C8pos-018	362.3046	9.586	3.91768E-02	up
CA-C8pos-019	447.2855	9.598	1.17149E-02	up
CA-C8pos-020	637.4777	10.123	1.24902E-02	down
CA-C8pos-021	707.5069	10.842	1.17149E-02	up

Results from C8/LC-MS with ESI in negative mode

No.	*Mass*	*Retention Time*	*p (Corr)*	*Regulation*
CA-C8neg-001	118.0628	3.176	1.59389E-02	down
CA-C8neg-002	219.1107	3.503	4.16151E-02	up
CA-C8neg-003	379.1054	4.367	8.88849E-16	up
CA-C8neg-004	413.0566	8.403	3.30937E-02	down
CA-C8neg-005	515.2917	8.629	4.79485E-17	down
CA-C8neg-006	508.2313	8.863	1.10850E-16	up
CA-C8neg-007	598.2002	8.864	8.88849E-16	up
CA-C8neg-008	688.169	8.864	3.30937E-02	up
CA-C8neg-009	530.213	8.864	1.36358E-16	up
CA-C8neg-010	666.1873	8.864	3.30937E-02	up
CA-C8neg-011	361.2826	9.260	3.30937E-02	down

Results from C18/LC-MS with ESI in positive mode

No.	*Mass*	*Retention Time*	*p (Corr)*	*Regulation*
CA-C18pos-001	674.5329	6.343	3.01724E-07	up

CA-C18pos-002	301.2973	6.407	1.03643E-07	up
CA-C18pos-003	301.2972	6.407	1.03643E-07	up
CA-C18pos-004	503.0962	7.413	8.14380E-09	down
CA-C18pos-005	349.2585	8.422	5.80877E-12	down
CA-C18pos-006	533.4988	8.592	3.53228E-12	down
CA-C18pos-007	533.499	8.672	8.94035E-09	up
CA-C18pos-008	683.3697	8.704	4.43461E-09	up
CA-C18pos-009	683.3697	8.991	1.66877E-07	down
CA-C18pos-010	407.3628	9.436	9.31795E-09	down
CA-C18pos-011	407.3617	9.457	9.31795E-09	down
CA-C18pos-012	407.3252	9.457	8.94035E-09	down
CA-C18pos-013	407.3251	9.457	8.94035E-09	down
CA-C18pos-014	407.3624	9.471	9.31795E-09	down
CA-C18pos-015	566.4143	10.152	4.53337E-08	up
CA-C18pos-016	680.2017	10.464	4.43461E-09	down
CA-C18pos-017	680.2008	10.468	4.43461E-09	down

Results from C18/LC-MS with ESI in negative mode

No.	***Mass***	***Retention Time***	***p (Corr)***	***Regulation***
CA-C18neg-001	408.2147	4.508	0.02959881	up
CA-C18neg-002	761.1557	5.157	0.017158514	down
CA-C18neg-003	212.1046	5.659	1.6168736E-10	up
CA-C18neg-004	768.5464	8.660	7.9252067E-7	up
CA-C18neg-005	636.2978	9.143	0.013028642	down
CA-C18neg-006	298.1585	9.152	8.970912E-9	up
CA-C18neg-007	266.1553	9.588	1.0206398E-5	down
CA-C18neg-008	356.1663	9.607	0.04066053	down
CA-C18neg-009	392.2154	9.607	7.9252067E-7	down
CA-C18neg-010	602.4516	9.609	8.432806E-10	down
CA-C18neg-011	431.3242	9.675	3.1974193E-10	up
CA-C18neg-012	513.2319	9.683	4.199384E-9	down
CA-C18neg-013	266.1548	9.851	5.963521E-7	up
CA-C18neg-014	947.3556	9.892	0.04066053	down
CA-C18neg-015	326.1918	9.901	9.834602E-7	up
CA-C18neg-016	930.3629	9.922	0.0040473435	up
CA-C18neg-017	410.266	10.268	5.6684817E-9	up
CA-C18neg-018	508.3761	10.562	0.020705163	up

Results from GC-EI-MS

No.	***Mass Base peak***	***Retention Time***	***p (Corr)***	***Regulation***
Polar fraction				
CA-GCMS-001	73.0467	6.668	1.21983E-03	down
CA-GCMS-002	73.0454	6.832	1.28918E-05	down
CA-GCMS-003	147.0657	7.449	2.41738E-02	down
CA-GCMS-004	147.0658	7.987	3.81510E-02	down
CA-GCMS-005	191.0017	10.383	7.88800E-07	down
CA-GCMS-006	147.0658	10.427	3.48916E-02	down
CA-GCMS-007	241.0476	10.744	2.47827E-04	down
CA-GCMS-008	193.0490	11.160	2.15478E-06	down
CA-GCMS-009	214.1257	11.721	2.46985E-03	down

CA-GCMS-010	239.1556	11.807	6.43795E-03	down
CA-GCMS-011	57.0698	12.373	3.48260E-03	up
CA-GCMS-012	172.0787	12.509	3.85944E-07	down
CA-GCMS-013	179.0235	12.673	1.28908E-02	down
CA-GCMS-014	172.0774	12.769	1.21983E-03	down
CA-GCMS-015	73.0467	16.556	6.47950E-03	up
CA-GCMS-016	73.0467	18.699	4.10233E-03	up
CA-GCMS-017	73.0467	19.333	2.88377E-03	up
CA-GCMS-018	73.0467	19.790	3.48916E-02	up
CA-GCMS-019	75.0262	21.354	3.81942E-03	up
Nonpolar fraction				
CA-GCMS-020	73.0452	7.984	1.33859E-03	up
CA-GCMS-021	73.0452	8.465	1.73166E-03	up
CA-GCMS-022	147.0656	9.870	1.09944E-02	up
CA-GCMS-023	172.0796	12.509	4.18256E-04	up
CA-GCMS-024	73.0454	18.701	3.12702E-02	down
CA-GCMS-025	57.0699	26.713	1.73166E-03	down

Supplementary Table 2. Differentiating metabolites between carnosol-treated cells and control cells.

Results from C8/LC-MS with ESI in positive mode

No.	*Mass*	*Retention Time*	*p (Corr)*	*Regulation*
CS-C8pos-001	291.2049	4.172	2.61331E-02	down
CS-C8pos-002	275.2102	5.426	1.74311E-02	down
CS-C8pos-003	347.2676	7.194	1.74311E-02	down
CS-C8pos-004	987.8173	8.163	2.61331E-02	up
CS-C8pos-005	434.1602	8.412	1.96612E-03	down
CS-C8pos-006	289.0676	8.452	1.11213E-02	down
CS-C8pos-007	317.2727	8.508	4.99146E-02	down
CS-C8pos-008	541.8991	8.510	2.34615E-03	down
CS-C8pos-009	315.2415	8.603	3.52535E-02	down
CS-C8pos-010	313.2263	8.849	2.34615E-03	up
CS-C8pos-011	313.2253	8.849	2.34615E-03	up
CS-C8pos-012	335.2081	8.850	2.34615E-03	up
CS-C8pos-013	542.2553	9.028	1.40476E-03	down
CS-C8pos-014	488.2078	9.036	2.61331E-02	down
CS-C8pos-015	365.253	9.038	2.61331E-02	up
CS-C8pos-016	325.2622	9.039	4.75483E-03	up
CS-C8pos-017	325.2622	9.039	4.75483E-03	up
CS-C8pos-018	343.271	9.040	4.75483E-03	up
CS-C8pos-019	341.2583	9.112	1.40476E-03	up
CS-C8pos-020	415.2573	9.115	3.52535E-02	down
CS-C8pos-021	386.3159	9.118	1.74311E-02	up
CS-C8pos-022	295.2521	9.209	6.49013E-03	up
CS-C8pos-023	315.2785	9.256	3.03553E-03	down
CS-C8pos-024	335.3048	9.596	2.74802E-02	down
CS-C8pos-025	335.2698	9.596	2.74802E-02	down
CS-C8pos-026	447.2855	9.598	4.75483E-03	up
CS-C8pos-027	376.319	9.699	1.98511E-02	down
CS-C8pos-028	333.2982	9.706	4.62199E-02	down
CS-C8pos-029	433.3771	10.101	4.62199E-02	down
CS-C8pos-030	637.4782	10.123	2.23095E-02	down

CS-C8pos-031	637.4777	10.123	1.36247E-02	down
CS-C8pos-032	707.5069	10.842	1.17686E-02	up

Results from C8/LC-MS with ESI in negative mode

No.	*Mass*	*Retention Time*	*p (Corr)*	*Regulation*
CS-C8neg-001	191.9361	0.474	1.91647E-02	up
CS-C8neg-002	967.008	0.483	1.91647E-02	down
CS-C8neg-003	147.0534	0.577	3.54929E-02	down
CS-C8neg-004	95.9328	0.577	2.13798E-03	down
CS-C8neg-005	214.8969	0.882	2.07082E-02	down
CS-C8neg-006	348.0501	0.904	2.32005E-02	up
CS-C8neg-007	348.0507	0.908	2.32005E-02	up
CS-C8neg-008	284.0758	3.047	5.14588E-04	down
CS-C8neg-009	118.0628	3.176	1.91647E-02	down
CS-C8neg-010	130.0631	3.934	1.91647E-02	down
CS-C8neg-011	509.9359	8.050	1.91647E-02	down
CS-C8neg-012	273.9849	8.117	1.91647E-02	up
CS-C8neg-013	509.9362	8.169	1.91647E-02	down
CS-C8neg-014	413.0566	8.403	3.66070E-15	down
CS-C8neg-015	515.2917	8.629	4.79485E-17	down
CS-C8neg-016	506.2156	8.646	2.06368E-02	up
CS-C8neg-017	344.163	9.036	1.86224E-02	up
CS-C8neg-018	491.1729	9.129	1.57560E-02	down
CS-C8neg-019	482.0457	9.242	9.95896E-04	down
CS-C8neg-020	361.2826	9.260	3.63407E-16	down
CS-C8neg-021	135.9021	9.855	2.56679E-02	down

Results from C18/LC-MS with ESI in positive mode

No.	*Mass*	*Retention Time*	*p (Corr)*	*Regulation*
CS-C18pos-001	317.1044	0.485	2.42014E-02	up
CS-C18pos-002	317.1049	0.485	2.42014E-02	up
CS-C18pos-003	187.1685	0.548	1.09649E-02	up
CS-C18pos-004	187.1685	0.548	1.09649E-02	up
CS-C18pos-005	201.2092	3.231	1.84768E-10	down
CS-C18pos-006	199.1933	3.282	3.87251E-12	down
CS-C18pos-007	185.214	4.083	1.56565E-04	down
CS-C18pos-008	185.2144	4.083	1.56565E-04	down
CS-C18pos-009	440.145	5.045	4.51837E-11	up
CS-C18pos-010	317.2931	5.272	5.83263E-12	down
CS-C18pos-011	317.2933	5.364	3.05996E-06	up
CS-C18pos-012	273.2668	5.385	1.05682E-02	down
CS-C18pos-013	273.2672	5.385	1.05682E-02	down
CS-C18pos-014	386.1727	5.675	4.51837E-11	up
CS-C18pos-015	386.173	5.893	4.85211E-11	down
CS-C18pos-016	386.1612	5.959	1.17968E-03	down
CS-C18pos-017	674.5329	6.343	3.00579E-09	up
CS-C18pos-018	528.3493	6.487	1.50557E-09	up
CS-C18pos-019	401.3859	7.203	4.65519E-11	up

CS-C18pos-020	512.381	7.330	2.85983E-02	down
CS-C18pos-021	429.3822	7.392	1.26717E-06	up
CS-C18pos-022	478.4848	8.299	6.04165E-10	down
CS-C18pos-023	478.4847	8.332	3.42657E-09	down
CS-C18pos-024	349.2585	8.422	3.87251E-12	down
CS-C18pos-025	478.4846	8.425	1.10249E-08	up
CS-C18pos-026	532.4942	8.580	7.03797E-08	down
CS-C18pos-027	533.4988	8.592	3.53228E-12	down
CS-C18pos-028	533.499	8.672	1.26717E-06	up
CS-C18pos-029	532.4951	8.676	1.68695E-07	up
CS-C18pos-030	683.3697	8.704	9.83304E-09	up
CS-C18pos-031	442.327	8.987	4.51837E-11	down
CS-C18pos-032	683.3697	8.991	8.61300E-08	down
CS-C18pos-033	586.5419	9.114	4.51837E-11	down
CS-C18pos-034	586.5429	9.125	2.92932E-11	down
CS-C18pos-035	317.3096	9.135	1.85627E-09	down
CS-C18pos-036	588.5578	9.146	2.50476E-09	down
CS-C18pos-037	586.5459	9.197	4.51837E-11	down
CS-C18pos-038	588.5612	9.214	2.50476E-09	down
CS-C18pos-039	407.3628	9.436	4.14131E-09	down
CS-C18pos-040	407.3617	9.457	4.14131E-09	down
CS-C18pos-041	407.3252	9.457	3.42657E-09	down
CS-C18pos-042	407.3251	9.457	3.42657E-09	down
CS-C18pos-043	407.3624	9.471	4.14131E-09	down
CS-C18pos-044	441.3928	9.637	7.58185E-07	down
CS-C18pos-045	441.3949	9.669	7.58185E-07	down
CS-C18pos-046	684.43	10.528	2.14948E-02	down
CS-C18pos-047	684.4306	10.553	4.11066E-02	down
CS-C18pos-048	662.4486	10.641	9.60633E-12	down
CS-C18pos-049	708.5113	10.685	6.11023E-10	down

Results from C18/LC-MS with ESI in negative mode

No.	***Mass***	***Retention Time***	***p (Corr)***	***Regulation***
CS-C18neg-001	132.021	0.589	1.60485E-07	down
CS-C18neg-002	1032.985	0.710	7.94891E-07	down
CS-C18neg-003	408.215	4.508	1.59982E-02	up
CS-C18neg-004	1028.281	5.148	1.22619E-02	down
CS-C18neg-005	413.056	5.151	3.90768E-04	down
CS-C18neg-006	1051.287	5.155	4.36218E-10	down
CS-C18neg-007	254.152	5.255	2.92206E-13	up
CS-C18neg-008	486.098	5.959	1.02755E-02	down
CS-C18neg-009	224.140	6.321	3.00335E-14	up
CS-C18neg-010	389.269	6.684	2.57643E-02	up
CS-C18neg-011	695.166	6.749	5.88663E-13	up
CS-C18neg-012	725.836	6.966	2.15062E-05	down
CS-C18neg-013	330.183	7.040	6.78587E-13	up
CS-C18neg-014	491.173	7.111	7.87015E-04	down
CS-C18neg-015	378.252	7.331	4.73967E-12	up
CS-C18neg-016	768.546	8.660	1.17733E-07	up
CS-C18neg-017	302.225	8.693	1.17737E-06	down
CS-C18neg-018	304.240	9.111	2.80415E-02	down
CS-C18neg-019	636.298	9.143	1.20935E-03	down
CS-C18neg-020	158.908	9.557	4.45221E-06	down
CS-C18neg-021	266.155	9.588	5.61945E-05	down

CS-C18neg-022	256.241	9.598	3.99162E-04	up
CS-C18neg-023	534.463	9.599	2.04870E-02	down
CS-C18neg-024	341.219	9.599	1.61034E-07	down
CS-C18neg-025	392.215	9.607	5.61009E-06	down
CS-C18neg-026	602.452	9.609	1.01879E-08	down
CS-C18neg-027	431.324	9.675	5.57751E-09	up
CS-C18neg-028	421.296	9.683	8.61102E-09	up
CS-C18neg-029	513.232	9.683	4.57355E-08	down
CS-C18neg-030	636.293	9.703	7.86545E-03	up
CS-C18neg-031	947.356	9.892	6.03945E-03	down
CS-C18neg-032	930.363	9.922	3.51629E-03	up
CS-C18neg-033	338.242	9.962	1.69675E-09	down
CS-C18neg-034	340.207	9.994	9.32829E-06	up
CS-C18neg-035	401.315	10.020	6.97629E-08	up
CS-C18neg-036	410.266	10.268	4.03489E-09	up
CS-C18neg-037	917.610	10.441	1.69675E-09	up
CS-C18neg-038	508.376	10.562	1.28171E-02	up
CS-C18neg-039	298.287	10.716	2.21665E-08	up

Results from GC-EI-MS

No.	***Mass Base pek***	***Retention Time***	***p (Corr)***	***Regulation***
Polar fraction				
CS-GCMS-001	73.0454	6.665	8.88585E-04	down
CS-GCMS-002	73.0454	6.830	1.89705E-05	down
CS-GCMS-003	116.0887	7.449	2.80239E-05	down
CS-GCMS-004	73.0468	7.718	1.59128E-02	up
CS-GCMS-005	147.0656	7.988	1.28537E-03	down
CS-GCMS-006	147.0656	8.271	2.67330E-03	down
CS-GCMS-007	158.1367	10.164	1.38744E-02	down
CS-GCMS-008	191.0017	10.407	4.39990E-06	down
CS-GCMS-009	147.0656	10.451	9.92216E-04	down
CS-GCMS-010	193.0487	11.188	2.72111E-04	down
CS-GCMS-011	73.0454	11.468	1.41233E-02	down
CS-GCMS-012	214.1257	11.754	4.09121E-04	down
CS-GCMS-013	239.1573	11.839	9.66914E-04	down
CS-GCMS-014	172.0787	12.544	4.73392E-06	down
CS-GCMS-015	172.0787	12.804	4.56645E-03	down
CS-GCMS-016	84.0922	13.301	3.65175E-02	down
CS-GCMS-017	299.0722	16.192	1.38744E-02	down
CS-GCMS-018	156.0839	17.636	1.38744E-02	down
CS-GCMS-019	73.0454	18.699	1.40705E-02	down
Nonpolar fraction				
CS-GCMS-020	170.1342	6.364	1.14939E-02	down
CS-GCMS-021	147.0658	7.984	1.37500E-08	down
CS-GCMS-022	73.0453	8.022	9.44289E-17	up
CS-GCMS-023	203.1801	10.919	1.00760E-05	up
CS-GCMS-024	73.0455	11.439	4.71886E-13	up
CS-GCMS-025	69.0697	13.150	9.44289E-17	up
CS-GCMS-026	239.1566	17.959	1.65219E-03	down
CS-GCMS-027	75.0257	20.419	1.25734E-03	down
CS-GCMS-028	73.0454	20.469	7.82361E-04	down
CS-GCMS-029	73.0453	20.525	5.20442E-03	down
CS-GCMS-030	98.0719	21.306	3.95634E-03	down

CS-GCMS-031	98.0719	21.358	1.14939E-02	down
CS-GCMS-032	73.0453	21.531	7.52667E-14	up
CS-GCMS-033	73.0453	21.745	2.47473E-05	down
CS-GCMS-034	57.0700	21.925	4.13982E-02	up
CS-GCMS-035	463.0863	26.081	8.71446E-03	up

Supplementary Table 3. Differentiating metabolites between rosmanol-treated cells and control cells.

Results from C8/LC-MS with ESI in positive mode

No.	*Mass*	*Retention Time*	*p (Corr)*	*Regulation*
RS-C8pos-001	235.065	0.504	1.89445E-02	up
RS-C8pos-002	231.033	0.505	1.86089E-02	up
RS-C8pos-003	139.061	0.598	1.07186E-02	up
RS-C8pos-004	208.085	3.117	1.15051E-02	up
RS-C8pos-005	302.064	3.263	1.15051E-02	up
RS-C8pos-006	219.111	3.516	5.59885E-13	up
RS-C8pos-007	291.205	4.172	1.15051E-02	down
RS-C8pos-008	129.152	4.337	4.91360E-02	up
RS-C8pos-009	199.194	5.290	1.15051E-02	up
RS-C8pos-010	275.210	5.426	2.24148E-11	down
RS-C8pos-011	607.379	5.980	1.15051E-02	down
RS-C8pos-012	170.142	7.109	3.86291E-02	up
RS-C8pos-013	347.268	7.194	9.38855E-13	down
RS-C8pos-014	447.172	7.574	9.97467E-17	up
RS-C8pos-015	651.247	7.761	3.24352E-16	up
RS-C8pos-016	987.994	8.154	1.15051E-02	up
RS-C8pos-017	1973.275	8.160	1.15051E-02	up
RS-C8pos-018	1863.328	8.167	1.15051E-02	up
RS-C8pos-019	218.168	8.231	2.88499E-02	up
RS-C8pos-020	263.226	8.232	4.27861E-03	down
RS-C8pos-021	544.193	8.238	1.15051E-02	up
RS-C8pos-022	539.239	8.239	3.24352E-16	up
RS-C8pos-023	469.128	8.406	1.02144E-02	down
RS-C8pos-024	434.160	8.412	1.99354E-02	down
RS-C8pos-025	317.273	8.508	2.02527E-02	down
RS-C8pos-026	541.899	8.510	4.18800E-06	down
RS-C8pos-027	287.247	8.533	1.33544E-02	up
RS-C8pos-028	315.242	8.603	4.73282E-03	down
RS-C8pos-029	224.189	8.689	3.64626E-02	up
RS-C8pos-030	427.917	8.786	1.15051E-02	up
RS-C8pos-031	337.259	8.820	1.15051E-02	up
RS-C8pos-032	358.320	8.846	1.15051E-02	up
RS-C8pos-033	313.225	8.849	3.02443E-04	up
RS-C8pos-034	335.208	8.850	1.89339E-04	up
RS-C8pos-035	356.950	8.859	3.24352E-16	down
RS-C8pos-036	569.923	8.860	1.48567E-14	down
RS-C8pos-037	611.368	8.912	3.74534E-13	down
RS-C8pos-038	333.229	8.940	4.82956E-02	down
RS-C8pos-039	422.083	9.023	1.15051E-02	up
RS-C8pos-040	542.255	9.028	7.69424E-07	down
RS-C8pos-041	208.147	9.031	8.75878E-03	down
RS-C8pos-042	343.115	9.032	1.99641E-06	down

RS-C8pos-043	488.208	9.036	1.15051E-02	down
RS-C8pos-044	365.253	9.038	3.27277E-03	up
RS-C8pos-045	325.262	9.039	1.27213E-04	up
RS-C8pos-046	325.262	9.039	1.12514E-04	up
RS-C8pos-047	343.271	9.040	3.02443E-04	up
RS-C8pos-048	588.062	9.051	1.11920E-02	down
RS-C8pos-049	341.258	9.112	3.86436E-04	up
RS-C8pos-050	399.312	9.114	2.28962E-02	down
RS-C8pos-051	386.316	9.118	2.17609E-03	up
RS-C8pos-052	453.286	9.127	1.15051E-02	up
RS-C8pos-053	295.252	9.209	3.86436E-04	up
RS-C8pos-054	315.279	9.256	1.30914E-03	down
RS-C8pos-055	195.163	9.300	1.54396E-03	down
RS-C8pos-056	293.200	9.338	1.91973E-02	down
RS-C8pos-057	516.466	9.391	8.68807E-15	up
RS-C8pos-058	204.079	9.443	1.62451E-02	down
RS-C8pos-059	278.153	9.444	1.86089E-02	down
RS-C8pos-060	318.241	9.594	3.52638E-02	down
RS-C8pos-061	335.305	9.596	3.16769E-03	down
RS-C8pos-062	335.270	9.596	3.57510E-03	down
RS-C8pos-063	447.286	9.598	1.30914E-03	up
RS-C8pos-064	643.489	9.829	1.89445E-02	down
RS-C8pos-065	653.508	10.044	1.52087E-02	down
RS-C8pos-066	609.482	10.058	1.86089E-02	down
RS-C8pos-067	565.456	10.071	1.89445E-02	down
RS-C8pos-068	422.245	10.088	1.33544E-02	down
RS-C8pos-069	477.404	10.093	1.02144E-02	down
RS-C8pos-070	433.377	10.101	1.15051E-02	down
RS-C8pos-071	482.359	10.109	6.36214E-13	up
RS-C8pos-072	461.408	10.116	1.15051E-02	up
RS-C8pos-073	627.186	10.208	3.24352E-16	down
RS-C8pos-074	707.507	10.842	1.80387E-05	up

Results from C8/LC-MS with ESI in negative mode

No.	***Mass***	***Retention Time***	***p (Corr)***	***Regulation***
RS-C8neg-001	191.936	0.474	2.54501E-02	up
RS-C8neg-002	967.008	0.483	1.12986E-02	down
RS-C8neg-003	113.993	0.515	1.56491E-02	down
RS-C8neg-004	216.040	0.570	2.04185E-02	up
RS-C8neg-005	147.053	0.577	3.08855E-03	down
RS-C8neg-006	168.028	0.883	1.03519E-02	down
RS-C8neg-007	303.073	3.033	4.27693E-02	up
RS-C8neg-008	284.076	3.047	4.09642E-05	down
RS-C8neg-009	635.078	3.073	7.30803E-03	up
RS-C8neg-010	118.063	3.176	4.40358E-04	down
RS-C8neg-011	219.111	3.503	1.06118E-05	up
RS-C8neg-012	130.063	3.934	3.34368E-03	down
RS-C8neg-013	565.102	4.268	7.84584E-03	down
RS-C8neg-014	563.107	4.268	1.12986E-02	down
RS-C8neg-015	339.018	4.270	3.92549E-02	down
RS-C8neg-016	380.960	4.324	9.46160E-03	down
RS-C8neg-017	379.105	4.367	8.64000E-03	up
RS-C8neg-018	173.999	4.459	2.50434E-03	down

RS-C8neg-019	264.111	4.707	3.78390E-16	up
RS-C8neg-020	465.182	7.581	1.57674E-18	up
RS-C8neg-021	487.165	7.583	1.21485E-16	up
RS-C8neg-022	673.228	7.813	1.39437E-15	up
RS-C8neg-023	651.246	7.814	1.49390E-16	up
RS-C8neg-024	408.215	7.958	1.41821E-02	up
RS-C8neg-025	447.226	7.964	1.05572E-14	up
RS-C8neg-026	509.936	8.050	2.05277E-03	down
RS-C8neg-027	556.880	8.088	4.27693E-02	down
RS-C8neg-028	334.099	8.100	3.85505E-02	up
RS-C8neg-029	901.824	8.113	4.82985E-03	down
RS-C8neg-030	509.936	8.169	1.85214E-03	down
RS-C8neg-031	522.210	8.247	1.49390E-16	up
RS-C8neg-032	435.172	8.309	8.64444E-03	up
RS-C8neg-033	442.167	8.343	1.73687E-03	up
RS-C8neg-034	413.057	8.403	1.09821E-15	down
RS-C8neg-035	306.089	8.551	1.41821E-02	up
RS-C8neg-036	515.292	8.629	7.84584E-03	down
RS-C8neg-037	346.179	8.669	2.88120E-13	up
RS-C8neg-038	240.067	8.690	2.42322E-02	up
RS-C8neg-039	376.135	8.906	6.38027E-24	up
RS-C8neg-040	376.135	8.986	1.29265E-14	up
RS-C8neg-041	195.089	8.999	1.91803E-04	up
RS-C8neg-042	376.135	9.108	1.57264E-12	up
RS-C8neg-043	491.173	9.129	1.80989E-03	down
RS-C8neg-044	376.135	9.216	3.50940E-17	up
RS-C8neg-045	482.046	9.242	7.73474E-05	down
RS-C8neg-046	361.283	9.260	1.21485E-16	down
RS-C8neg-047	222.162	9.333	1.34010E-03	up
RS-C8neg-048	166.048	9.473	9.85099E-03	up
RS-C8neg-049	279.184	9.592	4.27693E-02	up
RS-C8neg-050	357.156	9.600	7.30803E-03	up
RS-C8neg-051	260.847	9.825	8.64444E-03	down
RS-C8neg-052	135.902	9.855	1.66262E-03	down
RS-C8neg-053	360.158	9.857	3.38703E-18	up
RS-C8neg-054	284.112	9.867	8.64444E-03	up
RS-C8neg-055	426.135	10.082	1.13636E-15	up

Results from C18/LC-MS with ESI in positive mode

No.	***Mass***	***Retention Time***	***p (Corr)***	***Regulation***
RS-C18pos-001	154.147	2.739	2.38488E-14	down
RS-C18pos-002	154.146	2.739	2.38488E-14	down
RS-C18pos-003	201.209	3.231	1.03470E-10	down
RS-C18pos-004	199.193	3.282	9.68128E-13	down
RS-C18pos-005	171.126	3.490	8.06320E-03	down
RS-C18pos-006	171.126	3.490	8.06320E-03	down
RS-C18pos-007	183.126	3.751	8.26486E-03	down
RS-C18pos-008	183.126	3.751	8.26486E-03	down
RS-C18pos-009	185.214	4.083	1.33881E-04	down
RS-C18pos-010	185.214	4.083	1.33881E-04	down
RS-C18pos-011	170.142	4.206	1.23982E-02	down
RS-C18pos-012	170.142	4.207	1.80677E-03	down
RS-C18pos-013	272.156	4.496	8.86242E-13	down
RS-C18pos-014	226.157	4.990	3.89336E-02	down

RS-C18pos-015	317.293	5.272	1.79465E-12	down
RS-C18pos-016	317.293	5.364	5.11887E-07	up
RS-C18pos-017	386.173	5.675	5.89873E-10	up
RS-C18pos-018	386.173	5.893	3.00369E-11	down
RS-C18pos-019	408.140	5.961	3.65629E-14	down
RS-C18pos-020	408.149	5.962	3.65629E-14	down
RS-C18pos-021	703.461	6.028	2.72733E-06	up
RS-C18pos-022	310.178	6.232	3.25781E-02	up
RS-C18pos-023	310.178	6.232	3.25781E-02	up
RS-C18pos-024	299.283	6.249	5.89873E-10	up
RS-C18pos-025	311.246	6.282	2.17995E-02	down
RS-C18pos-026	315.277	6.283	6.94912E-04	up
RS-C18pos-027	315.278	6.285	3.42646E-03	up
RS-C18pos-028	674.533	6.343	5.46078E-08	up
RS-C18pos-029	792.474	6.368	1.62409E-03	down
RS-C18pos-030	792.471	6.368	1.59387E-03	down
RS-C18pos-031	1150.710	6.371	9.68128E-13	down
RS-C18pos-032	574.858	6.373	3.51982E-11	down
RS-C18pos-033	1150.711	6.374	9.68128E-13	down
RS-C18pos-034	722.581	6.422	1.09770E-04	up
RS-C18pos-035	361.290	6.474	2.34013E-08	up
RS-C18pos-036	329.330	6.643	1.04451E-04	up
RS-C18pos-037	329.329	6.645	1.04451E-04	up
RS-C18pos-038	373.355	6.655	3.77185E-09	up
RS-C18pos-039	311.246	6.700	3.44065E-02	down
RS-C18pos-040	311.246	6.700	3.44065E-02	down
RS-C18pos-041	285.303	6.719	1.20307E-08	up
RS-C18pos-042	425.316	6.953	1.03470E-10	down
RS-C18pos-043	341.212	7.027	1.38332E-03	up
RS-C18pos-044	425.313	7.081	6.40408E-06	up
RS-C18pos-045	437.350	7.136	1.04747E-11	down
RS-C18pos-046	401.386	7.203	5.89873E-10	up
RS-C18pos-047	401.386	7.282	5.89873E-10	up
RS-C18pos-048	401.386	7.282	5.89873E-10	up
RS-C18pos-049	401.386	7.282	5.89873E-10	up
RS-C18pos-050	429.382	7.392	5.05066E-11	up
RS-C18pos-051	503.096	7.413	1.11052E-09	down
RS-C18pos-052	295.251	7.421	4.48826E-02	up
RS-C18pos-053	443.323	7.739	6.21668E-07	down
RS-C18pos-054	443.325	7.740	6.21668E+00	down
RS-C18pos-055	455.398	7.997	4.65113E-12	down
RS-C18pos-056	455.397	8.017	3.48993E-10	down
RS-C18pos-057	278.151	8.048	1.18153E-02	down
RS-C18pos-058	278.151	8.048	1.18153E-02	down
RS-C18pos-059	148.016	8.049	2.49889E-02	down
RS-C18pos-060	148.016	8.049	2.49889E-02	down
RS-C18pos-061	488.434	8.178	1.51592E-11	down
RS-C18pos-062	488.434	8.242	1.68333E-09	up
RS-C18pos-063	478.485	8.299	3.23660E-10	down
RS-C18pos-064	478.485	8.332	1.71328E-09	down
RS-C18pos-065	281.271	8.365	4.36890E-02	down
RS-C18pos-066	697.349	8.380	8.28565E-08	down
RS-C18pos-067	327.277	8.400	1.71122E-02	down
RS-C18pos-068	327.277	8.404	1.49279E-02	down
RS-C18pos-069	349.259	8.422	9.68128E-13	down
RS-C18pos-070	478.485	8.425	2.71550E-10	up

RS-C18pos-071	532.494	8.580	3.57863E-08	down
RS-C18pos-072	533.499	8.592	5.04612E-13	down
RS-C18pos-073	533.499	8.672	1.02368E-07	up
RS-C18pos-074	532.495	8.676	3.85688E-08	up
RS-C18pos-075	683.370	8.704	7.71711E-10	up
RS-C18pos-076	683.371	8.704	8.72773E-03	down
RS-C18pos-077	683.370	8.704	8.86740E-03	down
RS-C18pos-078	199.194	8.903	2.90011E-03	down
RS-C18pos-079	199.194	8.903	2.90011E-03	down
RS-C18pos-080	442.327	8.987	1.99228E-11	down
RS-C18pos-081	255.256	8.987	1.95210E-02	down
RS-C18pos-082	683.370	8.991	4.37710E-08	down
RS-C18pos-083	586.542	9.114	2.48510E-11	down
RS-C18pos-084	317.310	9.135	7.95545E-10	down
RS-C18pos-085	681.361	9.152	1.21358E-02	down
RS-C18pos-086	681.359	9.152	1.21358E-02	down
RS-C18pos-087	451.351	9.425	5.89873E-10	down
RS-C18pos-088	407.363	9.436	2.19246E-09	down
RS-C18pos-089	407.362	9.457	2.19246E-09	down
RS-C18pos-090	407.325	9.457	1.71198E-09	down
RS-C18pos-091	407.325	9.457	1.71198E-09	down
RS-C18pos-092	407.362	9.471	2.19246E-09	down
RS-C18pos-093	521.591	9.514	1.84611E-08	up
RS-C18pos-094	441.393	9.637	3.84751E-07	down
RS-C18pos-095	406.289	9.659	1.60326E-08	down
RS-C18pos-096	406.289	9.661	1.77322E-08	down
RS-C18pos-097	441.395	9.669	3.84751E-07	down
RS-C18pos-098	567.422	10.159	5.74147E-10	down
RS-C18pos-099	405.323	10.281	1.88587E-11	down
RS-C18pos-100	405.323	10.281	2.79922E-10	down
RS-C18pos-101	405.324	10.282	8.32744E-10	down
RS-C18pos-102	695.265	10.303	5.79970E-14	down
RS-C18pos-103	695.263	10.305	9.37482E-15	down
RS-C18pos-104	680.202	10.464	5.89873E-10	down
RS-C18pos-105	680.201	10.468	5.89873E-10	down
RS-C18pos-106	722.508	10.488	1.32859E-07	down
RS-C18pos-107	685.435	10.638	4.55708E-09	down
RS-C18pos-108	662.449	10.641	3.43083E-12	down
RS-C18pos-109	708.511	10.685	3.37116E-10	down
RS-C18pos-110	707.508	10.712	3.94756E-02	down

Results from C18/LC-MS with ESI in negative mode

No.	***Mass***	***Retention Time***	***p (Corr)***	***Regulation***
RS-C18neg-001	407.231	3.575	8.86540E-03	up
RS-C18neg-002	408.215	4.508	1.40208E-03	up
RS-C18neg-003	447.226	4.511	1.39513E-12	up
RS-C18neg-004	926.562	4.873	4.02158E-02	up
RS-C18neg-005	1028.281	5.148	1.49765E-03	down
RS-C18neg-006	1038.310	5.149	8.26057E-03	down
RS-C18neg-007	1039.313	5.149	9.37743E-03	down
RS-C18neg-008	1036.315	5.149	7.67409E-03	down
RS-C18neg-009	413.056	5.151	9.09139E-04	down
RS-C18neg-010	1010.316	5.153	1.37285E-11	down
RS-C18neg-011	1051.287	5.155	5.20847E-12	down

RS-C18neg-012	254.152	5.255	3.96568E-13	up
RS-C18neg-013	486.098	5.959	3.70340E-03	down
RS-C18neg-014	471.202	6.379	3.96568E-13	up
RS-C18neg-015	258.056	6.509	5.16764E-12	down
RS-C18neg-016	294.183	6.540	1.90164E-02	up
RS-C18neg-017	389.269	6.684	3.03515E-02	up
RS-C18neg-018	435.273	6.684	1.31872E-02	up
RS-C18neg-019	725.836	6.966	1.97792E-06	down
RS-C18neg-020	491.173	7.111	6.05250E-04	down
RS-C18neg-021	541.338	7.133	9.09139E-04	up
RS-C18neg-022	481.317	7.986	1.90164E-02	up
RS-C18neg-023	636.298	9.143	6.05250E-04	down
RS-C18neg-024	683.300	9.586	6.89476E-12	down
RS-C18neg-025	266.155	9.588	5.90897E-06	down
RS-C18neg-026	256.241	9.598	2.36629E-03	up
RS-C18neg-027	341.219	9.599	6.29629E-09	down
RS-C18neg-028	715.559	9.600	3.84770E-02	up
RS-C18neg-029	392.215	9.607	4.06493E-07	down
RS-C18neg-030	1015.819	9.607	3.96568E-13	up
RS-C18neg-031	602.452	9.609	2.29986E-10	down
RS-C18neg-032	652.331	9.665	2.36629E-03	up
RS-C18neg-033	431.324	9.675	1.15418E-09	up
RS-C18neg-034	513.232	9.683	1.19982E-09	down
RS-C18neg-035	636.293	9.703	1.23716E-03	up
RS-C18neg-036	354.209	9.775	4.66062E-02	down
RS-C18neg-037	947.356	9.892	8.35343E-04	down
RS-C18neg-038	920.333	9.913	1.06617E-07	up
RS-C18neg-039	930.363	9.922	9.86538E-04	up
RS-C18neg-040	338.242	9.962	2.27874E-11	down
RS-C18neg-041	340.207	9.994	1.01999E-05	up
RS-C18neg-042	401.315	10.020	8.70756E-10	up
RS-C18neg-043	326.191	10.272	3.77135E-02	down
RS-C18neg-044	529.423	10.358	1.48254E-02	up
RS-C18neg-045	917.610	10.441	7.00183E-11	up
RS-C18neg-046	508.376	10.562	2.77788E-03	up

Results from GC-EI-MS

No.	***Mass Base peak***	***Retention Time***	***p (Corr)***	***Regulation***
Polar fraction				
RS-GCMS-001	73.0454	6.668	4.40935E-03	down
RS-GCMS-002	73.0454	6.832	3.95215E-08	down
RS-GCMS-003	147.0655	7.450	7.59181E-04	down
RS-GCMS-004	244.1231	7.527	3.45225E-03	down
RS-GCMS-005	147.0655	7.989	4.93436E-05	down
RS-GCMS-006	147.0655	8.271	2.37276E-02	down
RS-GCMS-007	179.0235	9.568	1.07300E-08	down
RS-GCMS-008	300.0737	9.856	6.16240E-03	down
RS-GCMS-009	191.0017	10.405	1.10773E-04	down
RS-GCMS-010	147.0655	10.450	1.57913E-04	down
RS-GCMS-011	241.0482	10.769	1.10773E-04	down
RS-GCMS-012	73.0454	11.077	2.22225E-02	down
RS-GCMS-013	193.0493	11.187	4.35674E-06	down
RS-GCMS-014	214.1257	11.755	2.43915E-03	down

RS-GCMS-015	239.1569	11.837	5.99067E-04	down
RS-GCMS-016	71.0845	12.497	4.34898E-03	down
RS-GCMS-017	172.0793	12.542	5.59825E-04	down
RS-GCMS-018	84.0917	13.301	6.62359E-03	down
RS-GCMS-019	73.0454	15.947	2.07751E-02	down
RS-GCMS-020	147.0655	17.368	1.83177E-03	up
RS-GCMS-021	147.0655	17.430	7.02355E-03	up
RS-GCMS-022	73.0452	17.527	3.83086E-03	up
RS-GCMS-023	73.0454	19.333	2.43915E-03	down
Nonpolar fraction				
RS-GCMS-024	75.0257	6.137	1.22651E-04	up
RS-GCMS-025	147.0655	6.832	5.23084E-03	down
RS-GCMS-026	154.9924	7.594	4.13745E-02	down
RS-GCMS-027	147.0655	8.065	3.22940E-02	up
RS-GCMS-028	73.0454	8.465	6.51918E-04	up
RS-GCMS-029	73.0466	11.441	5.15894E-03	up
RS-GCMS-030	172.0786	12.509	1.67529E-04	up
RS-GCMS-031	73.0454	18.704	1.39007E-02	down
RS-GCMS-032	75.0257	20.419	3.32920E-04	down
RS-GCMS-033	73.0454	20.469	2.54851E-05	down
RS-GCMS-034	73.0454	20.524	2.69404E-05	down
RS-GCMS-035	69.0698	20.879	3.15617E-02	down
RS-GCMS-036	98.0723	21.306	2.76823E-04	down
RS-GCMS-037	98.0723	21.357	5.16301E-05	down
RS-GCMS-038	85.1006	21.580	4.32664E-02	down
RS-GCMS-039	69.0698	25.295	6.41904E-07	down
RS-GCMS-040	463.0875	26.081	3.86560E-02	up

CAPÍTULO 5

Discusión general

5. DISCUSIÓN GENERAL

Los resultados de esta Tesis Doctoral muestran nuevas aproximaciones metodológicas para el desarrollo de herramientas metabolómicas utilizando una multiplataforma analítica que combina el uso de técnicas de CE-MS, LC-MS y GC-MS, así como su aplicación en investigaciones relacionadas con la Alimentómica. En concreto el Capítulo 3 muestra un nuevo desarrollo metodológico para CE-MS en el que se emplea un nuevo recubrimiento capilar catiónico y se demuestra su utilidad para el análisis rápido y estable de metabolitos aniónicos y la separación de péptidos y proteínas básicas reduciendo los fenómenos de adsorción, dos problemas analíticos en el análisis por CE-MS. En el Capítulo 4, se muestra la aplicación de la metabolómica para evaluar el efecto de los principales diterpenos fenólicos del romero (ácido carnósico, carnosol y rosmanol) en células HepaRG, un modelo celular que permite determinar la posible toxicidad de compuestos sin emplear animales. A continuación se discuten de una manera pormenorizada los resultados de cada uno de los mencionados capítulos.

Para ayudar a situar en el marco adecuado de los resultados del Capítulo 3, es interesante mencionar que la CE-MS es una potente herramienta analítica complementaria a los acoplamientos LC-MS y GC-MS, ya que permite el análisis de compuestos iónicos o de mayor polaridad que son difíciles de analizar mediante las otras técnicas. El acoplamiento CE-MS presenta ciertas dificultades técnicas que limitan la robustez de la técnica y que comprometen la sensibilidad y la reproducibilidad de los tiempos de migración, lo que limita la aplicabilidad de la técnica, especialmente en el campo del análisis de proteínas y metabolitos aniónicos. En esta Tesis Doctoral hemos avanzado en el desarrollo de recubrimientos poliméricos con el fin de disminuir estas limitaciones y hemos demostrado su gran potencial en el análisis de alimentos.

En concreto, se han investigado las propiedades de diferentes recubrimientos capilares poliméricos basados en un homopolímero catiónico de TEDETAMA y tres copolímeros de TEDETAMA, estos últimos sintetizados con unidades neutras de HPMA en diferentes porcentajes molares (25%, 50% y 75%). Con fines comparativos, se incluyeron en el estudio un capilar de sílice fundida sin recubrir y un capilar recubierto con un polímero catiónico comercial. Tal y como se esperaba, se observó el típico EOF catódico en el capilar de sílice fundida, mientras que en los capilares recubiertos con los polímeros catiónicos de TEDETAMA se observó un flujo electroosmótico anódico en todo el intervalo de pH estudiado (1.9-10), con valores de EOF próximos a cero a pHs cerca de 10. Este comportamiento se puede explicar debido a la desprotonación de los grupos amino de los polímeros TEDETAMA, puesto que el pKa de las aminas alifáticas terciarias de su estructura es en torno a 8.5. La reproducibilidad de los tiempos de migración presentó valores de %RSD inferiores a 2.4% para todos los copolímeros de TEDETAMA. La separación a línea base de las proteínas básicas se obtuvo únicamente con los copolímeros de TEDETAMA con 75% y 50% de HPMA, siendo éste último porcentaje el que aportaba los tiempos de migración más cortos. Así, se alcanzó un compromiso óptimo entre tiempo de migración y resolución con el capilar recubierto con el polímero TEDETAMA-co-HPMA (50:50). En estas condiciones, se obtuvo una buena reproducibilidad en el mismo día de los tiempos de migración y las

áreas de pico, con %RSD por debajo de 0.7% y 2%, respectivamente. Se demostró además que el polímero no afecta a la señal de MS y permite el análisis de péptidos y proteínas en tiempos cortos de migración y con buena resolución. Con el fin de demostrar la utilidad de este recubrimiento polimérico, se llevó a cabo el análisis de la proteína lisozima en queso comercial. Se seleccionó esta aplicación además de por ser la lisozima un agente potencialmente alergénico, por ser una proteína con una elevada carga positiva al presentar un punto isoeléctrico superior a 11, lo que supone un reto analítico ya que tiende a adsorberse fuertemente sobre la pared de sílice fundida del capilar con carga negativa. El método por CE-MS empleando el recubrimiento polimérico capilar demostró ser eficaz para el análisis de lisozima en muestras de queso y también permitió la identificación de proteínas del suero lácteo, tales como alfa-lactoalbúmina y beta-lactoglobulinas, demostrando que el recubrimiento permite el análisis de proteínas tanto básicas (lisozima) como ácidas (proteínas de suero).

El empleo de CE-MS en el campo de la metabolómica es inferior comparada con otras técnicas analíticas como LC-MS y GC-MS, si bien como ya se ha comentado, proporciona información complementaria. El análisis de metabolitos aniónicos por CE-MS presenta ciertas dificultades técnicas que limitan la robustez de la técnica y comprometen la sensibilidad y la reproducibilidad de los tiempos de migración. La capacidad del polímero TEDETAMA-co-HPMA (50:50) de invertir y estabilizar el EOF en CE-MS, se utilizó para llevar a cabo una investigación empleando capilares recubiertos con este copolímero para el análisis de compuestos aniónicos por CE-MS en polaridad inversa. Para la optimización de las condiciones óptimas de separación se llevó a cabo la evaluación de diferentes electrolitos con pHs comprendidos entre 1.8 y 10, así como el empleo de modificadores orgánicos, obteniéndose una buena separación con una solución 1 M de ácido fórmico en agua a pH 2.4. El método presentó una buena reproducibilidad, con valores de %RSD para los tiempos de migración inferiores a 0.1 y 0.6 %, en el mismo día y en tres días diferentes, respectivamente. Se obtuvieron, por otro lado, valores de %RSD para las áreas de pico por debajo de 0.5% en el mismo día, y valores de RSD inferiores a 7.3% en días diferentes. Los límites de detección y los límites de cuantificación del método fueron inferiores a 16.4 y 54.6 ppm, respectivamente. De forma global, los datos indican que empleando el recubrimiento polimérico se logran análisis de metabolitos aniónicos con alta reproducibilidad y eficacia. Con el fin de demostrar la utilidad del método en muestras reales, se llevó a cabo el análisis del perfil de metabolitos aniónicos en muestras de zumo de naranja y de vino tinto. La aplicación del método optimizado permitió la detección de 87 metabolitos en zumo de naranja y 142 metabolitos en vino tinto en menos de 15 minutos. Muchos de los metabolitos detectados desempeñan un importante papel en la calidad nutricional del zumo de naranja, así como, en las características organolépticas del vino tinto. Estos resultados demuestran las magníficas posibilidades del uso combinado de CE-MS y recubrimientos poliméricos para metabolómica de alimentos.

En relación al Capítulo 4 de esta Tesis Doctoral, es importante resaltar que en los últimos años el grupo de Alimentómica (Instituto de Investigación en Ciencias de la Alimentación, CIAL, CSIC-UAM) ha realizado diversos trabajos para profundizar en el conocimiento del efecto de los compuestos bioactivos

procedentes del romero (*Rosmarinus officinallis* L.) a nivel molecular en líneas celulares de cáncer de colon empleando una aproximación alimentómica (combinando Transcriptómica, Proteómica y Metabolómica) (Valdés y col., 2013; Valdés y col., 2017a; Ibañez y col., 2012a; Ibañez y col., 2012b). Los resultados de esta investigación han demostrado que los compuestos bioactivos de romero tienen actividad antiproliferativa en distintos modelos celulares de cáncer e indican que la capacidad de inhibir la proliferación de células de cáncer está relacionada con diferentes mecanismos de acción. La mayoría de las actividades anticancerígenas del extracto de romero se atribuyen principalmente a los diterpenos fenólicos ácido carnósico, carnosol y en menor proporción al rosmanol (Chun y col., 2014; Manoharan y col., 2010; Petiwala y col., 2015), sin embargo aún se tiene poca información acerca de la toxicidad de estos compuestos en el organismo. Con el objetivo de investigar la toxicidad de los tres diterpenos fenólicos más activos (ácido carnósico, carnosol y rosmanol), se llevó a cabo un experimento para evaluar la viabilidad de células hepáticas HepaRG diferenciadas y no diferenciadas expuestas durante 24h a un intervalo de concentraciones creciente (de 10 a 100 µM) de estos tres diterpenos fenólicos. Se ha demostrado que estos diterpenos presentan a estas concentraciones actividad antiproliferativa frente a células de cáncer de colon humano HT-29 y HCT116, evolucionando a un efecto citotóxico conforme aumenta la concentración del diterpeno. En estas condiciones las células hepáticas HepaRG diferenciadas presentaron una mayor resistencia a la toxicidad de los diterpenos fenólicos comparadas con las células HepaRG no diferenciadas y con las células de cáncer de colon, lo que es coherente con la gran capacidad detoxificante que las células HepaRG alcanzan durante el proceso de diferenciación. Al diferenciarse en determinadas condiciones de cultivo, las células HepaRG logran funciones muy similares al hígado humano, lo que hace que sean un modelo celular muy útil para la investigación de la toxicidad de xenobióticos *in vitro*. Entre los tres diterpenos fenólicos estudiados, el rosmanol demostró ejercer un mayor impacto en la viabilidad de las células hepáticas diferenciadas. En concentraciones de 60 µM el rosmanol redujo aproximadamente 19% de la viabilidad de las células, mientras que las mismas concentraciones de ácido carnósico y carnosol no presentaron un efecto significativo ($p > 0.05$). Con el fin de obtener una información más detallada a nivel molecular del efecto de los diterpenos fenólicos en las células HepaRG, se realizó un estudio metabolómico de las células hepáticas expuestas a 60 µM de ácido carnósico, carnosol y rosmanol. Para ello, se combinó el uso de un método de extracción simultáneo de metabolitos polares y apolares con el empleo de múltiples plataformas analíticas como GC-TOF MS y UHPLC-TOF MS, empleando en el último caso diferentes modalidades de separaciones cromatográficas en fase reversa (con columnas tipo C8 y C18). El PCA del conjunto de datos obtenidos por las diferentes técnicas analíticas demostró la separación entre el grupo de células HepaRG control y aquellas tratadas con los diterpenos fenólicos, el método estadístico no supervisado también reveló diferencias entre los tratamientos con los tres diterpenos, que se encontraron parcialmente separados. Además la integración de los resultados procedentes de las múltiples plataformas analíticas complementarias permitió la detección de un gran número de metabolitos significativamente alterados en las células hepáticas tratadas con los diterpenos. De estos, solamente diez metabolitos fueron comúnmente detectados por C8/C18-UHPLC-

TOF MS y GC-TOF MS, demostrando la gran complementariedad de las técnicas analíticas y la amplia cobertura metabólica alcanzada mediante el empleo de múltiples plataformas. Los resultados obtenidos indican que 60 µM de ácido carnósico, carnosol y rosmanol pueden presentar efectos comunes, así como alteraciones específicas de cada diterpeno fenólico. En general, el tratamiento con rosmanol indujo una mayor alteración en el metaboloma de las células hepáticas que los tratamientos con ácido carnósico y carnosol, lo que demuestra que el rosmanol genera un mayor desequilibrio metabólico en las células, lo cual es concordante con su efecto citotóxico anteriormente observado. De hecho, se observó una alta correlación entre los cambios de marcadores oxidativos y la toxicidad celular observada en las células tratadas con rosmanol. Entre estos cambios cabe destacar las alteraciones detectadas en los niveles de glutatión reducido (GSH) y glutatión oxidado (GSSG) en las células tratadas con 60 µM de rosmanol en comparación con el grupo control, los cuales son indicativos de la alteración de la homeostasis redox celular, aumentando las posibilidades de daño por estrés oxidativo, una condición que puede desencadenar la muerte celular. Por otro lado, al igual que el rosmanol, el tratamiento con carnosol también indujo una disminución de los niveles de GSH, sin embargo con este tratamiento no se observaron cambios significativos en los niveles de GSSG. Los efectos observados por el tratamiento con carnosol son similares a los resultados reportados en un estudio realizado por Valdés y col. (2016a) acerca de la actividad prooxidante de los diterpenos de romero en concentraciones de aproximadamente 40 µM en células HT-29. Por otro lado, Chen y col. (2011) describieron un aumento de GSH en células HepG2 tras 12h de tratamiento con concentraciones no toxicas de carnosol (≤10 µM). Los autores de este trabajo sugieren que el aumento de los niveles de GSH está relacionado con un efecto de protección contra el estrés oxidativo, el cual asocian a la inducción de la expresión de genes que controlan la síntesis de GSH mediada por el factor de trascripción NRF2. No obstante, recientes estudios proteómicos con células HT-29 han demostrado que concentraciones de 40-70 µM de carnosol, concentración en las cuales posee un efecto citoestático y citotóxico en las células, también inducen una respuesta antioxidante mediada por NRF2 que incluye la expresión de genes que controlan la síntesis de GSH (Valdés y col., 2017a). Estos resultados indican que carnosol induce una respuesta mediante la activación del factor NRF2 independientemente del tipo celular o de la concentración en estudio, mientras que su capacidad de alterar los niveles intracelulares de GSH y GSSG puede depender de su concentración y esta alteración puede estar relacionada en algunos casos con cierta toxicidad.

Además de las alteraciones en el estado redox celular, se observaron importantes cambios en el metabolismo de los lípidos de las células HepaRG tratadas con los diterpenos fenólicos, en especial esfingolípidos y glicerofosfolípidos. Los nieveles de los esfingolípidos detectados, tales como esfingomielina SM (d18:1/14:0), fitoesfingosina, esfingosine, entre otros, fueron mayores en células tratadas con ácido carnósico, carnosol y rosmanol en comparación con el grupo control. Diferentes trabajos indican que los esfingolípidos son importantes reguladores de apoptosis en distintos modelos celulares (Hung y col., 1999; Huang y col., 2015). Sin embargo, todavía son necesarios más estudios para

poder comprender los mecanismos por los cuales el ácido carnósico, el carnosol y el rosmanol regulan el metabolismo de los esfingolípidos.

Algunas evidencias científicas han demostrado que el extracto de romero enriquecido con ácido carnósico aumenta el consumo de glucosa y glucólisis en células HepG2 por la activación de la ruta AMPK-ACC (proteína quinasa activada por adenosín monofosfato - acetil-CoA carboxilasa) y altera la expresión de los genes SIRT1, PGC-1α y G6Pase (Tu y col., 2013). Este efecto regulador del metabolismo energético sugiere que algunos compuestos procedentes del romero juegan un papel importante en el bloqueo de la síntesis de ácidos grasos y en el aumento de las reacciones de *β*-oxidación de los mismos. De manera similar, Wang y col., (2012) también han demostrado que el ácido carnósico activa AMPK e inhibe la acumulación de lípidos en células HepG2 y que el tratamiento con ácido carnósico disminuye la acumulación de grasa en hepatocitos de ratones ob/ob deficientes en leptina (un modelo de diabetes tipo 2 con hiperglucemia y obesidad relativamente leves). En el presente estudio también hemos observado una disminución de los niveles de ácidos grasos insaturados de las células HepaRG expuestas al ácido carnósico. Además se detectaron alteraciones en los niveles de tres acilcarnitinas en las células tratadas con este diterpeno. La principal función de las acilcarnitinas es el transporte de los ácidos grasos de cadena larga hacia la mitocondria para la *β*-oxidación de los mismos. Dado que las acilcarnitinas son transformadas en las reacciones de *β*-oxidación, su acumulación normalmente sugiere una disfunción mitocondrial (McGill y col., 2014). Sin embargo, en este estudio el acúmulo o disminución de los niveles de acilcarnitinas varían de acuerdo con el tipo de acilcarnitina.

Recientes estudios indican que los extractos de romero enriquecidos con ácido carnósico inducen las vías catabólicas y el aumento de la glucólisis, así como la inhibición de las vías anabólicas como la síntesis de glucógeno y la gluconeogénesis en células HepG2 (Tu y col., 2013). Los resultados observados en el presente estudio indicaron que el tratamiento con los diterpenos fenólicos provoca alteraciones en diferentes metabolitos relacionados con la glucólisis y metabolitos intermediarios del ciclo del ácido cítrico. Por ejemplo, se observó una disminución significativa de los niveles de ácido pirúvico, ácido láctico y ácido succínico para todos los tratamientos con los diterpenos fenólicos, mientras que un acúmulo en los niveles de glucosa sólo se observó en células tratadas con rosmanol. La acumulación de los niveles de glucosa en las células tratadas con rosmanol sugiere que este diterpeno fenólico disminuye la utilización de la glucosa, efecto que no se detectó en las células tratadas con ácido carnósico y carnosol. En relación al metabolismo de la glucosa también se observó un acúmulo de S-lactoil-glutatión en las células tratadas con rosmanol. Este metabolito es un intermediario de la detoxificación del metilglioxal. El metilglioxal es normalmente considerado un producto tóxico del metabolismo de las proteínas y de los ácidos grasos, sin embargo la vía glucolítica representa la fuente endógena más importante de metilglioxal. Altos niveles de este agente glicante aparecen cuando las concentraciones de sus precursores son elevadas, como en aquellas condiciones en las cuales el uso de la glucosa está alterada, siendo su acumulación altamente tóxica para la célula (Allaman y col., 2015). Adicionalmente a los metabolitos endógenos, también se detectó la acumulación significativa de los diterpenos en su forma

oxidada. Por ejemplo, en células tratadas con carnosol se detectó un acúmulo de carnosol y rosmadial (producto de oxidación del rosmanol), lo que sugiere que el tiempo de exposición no fue suficiente para la total eliminación del diterpeno a una concentración de 60 µM y de sus productos de oxidación.

CAPÍTULO 6

Conclusiones

6. CONCLUSIONES

Las conclusiones más relevantes del trabajo realizado en esta Tesis Doctoral se enumeran a continuación:

1. Se ha investigado el empleo de nuevos recubrimientos poliméricos de capilares basados en un homopolímero de TEDETAMA y tres copolímeros de TEDETAMA con diferentes porcentajes molares de unidades neutras de HPMA para el análisis de péptidos y proteínas por CE-UV y CE-MS. Todos los capilares recubiertos con el homopolímero y los copolímeros de TEDETAMA presentaran un flujo electroosmótico anódico en un intervalo de pH de 1.9-10. La incorporación de unidades neutras de HPMA modula la interacción del polímero con la pared del capilar, reduciendo el flujo electroosmótico anódico, de modo que la separación puede ser ajustada según la composición del copolímero. El capilar recubierto con el copolímero de TEDETAMA con la incorporación de 50% de HPMA ha presentado los mejores resultados en cuanto a la resolución y el tiempo de análisis de las proteínas, así como una buena reproducibilidad de los tiempos de migración y de áreas de pico. Además, el polímero es compatible con la detección por MS y permite el análisis de péptidos y proteínas en tiempos cortos de migración y con buena resolución mediante CE-MS. El método desarrollado con el recubrimiento polimérico capilar TEDETAMA-co-HPMA (50:50) también ha demostrado ser eficaz para el análisis de lisozima en muestras de queso mediante CE-MS.

2. Se ha desarrollado un nuevo procedimiento de análisis rápido y robusto mediante CE-MS para la obtención del perfil de metabolitos aniónicos. Dicho método se basa en el uso del recubrimiento capilar catiónico con el copolímero TEDETAMA-co-HPMA (50:50) para invertir y estabilizar el EOF en CE-MS y llevar a cabo el análisis de compuestos aniónicos en polaridad inversa. El método ha presentado límites de detección y límites de cuantificación inferiores a 16.4 y 54.6 ppm, respectivamente, así como una buena reproducibilidad, con valores de RSD inferiores 0.1 y 0.6% para los tiempos de migración para un mismo día (n= 5 inyecciones) y en días diferentes (n= 15 inyecciones), y RSDs inferiores a 0.5 % y 7.3% para los valores de área de pico para un mismo día (n= 5 inyecciones) y tres diferentes días (n= 15 inyecciones). Además, ha sido aplicado con éxito al análisis del perfil de metabolitos aniónicos en muestras de zumo de naranja y de vino tinto, permitiendo la detección de 87 y 142 metabolitos, respectivamente, en menos de 15 minutos de análisis.

3. Se ha utilizado una aproximación metabolómica para investigar los cambios metabólicos originados por los diterpenos ácido canósico, carnosol y rosmanol, compuestos bioactivos procedentes del romero, en células de hígado humano HepaRG. La combinación de los resultados obtenidos mediante el uso de diferentes plataformas analíticas complementarias como GC-TOF MS y C8/C18-UHPLC-TOF MS, ha permitido detectar un mayor número de metabolitos cuya expresión varía significativamente en células HepaRG tratadas con los diterpenos. Además, la aproximación metabolómica empleada proporciona una elevada sensibilidad para identificar

diferencias entre la actividad de los diterpenos. Así, se observó que el rosmanol origina una mayor alteración en el metaboloma de las células HepaRG que el carnosol o el ácido carnósico; estos cambios a nivel molecular están en consonancia con la mayor citotoxicidad observada para el rosmanol. Así, el tratamiento de las células hepáticas con 60 µM de los diterpenos fenólicos (principalmente con rosmanol) reveló cambios significativos en metabolitos involucrados en reacciones redox y de desintoxicación de xenobióticos, así como alteraciones en el metabolismo de los lípidos y de la glucosa, indicando modificaciones en el metabolismo energético y de la homeostasis redox celular. Estos resultados corroboran la utilidad de la aproximación empleada (metabolómica y células HepaRG) para el estudio de la toxicidad de compuestos y confirman la mayor toxicidad del diterpeno rosmanol respecto al ácido carnósico y al carnosol.

Bibliografía

Bibliografía

Afonso, M.S., de O Silva, A.M., Carvalho, E.B., Rivelli, D.P., Barros, S.B., Rogero, M.M., Lottenberg, A.M., Torres, R.P., Mancini-Filho, J., 2013. Phenolic compounds from Rosemary (*Rosmarinus officinalis* L.) attenuate oxidative stress and reduce blood cholesterol concentrations in diet-induced hypercholesterolemic rats. Nutr. Metab. 10, 19. doi:10.1186/1743-7075-10-19

Aguilar, F., Autrup, H., Barlow, S., Castle, L., Crebelli, R., Dekant, W., Engel, K.-H., Gontard, N., Gott, D., Grilli, S., Gürtler, R., Chr Larsen, J., Leclercq, C., Leblanc, J.-C., Xavier Malcata, F., Mennes, W., Milana, M. R., Pratt, I., Rietjens, I., Tobback, P., Toldrá, F., 2008. Use of rosemary extracts as a food additive Scientific Opinion of the Panel on Food Additives, Flavourings, Processing Aids and Materials in Contact with Food Panel Members. EFSA J. 721, 1–29. doi:10.2903/j.efsa.2008.721.

Albalat, A., Husi, H., Siwy, J., Nally, J.E., McLauglin, M., Eckersall, P.D., Mullen, W., 2014. Capillary electrophoresis interfaced with a mass spectrometer (CE-MS): technical considerations and applicability for biomarker studies in animals. Curr. Protein Pept. Sci. 15, 23–35.

Allaman, I., Bélanger, M., Magistretti, P.J., 2015. Methylglyoxal, the dark side of glycolysis. Front. Neurosci. 9, 1–12.

Al-Sereiti, M.R., Abu-Amer, K.M., Sen, P., 1999. Pharmacology of rosemary (*Rosmarinus officinalis* Linn.) and its therapeutic potentials. Indian J. Exp. Biol. 37, 124–130.

Alves, M.J., Ferreira, I.C.F.R., Froufe, H.J.C., Abreu, R.M. V, Martins, A., Pintado, M., 2013. Antimicrobial activity of phenolic compounds identified in wild mushrooms, SAR analysis and docking studies. J. Appl. Microbiol. 115, 346–357.

Anadón, A., Martínez-Larrañaga, M.R., Martínez, M. A, Ares, I., García-Risco, M.R., Señoráns, F.J., Reglero, G., 2008. Acute oral safety study of rosemary extracts in rats. J. Food Prot. 71, 790–795.

Aninat, C., Piton, A., Glaise, D., Le Charpentier, T., Langouët, S., Morel, F., Guguen-Guillouzo, C., Guillouzo, A., 2006. Expression of Cytochrome P450 Enzymes and Nuclear Receptors in Human Hepatoma HepaRG Cells. Drug Metab. Dispos. 34, 75–83.

Aruoma, O. I., Halliwell, B., Aeschbach, R. Loligers, J., 1992. Antioxidant and pro-oxidant properties of active rosemary constituents: carnosol and carnosic acid. Xenobiotica 22, 257–268.

Avila-Sosa, R., Navarro-cruz, A.R., Vera-lópez, O., Dávila-márquez, R.M., Melgoza-palma, N., Meza-pluma, R., 2011. Romero (*Rosmarinus officinalis*): Una revisión de sus usos no culinarios. Cinc. Mar. 52, 23–36.

Azmir, J., Zaidul, I.S.M., Rahman, M.M., Sharif, K.M., Mohamed, A., Sahena, F., Jahurul, M.H.A., Ghafoor, K., Norulaini, N.A.N., Omar, A.K.M., 2013. Techniques for extraction of bioactive compounds from plant materials: A review. J. Food Eng. 117, 426–436.

Babushok, V.I., Linstrom, P.J., Reed, J.J., Zenkevich, I.G., Brown, R.L., Mallard, W.G., Stein, S.E., 2007. Development of a database of gas chromatographic retention properties of organic compounds. J. Chromatogr. A 1157, 414–421.

Bai, N., He, K., Roller, M., Lai, C.S., Shao, X., Pan, M.H., Ho, C.T., 2010. Flavonoids and phenolic compounds from *Rosmarinus officinalis*. J. Agric. Food Chem. 58, 5363–5367.

Balasundram, N., Sundram, K., Samman, S., 2006. Phenolic compounds in plants and agri-industrial by-products: Antioxidant activity, occurrence, and potential uses. Food Chem. 99, 191–203.

Barding, G.A., Salditos, R., Larive, C.K., 2012. Quantitative NMR for bioanalysis and metabolomics. Anal. Bioanal. Chem. 404, 1165–1179.

Barni, M. V., Carlini, M.J., Cafferata, E.G., Puricelli, L., Moreno, S., 2012. Carnosic acid inhibits the proliferation and migration capacity of human colorectal cancer cells. Oncol. Rep. 27, 1041–1048.

Berrington, D., Lall, N., 2012. Anticancer activity of certain herbs and spices on the cervical epithelial carcinoma (HeLa) cell line. Evidence-based Complement. Altern. Med. 2012, 1–11.

Bi, H., Krausz, K.W., Manna, S.K., Li, F., Johnson, C.H., Gonzalez, F.J., 2013. Optimization of harvesting, extraction, and analytical protocols for UPLC-ESI-MS-based metabolomic analysis of adherent mammalian cancer cells. Anal. Bioanal. Chem. 405, 5279–5289.

Biasioli, F., Yeretzian, C., Märk, T.D., Dewulf, J., Van Langenhove, H., 2011. Direct-injection mass spectrometry adds the time dimension to (B)VOC analysis. TrAC - Trends Anal. Chem. 30, 1003–1017.

Birungi, G., Chen, S.M., Loy, B.P., Ng, M.L., Fong, S., Li, Y., 2010. Metabolomics Approach for Investigation of Effects of Dengue Virus Infection Using the EA . hy926 Cell Line research articles. J. Proteome Res. 9, 6523–6534.

Boccard, J., Veuthey, J.L., Rudaz, S., 2010. Knowledge discovery in metabolomics: An overview of MS data handling. J. Sep. Sci. 33, 290–304.

Bolton, E.E., Wang, Y., Thiessen, P.A., Bryant, S.H., 2008. PubChem: Integrated Platform of Small Molecules and Biological Activities, in: Wheeler, R. A. and Spellmeyer D. C. (Eds.), Annual Reports in Computational Chemistry. Elsevier B.V., pp. 217–241.

Borrás-Linares, I., Stojanovic, Z., Quirantes-Piné, R., Arráez-Román, D., Švarc-Gajić, J., Fernández-Gutiérrez, A., Segura-Carretero, A., 2014. *Rosmarinus officinalis* leaves as a natural source of bioactive compounds. Int. J. Mol. Sci. 15, 20585–20606.

Bozin, B., Mimica-Dukic, N., Samojlik, I., Jovin, E., 2007. Antimicrobial and antioxidant properties of Rosemary and Sage (*Rosmarinus officinalis* L. and *Salvia officinalis* L., Lamiaceae) essential oils. J. Agric. Food Chem. 55, 7879–7885.

Bravo, L., Sources, D., Significance, N., 1998. Polyphenols: chemistry, dietary sources, metabolism, and nutritional significance. Nutr. Rev. 56, 317–333.

Brennan, L., 2014. NMR-based metabolomics: From sample preparation to applications in nutrition research. Prog. Nucl. Magn. Reson. Spectrosc. 83, 42–49.

Carocho, M., Ferreira, I.C.F.R., 2013. The role of phenolic compounds in the fight against cancer - A review. Anticancer. Agents Med. Chem. 13, 1236–1258.

Català-Clariana, S., Benavente, F., Giménez, E., Barbosa, J., Sanz-Nebot, V., 2013. Identification of bioactive peptides in hypoallergenic infant milk formulas by CE-TOF-MS assisted by semiempirical model of electromigration behavior. Electrophoresis 34, 1886–1894.

Chen, C., Chen, H., Hsieh, C., Yang, Y., Wung, B., 2011. Upregulation of NF-E2-related factor-2-dependent glutathione by carnosol provokes a cytoprotective response and enhances cell survival. Acta Pharmacol. Sin. 32, 62–69.

Chun, K.S, Kundu, J., Chae, I.G., Kundu, J.K., 2014. Carnosol: A Phenolic Diterpene With Cancer Chemopreventive Potential. J. Cancer Prev. 1919, 103–110.

Cifuentes, A., 2009. Food analysis and foodomics. J. Chromatogr. A 1216, 7109.

Cooks, R.G., Ouyang, Z., Takats, Z., Wiseman, J.M., 2006. Ambient Mass Spectrometry. Science. 311, 1566–1570.

Dai, J., Mumper, R.J., 2010. Plant phenolics: Extraction, analysis and their antioxidant and anticancer properties. Molecules 15, 7313–7352.

de Oliveira, M.R., 2016. The Dietary Components Carnosic Acid and Carnosol as Neuroprotective Agents: a Mechanistic View. Mol. Neurobiol. 53, 6155–6168.

de Pascual-Teresa, S., Moreno, D.A., García-Viguera, C., 2010. Flavanols and anthocyanins in cardiovascular health: A review of current evidence. Int. J. Mol. Sci. 11, 1679–1703.

Del Baño, M.J., Lorente, J., Castillo, J., Benavente-García, O., Marín, M.P., Del Río, J.A., Ortuño, A., Ibarra, I., 2004. Flavonoid distribution during the development of leaves, Flowers, stems, and roots of *Rosmarinus officinalis*. Postulation of a biosynthetic pathway. J. Agric. Food Chem. 52, 4987–4992.

Dettmer, K., Almstetter, M.F., Wachsmuth, C.J. ,Oefner, P.J., 2013. Comprehensive Two-Dimensional Gas Chromatography for Metabolomics, in: Weckwerth, W., Kahl, and G. (Eds.), The Handbook of Plant Metabolomics. Wiley-VCH Verlag GmbH & Co. KGaA, Weinheim, Germany, pp. 77–91.

Dettmer, K., Aronov, P.A., Hammock, B.D., 2007. Mass spectrometry-based metabolomics. Mass Spectrom. Rev. 26, 51–78.

Doherty, E.A.S., Meagher, R.J., Albarghouthi, M.N., Barron, A.E., 2003. Microchannel wall coatings for protein separations by capillary and chip electrophoresis. Electrophoresis 24, 34–54.

Dolník, V., 2008. Capillary electrophoresis of proteins 2005-2007. Electrophoresis 29, 143–156.

Draper, J., Lloyd, A.J., Goodacre, R., Beckmann, M., 2013. Flow infusion electrospray ionisation mass spectrometry for high throughput, non-targeted metabolite fingerprinting: A review. Metabolomics 9, 4–29.

Dummer, J., Storer, M., Swanney, M., McEwan, M., Scott-Thomas, A., Bhandari, S., Chambers, S., Dweik, R., Epton, M., 2011. Analysis of biogenic volatile organic compounds in human health and disease. TrAC - Trends Anal. Chem. 30, 960–967.

Dunn, W.B., Bailey, N.J.C., Johnson, H.E., 2005. Measuring the metabolome: current analytical technologies. Analyst 130, 606–625.

Dunn, W.B., Ellis, D.I., 2005. Metabolomics: Current analytical platforms and methodologies. TrAC - Trends Anal. Chem. 24, 285–294.

Edwards, J.L., Kennedy, R.T., 2005. Metabolomic analysis of eukaryotic tissue and prokaryotes using negative mode MALDI time-of-flight mass spectrometry. Anal. Chem. 77, 2201–2209.

EFSA Panel on Food Additives and Nutrient Sources added to Food, 2015. Extension of use ofextracts of rosemary (E 392) in fat-based spreads. EFSA J. 13, 4090. doi:10.2903/j.efsa.2015.4090.

Ellinger, J.J., Chylla, R.A, Ulrich, E.L., Markley, J.L., 2013. Databases and Software for NMR-Based Metabolomics. Curr. Metabolomics 1, 1–22.

Estruch, R., Ros, E., Salas-Salvadó, J., Covas, M., Corella, D., Arós, F., Gómez-Gracia, E., Ruiz-Gutiérrez, V., Fiol, M., Lapetra, J., Lamuela-Raventos, R., Serra-Majem, L., Pintó, X., Basora, J., Muñoz, M., Sorlí, J., Martínez, J.A., Martínez-González, M.A., 2013. Primary prevention of cardiovascular disease with a Mediterranean diet. N. Engl. J. Med. 368, 1279–1290.

Ewing, A.G., Wallingford, R.A., Olefirowicz, T.M., 1989. Capillary Electrophoresis. Anal. Chem. 61, 292A–303A.

Fiehn, O., 2001. Combining Genomics, Metabolome Analysis, and Biochemical Modelling to Understand Metabolic Networks. Comp. Funct. Genomics 2, 155–168.

Fornari, T., Vicente, G., Vázquez, E., García-Risco, M.R., Reglero, G., 2012. Isolation of essential oil from different plants and herbs by supercritical fluid extraction. J. Chromatogr. A 1250, 34–48.

Fresco, P., Borges, F., Diniz, C., Marques, M.P.M., 2006. New insights on the anticancer properties of dietary polyphenols. Med. Res. Rev. 26, 747–766.

Galati, G., O'Brien, P.J., 2004. Potential toxicity of flavonoids and other dietary phenolics: Significance for their chemopreventive and anticancer properties. Free Radic. Biol. Med. 37, 287–303.

Gao, X., Pujos-Guillot, E., Martin, J.F., Galan, P., Juste, C., Jia, W., Sebedio, J.L., 2009. Metabolite analysis of human fecal water by gas chromatography/mass spectrometry with ethyl chloroformate derivatization. Anal. Biochem. 393, 163–175.

García, A., Godzien, J., López-Gonzálvez, Á., Barbas, C., 2017 Capillary electrophoresis mass spectrometry as a tool for untargeted metabolomics. Bioanalysis 9, 99–130.

García-Cañas, V., Simó, C., Herrero, M., Ibáñez, E., Cifuentes, A., 2012. Present and future challenges in food analysis: Foodomics. Anal. Chem. 84, 10150–10159.

Gerber, M., Hoffman, R., 2015. The Mediterranean diet: health, science and society. Br. J. Nutr. 113, S4–S10.

Ghaste, M., Mistrik, R., Shulaev, V., 2016. Applications of fourier transform ion cyclotron resonance (FT-ICR) and orbitrap based high resolution mass spectrometry in metabolomics and lipidomics. Int. J. Mol. Sci. 17, 816. doi:10.3390/ijms17060816.

Gika, H.G., Theodoridis, G.A., Plumb, R.S., Wilson, I.D., 2014. Current practice of liquid chromatography-mass spectrometry in metabolomics and metabonomics. J. Pharm. Biomed. Anal. 87, 12–25.

González-Vallinas, M., Molina, S., Vicente, G., Sánchez-Martínez, R., Vargas, T., García-Risco, M.R., Fornari, T., Reglero, G., Ramírez de Molina, A., 2014a. Modulation of estrogen and epidermal growth factor receptors by rosemary extract in breast cancer cells. Electrophoresis 35, 1719–1727.

González-Vallinas, M., Molina, S., Vicente, G., Zarza, V., Martín-Hernández, R., García-Risco, M.R., Fornari, T., Reglero, G., De Molina, A.R., 2014b. Expression of MicroRNA-15b and the glycosyltransferase GCNT3 correlates with antitumor efficacy of rosemary diterpenes in colon and pancreatic cancer. PLoS One 9, 1–10.

González-Vallinas, M., Reglero, G., Ramírez de Molina, A., 2015. Rosemary (*Rosmarinus officinalis* L .) extract as a potential complementary agent in anticancer therapy. Nutr. Cancer 67, 1223–1231.

Gripon, P., Rumin, S., Urban, S., Le Seyec, J., Glaise, D., Cannie, I., Guyomard, C., Lucas, J., Trepo, C., Guguen-Guillouzo, C., 2002. Infection of a human hepatoma cell line by hepatitis B virus. Proc. Natl. Acad. Sci. U. S. A. 99, 15655–60.

Gross, J.H., 2014. Direct analysis in real time-a critical review on DART-MS. Anal. Bioanal. Chem. 406, 63–80.

Guillarme, D., Schappler, J., Rudaz, S., Veuthey, J.-L., 2010. Coupling ultra-high-pressure liquid chromatography with mass spectrometry. TrAC Trends Anal. Chem. 29, 15–27.

Guillouzo, A., Corlu, A., Aninat, C., Glaise, D., Morel, F., Guguen-Guillouzo, C., 2007. The human hepatoma HepaRG cells: A highly differentiated model for studies of liver metabolism and toxicity of xenobiotics. Chem. Biol. Interact. 168, 66–73.

Habtemariam, S., 2016. The Therapeutic Potential of Rosemary (*Rosmarinus officinalis*) Diterpenes for Alzheimer's Disease. Evidence-based Complement. Altern. Med. 2016, ID2680409. doi:10.1155/2016/2680409

Harris, G.A., Galhena, A.S., Fern, F.M., 2011. Ambient Sampling/Ionization Mass Spectrometry : Applications and Current Trends. Anal. Chem. 83, 4508–4538.

Haselberg, R., de Jong, G.J., Somsen, G.W., 2013. CE-MS for the analysis of intact proteins 2010-2012. Electrophoresis 34, 99–112.

Hernández-Aguilera, A., Rull, A., Rodríguez-Gallego, E., Riera-Borrull, M., Luciano-Mateo, F., Camps, J., Menéndez, J.A., Joven, J., 2013. Mitochondrial dysfunction: A basic mechanism in inflammation-related non-communicable diseases and therapeutic opportunities. Mediators Inflamm. 2013, ID 135698. doi:10.1155/2013/135698

Herrero, M., Plaza, M., Cifuentes, A., Ibáñez, E., 2010. Green processes for the extraction of bioactives from Rosemary: Chemical and functional characterization via ultra-performance liquid chromatography-tandem mass spectrometry and in-vitro assays. J. Chromatogr. A 1217, 2512–2520.

Hewer, R., Vorster, J., Steffens, F.E., Meyer, D., 2006. Applying biofluid 1H NMR-based metabonomic techniques to distinguish between HIV-1 positive/AIDS patients on antiretroviral treatment and HIV-1 negative individuals. J. Pharm. Biomed. Anal. 41, 1442–1446.

Hirayama, A., Wakayama, M., Soga, T., 2014. Metabolome analysis based on capillary electrophoresis-mass spectrometry. TrAC - Trends Anal. Chem. 61, 215–222.

Hommerson, P., Khan, A.M., de Jong, G.J., Somsen, G.W., 2011. Ionization techniques in capillary electrophoresis-mass spectrometry: Principles, design, and application. Mass Spectrom. Rev., 30, 1096–1120.

Horai, H., Arita, M., Kanaya, S., Nihei, Y., Ikeda, T., Suwa, K., Ojima, Y., Tanaka, K., Tanaka, S., Aoshima, K., Oda, Y., Kakazu, Y., Kusano, M., Tohge, T., Matsuda, F., Sawada, Y., Hirai, M.Y., Nakanishi, H., Ikeda, K., Akimoto, N., Maoka, T., Takahashi, H., Ara, T., Sakurai, N., Suzuki, H., Shibata, D., Neumann, S., Iida, T., Tanaka, K., Funatsu, K., Matsuura, F., Soga, T., Taguchi, R., Saito, K., Nishioka, T., 2010. MassBank: A public repository for sharing mass spectral data for life sciences. J. Mass Spectrom. 45, 703–714.

Huang, C., Freter, C., 2015. Lipid metabolism, apoptosis and cancer therapy. Int. J. Mol. Sci. 16, 924–949.

Huhn, C., Ramautar, R., Wuhrer, M., Somsen, G.W., 2010. Relevance and use of capillary coatings in capillary electrophoresis-mass spectrometry. Anal. Bioanal. Chem. 396, 297–314.

Hung, W.C., Chang, H.C., Chuang, L.Y., 1999. Activation of caspase-3-like proteases in apoptosis induced by sphingosine and other long-chain bases in Hep3B hepatoma cells. Biochem. J. 338, 161–166.

Ibáñez, C., Simó, C., García-Cañas, V., Cifuentes, A., Castro-Puyana, M., 2013. Metabolomics, peptidomics and proteomics applications of capillary electrophoresis-mass spectrometry in Foodomics: A review. Anal. Chim. Acta 802, 1–13.

Ibáñez, C., Simó, C., García-Cañas, V., Gómez-Martínez, Á., Ferragut, J.A., Cifuentes, A., 2012a. CE/LC-MS multiplatform for broad metabolomic analysis of dietary polyphenols effect on colon cancer cells proliferation. Electrophoresis 33, 2328–2336.

Ibáñez, C., Valdés, A., García-Cañas, V., Simó, C., Celebier, M., Rocamora-Reverte, L., Gómez-Martínez, Á., Herrero, M., Castro-Puyana, M., Segura-Carretero, A., Ibáñez, E., Ferragut, J.A., Cifuentes, A., 2012b. Global Foodomics strategy to investigate the health benefits of dietary constituents. J. Chromatogr. A 1248, 139–153.

Idborg-Björkman, H., Edlund, P.O., Kvalheim, O.M., Schuppe-Koistinen, I., Jacobsson, S.P., 2003. Screening of biomarkers in rat urine using LC/electrospray ionization-MS and two-way data analysis. Anal. Chem. 75, 4784–4792.

Jacobs, D.M., Fuhrmann, J.C., Van Dorsten, F.A., Rein, D., Peters, S., Van Velzen, E.J.J., Hollebrands, B., Draijer, R., Van Duynhoven, J., Garczarek, U., 2012. Impact of short-term intake of red wine and grape polyphenol extract on the human metabolome. J. Agric. Food Chem. 60, 3078–3085.

Jeong, J., Zhang, X., Shi, X., Kim, S., Shen, C., 2013. An efficient post-hoc integration method improving peak alignment of metabolomics data from GCxGC/TOF-MS. BMC Bioinformatics 14, 123. doi:10.1186/1471-2105-14-123

Jossé, R., Aninat, C., Glaise, D., Dumont, J., Fessard, V., Morel, F., Poul, J., Guguen-Guillouzo, C. Guillouzo, A., 2008. Long-Term Functional Stability of Human HepaRG Hepatocytes and Use for Chronic Toxicity and Genotoxicity Studies Drug Metab. Dispos. 36, 1111–1118.

Junot, C., Fenaille, F., Colsch, B., Bécher, F., 2014. High resolution mass spectrometry based techniques at the crossroads of metabolic pathways. Mass Spectrom. Rev. 33, 471–500.

Kanehisa, M., 1997. A database for post-genome analysis. Trends Genet. 13, 375–376.

Katajamaa, M., Orešič, M., 2005. Processing methods for differential analysis of LC/MS profile data. BMC Bioinformatics 6, 179. doi:10.1186/1471-2105-6-179

Katajamaa, M., Orešič, M., 2007. Data processing for mass spectrometry-based metabolomics. J. Chromatogr. A 1158, 318–328.

Kaur, C., Kapoor, H.C., 2001. Antioxidants in fruits and vegetables - The millennium's health. Int. J. Food Sci. Technol. 36, 703–725.

Kim, D.H., Park, K.W., Chae, I.G., Kundu, J., Kim, E.H., Kundu, J.K., Chun, K.S., 2016. Carnosic acid inhibits STAT3 signaling and induces apoptosis through generation of ROS in human colon cancer HCT116 cells. Mol. Carcinog. 55, 1096–1110.

Kind, T., Wohlgemuth, G., Lee, D.Y., Lu, Y., Palazoglu, M., Shahbaz, S., Fiehn, O., 2009. FiehnLib: Mass spectral and retention index libraries for metabolomics based on quadrupole and time-of-flight gas chromatography/mass spectrometry. Anal. Chem. 81, 10038–10048.

Klepacka, J., Gujska, E., Michalak, J., 2011. Phenolic Compounds as Cultivar- and Variety-distinguishing Factors in Some Plant Products. Plant Foods Hum. Nutr. 66, 64–69.

Koek, M.M., Jellema, R.H., Van der Greef, J., Tas, A.C., Hankemeier, T., 2011. Quantitative metabolomics based on gas chromatography mass spectrometry: Status and perspectives. Metabolomics 7, 307–328.

Koek, M.M., Muilwijk, B., Van Der Werf, M.J., Hankemeier, T., 2006. Microbial metabolomics with gas chromatography/mass spectrometry. Anal. Chem. 78, 1272–1281.

Kondeková, M., Maier, V., Ginterová, P., Marák, J., Ševčík, J., 2014. Analysis of lysozyme in cheese samples by on-line combination of capillary zone electrophoresis and mass spectrometry. Food Chem. 153, 398–404.

Kopka, J., Schauer, N., Krueger, S., Birkemeyer, C., Usadel, B., Bergmüller, E., Dörmann, P., Weckwerth, W., Gibon, Y., Stitt, M., Willmitzer, L., Fernie, A.R., Steinhauser, D., 2005. GMD@CSB.DB: The Golm metabolome database. Bioinformatics 21, 1635–1638.

Law, W.S., Huang, P.Y., Ong, E.S., Ong, C.N., Li, S.F. Y., Pasikanti, K.K., Chan, E.C.Y., 2008. Metabonomics investigation of human urine after ingestion of green tea with gas chromatography/mass spectrometry, liquid chromatography/mass spectrometry and 1H NMR spectroscopy.Rapid Commun. Mass Spectrom. 22, 2436–2446.

Lei, Z., Huhman, D.V., Sumner, L.W., 2011. Mass spectrometry strategies in metabolomics. J. Biol. Chem. 286, 25435–25442.

Lenz, E.M., Bright, J., Knight, R., Wilson, I.D., Major, H., 2004. Cyclosporin A-induced changes in endogenous metabolites in rat urine: A metabonomic investigation using high field 1H NMR spectroscopy, HPLC-TOF/MS and chemometrics. J. Pharm. Biomed. Anal. 35, 599–608.

Lin, C.Y., Wu, H., Tjeerdema, R.S., Viant, M.R., 2007. Evaluation of metabolite extraction strategies from tissue samples using NMR metabolomics. Metabolomics 3, 55–67.

Lindon, J.C., Holmes, E., Nicholson, J.K., 2001. Pattern recognition methods and applications in biomedical magnetic resonance. Prog. Nucl. Magn. Reson. Spectrosc. 39, 1–40.

Lindon, J.J.C., Holmes, E., Nicholson, J.K., 2003. So what's the deal with metabonomics? Anal. Chem. 75, 384A–391A.

Lucy, C.A., MacDonald, A.M., Gulcev, M.D., 2008. Non-covalent capillary coatings for protein separations in capillary electrophoresis. J. Chromatogr. A 1184, 81–105.

Manach, C., Scalbert, A., Morand, C., Scalbert, A., Morand, C., Rémésy, C., Jiménez, L., 2004. Polyphenols: food sources and bioavailability. Am. J. Clin. Nutr. 79, 727–747.

Manoharan, S., VasanthaSelvan, M., Silvan, S., Baskaran, N., Kumar Singh, A., Vinoth Kumar, V., 2010. Carnosic acid: A potent chemopreventive agent against oral carcinogenesis. Chem. Biol. Interact. 188, 616–622.

Mansor, R., Mullen, W., Albalat, A., Zerefos, P., Mischak, H., Barrett, D.C., Biggs, A., Eckersall, P.D., 2013. A peptidomic approach to biomarker discovery for bovine mastitis. J. Proteomics 85, 89–98.

Martin, F.P.J., Rezzi, S., Peré-Trepat, E., Kamlage, B., Collino, S., Leibold, E., Kastler, J., Rein, D., Fay, L.B., Kochhar, S., 2009. Metabolic effects of dark chocolate consumption on energy, gut microbiota, and stress-related metabolism in free-living subjects. J. Proteome Res. 8, 5568–5579.

McGill, M.R., Li, F., Sharpe, M.R., Williams, C.D., Curry, S.C., Ma, X., Jaeschke, H., 2014. Circulating acylcarnitines as biomarkers of mitochondrial dysfunction after acetaminophen overdose in mice and humans. Arch. Toxicol. 88, 391–401.

Mellert, W., Kapp, M., Strauss, V., Wiemer, J., Kamp, H., Walk, T., Looser, R., Prokoudine, A., Fabian, E., Krennrich, G., Herold, M., van Ravenzwaay, B., 2011. Nutritional impact on the plasma metabolome of rats. Toxicol. Lett. 207, 173–181.

Michopoulos, F., Lai, L., Gika, H., Theodoridis, G., Wilson, I., 2009. UPLC-MS-based analysis of human plasma for metabonomics using solvent precipitation or solid phase extraction. J. Proteome Res. 8, 2114–2121.

Miura, D., Fujimura, Y., Tachibana, H., Wariishi, H., 2010. Highly sensitive matrix-sssisted laser desorption ionization-mass spectrometry for high-throughput metabolic profiling. Anal. Chem. 82, 498–504.

Mondello, L., Tranchida, P.Q., Dugo, P., Dugo, G., 2008. Comprehensive two-dimensional gas chromatography-mass spectrometry: A review. Mass Spectrom. Rev. 27, 101–124.

Monge, M.E., Harris, G.A., Dwivedi, P., Fernández, F.M., 2013. Mass spectrometry: Recent advances in direct open air surface sampling/ionization. Chem. Rev. 113, 2269–2308.

Moreno, S., Scheyer, T., Romano, C.S., Vojnov, A.A., 2006. Antioxidant and antimicrobial activities of rosemary extracts linked to their polyphenol composition. Free Radic. Res. 40, 223–231.

Morton, L.W., Abu-Amsha Caccetta, R., Puddey, I.B., Croft, K.D., 2000. Chemistry and biological effects of dietary phenolic compounds: relevance to cardiovascular disease. Clin. Exp. Pharmacol. Physiol. 27, 152–159.

Mueller, S.O., Guillouzo, A., Hewitt, P.G., Richert, L., 2015. Drug biokinetic and toxicity assessments in rat and human primary hepatocytes and HepaRG cells within the EU-funded Predict-IV project. Toxicol. Vitr. 30, 19–26.

Naczk, M., Shahidi, F., 2006. Phenolics in cereals, fruits and vegetables: Occurrence, extraction and analysis. J. Pharm. Biomed. Anal. 41, 1523–1542.

Paglia, G., Astarita, G., 2017. Metabolomics and lipidomics using traveling-wave ion mobility mass spectrometry. Nat. Protoc. 12, 797–813.

Pandey, K.B., Rizvi, S.I., 2009. Plant polyphenols as dietary antioxidants in human health and disease. Oxid. Med. Cell. Longev. 2, 270–278.

Peng, C.-H., Su, J.-D., Chyau, C.-C., Sung, T.-Y., Ho, S.-S., Peng, C.-C., Peng, R.Y., 2007. Supercritical Fluid Extracts of Rosemary Leaves Exhibit Potent Anti-Inflammation and Anti-Tumor Effects. Biosci. Biotechnol. Biochem. 71, 2223–2232.

Petiwala, S.M., Berhe, S., Li, G., Puthenveetil, A.G., Rahman, O., Nonn, L., Johnson, J.J., 2014. Rosemary (*Rosmarinus officinalis*) extract modulates CHOP/GADD153 to promote androgen receptor degradation and decreases xenograft tumor growth. PLoS One 9, e89772. doi:10.1371/journal.pone.0089772

Petiwala, S.M., Johnson, J.J., 2015. Diterpenes from rosemary (*Rosmarinus officinalis*): Defining their potential for anti-cancer activity. Cancer Lett. 367, 93–102.

Petiwala, S.M., Puthenveetil, A.G., Johnson, J.J., 2013. Polyphenols from the Mediterranean herb rosemary (*Rosmarinus officinalis*) for prostate cancer. Front. Pharmacol. 4, 1–4.

Psychogios, N., Hau, D.D., Peng, J., Guo, A.C., Mandal, R., Bouatra, S., Sinelnikov, I., Krishnamurthy, R., Eisner, R., Gautam, B., Young, N., Xia, J., Knox, C., Dong, E., Huang, P., Hollander, Z., Pedersen, T.L., Smith, S.R., Bamforth, F., Greiner, R., McManus, B., Newman, J.W., Goodfriend, T., Wishart, D.S., 2011. The human serum metabolome. PLoS One 6, e16957. doi:10.1371/journal.pone.0016957

Rajasekaran, D., Manoharan, S., Silvan, S., Vasudevan, K., Baskaran, N., Palanimuthu, D., 2012. Proapoptotic, anti-cell proliferative, anti-inflammatory and anti-angiogenic potential of carnosic acid during 7,12 dimethylbenz[a]anthracene-induced hamster buccal pouch carcinogenesis. Afr. J. Tradit. Complement. Altern. Med. 10, 102–112.

Ramassamy, C., 2006. Emerging role of polyphenolic compounds in the treatment of neurodegenerative diseases: A review of their intracellular targets. Eur. J. Pharmacol. 545, 51–64.

Ramautar, R., Somsen, G.W., De Jong, G. J., 2017. CE-MS for metabolomics: developments and applications in the period 2014–2016. Electrophoresis 38, 190–202.

Ramautar, R.,Somsen, G.W., De Jong, G.J., 2013. CE-MS for metabolomics: Developments and applications in the period 2010–2012. Electrophoresis 34, 86–98.

Reo, N.V., 2002. NMR-Based Metabolomics. Drug Chem. Toxicol. 25, 375–382.

Rico, E., González, O., Blanco, M.E., Alonso, R.M., 2014. Evaluation of human plasma sample preparation protocols for untargeted metabolic profiles analyzed by UHPLC-ESI-TOF-MS. Anal. Bioanal. Chem. 406, 7641–7652.

Ríos, J.L., Recio, M.C., Escandell, J.M., Andújar, I., 2009. Inhibition of transcription factors by plant-derived compounds and their implications in inflammation and cancer. Curr. Pharm. Des. 15, 1212–1237.

Rodriguez-Aller, M., Gurny, R., Veuthey, J.-L., Guillarme, D., 2012. Coupling ultra high-pressure liquid chromatography with mass spectrometry: Constraints and possible applications. J. Chromatogr. A 1292, 2–18.

Roessner, U., Wagner, C., Kopka, J., Trethewey, R.N., Willmitzer, L., 2000. Simultaneous analysis of metabolites in potato tuber by gas chromatography-mass spectrometry. Plant J. 23, 131–142.

Sancheti, G., Goyal, P. K., 2006. Effect of *Rosmarinus officinalis* in modulating 7, 12-dimethylbenz (a) anthracene induced skin tumorigenesis in mice. Phytother. Res. 20, 981–986.

Saric, J., Want, E.J., Duthaler, U., Lewis, M., Keiser, J., Shockcor, J.P., Ross, G.A., Nicholson, J.K., Holmes, E., Tavares, M.F.M., 2012. Systematic Evaluation of Extraction Methods for Multiplatform-Based Metabotyping: Application to the Fasciola hepatica Metabolome. Anal. Chem. 84, 6963–6972.

Satoh, T., Kosaka, K., Itoh, K., Kobayashi, A., Yamamoto, M., Shimojo, Y., Kitajima, C., Cui, J., Kamins, J., Okamoto, S.I., Izumi, M., Shirasawa, T., Lipton, S.A., 2008. Carnosic acid, a *catechol-type* electrophilic compound, protects neurons both *in vitro* and *in vivo* through activation of the Keap1/Nrf2 pathway via S-alkylation of targeted cysteines on Keap1. J. Neurochem. 104, 1116–1131.

Schrader, M., Schulz-Knappe, P., 2001. Peptidomics technologies for human body fluids. Trends Biotechnol. 19, S55–S60.

Sedighi, R., Zhao, Y., Yerke, A., Sang, S., 2015. Preventive and protective properties of rosemary (*Rosmarinus officinalis* L.) in obesity and diabetes mellitus of metabolic disorders: A brief review. Curr. Opin. Food Sci. 2, 58–70.

Shah, V., Castro-Perez, J.M., McLaren, D.G., Herath, K.B., Previs, S.F., Roddy, T.P., 2013. Enhanced data-independent analysis of lipids using ion mobility-TOFMS E to unravel quantitative and qualitative information in human plasma. Rapid Commun. Mass Spectrom. 27, 2195–2200.

Simó, C., Domínguez-Vega, E., Marina, M.L., García, M.C., Dinelli, G., Cifuentes, A., 2010. CE-TOF MS analysis of complex protein hydrolyzates from genetically modified soybeans - A tool for foodomics. Electrophoresis 31, 1175–1183.

Smith, C.A., Maille, G.O., Want, E.J., Qin, C., Trauger, S.A., Brandon, T.R., Custodio, D.E., Abagyan, R., Siuzdak, G., 2005. Metlin: A metabolite mass spectral database. Ther. Drug Monit. 27, 747–751.

Smith, C.A., Want, E.J., Maille, G.O., Abagyan, R., Siuzdak, G., 2006. XCMS: Processing Mass Spectrometry Data for Metabolite Profiling Using Nonlinear Peak Alignment, Matching, and Identification 78, 779–787.

Smolinska, A., Blanchet, L., Buydens, L.M.C., Wijmenga, S.S., 2012. NMR and pattern recognition methods in metabolomics: From data acquisition to biomarker discovery: A review. Anal. Chim. Acta 750, 82–97.

Sofi, F., Abbate, R., Gensini, G.F., Casini, A., 2010. Accruing evidence on benefits of adherence to the Mediterranean diet on health : an updated systematic review and meta-analysis. Am. J. Clin. Nutr. 92, 1189–1196.

Southam, A.D., Weber, R.J.M., Engel, J., Jones, M.R., Viant, M.R., 2017. A complete workflow for high-resolution spectral-stitching nanoelectrospray direct-infusion mass-spectrometry-based metabolomics and lipidomics. Nat. Protoc. 12, 255–273.

Spencer, J.P.E., Abd El Mohsen, M.M., Minihane, A.-M., Mathers, J.C., 2008. Biomarkers of the intake of dietary polyphenols: strengths, limitations and application in nutrition research. Br. J. Nutr. 99, 12–22

Stalmach, A., Albalat, A., Mullen, W., Mischak, H., 2013. Recent advances in capillary electrophoresis coupled to mass spectrometry for clinical proteomic applications. Electrophoresis 34, 1452–1464.

Sud, M., Fahy, E., Cotter, D., Brown, A., Dennis, E.A., Glass, C.K., Merrill, A.H., Murphy, R.C., Raetz, C.R.H., Russell, D.W., Subramaniam, S., 2007. LMSD: LIPID MAPS structure database. Nucleic Acids Res. 35, 527–532.

Sugimoto, M., Kawakami, M., Robert, M., Soga, T., Tomita, M., 2012. Bioinformatics Tools for Mass Spectroscopy-Based Metabolomic Data Processing and Analysis. Curr. Bioinform. 7, 96–108.

Suhre, K., Meisinger, C., Döring, A., Altmaier, E., Belcredi, P., Gieger, C., Chang, D., Milburn, M. V., Gall, W.E., Weinberger, K.M., Mewes, H.W., Angelis, M.H., Wichmann, H.E., Kronenberg, F., Adamski, J., Illig, T., 2010. Metabolic footprint of diabetes: A multiplatform metabolomics study in an epidemiological setting. PLoS One 5, e13953. doi:10.1371/journal.pone.0013953

Szmitko, P.E., Verma, S., 2005. Antiatherogenic potential of red wine: clinician update. Am. J. Physiol. Heart Circ. Physiol. 288, H2023–H2030.

Tai, J., Cheung, S., Wu, M., Hasman, D., 2012. Antiproliferation effect of Rosemary (*Rosmarinus officinalis*) on human ovarian cancer cells in vitro. Phytomedicine 19, 436–443.

Takats, Z., Wiseman, J. M., Gologan, B., Cooks, R. G., 2004. Mass spectrometry sampling under ambient conditions with desorption electrospray ionization. Science 306, 471–473.

Temmerman, L., De Livera, A.M., Bowne, J.B., Sheedy, J.R., Callahan, D.L., Nahid,A., De Souza D.P., Schoofs, L., Tull, D.L., McConville, M.J., Roessner, U., Wentworth , J.M., 2013. Cross-Platform Urine Metabolomics of Experimental Hyperglycemia in Type 2 Diabetes. J. Diabetes Metab. S6, 002. doi:10.4172/2155-6156.S6-002.

Theodoridis, G., Gika, H.G., Wilson, I.D., 2011. Mass spectrometry-based holistic analytical approaches for metabolite profiling in systems biology studies. Mass Spectrom. Rev. 30, 884–906.

Theodoridis, G.A., Gika, H.G., Want, E.J., Wilson, I.D., 2012. Liquid chromatography-mass spectrometry based global metabolite profiling: A review. Anal. Chim. Acta 711, 7–16.

Tiziani, S., Emwas, A.-H., Lodi, A., Ludwig, C., Bunce, C.M., Viant, M.R., Günther, U.L., 2008. Optimized metabolite extraction from blood serum for 1H nuclear magnetic resonance spectroscopy. Anal. Biochem. 377, 16–23.

Triba, M.N., Moyec, L.L., Amathieu, R., Goossens, C., Bouchemal, N., Nahon, P., Rutledge, D.N., Savarin, P., 2014. PLS/OPLS models in metabolomics: the impact of permutation of dataset rows on the K-fold cross-validation quality parameters. Mol. Biosyst. 11, 13–19.

Tu, Z., Moss-Pierce, T., Ford, P., Jiang, T.A., 2013. Rosemary (*Rosmarinus officinalis* L.) extract regulates glucose and lipid metabolism by activating AMPK and PPAR pathways in HepG2 cells. J. Agric. Food Chem. 61, 2803–2810.

Vaidyanathan, S., Gaskell, S., Goodacre, R., 2006. Matrix-suppressed laser desorption/ionisation mass spectrometry and its suitability for metabolome analyses. Rapid Commun. Mass Spectrom. 20, 1192–1198.

Valdés, A., García-Cañas, V., Artemenko, K.A., Simó, C., Bergquist, J., Cifuentes, A., 2017a. Nano-liquid Chromatography-orbitrap MS-based Quantitative Proteomics Reveals Differences Between the Mechanisms of Action of Carnosic Acid and Carnosol in Colon Cancer Cells. Mol. Cell. Proteomics. 16, 8–22.

Valdés, A., Artemenko, K.A., Bergquist, J., García-Cañas, V., Cifuentes, A., 2016b. Comprehensive proteomic study of the antiproliferative activity of a polyphenol-enriched rosemary extract on colon cancer cells using nanoliquid chromatography-Orbitrap MS/MS. J. Proteome Res. 15, 1971–1985.

Valdés, A., García-Cañas, V., Koçak, E., Simó, C., Cifuentes, A., 2016a. Foodomics study on the effects of extracellular production of hydrogen peroxide by rosemary polyphenols on the anti-proliferative activity of rosemary polyphenols against HT-29 cells. Electrophoresis 37, 1795–1804.

Valdés, A., García-Cañas, V., Pérez-Sánchez, A., 2017b. Shotgun proteomic analysis to study the decrease of xenograft tumor growth after rosemary extract treatment. Chromatogr. A 1499, 90–100.

Valdés, A., García-Cañas, V., Rocamora-Reverte, L., Gómez-Martínez, Á., Ferragut, J.A., Cifuentes, A., 2013. Effect of rosemary polyphenols on human colon cancer cells: Transcriptomic profiling and functional enrichment analysis. Genes Nutr. 8, 43–60.

Valdés, A., García-Cañas, V., Simó, C., Ibáñez, C., Micol, V., Ferragut, J.A., Cifuentes, A., 2014. Comprehensive foodomics study on the mechanisms operating at various molecular levels in cancer cells in response to individual rosemary polyphenols. Anal. Chem. 86, 9807–9815.

Valdés, A., Simó, C., Ibáñez, C., Rocamora-Reverte, L., Ferragut, J.A., García-Cañas, V., Cifuentes, A., 2012. Effect of dietary polyphenols on K562 leukemia cells: A Foodomics approach. Electrophoresis 33, 2314–2327.

Valdés, A., Sullini, G., Ibáñez, E., Cifuentes, A., García-Cañas, V., 2015. Rosemary polyphenols induce unfolded protein response and changes in cholesterol metabolism in colon cancer cells. J. Funct. Foods 15, 429–439.

van Dorsten, F.A., Grün, C.H., van Velzen, E.J.J., Jacobs, D.M., Draijer, R., van Duynhoven, J.P.M., 2010. The metabolic fate of red wine and grape juice polyphenols in humans assessed by metabolomics. Mol. Nutr. Food Res. 54, 897–908.

Vicente, G., Molina, S., González-Vallinas, M., García-Risco, M.R., Fornari, T., Reglero, G., De Molina, A.R., 2013. Supercritical rosemary extracts, their antioxidant activity and effect on hepatic tumor progression. J. Supercrit. Fluids 79, 101–108.

Visioli, F., Galli, C., 2001. Antiatherogenic components of olive oil. Curr. Atheroscler. Rep. 3, 64–7.

Vuckovic, D., 2012. Current trends and challenges in sample preparation for global metabolomics using liquid chromatography-mass spectrometry. Anal. Bioanal. Chem. 403, 1523–1548.

Wang, Q.L., Li, H., Li, X.X., Cui, C.Y., Wang, R., Yu, N.X., Chen, L.X., 2012. Acute and 30-day oral toxicity studies of administered carnosic acid. Food Chem. Toxicol. 50, 4348–4355.

Wang, T., Takikawa, Y., Tabuchi, T., Satoh, T., Kosaka, K., Suzuki, K., 2012. Carnosic acid (CA) prevents lipid accumulation in hepatocytes through the EGFR/MAPK pathway. J. Gastroenterol. 47, 805–813.

Wasinger, V.C., Cordwell, S.J., Cerpa-Poljak, A., Yan, J.X., Gooley, A.A., Wilkins, M.R., Duncan, M.W., Harris, R., Williams, K.L., Humphery-Smith, I., 1995. Progress with gene-product mapping of the Mollicutes: Mycoplasma genitalium. Electrophoresis 16, 1090–1094.

Wenz, C., Barbas, C., López-Gonzálvez, Á., Garcia, A., Benavente, F., Sanz-Nebot, V., Blanc, T., Freckleton, G., Britz-McKibbin, P., Shanmuganathan, M., De L'Escaille, F., Far, J., Haselberg, R., Huang, S., Huhn, C., Pattky, M., Michels, D., Mou, S., Yang, F., Neususs, C., Tromsdorf, N., Baidoo, E.E.K., Keasling, J.D., Park, S.S., 2015. Interlaboratory study to evaluate the robustness of capillary electrophoresis-mass spectrometry for peptide mapping. J. Sep. Sci. 38, 3262–3270.

Weston, D.J., 2010. Ambient ionization mass spectrometry: current understanding of mechanistic theory; analytical performance and application areas. Analyst. 135, 661–668.

Wilson, I.D., Nicholson, J.K., Castro-Perez, J., Granger, J.H., Johnson, K.A., Smith, B.W., Plumb, R.S., 2005. High resolution "ultra performance" liquid chromatography coupled to oa-TOF mass spectrometry as a tool for differential metabolic pathway profiling in functional genomic studies. J. Proteome Res. 4, 591–598.

Wishart, D.S., Knox, C., Guo, A.C., Eisner, R., Young, N., Gautam, B., Hau, D.D., Psychogios, N., Dong, E., Bouatra, S., Mandal, R., Sinelnikov, I., Xia, J., Jia, L., Cruz, J.A., Lim, E., Sobsey, C.A., Shrivastava, S., Huang, P., Liu, P., Fang, L., Peng, J., Fradette, R., Cheng, D., Tzur, D., Clements, M., Lewis, A., de souza, A., Zuniga, A., Dawe, M., Xiong, Y., Clive, D., Greiner, R., Nazyrova, A., Shaykhutdinov, R., Li, L., Vogel, H.J., Forsythei, I., 2009. HMDB: A knowledgebase for the human metabolome. Nucleic Acids Res. 37, 603–610.

Wu, H., Southam, A.D., Hines, A., Viant, M.R., 2008. High-throughput tissue extraction protocol for NMR- and MS-based metabolomics. Anal. Biochem. 372, 204–212.

Xiang, Q., Liu, Q., Xu, L., Qiao, Y., Wang, Y., Liu, X., 2013. Carnosic acid protects biomolecules from free radical-mediated oxidative damage *in vitro*. Food Sci. Biotechnol. 22, 1381–1388.

Yan, M., Li, G., Petiwala, S.M., Householter, E., Johnson, J.J., 2015. Standardized rosemary (*Rosmarinus officinalis*) extract induces Nrf2/sestrin-2 pathway in colon cancer cells. J. Funct. Foods 13, 137–147.

Yesil-Celiktas, O., Sevimli, C., Bedir, E., Vardar-Sukan, F., 2010. Inhibitory effects of rosemary extracts, carnosic acid and rosmarinic acid on the growth of various human cancer cell lines. Plant Foods Hum. Nutr. 65, 158–163.

Zgórka, G., Glowniak, K., 2001. Variation of free phenolic acids in medicinal plants belonging to the Lamiaceae family. J. Pharm. Biomed. Anal. 26, 79–87.

ANEXOS

ANEXO I

Lista de publicaciones relacionadas con esta Tesis Doctoral

LISTA DE PUBLICACIONES

El desarollo de la presente Tesis Doctoral ha dado lugar a las publicaciones científicas que se describen a continuación:

Revistas SCI

Tanize Acunha, Clara Ibáñez, María Isabel Pascual Reguera, Mariagiovanna Sarò, Rodrigo Navarro, Juan Alfonso Redondo, Helmut Reinecke, Alberto Gallardo, Carolina Simó, Alejandro Cifuentes.
"*Potential of prodendronic polyamines with modulated segmental charge density as novel coating for fast and efficient analysis of peptides and basic proteins by CE and CE-MS*".
Electrophoresis 36, 1564–1571 (2015).

Clara Ibáñez, Carolina Simó, Virginia García-Cañas, Tanize Acunha, Alejandro Cifuentes
"*The role of direct high-resolution mass spectrometry in foodomics*".
Analytical and Bioanalytical Chemistry 407, 6275–6287 (2015).

Tanize Acunha, Carolina Simó, Clara Ibáñez, Alberto Gallardo, Alejandro Cifuentes
"*Anionic metabolite profiling by capillary electrophoresis–mass spectrometry using a noncovalent polymeric coating. Orange juice and wine as case studies*".
Journal Chromatography A 1428, 326–335 (2016).

Tanize Acunha, Clara Ibáñez, Virginia García-Cañas, Carolina Simó, Alejandro Cifuentes
"*Recent advances in the application of capillary electromigration methods for food analysis and Foodomics*".
Electrophoresis 37, 111–141 (2016).

Guillaume L. Erny, Tanize Acunha, Carolina Simó, Alejandro Cifuentes, Arminda Alves
"*Algorithm for comprehensive analysis of datasets from hyphenated high resolution mass spectrometric techniques using single ion profiles and cluster analysis*".
Journal of Chromatography A 1429, 134–141 (2016).

Guillaume L. Erny, Tanize Acunha, Carolina Simó, Alejandro Cifuentes, Arminda Alves
"*Finnee —A Matlab toolbox for separation techniques hyphenated high resolution mass spectrometry dataset*".
Chemometrics and Intelligent Laboratory Systems 155, 138–144 (2016).

Guillaume L. Erny, Tanize Acunha, Carolina Simó, Alejandro Cifuentes, Arminda Alves
"*Background correction in separation techniques hyphenated to high-resolution mass spectrometry – Thorough correction with mass spectrometry scans recorded as profile spectra*".
Journal of Chromatography A 1492, 98–105 (2017).

Tanize Acunha, Virginia García, Alberto Valdés, Alejandro Cifuentes, Carolina Simó
"*Metabolomics of early metabolic changes in hepatic HepaRG cells in response to rosemary diterpenes exposure*".
Analytica Chimica Acta, 2017 (Enviado)

Capítulos de Libro

Clara Ibáñez, Tanize Acunha, Alberto Valdés, Virginia García-Cañas, Alejandro Cifuentes, Carolina Simó.
"*Capillary Electrophoresis in Food and Foodomics*". In: In Capillary Electrophoresis: Methods and Protocols, Edited by Philippe Schmitt-Kopplin. Series: Methods in Molecular Biology. Editorial: Springer Science, New York 2016, pp. 471–507.

Tanize Acunha, Clara Ibáñez, Virginia García-Cañas, Alejandro Cifuentes, Carolina Simó
"*CE-MS in food analysis and Foodomics*". In Capillary Electrophoresis–Mass Spectrometry (CE-MS): Principles and Applications, Edited by Gerhardus de Jong. Editorial: Wiley-VCH, Weinheim, Germany 2016, pp. 193–215.

Bienvenida Gilbert-López, Alberto Valdés, Tanize Acunha, Virginia García-Cañas, Carolina Simó, Alejandro Cifuentes
"*Foodomics: LC and LC-MS-based omics strategies in food science and nutrition*". In Liquid Chromatography. Volume Two: Applications, Second Edition, Edited by: Salvatore Fanali, Paul R. Haddad, Colin Poole and Marja-Liisa Riekkola. (2017) Elsevier, Cambridge. ISBN: 9780128053928.

ANEXO II

Algorithm for comprehensive analysis of datasets from hyphenated high resolution mass spectrometric techniques using single ion profiles and cluster analysis

Erny,G. L., Acunha,T., Simó, C., Cifuentes, A., Alves, A.

Journal of Chromatography A **1429,** 134–141 (2016).

DOI: 10.1016/j.chroma.2015.12.005.

Journal of Chromatography A, 1429 (2016) 134–141

Contents lists available at ScienceDirect

Journal of Chromatography A

journal homepage: www.elsevier.com/locate/chroma

Algorithm for comprehensive analysis of datasets from hyphenated high resolution mass spectrometric techniques using single ion profiles and cluster analysis

Guillaume L. Erny[a,*], Tanize Acunha[b], Carolina Simó[b], Alejandro Cifuentes[b], Arminda Alves[a]

[a] LEPABE – Laboratory for Process Engineering, Environment, Biotechnology and Energy, Faculdade de Engenharia da Universidade do Porto, Rua Dr. Roberto Frias, 4200-465 Porto, Portugal
[b] Laboratory of Foodomics, CIAL, CSIC, Nicolas Cabrera 9, 28049 Madrid, Spain

ARTICLE INFO

Article history:
Received 9 October 2015
Received in revised form
27 November 2015
Accepted 1 December 2015
Available online 11 December 2015

Keywords:
Chemometrics
Hyphenated techniques
Data mining
Representation

ABSTRACT

Various algorithms have been developed to improve the quantity and quality of information that can be extracted from complex datasets obtained using hyphenated mass spectrometric techniques. While different approaches are possible, the key step often consists in arranging the data into a large series of profiles known as extracted ion profiles. Those profiles, similar to mono-dimensional separation profiles, are then processed to detect potential chromatographic peaks. This allows extracting from the dataset a large number of peaks that are characteristics of the compounds that have been separated. However, with mass spectrometry (MS) detection, the response is usually a complex signal whose pattern depends on the analyte, the MS instrument and the ionization method. When converted to ionic profiles, a single separated analyte will have multiple images at different m/z range. In this manuscript we present a hierarchical agglomerative clustering algorithm to group profiles with very similar feature. Each group aims to contain all profiles that are due to the transport and monitoring of a single analyte. Clustering results are then used to generate a 2 dimensional representation, called clusters plot, which allows an in-depth analysis of the MS dataset including the visualization of poorly separated compounds even when their intensity differs by more than two orders of magnitude. The usefulness of this new approach has been validated with data from capillary electrophoresis time of flight mass spectrometry hyphenated via an electrospray ionization. Using a mixture of 17 low molecular endogenous compounds it was verified that ionic profiles belonging to each compounds were correctly clustered even with very low degree of separation (R below 0.03). The approach was also validated using a urine sample. While with the total ion profile 15 peaks could be distinguished, 70 clusters were obtained allowing a much thorough analysis. In this particular example, the total computing took less than 10 min.

1. Introduction

Separation techniques coupled with high resolution mass spectrometry (X-HRMS, where X stands for GC, LC, CE...) are key analytical hyphenated instruments in many areas of research [1–8]. In these configurations, the mass spectrometer is placed at the outlet of the separation device, allowing recording full mass spectra at regular intervals. Initially aimed as a technique to identify the main peaks in a profile (following the recommendation of the IUPAC, profile can be an electropherogram, chromatogram or any continuous trace recorded by an analytical instrument [9]), X-HRMS is now essential for analysing complex matrices. MS instruments are considered almost universal detectors while extremely selective and sensitive. As a result, a typical non-targeted analysis by X-HRMS comprises a huge amount of information in a dataset practically impossible to handle in a manual way. A typical approximation during any X-HRMS analysis is to narrow the mass range of the MS detector to only detect those ions whose m/z are within the selected range. While this can be done via the instruments setting, the easiest way is often done by filtering the resulting dataset to obtain the extracted ion profile (EIP). Interestingly, filtering can be used multiple times using the same dataset, thereby, obtaining profiles that are selective to potentially represent every analyte present in the sample. However, knowledge of the target mass interval is a

* Corresponding author.
E-mail address: guillaume@fe.up.pt (G.L. Erny).

http://dx.doi.org/10.1016/j.chroma.2015.12.005
0021-9673/

key requirement for minor components as they will only be visible if the dataset is adequately filtered. This is the main limitation in non-targeted X-HRMS analysis. Because it is important in many fields to obtain a complete analysis of the sample, especially of unknown or unexpected components, many algorithms have been proposed to improve the quality and quantity of information that can be obtained after a non-targeted X-HRMS analysis [10].

Automatic processing of hyphenated dataset often starts with the transformation of the raw MS data into centroid data. This can be done by various algorithms that detect in each MS scan every peak and calculate for each of them the centroid mass (also called the accurate mass [9]). The centroid data only records the centroid m/z value and the peak amplitude. This allows a drastic reduction of the data size, and as a consequence, faster computational speed. Centroid data can be sometimes obtained by the proprietary acquisition or associated software, such as, compassXport (Bruker) or Masslynx (Waters), or secondary software [11–13]. Those software also allow to export the data to formats such as mzML [14], mzXML [15] or JCAMP [16] that can easily be read by users [16]. It should be emphasized that the transformation to centroid data is an important transformation of the original data that can influence a subsequent quantitative analysis [17]. The information in the resulting file can be seen as a collection of 3 coordinates data point: the accurate mass m/z value (referred from now on as mass coordinate), the scan number and the peak intensity. Such dataset can be processed in two ways, either each MS scan is analyzed to detect peaks that are probably related to the same compounds (isotopic ions, common adducts, possible fragmentations) [18–20] or profiles characteristic of the transport and separation of the formed ions can be reconstituted and processed as chromatographic profiles. The latter is often the method of choice in hyphenated MS datasets [21–23].

Two approaches are used to obtain chromatographic profiles, i.e., the binning approach and the pure ion profile. In the binning approach, a series of EIPs are defined in such a way that each EIP will only contain data within a very narrow mass range, so, all the information is distributed along the EIPs [11]. The mass range is the key parameter and should be carefully optimized to avoid peak splitting. Algorithms have also been proposed to correct for this default [24]. The EIPs are then processed to detect for the presence of chromatographic peaks. Those are then measured and figure of merits (peak, center, amplitude, m/z, area...) recorded in a table [22,24–26]. Another recent alternative is the use of pure ion profile (PIP), which consists of scanning the dataset to find sequences of points that follow each other in their scan coordinate and does not differ in their mass coordinate by more than a certain threshold that corresponds to the variation in the accurate mass value determined for the same peak in the mass profile (original data) at different scan [27–29]. The advantage of PIP over EIP (or binning approach) is that in the PIP only the data points related to the target ions are obtained. This makes the use of peak picking algorithms redundant. However, while EIP can be obtained from centroid or profile dataset, PIP can only be calculated using centroid dataset. Automatic processing of EIP or PIP allows obtaining a large number of chromatographic peaks that are characteristic of the analytes of interest present in the sample. Most algorithms are able to retrieve peaks at very low intensity that would have never been detected manually without information on their mass.

Nevertheless, this is not sufficient for a comprehensive analysis of the whole X-HRMS dataset due to its intrinsic complexity. When processing the dataset, multiple EIE or PIP will be found for every analyte that has been separated. Thus, the remaining problem is to determine whether a minor peak is due to a new analyte or an image of an existing peak. Usually, this problem is bypassed by working in differential analysis [12,30,31]. However, PIP related to the same compounds are highly related with each other. All PIP due to isotopic ions, adducts or fragments are an image of the main profile where the only variation is the intensity of the peak. We have already used this concept in a previous work to propose a new representation [21]. The present work is a significant improvement from that previous approach. Here we use for the first time a hierarchical agglomerative cluster approach (HACA) [32] to classify the different profiles, based on similarity as measured by the correlation coefficient into clusters. Ideally, selected clusters should contain all profiles related to the same analyte. While peak aggregation as already been discussed [33,34], HACA has never been tested in this context. While previously published approaches [33,34] used classical figures of merits such at time at peak apex and peak width, the HACA designed in this work is based on the valor of the correlation coefficients between profiles. It is therefore less dependent on noise that can prevent the accurate determination of peak apex and peak width. In the present work, we demonstrate, using test and real complex samples, that HACA allows to rationally and systematically organize the various profiles in a limited amount of clusters. In this work, the clusters are used to provide a new two dimensional representation of the dataset, called clusters plot, which allows a comprehensive analysis of the results, making possible to distinguish analytes that are not well separated.

2. Materials and methods

2.1. Programing

Programing was done using Matlab 2013b and functions were run on a personal computer (Intel Pentium CPU G3320@3.00 GHz, 4.00 GB RAM, 64-bit operating system) with Windows 7. All the functions programmed and used during this work can be obtain by contacting the corresponding author.

2.2. Chemicals and samples

All reagents employed in the preparation of the CE buffer and sheath liquid (isopropanol, formic acid and ammonium hydroxide, all of MS grade) were from Sigma–Aldrich (St. Louis, MO, USA). A mixture of 17 small molecular mass compounds from Sigma–Aldrich was employed as a test mixture: 0.3 mM adenosine triphosphate (ATP), 7.8 mM nicotinic acid, 0.5 mM glutamic acid, 1.0 mM aspartic acid, 0.3 mM glutathione oxidized, 0.6 mM glutathione reduced, 2.7 mM iminodiacetic acid, 0.2 mM adenosine monophosphate (AMP), 0.2 mM panthotenic acid, 1.4 mM succinic acid, 0.1 mM gluconic acid, 0.4 mM hippuric acid, 0.3 mM malic acid, 0.2 mM citric acid, 0.2 mM tartaric acid, and 2.8 mM 1,4 piperazinediethanesulfonic acid (PIPES) and 156.5 mM malonic acid. The urine was filtered through 0.2 μm polyethersulfone filter before CE-MS analysis.

2.3. CE-TOF MS analysis

The capillary electrophoresis (CE) apparatus used was a P/ACE 5010 from Beckman (Fullerton, CA, USA). The CE instrument was controlled by a PC running System GOLD software from Beckman. The CE equipment was coupled to a time-of-flight (TOF) instrument "microTOF" from Bruker Daltonik. CE-TOF coupling was carried out via an ESI interface model G1607A from Agilent Technologies. Electrical contact at the electrospray needle tip was established via a flow of sheath liquid composed of 2-propanol-water (50:50, v/v) delivered by a 74900-00-05 Cole Palmer syringe pump (Vernon Hills, IL, USA) at a flow rate of 4 μL/min. Bare fused-silica capillary with 50 μm i.d. and 85 cm of total length was from Composite Metal Services (Worcester, England). The inner capillary wall was coated with a cationic TEDETAMA-co-HPMA copolymer [35]. CE separation was performed at −20 kV in an acidic BGE (1 M formic acid

adjusted to pH 2.4 with ammonium hydroxide). Nebulizer pressure was 0.4 bar, drying gas flow rate was 4 L/min, and ESI chamber temperature was set at 200 °C. TOF MS was operated in the negative ion mode (capillary voltage was 4 kV) and spectra were acquired in the range of 50–700 m/z.

2.4. Datasets

Two datasets were used in this work, both obtained under the same CE-MS analytical conditions. The first one was obtained from the CE-MS analysis of a test mixture (17 small molecules). The second dataset was obtained from a urine sample injected under the same CE-MS analytical conditions.

3. Programming

In this work, a series of functions, programmed in Matlab, were designed in order to obtain a true two dimensional representation of the CE-TOF-MS datasets. The workflow is illustrated in Fig. 1 and consists of four main tasks: loading the data, extracting the single ion profiles, classification and generation of the clusters plot.

3.1. Data loading

This initial step consists of loading the centroid dataset. Centroid dataset can be obtained using various freeware as well as some proprietary software. In the case of Bruker instruments, for example, the software exports the rough data as CSV files and allows obtaining a centroid dataset. CompassXport is a software freely available from Bruker and also allows obtaining profile or centroid datasets from files in various format (text, JCAMP, mzXML, mzML. . .). In this work, Matlab functions were developed for mzML, JCAMP or CSV files that were processed from original Bruker files using CompassXport. Such formats are text based and can be easily read. During data loading, the only modification was to round off the m/z values to a fixed number of decimals; namely, five decimals were used for all TOF MS data since a higher precision is meaningless.

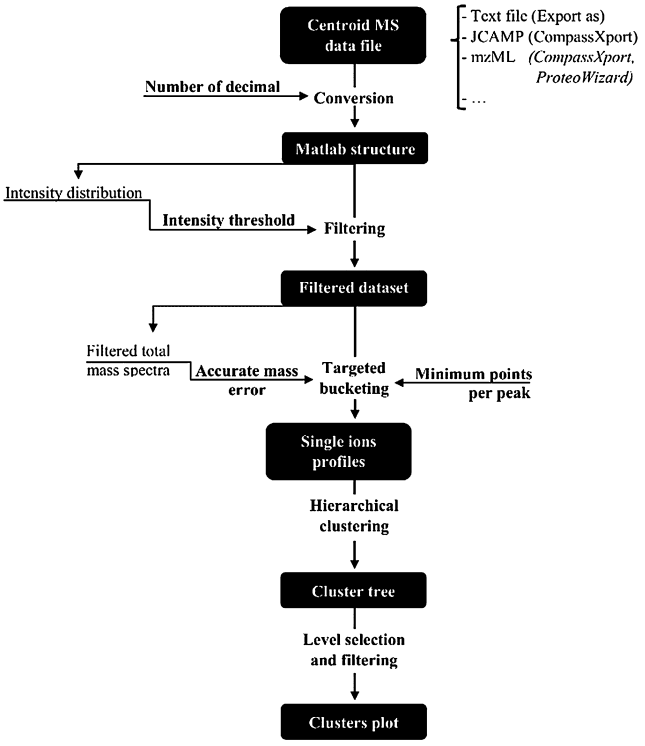

Fig. 1. Workflow used in this work.

3.2. Pure ion profiles (PIPs)

The quality and quantity of the PIPs is paramount to this approach. Functions have been developed with a particular attention to increase both the computing speed and the ability to extract from the dataset PIPs with very low intensity. In this work, PIPs are obtained in three steps. First the dataset is filtered to remove the random noise, this is done by rejecting all data points whose intensity is below a set threshold. Value of this threshold is an important experimental parameter and should be accurately determined. This can be done via the intensity frequency distribution of the dataset, i.e. the number of data points in the dataset whose intensity is equal, or between the set values. Such a distribution for the urine dataset is shown in Fig. 2A.

As it can be observed, while the intensities ranged from 1 to ~110,000 counts, a large fraction of the data has an intensity bellow 20 counts. This very low value can be used confidently as threshold to filter the dataset. Fig. 2B shows the comparison of the total ion current profiles (TICPs) obtained using all data points (top) and the one obtained (bottom) after removal of the random noise (intensities below 20). Fig. 2C shows the difference between the two TICPs. Using this threshold value, the data integrity is maintained while the size of the dataset has been reduced by more than 91%. Such values are consistent with other works and allow to drastically increasing the computing speed of the PIP algorithm.

In the work from Wang and co-workers [27], PIPs were obtained selecting a starting point and finding data in the time coordinate that does not differ in their m/z coordinate by more than a fixed value that is the uncertainty in the determination of the accurate mass. In the present work, we use a projection of the data to a mass axis to obtain the total mass profile (TMP) as shown in Fig. 3. This profile can be used to measure the accurate mass uncertainty as shown in inserts A to C. With the urine dataset this value can be estimated at 0.002 m/z for analyte peaks (insert A and C) and 0.005 m/z for background ions (insert B). The TMP can also be used to find mass intervals of interest (MII), determined as group of points in the TMP where the m/z value of each point does not differ from its neighbors by more than $x/\sqrt{(y-1)}$, where x is the mass uncertainty and y is the minimum number of consecutive points to define a single ion profile. PIPs are then selected as any sequence of at least y points whose time coordinate follow each other and belong to the same MII. Each PIP is recorded individually and figures of merit are measured and recorded in a table. Those include the average and standard deviation of the accurate mass measured with all the data points that build the PIP, the time and intensity of the most intense data points, as well as the PIP zeroth and first statistical moment (area and center). This is a very simple and robust approach to obtain single ion profiles with no assumption on their shape or intensity. A high number of PIPs are obtained in this way in a short time. For example with the urine sample 4779 PIPs ($x = 0.002$, $y = 5$) were obtained in less than 9 min. The computing speed depends on the size of the TMP that can be reduced by increasing the initial threshold. Using a threshold of 50 counts instead of 20, 1776 PIPs were obtained in 2 min. Interestingly, if only considering PIP with a maximum intensity higher than 100 (representing 0.05% of the highest intensity), 1262 PIPs were obtained with a threshold of 20, while 1231 PIPs were obtained with a threshold of 50 showing the robustness of the algorithm. Hereinafter, profiles whose maximum intensity are below 100 counts will be discarded. This filtering step attempts to keep only profiles whose maximum intensity is higher than 5 times the background noise and is a simple step to only work with PIPs of chromatographic relevance.

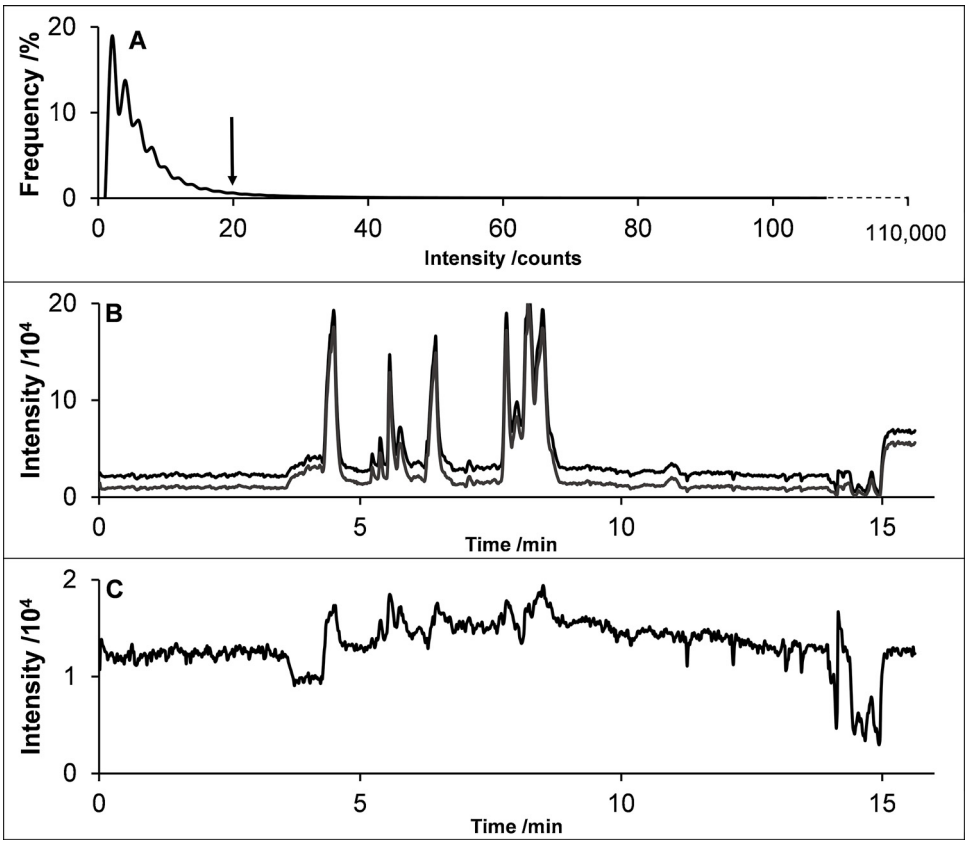

Fig. 2. (A) Frequency distribution; (B) TICP with full data (top) and filtered data (bottom) and (C) residual between the full and filtered data.

3.3. *Hierarchical agglomerative cluster analysis (HACA)*

The main novelty of this work is the use of HACA to group PIPs based on similarities, giving as result an arrangement of all the data in individual clusters. HACA is a "bottom up" approach. Initially each profile starts in its own cluster and a measuring is used to assess the similarity between every cluster. The two most similar clusters are merged into a new one and this step is repeated until one cluster remains. The hierarchical structure is formed by the clusters obtained at each step and can be analyzed by visualizing how the data relate with each other at a particular hierarchical level (HL). For this work, clusters were compared by calculating the matrix of correlation between the most intense profiles in each cluster. The correlation between two profiles X and Y is defined as:

$$p_{X,Y} = \frac{cov(X, Y)}{\sigma_X \sigma_Y} \quad (1)$$

Cov(X,Y) is the covariance of X and Y, and σ_X and σ_Y are the variances of X and Y, respectively. Correlation coefficients are normalized measurements with values between 1 and −1. This approach allows comparing profiles not only based on their position but also on their global shape.

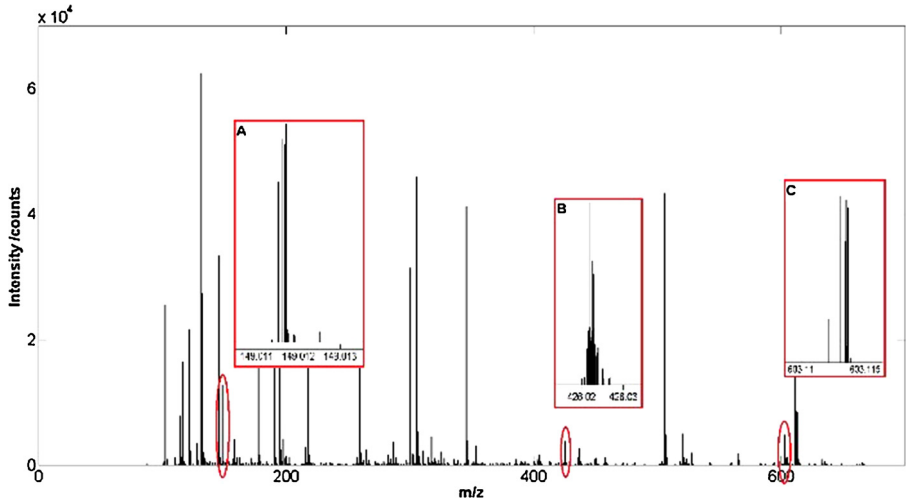

Fig. 3. Total mass profile obtained by projecting all data points of intensity higher than 20 counts on to a mass axis. Insert A, B and C are zooms of the encircled areas.

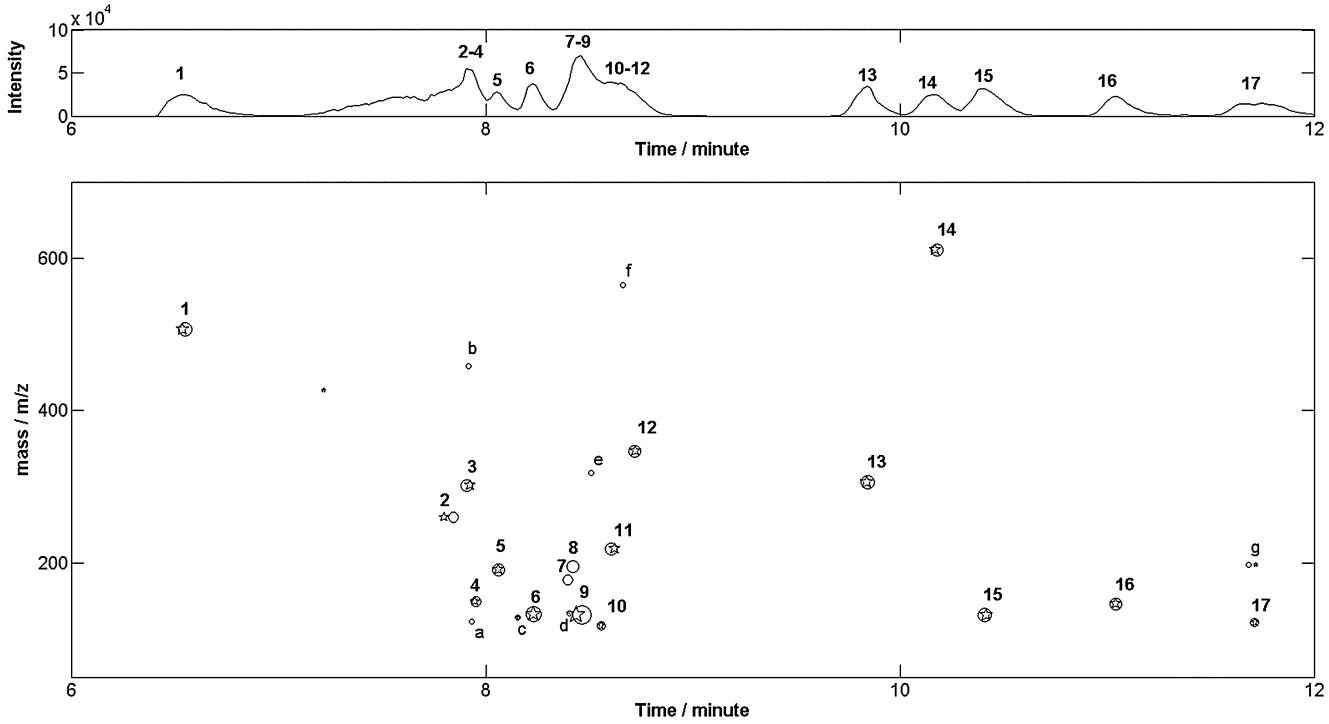

Fig. 4. Two clusters plots of the standard mix obtained for merging correlation coefficients of 0.8 (stars) and 0.95 (circles). Clusters plot obtained at 0.95 are also labeled with numbers and correspond to the following compounds (values between parentheses correspond to the exact mass and the average accurate mass respectively): (1) ATP (505.9985 – 505.9891 ± 0.0013); (2) malonic acid (103.0037 – 259.9258 ± 0.0014), (3) PIPES (301.0522 – 301.0538 ± 0.0004), (4) tartaric acid (149.0092 – 149.0118 ± 0.0005), (5) citric acid (191.0197 – 191.0207 ± 0.0003), (6) malic acid (133.0142 – 133.0174 ± 0.0001), (7) hippuric acid (178.0510 – 178.0518 ± 0.0013), (8) gluconic acid (195.0520 – 195.0523 ± 0.0009), (9) iminodiacetic acid (132.0291 – 132.0328 ± 0.0008), (10) succinic acid (117.0193 – 117.0226 ± 0.0005), (11) pantothenic acid (218.1034 – 218.1034 ± 0.0004), (12) AMP (346.0558 – 346.0551 ± 0.0010), (13) glutathione (306.0765 – 306.0753 ± 0.0010), (14) glutathione oxidized (611.1447 – 611.1430 ± 0.0006), (15) aspartic acid (132.0302 – 132.0334 ± 0.0009), (16) glutamic acid (146.0459 – 146.0482 ± 0.0006), (17) nicotinic acid (122.0248 – 122.0275 ± 0.0008). Clusters labeled with letters are impurities (some of them are discussed in the text).

3.4. Selection of the hierarchical level and cluster plot

While the HACA is systematic and does not require any input, the selection of the HL is critical for the final representation. HL can be defined as the number of iterations but it is more pertinent to use here the correlation between the two clusters merged at each iteration. Under these conditions, the HL can vary from 1, where each profile will be in an independent cluster, till zero where each profile will be in a single cluster.

An HL of 0.9 will indicate that within a cluster each PIP will be correlated by a value higher or equal to 0.9. The task here, is to find the HL where all isotopes and adduct ion profiles will be regrouped into the same cluster. Ideally, each cluster should only contain the profile related to only one component. Obviously, this will depend on the degree of separation between compounds in the sample. Optimization of the HL is achieved using a two dimensional representation of the clusters, named clusters plot, which is a two dimensional scatter plot of the main values representative of the clusters. An example of such plots can be seen in Fig. 4 where each circle depict a cluster. Its time coordinate corresponds to the average time at peak maxima of all PIPs in this cluster, its mass coordinate and size correspond to the accurate mass and intensity of the most intense profile respectively. Because an analyte should have more than one image profiles, the one corresponding to the molecular ions as well as the main isotopic ions and adducts, clusters than only contain one profile are discarded in such a representation. The use of the clusters plot to select the HL and to improve the visualization of key information from the dataset will be discussed in the following section.

4. Results and discussion

4.1. Test mixtures

The approach was first validated using the dataset obtained from the CE-TOF/MS analysis of the standard sample composed of 17 metabolites. With an intensity threshold of 20, $x = 0.002$ and $y = 5$, 2347 PIPs were obtained from the dataset in less than 5 min; among them, only 440 had a maximum intensity higher than 100. Those 440 PIPs were organized in the hierarchical structure in less than one minute. Final results will depend on the HL selected. The only task done manually by the operator consists of finding the right HL for which all image profiles of the same component fall within the same clusters, while separates the different analytes in different clusters. As illustrated in Fig. 4, the clusters plot allows the optimization of this parameter. In this figure two clusters plots are superposed, the plot obtained at HL = 0.8 (stars) and the plot obtained at HL = 0.95 (circles). The clusters labeled with a number were unambiguously assigned to one of the 17 compounds initially present in the test mixtures. The clusters labeled with a letter are either false positive or impurities. The main differences between both representations is in the clusters (circles) labeled as 7, 8 and 9 that were only obtained using a HL value of 0.95 while with HL = 0.8, a single cluster (star near 9) containing 37 profile was obtained. The distribution of the 20 most intense profiles collected in this single cluster at HL 8.0 in various clusters at HL 0.95 is summarized in Table 1. As it can be seen, those PIPs are organized in at least 5 clusters (7, 8, 9, d and e in Fig. 4). It can also be observed that the profiles in the 3 main clusters (labeled as 7, 8 and 9 in Fig. 4) are consistent

Table 1
Repartition of the 20 most intense profiles obtained in a single cluster at HL 0.8 in various cluster at HL 0.95. Each entry in this cluster correspond to the accurate mass and associated standard deviation of a PIP and the symbol of the cluster (Fig. 3, circle) where it was found at HL = 0.95.

m/z	@0.95	*m/z*	@0.95
132.0328 ± 0.0008	9	318.9867 ± 0.0007	NA
195.0523 ± 0.0009	8	413.0939 ± 0.0010	7
178.0518 ± 0.0013	7	391.1103 ± 0.0007	NA
317.9800 ± 0.0013	e	472.9995 ± 0.0025	e
134.0632 ± 0.0005	d	273.9887 ± 0.0010	NA
133.0342 ± 0.0013	9	197.0547 ± 0.0014	8
179.0554 ± 0.0006	7	154.0145 ± 0.0006	9
287.0498 ± 0.0007	9	175.0258 ± 0.0006	7
196.0556 ± 0.0014	8	381.0000 ± 0.0007	NA
303.0207 ± 0.0017	NA	135.0669 ± 0.0004	d

with the presence of the molecular ion and at least one isotope ion (7: 178.0518 and 179.0554; 8: 195.0523, 196.0556 and 197.0547; 9: 132.0328 and 133.0342). Using the most intense profiles in clusters 7 and 8, the resolution between two clusters was measured equal to 0.027. This demonstrates that clusters plots allow to visually detect analytes that are poorly separated even when their relative intensity differs significantly. For example the similarity between profiles from clusters d and 9 in Fig. 4 can be assessed in Fig. 5. The resolution between those two profiles is equal to 0.59 and their relative intensity differ by one order of magnitude. Although the PIPs from these clusters are very similar both in terms of *m/z* and migration time, they belong to different analytes and were rightly assigned at HL = 0.95 to two different clusters. At HL = 0.95, all standards, numbered as 1 to 17 in Fig. 4, were successfully separated and with the exception of malonic acid (cluster 2), the most intense PIP in each cluster corresponds to the molecular ions. Very good agreement were obtained between the exact mass and the accurate mass, this can be seen even with peaks poorly separated as hippuric acid (7), gluconic acid (8) and iminodiacetic acid (9). For malonic acid, the PIP corresponding to the molecular ions is the second most intense one.

The entire data processing necessary for obtaining the cluster plots (i.e., from the first step in which the original file was converted to mzML file till displaying the clusters plot) took less than 20 min. The list of the *m/z* values for all PIPs and each cluster can be found in supplementary material. For all tested datasets, HL = 0.95 always gave the best results and was used for all clusters plots. This value seems to be the highest value to accurately group all profiles related to the same analyte; however, co-clustering of more than one analyte was also observed with complex samples. This value may depend on the sampling frequency, peak efficiency and noise. The full listing of the *m/z* values of every PIP and cluster can be found in the supporting information.

4.2. Urine sample

The above data treatment was applied to the dataset obtained from the CE-TOF MS analysis of a urine sample. Under the same conditions used for the standard sample, 1262 PIPs were processed from the urine dataset with an intensity higher than 100. 177 of those PIPs were organized in 70 clusters with a maximum intensity ranging from 100,000 to 1000. The clusters plot is shown in Fig. 6. Not surprisingly, this representation is more complex than that obtained with the standard mixtures. To validate the approach, the clusters within the square were analyzed in detail below. Fig. 7 shows, for each cluster selected in Fig. 6, the most intense normalized PIPs. It can be observed that 6 out of 7 clusters clearly show pure profiles. Nevertheless, in all cases every cluster regroups at least one isotopic profile besides the main PIP (1. 135.0320 & 136.0347; 2. 191.0539 & 192.0603; 3. 165.0391 & 166.0439; 4. 195.0507 & 196.0544; 5. 263.1017 & 264.1037; 6. 149.0471 & 150.0516; 7. 179.0545 & 180.0573) allowing the identification of the component in each cluster unambiguously. The list of the *m/z* values for all PIPs and each cluster can be found in supplementary material. When working with real samples, numerous clusters seem to have more than one compound that could easily be identified and separated using common rules of adducts formation.

While the relevance of all clusters should be further studied using multiple datasets, with a single dataset it is also easy to study the profile and *m/z* values in each cluster, helping to determine whether a cluster is an artifact or contain one or more analytes. This represents a systematic and robust approach for a comprehensive analysis of complex datasets from hyphenated X-HRMS techniques. While with small molecules, clusters are generally low populated, preliminary experiments with macromolecules (protein digests) showed that this approach could be particularly relevant for these types of analytes as clusters are more populated increasing the confidence of the representation. This will be the topic of a future work.

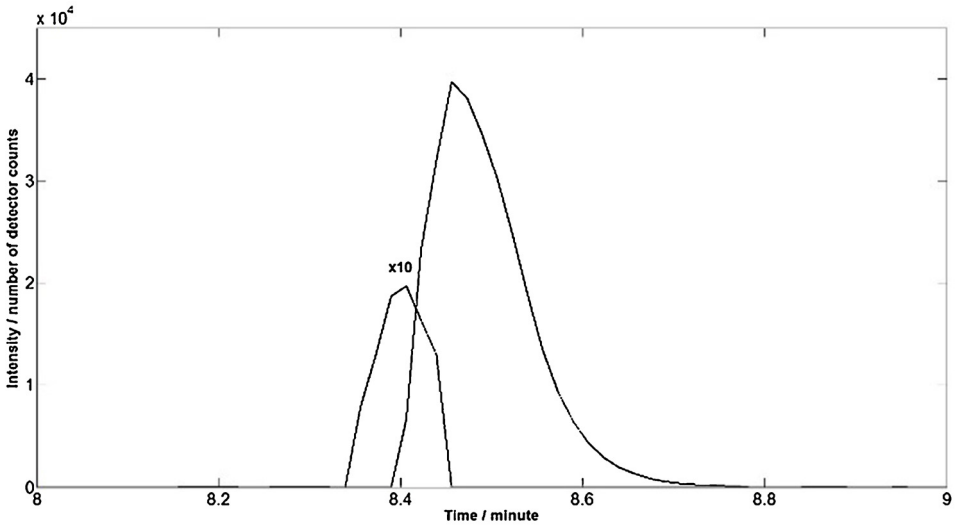

Fig. 5. Comparison of the intensity obtained for the most intense profile from cluster d (left) and the most intense profile from cluster 9 (right).

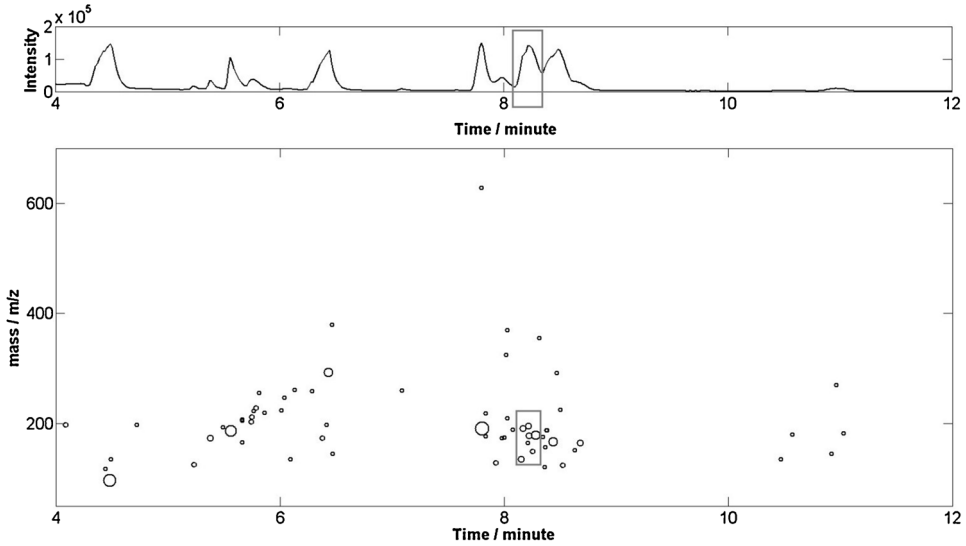

Fig. 6. Cluster plots of the dataset obtained from the CE-TOF MS analysis of a urine sample at a merging correlation coefficient of 0.95. The box highlights the clusters that are displayed in detail in Fig. 7.

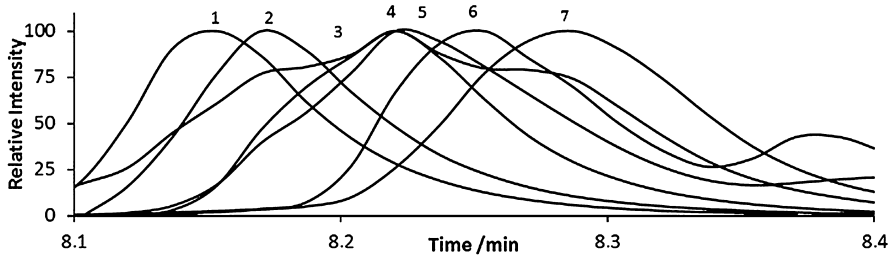

Fig. 7. Normalized most intense profiles in the clusters marked in Fig. 6 between 8.1 and 8.3 min. List of m/z values 1. 135.0320 ± 0.0015; 2. 191.0539 ± 0.0022; 3. 165.0391 ± 0.0045; 4. 195.0507 ± 0.0031; 5. 178.0502 ± 0.0016; 6. 149.0471 ± 0.0015; 7. 179.0545 ± 0.0023.

5. Conclusions

Hierarchical agglomerative cluster analysis is a logical and robust approach to order single ions profiles in clusters from complex X-HRMS datasets, as corroborated by the excellent results obtained in this paper for both a standard and a real sample analyzed by CE-TOF MS. The cluster plot, a two dimensional representation of the data, allows to easily determine the best hierarchical level as well as it provides an excellent visualization of the information contained in an X-HRMS dataset. This representation allows detecting poorly separated analytes even when one is at very low concentration. Another great advantage of the approach proposed in this work is that it is methodical and does not rely on any supervision from the operator. However, this approach relies on the consistency of the obtained PIPs. While the PIP algorithm presented here gave good results, it should also be compared with profiles obtained using other algorithms. In this work, because of the very narrow mass intervals obtained, no peak picking algorithms were used. However, with real sample, some of the PIPs clearly showed the presence of more than one ion. Peak picking algorithms may be introduced in a future work to resolve this issue. The approach developed here is particularly rapid allowing to test various conditions in order to optimize the results in a fast and straightforward way. Matlab files can be obtained on demand.

Acknowledgments

This work was supported by: Project UID/EQU/00511/2013-LEPABE, by the FCT/MEC with national funds and co-funded by FEDER in the scope of the P2020 Partnership Agreement; Project NORTE-07-0124-FEDER-000025 – RL2_ Environment&Health, by FEDER funds through Programa Operacional Factores de Competitividade – COMPETE, by the Programa Operacional do Norte (ON2) program by national funds through FCT – Fundação para a Ciência e a Tecnologia and AGL2014-53609-P project (Ministerio de Educación y Ciencia, Spain). This work was funded by FEDER funds through the Operational Program for Human Potential and by National Funds through FCT-Foundation for Science and Technology under the project IF/00528/2013. T.A. thanks the CAPES Foundation, Ministry of Education of Brazil for her pre-doctoral Scholarship-Proc. N 1532/13-8 TEDETAMA-co-HPMA copolymer was gently provided by Dr. Alberto Gallardo from Institute of Polymer Science and Technology (ICTP-CSIC).

Appendix A. Supplementary data

Supplementary data associated with this article can be found, in the online version, at http://dx.doi.org/10.1016/j.chroma.2015.12.005.

References

[1] A. Valdes, V. Garcia-Canas, C. Simo, C. Ibanez, V. Micol, J.A. Ferragut, A. Cifuentes, Comprehensive foodomics study on the mechanisms operating at various molecular levels in cancer cells in response to individual rosemary polyphenols, Anal. Chem. 86 (2014) 9807–9815.
[2] M. Herrero, C. Simó, V. García-Cañas, E. Ibáñez, A. Cifuentes, Foodomics: MS-based strategies in modern food science and nutrition, Mass Spectrom. Rev. 31 (2012) 49–69.

[3] C.C. Jacob, G. Dervilly-Pinel, G. Biancotto, F. Monteau, B. Le Bizec, Global urine fingerprinting by LC-ESI(+)-HRMS for better characterization of metabolic pathway disruption upon anabolic practices in bovine, Metabolomics 11 (2015) 184–197.
[4] S.D. Sarker, L. Nahar, Hyphenated techniques and their applications in natural products analysis, Methods Mol. Biol. (2012) 301–340.
[5] M. Petrović, M.D. Hernando, M.S. Díaz-Cruz, D. Barceló, Liquid chromatography–tandem mass spectrometry for the analysis of pharmaceutical residues in environmental samples: a review, J. Chromatogr. A 1067 (2005) 1–14.
[6] G.L. Erny, A. Cifuentes, Liquid separation techniques coupled with mass spectrometry for chiral analysis of pharmaceuticals compounds and their metabolites in biological fluids, J. Pharm. Biomed. Anal. 40 (2006) 509–515.
[7] W. Struck, M. Waszczuk-Jankowska, R. Kaliszan, M.J. Markuszewski, The state-of-the-art determination of urinary nucleosides using chromatographic techniques "hyphenated" with advanced bioinformatic methods, Anal. Bioanal. Chem. 401 (2011) 2039–2050.
[8] O.J. Pozo, J. Marcos, J. Segura, R. Ventura, Recent developments in MS for small molecules: application to human doping control analysis, Bioanalysis 4 (2012) 197–212.
[9] K.K. Murray, R.K. Boyd, M.N. Eberlin, G.J. Langley, L. Li, Y. Naito, Definitions of terms relating to mass spectrometry (IUPAC Recommendations 2013), Pure Appl. Chem. 85 (2013) 1515–1609.
[10] K. Kleparnik, Recent advances in combination of capillary electrophoresis with mass spectrometry: methodology and theory, Electrophoresis 36 (2015) 159–178.
[11] H. Gowda, J. Ivanisevic, C.H. Johnson, M.E. Kurczy, H.P. Benton, D. Rinehart, T. Nguyen, J. Ray, J. Kuehl, B. Arevalo, P.D. Westenskow, J.H. Wang, A.P. Arkin, A.M. Deutschbauer, G.J. Patti, G. Siuzdak, Interactive XCMS online: simplifying advanced metabolomic data processing and subsequent statistical analyses, Anal. Chem. 96 (2014) 6931–6939.
[12] C.A. Smith, E.J. Want, G. O'Maille, R. Abagyan, G. Siuzdak, XCMS: processing mass spectrometry data for metabolite profiling using nonlinear peak alignment, matching, and identification, Anal. Chem. 78 (2006) 779–787.
[13] J.D. Holman, D.L. Tabb, P. Mallick, Employing proteowizard to convert raw mass spectrometry data, Curr. Protoc. Bioinform. 46 (2014) 11–19.
[14] G. Mayer, L. Montecchi-Palazzi, D. Ovelleiro, A.R. Jones, P.-A. Binz, E.W. Deutsch, M. Chambers, M. Kallhardt, F. Levander, J. Shofstahl, S. Orchard, J.A. Vizcaino, H. Hermjakob, C. Stephan, H.E. Meyer, M. Eisenacher, H.-P Group, The HUPO proteomics standards initiative mass spectrometry controlled vocabulary, 2013, Database:bat009 (doi:10.1093/database/bat009).
[15] S.M. Lin, L.H. Zhu, A.Q. Winter, M. Sasinowski, W.A. Kibbe, What is mzXML good for? Expert Rev. Proteomics 2 (2005) 839–845.
[16] P. Lampen, H. Hillig, A.N. Davies, M. Linscheid, Jcamp-Dx for mass-spectrometry, Appl. Spectrosc. 48 (1994) 1545–1552.
[17] L. Vergeynst, H. Van Langenhove, P. Joos, K. Demeestere, Accurate mass determination, quantification and determination of detection limits in liquid chromatography–high-resolution time-of-flight mass spectrometry: challenges and practical solutions, Anal. Chim. Acta 789 (2013) 74–82.
[18] N. Huang, M. Siegel, G. Kruppa, F. Laukien, Automation of a Fourier transform ion cyclotron resonance mass spectrometer for acquisition, analysis, and E-mailing of high-resolution exact-mass electrospray ionization mass spectral data, J. Am. Soc. Mass Spectrom. 10 (1999) 1166–1173.
[19] D.M.A. Horn, R. Zubarev, F.W. McLafferty, Automated reduction and interpretation of high resolution electrospray mass spectra of large molecules, J. Am. Soc. Mass Spectrom. 11 (2000) 320–332.
[20] P. Kaur, P.B. O'Connor, Algorithms for automatic interpretation of high resolution mass spectra, J. Am. Soc. Mass Spectrom. 17 (2006) 459–468.
[21] G.L. Erny, C. Simo, A. Cifuentes, V.I. Esteves, Introducing the concept of centergram. A new tool to squeeze data from separation techniques-mass spectrometry couplings, J. Chromatogr. A 1330 (2014) 89–96.
[22] M. Katajamaa, M. Oresic, Data processing for mass spectrometry-based metabolomics, J. Chromatogr. A 1158 (2007) 318–328.
[23] G.L. Erny, A. Cifuentes, Simplified 2-D CE-MS mapping: analysis of proteolytic digests, Electrophoresis 28 (2007) 1335–1344.
[24] R. Tautenhahn, C. Bottcher, S. Neumann, Highly sensitive feature detection for high resolution LC/MS, BMC Bioinform. 8 (2008) 16.
[25] V. Andreev, T. Rejtar, H. Chen, E. Moskovets, A. Ivanov, B. Karger, A universal denoising and peak picking algorithm for LC–MS based on matched filtration in the chromatographic time domain, Anal. Chem. 75 (2003) 6314–6326.
[26] R. Stolt, R. Torgrip, J. Lindberg, L. Csenki, J. Kolmert, I. Schuppe-Koistinen, S. Jacobsson, Second-order peak detection for multicomponent high-resolution LC/MS data, Anal. Chem. 78 (2006) 975–983.
[27] S.-Y. Wang, C.-H. Kuo, Y.J. Tseng, Y.J. Ion, Trace detection algorithm to extract pure ion chromatograms to improve untargeted peak detection quality for liquid chromatography/time-of-flight mass spectrometry-based metabolomics data, Anal. Chem. 87 (2015) 3048–3055.
[28] E. Tengstrand, J. Lindberg, K.M. Aberg, racMass 2-A modular suite of tools for processing chromatography-full scan mass spectrometry data, Anal. Chem. 86 (2014) 3435–3442.
[29] K. Aberg, R. Torgrip, J. Kolmert, O. Schuppe-Koistinen, J. Lindberg, Feature detection and alignment of hyphenated chromatographic-mass spectrometric data extraction of pure ion chromatograms using Kalman tracking, J. Chromatogr. A 1192 (2008) 139–146.
[30] M. Katajamaa, M. Oresic, Processing methods for differential analysis of LC/MS profile data, BMC Bioinform. 6 (2005) 179.
[31] S.C. Grace, S. Embry, H. Luo, Haystack, a web-based tool for metabolomics research, BMC Bioinform. 15 (2014) 14.
[32] A.K. Jain, Data clustering: 50 years beyond K-means, Pattern Recogn. Lett. 31 (2010) 651–666.
[33] F. Fernandez-Albert, R. Llorach, C. Andres-Lacueva, A. Perera-Lluna, Peak aggregation as an innovative strategy for improving the predictive power of LC–MS metabolomic profiles, Anal. Chem. 86 (2014) 2320–2325.
[34] B.D. Fitz, B.C. Reaser, D.K. Pinkerton, J.C. Hoggard, K.J. Skogerboe, E.R. Synovec, Enhancing gas chromatography–time of flight mass spectrometry data analysis using two-dimensional mass channel cluster plots, Anal. Chem. 86 (2014) 3973–3979.
[35] T. Acunha, C. Ibáñez, M.I. Pascual Reguera, M. Sarò, R. Navarro, J. Alfonso Redondo, H. Reinecke, A. Gallardo, C. Simó, A. Cifuentes, Potential of prodendronic polyamines with modulated segmental charge density as novel coating for fast and efficient analysis of peptides and basic proteins by CE and CE-MS, Electrophoresis (2015), http://dx.doi.org/10.1002/elps.201400576.

ANEXO III

Finnee — A Matlab toolbox for separation techniques hyphenated to high resolution mass spectrometry dataset

Erny, G.L., Acunha, T., Simó, C., Cifuentes, A., Alves, A.

Chemometrics and Intelligent Laboratory Systems **155,** 138–144 (2016).

DOI: 10.1016/j.chemolab.2016.04.013.

Chemometrics and Intelligent Laboratory Systems 155 (2016) 138–144

Contents lists available at ScienceDirect

Chemometrics and Intelligent Laboratory Systems

journal homepage: www.elsevier.com/locate/chemolab

Software Description

Finnee — A Matlab toolbox for separation techniques hyphenated high resolution mass spectrometry dataset

Guillaume L. Erny [a,*], Tanize Acunha [b,c], Carolina Simó [b], Alejandro Cifuentes [b], Arminda Alves [a]

[a] LEPABE - Laboratory for Process Engineering, Environment, Biotechnology and Energy, Faculdade de Engenharia da Universidade do Porto, Rua Dr. Roberto Frias, 4200-465 Porto, Portugal
[b] Laboratory of Foodomics, CIAL, CSIC, Nicolas Cabrera 9, 28049 Madrid, Spain
[c] CAPES Foundation, Ministry of Education of Brazil, 70040-020 Brasília, DF, Brazil

ARTICLE INFO

Article history:
Received 23 February 2016
Received in revised form 13 April 2016
Accepted 21 April 2016
Available online 22 April 2016

Keywords:
Chemometrics
High resolution mass spectrometry
Hyphenated technique
Matlab
Tool box

ABSTRACT

Post processing of dataset obtained using separation techniques hyphenated with mass spectrometry can allow automation of the recovery of target information, improve the visualization of the data or allow for mathematical separations of convoluted data. Despite the growing popularity and proven successes, those techniques are still only used by few. This is mainly due to the supposed difficulty to open hyphenated dataset, as well as use or develop efficient chemometrics tools. However, due to the work of the Human Proteome Organization (HUPO), the IUPAC and others, there is now MS file formats that are vendor-neutral and can easily be open using various language such as Java, Python, Matlab or R. In the past decades, using those formats, various tools (commercially or freely available) have been designed to help in the post-processing of hyphenated datasets. For proteomic applications, the best known is probably XCMS. However, each of these software is designed for a particular purpose and will not fit all purposes. In the context of our work, we developed a Matlab toolbox that allows openning of MS files in the mzML format and perform various calculations. The aim of this manuscript is to present this toolbox, called Finnee, as well as some key functions. While it is necessary to own a working Matlab license, the toolbox can be used without any programing skills. Every function is protected with the BSD license allowing anyone to study the source code, modify and share it, as long as its copyright notices and the license's disclaimers of warranty are maintained. The source code is available and will be maintain in the GitHub repository (https://github.com/glerny/finnee). Updates and tutorials will be posted in https://finneeblog.wordpress.com/.

1. Introduction

Separation techniques hyphenated with mass spectrometry (X-MS, where X stands for a separation technique, typically gas chromatography, liquid chromatography or capillary electrophoresis) is a very powerful combination for the analysis of complex mixtures. Those instruments are often the center piece in analytical facilities. X-MS covers a very large variety of instruments with different capabilities, performances and prices. The data recorded by those instruments consists in a collection of MS scans acquired at the outlet of the separation channel along the time. Depending on the mass analyzer, the file may range from few megabytes to few gigabytes in size. Data manipulation and transformation play an important part when working with X-MS datasets. For example, centroidization algorithms are used to reduce the size of the file and calculate the accurate masses [1]. Total ion profile (TIP) and base peak profile (BPP) are filters that allow representation of the dataset using simple mono-dimensional profiles [2]. Extracted ion profiles (EIPs) allow generating from the dataset, profiles corresponding to the transport and detection of one theoretical ion defined by its m/z range. X-MS datasets, due to their high importance and complexity, are particularly relevant for complex automatic post-processing. In the past decades, various algorithms and software have been developed aiming to provide advanced representations, comparison of datasets, or automatizing the extraction of the relevant information from multiple runs [1,3–10]. An updated list of software for analysis of mass spectrometry data can be found in the ms-utils.org website [11]. However, despite the large choice of available freeware, they are often specific to an instrument configuration, field of application or target class of compounds. Moreover, they do not always provide all the necessary controls to assess the information that are lost or modified during the various steps. The aim of this manuscript is to present a series of Matlab functions that are part of the Finnee toolbox and were developed within the frame of our work [5,4,12]. This toolbox contains basic function to read mzML files, extract profiles and spectra as well as more advanced tools to calculate accurate masses, obtained pure ion profiles or draw clusters plots. Each function is annotated allowing anyone not only to use them but also to understand and modify them if needed. The functions and algorithms presented here have been developed for high resolution mass spectrometry instruments but should also be suitable for low resolution mass analysers as long as the original proprietary file can be converted to mzML format. The MatLab functions can be

* Correspondence author.
E-mail address: guillaume@fe.up.pt (G.L. Erny).

http://dx.doi.org/10.1016/j.chemolab.2016.04.013
0169-7439/

downloaded in GitHub [13], update and tutorial will be detail in https://finneeblog.wordpress.com/, and the mzML datasets used as example in this manuscript are available for download.[1]

2. The Finnee data architecture

2.1. Software environment

Finnee is developed under MATLAB R2013a environment and has been tested with MATLAB 2015a and 2016a. As far as we are aware no extra toolbox is required with any functions. All functions are run via the Matlab interface thus the working copy of the software is required.

2.2. The mzML format

The past decades have seen a rapid increase in freeware and software dedicated to the analysis of datasets from mass spectrometry and separation techniques hyphenated to mass spectrometry. This is largely due to the effort of various groups to develop and promote open, vendor-neutral, format for MS related files. Those formats are compatible with most mass spectrometers used as standalone instruments or as detectors of a separation technique [14–18]. Among the various formats, mzML, the format promoted by the Human Proteome Organization (HUPO) is now the best accepted. Most instrument manufacturers proposed freeware allowing converting their proprietary format to mzML. Software are also available to perform such conversion [19]. MatLab and Python include functions to read mzML and mzXML formats [9]. The mzML format is a html-like format that uses a control vocabulary (CV) to precisely categorize the information. A full description of the mzML CV can be found in the HUPO web site.[2]

Briefly, a mzML file is a structured way to maintain and share information. Each element has a start tag and an end tag, both enclosed between a '<' and a '>' character. The start tag can encompass a series of attribute = 'value' pairs that allow organizing the information. Text and child elements can be put inside a start tag and end tag to form the mzML structure. Decoding a mzML file often consists in looking for a particular attribute = 'value' within a specific tag.

2.3. Conversion to Matlab structure and associated binary file

While the MatLab function readmzxml.m allows working with mzXML files, this function is problematic with X-MS data files, especially when working with high resolution profile scans. This function will load all the data in memory, overloading it if the file is too large. To be able to work with high resolution datasets and maintain good performances independently of the size of the file, we developed the function domzML2Stc that should be used as below:

```
>> finneeStc = domzML2struct
```

where finneeStc is the Matlab structure that will receive all general information from the mzML file. With this function, MS scans are stored in a separated binary file whose path is kept in finneeStc. This structure will also store the position of each individual scan in the binary file. This allows working with very large files without compromising speed and accuracy.

2.4. The concept of datasets

In finneeStc, MS scans are organized in datasets, each dataset contains all the scans related to a particular run or transformation. While at creation only one dataset exists, the original one, additional datasets can be created. This will be the case for example, after centroidization of profile spectra, background corrections or bucketing. This enables to verify the data integrity after each transformation by comparing scans or profile in each dataset. Until now three formats for dataset are recognized, those that define how the data are organized. The recognized formats are 'profile spectrum', 'centroid spectrum' and 'ionic profile'. 'Profile spectrum' and 'centroid spectrum' are classical formats used by instrument manufacturers and have been well explained by the IUPAC [18]. In 'profile spectrum' datasets, each MS scan is as recorded by the instrument. It is a two column array with in the first column the *m/z* axis and in the second column the corresponding ion counts. In 'centroid spectrum' datasets, each MS scan has been processed with a centroid algorithm. In this case only the position and intensity of each peak originally present in the profile spectrum are recorded. Individual MS scans are also two column arrays with in the first column the accurate masses (centroid position of each peak) and in the second column the corresponding intensity at peak apexes. Ionic profile dataset are a transformation of a MS based architecture (MS scans as a function of time) to a chromatographic based architecture (profiles at different *m/z* values or ranges). Such dataset can be obtained after bucketing or via pure ion profiles. An 'ionic profile' is stored as a three column array; the first column contains the scan numbers, the second the corresponding intensities and the third the *m/z* coordinate or the accurate mass. With each dataset a series of traces are calculated. By default, they are the total ion profile (TIP), the base peak profile (BPP) and the *m/z* value at base peak value (mzBPP).

3. Test files

We provide four mzML files to test and experiment with Finnee. Those files were obtained using CompassXport with two already described experimental results [4]. For each experiment, the data were transformed to mzML using the 'centroid spectrum' and 'profile spectrum' option. standards_profile and standards_centroid are the mzML files related to the CE-TOFMS separation of 17 small molecular mass compounds (adenosine triphosphate, nicotinic acid, glutamic acid, aspartic acid, glutathione oxidized, glutathione reduced, iminodiacetic acid, adenosine monophosphate, panthotenic acid, succinic acid, gluconic acid, hippuric acid, malic acid, citric acid, tartaric acid, 1,4-piper-azinediethanesulfonic acid and malonic acid). urine_profile and urine_centroid are the mzML files obtained after separation of a urine sample by CE-TOFMS. Additional information can be found in the cited manuscript. Datasets are available for download.

4. Exploratory functions

Datasets can be explored using four basic functions. Those will generate a text and/or a figure output in Matlab providing all the necessary information. Additionally, in most cases, a structure will also be created allowing storing the results. Only the basic syntaxes are provided here, most functions also have optional parameters. A detail description can be obtained in Matlab using help *nameOfTheFunction*.

4.1. tellFinnee

This function allows having information about the original file, the number of datasets and associated traces and substructures. The basic syntax to use this function is:

```
>> tellFinnee(finneeStc)
```

4.2. getTrace

getTrace allows recovering and plotting a trace linked to a dataset, where a trace is any type of mono-dimensional representations (i.e. MS scans, base peak profile…). While not available at this time, it may

[1] https://onedrive.live.com/redir?resid=44D0236A062B67C5!4529&authkey=!AI4JV9psRYElepQ&ithint=folder%2c.

[2] http://www.psidev.info/mzml_1_0_0%20.

be possible to add additional traces to a dataset. The basic syntax to use this function is as follows:

```
>> traceOut = getTrace(finneeStc, 'n@m')
```

where traceOut is an output structure that contains information about the trace, finneeStc is the basic Finnee structure created by domzML2struct, and '*n@m*' is the address of the trace (*m* and *n* are the dataset and trace indexes respectively). This address can be found using tellFinnee. A more detail help can be obtained using:

```
>> help getTrace
```

getTrace will create a new figure with the requested information as displayed in Fig. 1. Matlab provides a menu bar that is particularly useful in this work. Not only it permits to zoom or annotate, it also allows the data cursor icon (1 in Fig. 1) to read data directly from the graph (2 in Fig. 1). Those can be used to obtain time values or interval of interest.

4.3. getSpectra

getSpectra allows extraction from the dataset, a mass spectrum at a particular time or scan number. This function can be used with the three types of datasets, 'profile spectrum'. 'centroid spectrum' and 'ionic profile'. The syntax and output are:

```
>> spectraOut = getSpectra(finneeStc, m, [t1 t2])
```

where spectraOut is a summary of the results, finneeStc is the Finnee structure, *m* is the index to the dataset and $[t_1 \cdot t_2]$ is the time interval of interest. A single value can be used instead of an interval.

4.4. getProfile

getProfile allows generating a profile spectrum along the separation by filtering every scan to only kept datapoints within a defined *m/z* interval. The syntax is:

```
>> profileOut = getProfile(finneeStc, m, [mz1 mz2])
```

where profileOut is a summary of the results, finneeStc is the Finnee structure, *m* is the index to the dataset and $[mz_1\ mz_2]$ defines the *m/z* interval. A single value can also be use, however this option is only relevant for 'profile spectrum' datasets.

5. Dataset manipulation

5.1. doCentroid

Centroidization consists in a peak picking routine of a 'profile spectrum' type scan to detect and measure every peak. The 'centroid spectrum' type scan is the conversion of the original continuous profile to a discrete spectrum where only the position and intensity of each original peak are recorded. The position of each peak is the centroid value of the peak and is known as the accurate mass [1]. Such an accurate measurement of the peak position is essential as it allows the identification of unknown compounds [20]. doCentroid is a function that will convert all 'profile spectrum' scans in the original dataset into 'centroid spectrum' scans. New data are recorded in the same original binary file and a new dataset will be created in the Finnee structure that will index the newly created spectra. This allows storing within the same files the original and centroid scans allowing easy comparison. The syntax is:

```
>> finneeStc = doCentroid (finneeStc, m)
```

where *m* is the index to the target dataset (it should be a 'profile spectrum' dataset). The centroid algorithm that is provided here has been optimized for the test datasets provided. In that example, the peaks in each profile spectrum are characterized by a very low number of points per peak (4 to 5) as well as very low noise. In this condition, a classical first derivative based algorithm does not allow separating peaks that are spaced by less than 2 *m/z* intervals even though those appear separated in the profile spectrum. We designed an alternative algorithm that calculates centroid spectrum by (1) detecting every local maxima and (2) calculating the accurate masses and associated intensities by fitting a polynomial of degree 2 to the local maxima and the two closest neighboring data points. Results are shown in Fig. 2. Fig. 2A

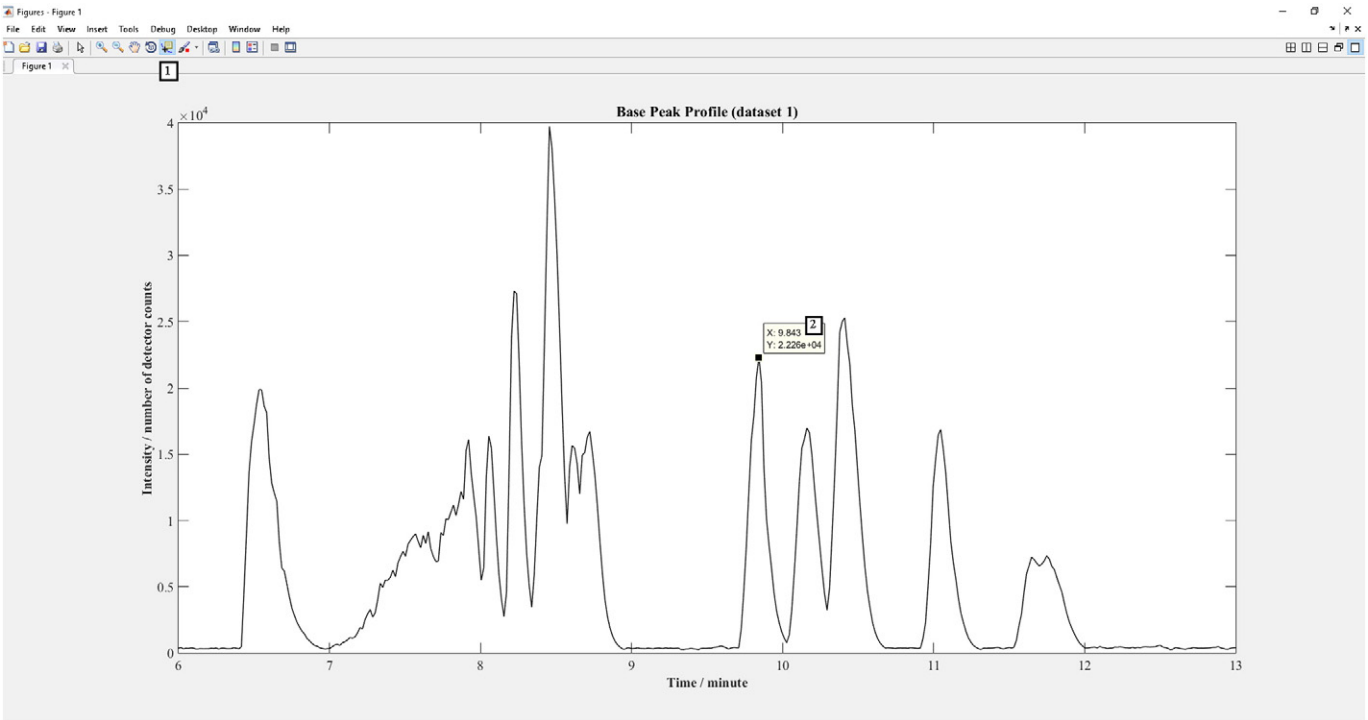

Fig. 1. Figure as displayed by Matlab when using the function getTrace. (1) indicates the data cursor icon and (2) the datatip.

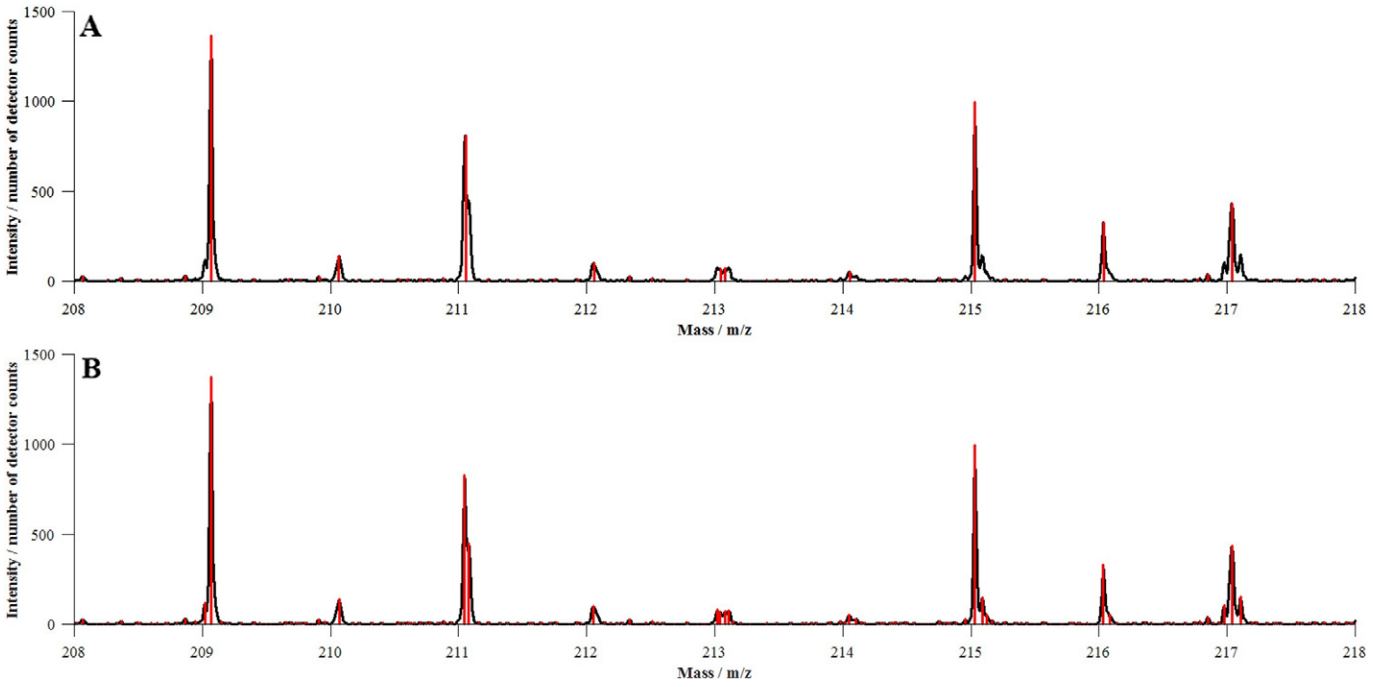

Fig. 2. Comparison of the profile spectrum (continuous) and centroid spectrum (bars) obtained at 8.48 min with the urine dataset. (A) shows the comparison with the centroid spectrum obtained by CompassXport and (B) with the doCentroid function.

shows the comparison between the profile spectrum and the centroid spectrum as calculated by CompassXport and Fig. 2B shows the comparison between the profile spectrum and the centroid spectrum as calculated by doCentroid. CompassXport is the freeware provided by Bruker that allows converting a baf Bruker proprietary file to an mzML file format and it allows converting a file either to 'profile spectrum' mode or to 'centroid spectrum' mode. While there is no information about the centroid algorithm, looking at Fig. 2A, it is likely that a derivative of the signal is used. As it can be seen such algorithm fails to separate closely related peaks (see around *m/z* 215 and 217 for example). The doCentroid, in this case, provide better results. However, it should be emphasize that this is data dependent and with a higher number of

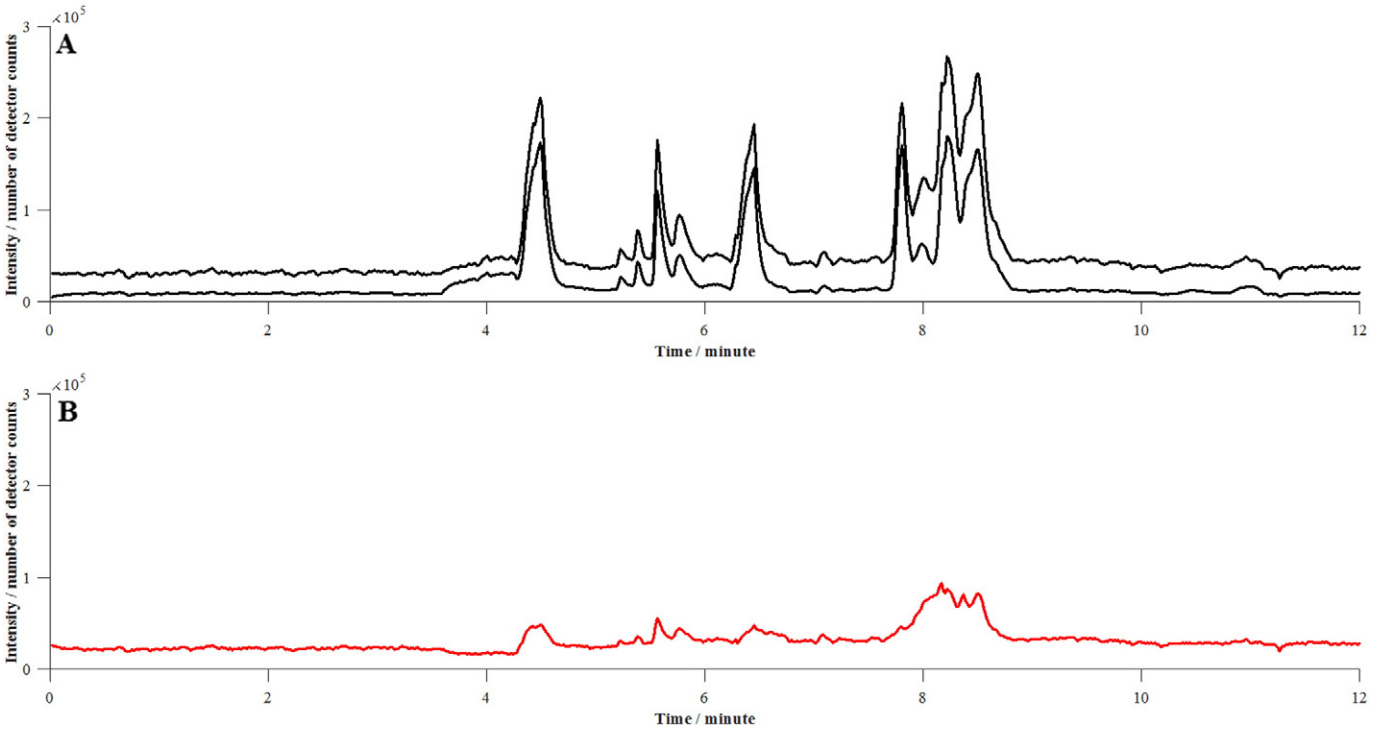

Fig. 3. (A) Comparison of the total ion profile from the centroid spectrum dataset (top) with the total ion profile from the ionic spectrum dataset (bottom), (B) differences between the two profiles.

points per peak or noise, it is likely that the result will be different. A quick tutorial allowing obtaining Fig. 2 is given below.

```
>> Urine_prf = doCentroid (Urine_prf, 1)
>> stra_CTR1 = getSpectra(Urine_ctr, 1, 8.488, 'noFig');
>> stra_PRF1 = getSpectra(Urine_prf, 1, 8.488, 'noFig');
>> stra_PRF2 = getSpectra(Urine_prf, 2, 8.488, 'noFig');
>>subplot(2,1,1)
>> plot(stra_PRF1.data(:,1), stra_PRF1.data(:,2), 'k')
>> hold on
>> stem(stra_CTR1.data(:,1), tra_CTR1.data(:,2), 'r', 'Marker', 'none')
>> xlabel([stra_CTR1.axes.axeX.label, ' / ', stra_CTR1.axes.axeX.unit])
>> ylabel([stra_CTR1.axes.axeY.label, ' / ', stra_CTR1.axes.axeY.unit])
>> hold off
>> subplot(2,1,2)
>> plot(stra_PRF1.data(:,1), stra_PRF1.data(:,2), 'k')
>> hold on
>> stem(stra_PRF2.data(:,1), stra_PRF2.data(:,2), 'r', 'Marker', 'none')
>> xlabel([stra_PRF2.axes.axeX.label, ' / ', stra_PRF2.axes.axeX.unit])
>> ylabel([stra_PRF2.axes.axeY.label, ' / ', stra_PRF2.axes.axeY.unit])
>> hold off
```

where Urine_ctr and Urine_prf are the Finnee structures created using the mzML files in centroid mode and profile mode respectively. Both structures were created using domzML2struct.

5.2. getPIP

When working with X-MS datasets, it is often convenient to transform the MS based dataset (i.e. a scan at each acquisition time) to a chromatographic based dataset (i.e. chromatographic type profile at different m/z intervals). This allows automatizing the treatment of the dataset using chromatographic related tools such as peak picking algorithms and chromatographic figures of merits (time at peak maxima, peak area, peak width, etc.) for each profile. To transform the dataset, two different approaches are usually used. In the bucketing approach, the data are organized in extracted ion profiles (EIPs), each of them corresponding to the sum of all ions within a set m/z interval. The difficulty in this approach is selecting the m/z intervals in such a way that each profile can only contain few ions, but that all the data related to the transport of one ion is not split between two EIPs [20]. Bucketing is often done with 'centroid spectrum' type dataset but can also be done with 'profile spectrum' type dataset. Alternatively, the dataset can be scanned to find sequence of points that should belong to the transport and detection of a single ion. Those are usually points in successive scans that do not differ in their accurate mass by more than a set valor. Profiles reconstituted by this approach are often termed as pure ion profiles (PIPs) [21,22,10,23]. This approach can only be done with 'centroid spectrum' type dataset. The getPIP algorithm has already been described in a previous work [3] and allows extracting PIP from a centroid dataset and, as with doCentroid, will create a new dataset with the results, this allowing verifying the performances of the algorithm. The syntax is:

```
>> [finneeStc, FOMOut] = getPIP( finneeStc, m, intThres, Dmz, pPP)
```

where m is the index to the dataset in 'profile spectrum' mode and *intThres*, *Dmz* and *pPP* are parameters that define the detection of PIPs. A PIP will be created with any sequence of at least *pPP* points with an intensity higher than *intThres* that does not differ in their accurate masses by more than *Dmz*. FOMOut is optional and is a structure that contains all the PIPs as well as key figure of merits. The list of all profiles will be found in the sub-structure FOMOut profiles while FOMOut. FOM lists key figure of merits (fom) for each of those profiles (mean accurate mass of all points that belong to this profile together with the associated standard deviation, the time at peak apex, the peak area, the peak center, etc.). With the test urine dataset, the PIP can be obtained using:

```
>> [Urine_prf, PIPOut] = getPIP(Urine_prf, 2, 25, 0.001, 4)
```

Under those conditions 5784 pure ion profiles were extracted from the dataset. Those profiles are characterized with a mean standard deviation of their accurate mass of 0.0014 ($\pm$0.0010). This value is as expected from a TOF mass analyzer. In Fig. 3A, the TIP obtained with the 'centroid spectrum' dataset (top trace) is compared with the TIP obtained with the 'ionic profile' dataset. Fig. 3B shows the difference between the two traces. As it can be seen from those figures a certain amount of relevant information is lost in the process. As with most chemometric approaches there is a tradeoff between the quality and quantity of information. The residual shows in Fig. 3B can be decreased by

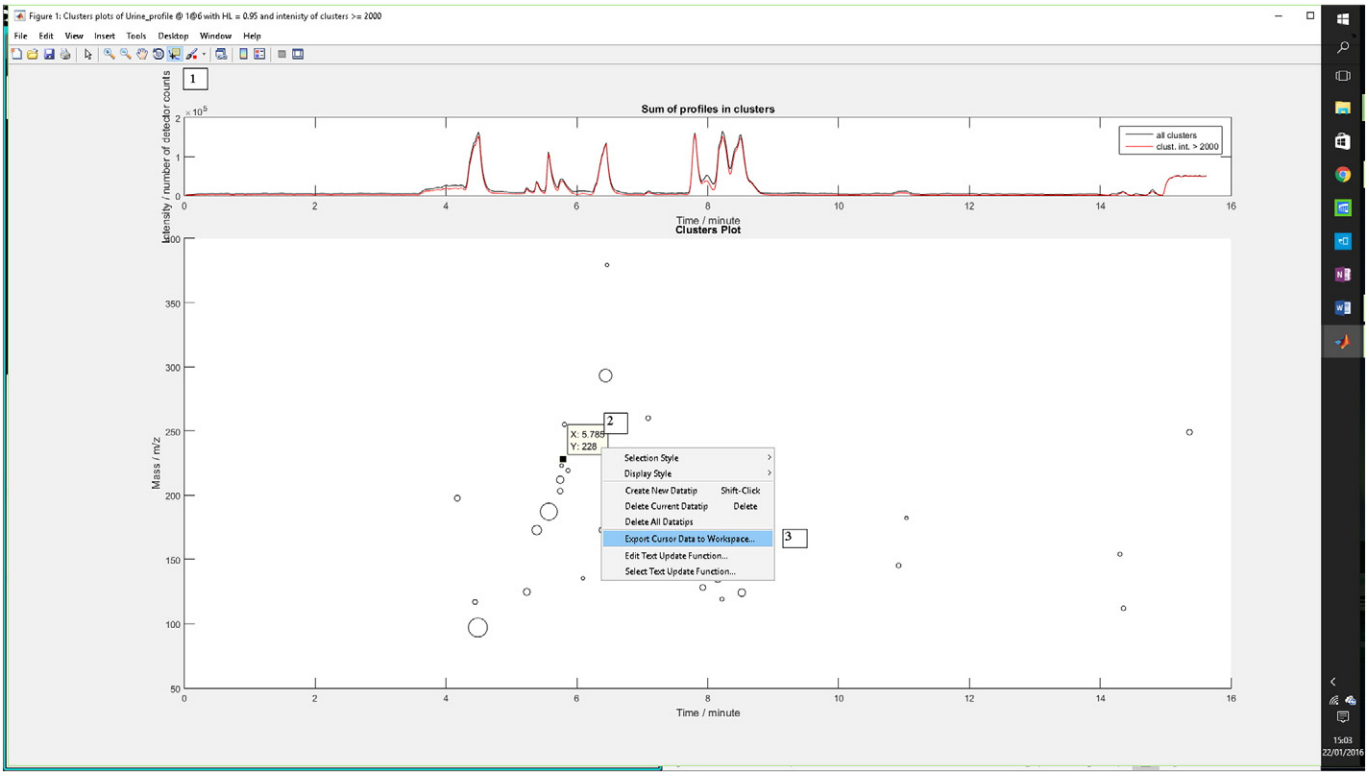

Fig. 4. Cluster plot of the urine dataset as obtained using the function doClusterPlot. (1) indicates the data cursor icon, (2) the data tip and (3) the menu that can be openned by right clicking on the data tip.

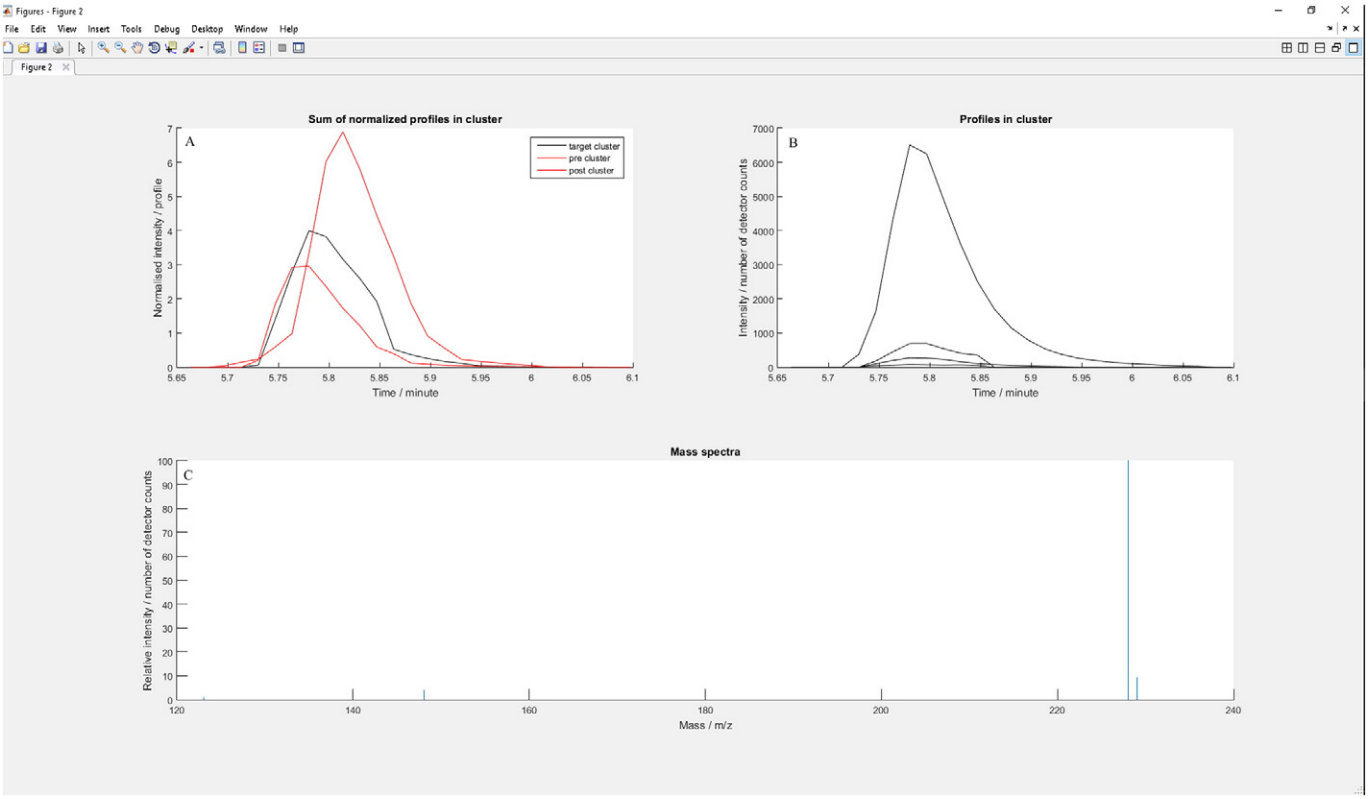

Fig. 5. Figure obtained using the function tellCluster. (A) is the comparison of the average of all profiles in the cluster with the profiles from the two closest clusters, (B) is the superposition of all profiles within the cluster and (C) the MS spectrum obtained using the data from the cluster.

decreasing *intThres* and/or *pPP*. However, doing so it will increase the number of profiles, including artifacts and noise.

6. Cluster plot

We recently proposed a new two dimensional representation of hyphenated dataset called cluster plot [3]. This method used an agglomerative hierarchical clustering approach to regroup similar profiles as measured by the correlation coefficient.

6.1. doHACA

doHACA is the function that will build the hierarchical structure. The syntax is:

```
>> finneeStc = doHACA(finneeStc, m)
```

m is the index to the dataset that should be with 'ionic profile' format. By default, doHACA will only use the 2000 most intense profiles and the hierarchical structure will stop when the highest correlation coefficient between the clusters is lower than 0.9. Both values can easily be changed in the option.

6.2. getClustersPlot

getClustersPlot allows generating the 2 dimensional scatter plot based on the hierarchical structure generated using doHACA. The syntax is:

```
>> clustersOut = doClustersPlot(finneeStc, 'l@m', HL, intThres)
```

'*l@m*' is the address of the hierarchical structure (HS) (*m* and *l* are the dataset and HS indexes respectively), *HL* is the target level in the HS defined by the value of the merging correlation coefficient and *intThres* defined the clusters to be plotted. Only clusters that contain at least one profile with intensity higher than *intThres* are retained. Fig. 4 shows the cluster plot obtained using the urine dataset.

```
>> Urine_prf = doHACA(Urine_prf)
>> clustersOut = doClustersPlot(Urine_prf, '1@6', 0.95, 2000)
```

Ideally every cluster will contain all profiles that are related to the transport and ionization of only one analyte. It is evident that to obtain such a representation a small amount of information is lost; it is therefore important to assess the data integrity at each step.

6.3. tellCluster

The function tellCluster allows visualizing the different PIPs that belong to a particular cluster. The selection of the cluster is done via Fig. 4 by clicking the data cursor icon (1 in Fig. 4) and selecting the target cluster. Right clicking the text box (2) opens a pop up menu that allows exporting the cursor data to the work space (3). Information about the cluster can be obtained using:

```
>> results = getCluster( clustersIn, cursor_info )
```

where clustersIn is the structure obtained after running doClustersPlot and cursor_info is the structure created when exporting the cursor data to the work space. tellCluster will generate two outputs a figure that, as shown in Fig. 5, is made of three panels and a text displayed in Matlab workspace. The panel A shows a profile in black that is the summation of all normalized profiles that belong to the clusters as well as the same profiles for the two closest (in time) clusters. The panel B shows the superposition of all profiles within the cluster and panel C is the stem plot of the *m/z* position as a function of the maximum intensity of all profiles. The text in the workspace summarized

the average accurate mass and associate standard deviation, relative intensity and correlation to the average cluster's profile.

```
>> results = getCluster(clustersIn, cursor info )

Time at peak maxima:                5.78
Maximum intensity:                  228
Sum of max intensities:             7549
Sum of PIP areas:                   672

 AcuMass     std        Intensity    corr2clustP

227.9953    0.0013      100.0        (0.992)
228.9980    0.0013      9.3          (0.994)
148.0403    0.0006      4.3          (0.993)
123.0090    0.0011      1.2          (0.985)
```

7. Conclusions

X-MS datasets contain a wealth of information that can be challenging to extract without any pre information (i.e. untargeted analysis). Chemometric tools have been developed to facilitate recovering this information. However, such tools often filter and/or modify some information and should be used with proper control and understanding. Moreover, the diversity of matrices and instruments means that optimization of condition and algorithms can be challenging. The Finnee toolbox has been design to allow an easy control of the data integrity after each transformation. It allows exploring the data and optimizing or designing algorithms to better fit the instrument particularities or experimental needs. Finnee is not aimed to be a finish product but rather an open solution where tools can easily be developed and tweaked. The GitHub repository has been designed for ease of use of end-users, to download the tools, keep track of updates and new developments, as well as to develope and share their own solutions. Update and news can be followed at https://github.com/glerny/finnee and https://finneeblog.wordpress.com/.

7.1. Independent testing

The Finnee toolbox has been tested by Dr. E Bergström, Centre of Excellence in Mass Spectrometry,

Department of Chemistry, University of York, York YO10 5DD, www.york.ac.uk/mass-spectrometry.

"This is a report reviewing the toolbox described in "Finnee - a Matlab toolbox for processing datasets from high resolution mass spectrometry hyphenated to separation techniques" by G L. Erny, T Acunha, C Simó, A Cifuentes and A Alvesa.

"I have tried all of the MATLAB functions in the Finee toolbox on the following LC–MS datasets: 1. A short LC run of a simple test mix with data collected on a Bruker HCT II ion trap (low resolution data), 2. A 30 min LC run of a real metabolomics sample with a Bruker maXis (high resolution Q-ToF) instrument.

The data was first exported in MZML format using the tool within the the Bruker DataAnalysis software.

Firstly all of the functions worked correctly, as described in the manuscript. The run times were fine for the smaller, low resolution, dataset.

The larger dataset was 220 MB in the Bruker data format which produced a 6 GB MZML file. The domzML2struct function took ~20 min and produced a 12 GB .dat file. The doCentroid function took ~15 min to run. The other functions were then quite quick to run.

For us it is quicker to use the Bruker DataAnalysis software working with the much smaller Bruker .d files. Overall I thought the functions would be useful and it's very good to be able".

Acknowledgments

This work was financially supported by: Project POCI-01-0145-FEDER-006939 (Laboratory for Process Engineering, Environment, Biotechnology and Energy – LEPABE) funded by FEDER funds through COMPETE2020 - Programa Operacional Competitividade e Internacionalização (POCI) – and by FEDER funds through the Operational Program for Human Potential and by National Funds through FCT-Foundation for Science and Technology under the project IF/00528/2013 and AGL2014-53609-P project (Ministerio de Educación y Ciencia, Spain).

References

[1] L. Vergeynst, H. Van Langenhove, P. Joos, K. Demeestere, Accurate mass determination, quantification and determination of detection limits in liquid chromatography–high-resolution time-of-flight mass spectrometry: challenges and practical solutions, Anal. Chim. Acta 789 (2013) 74–82.
[2] K.K. Murray, R.K. Boyd, M.N. Eberlin, G.J. Langley, L. Li, Y. Naito, Definitions of terms relating to mass spectrometry (IUPAC recommendations 2013), Pure Appl. Chem. 85 (2013) 1515–1609.
[3] L. Erny Guillaume, T. Acunha, C. Simó, A. Cifuentes, Algorithm for comprehensive analysis of datasets from hyphenated high resolution mass spectrometric techniques using single ion profiles and cluster analysis, J. Chromatogr. A. 1429 (2016) 134–141.
[4] G.L. Erny, C. Simo, A. Cifuentes, V.I. Esteves, Introducing the concept of centergram. A new tool to squeeze data from separation techniques-mass spectrometry couplings, J. Chromatogr. A. 1330 (2014) 89–96.
[5] G.L. Erny, A. Cifuentes, Simplified 2-D CE-MS mapping: analysis of proteolytic digests, Electrophoresis 28 (2007) 1335–1344.
[6] H. Gowda, J. Ivanisevic, C.H. Johnson, M.E. Kurczy, H.P. Benton, D. Rinehart, et al., Interactive XCMS online: simplifying advanced metabolomic data processing and subsequent statistical analyses, Anal. Chem. 86 (2014) 6931–6939.
[7] S.C. Grace, S. Embry, H. Luo, Haystack, a web-based tool for metabolomics research, BMC Biochem. 15 (2014) 14.
[8] M. Jalali-Heravi, H. Parastar, M. Kamalzadeh, R. Tauler, J. Jaumot, MCRC software: a tool for chemometric analysis of two-way chromatographic data, Chemom. Intell. Lab. Syst. 104 (2010) 155–171.
[9] H.L. Rost, U. Schmitt, R. Aebersold, L. Malmstrom, pyOpenMS: a Python-based interface to the OpenMS mass-spectrometry algorithm library, Proteomics 14 (2014) 74–77.
[10] E. Tengstrand, J. Lindberg, K.M. Aberg, TracMass 2-A modular suite of tools for processing chromatography–full scan mass spectrometry data, Anal. Chem. 86 (2014) 3435–3442.
[11] M. Palmblad, ms-utils.org2007 http://www.ms-utils.org/wiki/pmwiki.php/Main/SoftwareList (accessed January 6, 2016).
[12] G.L. Erny, T. Acunha, C. Simó, A. Cifuentes, A. Alves, Algorithm for comprehensive analysis of datasets from hyphenated high resolution mass spectrometric techniques using single ion profiles and cluster analysis, J. Chromatogr. A. (2015).
[13] G. Erny, Finnee, https://github.com/glerny/finnee.git2016.
[14] G. Mayer, L. Montecchi-Palazzi, D. Ovelleiro, A.R. Jones, P.-A. Binz, E.W. Deutsch, et al., The HUPO proteomics standards initiative — mass spectrometry controlled vocabulary, Database (Oxford) 2013 (2013) bat009, http://dx.doi.org/10.1093/database/bat009.
[15] E. Deutsch, mzML: a single, unifying data format for mass spectrometer output, Proteomics. 8 (2008) 2776–2777.
[16] S.M. Lin, L.H. Zhu, A.Q. Winter, M. Sasinowski, W.A. Kibbe, What is mzXML good for? Expert Rev. Proteomics. 2 (2005) 839–845.
[17] P.G. Pedrioli, J.K. Eng, R. Hubley, M. Vogelzang, E.W. Deutsch, B. Raught, et al., A common open representation of mass spectrometry data and its application to proteomics research, Nat. Biotechnol. 22 (2004) 1459–1466.
[18] P. Lampen, H. Hillig, A.N. Davies, M. Linscheid, Jcamp-Dx for mass-spectrometry, Appl. Spectrosc. 48 (1994) 1545–1552.
[19] J.D. Holman, D.L. Tabb, P. Mallick, Employing proteowizard to convert raw mass spectrometry data, Curr. Protoc. Bioinforma 46 (2014) 13 24 1–9.
[20] R. Tautenhahn, C. Bottcher, S. Neumann, Highly sensitive feature detection for high resolution LC/MS, BMC Biochem. 9 (2008) 16.
[21] K. Aberg, R. Torgrip, J. Kolmert, I. Schuppe-Koistinen, J. Lindberg, Feature detection and alignment of hyphenated chromatographic-mass spectrometric data extraction of pure ion chromatograms using Kalman tracking, J. Chromatogr. A. 1192 (2008) 139–146.
[22] S.-Y. Wang, C.-H. Kuo, Y.J. Tseng, Ion trace detection algorithm to extract pure ion chromatograms to improve untargeted peak detection quality for liquid chromatography/time-of-flight mass spectrometry-based metabolomics data, Anal. Chem. 87 (2015) 3048–3055.
[23] R. Stolt, R. Torgrip, J. Lindberg, L. Csenki, J. Kolmert, I. Schuppe-Koistinen, et al., Second-order peak detection for multicomponent high-resolution LC/MS data, Anal. Chem. 78 (2006) 975–983.

ANEXO IV

Background correction in separation techniques hyphenated to high-resolution mass spectrometry – Thorough correction with mass spectrometry scans recorded as profile spectra

Erny, G.L., Acunha, T., Simó, C., Cifuentes, A., Alves, A.

Journal of Chromatography A **1492,** 98–105 (2017).

DOI: 10.1016/j.chroma.2017.02.052.

Journal of Chromatography A, 1492 (2017) 98–105

Contents lists available at ScienceDirect

Journal of Chromatography A

journal homepage: www.elsevier.com/locate/chroma

Background correction in separation techniques hyphenated to high-resolution mass spectrometry – Thorough correction with mass spectrometry scans recorded as profile spectra☆

Guillaume L. Erny[a,*], Tanize Acunha[b,c], Carolina Simó[b], Alejandro Cifuentes[b], Arminda Alves[a]

[a] LEPABE – Laboratory for Process Engineering, Environment, Biotechnology and Energy, Faculdade de Engenharia da Universidade do Porto, Rua Dr. Roberto Frias, 4200-465 Porto, Portugal
[b] Laboratory of Foodomics, CIAL, CSIC, Nicolas Cabrera 9, 28049 Madrid, Spain
[c] CAPES Foundation, Ministry of Education of Brazil, 70040-020 Brasília, DF, Brazil

ARTICLE INFO

Article history:
Received 26 October 2016
Received in revised form 31 January 2017
Accepted 23 February 2017
Available online 1 March 2017

Keywords:
Chemometrics
Hyphenated techniques
Data mining
Profile spectrum
Baseline correction

ABSTRACT

Separation techniques hyphenated with high-resolution mass spectrometry have been a true revolution in analytical separation techniques. Such instruments not only provide unmatched resolution, but they also allow measuring the peaks accurate masses that permit identifying monoisotopic formulae. However, data files can be large, with a major contribution from background noise and background ions. Such unnecessary contribution to the overall signal can hide important features as well as decrease the accuracy of the centroid determination, especially with minor features. Thus, noise and baseline correction can be a valuable pre-processing step. The methodology that is described here, unlike any other approach, is used to correct the original dataset with the MS scans recorded as profiles spectrum. Using urine metabolic studies as examples, we demonstrate that this thorough correction reduces the data complexity by more than 90%. Such correction not only permits an improved visualisation of secondary peaks in the chromatographic domain, but it also facilitates the complete assignment of each MS scan which is invaluable to detect possible comigration/coeluting species.

1. Introduction

In separation techniques, the baseline should ideally be a constant shift of the signal intensity. In practice, however, especially with complex samples, various artefacts (e.g. drift, large featureless objects, dips, ghost peaks) can be visible. While some of those artefacts are related to instrumental problems and can be corrected, others are inherent to the matrix, the sample preparation (derivatization, digestion, dilution, etc.) or due to additives needed in the mobile phase or background electrolyte. Modern software is usually able to detect and measure the relevant peaks' figures of merit despite complicated background signals. In the most extreme cases, the method can be optimised to avoid baseline artefacts that are interfering with the part of the analytical signal that is of interest. However, even the simplest background signal can be challenging when using Parallel Factor Analysis (PARAFAC) and other multi-ways related chemometric tools [1–5]. Background signals are also problematic in hyphenated and two-dimensional separation techniques. For example, Pierce and colleagues demonstrated that baseline drift does not only hide important features, it also impairs the accurate determination of peaks areas and centres [6,7]. Similarly, Zhang et al. demonstrated the interest of intensive background subtraction for high-resolution LC/MS data to obtain clean product ion spectra [8].

Due to the growing importance of the above-cited techniques, many innovative algorithms for background correction have been proposed in the past decade [1,9–24]. While it is not the aim of this manuscript to compare those methods [21], two of those algorithms are particularly interesting because of their fast computing speed and their ability to model any baselines. Those were derived from the work of Eilers [18,25] and are the adaptive iteratively reweighted penalised least squares (airPLS) and the asymmetrically

☆ Selected paper from the 40th International Symposium on Capillary Chromatography and 13th GC×GC Symposium (RIVA 2016), 29 May–3 June 2016, Riva del Garda, Italy.

* Corresponding author.
E-mail address: guillaume@fe.up.pt (G.L. Erny).

http://dx.doi.org/10.1016/j.chroma.2017.02.052
0021-9673/

reweighted penalised least squares (arPLS) algorithms [15,19]. The aim of this work is to demonstrate the facility and rapidity in which a dataset obtained using separation techniques hyphenated with high-resolution mass spectrometry (CE-TOF MS and UHPLC-Q/TOF MS) can be thoroughly corrected using a modified arPLS algorithm. The key innovative concept in this work is to use MS scans recorded as profile spectrum rather than the usual centroid spectrum.

While MS instruments record scans as continuous profiles (known as profile spectrum), it is usual to transform each scan into a MS centroid spectrum, the prevalent bars type representation. To this effect, every peak within every MS scan is detected using a peak picking algorithm. For each of the detected peaks, only two figures of merits are measured and recorded: the peak centre and the peak maximum intensity. Such conversion allows reducing the size of the file by at least one order of magnitude. The peak centre is also an accurate measurement of the peak position in the m/z axis (hence the name accurate mass [26]), allowing higher selectivity [27] and better identification capability, this by equaling the accurate mass with putative isotopic formula [28,29]. Centroided data are typically calculated by the acquisition software and are often (if not always) the starting points in chemometric tools. However, Kaufmann and others [28,30,31] unambiguously proved that with complex samples, centroid values are not always exact. Most of the errors are due to poorly separated peaks in the MS profile that become merged as a single centroided object. Moreover, when using centroided data, ion profiles (extracted ion profile or pure ion profile) need to be reconstituted before performing the background correction. Various algorithms exist for extracting ion profiles [32–34] from complex datasets with MS scans recorded as centroid spectra. However, with those approaches, some of the data will be lost or merged in the process. On the other hand, working with MS scans recorded as profile spectra allows bypassing those issues. In this case, the m/z axis is the same for every scan and ion profiles are simply obtained by recording, in every scan, the intensity at a given m/z ordinate. In this manuscript, ion profiles refer to chromatographic-like profiles retrieved by selecting in each MS scan the intensity at a given m/z coordinate. They should not be mistaken with extracted ion profiles, single ion profiles or pure ion profiles constructed from MS scans that were converted to centroid spectrum format.

In this work, two metabolomics urine datasets will be used to highlight the interest of this approach. One dataset was obtained using CE-TOF MS instrument, the other with a UHPLC-Q/TOF MS instrument. All algorithms used in this work have been programmed using Matlab and a personal computer. The files are available at https://github.com/glerny/finneeFinnee2016/ as part of the Finnee toolbox. Additional information and tutorials will also be posted at https://finneeblog.wordpress.com/ as well as in the wiki associated with finnee2016 (https://github.com/glerny/Finnee2016/wiki).

2. Materials and methods

2.1. Programming

The Finnee toolbox, used for this work, was run under Matlab 2016b using a PC (Operating system: Windows 10 Pro 64-bit; CPU Intel Core i5 2400 @ 3.10 GHz; RAM: 8.00 GB Dual-Channel DDR3). The new functions programmed for this work are freely available in the Finnee repository https://github.com/glerny/finnee2016/. The Finnee toolbox uses the mzML file format. In this work those were obtained from the original data using either CompassXport (Bruker) or msConvert (freely available at http://proteowizard.sourceforge.net/).

2.2. CE-TOF MS analysis

CE-TOF MS analysis were carried out using a P/ACE 5010 CE system (Beckman, Fullerton, CA, USA) coupled to a time-of-flight (TOF) instrument "microTOF" from Bruker Daltonics (Bremen, Germany). The coupling was carried out via an ESI interface model G1607A from Agilent Technologies. Electrical contact at the electrospray needle tip was established via a sheath liquid composed of 2-propanol-water (50:50, v/v) delivered at a flow rate of 4 μL/min by a 74900-00-05 Cole Palmer syringe pump (Vernon Hills, IL, USA). Bare fused-silica capillary with 50 μm i.d. and 85 cm of total length was from Composite Metal Services (Worcester, England). The inner capillary wall was coated with a cationic TEDETAMA-co-HPMA copolymer. CE separation was performed at −20 kV in an acidic BGE (1 M formic acid adjusted to pH 2.4 with ammonium hydroxide). The nebuliser and drying gas conditions were 0.4 bar N_2 and 4 L/min N_2, respectively, maintaining the ESI chamber temperature at 200 °C. TOF MS was operated in the negative ion mode (capillary voltage was 4 kV) and spectra were acquired in the range of 50–700 m/z. External and internal calibration of the TOF MS instrument was performed by introducing a 5 mM sodium formate solution through the separation capillary. Masses for the calibration of the TOF MS were next: 180.9731, 248.9594, 316.9479, 384.9353, 452.9227 and 520.9102 m/z. The mass resolving power, RP(FWHM), was calculated at m/z = 243 equal to 8500. The numerical threshold was set to zero. The original data files were converted to mzML format using CompassXport. The mzML file is freely available [35].

2.3. UHPLC-Q/TOF MS analysis

UHPLC-Q/TOF analysis was carried out using a 1290 system (Agilent) coupled to a quadrupole-time-of-flight (Q/TOF) 6540 (Agilent) equipped with an orthogonal electrospray ionisation (ESI) source (Agilent Jet Stream, AJS). The separation was performed on a Zorbax Eclipse Plus C8 (2.1 × 100 mm, 1.8 μm) column using phase A (water with 0.1% (v/v) formic acid) and phase B (acetonitrile with 0.1% (v/v) formic acid) and following gradient program: the run was started at 0% B and maintained for 2 min. From 2–6 min phase, B increased linearly till 30%. From 6–8 min phase B was increased to 100% and maintained for 2 min (from 8 to 10). Before each run, the column was re-equilibrated for 3 min using the initial solvent composition. TOF-MS operation parameters were the following: capillary voltage, −4000 V; nebuliser pressure, 25 psi; drying gas flow rate, 7 L/min; gas temperature, 300 °C; skimmer voltage, 45 V; fragmentor voltage was 125 V; 50–1000 m/z mass scan in positive ionisation mode. External calibration of the TOF MS was carried out using a commercial mixture from Agilent with next m/z values: 118.0863, 322.0481, 622.0290, 1221.9906, 1521.9715, 1821.9523, 2121.9331, 2421.9139 and 2721.8948. The mass resolving power, RP(FWHM), was calculated at m/z = 265 equal to 16000. The numerical threshold was set to 200. The original data files were converted to mzML format using msConvert. The mzML file is freely available [36].

2.4. Chemicals and samples

All chemical used were of analytical reagent grade. Reagent and solvents employed in the preparation of the CE electrolytes, sheath liquid, and LC mobile phases were of MS grade: isopropanol, formic acid and ammonium hydroxide from Sigma-Aldrich (St. Louis, MO, USA) and acetonitrile from Labscan (Gliwice, Poland). The water was purified in a Milli-Q system from Millipore (Bedford, MA, USA). Urine sampleswere directly injected following simple filtration by using a 0.22 μm pore size regenerated cellulose filter.

3. Results and discussion

3.1. Selection of profiles

The first step in this work was to select the ion profiles that needed baseline subtraction. The initial motivation for such a task was to decrease the number of ion profiles to be corrected. For example, with the CE-TOF MS dataset, a MS scan is a 2 by 60512 array (m/z scan from 50 to 700, with an interval of 0.0044 at 50 m/z and 0.0167 at 700 m/z) with m/z values and intensities in the first and second column, respectively. The full dataset consists of 1265 scans spaced at relatively regular intervals, ion profiles are obtained by registering the intensity at given m/z values. Thus 60512 profiles will be collected, each containing 1265 points. Similarly, with the UHPLC-Q/TOF MS 141310 profiles (m/z scan from 50 to 1000, with an interval of 0.0025 at 50 and 0.0110 at 1000), each containing 3581 points, will have to be corrected. While the arPLS and airPLS algorithms are particularly fast to converge, it remains wise trying decreasing the number of ion profiles to correct.

While every ion profile is of the same length, with MS instruments, a zero value indicates that no ion was detected at this time and this m/z interval. The relative amount of zero values within a given profile is a strong indicator of the presence of background ions. Indeed, in the absence of background ions, the intensities in the profile will be different of zero only when an analyte entered the ion chamber and generated an ion whose m/z peak will be within the mass interval of interest. With high-resolution mass analyser, in the absence of noise and background ions, the signal will contain many zero values. However, if background ions are present, ionic profiles will contain few zero values as, by definition, the background ions are present during most of the separation time. Fig. 1 illustrates the repartition of profiles as a function of their relative amount of non-zeros values. In this figure, the profile relative lengths are represented in abscissa (non-zeros divided by the total number of values; discrete value with a 1% increment), and the number of profiles with such relative length are represented in ordinate. A similar figure was obtained with the CE-TOF MS data (additional figures, especially related to the CE-TOF MS are presented as supplementary materials, SM1). This graph is characteristic of the distribution of profiles, with no profiles with less than 10%, then a spike of profiles between 10 and 15% and a majority of profiles between 30 and 60%. This representation can be used to filter the dataset, by as in Fig. 2, grouping profiles based on their relative length.

Fig. 2(A–E) shows the base peak profiles (BPP) calculated using profiles with relative length between (A) 0 and 15%, (B) 0 and 25%, (C) 25 and 50%, (D) 50 and 75% and (E) 75% and 100%. BPPs in Fig. 2A and B contain a minimal amount of information, showing that profiles with a relative length below 25% contain neither background ions nor analytes and cen be used to estimate the instrumental noise in the absence of peaks.To do so, all the intensities from profiles with a relatve length below 25% were concatenate into a single vector.The noise was measured using six times the standard deviation of all values. The instrumental noise was equal to 50 a.u.for the UHPLC-Q/TOF MS and 20 a.u. for the CE-TOF MS. As was previously discussed, the BPP depicted in Fig. 2E presents a high baseline level, but also a strong analytical signal. Profiles used to construct this representation seem the most relevant for baseline correction. However, for a thorough correction of the dataset, profiles that contain more than 50% of non-zeros values were also included. Thus, with the UHPLC-Q/TOF MS dataset, 37,000 profiles are selected (for a total of 141310) for baseline correction. With the CE-TOF MS dataset, 3909 profiles were selected (for a total of 60512). It should be emphasised that while it may seem attractive to correct all profiles, most baseline correction algorithms will not perform well with profiles that only contain peaks without any baseline points.

3.2. Baseline correction algorithms

Basic requirements for the background correction algorithm are good robustness, high response speed, flexible; and parameters should be the same for every ion profile within a single dataset. While most existing algorithms were tested in this work, the airPLS and arPLS were of particular interest due to their easiness, good performance with various baseline drift profiles, and rapidity. Fig. 3A and C show the baseline obtained with both algorithms with profiles representative of the most complicated baselines found in the two datasets. This figure clearly indicates that the airPLS algorithm is not adequate when negative peaks, such artefacts (very common in CE analysis), are present (Fig. 3C). Moreover, the position of the baseline about the background noise depends on the

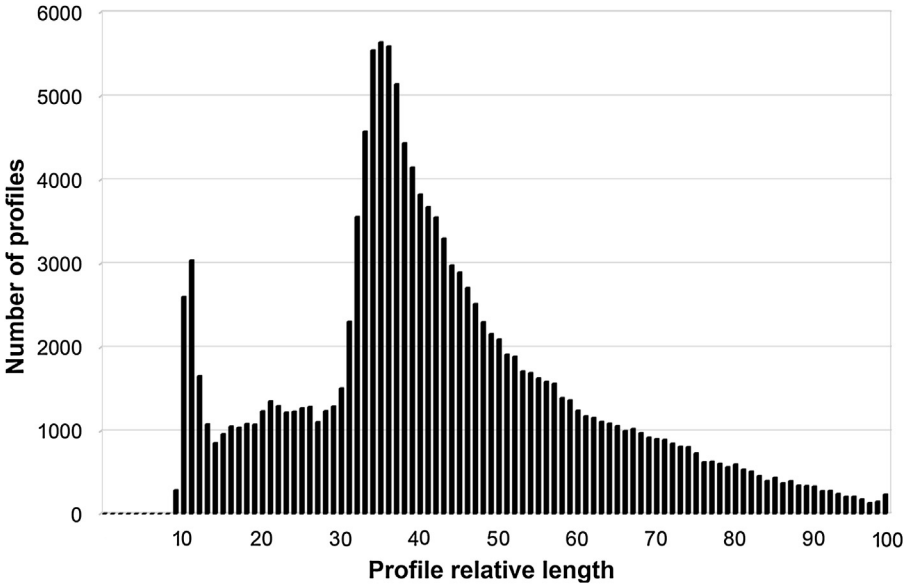

Fig. 1. Amount of profiles within the UHPLC-Q/TOF MS dataset with a given relative length, where the relative length is, for a given profile, the number of nonnull values divide by the total number of values.

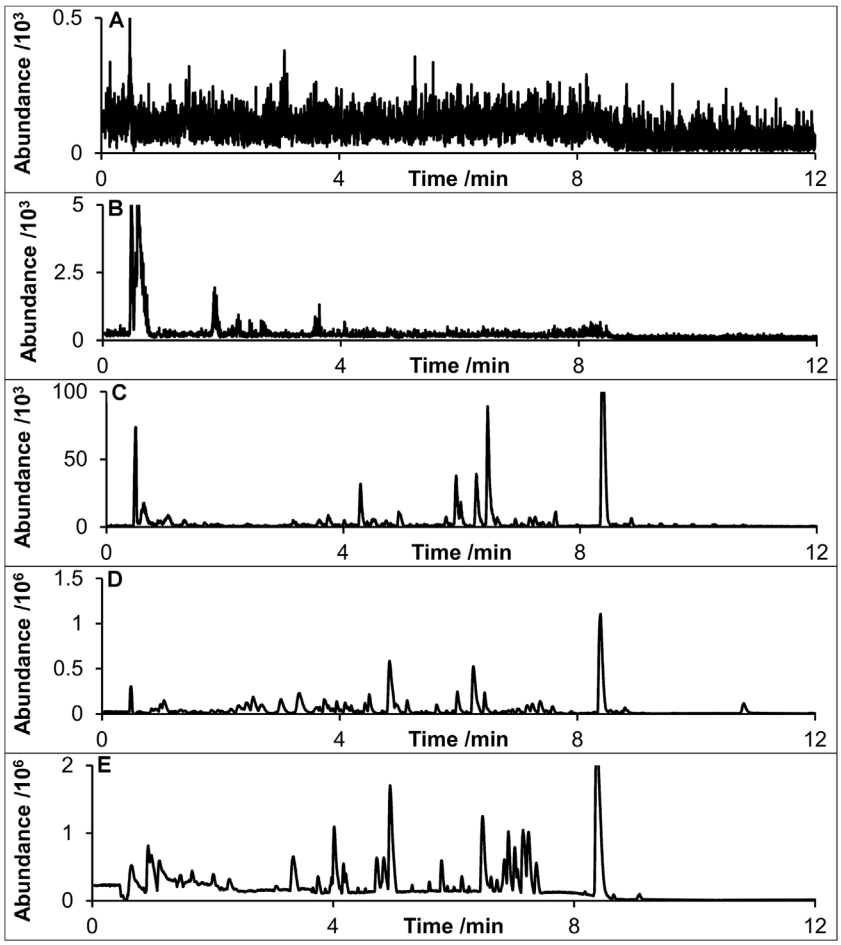

Fig. 2. Base peak profiles using selected ion profiles filtered based on the relative length. BPP calculated with profiles with relative lengths between (A) 0 and 15%, (B) 0 and 25%, (C) 25 and 50%, (D) 50 and 75% and (E) 75 and 100%.

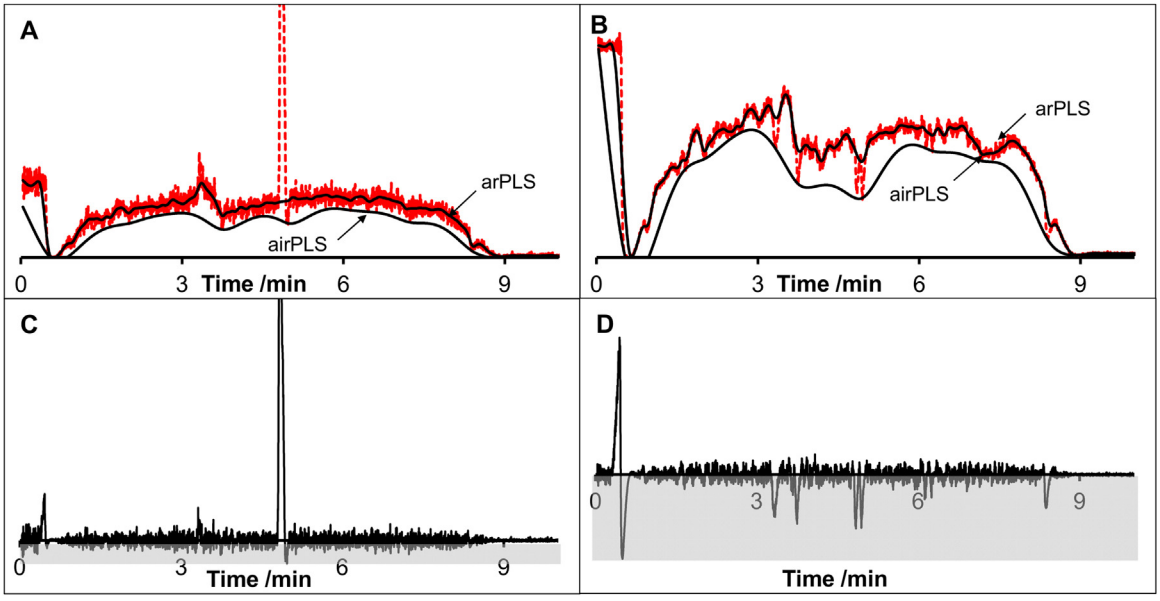

Fig. 3. (A) and (B) selected ion profiles and baselines calculated using the arPLS and airPLS algorithms, (C) and (D) corrected profiles using the arPLS algorithms.

asymmetry parameters. Such a parameter will have to be optimised for every profile depending on the signal to noise ratio. The arPLS appears better with profiles found in the two datasets. Not only this method works correctly with negative peaks, but the smoothness, the only necessary parameter, can be optimised once for all profiles within the dataset. The main limitation of the airPLS algorithm is that negative values can be under evaluated and will depend on the asymmetry factor. While the airPLS algorithm is suitable for convo-

luted profiles with many sharp peaks, the arPLS is clearly superior for profiles that consist of few peaks. Thus the arPLS algorithm was used to correct the selected ion profiles. It should be noted that the arPLS algorithm utilised in this work is slightly different from the original version. The code is introduced in supplementary material (SM2).

Figs. 3C and D show the baseline corrected profiles with the arPLS algorithm; all negative values (zone in grey) are arbitrary set to zero. Those figures indicate that the arPLS can correct baselines with very erratic fluctuations. Nevertheless, in cases of sharp variations of the baseline intensity a ghost peak may appear in the corrected profile (e.g. at 0.5 min in Fig. 3D). The intensity of this peak can be decreased using a lower smoothness value. However, an improperly low value will also modify the intensity of the analytical signal.

3.3. Thorough correction

Fig. 4 is a schematic representation of the algorithm utilised for the thorough baseline correction of the original MS dataset. The steps are as follow:

i Selection of profiles using the percentage of non-zeros values.
ii Estimation of the baseline for each profile using the arPLS algorithm. Each profile is corrected, and negative values are set to zeros.
iii MS scans are corrected by replacing the intensities in the *m*/*z* coordinates of the selected profiles.

Fig. 5 compares the total ion profile (TIP) calculated with (A) the original dataset and (B) the dataset where MS scans were baseline corrected. While the baseline level decreases after baseline correction, the level is still higher than zero. Rather than due to uncorrected (or poorly corrected) baselines this shift is believed to be due to the contribution from noise from every channel. Because individual scans are now corrected from background ions, a very simple noise removal strategy can be designed. Noise removal was done as follow: first, the intensity of the noise in the absence of peaks is estimated. Then, a moving window of size m*n is used to

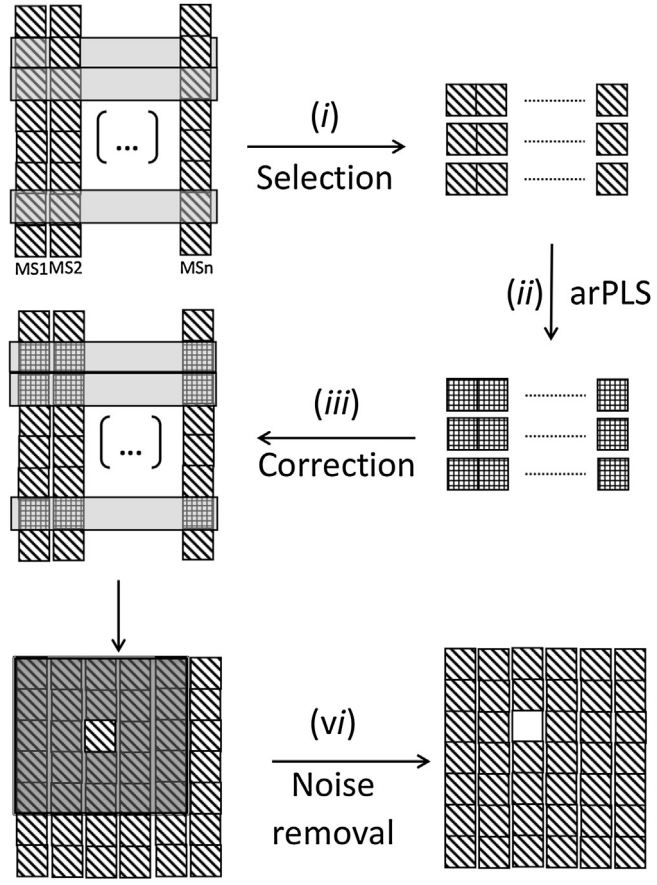

Fig. 4. Schematic representation of the baseline correction methodology. (*i*) Selection of the profiles that need to be corrected from baseline drift; (*ii*) correction using the arPLS algorithm; (*iii*) the selected profiles are replaced by the corrected profiles in the dataset: (*iv*) noise removal: for each point if the intensities within a set window are below the noise threshold, the intensity of the point of interest is set to zero.

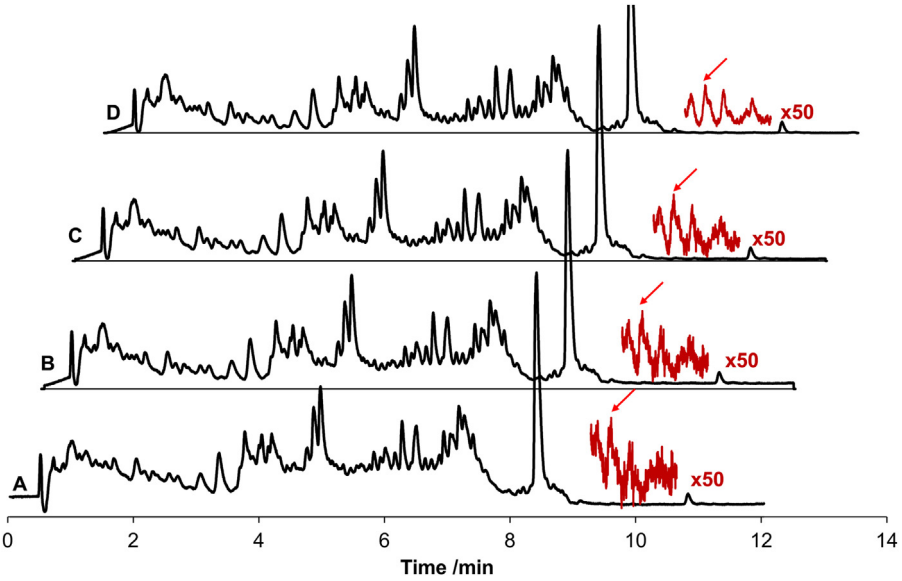

Fig. 5. Total ion profiles from the UHPLC-Q/TOF MS dataset with (A) original data, (B) corrected profiles, (C) corrected profiles and noise reduction using a noise value of 50 and a 7*5 moving window and (D) corrected profiles and noise reduction using a noise value of 200 and a 11*7 moving window. Traces in light grey are a 50-time enhancement of the signal between 9 and 10.5 min; the arrows indicate the peak of interest.

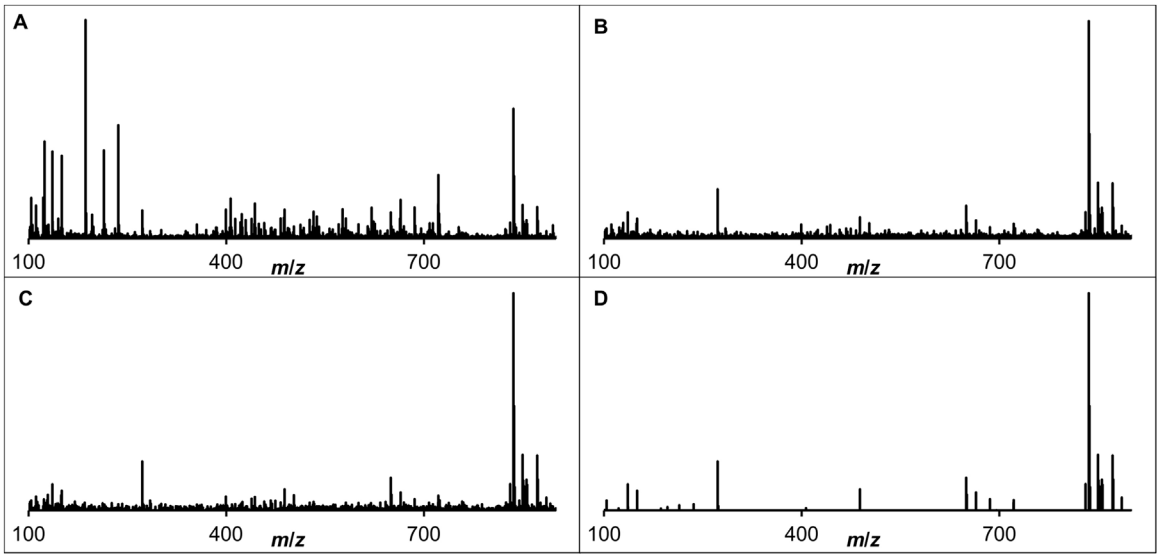

Fig. 6. Full MS scans (profile spectrum) recorded at 9.69 min with (A) original data, (B) corrected profiles, (C) corrected profiles and noise reduction using a noise value of 50 and (D) corrected profiles and noise reduction using a noise value of 200.

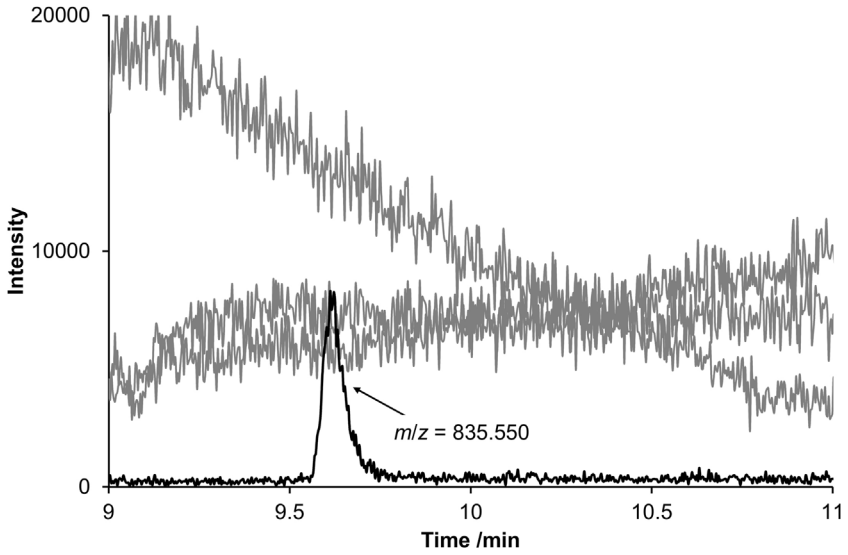

Fig. 7. Ion profiles from the original dataset selected based on the four most intense m/z peak in Fig. 6A. The ion profile obtained at $m/z = 835.550$ corresponds to the base peak after baseline correction (Fig. 6B–D).

measure the maximum intensity within this window. This window is applied to every data point and if the maximum window's intensity is lower than three times the estimated noise, the intensity of the investigated point is set to zero. The TIP, after noise correction, obtained with threshold noise values of 50 and 200 can be observed in Fig. 5C and D, respectively. The noise threshold of 50 is the instrumental noise as previously estimated (see 3.1). As it can be seen in Fig. 5C, while there is a slight improvement in comparison to Fig. 5C, the noise remains high. This is not the case when using a noise threshold of 200, as it can be observed in Fig. 5D. The combination of baseline and noise removal allowed correction from baseline fluctuation. As visible in the close-up (red traces in Fig. 5), this allows detecting easily minor peaks. The noise removal allowed to reduce the size of the data (i.e. value set to zero) by more than 98% with the UHPLC-Q/TOF MS (noise value 200; window size of 11*7). While removing unnecessary information is clearly attractive, it is evident that the data should be minimally modified for such approach to be valuable. The effect of baseline correction and noise removal algorithm on the MS scan is investigated in Fig. 6. The MS scans at 9.69 min (A, indicated by the arrows in Fig. 5) is compared to (B) the scan after baseline correction but without noise removal, (C) baseline and noise corrected with a noise parameter of 50 (windows of 7*5) and (D) baseline and noise corrected with a noise parameter of 200 (window of 11*7).

The baseline correction allows a drastic simplification of the MS scans. Usefulness of such data reduction methodology is exemplified in Fig. 7 where the ion profiles calculated based on the four most intense MS peaks in Fig. 6A are superposed. As it can be seen three of them are related to background ions, while one exhibits a peak at 9.69 min. The m/z index of this profile corresponds to the base peak after baseline correction in Fig. 6B–D. In this example, and as demonstrated in Fig. 7, the corrected scans allow to easily and reliably obtaining the base peak ions that were previously hidden by background ions. While not as striking, this is also true for

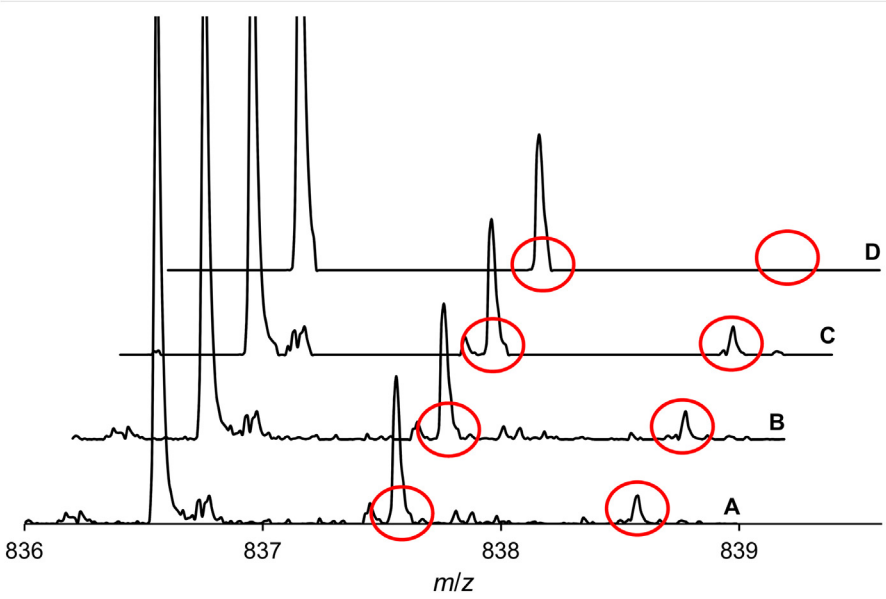

Fig. 8. Zoom between *m*/*z* 836 and 840 of the MS scans presented in Fig. 5. (A) original data, (B) corrected profiles, (C) corrected profiles and noise reduction using a noise value of 50 and (D) corrected profiles and noise reduction using a noise value of 200.

Table 1
Computing speed depending on the number of profiles to correct and dataset size.

CE-TOF MS		UHPLC-Q/TOFMS	
File size (mzML file)	650,000 kB	File size (mzML file)	2,900,000 kB
Selection of profiles	<1 min	Selection of profiles	5 min
Correction (1830 prof.)	<1 min	Correction (9000 prof.)	6 min
Correction (7145 prof.)	1.5 min	Correction (37000 prof.)	15 min
Data reduction by	99.4%	Data reduction by	98.0%

any scan, even with high-intensity peaks. In this case, baseline and noise removal facilitate a thorough analysis of the scans allowing to detect possible co-migration/co-elution.

In Fig. 8, the effects of the baseline and noise removal algorithms on the peak shapes were also investigated. In this figure, the shapes of the three first isotopic peaks were studied under different data manipulation. The filter is very conservative; the peak shapes barely change despite the removal of many data of low intensity. However, it is evident, that if using high values for the noise parameter, the peaks of lowest intensities may be filtered out as it is the case in Fig. 7D. Nevertheless, this may still be beneficial as it allows to reduce the data size by more the 98%, which not only allows much clearer TIP but should also be useful for subsequent chemometrics routine, including for centroid algorithms.

3.4. Computing speed

Computing speed is a crucial factor, however, because speed can vary a lot depending on the computer and complexity of the dataset, the speeds given in Table 1 are only indicative. Time has been measured using a personal computer and using the Matlab tic/toc functions that measure the CPU time. With a maximum time of 15 min, it demonstrates that manipulating large dataset can be done in reasonable times. The total computing speed varied from less than 2 min with the small CE-TOF MS dataset (0.7 GB) to 20 min with the larger dataset (2.9 GB), this excluding the conversion of the mzML file to the Matlab structure as previously described. Computing speed will also depend on the number or profiles to correct. While it is tempting to minimise this speed by reducing the number of profiles to correct, a thorough correction is clearly advantageous but will require overestimating the number of profiles to correct.

4. Conclusions

In this manuscript, the arPLS, a baseline correction algorithms and a new noise removal algorithm have been applied to thoroughly correct urine metabolome datasets. The baseline and noise correction allows a drastic reduction of the data complexity by more than 98%. Such data transformation allows easily detecting minor peaks that were previously hidden. The arPLS has been found to be reliable, robust and fast allowing to correct those large datasets in a reasonable time, e.g. less than 20 min for the larger dataset. The use of profile spectra instead of centroid spectra allows to easily obtain ion profiles. However, it is evident that centroid algorithms will then have to be performed in the corrected data set to calculate the accurate masses.

Acknowledgments

This work was financially supported by the projects: (i) POCI-01-0145-FEDER-006939 (Laboratory for Process Engineering, Environment, Biotechnology and Energy – UID/EQU/00511/2013) funded by the European Regional Development Fund (ERDF), through COMPETE2020 – Programa Operacional Competitividade e Internacionalização (POCI) and by national funds, through FCT – Fundaça˜o para a Ciência e a Tecnologia; (ii) NORTE-01-0145-FEDER-000005LEPABE-2-ECO-INNOVATION, LEPABE-2-*E*CO-INNOVATION, supported by North Portugal Regional Operational Programme (NORTE 2020), under the Portugal 2020 Partnership Agreement, through the European Regional Development Fund (ERDF); (iii) AGL2014-53609-P project (Ministerio de Educación y Ciencia, Spain); (iv) IF/00528/2013, supported by FEDER funds through the Operational Programme for Human Potential and by National Funds through FCT – Foundation for Science and Technology. T. A. thanks the CAPES Foundation, Ministry of Education of Brazil for her pre-doctoral Scholarship – Proc. N° 1532/13-8.

Appendix A. Supplementary data

Supplementary data associated with this article can be found, in the online version, at http://dx.doi.org/10.1016/j.chroma.2017.02.052.

References

[1] H.-Y. Fu, H.-D. Li, Y.-J. Yu, B. Wang, P. Lu, H.-P. Cui, et al., Simple automatic strategy for background drift correction in chromatographic data analysis, J. Chromatogr. A 2016 (1449) 89–99, http://dx.doi.org/10.1016/j.chroma.2016.04.054.

[2] J.W. McIlroy, R.W. Smith, V.L. McGuffin, Assessing the effect of data pretreatment procedures for principal components analysis of chromatographic data, Forensic Sci. Int. 257 (2015) 1–12, http://dx.doi.org/10.1016/j.forsciint.2015.07.038.

[3] J. Kuligowski, G. Quintás, R. Tauler, B. Lendl, M. De La Guardia, Background correction and multivariate curve resolution of online liquid chromatography with infrared spectrometric detection, Anal. Chem. 83 (2011) 4855–4862, http://dx.doi.org/10.1021/ac2004407.

[4] M. Jalali-Heravi, H. Parastar, Recent trends in application of multivariate curve resolution approaches for improving gas chromatography-mass spectrometry analysis of essential oils, Talanta 85 (2011) 835–849, http://dx.doi.org/10.1016/j.talanta.2011.05.045.

[5] R.B. Martí, J.F. Baldrich, Fundamentals of PARAFAC, in: A. Muñoz de la Peña, H.C. Goicoechea, G.M. Escandar, A.C. Olivieri (Eds.), Data Handl. Sci. Technol., first edition, Elsevier B.V., Amsterdam, Netherland, 2015, pp. 7–35, http://dx.doi.org/10.1016/B978-0-444-63527-3.00001-1.

[6] K.M. Pierce, B. Kehimkar, L.C. Marney, J.C. Hoggard, R.E. Synovec, Review of chemometric analysis techniques for comprehensive two dimensional separations data, J. Chromatogr. A 1255 (2012) 3–11, http://dx.doi.org/10.1016/j.chroma.2012.05.050.

[7] R.C. Allen, M.G. John, S.C. Rutan, M.R. Filgueira, P.W. Carr, Effect of background correction on peak detection and quantification in online comprehensive two-dimensional liquid chromatography using diode array detection, J. Chromatogr. A 1254 (2012) 51–61, http://dx.doi.org/10.1016/j.chroma.2012.07.034.

[8] H. Zhang, M. Grubb, W. Wu, J. Josephs, W.G. Humphreys, Algorithm for thorough background subtraction of high-Resolution LC/MS data: application to obtain clean product ion spectra from nonselective collision-Induced dissociation experiments, Anal. Chem. 81 (2009) 2695–2700, http://dx.doi.org/10.1021/ac8027189.

[9] R. Jabeen, Automated Baseline Estimation for Analytical Signals, Submitted in Partial Fulfilment of the Requirements for the Degree of Master of Science, Dalhousie University, 2013, http://dx.doi.org/10.1016/S0022-3913(12)00047-9.

[10] X. Liu, Z. Zhang, P.F.M. Sousa, C. Chen, M. Ouyang, Y. Wei, et al., Selective iteratively reweighted quantile regression for baseline correction, Anal. Bioanal. Chem. 406 (2014) 1985–1998, http://dx.doi.org/10.1007/s00216-013-7610-x.

[11] Y. Liu, W. Cai, X. Shao, Intelligent background correction using an adaptive lifting wavelet, Chemom. Intell. Lab. Syst. 125 (2013) 11–17, http://dx.doi.org/10.1016/j.chemolab.2013.03.010.

[12] M. Lopatka, A. Barcaru, M.J. Sjerps, G. Vivó-Truyols, Leveraging probabilistic peak detection to estimate baseline drift in complex chromatographic samples, J. Chromatogr. A 1431 (2016) 122–130, http://dx.doi.org/10.1016/j.chroma.2015.12.063.

[13] X. Ning, I.W. Selesnick, L. Duval, Chromatogram baseline estimation and denoising using sparsity (BEADS), Chemom. Intell. Lab. Syst. 139 (2014) 156–167, http://dx.doi.org/10.1016/j.chemolab.2014.09.014.

[14] Z. Wang, M. Zhang, P.D.B. Harrington, Comparison of three algorithms for the baseline correction of hyphenated data objects, Anal. Chem. 86 (2014) 9050–9057, http://dx.doi.org/10.1021/ac501658k.

[15] Z.-M. Zhang, S. Chen, Y.-Z. Liang, Baseline correction using adaptive iteratively reweighted penalized least squares, Analyst 135 (2010) 1138–1146, http://dx.doi.org/10.1039/b922045c.

[16] Y.-J. Yu, Q.-L. Xia, S. Wang, B. Wang, F.-W. Xie, X.-B. Zhang, et al., Chemometric strategy for automatic chromatographic peak detection and background drift correction in chromatographic data, J. Chromatogr. A 1359 (2014) 262–270, http://dx.doi.org/10.1016/j.chroma.2014.07.053.

[17] X. Liu, Z. Zhang, Y. Liang, P.F.M. Sousa, Y. Yun, L. Yu, Baseline correction of high resolution spectral profile data based on exponential smoothing, Chemom. Intell. Lab. Syst. 139 (2014) 97–108, http://dx.doi.org/10.1016/j.chemolab.2014.09.018.

[18] P.H.C. Eilers, H.F.M. Boelens, Baseline correction with asymmetric least squares smoothing, in: Unpubl. Manuscr, 2005, pp. 1–26 (accessed September 26, 2016) https://www.researchgate.net/publication/228961729_Baseline_Correction_with_Asymmetric_Least_Squares_Smoothing.

[19] S.-J. Baek, A. Park, Y.-J. Ahn, J. Choo, Baseline correction using asymmetrically reweighted penalized least squares smoothing, Analyst 140 (2015) 250–257, http://dx.doi.org/10.1039/C4AN01061B.

[20] J. Kuligowski, G. Quintás, S. Garrigues, M. de la Guardia, New background correction approach based on polynomial regressions for on-line liquid chromatography-Fourier transform infrared spectrometry, J. Chromatogr. A 1216 (2009) 3122–3130, http://dx.doi.org/10.1016/j.chroma.2009.01.110.

[21] L. Komsta, Comparison of several methods of chromatographic baseline removal with a new approach based on quantile regression, Chromatographia 73 (2011) 721–731, http://dx.doi.org/10.1007/s10337-011-1962-1.

[22] J. Kuligowski, G. Quintás, S. Garrigues, M. De La Guardia, Application of point-to-point matching algorithms for background correction in on-line liquid chromatography-Fourier transform infrared spectrometry (LC-FTIR), Talanta 80 (2010) 1771–1776, http://dx.doi.org/10.1016/j.talanta.2009.10.021.

[23] G.L. Erny, V. Calisto, V.I. Esteves, Noise normalisation in capillary electrophoresis using a diode array detector, J. Sep. Sci. 34 (2011) 1703–1707, http://dx.doi.org/10.1002/jssc.201100243.

[24] Z. Xu, X. Sun, P.B. Harrington, Baseline correction method using an orthogonal basis for gas chromatography/mass spectrometry data, Anal. Chem. 83 (2011) 7464–7471, http://dx.doi.org/10.1021/ac2016745.

[25] P.H.C. Eilers, A perfect smoother, Anal. Chem. 75 (2003) 3631–3636, http://dx.doi.org/10.1021/ac034173t.

[26] K.K. Murray, R.K. Boyd, M.N. Eberlin, G.J. Langley, L. Li, Y. Naito, Definitions of terms relating to mass spectrometry (IUPAC Recommendations 2013)*, Pure Appl. Chem. 85 (2013) 1515–1609, http://dx.doi.org/10.1351/PAC-REC-06-04-06.

[27] L. Vergeynst, H. Van Langenhove, P. Joos, K. Demeestere, Accurate mass determination, quantification and determination of detection limits in liquid chromatography–high-resolution time-of-flight mass spectrometry: challenges and practical solutions, Anal. Chim. Acta 789 (2013) 74–82, http://dx.doi.org/10.1016/j.aca.2013.06.024.

[28] A. Kaufmann, The current role of high-resolution mass spectrometry in food analysis, Anal. Bioanal. Chem. 403 (2012) 1233–1249, http://dx.doi.org/10.1007/s00216-011-5629-4.

[29] I. Ojanperä, M. Kolmonen, A. Pelander, Current use of high-resolution mass spectrometry in drug screening relevant to clinical and forensic toxicology and doping control, Anal. Bioanal. Chem. (2012), http://dx.doi.org/10.1007/s00216-012-5726-z.

[30] A.W.T. Bristow, K.S. Webb, Intercomparison study on accurate mass measurement of small molecules in mass spectrometry, J. Am. Soc. Mass Spectrom. 14 (2003) 1086–1098, http://dx.doi.org/10.1016/S1044-0305(03)00403-3.

[31] A. Kaufmann, P. Butcher, Strategies to avoid false negative findings in residue analysis using liquid chromatography coupled to time-of-flight mass spectrometry, Rapid Commun. Mass Spectrom. 20 (2006) 3566–3572, http://dx.doi.org/10.1002/rcm.2762.

[32] S.-Y.Y. Wang, C.-H.H. Kuo, Y.J. Tseng, Ion trace detection algorithm to extract pure ion chromatograms to improve untargeted peak detection quality for liquid chromatography/time-of-flight mass spectrometry-based metabolomics data, Anal. Chem. 87 (2015) 3048–3055, http://dx.doi.org/10.1021/ac504711d.

[33] T. Pluskal, S. Castillo, A. Villar-Briones, M. Oresic, MZmine 2: modular framework for processing, visualizing, and analyzing mass spectrometry-based molecular profile data, BMC Bioinf. 11 (2010) 395, http://dx.doi.org/10.1186/1471-2105-11-395.

[34] R. Tautenhahn, C. Bottcher, S. Neumann, Highly sensitive feature detection for high resolution LC/MS, BMC Bioinf. 9 (2008) 16, http://dx.doi.org/10.1186/1471-2105-9-504.

[35] G. Erny, CE-TOFMS data from a urine sample – mzML files with scans in profile or centroid spectrum format, Mendeley Data (2017) v2, http://dx.doi.org/10.17632/cb4hv9cp2c.2.

[36] G. Erny, UHPLC-QTOFMS data from a urine sample – mzML files with scans in profile or centroid spectrum format, Mendeley Data (2017) v1, http://dx.doi.org/10.17632/6rn82jdv8d.1.